HAL open science

Evolution temporelle en théorie des cordes

François Bourliot

To cite this version:

François Bourliot. Evolution temporelle en théorie des cordes. Physics [physics]. Ecole Polytechnique X, 2010. English. NNT : . pastel-00006168

HAL Id: pastel-00006168

https://pastel.hal.science/pastel-00006168

Submitted on 30 Jun 2010

HAL is a multi-disciplinary open access archive for the deposit and dissemination of scientific research documents, whether they are published or not. The documents may come from teaching and research institutions in France or abroad, or from public or private research centers.

L'archive ouverte pluridisciplinaire **HAL**, est destinée au dépôt et à la diffusion de documents scientifiques de niveau recherche, publiés ou non, émanant des établissements d'enseignement et de recherche français ou étrangers, des laboratoires publics ou privés.

ECOLE POLYTECHNIQUE

THESE

pour obtenir le grade de

Docteur en Science de l'Ecole Polytechnique

préparée au laboratoire **CPHT**

dans le cadre de l'Ecole Doctorale **EdX**

présentée par **François Bourliot**

le 8 Juin 2010

Titre:

Evolution temporelle en théorie des cordes

Directeur de thèse: **Marios Petropoulos**

Jury

M. Marios Petropoulos,	Directeur de thèse
M. Costas Bachas,	Rapporteur
M. Iosif Bena,	Rapporteur
M. Carlo Angelantonj,	Examinateur
M. Christos Charmousis,	Examinateur
M. Pierre Binétruy,	Examinateur
M. Nicolaos Toumbas,	Examinateur

Table des matières

Table des matières **1**

Table des figures **5**

Remerciements **7**

1 Introduction **9**

1 Cordes et cosmologie 9

1.1 Une rapide histoire de l'Univers 9

1.2 Pourquoi la théorie des cordes ? 10

1.3 De la transition d'Hagedorn vers la transition électrofaible . . 12

2 Flots géométriques et applications 13

3 Travaux non détaillés dans ce rapport 13

3.1 Classification des solutions statiques à symétrie sphérique . . . 14

3.2 Perturbations cosmologiques des théories Einstein-Ether . . . 15

4 Plan 15

2 Éléments de théorie des cordes et de cosmologie **17**

1 Éléments de théorie des cordes 17

1.1 Corde bosonique 17

1.2 Supersymétrie et supercordes 21

1.3 Interactions de cordes et fonction de partition 28

2 Modèle standard $\Lambda-$CDM 35

3 Cosmologie en théorie des supercordes **39**

1 Pourquoi étudier la cosmologie des supercordes ? 39

1.1 Cosmologie des supercordes : idées standard 39

1.2 Notre modèle 42

2 Notations et conventions 43
2.1 Thermodynamique d'un gaz de cordes 44
2.2 Modèle considéré 45
3 On introduit la brisure de supersymétrie 48
3.1 Brisure de supersymétrie sans orbifold simultané 48
3.2 Brisure de supersymétrie et orbifold simultanés 53
4 Deux dimensions internes dynamiques 54
4.1 Deux dimensions internes brisant la supersymétrie 54
4.2 UDR et stabilisation de modules 55
5 Conclusions et perspectives 66
5.1 Résumé 66
5.2 Extensions 66

4 Flots géométriques et instantons gravitationnels 69
1 Espaces homogènes et groupes de Bianchi 69
1.1 Espaces homogènes 69
1.2 Groupes de Bianchi 70
2 Instantons gravitationnels 71
3 Flots géométriques 79

5 Flots géométriques et systèmes gravitationnels 83
1 Espaces auto-duaux en quatre dimensions 84
1.1 Rappels du chapitre 4 84
1.2 Classification 85
2 Espaces homogènes auto-duaux et flots de Ricci 87
2.1 Posons le problème... 87
2.2 Notre classification 90
2.3 Les autres algèbres unimodulaires de la classification 95
3 Théorie d'Hořava et flots géométriques 97
3.1 Flot de Ricci+Cotton normalisé 100
3.2 Flot de Ricci+Cotton non normalisé 105
3.3 Quelques résultats quand $\Lambda_W \neq 0$ 109
3.4 Approche canonique de la théorie d'HL 111

6 Conclusions et ouvertures 113

A Savoir utiliser les fonctions modulaires **115**

1 Fonctions θ 115

2 Resommation de Poisson 118

3 Comment intégrer sur le domaine fondamental ? 119

B Classification de Bianchi **121**

1 Classification de Bianchi 121

2 Quelques tenseurs 123

3 Formalisme de Cartan 123

C Publication 1 : F. Bourliot, C. Kounnas and H. Partouche, "Attraction to a radiation-like era in early superstring cosmologies," Nucl. Phys. B 816 (2009) 227 [arXiv :0902.1892 [hep-th]]. **125**

D Publication 2 : F. Bourliot, J. Estes, C. Kounnas and H. Partouche, "Cosmological Phases of the String Thermal Effective Potential," Nucl. Phys. B 830 (2010) 330 [arXiv :0908.1881 [hep-th]]. **127**

E Publication 3 : F. Bourliot, J. Estes, C. Kounnas and H. Partouche, "Thermal and quantum induced early superstring cosmology," arXiv :0910.2814 [hep-th], *accepted for publication by NOVA publishers.* **129**

F Publication 4 : F. Bourliot, J. Estes, P. M. Petropoulos and Ph. Spindel, "Gravitational instantons, self-duality and geometric flows," Phys. Rev. D 81 (2010) 104001 [arXiv :0906.4558 [hep-th]]. **131**

G Publication 5 : F. Bourliot, J. Estes, P. M. Petropoulos and Ph. Spindel, "G3-homogeneous gravitational instantons," Class. Quant. Grav. 27 (2010) 105007 [arXiv :0912.4848 [hep-th]]. **133**

H Publication 6 : I. Bakas, F. Bourliot, D. Lust and M. Petropoulos, "Mixmaster universe in Horava-Lifshitz gravity," Class. Quant. Grav. 27 (2010) 045013 [arXiv :0911.2665 [hep-th]]. **135**

I Publication 7 : I. Bakas, F. Bourliot, D. Lust and M. Petropoulos, "Geometric flows in Horava-Lifshitz gravity," JHEP 1004 (2010) 131 [arXiv :1002.0062 [hep-th]]. **137**

Bibliographie **139**

Table des figures

2.1 Corde ouverte et corde fermée. Les positions initiales et finales des cordes sont notées en vert. 18

2.2 Ligne d'univers et surface d'univers (Σ). 18

2.3 Interactions en théorie des cordes et son développement en perturbations 30

2.4 Domaine fondamental d'un tore. 30

2.5 Schéma descriptif de l'orbifold $\mathbb{Z}_2$ 33

3.1 La forme du potentiel $V(z)$ dépend du rapport $\mathcal{R}$. Les cas (a), (b) et (c) sont détaillés ci-dessous. 50

3.2 Oscillations amorties pour z (courbe solide) et convergence vers 0 de $\dot{\phi}_\perp$ (courbe en pointillés) 52

3.3 L' allure du potentiel $\tilde{V}(z)$ dépend du rapport $\mathcal{R}$. Les cas (IIa), (IIb) et (IIc) sont des extensions des cas (a), (b) et (c) ci-dessus. En particulier, les cas (IIa) et (IIb) sont désormais identiques. 54

3.4 $P(\zeta)$ varie quand $n_V > 0$. Si $n_V < 0$, c'est uniquement possible si $z \ll -1$. 64

3.5 Phase III pour $z \gg 1$ et $n_V < 0$. Une telle phase n'existe pas pour $n_V > 0$. La phase V est T-duale. 64

4.1 Comportement de la solution anisotrope avec $\Omega_1(0) < \Omega_2(0) < \Omega_3(0)$. De haut en bas nous avons $\Omega_3(T)$, $\Omega_2(T)$ et $\Omega_1(T)$. 79

5.1 Principe de la décomposition ADM. On peut voir cette dernière comme une généralisation du théorème de Pythagore, et on comprend mieux le sens physique des différents termes de cette décomposition. 97

5.2 $\beta(\lambda)$ 101

5.3 Point fixe isotrope pour $\mu > 0$ ($\mu = 2$ ici). 104

5.4 Points fixes pour $-3 < \mu < 0$ (ici $\mu = -2$). 104

5.5 Points fixes pour $-6 \cdot 2^{1/3} < \mu < -3$ (ici $\mu = -5$). 105

5.6 Points fixes pour $\mu < -6\,2^{1/3}$ (ici $\mu = -10$). 105

A.1 Effets de transformations modulaires S et T successives sur le domaine fondamental en gris. L'ensemble des valeurs de τ_1, τ_2 peut ainsi être atteint. Tirée de [**?**]. 117

Remerciements

L'accomplissement de cette thèse aurait été impossible sans le soutien sans faille de mes parents. C'est grâce à ce soutien permanent que j'ai pu avancer sur les chemins sinueux de la recherche, mais pas seulement. Jamais je ne les remercierai assez. Ensuite je tiens à remercier Florence pour nombre de choses qui seraient trop longues à énumérer ici.

Sur un plan plus professionnel, je tiens à remercier mon directeur de thèse, Marios, pour avoir eu la gentillesse de me prendre comme étudiant et la patience digne d'une entrée dans le livre des records de supporter mes nombreuses questions et mon envie de travailler dans différents domaines de la physique théorique. Cette thèse est aussi le résultat d'une collaboration avec de nombreux chercheurs et post-doctorants que je remercie ici : I. Bakas, J. Estes, P. Ferreira, C. Kounnas, D. Lüst, H. Partouche, P. Spindel, G. Starkman, T. Zlosnik and J. Zuntz.

Je remercie également l'équipe pédagogique de l'école Georges Gusdorff qui a eu la grande gentillesse d'accepter que j'intervienne devant leur élèves afin de leur faire partager ma passion pour la science.

Je pourrais m'étendre plus dans ces remerciements, mais que ce rapport commence !

à P.P, cette thèse est la tienne

Chapitre 1

Introduction

1 Cordes et cosmologie

1.1 Une rapide histoire de l'Univers

Lorsque nous regardons autour de nous, nous découvrons différents objets, différentes formes, différentes personnes. A la tombée de la nuit, nous pouvons même prendre part à un voyage fabuleux à travers les étoiles et les âges simplement en levant les yeux et en admirant le ciel constellé de milliers d'étoiles. Ces étoiles nous apparaissent à chacun comme impossibles à atteindre, voir comme faisant partie d'un univers différent du nôtre, de celui *palpable* auquel on est habitué. Pourtant, en utilisant des télescopes et autres astuces, les astronomes ont découvert que cet univers qui nous parait si différent, n'est en fait qu'une infime partie d'un vaste réseau où chaque maille n'est pas très différente de ses voisines : notre Univers. L'étude poussée des observations astronomiques a également montré en quoi nous n'avions ni une place privilégiée dans l'Univers, ni une place insignifiante. Bien que l'Univers évolue sans trop se soucier de notre existence, nous avons été placé à un endroit où, localement, la vie et la connaissance ont pu se développer. Au cours des siècles qui nous ont précédé, nous n'avons cessé de chercher à comprendre l'Univers qui nous entoure. Dés lors que notre Univers fut mieux *cartographié* par les astronomes, les physiciens de divers horizons ont émis des quantités incroyables d'idées, hypothèses (vraies ou fausses), de théories, pour expliquer pourquoi ce que l'on observe se produit. Il a fallu des siècles, des millénaires même, avant que nous ne puissions expliquer pourquoi le ciel est bleu, que la terre tourne autour du Soleil, que la matière (toute matière) est faite d'atomes, eux mêmes composés de particules plus petites, les protons et neutrons ainsi que les électrons. Les protons et neutrons, comme bien d'autres particules élémentaires trouvées par les physiciens, sont composés de particules encore plus petites et plus légères : les quarks. Pour donner un ordre d'idée sur les grandeurs impliquées, la masse d'un proton et son rayon sont de l'ordre de

$$m_p \approx 10^{-27}\text{kg et } r_p \approx 8 \cdot 10^{-16}\text{m}. \tag{1.1}$$

C'est seulement vers 1967 que Bjorken et Feynman entre autres développent l'idée selon laquelle les quarks existeraient. Murray Gell-Mann, en 1969, reçoit le prix

nobel de physique pour ses travaux sur la théorie de quarks. Ses prédictions purement théoriques, en partie à l'aide de la théorie du groupe $SU(3)$, ont notamment permis de prédire plusieurs résultats expérimentaux et même l'existence d'une particule nouvelle dont les caractéristiques principales (masse et nombres quantiques) furent pleinement déterminées par la théorie de Gell-mann. En 1975, une preuve expérimentale est finalement apportée pour confirmer cette hypothèse, mais depuis, aucune entité plus fondamentale que le quark n'a été découverte. Les quarks, comme les électrons et toutes les autres particules, interagissent avec le reste de la matière. Il est remarquable qu'après des siècles d'efforts, les physiciens aient compris que l'ensemble de ces interactions était en fait classifiable. Cette classification, que nous élaborerons dans la suite, ne constitue en aucune façon un dogme intangible de la science. De nombreuses expériences et travaux théoriques ont tenté de montrer qu'il existe au moins une autre force par rapport à celles introduites. Tous ces travaux se sont soldés par des échecs, certes, mais nul ne peut affirmer avec absolue certitude qu'il n'existe que quatre interactions fondamentales dans l'Univers. Ceci dis, on ne prend pas un énorme risque en prétendant qu'il n'y a que quatre interactions. Afin de bien comprendre la révolution intellectuelle qu'a engendré la théorie des cordes, il convient de saisir que toutes les grandes percées scientifiques depuis l'antiquité ont été accompagnées de vérifications (plus ou moins rigoureuses) expérimentales. Or la grande révolution de la théorie des cordes est de vouloir expliquer tout ou partie des grands mystères de l'Univers, sans être suffisamment proche de la réalité expérimentale pour être jugée.

1.2 Pourquoi la théorie des cordes ?

Quatre interactions fondamentales décrivent l'ensemble des phénomènes physiques observables dans la nature : la gravitation, les interactions forte et faible, et l'interaction électromagnétique. Chacune de ces interactions a, après de nombreux essais et échecs, trouvé un cadre mathématique et physique satisfaisant dans lequel elle pouvait s'immerger. En effet, la Relativité Générale d'Albert Einstein [1] utilisant la géométrie Riemannienne décrit la gravitation, tandis que la théorie des groupes et la théorie des champs (classique et quantique) aident énormément à la compréhension des trois autres interactions. Cependant la plus ancienne des quatre interactions, la gravitation, semble être la plus mal comprise. Pour s'en convaincre, on peut se rappeler que les trois autres interactions sont portées par des particules médiatrices de ces interactions, des *bosons de jauge* en termes savants. Le photon véhicule l'onde électromagnétique alors que les interactions faible et forte sont véhiculées respectivement par des bosons $Z_0, W^{\pm}$ d'un côté et les gluons de l'autre. La gravitation est sans doute portée par un boson de jauge, le *graviton*, mais celui ci n'a encore jamais été détecté, contrairement à ses homologues qui ont chacun été confirmés dans leurs fonctions par l'expérience. En termes plus savants, s'il est possible de décrire les interactions faible, forte et électromagnétique par la théorie quantique des champs (TQC), il n'est toujours pas possible d'inclure la gravitation dans ce schéma unificateur. Que la gravitation ne soit pas facile à inclure avec les autres forces n'est pas compliqué à comprendre quand on sait qu'elle décrit les phénomènes d'attraction aux très grandes échelles, celles des galaxies, alors que la mécanique

quantique avec qui on aimerait marier la gravitation, ne s'intéresse qu'aux très petites échelles (particules élémentaires). Si le doux rêve d'une théorie quantique des champs unifiant les quatre interactions a longtemps existé, il y a fort à parier qu'il nous faille dépasser les cadres conceptuels actuels pour réaliser cette unification.

Avant de s'aventurer sur la piste glissante des conjectures, il est fondamental de bien comprendre que nous n'avons aucune idée de la façon dont la gravitation et la mécanique quantique s'harmonisent dans leur domaine commun. Peut être qu'une théorie quantique de la gravitation est extraordinairement plus compliquée à construire qu'il nous paraît. Il se peut aussi que dans le domaine quantique la gravitation requiert une physique tellement différente que celle que nous maîtrisons, qu'il soit prématuré de chercher à mélanger gravitation et mécanique quantique. Ce clivage profond entre théories quantiques d'une part et gravitation d'autre part a donné lieu à un nombre colossal de travaux depuis les années 1920 et l'avènement de la mécanique quantique. Bien que quantitativement très nombreux, ces travaux n'ont, pour l'instant, pas encore apporté de solutions fermes et définitives à propos de ce problème. De nombreuses tentatives pour décrire la gravitation à des échelles quantiques ont vu le jour. Que ce soient la théorie des cordes [2], la Gravité Quantique à Boucle [3] et la Géométrie Non Commutative [4], pour ne citer que ces approches ; aucune de ces théories n'est capable de dépasser le stade très formel que lui confère son arsenal mathématique tout en gardant une capacité suffisante de prédictions physiques pouvant être réfutées ou validées par des expériences dans un avenir proche. La théorie des cordes apparaît néanmoins comme une piste intéressante et continue de faire l'objet d'une recherche très active. Cette théorie prétend à la base que toute les particules élémentaires ne sont que des fluctuations d'entités encore plus petites, et donc fondamentales, les cordes. Comme nous le verrons dans le chapitre suivant, les théoriciens des cordes ont inventé des cordes ouvertes tout comme des cordes fermées. La théorie des cordes a d'ores et déjà engendré de nombreux résultats en mathématiques et en physique et a stimulé de nombreuses recherches et perspectives dans ces domaines. L'étude des variétés de Calabi-Yau [5] et l'étude poussée de la théorie conforme des champs [6], par exemple, ont ainsi vu leur activité s'accroître grâce à la théorie des cordes. La description de certaines propriétés des trous noirs [7] et la correspondance ADS/CFT [8] sont deux exemples de sujets où la théorie des cordes fournit une aide précieuse. De plus il est possible d'étudier le premier ordre de perturbation de la théorie des cordes de manière assez rigoureuse et d'en obtenir de nombreux résultats. Appliquant ce leitmotiv à des domaines de la physique tels que la physique des particules ou l'astrophysique des très hautes énergies dont la cosmologie fait partie, de nombreux résultats parfois en contradiction ont ainsi été obtenus.

La théorie des cordes est censée décrire entre autres comment la gravitation se comporte aux petites échelles, c'est à dire comment gravitation et mécanique quantique peuvent se combiner. La cosmologie est fondée sur la gravitation, mais la compréhension du début de l'Univers ainsi que des processus très énergétiques (comme ceux au voisinage de trous noirs) nécessitent une théorie quantique de la gravité. C'est pourquoi les tentatives de relier la théorie des cordes avec l'expérience ont souvent eu pour cadre la cosmologie primordiale. L'inflation, période encore très

spéculative du début de l'histoire de l'Univers, est un exemple parfait d'aire de jeux pour la théorie des cordes. On comprend dés lors mieux pourquoi il est facile, en parcourant les différents travaux de recherches, de constater l'inflation de scénarios différents obtenus pour... l'inflation cosmologique. Il en va de même concernant la constante cosmologique. Devant une telle activité et une telle diversité de résultats, il est très difficile de tirer des conclusions à la fois robustes et pertinentes. Une des grandes difficultés de la théorie des cordes est d'être extrêmement riche, et donc de fournir un nombre très grand de modèles *a priori* différents à partir desquels on peut travailler[1].

1.3 De la transition d'Hagedorn vers la transition électrofaible

Une partie de ce travail de thèse consiste en la description, dans des modèles de théorie des cordes bien définis sur le plan théorique, de la cosmologie de l'Univers primordial entre la transition de Hagedorn et la transition électrofaible. Chaque transition se matérialise en terme de température (ou énergie) critique. La transition d'Hagedorn est issue de la théorie des cordes : elle traduit simplement qu'au delà d'une certaine énergie notre modèle est caduque (instable notamment) et un modèle plus raffiné doit être utilisé. La transition électrofaible est quand à elle beaucoup plus universelle car elle décrit simplement le moment où dans le passé de l'Univers les interactions électromagnétique et faible se sont découplées d'une interaction unique : *l'interaction electrofaible.*

En effet, ce domaine de la physique des très hautes énergies est peut-être l'un des plus passionnants et excitants que nous ayons à étudier. Évidemment ce domaine est extrêmement compliqué et de nombreuses tentatives d'études de l'Univers primordial ont vu le jour. Expérimentalement nous ne connaissons quasiment rien de l'Univers primordial. La seule approche que nous ayons à notre disposition est l'interpolation de la physique pré-ère de rayonnement à partir de l'ère de rayonnement qui constitue le début de la cosmologie observationnelle. Nous tentons dans ce travail d'utiliser une approche prédictive en considérant des modèles de théorie des cordes et en supposant que ces modèles décrivent le gaz de cordes qui composait notre Univers. La physique de l'Univers primordial peut se décomposer en plusieurs étapes bien distinctes. Il y a d'abord la physique pré Big-Bang, domaine spéculatif dont nous ne dirons pas un mot. Ensuite, nous pouvons distinguer la physique pré-Hagedorn de la physique post-Hagedorn. La première peut s'étudier avec des méthodes de théorie conforme des champs. Nous ne poursuivrons pas cette possibilité. La seconde physique possible, celle post Hagedorn, est précisément celle qui nous intéresse. C'est durant cette période, si on en croit le modèle standard de cosmologie, que l'inflation cosmologique a eu lieu. On comprend donc aisément que cette période de l'histoire de l'Univers est très intéressante à étudier. La théorie des cordes fournit justement un cadre conceptuel permettant de l'aborder avec des moyens de

[1] Voir le chapitre 2 pour une meilleure compréhension de la théorie des cordes. Initialement bien définie en 26 (ou 10) dimensions, sans paramètres arbitraires, sa réduction à 4 dimensions est source d'arbitraire dans la théorie.

gravité quantique. Gardons nous cependant de ranger cette étude parmi les succès de la théorie des cordes.

Il convient également de préciser que depuis le début de l'étude de la théorie des cordes, la vision de cette dernière a énormément évolué. De théorie de grande unification on est passé par diverses étapes pour aujourd'hui arriver à un consensus qui stipule que, certes, la théorie des cordes est une très grande idée qui a permis l'émergence de nombreux travaux et l'établissement de nombreuses connaissances, mais son incapacité à se conformer à l'expérience et son incroyable complexité dans certains cas impliquent que peut être nous faisons fausse route. Il est impossible de dire si nous sommes sur le bon chemin pour trouver la théorie quantique de la gravitation, ni même si cette théorie est compréhensible par nos outils actuels La théorie des cordes est la candidate la plus étudiée à l'obtention d'une théorie quantique de la gravitation, et c'est en ce sens que nous allons l'utiliser.

2 Flots géométriques et applications

Nous nous sommes beaucoup intéressé pendant cette thèse aux flots géométriques, de manière assez large. Un *flot géométrique* nous renseigne sur l'évolution des propriétés typiques d'un espace (taille, volume, $\cdots$) en fonction d'un paramètre. Ces flots géométriques ont énormément servi en mathématique durant ces dernières années (voir chapitre 4). Ils ont engendré de tels résultats que leur étude est devenue un sujet de recherche à part entière.

Les flots géométriques ont également beaucoup été interprétés en physique, quoique du travail reste encore à faire dans cette direction. C'est justement vers celle-ci que nous nous sommes dirigé, et ce avec diverses applications en tête. D'une part nous avons étudié avec P.M. Petropoulos, Ph. Spindel et J. Estes une relation précise entre flots géométriques et espaces auto-duaux, et d'autre part, avec P.M. Petropoulos, D.Lüst et I. Bakas, nous avons analysé les flots géométriques intervenant dans la théorie de la gravitation connus sous le nom de théorie d'Hořava-Lifshitz.

3 Travaux non détaillés dans ce rapport

Différents sujets ont été étudiés dans cette thèse. Cette grande liberté de choix des sujets a eu pour important effet de donner lieu à des travaux très différents : cosmologie de super cordes, flots géométriques, perturbations cosmologiques dans les théories Einstein-Ether, classification des solutions statiques à symétrie sphérique d'une large classe de théories, reformulation de l'électromagnétisme comme gravitation avec torsion non nulle. N'ont été cités que les travaux ayant donné lieu à des rapports publiés. D'autres travaux, un peu moins étoffés, ont également vu le jour sur d'autres sujets comme la supergravité dans les théories de la gravitation $F(R)$. Afin de gagner en clarté et d'éviter un rapport de thèse trop long et diversifié, tous ces travaux ne seront pas détaillés ici. Les deux premiers sujets sont abordés de façn

approfondie et constituent le cœur de ce rapport. Nous profitons cependant de cette introduction pour parler de travaux annexes, [9] et [10].

3.1 Classification des solutions statiques à symétrie sphérique

La seule solution quadridimensionnelle statique à symétrie sphérique de la Relativité Générale est la solution de Schwarzschild, caractérisée par une masse m et définie par la métrique

$$ds^2 = -\left(1 - \frac{m}{r}\right) dt^2 + \frac{dr^2}{1 - \frac{m}{r}} + r^2 \left[d\theta^2 + \sin(\theta)^2 d\phi^2\right]. \tag{1.2}$$

On peut dés lors s'interroger sur l'extension de ce résultat au cas de théories plus compliquées. Par exemple, nous pouvons inclure un champ électromagnétique de Maxwell et couplé minimalement, on obtient alors la solution de Reissner-Nordström caractérisée par une masse m et une charge Q et donnée par la métrique

$$ds^2 = -\left(1 - \frac{m}{r} + \frac{Q}{r^2}\right) dt^2 + \frac{dr^2}{1 - \frac{m}{r} + \frac{Q}{r^2}} + r^2 \left[d\theta^2 + \sin(\theta)^2 d\phi^2\right]. \tag{1.3}$$

Si on choisit d'inclure des champs scalaire, la classification des solutions statiques à symétrie sphérique est bien plus subtile. Dans le cas le plus simple où nous avons la RG couplée à un champ scalaire de manière minimale, il a été établi la forme la plus générale des métriques statiques à symétrie sphérique (métriques SSS), de manière implicite. Néanmoins ce résultat n'a pas été généralisé aux cas plus compliqués de plusieurs champs couplés de façon non minimale, et même dans le cas le plus simple, la classification est implicite et demande à être étoffée pour mieux comprendre le comportement des différentes fonctions de la métrique. Bien entendu, plusieurs travaux ont été effectués dans le but de classifier (ou simplement trouver une solution particulière) les solutions SSS de diverses théories. Le but de mes travaux sur les solutions SSS d'une vaste classe de théories a été de déterminer précisément les différents comportements de ces solutions SSS. On a étudié avec un certain souci du détail la classe de théories donnée par (on notera $g^{\mu\nu} X_\mu Y_\nu = X \cdot Y$ dans cette thèse)

$$S = \int d^4x \sqrt{|g|} \left[R - \sum_i \epsilon_i \mathcal{F}_i(\phi_j)^2 \nabla\phi_j \cdot \nabla\phi^j\right], \tag{1.4}$$

avec $\epsilon_i = \pm 1$, ϕ_j des champs scalaires et $\mathcal{F}_i(\phi_j)$ des fonctions arbitraires. On a cherché les solutions du type

$$ds^2 = -e^{2\Phi(r)} dt^2 + \frac{dr^2}{1 - \frac{b(r)}{r}} + r^2 \left[d\theta^2 + \sin(\theta)^2 d\phi^2\right], \tag{1.5}$$

où $b(r)$ et $\Phi(r)$ sont deux fonctions ne dépendant que de r. Différentes solutions, au nombre de 7, ont été obtenues. Certaines vérifient $b(r) > 0$, d'autres $b(r) < 0$, alors que certaines solutions n'ont pas de signe constant pour la fonction $b(r)$. En plus de la solution de Schwarzschild et du trou de ver traditionnels, on trouve des solutions

où il est possible de confiner des particules grâce au concours simultané de la gravité et de l'anti-gravité. Si on ajoute à (1.4) un terme de champ vectoriel ou bien un potentiel pour les champs scalaires, il est possible d'obtenir d'autres solutions avec des comportements très différents, où il est possible de confiner des particules-test dans une région bien spécifique de l'espace. Enfin, nous avons essayé d'étudier les propriétés de stabilité des différentes solutions obtenues. Cependant, la très forte nécessité d'outils numériques et mes compétences limitées en la matière ne m'ont pas permis de tirer des conclusions définitives à ce sujet.

3.2 Perturbations cosmologiques des théories Einstein-Ether

L'extension de la Relativité Générale à des modèles classiques expliquant l'Univers dans le régime des faibles accélérations est un sujet passionnant. Outre la cosmologie induite par TeVeS, la version relativiste de MOND telle que formulée par Bekenstein, qui fut le sujet de [11], on a également étudié les perturbations cosmologiques dans les théories Einstein-Ether de la gravitation. L'intérêt premier de cette étude était de placer des contraintes sur les paramètres libres et la fonction libre dans ces modèles. Ces derniers sont décris par l'action

$$S_{EE} = \int d^4x\sqrt{-g}\,[R - F(K)]\,,\ K = K^{abcd}\nabla_a A_b \nabla_c A_d, \tag{1.6}$$

où $K_{abcd} = c_1 g_{ab}g_{cd} + c_2\delta_{ab}\delta_{cd} + c_3\delta_{ac}\delta_{bd}$. La fonction $F(K)$ tout comme les constantes c_i sont arbitraires. Si on impose que ces modèles ont le même succès que la relativité générale, on obtient des conditions très strictes sur la fonction F et les c_i. L'étude des perturbations cosmologiques permet également de mettre en exergue la vitesse de propagation des petites perturbations. Demander que ces vitesses soient sub-luminales place également des contraintes sur les paramètres F et c_i. C'est précisément ici que mon travail a eu lieu. Malgré une complexité évidente des modèles étudiés, nous avons pu mener à bien cette étude.

4 Plan

Le plan de cette dissertation est le suivant. Après cette introduction qualitative, on présente des notions de base en théorie des cordes et cosmologie afin de pleinement apprécier les travaux [12] et [13] appelés ci dessous respectivement publication 1 et 2. L'étude des résultats obtenus dans ces travaux sera le sujet du chapitre 3. La publication 3, [14], est également une revue de ces travaux. Ensuite, nous verrons dans le chapitre suivant comment les espaces auto-duaux (instantons gravitationnels quand ils sont réguliers) peuvent être décrits en terme de flots géométriques, le sujet des publications 4 et 5, resp. [15, 16]. Un flot de Ricci-Cotton modifié, exemple de flot géométrique, sera étudié dans le chapitre 5 dans le but de mieux comprendre la théorie non relativiste de la gravitation proposée par Horava [17]. Ce chapitre est basé sur les publications 6 et 7, resp. [18, 19]. Le chapitre 6 sera celui des conclusions et perspectives pour un travail de recherche future.

Chapitre 2

Éléments de théorie des cordes et de cosmologie

Un rapide aperçu des notions et éléments nécessaires pour comprendre les publications 1, 2 et 3 est donné ici. Dans un premier temps nous donnons des éléments de théorie des cordes et dans un second temps nous présentons les notions de cosmologie nécessaires.

1 Éléments de théorie des cordes

On présente ici certaines notions de la théorie des cordes. Seules les notions utilisées pendant ce travail de thèse sont présentée ; pour une introduction plus détaillée consulter par exemple [2]. Après une description de la corde bosonique et de la super corde, quelques éléments sur le mécanisme de Scherk-Schwarz et le calcul de fonctions de partitions en théorie des cordes sont présentés.

1.1 Corde bosonique

La révolution de la théorie des cordes a été de proposer que la matière qui compose l'Univers est constituée de cordes élémentaires. Ces cordes dont la taille est minuscule, de l'ordre de la longueur de Planck $l_p \approx 1.6 \cdot 10^{-35} m$, décrivent les différents types de particules par leurs divers modes de vibration. Il existe deux types de cordes montrés sur la Fig. 2.1 : les cordes fermées et les cordes ouvertes. Les cordes fermées (resp. ouvertes) véhiculent la gravitation (resp. les autres interactions). Lorsqu'une particule ponctuelle se déplace dans l'espace-temps, elle décrit une ligne d'univers, la généralisation de ce concept au cas d'une corde est naturellement la *surface d'univers* Σ, Fig. 2.2. Considérons une particule ponctuelle de masse m se propageant dans un espace-temps à D dimensions décrit par des coordonnées x^μ, $\mu = 0, ..., D-1$ et doté d'une métrique $g_{\mu\nu}$. Considérer une ligne d'univers de la particule revient à considérer une séquence d'histoires $x^\mu(\tau)$ de la particule (Fig. 2.2). On peut écrire une action décrivant la propagation de cette particule, en cas

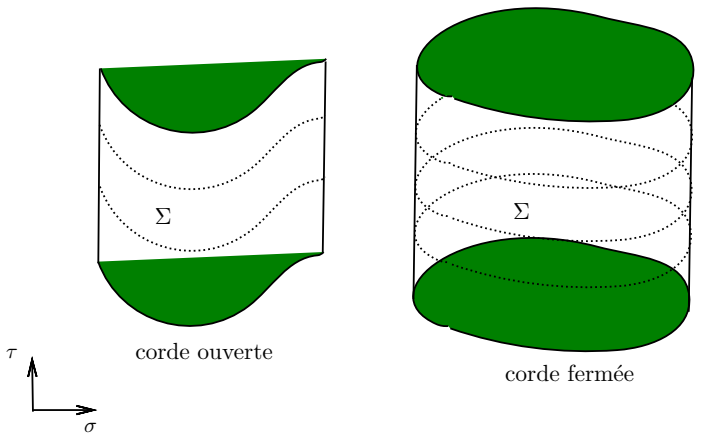

FIG. 2.1 – Corde ouverte et corde fermée. Les positions initiales et finales des cordes sont notées en vert.

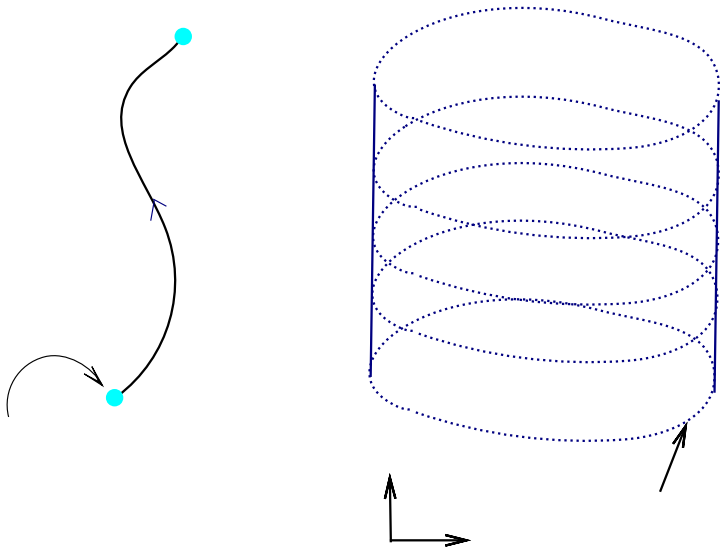

FIG. 2.2 – Ligne d'univers et surface d'univers (Σ).

de masse non nulle, comme ($\tau_{i,f}$ dénotant respectivement les valeurs initiale et finale du paramètre τ)

$$S_p = m\int_{\tau_i}^{\tau_f} \frac{ds}{d\tau}d\tau,\ ds = \sqrt{|g_{\mu\nu}dx^\mu dx^\nu|}. \tag{2.1}$$

Dans le cas de masse nulle, l'action (2.1) peut se généraliser en

$$S_p = -\frac{1}{2}\int d\tau \frac{g_{\mu\nu}\dot{x}^\mu\dot{x}^\nu}{e(\tau)},\ \dot{x}^\mu = \frac{dx^\mu}{d\tau} \tag{2.2}$$

où $e(\tau)$ est un nouveau champ non dynamique introduit sur la ligne d'univers. Ce champ décris une métrique sur la ligne d'univers et agit comme un multiplicateur de Lagrange. D'après ce que l'on a dit, il est aisé de dériver une action pour la propagation d'une corde. Pour cela, on décrit la surface d'univers par deux coordonnées, une temporelle (τ) et une spatiale (σ)[1]. Nous notons $x^{\mu'} = \frac{dx^\mu}{d\sigma}$, $\dot{x}^\mu = \frac{dx^\mu}{d\tau}$ et nous introduisons un élément d'aire de la surface d'univers

$$ds_A^2 = g_{\mu\nu}dx^\mu dx^\nu = h_{ij}d\zeta^i d\zeta^j,\ \zeta^0 = \tau,\ \zeta^1 = \sigma, \tag{2.4}$$

où $h_{ij} = g_{\mu\nu}\frac{\partial x^\mu}{\partial \zeta^i}\frac{\partial x^\nu}{\partial \zeta^j}$. Une fois cette opération effectuée, nous pouvons de manière naturelle écrire une action de Nambu-Goto décrivant la propagation d'une corde relativiste de *tension* T :

$$S_{NG} = -T\int d^2\zeta\sqrt{|\det(h_{ij})|}. \tag{2.5}$$

La présence d'une racine carrée dans cette expression pose des difficultés pratiques pour la quantification. Il est possible d'écrire une seconde action, dite action de Polyakov, dont les équations du mouvement sont identiques à celles de Nambu-Goto. Cette action est

$$S_{Pol} = -\frac{T}{2}\int d^2\zeta\sqrt{|\det(e)|}e^{ij}\partial_i X^\mu \partial_j X^\nu g_{\mu\nu}, \tag{2.6}$$

où $e_{ij}(\zeta^k) = \partial_i X^\mu \partial_j X_\mu$, d'après les équations du mouvement. C'est la généralisation du champ $e(\tau)$ de la particule élémentaire, elle joue le rôle de métrique sur la surface d'univers, et est un multiplicateur de Lagrange. Avant d'aller plus loin il convient de signaler que l'action (2.6) n'est pas la plus générale que l'on puisse écrire. Implicitement, par métrique de l'espace-temps $g_{\mu\nu}$ il faut comprendre un tenseur de rang 2 symétrique. Certaines théories de la gravitation [20], *ad-hoc* en général, utilisent des métriques avec une partie antisymétrique et/ou une connexion avec torsion à partir de laquelle on construit le tenseur de Riemann et le scalaire de Ricci de manière standard. Nous ne suivrons pas ce chemin ici préférant la connexion de Levi-Civita standard et une métrique symétrique. Ceci dit, si nous voulions écrire l'action la plus

[1]Pour une corde fermée, $0 \leq \sigma \leq 2\pi$ alors que pour une corde ouverte $0 \leq \sigma \leq \pi$. Dans ce dernier cas deux conditions aux bords existent : conditions de *Neumann* et *Dirichlet*. Les premières consistent à poser

$$X^{\mu'}(\tau, 0) = X^{\mu'}(\tau, \pi) = 0 \tag{2.3}$$

alors que les secondes imposent que les bouts des cordes ouvertes soient fixes.

générale d'une surface d'univers possédant les propriétés d'être invariante conforme et purement bosonique, nous pourrions écrire :

$$S_{Pm} = -\frac{T}{2}\int d^2\zeta\sqrt{|\det(e)|}e^{ij}\partial_i X^\mu \partial_j X^\nu g_{\mu\nu} + \epsilon^{ij}\partial_i X^\mu \partial_j X^\nu b_{\mu\nu} + \phi R^{(2)} + \Psi(X^\mu)\epsilon^{ij}F_{ij}. \tag{2.7}$$

Dans (2.7) nous avons introduit un tenseur de rang 2 antisymétrique $b_{\mu\nu}$ (champ de Kalb Ramond, KR) et un scalaire ϕ ainsi que le scalaire de Ricci de la connexion associée à la métrique e_{ij} : $R^{(2)}$. Comme e_{ij} est un objet bidimensionnel, l'invariance par reparamétrisation $\zeta_i \to \zeta_i + \delta\zeta_i$ permet de choisir la métrique

$$e_{ij} = e^\sigma \eta_{ij},\ R^{(2)} = \Box\sigma. \tag{2.8}$$

Il est immédiat de constater qu'à des termes de bords près, (2.6) et (2.7) sont égales dans le cas où le champ de KR et le dilaton sont constants. Une constante cosmologique dans (2.7) n'est pas permise par invariance conforme. Enfin, le dernier terme de (2.7) est un terme de connexion de jauge A_i sur la surface d'univers. Avec un champ scalaire quelconque $\Psi(X^\mu)$ et le tenseur de Maxwell standard

$$F_{ij} = \partial_i A_j - \partial_j A_i, \tag{2.9}$$

ce terme est également invariant conforme en deux dimensions. Dans le cas $\Psi(X^\mu) =$ const., ce terme donne un terme de bord. **Dans toute cette thèse, nous supposerons constants le champ de KR et la connexion de jauge A_i. De plus nous supposerons qu'au moins localement, nous pouvons approximer la métrique $g_{\mu\nu}$ à la métrique de Minkowski $\eta_{\mu\nu}$.** L'extension des résultats obtenus dans cette thèse dans les cas où les hypothèses ci-dessus sont relaxées constitue un ambitieux et intéressant programme.

Une fois la métrique e_{ij} fixée par son équation du mouvement, celle de la coordonnée bosonique X^μ dérivée de (2.6) est

$$\partial_+\partial_- X^\mu = 0,\ \partial_\pm = \frac{\partial}{\partial\zeta_\pm},\ \zeta_\pm = \tau \pm \sigma. \tag{2.10}$$

Les coordonnées $\zeta_\pm$ sont dites **coordonnées du cône de lumière**. La solution de (2.10) est, dans le cas d'une corde fermée ($X^\mu(\tau, \sigma + 2\pi) = X^\mu(\tau, \sigma)$ par périodicité de la corde),

$$X^\mu(\tau, \sigma) = X^\mu_L(\zeta_+) + X^\mu_R(\zeta_-) \tag{2.11}$$

où

$$X^\mu_L(\zeta_+) = \frac{x^\mu}{2} + \frac{p^\mu}{4\pi T}\zeta_+ + \frac{i}{\sqrt{4\pi T}}\sum_{k\in\mathbb{Z}^*}\frac{\tilde{\alpha}^\mu_k}{k}e^{-ik\zeta_+}, \tag{2.12}$$

$$X^\mu_R(\zeta_-) = \frac{x^\mu}{2} + \frac{p^\mu}{4\pi T}\zeta_- + \frac{i}{\sqrt{4\pi T}}\sum_{k\in\mathbb{Z}^*}\frac{\alpha^\mu_k}{k}e^{-ik\zeta_-}. \tag{2.13}$$

Nous avons introduit des modes de Fourier $\alpha^\mu_k, \tilde{\alpha}^\mu_k$. Étant donné que les fonctions x^μ, p^μ et $X^\mu(\tau, \sigma)$ sont réelles, nous avons

$$(\alpha^\mu_k)^* = \alpha^\mu_{-k},\ (\tilde{\alpha}^\mu_k)^* = \tilde{\alpha}^\mu_{-k}. \tag{2.14}$$

Les champs bosoniques X^μ sont donc décrit par une composante gauche X_L et une composante droite X_R. Chaque composante décrit des états gauche/droit. Dans le cas d'une corde ouverte, avec les conditions aux bords de Neumann :

$$X^{\mu'}(\tau,\sigma)_{\sigma=0,\pi} = 0. \tag{2.15}$$

Nous obtenons alors la décomposition en mode

$$X^\mu(\tau,\sigma) = x^\mu + \frac{p^\mu \tau}{\pi T} + \frac{i}{\sqrt{\pi T}} \sum_{k\in\mathbb{Z}^*} \frac{\alpha_k^\mu}{k} e^{-ik\tau} \cos(k\sigma). \tag{2.16}$$

Il est possible de relier la masse d'excitation des cordes aux modes de Fourier de l'excitation : $\alpha' M^2 = 4(N-1)$, où $\alpha' = \frac{1}{2\pi T}$ et

$$N = \sum_{m=1}^{\infty} \alpha_{-m} \cdot \alpha_m. \tag{2.17}$$

Dés lors, il est immédiat de voir que pour $N = 0$, nous avons $M^2 = -\frac{4}{\alpha'} < 0$. Ainsi, la corde bosonique a un problème : elle possède un tachyon, donc son vide est instable. La compatibilité de la théorie des cordes et de l'invariance de Lorentz, mais aussi la compatibilité des spectres de masse d'une théorie de cordes obtenus par différentes méthodes, imposent que la dimension de l'espace-temps soit 26. Une propriété fondamentale de la théorie des cordes apparaît alors : l'existence de dimensions supplémentaires. Cette profusion de dimensions supplémentaires est à l'origine d'un des plus importants problèmes de la théorie des cordes : l'existence d'un nombre important de modèles de physique de basse énergie sous-jacent. En effet, bien qu'en dimension 26 la théorie des cordes soit une théorie bien définie et sans aucun paramètre libre, revenir à un nombre de dimensions inférieur ne se fait pas de manière unique et sans équivoque. Ce processus de compactification introduit beaucoup d'arbitraire et d'indéterminations, la physique de basse-énergie dépend du modèle de compactification considéré. Dans cette thèse on ne procédera pas à une étude quantitative de différents modèles et de comparer les résultats obtenus. Au contraire, nous nous limiterons à des modèles bien précis, sélectionnés pour leur simplicité physique et calculatoire, et nous tenterons d'en tirer des conclusions pertinentes.

1.2 Supersymétrie et supercordes

quelques notions essentielles de supersymétrie

Apparue dans les années 1970 (voir [21] pour les articles fondateurs et [22] pour une introduction plus moderne), la supersymétrie est présente en théorie des cordes. La caractéristique principale d'une théorie supersymétrique est l'égalité entre le nombre de degrés de liberté bosoniques et fermioniques. En théorie quantique des champs (TQC), la supersymétrie joue un rôle primordial. En effet, les corrections dues à des boucles de bosons et de fermions ne sont pas comptées avec le même signe,

il apparaît donc que lorsque nous avons autant de degrés de liberté d'un côté que de l'autre, des corrections puissent s'annuler. En théorie des cordes, la supersymétrie d'espace-temps permet de s'affranchir du tachyon.

Si la nature possédait cette symétrie aux échelles d'énergies qui nous sont accessibles, nous serions en mesure d'associer à chaque particule sa particule miroir par supersymétrie : à tout boson correspondrait un fermion et vice-versa[2]. Or nous savons que ce n'est pas le cas, donc si nous voulons inclure le modèle standard dans une théorie supersymétrique, nous devons également étudier des moyens de briser la supersymétrie en deçà d'une certaine échelle (plus élevée que la plus haute échelle d'énergie testée à ce jour). Bien qu'il existe une pléthore de scénarios de brisure de la supersymétrie, aucun ne semble pour l'instant se dégager comme étant *le bon*, la nature ayant pu choisir parmi plusieurs scénarios différents. Le mécanisme de brisure de supersymétrie qui a été utilisé dans ce rapport est un mécanisme de brisure spontanée appelé mécanisme de Scherk-Schwarz. On dit qu'une symétrie est brisée *spontanément* lorsque cette dernière, associée à un groupe G, étant la symétrie d'une théorie (de son lagrangien, de son action), n'est plus symétrie de l'espace des vides de la théorie. En fait, un sous groupe de G, H, reste à la fois symétrie de la théorie et des vides. Le mécanisme de Scherk-Schwarz permet de briser spontanément une symétrie. Introduit dans [23], ce mécanisme fut d'abord appliqué à la théorie des champs, l'idée étant la suivante. Considérons une théorie en dimension $D+d$, avec des coordonnées $X^I,\ I=0,\cdots,D-1$ et $Y^a,\ a=D,\cdots,D+d-1$. Les coordonnées X^I décrivent une réduction de cette théorie en D dimensions et les coordonnées Y^a décrivent l'espace interne de dimension d. Supposons l'existence de symétries dans la théorie en $D+d$ dimensions générées par des opérateurs Q_I, l'idée du mécanisme de Scherk-Schwarz est de compactifer de $D+d$ à D dimensions de façon à ce que les champs de la théorie aient une dépendance en les dimensions internes non triviales, dirigée par les symétries de la théorie en $D+d$ dimensions. Si nous introduisons un paramètre réel q, définissant

$$\hat{\Phi}_i(X^I,Y^a) = [e^{qQ_aY^a}]_i^j\Phi_j(X^I,Y^a), \tag{2.18}$$

il est facile de constater que

$$\partial_I\hat{\Phi}^i\partial^I\hat{\Phi}_i + \partial_a\hat{\Phi}^i\partial^a\hat{\Phi}_i = \partial_I\Phi^i\partial^I\Phi_i + \partial_a\Phi^i\partial^a\Phi_i + q^2\Phi_i\mathrm{Tr}[Q_k^iQ_j^k]\Phi^j. \tag{2.19}$$

On crée ainsi un terme de masse pour les champs Φ_i ! Plus on a de coordonnées internes impliquées et de générateurs de symétries Q_I, plus il est possible d'obtenir des mécanismes de Higgs divers et variés. Ce schéma de brisure spontanée peut se généraliser à la théorie des cordes [23]. En fait, ce type de brisure de symétrie est très naturel en théorie des cordes, puisque les compactifications y jouent un rôle primordial.

Supercordes

La présence de tachyons et l'absence de fermions d'espace-temps rendent la corde bosonique insuffisante et trop simplificatrice. En effet, les tachyons engendrent

[2]Les partenaires supersymétriques devraient avoir même masse

souvent des instabilités, et bien que les tachyons de cordes ouvertes soient assez bien compris, il n'en est pas de même pour ceux de la corde fermée. De plus, l'absence de fermions dans une théorie visant à décrire le modèle standard et donc notamment les quarks est préjudiciable. Le fait qu'il soit possible de corriger simultanément les deux problèmes est assez remarquable. Ce faisant, la supersymétrie apparaît alors comme la seule solution possible. Néanmoins il existe deux approches pour introduire la supersymétrie en théorie des cordes :

- **Supersymétrie de surface d'univers**, ou formalisme de **Ramond-Neveu-Schwarz (RNS)**. C'est le formalisme qui va être utilisé dans la suite.
- **Supersymétrie d'espace-temps**, ou formalisme de **Green Schwarz (GS)**. Au moins dans le cas d'un espace-temps à 10 dimensions, ces deux formalismes sont équivalents.

En plus des bosons X^μ, il faut désormais introduire des champs fermioniques ψ^μ_α où α désigne un indice spinoriel et μ un indice d'espace-temps. En effet, ces fermions sont des spineurs à deux composantes sur la surface d'univers et des vecteurs sous les transformations de Lorentz de l'espace-temps à D dimensions. Il est possible de construire plusieurs actions pour la surface d'univers d'une corde, dépendant du nombre de supersymétries que l'on souhaite imposer. Les seules théories admettant des fermions chiraux et donc susceptibles de décrire (une fois la supersymétrie brisée par un mécanisme à préciser) la physique du modèle standard sont les théories $N = 1$. Dans ce cas-ci, la métrique sur la surface d'univers, e_{ij}, est associée à un gravitino χ_i avec lequel elle forme un multiplet de supersymétrie en deux dimensions. L'analogue de l'action de Polyakov (2.6) est alors

$$S^{II}_{Pol} = \frac{1}{4\pi\alpha'} \int \sqrt{e} \left[e^{ij}\partial_i X \cdot \partial_j X + \frac{i}{2}\psi \cdot \partial\!\!\!/ \psi + \frac{i}{2}(\chi_i \gamma^j \gamma^i \psi^\mu) \left(\partial_j X_\mu - \frac{i}{4}\chi_j \psi_\mu \right) \right]. \tag{2.20}$$

Cette action est invariante sous les transformations locales de supersymétrie $N = 1$:

$$\delta e_{ij} = i\epsilon(\gamma_i \chi_j + \gamma_j \chi_i),\ \delta\chi_i = 2\nabla_i \epsilon, \tag{2.21}$$

$$\delta X^\mu = i\epsilon\psi^\mu,\ \delta\psi^\mu = \gamma^i \left(\partial_i X^\mu - \frac{i}{2}\chi_i \psi^\mu \right) \epsilon,\ \delta\overline{\psi}^\mu = 0 \tag{2.22}$$

où ϵ est un spineur de Majorana-Weyl polarisé gauche. De la même façon, on a une transformation de supersymétrie locale $N = 1$ avec un spineur de Majorana-Weyl $\overline{\epsilon}$ et des transformations (2.21) et (2.22) où $\psi \to \overline{\psi}$ et $\epsilon \to \overline{\epsilon}$. On dit alors que l'on a une supersymétrie (1,1). Dans les expressions ci dessus, nous avons introduit les matrices de Dirac γ^i satisfaisant l'algèbre $\gamma^i\gamma^j + \gamma^j\gamma^i = 2\eta^{ij}$ et données par

$$\gamma^0 = \begin{pmatrix} 0 & -1 \\ 1 & 0 \end{pmatrix} \text{ et } \gamma^1 = \begin{pmatrix} 0 & 1 \\ 1 & 0 \end{pmatrix}. \tag{2.23}$$

Les opérateurs de Virasoro tels que définis pour la corde bosonique existent toujours sous cette forme pour la supercorde, on peut également introduire de nouveaux opérateurs appelés **super-courants** et dont l'algèbre avec ceux de Virasoro définie l'algèbre de supersymétrie $N = 1$. Ces courants sont définis par

$$G = i\psi \cdot \partial X,\ \overline{G} = i\overline{\psi} \cdot \overline{\partial} X. \tag{2.24}$$

De la même façon que l'on montre que la corde bosonique nécessite 26 dimensions, on peut montrer que les super-cordes requièrent l'existence de 10 dimensions. Bien que le nombre de dimensions supplémentaires soit plus petit que pour la corde bosonique, la théorie des supercordes autorise une grande variété de modèles différents possibles. En effet, s'il n'existe qu'un seul type de corde bosonique, il en existe au moins trois de super-cordes, appelés type I, II et corde hétérotique. On peut également subdiviser les deux derniers en deux sous-types : types IIA et IIB d'une part et corde hétérotique $E_8 \times E_8$ et $SO(32)$ d'autre part. Il est également possible d'étudier d'autres modèles de cordes, avec ou sans supersymétrie, avec ou sans tachyons, mais nous ne le ferons pas car ces modèles n'ont pas été utilisés dans nos différents travaux. La suite de cette section consistera donc en le détail de certaines propriétés des super-cordes de type I, II et hétérotiques.

Supercordes de type II fermées

Le développement en modes des coordonnées bosoniques X^μ étant le même que pour le cas de la corde bosonique, il convient de chercher celui des spineurs ψ^μ. Nous posons $\psi_\pm = \psi_0 \pm \psi_1$. Les équations du mouvement sont alors

$$\partial_+ \psi_- = \partial_- \psi_+ = 0. \tag{2.25}$$

Néanmoins il subsiste des termes de bord après variation de l'action :

$$\delta S_b = \int d\tau \left\{ (\psi_+ \delta\psi_+ - \psi_- \delta\psi_-)_{\sigma=\pi} - (\psi_+ \delta\psi_+ - \psi_- \delta\psi_-)_{\sigma=0} \right\}. \tag{2.26}$$

La discussion de ces termes de bord dépend alors de la nature des cordes : ouvertes ou fermées. Dans ce but on introduit la notation $\sigma_\pm = \sigma \pm \tau$.

cordes ouvertes Dans ce cas, $\sigma = 0, \pi$ désignant les extrémités des cordes ouvertes les deux termes de bord doivent s'annuler indépendamment l'un de l'autre, ce qui est vérifié pour $\psi_+ = \pm\psi_-$. Sans manquer de généralités nous pouvons aussi poser $\psi_+^\mu|_{\sigma=0} = \psi_-^\mu|_{\sigma=0}$, ce qui donne les deux choix possibles :

- condition de Ramond (R) : $\psi_+^\mu|_{\sigma=\pi} = \psi_-^\mu|_{\sigma=\pi}$. Dans ce secteur, le développement en mode est alors

$$\psi_\pm^\mu(\sigma,\tau) = \frac{1}{\sqrt{2}} \sum_{n\in\mathbb{Z}} d_n^\mu e^{-in\sigma_\pm}. \tag{2.27}$$

  La condition de réalité d'un spineur de Majorana implique $d_{-n}^\mu = d_n^{\mu\dagger}$.
- condition de Neveu-Schwarz (NS) : $\psi_+^\mu|_{\sigma=\pi} = -\psi_-^\mu|_{\sigma=\pi}$. Dans ce secteur, le développement en mode est alors

$$\psi_\pm^\mu(\sigma,\tau) = \frac{1}{\sqrt{2}} \sum_{r\in\mathbb{Z}+\frac{1}{2}} b_r^\mu e^{-ir\sigma_\pm}. \tag{2.28}$$

  La condition de réalité d'un spineur de Majorana implique $b_{-r}^\mu = b_r^{\mu\dagger}$.

Il existe donc deux secteurs différents dans le cas de cordes ouvertes. Étant donné que naïvement il est possible de considérer une corde fermée comme deux cordes ouvertes dont on a joint les bouts, il n'est pas surprenant qu'il existe quatre secteurs différents pour la supercorde fermée. Chaque secteur est détaillé ici et part du fait qu'il n'existe que deux conditions au bord possible : $\psi_\pm(\sigma) = \pm\psi_\pm(\sigma+\pi)$. Le secteur $+$ correspond à des conditions au bord périodiques (R) tandis que le secteur $-$ correspond à des conditions au bord anti-périodiques (NS). Ainsi, quatre configurations existent :

$$\text{R-R, R-NS, NS-R, NS-NS,} \tag{2.29}$$

où la configuration $X - Y$ décrit des états gauche dans le secteur X et des états droit dans le secteur Y. Le développement en modes est alors le même dans chaque secteur que pour la corde ouverte, à l'exception que $\zeta_\pm \to 2\zeta_\pm$.

Les états de corde dans les secteurs NS-NS et R-R sont des bosons d'espace-temps car ils se transforment dans des représentations tensorielles du groupe de rotations alors que ceux dans les secteurs R-NS et NS-R sont des fermions d'espace-temps (car ils se transforment dans des représentations spinorielles du groupe de rotations). Il est possible d'obtenir une formule de masse analogue à celle obtenue pour la corde bosonique dans le cadre de supercorde. Étant donné que nous n'avons pas l'utilité des détails de ce calcul, seuls les résultats finals sont ici présentés :

$$\alpha^{'} M^2 = \sum_{n=1}^{\infty} \alpha^i_{-n}\alpha^i_n + \sum_{r=1/2}^{\infty} r b^i_{-r} b^i_r - \frac{1}{2},\ (NS), \tag{2.30}$$

$$\alpha^{'} M^2 = \sum_{n=1}^{\infty} \alpha^i_{-n}\alpha^i_n + \sum_{n=1}^{\infty} n d^i_{-n} d^i_n,\ (R). \tag{2.31}$$

Il est clair que dans le secteur R il n'y a plus de tachyon, alors que dans le secteur NS ce dernier demeure. De plus, une analyse fine du spectre de masse nous montrerait l'absence de symétrie entre bosons et fermions. L'exemple le plus frappant étant clairement le tachyon bosonique sans contre-partie fermionique. L'absence de supersymétrie d'espace-temps est clairement reliée au choix de décrire la supercorde dans le formalisme RNS au lieu du formalisme GS. Néanmoins il est possible d'obtenir un spectre supersymétrique en projetant certains états. Cela s'effectue au travers de la projection GSO[3] qui consiste à introduire un opérateur de parité, G, dépendant du secteur considéré et à ne considérer comme physiques que les états de parité positive ou négative. Étant donné que quelque soit l'état physique $|\chi\rangle$ nous avons $G^2_{NS,R}|\chi\rangle = |\chi\rangle$, alors

$$G_{NS,R}|\chi\rangle = \epsilon_{NS,R}|\chi\rangle,\ \epsilon_{NS,R} = \pm 1. \tag{2.32}$$

Les états avec $\epsilon_{NS,R} = 1$ sont dit de chiralité positive alors que les autres sont de chiralité négative. Afin d'obtenir un spectre supersymétrique d'espace-temps, il faut garder les états du secteur NS avec $\epsilon_{NS} = 1$. Dans le secteur R décrivant des spineurs s'espace-temps, dépendant de la chiralité de l'état fondamental du spineur,

[3] elle fut introduite par Gliozzi, Scherk et Olive [24]

nous pouvons sélectionner les états avec $\epsilon_R = \pm 1$. Il est facile de constater que le tachyon du secteur NS caractérisé par $\alpha_n^i = b_r^i = 0$, $\forall n, r$ est éliminé par la projection GSO.

Dans le but de trouver le spectre des états de masse nulle, notons $|0\rangle$ l'état de cordes avec une impulsion nulle et $|p\rangle$ l'état avec une impulsion $p = \sqrt{|p^\mu p_\mu|}$. Un état de cordes sera alors le résultat de l'action d'oscillateurs bosoniques et/ou fermioniques sur un état $|p\rangle$. Dans le cas de la corde de type II, les états de masse nulle se répartissent en quatre groupes, chacun issu d'un des quatre secteurs de la théorie. Dans le secteur NS-NS nous avons les états

$$\psi^\mu_{-1/2}\psi^\nu_{-1/2}|p\rangle, \tag{2.33}$$

donnant lieu à un tenseur d'ordre 2 symétrique et sans trace (graviton $g_{\mu\nu}$), un tenseur d'ordre 2 antisymétrique (champ de Kalb-Ramond $B_{\mu\nu}$), et un scalaire (dilaton ϕ). Dans le secteur NS-R nous avons des fermions d'espace-temps, et les états de masse nulle sont

$$\psi^\mu_{-1/2}|p, \overline{S}\rangle, \tag{2.34}$$

où S est un spineur de chiralité positive par convention. L'état $|p, \overline{S}\rangle$ est le produit tensoriel des états de corde $|p\rangle >$ et $|\overline{S}\rangle >$. Ce dernier est un des deux états de plus basse énergie du secteur R. Le secteur R-NS est sensiblement le même que le précédent, à la différence que deux solutions sont possibles pour les états de masse nulle :

$$\overline{\psi}^\mu_{-1/2}|p, S\rangle \text{ et } \overline{\psi}^\mu_{-1/2}|p, C\rangle, \tag{2.35}$$

où C est un spineur de chiralité négative. Du choix du spineur, S ou C, dépend le type de théorie considéré : type IIB si le spineur est aussi S, type IIA sinon. Comme pour le secteur NS-R, les états (2.35) sont des fermions d'espace-temps. Enfin, dans le secteur R-R, les états de masse nulle dépendent du type de théorie considéré (IIA ou IIB). Dans le premier cas, les états cherchés sont $|S, \overline{C} >$ qui se décomposent selon un vecteur et un tenseur antisymétrique de rang 3. En type IIB les états sont $|S, \overline{S} >$, ou encore un scalaire, un tenseur antisymétrique de rang 2 et un tenseur antisymétrique de rang 4. De manière générale, les oscillateurs bosoniques n'interviennent pas dans le spectre d'états de masse nulle, mais ils interviennent dans le spectre des états massifs. Les théories de type IIA et IIB se différencient notamment au niveau de la chiralité : la première étant non-chirale alors que la seconde est chirale. Dans les publications 1, 2 et 3, nous avons utilisé des modèles de corde de type II mais aussi hétérotiques. Nous verrons dans ce chapitre que les différentes théories des cordes sont en fait reliées par un réseau de dualités. Nous ne donnons aucun détail concernant les supercordes de type I car nous ne les avons pas utilisé dans nos travaux.

Supercordes hétérotiques

Une théorie de cordes fermées est composée de deux types d'états : des états gauche et droit. Chaque état est décrit par des oscillateurs de cordes et une impulsion. Jusqu'ici, la seule théorie des cordes qui soit symétrique droite-gauche que nous

ayons à notre disposition est la théorie de type IIB. La corde hétérotique est une théorie asymétrique droite-gauche [?]. Nous choisirons la convention de construction suivante : les états gauches vivent dans une théorie de cordes bosoniques alors que les états droits vivent dans une théorie de supercordes. Le secteur gauche de la théorie est décrit par une théorie de cordes bosoniques avec 26 dimensions et le secteur droit de la théorie est par contre une théorie de supercordes vivant en dix dimensions. On peut ainsi paramétrer l'espace-temps par dix coordonnées bosoniques gauches et droites X^μ, $\mu = 0, \cdots, 9$ paramétrant l'espace-temps, dix coordonnées fermioniques droites ψ^α, $\alpha = 0, \cdots, 9$ et 16 coordonnées bosoniques gauches $X^I, I = 0, \cdots, 15$. On peut regrouper ces coordonnées en 10 coordonnées complexes

$$Z^\mu = X^\mu + i\psi^\mu, \ \mu = 0, \cdots, 9; \tag{2.36}$$

et 16 coordonnées bosoniques $X^I, \ I = 0, \cdots, 15$. Nous ne pouvons pas choisir les champs X^I au hasard. En effet, pour des raisons d'invariance modulaire[4], les coordonnées X^I doivent être compactes. Plus précisément, elles doivent décrire un réseau en 16 dimensions[5], L_{16}. Nous avons vu plus haut que la théorie des cordes bosoniques possède un tachyon, or la corde hétérotique possède un secteur de corde bosonique, donc il y a un tachyon ! De plus, on sait également que le secteur NS de la théorie des supercordes possède un tachyon, donc nous avons deux tachyons ! Néanmoins, on sait éliminer le second au travers de la projection GSO, que nous imposons alors. La corde hétérotique possède cependant le tachyon de la corde bosonique.

La corde hétérotique possède comme toute théorie des cordes des dimensions supplémentaires. Supposons donc que n dimensions soient compactifiées et que la métrique de l'espace-temps total soit donnée par

$$ds^2 = \sum_{\mu,\nu=0}^{d-1} dX \cdot dX + \sum_{I,J=1}^{n} G_{IJ} dY^I dY^J, \ d + n = 26. \tag{2.37}$$

Les coordonnées bosoniques compactes sont données par

$$Y^I(\sigma, \tau) = Y^I_L(\zeta_+) + Y^I_R(\zeta_-), \tag{2.38}$$

avec

$$Y^I_{L,R}(\zeta_\pm) \ = \ \frac{y^I}{2} + p^I_{L,R}\zeta_\pm + \frac{i}{2}\sum_{n\neq 0} \frac{\hat{\alpha}^I_n}{n} e^{-2in\zeta_\pm}, \tag{2.39}$$

avec $\hat{\alpha} = \alpha$ pour le secteur L et $\hat{\alpha} = \tilde{\alpha}$ pour le secteur R. De plus, si on compactifie une corde fermée sur un cercle, nous avons alors la condition de périodicité $Y^I(\sigma + 2\pi, \tau) = Y^I(\sigma, \tau) + 2\pi n^I$ où n^I caractérise le nombre de fois que la corde s'enroule autour de la dimension compactifié, on l'appelle *nombre d'enroulement*. De façon similaire, la quantité $p^I_L + p^I_R$ doit être quantifiée. En présence d'une métrique G^{IJ} et d'un champ de KR B_{JK}, nous pouvons écrire

$$p^I_{L,R} = \pm n^I + G^{IJ}\left(\frac{m_J}{2} - B_{JK}n^K\right), \tag{2.40}$$

[4]Nous expliquons cette notion plus bas
[5]voir Annexe A

où m_J est un *nombre de moment* venant de la quantification de $p_L^I + p_R^I$. La masse d'excitations de cordes dans ce modèle s'obtient en additionnant les contributions des moments, des oscillateurs, et de la charge centrale. Nous avons donc

$$M^2 = \frac{1}{2} G_{IJ} p_L^i p_L^J + N_L - 1 = \frac{1}{2} G_{IJ} p_R^I p_R^J + N_R - \epsilon, \tag{2.41}$$

soit

$$M^2 = M_0^2 + \frac{N_R + N_L - (1+\epsilon)}{2} \text{ avec } M_0^2 = \frac{G_{IJ}}{4}(p_L^I p_L^J + p_R^I p_R^J), \tag{2.42}$$

où $N_{L,R} = \sum_n \hat{\alpha}_n^I \cdot \hat{\alpha}_{-n}^I$ et $\epsilon = 1, \frac{1}{2}$ suivant que l'on considère la corde bosonique ou la corde hétérotique. Une façon élégante d'écrire ces relations est donnée par

$$4M_0^2 = (n,m)\mathcal{G}^{-1} \begin{pmatrix} n \\ m \end{pmatrix}, \ \mathcal{G} = \begin{pmatrix} \frac{G^{-1}}{2} & -G^{-1}B \\ BG^{-1} & 2(G - BG^{-1}B) \end{pmatrix}. \tag{2.43}$$

On peut ainsi écrire (2.42) sous la forme (corde hétérotique)

$$M^2 = 4(n^I, m_I)\mathcal{G}^{-1} \binom{n_I}{m_I} + 2(N_R + N_L) - \frac{3}{2}. \tag{2.44}$$

Cette formule est invariante sous l'échange moments-enroulements et l'inversion de la métrique $\mathcal{G}$. On peut ainsi montrer après plusieurs étapes que le réseau des vecteurs de moment $\vec{P} = (p_L, p_R)$ peut être relié aux algèbres de Lie des groupes $SO(32)$ et $E_8 \times E_8$. C'est pourquoi nous parlons de théorie hétérotique $SO(32)$ et $E_8 \times E_8$. Les groupes $SO(32)$ et E_8 sont très connus dans la communauté des physiciens des particules car incluent comme sous-groupe celui du modèle standard.

1.3 Interactions de cordes et fonction de partition

Jusqu'à présent, nous avons étudié brièvement la propagation de cordes libres, et détaillé les différents espace-temps possibles pour cette propagation, dépendant de la théorie considérée. Néanmoins, il est évident que les cordes considérées, en se mouvant dans l'espace-temps, vont interagir, subir des interactions. Étudier de manière exhaustive et rigoureuse les interactions de cordes est une tâche évidemment très ardue. Selon les même principes qu'en théorie des champs, l'interaction de N cordes peut se décrire dans un premier temps par une interaction à l'ordre des arbres, puis doit être affinée par des corrections à une et/ou plusieurs boucles. Cependant, comme en théorie des champs, il y a aussi des contributions venant d'effets non-perturbatifs, c'est à dire ne pouvant pas se décrire dans le cadre d'un développement perturbatif. Il est souvent très difficile de calculer ces effets en théorie des champs, et encore plus en théorie des cordes. Dans ce travail de thèse, nous n'avons à aucun moment eu à étudier en profondeur de tels effets non-perturbatifs, nous n'en dirons donc pas plus si ce n'est que la meilleure façon de les décrire reste souvent l'utilisation des dualités.

Montrons cependant comment on peut calculer des corrections à une boucle en théorie des cordes. Le calcul similaire à plusieurs boucles ne fais pas partie des

préoccupations présentes et futures. De plus, on se limite au cas des cordes fermées car c'est ce qui nous intéresse. Avant toute chose il convient cependant de décrire ce que l'on entend par *ordre des arbres*, ou *perturbations à n boucles* d'une interaction. La figure 2.3 montre comment représenter des processus à l'ordre des arbres mais aussi à une et deux boucles. Les figures de gauche schématisent l'interaction alors que celles de droite sont les contractions de celles de gauche. Les points noirs sur les surfaces de droite sont les résultats de la contraction des pattes caractérisées par les cordes fermées se propageant après interactions. Mathématiquement, on caractérise l'action des états décrit par ces cordes fermées par des *opérateurs de vertex*. Les surfaces où vivent ces opérateurs de vertex sont des **surfaces de Riemann** standard. Pour la corde fermée on a à l'ordre des arbres une sphère, un tore à une boucle, un double tore à deux boucles,$\cdots$. Pour la corde ouverte non dessinée, on devine aisément que les surfaces équivalentes respectives sont le disque, le cercle, deux cercles attachés,$\cdots$. Pour la corde fermée, les opérateurs de vertex sont attachés à la surface de la surface de Riemann alors que pour la corde ouverte ils le sont sur les bords des surfaces. Chaque surface de Riemann peut se décrire au travers de coordonnées z^a, de plus la valeur d'un opérateur de vertex dépend de sa position sur la surface de Riemann.

Avant d'effectuer tout calcul, il nous faut décrire la première surface de Riemann non triviale : le tore. Le tore est une surface de genre $g = 1$ et de nombre d'Euler $\chi = 0$. On peut choisir par normalisation le volume du tore $V = 1$, on peut donc le paramétrer par deux coordonnées $\sigma_{1,2} \in [0, 1]$. La métrique d'un tore s'exprime en fonction d'un troisième paramètre, $\tau = \tau_1 + i\tau_2$, complexe. Elle est donnée par

$$ds^2 = g_{ij} d\sigma_i d\sigma_j = \frac{1}{\tau_2} |d\sigma_1 + \tau d\sigma_2|^2. \tag{2.45}$$

τ est le module du tore, ou sa *structure complexe*, et ne peut être modifié par difféomorphismes infinitésimaux ou transformations de Weyl. Il peut par contre être modifié par difféomorphismes globaux. La périodicité du tore : $\sigma_i \to \sigma_i + 1$, entraine

$$\omega \to \omega + 1, \ \omega \to \omega + \tau, \tag{2.46}$$

avec $\omega = \sigma_1 + \tau\sigma_2$. L'ensemble des paramètres τ équivalents (décrivant le même tore), forme le groupe modulaire du tore. Il est possible de montrer que ce dernier est engendré par deux transformations :

$$\begin{aligned} T &: \ \tau \to \tau + 1, \\ S &: \ \tau \to -\frac{1}{\tau}. \end{aligned} \tag{2.47}$$

La transformation la plus générale est alors

$$\tau \to \frac{a\tau + b}{c\tau + d}, \ A = \begin{pmatrix} a & b \\ c & d \end{pmatrix}, \tag{2.48}$$

où $\det(A) = 1$ et a, b, c, d sont des entiers. L'ensemble de ces matrices est le groupe $SL(2, \mathbb{Z})$. Graphiquement, l'ensemble des paramètres τ inéquivalents est décris sur la figure 2.4. Pour plus de détails, voir l'annexe B. Il est maintenant possible de

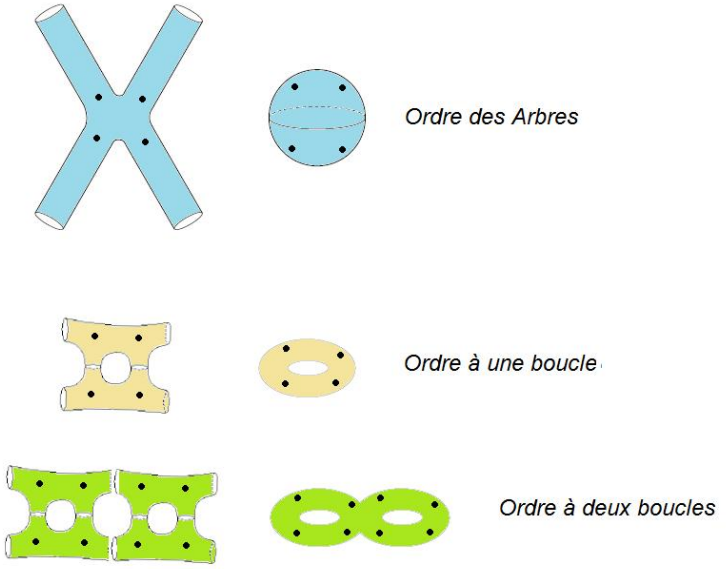

FIG. 2.3 – Interactions en théorie des cordes et son développement en perturbations

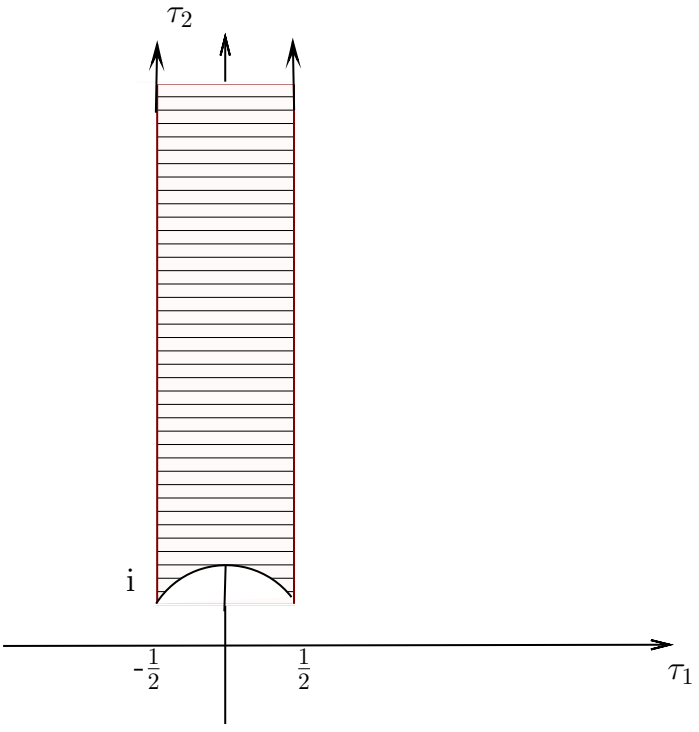

FIG. 2.4 – Domaine fondamental d'un tore.

calculer une fonction de partition sur un tore connaissant l'action de départ. A ce titre, à toute action S_E (euclidienne) ; on peut associer une fonction de partition $Z = \int d\mu e^{-S_E}$ où $d\mu$ est une mesure impliquant les différents champs dont dépend l'action.

Illustrons ce propos par le cas d'un boson compactifié sur un tore, décri par l'action

$$S = \frac{1}{4\pi}\int d^2\sigma\sqrt{g}g^{ij}\partial_i X\cdot\partial_j X = -\frac{1}{4\pi}\int d^2\sigma X\Box X, \tag{2.49}$$

où $\Box = \frac{1}{\tau_2}|\tau\partial_1 - \partial_2|^2$ et $\partial_i = \frac{\partial}{\partial\sigma_i}$. La stratégie usuelle consiste à déterminer les solutions classiques des champs dérivées de l'action ci dessus, développer ces champs autour de leur solution classique, et effectuer les intégrales. L'équation du mouvement classique pour X^μ est

$$\Box X = 0,\ \rightarrow X_{class} = 2\pi R(n\sigma_1 + m\sigma_2),\ m,n\in\mathbb{Z}. \tag{2.50}$$

On obtient après de nombreux calculs la fonction de partition

$$Z(R) = \frac{R}{\sqrt{\tau_2}|\eta|^2}\sum_{m,n\in\mathbb{Z}} e^{-\frac{\pi R^2}{\tau_2}|m-n\tau|^2}. \tag{2.51}$$

C'est la forme *lagrangienne* de la fonction de partition. En utilisant la technique de la resommation de Poisson, nous pouvons obtenir la forme *hamiltonienne* :

$$Z(R) = \sum_{m,n\in\mathbb{Z}} \frac{q^{\frac{P_L^2}{2}}\overline{q}^{\frac{P_R^2}{2}}}{\eta\overline{\eta}}, \tag{2.52}$$

où nous avons défini les moments

$$P_L = \frac{1}{\sqrt{2}}\left(\frac{m}{R} + nR\right),\ P_R = \frac{1}{\sqrt{2}}\left(\frac{m}{R} - nR\right). \tag{2.53}$$

Un résultat simple que l'on peut dériver à partir de (2.52) est la valeur de la fonction de partition pour un boson non-compact, *ie* $R\rightarrow\infty$. Nous obtenons alors

$$Z(R) = \frac{R}{\sqrt{\tau_2}\eta\overline{\eta}},\ R\rightarrow\infty. \tag{2.54}$$

L'étape suivante dans notre introduction au calcul des fonctions de partition et à la théorie des cordes est l'équivalent du calcul précédent en remplaçant un boson par un fermion (et en gardant la taille caractéristique R finie). La version du calcul présentée est basée sur l'étude des valeurs propres d'un déterminant. L'action du fermion est donnée par

$$S = -\frac{1}{8\pi}\int d^2z\psi\overline{\partial}\psi. \tag{2.55}$$

Nous savons d'après la brève introduction donnée dans cette section que le spineur ψ a deux conditions de périodicité possibles :

$$\begin{aligned}\psi(\sigma+2\pi) &= -\psi(\sigma),\ NS\rightarrow A\\ \psi(\sigma+2\pi) &= \psi(\sigma),\ R\rightarrow P.\end{aligned} \tag{2.56}$$

Dans chaque secteur, les développements en modes de ψ ont été donné aux équations (2.27,2.28). La fonction de partition d'un fermion libre de Majorana-Weyl est simplement donnée par

$$Z_f = \int \mathcal{D}\psi e^{-S} = \sqrt{\det(\partial)}. \tag{2.57}$$

Un tore peut mathématiquement se voir comme un produit cartésien de deux cercle, $\mathbb{T}^2 = S^1 \times S^1$, donc il existe quatre solutions pour les conditions au bord du fermion sur le tore : (P,P), (A,P), (P,A) et (A,A). Le calcul de $\det(\partial)$ se fait au travers des valeurs propres de ∂ qui dans le secteur (A,A) sont

$$\lambda_{AA} = \left(m_1 + \frac{1}{2}\right)\tau + \left(m_2 + \frac{1}{2}\right), \; m_{1,2} \in \mathbb{Z}, \tag{2.58}$$

donnant $(\det(\partial))_{AA} = \frac{\theta_3(\tau)}{\eta(\tau)}$[6]. Dans le secteur (A,P), les valeurs propres sont

$$\lambda_{AA} = \left(m_1 + \frac{1}{2}\right)\tau + m_2, \; m_{1,2} \in \mathbb{Z}, \tag{2.59}$$

donnant $(\det(\partial))_{AP} = \frac{\theta_4(\tau)}{\eta(\tau)}$. Dans le secteur (P,A), les valeurs propres sont

$$\lambda_{AA} = m_1\tau + \left(m_2 + \frac{1}{2}\right), \; m_{1,2} \in \mathbb{Z}, \tag{2.60}$$

donnant $(\det(\partial))_{PA} = \frac{\theta_2(\tau)}{\eta(\tau)}$. Finalement, le secteur (P,P) donne une contribution nulle car pour $m_{1,2} = 0$ nous avons une valeur propre nulle. Il est plus élégant de noter les résultats sous la forme

$$(\det \partial) \left[{a \atop b}\right] = \frac{\theta \left[{a \atop b}\right](\tau)}{\eta(\tau)}, \tag{2.61}$$

où $a = 0, 1$ indique des conditions aux bords A,P autour d'un des cercles du tore et $b = 0, 1$ indique des conditions aux bords A,P autour de l'autre des cercles du tore. Les différents secteurs d'un fermion sur un tore ne sont pas totalement indépendants. En fait, un simple regard aux transformations modulaires données en annexe B montre que les secteurs (A,A), (A,P) et (P,A) sont reliés entre eux alors que le secteur (P,P) forme une orbite à lui seul du groupe modulaire. Introduisant un fermion droit comme partenaire du fermion précédent considéré comme fermion gauche, la fonction de partition est alors

$$Z_f = \frac{1}{2}\sum_{a,b=0}^{1} \left|\frac{\theta \left[{a \atop b}\right]}{\eta}\right|. \tag{2.62}$$

Cette expression est invariante modulaire comme il est facile de le montrer en utilisant les résultats de l'annexe B. L'invariance modulaire est fondamentale en théorie des cordes, et imposer que la fonction de partition d'une théorie le soit permet de s'affranchir de nombreuses pathologies pour la théorie. En combinant des bosons et

[6] voir l'annexe B pour les définitions des fonctions θ entre autres.

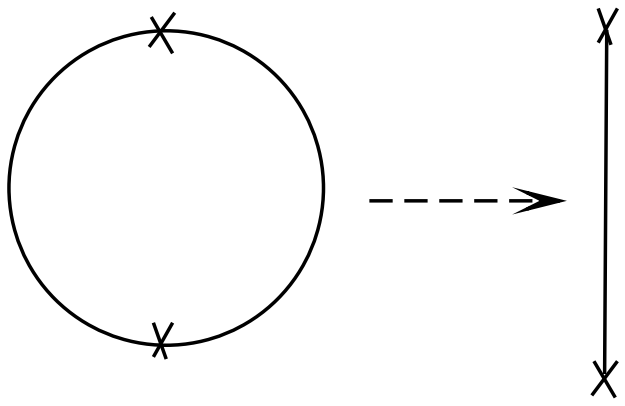

FIG. 2.5 – Schéma descriptif de l'orbifold $\mathbb{Z}_2$

des fermions, il est possible de d'obtenir différents modèles desquels on peut tirer des fonctions de partition invariantes modulaires.

Avant de décrire certains de ces systèmes, il est intéressant de noter qu'après quelques manipulations élémentaires et transformations de Poisson, la fonction de partition Z_f peut s'écrire comme

$$Z_f = \frac{1}{\sqrt{2\tau_2}} \sum_{m,n\in\mathbb{Z}} e^{-\frac{\pi}{2\tau_2}|n+\tau m|^2}, \tag{2.63}$$

ce qui est la même expression que pour un boson compactifié sur un cercle de rayon $R = \frac{1}{\sqrt{2}}$. Un couple de deux fermions libres de Majorana-Weyl (gauche et droit) est donc équivalent à un boson compact de rayon $R = \frac{1}{\sqrt{2}}$.

L'étape suivante est le calcul de la fonction de partition d'un orbifold simple d'un boson sur un cercle de rayon R. l'orbifold utilisé est celui décrit sur la figure 2.5 Mathématiquement, nous partons du cercle S^1, appliquons l'identification $\mathbb{Z}_2$: $X \to -X$ et obtenons l'orbifold $\frac{S^1}{\mathbb{Z}_2}$. L'ensemble des états d'un orbifold[7] peut se décomposer en deux groupes. Le premier est composé des états *non twistés*, dont les conditions de périodicité sont indépendantes de la présence ou non de l'orbifold, et le second est composé des états *twistés*, dont les conditions de périodicité sont dictées par l'orbifold. Un orbifold n'est autre que l'identification de points d'une variété a priori inéquivalents en points équivalents. Ainsi, en plus des états d'origine associés à la variété de départ, nous avons des états qui apparaissent du fait de l'orbifold. La fonction de partition peut donc s'écrire

$$Z = Z_{untw} + Z_{tw}, \tag{2.64}$$

[7] un orbifold est une variété sur laquelle on fait agir un groupe d'opérations identifiant différents points de la variété à un seul point. Chaque élément de l'orbifold est en fait une classe d'équivalence pour une certaine relation donnée.

Soit h l'inversion de l'orbifold, $h : X \to -X$, de sorte que l'opérateur

$$P = \frac{1+h}{2} \tag{2.65}$$

soit un projecteur. L'orbifold échangeant X en $-X$, les moments et enroulements deviennent donc

$$(m,n) \to (-m,-n), \tag{2.66}$$

soit : $h|m,n\rangle = |-m,-n\rangle$. Nous avons donc

$$h\left[\prod_{i=1}^{N} a_{-n_i} \prod_{j=1}^{\tilde{N}} \tilde{a}_{\tilde{n}_j}|m,n\rangle\right] = (-1)^{N+\tilde{N}}\left[\prod_{i=1}^{N} a_{-n_i} \prod_{j=1}^{\tilde{N}} \tilde{a}_{\tilde{n}_j}|-m,-n\rangle\right], \tag{2.67}$$

ce qui implique ($L_0 = \frac{1}{2}\sum_n \alpha_{-n}\alpha_n,\ \tilde{L}_0 = \frac{1}{2}\sum_n \tilde{\alpha}_{-n}\tilde{\alpha}_n$).

$$Z(R)_{untw} = \frac{1}{2}Z(R) + \frac{1}{2}\mathrm{Tr}[hq^{L_0-1/24}\overline{q}^{\overline{L}_0-1/24}]. \tag{2.68}$$

Les états $|m,n\rangle$ satisfaisant la relation

$$\langle m_1,n_1|m_2,n_2\rangle \simeq \delta_{m_1+m_2}\delta_{n_1+n_2}, \tag{2.69}$$

il est facile de constater que seuls les états de moment et d'enroulement nuls vont contribuer, nous avons donc, après utilisation des formules de l'annexe B :

$$\frac{1}{2}\mathrm{Tr}[hq^{L_0-1/24}\overline{q}^{\overline{L}_0-1/24}] = \left|\frac{\eta}{\theta_2}\right| \Longrightarrow Z_{untw} = \frac{1}{2}Z(R) + \left|\frac{\eta}{\theta_2}\right|. \tag{2.70}$$

Cependant cette fonction de partition n'est pas invariante modulaire, comme il est facile de le vérifier avec l'annexe B. La raison de ceci est évidente, nous n'avons considéré que les états vérifiant la condition de périodicité $X(\sigma+2\pi) = X(\sigma)$ et nous avons regardé lesquels de ces états sont gardés dans le spectre par le projecteur P. Comme énoncé plus haut, l'orbifold permet également d'identifier des états a priori inéquivalents en états équivalents, ici X et $-X$. Ainsi, la condition de périodicité

$$X(\sigma+2\pi) = hX(\sigma) = -X(\sigma) \tag{2.71}$$

imposée sur l'équation du mouvement pour X implique le nouveau développement en modes du champ X_t où l'indice t signifie *twisté* :

$$X_t(\sigma,\tau) = x_0 + \frac{i}{\sqrt{4\pi T}}\sum_{n\in\mathbb{Z}}\left(\frac{a_{n+1/2}}{n+1/2}e^{i(n+1/2)(\sigma+\tau)} + \frac{\overline{a}_{n+1/2}}{n+1/2}e^{i(n+1/2)(\sigma+\tau)}\right), \tag{2.72}$$

où le mode 0 doit satisfaire $x_0 = 0, \pi R$ selon l'orbifold. Nous pouvons ensuite calculer

$$Z_{twisted} = \frac{1}{2}\mathrm{Tr}\left[(1+h)q^{L_0-1/24}\overline{q}^{\overline{L}_0-1/24}\right] = \left|\frac{\eta}{\theta_4}\right| + \left|\frac{\eta}{\theta_3}\right|. \tag{2.73}$$

Nous rassemblons les deux parties pour finalement obtenir

$$Z_{orb} = Z_{untw} + Z_{twisted} = \frac{1}{2}Z(R) + \left|\frac{\eta}{\theta_2}\right| + \left|\frac{\eta}{\theta_4}\right| + \left|\frac{\eta}{\theta_3}\right|, \tag{2.74}$$

qui possède la propriété d'être invariante modulaire. Comme dans le cas du fermion sur un cercle, nous pouvons écrire cette fonction de partition plus agréablement en introduisant deux entiers g, h tels que

- $h = 0, 1$ désigne respectivement les secteurs non-twistés et twistés,
- $g = 0, 1$ implique respectivement aucune projection et une projection.

Nous pouvons alors écrire

$$Z_{orb} = \frac{1}{2} \sum_{h,g=0}^{1} Z \left[\begin{smallmatrix} h \\ g \end{smallmatrix}\right], \tag{2.75}$$

avec $Z \left[\begin{smallmatrix} 0 \\ 0 \end{smallmatrix}\right] = Z(R)$ et $Z \left[\begin{smallmatrix} h \\ g \end{smallmatrix}\right] = 2 \left| \frac{\eta}{\theta \left[\begin{smallmatrix} 1-h \\ 1-g \end{smallmatrix}\right]} \right|$, $(h, g) \neq (0, 0)$. Les transformations modulaires sont alors données par

$$T(\tau) \to Z \left[\begin{smallmatrix} h \\ g \end{smallmatrix}\right] \to Z \left[\begin{smallmatrix} h \\ h+g \end{smallmatrix}\right], \tag{2.76}$$

et

$$S(\tau) \to Z \left[\begin{smallmatrix} h \\ g \end{smallmatrix}\right] \to Z \left[\begin{smallmatrix} g \\ h \end{smallmatrix}\right]. \tag{2.77}$$

Nous avons ainsi vu une nouvelle façon de construire des fonctions de partition invariantes modulaires.

Une remarque **fondamentale** doit être faite à propos de Z_{orb} : $Z_{orb}(R) = Z_{orb}\left(\frac{1}{R}\right)$, qui peut se vérifier en utilisant la resommation de Poisson. Cette symétrie appelée $T-$dualité est fondamentale en théorie des cordes. Cette symétrie peut permettre, en utilisant la resommation de Poisson, de simplifier le calcul des fonctions de partitions en se focalisant seulement sur certains termes à calculer.

Considérons enfin un autre orbifold $\frac{S^1}{\mathbb{Z}_2}$ où l'élément du groupe g de l'orbifold agit tel que

$$g \cdot X = X + \pi R, \;\; g|m, n\rangle = (-1)^m |m, n\rangle. \tag{2.78}$$

Appliquant la même méthode que ci dessus, nous trouvons la fonction de partition invariante modulaire

$$Z_{orb} = \frac{1}{2} \sum_{h,g=0}^{1} Z \left[\begin{smallmatrix} h \\ g \end{smallmatrix}\right], \tag{2.79}$$

avec $Z \left[\begin{smallmatrix} 0 \\ 0 \end{smallmatrix}\right] = Z(R)$ et

$$Z \left[\begin{smallmatrix} h \\ g \end{smallmatrix}\right] = \frac{R}{\sqrt{\tau_2}\eta\overline{\eta}} \sum_{m,n\in\mathbb{Z}} e^{-\frac{\pi R^2}{\tau_2}\left|m+\frac{g}{2}+\left(n+\frac{h}{2}\right)\tau\right|^2} \;\; (h, g) \neq (0, 0). \tag{2.80}$$

Le premier orbifold étudié avait deux points fixes, marqués par deux croix sur la figure (2.5), alors que l'orbifold ci-dessus n'en a pas. Un point fixe se traduit sur la variété finale par une singularité.

2 Modèle standard $\Lambda-$CDM

La cosmologie est l'une des plus anciennes sciences étudiée par l'homme. Pourtant, le seul modèle cohérent décrivant l'Univers (son passé et son évolution) dont

nous disposons, appelé modèle $\Lambda-$CDM, nécessite que 96% du contenu énergétique de l'Univers soit décrit par de la matière *sombre* et de *l'énergie du vide*. Ces deux quantités n'ont toujours pas été détectées à proprement parler, et de très nombreux travaux ont été effectués à ce sujet. Cependant, à ce jour, aucune description théorique cohérente de la matière sombre et/ou de la constante cosmologique n'existe.

Le modèle $\Lambda-$CDM suppose que l'Univers est homogène et isotrope à suffisamment grandes échelles[8]. Partant de ce principe, et en supposant que nous vivons en D dimensions avec $D-1$ dimensions spatiales décrites par les coordonnées x^i, $i = 1, ..., D-1$, il est possible de montrer que la métrique décrivant un tel espace-temps est donnée par celle de Friedmann-Lemaître-Robertson-Walker (FLRW) :

$$ds^2 = -dt^2 + a(t)^2 \sum_i dx^{i\ 2}, \tag{2.81}$$

où $a(t)$ est le *facteur d'échelle* de l'Univers. Dans ce formalisme nous supposons que la courbure de l'espace est nulle. Dans le modèle $\Lambda-$CDM, l'Univers est composé de matière non-relativiste sans pression de densité ρ_m, rayonnement de densité ρ_r, matière noire froide de densité ρ_{CDM} et constante cosmologique Λ de densité ρ_Λ. Chacun de ces fluides est caractérisé par une équation d'état $P_X = \omega_X \rho_X$ où P_X est la pression du fluide X et ω_X est le paramètre d'équation d'état. Nous avons

$$\omega_m = \omega_{CDM} = 0,\ \omega_r = \frac{1}{3},\ \omega_\Lambda = -1. \tag{2.82}$$

La nature de la matière noire et de la constante cosmologique Λ est toujours inconnue (existent elles seulement, où sont-elles le fruit de notre ignorance en matière de gravitation ?).

L'idée standard en cosmologie est que la théorie décrivant l'Univers et son évolution de la meilleure des façons est la Relativité Générale (RG) décrite par l'équation

$$G_{\mu\nu} = R_{\mu\nu} - \frac{1}{2} R g_{\mu\nu} = T_{\mu\nu} \tag{2.83}$$

dans des unités appropriées. Dans (2.83), $R_{\mu\nu}$ est le tenseur de Ricci alors que $T_{\mu\nu}$ est le tenseur énergie impulsion qui dans l'approximation du fluide parfait peut s'écrire comme

$$T_{\mu\nu} = (P + \rho) u_\mu u_\nu + P g_{\mu\nu}, \tag{2.84}$$

où u^μ est la quadrivitesse du fluide cosmique.

Le scénario d'évolution de l'Univers communément admis est le suivant. Tout d'abord il y a la naissance de l'Univers (Big-Bang ?) et la période la suivant, mais s'arrêtant avant l'inflation : la période pré-Inflation. Domaine assez spéculatif, différents scénarios existent mais il est très difficile de l'étudier alors que l'on ne connait assez mal ce qu'il se passe juste après.

L'inflation est une idée qui a le mérite d'expliquer un grand nombre de problèmes de la cosmologie, mais il en existe d'autres, comme la possibilité que notre

[8] pour une étude d'Univers inhomogènes et anisotropes, le lecteur peut se référer à [26] pour une approche nouvelle et instructive.

Univers soit cyclique, phénix,$\cdots$. Nous supposerons cependant qu'il est admis que l'Univers a subi une courte mais très intense période d'accélération au cours de laquelle sa taille a augmenté exponentiellement : l'inflation. Cette période, qui peut être décomposée en plusieurs de durées et importances inégales, a eu pour effet de diluer les premiers défauts topologiques présents, diluer les inhomogénéités primordiales, et rendre l'Univers spatialement quasi-plat. Après cette période d'inflation, le *réchauffement* a permis à l'Univers, dont la température a fortement baissé dû à la forte augmentation de sa taille, de se réchauffer suffisamment pour débuter les relations thermonucléaires de nucléosynthèse et ainsi produire les premiers éléments. Il faut cependant noter que lors de ce réchauffement, l'Univers peut produire des particules suffisamment lourdes et nombreuses pour entrainer une contraction de l'Univers sous son propre poids. Une seconde phase d'inflation, en générale d'intensité plus faible que la première, peut être utilisée pour diluer ces particules. Nous entrons ensuite dans la période de domination par le rayonnement où le facteur d'échelle évolue comme $a(t) \propto t^{\frac{1}{2}}$. Comme la matière non relativiste se dilue moins vite que le rayonnement, il arrive un moment où la matière domine, et le facteur d'échelle évolue comme $a(t) \propto t^{\frac{2}{3}}$. S'il existe encore beaucoup d'arbitraire dans cette grande histoire de l'Univers, une ère de domination de la matière assez longue est indéniable de par le fait que nous existons et que des structures organisées de matière se sont formées (galaxies, étoiles, planètes,$\cdots$). Enfin, pour expliquer la récente accélération de l'Univers observée d'après les résultats de mesures sur les supernovae et le CMB (Fond diffus cosmologique) [27], l'ère de domination par la matière cède la place à une ère de domination par la constante cosmologique où le facteur d'échelle croît exponentiellement : $a(t) \propto e^{Ht}$.

Si la théorie des cordes veut décrire efficacement les phénomènes de gravité quantique, elle doit être en mesure d'expliquer ce qui s'est passé très tôt dans l'histoire de l'Univers, c'est à dire *grosso modo* avant la domination par la matière. En fait, l'inflation constitue le terrain de jeux par excellence pour la théorie des cordes, d'où le grand nombre de travaux plus ou moins phénoménologiques s'y rapportant. L'inflation doit permettre de décrire comment à partir de fluctuations primordiales l'Univers les a dilués pour rendre le tout quasi-homogène. Les résidus de ces fluctuations primordiales donneront les perturbations de densité qui elles mêmes vont engendrer des puits de potentiel gravitationnel où la matière va pouvoir évoluer et se rassembler pour former des structures (galaxies, amas de galaxies,...). Il est possible d'observer la trace de ces fluctuations primordiales de densité en observant le CMB. De plus, il est également possible de déterminer à partir du CMB la proportion de chaque composante du fluide cosmique dans l'Univers. Cette manœuvre est cependant très délicate car très sujette à approximations et hypothèses. La théorie des cordes est actuellement très loin de pouvoir expliquer ou prédire des phénomènes visibles dans les prochaines expériences sur le CMB. Dans le chapitre suivant, nous verrons néanmoins qu'il est possible, dans un cadre rigoureux et précis, d'obtenir des informations sur l'évolution de l'Univers primordial engendrée par des modèles de cordes précis. Nous verrons comment dans les cas étudiés la dynamique de l'Univers tend vers celle d'un univers dominé par le rayonnement et comment on peut espérer décrire les étapes ultérieures de l'évolution de l'Univers par des généralisations minimales des modèles de cordes employés.

Les travaux présentés dans ce rapport sont très différents de la majorité des travaux traitant de cosmologie de super-cordes. Nous noterons au moins deux différences majeures.

- Dans les travaux présentés ici, certes nous utiliserons des théories des champs effectives, mais nous les dérivons à partir de la théorie des cordes. Certaines approches de supergravité manquent d'un tel lien avec la théorie des cordes, ou tout simplement avec une théorie microscopique.
- Nous ne dérivons aucune information cosmologique autre que l'allure du facteur d'échelle en fonction du temps. Il est dangereux, à mon avis, de dériver à partir de tels modèles des informations trop précises sur les modèles cosmologiques étudiés (indice spectral, paramètre de non gaussianités). Pour être franc, ce n'est pas la dérivation en elle même qui est dangereuse, c'est la comparaison avec l'expérience. Nous pourrions être tentés d'oublier ou encenser certains modèles alors que les expériences risquent fort encore de changer de verdicts dans ce domaine de la physique.

Chapitre 3

Cosmologie en théorie des supercordes

Ce long chapitre décrit le contenu des publications 1 et 2. Un résumé plus qualitatif et plus concis de ce chapitre est fourni dans la publication 3. L'intérêt de cette dernière étant d'écrire une revue des progrès effectués dans le cadre de cosmologie des supercordes étudié ici, la présentation y est assez concise en termes de détails techniques. C'est une reprise de ce travail, étoffée de détails techniques, qui est présentée ici.

Ce chapitre débute par des rappels concernant la cosmologie des supercordes. Nous préciserons en quoi il est difficile de mener à bien une telle analyse et pourquoi la nôtre est intéressante à suivre. Nous ne prétendons pas présenter une classification exhaustive des modèles cosmologiques induits par nos constructions de supercordes. Il n'est pas exclu par conséquent que des comportements différents de ceux étudiés ici puissent être obtenus avec des modèles relativement proches de ceux étudiés dans ce chapitre. Après cette introduction, nous illustrerons les principes de notre approche sur un exemple très simple nous permettant de retrouver la loi de Stefan et de mettre au point les conventions et outils de base. Ensuite nous compliquerons les modèles considérés en introduisant une dynamique interne plus riche. Cette dynamique pouvant être de deux types au moins : *portant une brisure spontanée de supersymétrie ou non*. Pour conclure ce chapitre nous évoquerons quelques perspectives pour des travaux ultérieurs.

1 Pourquoi étudier la cosmologie des supercordes ?

1.1 Cosmologie des supercordes : idées standard

Il est communément admis que la cosmologie et donc l'histoire de l'Univers peuvent se décrire par des théories des champs appropriées. Dans ce cadre, il est possible [11], en demandant l'ajout de divers champs de matière, de décrire l'histoire de l'Univers en incluant la matière noire et la constante cosmologique en ne tenant compte uniquement que de la matière non relativiste et sans pression et du

rayonnement. Bien que très intéressant, ce type d'approche manque d'une théorie microscopique de la gravitation à sa base. Certes, rien ne nous dit qu'une telle théorie microscopique de la gravitation doit exister, ou ben même que les lois gouvernant l'évolution de l'Univers à certaines échelles doivent dériver d'une action et d'un principe variationnel. Gardant ceci à l'esprit, nous ne pouvons en aucune façon discriminer certains modèles et scénarios plutôt que d'autres, seule l'expérience est mère de certitudes en physique. Néanmoins, nous allons tenter de développer des modèles cosmologiques dans un scénario théoriquement plus abouti que celui utilisé notamment dans [11]. Bien entendu, nous ne pourrons pas être aussi précis ici que dans l'application de TeVeS à la cosmologie. Dans ce chapitre, nous travaillons avec la théorie des cordes en 10 dimensions et la réduisons en une théorie en dimension D. A l'action de l'espace-temps qui en découle, nous devons ajouter de la matière s'y couplant. Dans les approches conventionnelles de cosmologie, mais aussi de cosmologie des supercordes, la matière est décrite par un fluide parfait décrit par sa pression P et sa densité ρ, reliés par une équation d'état $P = \omega\rho$ avec ω le paramètre de l'équation d'état. Cette procédure *ad-hoc* ne sera cependant pas suivie ici. Nous verrons dans la section suivante comment nous pouvons déterminer à partir d'arguments microscopiques la densité et la pression d'un gaz de cordes associé à un modèle précis.

Bien que nous puissions étudier de manière théorique des échelles d'énergie bien plus grandes que celles testées jusqu'à présent par l'expérience, il existe dans de nombreux modèles de cordes une singularité appelée *transition d'Hagedorn* [28]. Cette transition est due à la théorie des cordes. Physiquement cette transition est caractérisée par une température T_H et un rayon R_H. Si l'Univers décrit par un modèle de cordes possédant une singularité de type Hagedorn a une taille plus petite que ce rayon R_H ou si sa température est plus élevée que T_H alors nous sommes en présence d'une contradiction car des tachyons apparaissent dans le modèle de cordes à la transition d'Hagedorn. La fonction de partition devient infinie et nous ne pouvons rien dire concernant la cosmologie

Malgré de nombreux efforts vers l'étude de la cosmologie en théorie des cordes ces dernières années, peu de résultats significatifs sont à noter, et beaucoup de travail reste à faire dans le domaine de la dynamique de cordes dans un espace-temps en évolution temporelle. Le but du travail présenté ici est de présenter une classe de modèles de cordes à partir desquels nous pouvons étudier de manière aussi rigoureuse que possible quelques questions cosmologiques. Au niveau classique de la théorie des cordes, il apparaît difficile d'obtenir des solutions cosmologiques exactes. En effet, après de nombreux travaux dans le domaine des compactifications de supercordes (avec ou sans flux), les résultats obtenus apparaissent comme inappropriés à la cosmologie. Dans la plupart des cas, l'espace-temps classique est celui d'Anti-de-Sitter (AdS) ou bien celui de Minkowski. Aucun espace-temps ayant un intérêt cosmologique n'apparait. Le même problème se pose dans les théories effectives de supergravité. Naïvement, les résultats ainsi obtenus amènent à la conclusion que des espace-temps cosmologiquement non triviaux ne peuvent pas être obtenus en théorie des supercordes. Cependant, cette conclusion ne peut être correcte à ce niveau car elle ne tient pas compte des corrections thermiques et quantiques. Ces corrections,

lorsque l'on en tient compte, permettent d'aller au delà de l'approximation classique de la théorie. La direction que l'on choisit de suivre ici consiste précisément à étudier les *cosmologies quantiques et thermales* générées dynamiquement au niveau quantique de la théorie des cordes. Bien que cette étude paraisse très difficile à première vue, il apparaît que dans certains cas, les corrections quantiques et thermiques sont sous contrôle grâce à la structure particulière de la théorie effective de supergravité dans sa phase de brisure spontanée de supersymétrie.

Nous voulons faire remarquer dans cette section que quelques modèles simples de théorie des cordes peuvent engendrer des prédictions intéressantes pour la cosmologie.

Dans le but de voir comment des solutions intéressantes du point de vue cosmologique apparaissent, considérons le cas d'un espace-temps plat en théorie des cordes. Cet espace-temps contient un gaz de cordes, que l'on supposera **libre**. A température finie, les fluctuations thermiques produisent une densité d'énergie non nulle qui est calculable perturbativement au niveau de la théorie des cordes. Les interactions entre les différents champs donnent lieu à une évolution cosmologique bien spécifique. Pour des températures plus basses que la température d'Hagedorn, l'évolution de l'Univers est déterminée comme étant dominée par le rayonnement.

Des cas plus intéressants sont donnés par ceux où la supersymétrie est spontanément brisée au niveau des cordes par des flux.

Très tôt dans l'Univers, quand la température est plus faible que celle d'Hagedorn, nous sommes face à des singularités de notre modèle. Cette obstruction issue de la théorie des cordes peut être occultée en ne considérant que des énergies (températures) petites devant celle d'Hagedorn. Cette ère n'existe que pour $t \gg t_H$. Ainsi, pour $t \gg t_H$ nous supposons l'émergence d'au moins trois grandes dimensions spatiales avec de possibles dimensions internes de taille intermédiaire. La taille de ces dimensions internes caractérise la brisure de supersymétrie, ou plus généralement *l'échelle de brisure de symétries* (de jauge ou non). Si nous désignons par t_E le temps à partir duquel l'Univers sort du régime d'Hagedorn, nous pouvons masquer notre ignorance des phénomènes à $t \ll t_E$ en imposant des conditions aux bords sur l'hypersurface $t = t_E$. Dans ce travail, nous nous focaliserons sur l'ère définie par

$$ICE : t_E \ll t \ll t_w, \tag{3.1}$$

soit après la transition d'Hagedorn et avant celle de la brisure de symétrie électrofaible. Dans nos modèles, la description de l'Univers est sous contrôle modulo les conditions initiales à $t = t_E$. Ce n'est qu'en imposant ces conditions initiales que l'on peut déterminer certaines informations sur l'Univers comme la valeur de certains modules. Le module de Kähler $r = \frac{R_{s1}}{R_{s2}}$ représentant le rapport de deux rayons de dimensions spatiales différentes en est un exemple.

Notons au passage que [29] a développé un scénario alternatif à la cosmologie standard et à l'inflation. Ce scénario suppose que la présence de moments et d'enroulements implique que l'Univers ait subi une phase de rebond, l'empêchant ainsi de passer par des régimes où la température est trop élevée (dépassant celle d'Hagedorn par exemple). Dans cette approche nous n'avons pas à nous soucier de

la transition d'Hagedorn car elle n'existe pas. On peut également mentionner que les univers à rebonds ont beaucoup été étudiés dans la littérature, et qu'ils présentent le grand avantage de ne pas avoir besoin d'inflation en général.

1.2 Notre modèle

Dans ce travail, nous avons restreint notre attention aux espace-temps de dimension quatre avec une supersymétrie d'espace-temps initiale $N = 4, 2, 1$, obtenue par compactifications de modèles de super-cordes hétérotiques ou de type II, avec ou sans orbifold. Comme pour la température, la brisure de supersymétrie est implémentée par un orbifold agissant librement.

Différentes présentations des publications 1, 2 et 3 sont possibles. Par souci de clarté et de pédagogie, la démarche choisie ici est progressive, dans le sens où nous compliquons les modèles au fur et à mesure que l'on progresse, et destinée à mettre en valeur les différents résultats obtenus. Le but de ce travail est de montrer clairement qu'une approche par la théorie des cordes, même si dans certains cas simples elle peut paraître superflue, permet dans des cas plus complexes d'obtenir des modèles phénoménologiques très puissants et nouveaux, ne pouvant pas s'obtenir par une simple théorie des champs. On verra que les modèles obtenus peuvent pour les plus compliqués être décrits par une succession de théories des champs convenablement reliées entre elles. Nous ne traiterons qu'un nombre restreint de modèles de cordes. Dans ces modèles, deux types de dimensions internes émergent : celles brisant la supersymétrie et celles dont la taille peut être de l'ordre de celle d'une dimension décompactifiée ou bien de celle d'une dimension compactifiée. Il est évident que chacune de ces fonctions peut être jouée par une ou plusieurs dimensions. Pour simplifier, nous ne considérons au maximum que deux dimensions internes non compactifiées. Des commentaires qualitatifs sur ce que l'on obtient en relaxant cette hypothèse sont donnés ci dessous.

Le plan de ce chapitre est le suivant. Après cette brève introduction qualitative, la section 2 décrit la thermodynamique d'un gaz de cordes. Nous étudions également un premier exemple simple où uniquement la température est introduite. Cet exemple un peu simpliste permet cependant de bien commencer à comprendre quels sont les états qui contribuent à la théorie effective et de se familiariser avec les techniques de calculs à utiliser. Dans la section suivante nous ajoutons à ce modèle de base une brisure de supersymétrie d'une part, et une dimension interpolatrice d'autre part. Enfin, en section 4 nous analysons ce qui se passe lorsque deux dimensions internes deviennent dynamiques, en variant leurs fonctions. Nous concluons ensuite avec diverses pistes de recherche.

L'organisation de ce chapitre doit permettre de se rendre compte que, au fur et à mesure que l'on complique les modèles étudiés, d'une part les étapes de calcul sont les mêmes (calculer la fonction de partition du gaz de cordes, déterminer l'action effective et les équations du mouvement des différents champs du modèle, résoudre ces équations pour en déduire l'évolution de l'Univers décrit par ce modèle), et d'autre part les conclusions se rejoignent toutes. Pour éviter un rapport trop long et trop

calculatoire, nous présentons pour les modèles les plus simples divers calculs (stabilité par exemple) qui sont volontairement omis pour les modèles les plus compliqués (mais les conclusions restent les mêmes comme nous le verrons). Sans rentrer dans des calculs interminables nous espérons que cette présentation permet d'une part de présenter l'ensemble des conclusions physiques et des méthodes de calcul.

2 Notations et conventions

Tous les modèles que nous considérons appartiennent à la classe d'espace-temps

$$S^1(R_0) \times \underbrace{T^D}_{\text{partie spatiale}} \times \underbrace{M_{9-D}}_{\text{variété interne}} . \tag{3.2}$$

La direction temporelle, de rayon R_0, est supposée être compacte dans l'euclidien (pas dans le Minkowskien, bien évidemment), comme la partie spatiale T^D que nous prenons D-dimensionnelle. Notons que nous pouvons voir ces espaces-temps comme inclus dans une boîte de grande taille pour ce qui est des directions spatiales externes, et de taille minuscule pour ce qui est des dimensions internes. Afin de bien fixer les idées, nous supposerons dans tout ce chapitre que la taille caractéristique d'une dimension spatiale externe, R_{box}, la taille caractéristique d'une direction interne brisant la supersymétrie ou interpolant, R_S, et celle d'une direction interne compactifiée, sont reliées par

$$R_{box} \gg R_S \geq R_I. \tag{3.3}$$

Quand la dimension de l'espace-temps change, les résultats varient quantitativement bien que qualitativement ils soient identiques.

La partie spatiale est compactifiée dans le but d'éliminer notamment les divergences infra-rouge. Naïvement, nous nous retrouvons avec un espace-temps vivant dans une boîte que le gaz de cordes remplit. Des équations du mouvement, on déduit qu'une fois les conditions aux bords bien définies selon la direction temporelle et les directions internes compactifiées, les champs sont bien définis dans la boîte d'espace-temps. Les différents modèles de cordes que nous allons étudier sont donnés par

- $M_6 = T^6,\ D = 3$, où seulement la température est incluse. Ce modèle est étudié à la fin de cette section. On retrouve notamment la loi de Stefan.
- $M_6 = S^1(R_4) \times S^1 \times \frac{T^4}{\mathbb{Z}_2 \times \mathbb{Z}_2}$, où une brisure spontanée de supersymétrie intervient également le long de la direction 4 de rayon R_4. Ce modèle sera étudié dans la section suivante. L'attraction vers des Univers Dominés par le Rayonnement (UDR) est la principale conclusion de cette étude.
- $M_6 = \frac{S^1(R_4) \times S^1}{\mathbb{Z}_2} \times \frac{T^2}{\mathbb{Z}_2} \times T^2$, où la direction 4 de brisure de supersymétrie porte également un orbifold. Ce modèle comme le précédent sera aussi étudié à la prochaine section.
- $M_6 = S^1(R_4) \times S^1(R_5) \times \frac{T^4}{\mathbb{Z}_2 \times \mathbb{Z}_2}$, où la brisure interne de supersymétrie est cette fois-ci portée par les directions 4 et 5 de rayons respectifs $R_4,\ R_5$. La

direction 5 peut également être remplacée par une dimension interpolatrice de rayon R_9. Ces modèles seront considérés en section 4 car ils mettent à nu de nouveaux phénomènes tels que la compactification spontanée de modules de Kähler internes, et sont globalement plus compliqués.

Les corrections thermiques sont introduites en couplant le nombre de fermions d'espace-temps, Q_F, aux nombres de moment et d'enroulement associés à la direction du temps euclidien compactifiée sur un cercle $S^1(T)$ alors que la brisure de supersymétrie est introduite par un couplage similaire d'une charge interne de $R-$symétrie, Q_R, aux nombres de moment et d'enroulement associés à la direction interne de brisure de supersymétrie $S^1(M)$ que nous choisissons par conventions comme étant la direction 4. La brisure de supersymétrie et l'introduction de la température se font au travers de la généralisation à la théorie des cordes des compactifications de Scherk-Schwarz [23]. Deux échelles de brisure de supersymétrie sont à distinguer : l'échelle de température $T \propto \frac{1}{2\pi R_0}$ et l'échelle de brisure de la supersymétrie $M \propto \frac{1}{2\pi R_4}$, avec R_0 et R_4 les rayons des directions temporelles et 4 respectivement. La dégénérescence dans le spectre des états de masses des bosons et fermions est levée de manière proportionnelle à T et M. Cette levée de dégénérescence est un signe de la brisure de supersymétrie et de la valeur non nulle de l'énergie libre.

A faible couplage, l'énergie libre du gaz de cordes peut s'obtenir à partir de la fonction de partition euclidienne d'un gaz de cordes à une boucle. Les amplitudes de cordes perturbatives sont libres des ambiguïtés UV usuelles qui nuisent toute approche à la cosmologie et la gravité quantique par la théorie des champs. La raison de cette absence est bien entendu la nature étendue des cordes. Pour R_0 et R_4 suffisamment larges, le système est également libre de tachyons. Par conséquent, la densité d'énergie et la pression du gaz de cordes peuvent être déterminées sans ambiguïtés, et nous pouvons les utiliser comme sources aux équations d'Einstein pour obtenir des solutions cosmologiques non triviales. Cette approche perturbative perd son sens près de la singularité de genre espace d'Hagedorn.

2.1 Thermodynamique d'un gaz de cordes

Nous considérons un gaz de cordes que l'on peut traiter par les techniques de l'ensemble canonique, ce qui est vrai pour $t \gg t_E$ (car la fonction de partition est finie). Dans cet esprit, considérons la fonction de partition thermique de la théorie

$$Z_{th} = \int \mathcal{D}\phi e^{-S_E[\phi]}. \tag{3.4}$$

C'est la somme des diagrammes de Feynman connectés et disconnectés. Comme nous supposons que le gaz de cordes est faiblement couplé, nous réduisons la liste des diagrammes de Feynman à ceux n'ayant qu'une boucle. Le seul diagramme de ce type, connecté, est le diagramme *circulaire*, nous avons donc

$$Z_{th}^{1-loop} = \ln Z_{th}, \tag{3.5}$$

où Z_{th} est appelée *l'énergie du vide* de notre gaz de cordes.[1]. Dans notre limite de basse énergie, l'énergie du vide est reliée à l'énergie libre $\mathcal{F}$ par

$$\mathcal{F} = -\frac{Z_{th}^{1-loop}}{\beta}. \tag{3.6}$$

Les corrections à une boucle dues à cette énergie du vide pour l'action effective sont données par l'action

$$S_m = \int d^4x \sqrt{|g|} V_s, \; V_s = \mathcal{F}, \tag{3.7}$$

de sorte que l'action totale soit $S = S_{cl} + S_m$. L'action S_m peut ainsi être comprise comme l'action décrivant la matière dans notre modèle. Nous la couplons à la gravitation en lui associant un tenseur d'énergie-impulsion

$$T_{\mu\nu} = \frac{1}{\sqrt{|g|}} \frac{\delta}{\delta g_{\mu\nu}} \left(\sqrt{|g|} F \right) \tag{3.8}$$

de sorte que notre gaz de cordes puisse être décris dans la limite de couplage faible par la pression $P = \frac{T_{ii}}{V_{space}}$ et la densité d'énergie $\rho = \frac{T_{00}}{V_{space}}$ qui satisfont

$$P = -\frac{\partial F}{\partial V_s}, \; \rho = T\frac{\partial P}{\partial T} - P. \tag{3.9}$$

Ces résultats sont en parfait accord avec ceux obtenus par la thermodynamique.

Divergences IR et UV Deux types de divergences peuvent apparaître en théorie des champs : IR et UV. Les premières peuvent s'éliminer en imposant un cut-off à large distance ou par des conditions aux bords appropriées. Par conséquent, *en plaçant l'Univers dans une boîte*, nous pouvons éliminer les divergences IR. Les divergences UV peuvent également être supprimées en imposant un cut-off à faible distance. En étudiant comment la théorie des cordes peut décrire un Univers dans une boîte, on est en mesure de supprimer les deux types de divergences.

2.2 Modèle considéré

Tout d'abord, dans cette section et dans la suivante, nous supposerons que $D = 3$. Nous laisserons la dimension de l'Univers, D, arbitraire dans la dernière section, bien que les différences ne soient que qualitatives. Nous débutons avec le modèle le plus simple où seule la température est incluse. Nous sommes donc intéressés par la fonction de partition de bosons et fermions à température finie. L' équilibre

[1] Cette énergie du vide représente la différence entre celle due aux bosons et celle due aux fermions. Ici, nous partons de modèles initialement supersymétriques où bosons et fermions donnent exactement la même contribution à Z_{th}^{1-loop}, de sorte que l'énergie du vide s'annule. Quand nous introduisons des termes de brisure de supersymétrie, les bosons et fermions couplent aux $R-$charges de manière *a priori* différentes, de sorte que leurs masses changent et l'énergie du vide n'est plus nulle (elle peut être des deux signes). On verra que cela implique même que la pression du gaz de cordes peut prendre les deux signes

thermique va briser la supersymétrie de telle sorte que même si classiquement $Z = 0$ par supersymétrie, à une boucle, nous obtenons *in fine* une énergie libre non nulle. Ce n'est pas un résultat très surprenant étant donné que la supersymétrie est spontanément brisée. De plus, nous savons depuis le travail de Planck que des particules dans un bain thermique décrivent un gaz de pression $P \propto T^4$. Nous allons retrouver cet élégant résultat. Pour ce faire, considérons un gaz de cordes hétérotiques. Dans ce cas, la fonction de partition à une boucle prend la forme[2]

$$Z = R_0 R_{box}^3 \int_F \frac{d\tau_1 d\tau_2}{2\tau_2^{5/2}} \frac{1}{2} \sum_{a,b} (-)^{a+b+ab} \frac{\theta[^a_b]^4}{\eta^4} \sum_{n_0,\tilde{m}_0} e^{-\frac{\pi R_0^2}{\tau_2}|\tilde{m}_0+n_0\tau|^2} (-)^{a\tilde{m}_0+bn_0+\tilde{m}_0 n_0} Z_{(6,22)}, \tag{3.10}$$

où R_{box} est le rayon caractéristique de T^3 et nous rappelons que le domaine fondamental est

$$F \equiv \left\{ \tau \in \mathbb{C} / |\mathrm{Re}(\tau)| \leq \frac{1}{2} \text{ et } |\tau| > 1 \right\}. \tag{3.11}$$

$Z_{(6,22)}$ est la contribution des modes zéros et des oscillateurs bosoniques de l'espace interne. Par exemple, pour un espace interne torique T^6, nous avons

$$Z_{(6,22)} = \frac{\Gamma_{(6,6)}\Gamma_{(0,16)}}{\eta^8\, \bar{\eta}^{24}}, \tag{3.12}$$

où $\Gamma_{(i,j)}$ désigne un réseau de Narain[3], mais des modèles plus complexes avec des actions d'orbifold peuvent être considérés. R_0 est le rayon de la direction temporelle euclidienne le long de laquelle les bosons ($a = 0$) et fermions ($a = 1$) ont différentes conditions aux bords, de telle sorte que toutes les supersymétries soient brisées spontanément par des effets thermiques. Après réduction dimensionnelle en quatre dimensions, l'action décrivant notre modèle est

$$S = \int d^4x \sqrt{-g_{st}} \left[e^{-2\phi} \left(\frac{R_{st}}{2} + 2(\partial\phi)^2 + \cdots \right) + \frac{Z}{\beta V_{box}} \right], \tag{3.13}$$

où ϕ est le dilaton en D dimensions. Les points de suspension désignent les autres états sans masse alors que $\beta = 2\pi R_0$, $V_{box} = (2\pi R_{box})^3$ et R_{box} est la taille d'une dimension compacte. Afin de calculer Z, il convient de préciser exactement quels sont les états sans masse et massifs qui interviennent. Tout d'abord il y a les états de masse nulle, qui doivent être gardés. Ensuite nous avons deux types d'états massifs : ceux de la variété interne, et ceux venant de la compactification du temps. Les premiers sont extrêmement massifs car proportionnels à $\frac{1}{R_I}$ où R_I est de l'ordre de 1 en unités de cordes, par conséquent ces états peuvent être négligés devant les autres états massifs : ceux de la direction 0. Parmi ces derniers nous avons les états avec et sans enroulement. Les premiers sont plus massifs que les seconds et interviennent dans Z avec une contribution de la forme

$$e^{-\pi\tau_2 \frac{M^2}{\alpha'}} \ll 1, \tag{3.14}$$

[2]Nos conventions pour les fonctions θ et blocs conformes sont celles de [30]. Quand ce n'est pas explicitement mentionné, nous travaillons avec $\alpha' = 1$. Nous notons également $Z = Z_{th}^{1-loop}$.

[3]Un réseau de Narain est un réseau décrivant les nombres discrets de moment et d'enroulement associés à $16+n$ directions droites compactifiées et n directions gauches compactifiées d'une théorie de cordes.

car $\frac{M^2}{\alpha'} \propto \frac{R_0^2}{R_I^2} \gg 1$. Les états massifs de la direction 0, sans enroulement, contribuent quand à eux à Z et donnent une somme discrète sur les états de Kaluza-Klein. Nous obtenons ainsi

$$Z = \frac{R_0 R_{box}^3}{R_0^4} n_T c_4 \qquad \text{où} \qquad c_4 = \frac{1}{\pi^2} \sum_{\tilde{k}_0} \frac{1}{|2\tilde{k}_0 + 1|^4} . \tag{3.15}$$

n_T est le nombre de paires boson-fermion sans masse dans le modèle de départ supersymétrique où la température n'est pas introduite. Il est facile d'obtenir la métrique dans le repère d'Einstein [4]

$$S = \int d^4x \sqrt{-g} \left[\frac{R}{2} - \frac{1}{2}(\partial\phi_\perp)^2 + \cdots - \mathcal{F} \right] , \tag{3.16}$$

où

$$\mathcal{F} = -T^4 n_4 c_4 , \qquad T = \frac{1}{2\pi R_0 e^{-\frac{2\phi}{2}}} , \qquad \phi_\perp = \sqrt{2}\phi . \tag{3.17}$$

Nous ne nous intéressons uniquement qu'aux extrema homogènes et isotropes de cette action. Nous considérons l'ansatz pour la métrique et le dilaton

$$\begin{aligned} ds^2 &= -N(t)^2 dt^2 + a(t)^2 \left[(dx^1)^2 + \cdots + (dx^3)^2 \right] , \qquad \phi_\perp(t) , \\ \text{où} \qquad N(t) &\equiv 2\pi R_0 e^{-\phi} \equiv \frac{1}{T(t)} , \qquad a(t) \equiv 2\pi R_{box} e^{-\phi} , \end{aligned} \tag{3.18}$$

avec une ansatz triviale pour les autres états sans masse. Comme $P = -\mathcal{F}$, nous retrouvons la loi de Stefan. Par conséquent, la cosmologie sous-jacente est celle dictée par un Univers dominé par le rayonnement :

$$a(t) = t^{1/4} \times \left(\frac{C_r}{3} \right)^{1/D} = \frac{1}{T(t)} \times (a_0 T_0) , \qquad \phi_\perp = cst. \tag{3.19}$$

Nous obtenons en particulier le résultat standard $a(t) \propto \frac{1}{T(t)}$.

Nous avons ainsi obtenu les résultats de base pour un Univers dominé par le rayonnement. Bien que nous soyons partis de la théorie des cordes, nous avons finalement obtenu des résultats standard de théorie des champs après s'être restreint aux états de masse nulle et de faible masse. Comme nous l'avons dit, cette restriction est parfaitement légitime. A ce stade du travail, il est naturel d'être suspicieux du réel intérêt de la théorie des cordes dans notre approche. En effet, nous n'obtenons rien d'autre que des résultats standard de théorie des champs. Cependant, nous allons voir dans la suite de ce chapitre que certains résultats ne peuvent pas s'obtenir à partir de la théorie des champs. Bien qu'à la fin du travail, les modèles obtenus ne soient ni plus ni moins qu'une succession de théories des champs plus ou moins bien connectées, ces connexions non triviales apportées par la théorie des cordes rendent la physique nouvelle et l'approche très intéressante et enrichissante.

Dans la section suivante nous enrichissons notre modèle de base en introduisant premièrement une brisure interne de supersymétrie et deuxièmement un orbifold le long de cette direction.

[4] valable seulement pour $D \geq 3$.

3 On introduit la brisure de supersymétrie

Jusqu'à la fin de ce chapitre, nous travaillons avec l'exemple simple $D = 3$ pour donner les idées. Les autres dimensions sont équivalentes du point de vue des techniques analytiques et numériques utilisées.

3.1 Brisure de supersymétrie sans orbifold simultané

On suppose que la direction 4 est compactifiée sur un cercle de taille R_4. Nous introduisons des conditions aux bords appropriées le long de cette direction de telle façon à briser spontanément la supersymétrie avant même l'équilibre thermique de l'Univers. Le résultat simple $\mathcal{F} = \mathcal{F}(T)$ trouvé dans la section précédente n'est clairement plus possible ici. En effet, il existe une nouvelle échelle de masse M, la masse de brisure de supersymétrie. Cette masse est reliée à R_4 et le dilaton ϕ par

$$M = \frac{1}{2\pi R_4 e^{-\phi}}. \tag{3.20}$$

Nous verrons que l'énergie libre peut alors s'exprimer comme $P = P(T, z)$ où $z = \ln\left(\frac{M}{T}\right)$ est un module du problème.

Pour implémenter la température et la brisure de supersymétrie, les termes de réseaux le long de la direction temporelle et le tore T^n sont déformés par des phases additionnelles. L'invariance modulaire dicte alors la forme de ces phases, et le résultat final nécessite donc le remplacement des termes de réseaux

$$\begin{aligned}
\Gamma_{(1,1)}(R_0) &\rightarrow \sum_{\tilde{k},\tilde{l}} R_0 \tau_2^{-\frac{1}{2}} \exp(-\pi R_0^2 |\tilde{k} + \tilde{l}\tau|^2/\tau_2)(-1)^{\tilde{k}a+\tilde{l}b+\tilde{k}\tilde{l}}, \\
\Gamma_{(1,1)}(R_i) &\rightarrow \sum_{\tilde{k},\tilde{l}} R_i \tau_2^{-\frac{1}{2}} \exp(-\pi R_i^2 |\tilde{k} + \tilde{l}\tau|^2/\tau_2)(-1)^{\tilde{k}(a+Q_i)+\tilde{l}(b+L_i)+\varepsilon_i\tilde{k}\tilde{l}}.
\end{aligned} \tag{3.21}$$

Ces phases couplent les nombres de moment et d'enroulement des directions brisant la supersymétrie aux phases a, b ainsi qu'aux charges de $R-$ symétries , L introduites pour la brisure spontanée de supersymétrie. Ces phases doivent être vues comme des conditions aux bords particulières que l'on impose aux différents champs composant l'Univers, vu on le rappelle comme une boîte. Le calcul de la fonction de partition est élémentaire une fois ciblés les secteurs contribuant pour une valeur non nulle. Ensuite nous ne gardons, comme dans le cas purement thermal, dans les différents secteurs que les états de masse nulle et ceux de faible masse. Ils sont de deux sortes : les Kaluza-Klein des directions 0 et 4. Enfin, nous utilisons l'invariance modulaire (cf [31]) pour simplifier le domaine d'intégration en remplaçant le domaine fondamental par un domaine d'intégration plus simple. L'intégrale sur τ_1 a pour effet d'imposer que la masse d'états de cordes gauche est la même que celle des états droits. Après tout ce travail, l'intégrale sur τ_2 est relativement aisée. Après ces longues étapes calculatoires, nous obtenons la pression

$$p(z) = f(z) + \mathcal{R}\tilde{f}(z), \tag{3.22}$$

où

$$\frac{\Gamma(5/2)}{\pi^{5/2}} \sum_{k_0,k_4\in\mathbb{Z}} \frac{e^{4z}}{[(2k_0+1)^2 e^{2z} + (2k_4)^2]^{5/2}}, \quad \tilde{f}(z) = e^{3z} f(-z). \tag{3.23}$$

Nous avons

$$-1 \leq \mathcal{R} \leq 1. \tag{3.24}$$

Selon la valeur précise du rapport $\mathcal{R}$, différents modèles et différentes cosmologies sont possibles. Nous verrons que pour une large gamme de valeurs du paramètre $\mathcal{R}$, une solution cosmologique décrite par une ère de rayonnement existe et est stable.

La source de matière décrite par la pression P résulte d'une correction à une boucle. Elle interagit avec l'espace-temps Lorentzien classique en 4 dimensions, au travers de la théorie effective

$$S = \int d^4x\sqrt{-g}\left[\frac{1}{2}R - g^{\mu\nu}\left(\partial_\mu\phi_D\,\partial_\nu\phi_D + \frac{1}{2}\frac{\partial_\mu R_4\,\partial_\nu R_4}{R_4^2}\right) + P\right], \tag{3.25}$$

où nous mentionnons seulement les champs de dynamique non triviale. Avant d'écrire les équations du mouvement, il est utile de définir les champs

$$\phi := \sqrt{\frac{2}{3}}\,(\phi_D - \ln R_4)\,, \qquad \phi_\perp := \frac{1}{\sqrt{3}}\,(2\phi_D + \ln R_4)\,, \tag{3.26}$$

de sorte que l'action devienne

$$S = \int d^4x\sqrt{-g}\left[\frac{1}{2}R - \frac{1}{2}\left((\partial\phi)^2 + (\partial\phi_\perp)^2\right) + P\right], \tag{3.27}$$

où la pression et l'échelle de brisure de supersymétrie M prennent la forme

$$P = M^4\,e^{-4z}p(z)\,, \qquad e^z = \frac{M}{T}\,, \qquad M = \frac{e^{\alpha\phi}}{2\pi} \qquad \text{avec} \qquad \alpha = \sqrt{\frac{3}{2}}\,. \tag{3.28}$$

Supposant une métrique homogène et isotrope avec un sous-espace plat tri-dimensionnel, on obtient les équations du mouvement

$$2\dot{H} + 3H^2 = -\frac{1}{2}\dot{\phi}^2 - \frac{1}{2}\dot{\phi}_\perp^2 - P\,, \tag{3.29}$$

$$\ddot{\phi} + 3H\dot{\phi} = \frac{\partial P}{\partial\phi} \equiv \alpha(3P - \rho)\,, \tag{3.30}$$

$$\ddot{\phi}_\perp + 3H\dot{\phi}_\perp = 0 \qquad \Longrightarrow \qquad \dot{\phi}_\perp = \sqrt{2}\,\frac{c_\perp}{a^3}\,, \tag{3.31}$$

où $c_\perp$ est une constante d'intégration arbitraire. Nous pouvons obtenir une équation pour z, montrant que $z = \text{cst.}$ est une solution si et seulement si $V_z = 0$ où

$$V_z(z) = r - 4\,p\,. \tag{3.32}$$

La forme de $V(z)$ dépend de la valeur du paramètre

$$\mathcal{R} \in [-1, 1] \tag{3.33}$$

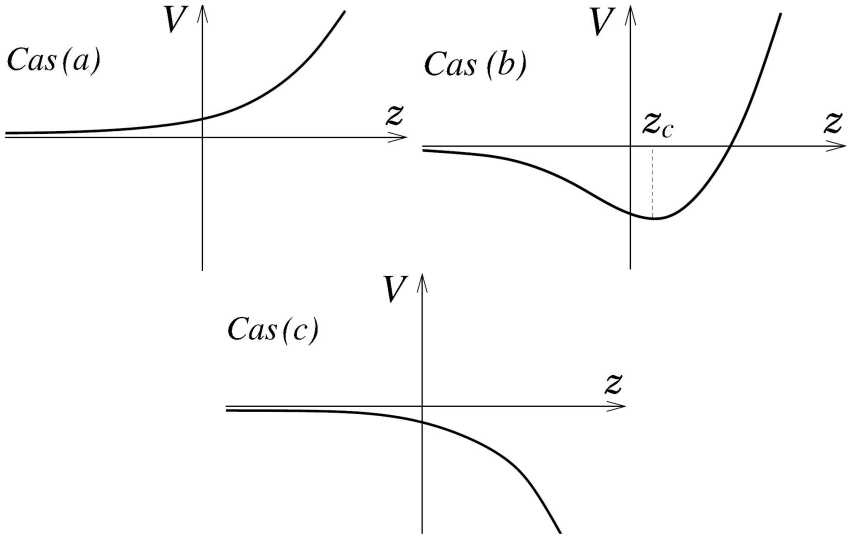

FIG. 3.1 – La forme du potentiel $V(z)$ dépend du rapport $\mathcal{R}$. Les cas (a), (b) et (c) sont détaillés ci-dessous.

3 cas distincts existent et sont montrés sur la Fig.3.3 :

- *Cas (a) :* Pour $\mathcal{R} < -1/15$, V croît de façon monotone.
- *Cas (b) :* Pour $-1/15 < \mathcal{R} < 0$, V a un unique minimum en z_c, et $p(z_c) > 0$.
- *Cas (c) :* Pour $0 < \mathcal{R}$, V décroît de façon monotone.

Nous nous intéressons uniquement aux solutions stables, par conséquent on ne tiendra compte uniquement que du cas (b). Dans ce cas, z est fixé à une valeur critique z_c. Les équations de Friedmann donnent le résultat simple

$$a(t) = \left(\frac{t}{\tilde{t}_0}\right)^{2/d} \tilde{a}_0 \qquad \text{où} \qquad \frac{\tilde{a}_0}{\tilde{t}_0^{2/d}} = \left(\frac{d^2\,\tilde{c}_r}{2(d-2)(d-1)}\right)^{1/d},$$
$$T(t) = M(t)\,e^{-\tilde{z}_c} = \frac{1}{a(t)}\,e^{-\tilde{z}_c}\tilde{a}_0\tilde{M}_0\,, \qquad \phi_\perp(t) = \phi_{\perp 0}\,, \qquad \zeta(t) = 0\,. \tag{3.34}$$

Cette évolution particulière se caractérise par la relation

$$a(t) \propto T(t) \propto M(t). \tag{3.35}$$

Cette solution décrit une ère de rayonnement en 4 dimensions (valable également en dimension arbitraire avec un module $\phi_\perp$. Il est facile de vérifier analytiquement que les UDR ainsi trouvés sont stables pour toute petite fluctuation autour du minimum. Pour ce faire, nous obtenons d'abord la relation $\alpha\overset{\circ}{\phi} = \mathcal{A}_z(z)\overset{\circ}{z} - 1$ avec

$$\mathcal{A}_z(z) = \frac{4r - r_z}{3(r+p)}. \tag{3.36}$$

Nous obtenons alors $M = \frac{e^{\mathcal{A}(z)+c^2}}{a}$ avec une constante c. En manipulant l'équation de Friedmann nous avons $H^2 = h(z)T^4$ avec

$$h(z) = \frac{r(z)}{3 - \mathcal{K}(z, \overset{\circ}{z}, \overset{\circ}{\phi}_\perp)}, \quad \mathcal{K} = \frac{1}{2\alpha^2}\left(\mathcal{A}_z(z)\overset{\circ}{z} - 1\right)^2 + \frac{\overset{\circ}{\phi}{}_\perp^2}{2}. \tag{3.37}$$

Les équations pour z et $\phi_\perp$ deviennent alors

$$\begin{cases} \dfrac{r(z)}{3-\mathcal{K}(z,\overset{\circ}{z},\overset{\circ}{\phi}_\perp)}\left(\mathcal{A}_z(z)\,\overset{\circ\circ}{z}+\mathcal{A}_{zz}(z)\,\overset{\circ}{z}{}^2\right)+\dfrac{r(z)-p(z)}{2}\,\mathcal{A}_z(z)\,\overset{\circ}{z}+V_z(z)=0, \\ \dfrac{r(z)}{3-\mathcal{K}(z,\overset{\circ}{z},\overset{\circ}{\phi}_\perp)}\,\overset{\circ\circ}{\phi}_\perp+\dfrac{r(z)-p(z)}{2}\,\overset{\circ}{\phi}_\perp=0. \end{cases} \tag{3.38}$$

Nous avons introduit $V_z(z)=r(z)-4p(z)$, et pour la suite nous utilisons $\alpha^2=\frac{3}{2}$. Si nous posons $z(\lambda)=z_c+\epsilon(\lambda)$ et $\overset{\circ}{\phi}_\perp(\lambda)=\overset{\circ}{\epsilon}_\perp(\lambda)$ pour ϵ et $\epsilon_\perp$ petits. Au premier ordre, le système (3.38) est donné par

$$\begin{cases} \overset{\circ\circ}{\epsilon}+\overset{\circ}{\epsilon}+\xi\,\epsilon=0 \qquad \text{où} \qquad \xi=10\left.\dfrac{p-p_{zz}}{19p+p_{zz}}\right|_{z_c}, \\ \overset{\circ\circ}{\epsilon}_\perp+\overset{\circ}{\epsilon}_\perp=0\,. \end{cases} \tag{3.39}$$

ξ est en fait une fonction de $\mathcal{R}$. Si $\mathcal{R}\in\left[-\frac{1}{15},0\right]$ alors on peut montrer numériquement que $\xi>0$. ϵ et $\epsilon_\perp$ sont ainsi donnés par

$$\overset{\circ}{\epsilon}_\perp(\lambda)=c_3\,e^{-\lambda}\ ,\ \epsilon(\lambda)=\begin{cases} c_1\,e^{-\lambda(1+\sqrt{1-4\xi})/2}+c_2\,e^{-\lambda(1-\sqrt{1-4\xi})/2} & \text{si}\ \ 0<\xi<1/4 \\ e^{-\lambda/2}(c_1+c_2\,\lambda) & \text{si}\ \ \xi=1/4 \\ e^{-\lambda/2}\left(c_1\cos\left(\lambda\sqrt{\xi-1/4}\right)+c_2\sin\left(\lambda\sqrt{\xi-1/4}\right)\right) & \text{si}\ \ \xi>1/4 \end{cases} \tag{3.40}$$

où $c_{1,2,3}$ sont des constantes d'intégration dépendant des conditions initiales. Il est aisé de constater que $\epsilon_\perp$ et ϵ convergent vers 0 indépendamment de ξ. Si $0<\xi<\frac{1}{4}$ alors $\epsilon(\lambda)$ oscille tout en ayant une amplitude décroissante, alors que pour $\xi\geq\frac{1}{4}$, $\epsilon(\lambda)$ converge exponentiellement vers 0.

Nous pouvons aussi trouver explicitement les petites fluctuations du facteur d'échelle $a(t)$ autour de sa valeur d'attraction : $a(t)\propto t^{1/2}$. On va ainsi montrer que ces fluctuations peuvent être oscillantes, donnant lieu à un comportement très intéressant du facteur d'échelle total. On introduit pour cela le temps $\eta=\ln t$, et on note

$$X'=\frac{dX}{d\eta},\ a(\eta)=a_0t^{1/2}+\alpha(\eta). \tag{3.41}$$

Nous avons alors l'équation

$$4\alpha''-\alpha=e^{\eta/2}[C_1\epsilon+C_2\frac{d\epsilon}{d\lambda}]. \tag{3.42}$$

Les trois comportements différents pour $\epsilon(\lambda)$ donnent lieu à trois équations différentielles différentes pour $\alpha(\eta)$, qui sont

$$4\alpha''-\alpha=D_0e^{\lambda(1-\delta_+)}+D_1e^{\lambda(1-\delta_-)}, \tag{3.43}$$

$$4\alpha''-\alpha=e^{\lambda/2}[D_2+D_3\lambda], \tag{3.44}$$

$$4\alpha'' - \alpha = e^{\lambda/2}[D_4 \cos(\delta\lambda) + D_5 \sin(\delta\lambda)]. \tag{3.45}$$

Il est facile de trouver l'expression de $\alpha(\eta)$ dans les trois cas différents. Dans le premier cas nous avons ($\delta_\pm = \mp\sqrt{1-4\xi}$).

$$\frac{\alpha(t)}{a(t)} = \frac{\alpha_1}{t} + \alpha_2 t^{-\delta_+/2} + \alpha_3 t^{-\delta_-/2}. \tag{3.46}$$

Dans le second cas, une expression exacte ne peut être obtenue que pour $a_0 = 1$, tout comme dans le dernier cas. Dans le second cas nous avons

$$\frac{\alpha(t)}{a(t)} \propto t^{-1/4}, \tag{3.47}$$

alors que dans le troisième cas nous avons

$$\frac{\alpha(t)}{a(t)} \propto t^{-1/4}[C_0 \cos(\delta t/2) + C_1 \sin(\delta t/2)], \delta = \sqrt{\xi - \frac{1}{4}}. \tag{3.48}$$

Ce dernier résultat est remarquable et très intéressant. En effet il permet de montrer que le facteur d'échelle subit des oscillations dans ce cas. Ces oscillations sont dues aux oscillations de la variable z qui effectue des va-et-vient autour de son minimum. De plus ces oscillations sont amorties dans le sens où bien que leur amplitude augmente, l'amplitude relative, décroît.

Les UDR sont également stables pour des grandes fluctuations comme le montre la Fig .3.2 dans le cas d'un espace-temps quadri-dimensionnel ($\lambda = \ln a$) avec pour conditions initiales $(z_0, \overset{\circ}{z}_0, \overset{\circ}{\phi}_{\perp 0}) = (0.4, 0.8, 0.5)$ et $\mathcal{R} = -0.02$. Nous avons $z \to 0.272$ alors que $\overset{\circ}{\phi}_\perp \to 0$ comme prévu. Nous ne décrivons pas ici les autres solutions car

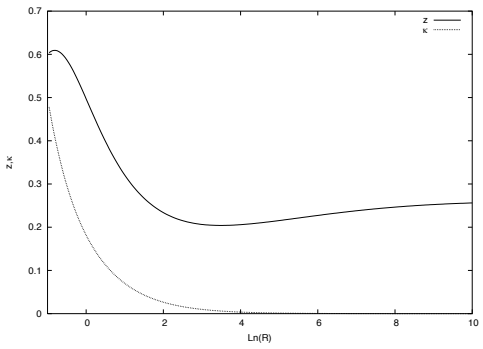

FIG. 3.2 – Oscillations amorties pour z (courbe solide) et convergence vers 0 de $\dot{\phi}_\perp$ (courbe en pointillés)

elles ne sont pas intéressantes pour nous.

Le cas (a) est plus compliqué dans le sens où il nécessite que nous réinterprétions notre calcul en une dimension de plus, sans brisure de supersymétrie alors

que le cas (c) a seulement des solutions cosmologiques de type Big-Crunch. Une remarque intéressante que l'on peut faire concerne la présence d'inflation ou non dans nos différents modèles. Une analyse numérique montre que les conditions à remplir pour avoir inflation sont $\mathcal{R} < 0$ et $\mathcal{K} < \mathcal{I} = -\frac{3p-\frac{p_z}{2}}{p-\frac{p_z}{2}}$. La dernière condition requiert $z \gg 1$. Les seules solutions permettant de satisfaire les deux conditions sont les UDR. Lorsque z oscille autour de z_c, si les conditions initiales sont favorables, on peut passer rapidement par une zone où $z \gg 1$. Dans cette zone, il est possible d'avoir inflation. Numériquement et analytiquement, on peut montrer que le nombre maximum d'e-folds obtenu est 0.2. Il est facile de comprendre que ce nombre très petit est une borne supérieure à la quantité d'inflation quand on augmente le nombre de directions internes brisant la supersymétrie. De plus, ce nombre est petit car le potentiel pour z est très pentu dans la région $z \gg 1$, on est donc rapidement amené vers des valeurs de z plus petites. L'inflation cosmologique requiert la présence d'au moins 60 e-folds, ce qui est de très loin supérieur à notre borne maximale.

Avec ce premier exemple non-trivial, l'intérêt de partir de la théorie des cordes semble évident. Entre autre, des théories de champs assez compliquées peuvent être obtenues. Dans la suite de ce chapitre nous verrons comment on peut décrire un ensemble de théories des champs, bien connectées entre elles, grâce à la théorie des cordes. Pour le moment, analysons ce qu'il se passe lorsque la direction 4 porte en plus de la brisure de supersymétrie l'action d'un orbifold.

3.2 Brisure de supersymétrie et orbifold simultanés

Nous répétons toutes les étapes ci-dessus et donnons les résultats les plus pertinents. Nous considérons des modèles $\mathcal{N} = 2$ spontanément brisés vers $\mathcal{N} = 0$. La pression prend la forme

$$P = T^4 \left(n_T f_T(z) + \tilde{n}_T c_4 + n_V f_V(z) \right), \tag{3.49}$$

où n_T, n_V, $f_T(z)$ et $f_V(z)$ ont été définies plus haut et $\tilde{n}_T > 0$, $c_4 = \frac{\pi^2}{48}$. Les premier et troisième termes sont les mêmes que ceux obtenus dans le modèle précédent alors que le second terme est nouveau. Les analogues du potentiel $V(z)$ dans les cas (a), (b) et (c) sont donnés par les cas (IIa), (IIb) et (IIc) pour le potentiel $\tilde{V}(z)$ représenté sur la figure (3.3). Pour simplifier, il existe un extremum de $\tilde{V}$ pour $n_V < 0$ et aucun extremum pour $n_V > 0$. Le cas (IIa) est semblable au cas (IIb), par conséquent nous atteignons un UDR stable dans les deux cas.

La conclusion principale de cette section est que l'Univers, dans beaucoup de cas intéressants, est décrit après suffisamment longtemps par un gaz de cordes se comportant comme du rayonnement. De plus, cette ère de rayonnement est stable pour les petites et grandes fluctuations autour de cette ère d'équilibre. Dans la section suivante nous augmentons la complexité de ces modèles en analysant le cas où deux dimensions internes deviennent dynamiques. Dans un cas, ces deux directions brisent spontanément la supersymétrie alors que dans le second cas, une direction brise la supersymétrie alors que l'autre interpole entre très petite et très grande taille (c'est à dire entre la taille d'une dimension compactifiée et celle d'une dimension externe).

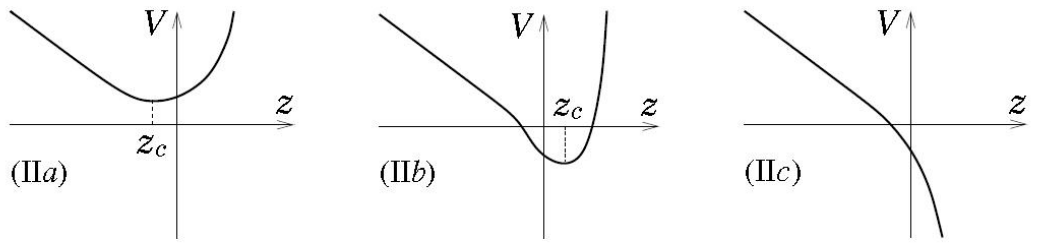

FIG. 3.3 – L' allure du potentiel $\tilde{V}(z)$ dépend du rapport $\mathcal{R}$. Les cas (IIa), (IIb) et (IIc) sont des extensions des cas (a), (b) et (c) ci-dessus. En particulier, les cas (IIa) et (IIb) sont désormais identiques.

4 Deux dimensions internes dynamiques

Dans cette section nous montrons que les conclusions obtenues dans les modèles ci-dessus paraissent être assez générales. En effet ces conclusions vont être obtenues de nouveau pour des modèles plus compliqués avec deux dimensions internes dynamiques. Les deux cas distincts présentés ici ont néanmoins des similitudes et des propriétés communes remarquables. Cependant, ils possèdent également des différences importantes. Avant d'expliquer le travail développé dans la publication 2, analysons le cas plus simple où deux dimensions internes brisent la supersymétrie.

4.1 Deux dimensions internes brisant la supersymétrie

Considérons l'espace-temps

$$S^1(R_0) \times T^3 \times S^1(R_4) \times S^1(R_5) \times M_4, \tag{3.50}$$

où la taille caractéristique de M_4 est très petite devant les tailles des autres dimensions. En plus de la température T, il est facile de montrer que l'énergie libre dépend également des deux quantités

$$z = \ln \frac{R_0}{\sqrt{R_4 R_5}}, \;\; Z = \ln \frac{R_5}{R_4}. \tag{3.51}$$

Il est possible de choisir une classe de modèles où l'énergie libre a la forme

$$\mathcal{F} = -VT^4 p(z, Z, \mathcal{R}). \tag{3.52}$$

Une fois l'analyse des équations du mouvement effectuée, on peut montrer que z et Z ne convergent pas vers une constante, donnant lieu à des modèles cosmologiques ne nous intéressant pas ; ou bien alors $Z \to 0$ et $z \to z_c$. Cette seconde possibilité est une généralisation triviale des résultats présentés dans la section précédente. La limite entre les deux comportements est donnée par $\mathcal{R} = \mathcal{R}_{c2}$ avec $\mathcal{R}_{c2} < -\frac{1}{15}$. Pour $\mathcal{R} < \mathcal{R}_{c2}$ il n'y a pas d'attraction vers un UDR alors que pour $\mathcal{R}_{c2} < \mathcal{R} < 0$ il y a une telle attraction. Pour $\mathcal{R} > 0$ nous trouvons à nouveau des Big-Crunch.

L'intérêt d'un tel modèle est de montrer qu'il est possible de stabiliser dynamiquement des modules de structure complexe (comme Z) de façon relativement simple. Cependant, jusqu'à maintenant nous avons uniquement considéré le cas le plus simple où aucune dimension interne n'interpole. Toutes nos dimensions internes sont soit très petites, et font partie de la variété interne compactifiée, soit très grandes, et elles portent la brisure de supersymétrie. Dans la suite, nous montrons qu'il est possible d'étudier un cas plus général où une dimension interne peut interpoler entre petite et grande taille.

4.2 UDR et stabilisation de modules

Dans la section 4.2, cinq phases distinctes pour le potentiel effectif thermique $V(T, M)$ ont été identifiées dans le cadre de la corde hétérotique. Nous analysons ici en détail le comportement du système dans les trois premières phases. La phase IV peut être identifiée à la phase II par T-dualité tout comme les phases III et V. Nous n'avons donc pas besoin d'étudier toutes ces phases. Nous montrons que pour chacune de ces phases, il existe un extremum ou une région plate du potentiel effectif V qui admet une solution d'UDR. Pour les phases I, II et IV, l'UDR est en d dimensions, alors que pour les phases III et V, il peut être en d ou d+1 dimensions, dépendant des conditions initiales. Nous montrons que ces solutions *sont stables devant les petites fluctuations*. En particulier, pour la phase I, le module spectateur R_9 est stabilisé au point self-dual, alors que pour les phases III et V, il décrit une dimension décompactifiée. Pour les phases II et IV, le module spectateur est stabilisé assez mollement par la présence de friction gravitationnelle due à l'expansion de l'Univers.

Modèle considéré

Nous considérons la variété d'espace-temps

$$S_E^1 \times T^{d-1} \times T^D \times T^n \times M_{10-d-D-n} \tag{3.53}$$

[5]où S_E^1 est la direction temporelle euclidienne compactifiée, le tore T^n contient des flux qui génèrent la brisure de supersymétrie alors que le tore T^D n'en contient pas. Nous considérons à la fois la température et la brisure de supersymétrie comme étant faibles, tout en autorisant les rayons caractéristiques du tore T^D à être arbitraires. Un des enjeux de notre étude est la détermination de l'effet de $V(T, M)$ sur les modules de T^D. Dans ce cas, la fonction de partition peut être calculée exactement pour la corde hétérotique et la supercorde de type II. Nous nous focalisons sur le premier cas d'abord, appliquant ces résultats au cas plus simple de la corde de type II. Nous utilisons les indices k, l pour noter une somme sur le tore T^D et les indices m, n pour noter une somme sur le tore T^n. La température est incluse en couplant le nombre fermionique d'espace-temps aux moments et enroulements du cercle S_E^1. En suivant [32], nous couplons également une $R-$charge aux nombres de moment

[5]Un orbifold peut également agir le long du tore T^n, nous n'étudions pas ce cas

et enroulement du tore T^n. Ce couplage brise la supersymétrie même à température nulle au travers de la généralisation à la théorie des cordes du mécanisme de Scherk-Schwarz. En général, cette charge de brisure de supersymétrie inclut le nombre de fermions d'espace-temps ainsi que d'autres charges additionnelles venant du réseau $E_8 \times E_8'$ ainsi que des charges de $R-$symétrie dans le cas d'orbifold $\mathbb{Z}_2$. Dans le cas où $d = 4$, la fonction de partition est donnée par

$$\begin{aligned} Z &= \int_F \frac{d\tau d\bar{\tau}}{4\tau_2} \frac{1}{2} \sum_{a,b} (-1)^{a+b+ab} \frac{\vartheta^4 \left[\begin{smallmatrix} a \\ b \end{smallmatrix}\right]}{\eta^4} \frac{\Gamma_{(0,16)}}{\eta^8 \bar{\eta}^{24}} \times \\ &\qquad \Gamma_{(1,1)}(R_0) \times \prod_{p=1}^{D} \Gamma_{(1,1)}(R_p) \times \prod_{i=1}^{n} \Gamma_{(1,1)}(R_i). \end{aligned} \tag{3.54}$$

Température et brisure de supersymétrie Afin d'implémenter la température et la brisure de supersymétrie, nous avons vu qu'il suffit d'effectuer les remplacements

$$\begin{aligned} \Gamma_{(1,1)}(R_0) &\rightarrow \sum_{\tilde{k},\tilde{l}} R_0 \tau_2^{-\frac{1}{2}} \exp(-\pi R_0^2 |\tilde{k} + \tilde{l}\tau|^2/\tau_2)(-1)^{\tilde{k}a + \tilde{l}b + \tilde{k}\tilde{l}}, \\ \Gamma_{(1,1)}(R_i) &\rightarrow \sum_{\tilde{k},\tilde{l}} R_i \tau_2^{-\frac{1}{2}} \exp(-\pi R_i^2 |\tilde{k} + \tilde{l}\tau|^2/\tau_2)(-1)^{\tilde{k}(a+Q_i) + \tilde{l}(b+L_i) + \varepsilon_i \tilde{k}\tilde{l}}. \end{aligned} \tag{3.55}$$

Nous obtenons alors pour la fonction de partition

$$\begin{aligned} Z &= -\int_F \frac{d\tau d\bar{\tau}}{4\tau_2} \sum_{\{\tilde{g}_i\},\{\tilde{h}_i\}} (-1)^{\sum_{i=0}^n \tilde{g}_i(1+Q_i)} (-1)^{P(\tilde{g}_i,h_i,Q_i,L_i,\epsilon_i)} \vartheta^4 \left[\begin{smallmatrix} 1+\sum_{i=0}^n \tilde{h}_i \\ 1+\sum_{i=0}^n \tilde{g}_i \end{smallmatrix}\right] \\ &\qquad \prod_{i=0}^{n} \Gamma_{(1,1)} \left[\begin{smallmatrix} \tilde{h}_i \\ \tilde{g}_i \end{smallmatrix}\right](R_i) \times \prod_{p=1}^{D} \Gamma_{(1,1)}(R_p) \times \frac{\Gamma_{(0,16)}}{\eta^{12} \bar{\eta}^{24}} \end{aligned} \tag{3.56}$$

où nous avons introduit les sommes de réseaux twistées

$$\Gamma_{(1,1)} \left[\begin{smallmatrix} a \\ b \end{smallmatrix}\right](R) = \sum_{\tilde{k},\tilde{l}} R \tau_2^{-\frac{1}{2}} \exp(-\pi R^2 |2\tilde{k} + b + (2\tilde{l} + a)\tau|^2/\tau_2). \tag{3.57}$$

Calcul de Z Nous pouvons faire une remarque importante : dans les secteurs où simultanément

$$\sum_{i=0}^{n} \tilde{g}_i = 0 \bmod 2 \text{ et } \sum_{i=0}^{n} \tilde{h}_i = 0 \bmod 2, \tag{3.58}$$

les phases additionnelles dans (3.55) valent 1 et nous nous retrouvons avec le cas de température nulle. Leur contribution à la fonction de partition est par conséquent

nulle ($\vartheta_1 = 0$). Dans la limite de grand R les réseaux admettent le développement

$$\begin{aligned}
\Gamma_{(1,1)}{}^{[0]}_{[0]}(R) &= R\tau_2^{-\frac{1}{2}}\Big(1+\sum_{\tilde{k}\neq 0}\exp(-\pi R^2(2\tilde{k})^2/\tau_2)+\mathcal{O}(\exp(-\pi R^2\tau_2)+...\Big),\\
\Gamma_{(1,1)}{}^{[1]}_{[b]}(R) &= R\tau_2^{-\frac{1}{2}}\Big(\mathcal{O}(\exp(-\pi R^2\tau_2)+...\Big),\\
\Gamma_{(1,1)}{}^{[0]}_{[1]}(R) &= R\tau_2^{-\frac{1}{2}}\Big(\sum_{\tilde{k}}\exp(-\pi R^2(2\tilde{k}+1)^2/\tau_2)+\mathcal{O}(\exp(-\pi R^2\tau_2)+...\Big),
\end{aligned} \tag{3.59}$$

où les termes négligés ont une contribution en puissance de $\exp(-\pi R^2)$. De cette analyse, nous voyons que tout secteur avec $\tilde{h}_i \neq 0$ donne une contribution négligeable à notre étude. De plus, le secteur avec

$$\sum_{i=0}^{n}\tilde{h}_i = 0 \text{ et } \sum_{i=0}^{n}\tilde{g}_i = 0 \bmod 2 \tag{3.60}$$

donne une contribution nulle à cause de la supersymétrie comme discuté précédemment. Par conséquent, seulement les secteurs avec tous les $\tilde{h}_i = 0$ et $\sum_{i=0}^{n}\tilde{g}_i = 1 \bmod 2$ contribuent dans la limite où R_0 et les R_i sont grand. De plus, seule la partie pour τ_2 grand va contribuer à la fonction de partition. Pour résumer, nous nous concentrons sur les secteurs avec

$$\tilde{h}_i = 0, \qquad \sum_{i=0}^{n}\tilde{g}_i = 1 \bmod 2 \tag{3.61}$$

et remplaçons le domaine fondamental par la demi-bande[6] $|| \equiv \left\{\tau \in \mathbb{C}/|\mathrm{Re}(\tau)| \leq \frac{1}{2}\right\}$. La fonction de partition se réduit alors à

$$\begin{aligned}
Z &= \int_{||}\frac{d\tau d\bar{\tau}}{4\tau_2}\sum_{\{\tilde{g}_i,\sum\tilde{g}_i=1\}}(-1)^{\sum_{i=0}^{n}\tilde{g}_iQ_i}\vartheta^4{}^{[1]}_{[0]}\\
&\qquad \prod_{i=0}^{n}\Gamma_{(1,1)}{}^{[0]}_{[\tilde{g}_i]}(R_i)\times\prod_{p=1}^{D}\Gamma_{(1,1)}(R_p)\times\frac{\Gamma_{(0,16)}}{\eta^{12}\bar{\eta}^{24}}.
\end{aligned} \tag{3.62}$$

Ayant pu remplacer l'intégrale sur le domaine fondamental par une intégrale sur la demi-bande supérieure, l'intégration sur τ_1 impose l'égalité de la masse d'états gauche et droit. Nous supposons ensuite que R_0 et R_i sont plus grands que les échelles caractéristiques dans la variété interne. En général, la partie interne de la fonction de partition prend la forme

$$(-1)^{\sum_{i=0}^{n}\tilde{g}_iQ_i}\frac{\vartheta^4{}^{[1]}_{[0]}}{\eta^{12}\bar{\eta}^{24}}\Gamma_{(0,16)} = 2^4\Big((\bar{q})^{-1}+D_0(\tilde{g}_i,Q_i)+\mathcal{O}(q,\bar{q})\Big) \tag{3.63}$$

[6]En suivant le travail de [31], il est possible de simplifier le calcul de beaucoup d'intégrales sur le domaine fondamental comme ici.

où $q = \exp(2\pi i\tau)$ et $D_0(\tilde{g}_i, Q_i)$ est la somme sur tous les états sans masse avec chaque mode pondéré par $(-1)^{\sum_{i=0}^{n} \tilde{g}_i Q_i}$. Nous obtenons après calculs

$$\begin{aligned}
\prod_{p=1}^{D} \Gamma_{(1,1)}(R_p) &= \prod_{p=1}^{D} \Bigg[\sum_{\{m_p\}} \exp\Big(-\pi\tau_2 (m_p/R_p)^2 \Big) \\
&\qquad + 2\exp\Big(-\pi\tau_2 (\frac{1}{R_p^2} + R_p^2) \Big) \exp\Big(-2\pi i \tau_1 \Big) \Bigg] + \mathcal{O}(e^{-\pi\tau_2}) \\
&= \prod_{p=1}^{D} \Bigg[\sum_{\{m_p\}} \exp\Big(-\pi\tau_2 (m_p/R_p)^2 \Big) \Bigg] \\
&\quad + \sum_{q=1}^{D} \Bigg\{ \prod_{p=1, p\neq q}^{D} \Bigg[2\exp\Big(-\pi\tau_2 (\frac{1}{R_q^2} + R_q^2) \Big) \exp\Big(-2\pi i \tau_1 \Big) \Bigg] \\
&\qquad \Bigg[\sum_{\{m_p\}} \exp\Big(-\pi\tau_2 (m_p/R_p)^2 \Big) \Bigg] \Bigg\} + \mathcal{O}(e^{-\pi\tau_2}). \qquad (3.64)
\end{aligned}$$

Dans le régime où R_0 et R_i sont grands ($R_{0,i} \gg 1$), après calculs et en ne considérant que les termes dominants, nous obtenons la forme réduite de la fonction de partition

$$\begin{aligned}
Z &= \Big(\prod_{j=0}^{n} R_j \Big) \sum_{\{\tilde{g}_i, \sum \tilde{g}_i = 1\}} \int_{||} \frac{d\tau d\bar{\tau}}{4\tau_2^{(n+2)/2}} \Big(\sum_{\{\tilde{k}_i\}} \exp(-\frac{\pi}{\tau_2} \sum_{i=0}^{n} R_i^2 (2\tilde{k}_i + \tilde{g}_i)^2) \Big) \\
&\quad \Bigg\{ \sum_{q=1}^{D} \Bigg[2^4 2 \exp\Big(-\pi\tau_2 (\frac{1}{R_q^2} + R_q^2 - 2) \Big) \sum_{\{m_p, \not{m}_q\}}^{D} \exp\Big(-\pi\tau_2 \sum_{p=1, p\neq q} (m_p/R_p)^2 \Big) \Bigg] \\
&\qquad + \sum_{\{m_p\}} 2^4 D_0(\tilde{g}_i, Q_i) \exp\Big(-\pi\tau_2 \sum_{p=1}^{D} (m_p/R_p)^2 \Big) \Bigg\}. \qquad (3.65)
\end{aligned}$$

La prochaine étape consiste à intégrer sur τ_2. Il est alors pratique d'introduire un paramètre Δ et de séparer le tore T^D en $T^{D-\Delta} \times T^{\Delta}$. La raison de cette subtilité supplémentaire est que nous allons considérer dans la suite des modèles cosmologiques en d et $d+1$ dimensions. Nous effectuons ensuite une resommation de Poisson sur le réseau de $T^{D-\Delta}$. Pour $R_p \approx 1$, la formulation hamiltonienne est la plus pratique alors que pour $R_p \gg 1$, c'est la formulation lagrangienne. Après resommation de

Poisson et intégration, la fonction de partition devient

$$
\begin{aligned}
Z \;=\; & \left(\prod_{j=0}^{n} R_j\right)\left(\prod_{q\in T^{D-\Delta}} R_q\right) \sum_{\{\tilde g_i,\sum \tilde g_i=1\},\{\tilde k_i\}} \Bigg\{ \\
& \sum_{\{m_p\},\{\tilde m_p\}} 2^4 D_0(\tilde g_i, Q_i)\left(\frac{G_3}{F_3}\right)^{\frac{D-\Delta+n}{4}} K_{\frac{D-\Delta+n}{4}}(2\pi\sqrt{F_3G_3}) \\
& + \sum_{q\in T^{\Delta}} \sum_{\{m_p,\not{m}_q\},\{\tilde m_p\}} 2^4 2\left(\frac{G_1}{F_1}\right)^{\frac{D-\Delta+n}{4}} K_{\frac{D-\Delta+n}{4}}(2\pi\sqrt{F_1G_1}) \\
& + \sum_{q\in T^{D-\Delta}} \sum_{\{m_p\},\{\tilde m_p,\not{m}_q\}} \frac{2^4 2}{R_q}\left(\frac{G_2}{F_2}\right)^{\frac{D-\Delta+n-1}{4}} K_{\frac{D-\Delta+n-1}{4}}(2\pi\sqrt{F_2G_2})\Bigg\},
\end{aligned}
\tag{3.66}
$$

où $K_n(z)$ est une fonction de Bessel modifiée du second type, et nous introduisons les notations

$$
\begin{aligned}
F_1 &= \sum_{i=0}^{n} R_i^2(2\tilde k_i+\tilde g_i)^2 + \sum_{p\in T^{D-\Delta}} R_p^2\tilde m_p^2, & G_1 &= \left(\frac{1}{R_q}-R_q\right)^2 + \sum_{p\in T^{\Delta},p\neq q}\frac{{m_p}^2}{R_p}, \\
F_2 &= \sum_{i=0}^{n} R_i^2(2\tilde k_i+\tilde g_i)^2 + \sum_{p\in T^{D-\Delta},p\neq q} R_p^2\tilde m_p^2, & G_2 &= \left(\frac{1}{R_q}-R_q\right)^2 + \sum_{p\in T^{\Delta}}\frac{{m_p}^2}{R_p}, \\
F_3 &= \sum_{i=0}^{n} R_i^2(2\tilde k_i+\tilde g_i)^2 + \sum_{p\in T^{d-\Delta}} R_p^2\tilde m_p^2, & G_3 &= \sum_{p\in T^{\Delta}}\frac{{m_p}^2}{R_p}.
\end{aligned}
\tag{3.67}
$$

En guise de rappel, l'équation (3.66) est valide pour tout $R_p \geq 1$. L'expression avec $R_q \leq 1$ peut être obtenue en prenant le T-dual de l'expression ci-dessus et en remplaçant R_q par $\frac{1}{R_q}$.

Type II La fonction de partition dans le cas de la théorie de type II sur $S^1_E \times T^D \times T^n$ prend la forme

$$
\begin{aligned}
Z_{II} \;=\; & \int_F \frac{d\tau d\bar\tau}{4\tau_2}\frac{1}{2\eta^8}\sum_{a,b}(-1)^{a+b+ab}\frac{\vartheta^4\left[{a \atop b}\right]}{\eta^4}\frac{1}{2\bar\eta^8}\sum_{\bar a,\bar b}(-1)^{\bar a+\bar b+\bar a\bar b}\frac{\bar\vartheta^4\left[{\bar a \atop \bar b}\right]}{\bar\eta^4} \\
& \Gamma_{(1,1)}(R_0)\times\prod_{p=1}^{D}\Gamma_{(1,1)}(R_p)\times\prod_{i=1}^{n}\Gamma_{(1,1)}(R_i).
\end{aligned}
\tag{3.68}
$$

Une fois de plus, nous avons écrit la fonction de partition de telle sorte à bien comprendre l'origine des différents termes. La température et la brisure de supersymétrie sont une fois de plus introduites en modifiant les sommes de réseaux le long de S^1_E et T^n comme dans (3.55), cependant, dans la théorie de type II, nous introduisons des phases gauche et droite. En répétant les étapes ci-dessus nous arrivons à la fonction

de partition

$$Z_{II} = \left(\prod_{j=0}^{n} R_j\right)\left(\prod_{q\in T^{D-\Delta}} R_q\right) \sum_{\{\tilde{g}_i,\sum \tilde{g}_i=1\},\{m_i\}} \Bigg\{ \sum_{\{m_p\},\{\tilde{m}_p\}} 2^4 D_0(\tilde{g}_i, Q_i)\left(\frac{G_3}{F_3}\right)^{\frac{D-\Delta+n}{4}} K_{\frac{D-\Delta+n}{4}}(2\pi\sqrt{F_3G_3})\Bigg\} \quad (3.69)$$

Équations du mouvement Par souci de simplicité, nous simplifions le calcul ci-dessus avec les hypothèses suivantes :

- Les directions $1...d-1$ sont considérées comme décompactifiées et de taille caractéristique $R \gg 1$ et forment un espace-temps $d-$ dimensionnel avec la direction temporelle
- la direction d de rayon arbitraire R_d est interne si R_d est petit alors qu'elle fait partie de l'espace-temps si son rayon est large.
- La brisure de supersymétrie le long des dimensions internes est effectuée le long d'une dimension interne, $n = 1$.
- Les rayons des dimensions restantes, $d+1, ..., 8$ sont considérées comme fixes et de l'ordre de 1 dans les unités de la longueur d'une corde.

Par conséquent, le calcul de la fonction de partition à une boucle donnée plus haut est appliqué à l'espace-temps Euclidien

$$S^1(R_0) \times T^{d-1} \times S^1(R_d) \times \mathcal{M} \times S^1(R_9). \quad (3.70)$$

De plus, $\mathcal{M} = T^{8-d}$ (ou $\frac{T^4}{\mathbb{Z}_2\times\mathbb{Z}_2} \times T^{4-d}$). Les échelles de brisure de supersymétrie, M et T sont définies par $1/R_9$ et $1/R_0$ respectivement. Nous supposons R_0 et R_9 grands mais bien plus petits que les rayons du tore T^{d-1} de sorte que nous ayons les inégalités

$$R_1, ..., R_{d-1} \gg R_0, R_9 \gg 1. \quad (3.71)$$

Quand R_d est de l'ordre de 1 en unités de longueur de cordes, cette dimension fait partie de l'espace interne et la dimension effective de l'espace-temps est d. Étant donné que R_d peut varier de façon arbitraire, la dimension d peut aussi faire partie de l'espace-temps, et dans ce cas la dimension effective de l'espace temps est $d+1$. L'action effective à basse énergie, S, peut être écrite en termes d'un ensemble de champs, éventuellement redéfinis. Nous sommes intéressés par des espace-temps isotropes, par conséquent nous considérons les champs de jauge comme des pures jauges et l'espace-temps résultant ne dépend que du temps. Plus exactement, les espace-temps que nous considérons sont non-triviaux pour la métrique $g_{\mu\nu}$, le dilaton d-dimensionnel ϕ_d ainsi que les scalaires

$$\zeta := \ln R_d\ , \qquad \eta := \ln R_9. \quad (3.72)$$

Les modules restants sont fixés et de l'ordre de 1 en unité de longueur de corde. Nous ne détaillons pas la réduction dimensionnelle de 10 dimensions à d dimensions

qui ne ferait qu'alourdir le propos. Le cas considéré ici est $n = 1$, $\Delta = 1$ alors que l'action effective est

$$S = \int d^d x \sqrt{-g} \left(\frac{R}{2} - \frac{1}{2}(\partial\Phi)^2 - \frac{1}{2}(\partial\phi_\perp)^2 - \frac{1}{2}(\partial\zeta)^2 + P \right) , \tag{3.73}$$

où nous avons défini les champs normalisés

$$\Phi := \frac{2}{\sqrt{(d-2)(d-1)}}\,\phi_{\rm dil} - \sqrt{\frac{d-2}{d-1}}\,\eta\,, \qquad \phi_\perp := \frac{2}{\sqrt{d-1}}\,\phi_{\rm dil} + \frac{1}{\sqrt{d-1}}\,\eta\,. \tag{3.74}$$

La source P résulte du potentiel effectif à 1 boucle et est reliée à la fonction de partition à une boucle

$$P = e^{\frac{2d}{d-2}\phi_{\rm dil}}\,\frac{Z}{V_{0,\ldots,d-1}}\,, \tag{3.75}$$

où $V_{0,\ldots,d-1}$ est le volume de l'espace-temps en d dimensions (dans le repère de cordes) et Z est la fonction de partition calculée plus haut. Nous sommes intéressés à l'effet du potentiel effectif sur les différents champs présents. les équations du mouvement pour les différents champs sont données par

$$\mathcal{F}(\overset{\circ\circ}{z}, \overset{\circ\circ}{\phi}_\perp, \overset{\circ\circ}{\zeta}, \overset{\circ}{z}, \overset{\circ}{\phi}_\perp, \overset{\circ}{\zeta}) + V_z = 0\,, \tag{3.76}$$

$$\overset{\circ\circ}{\phi}_\perp + \frac{1}{d-2}\,(r-p)\,\overset{\circ}{\phi}_\perp - \frac{1}{\sqrt{d-1}}\,p_\eta = 0\,, \tag{3.77}$$

$$\overset{\circ\circ}{\zeta} + \frac{1}{d-2}\,(r-p)\,\overset{\circ}{\zeta} - p_\zeta = 0\,, \tag{3.78}$$

où $\mathcal{F}(\overset{\circ\circ}{z}, \overset{\circ\circ}{\phi}_\perp, \overset{\circ\circ}{\zeta}, \overset{\circ}{z}, \overset{\circ}{\phi}_\perp, \overset{\circ}{\zeta})$ est une fonction qui s'annule quand tous ses arguments sont nuls et p et ρ sont définis par Eq. (3.82) et $e^z := \frac{M}{T} = \frac{R_0}{R_9}$. Nous avons reparamétrisé nos fonctions en terme de $\ln a$ de sorte que les dérivées temporelles soient remplacées par des dérivées par rapport à $\ln a$ notées comme $\overset{\circ}{f} = \frac{\partial f}{\partial \ln a}$. Les solutions stationnaires sont données par

$$p_\eta = p_\zeta = V_z = 0. \tag{3.79}$$

Pour la théorie hétérotique, la fonction de partition est donnée par (3.65) et peut être écrite sous la forme

$$Z = \left(\prod_{i=0}^{d-1} R_i \right) R_9 \frac{2^4}{2} \sum_{\tilde{g}_0 + \tilde{g}_9 = 1} (\mathcal{Z}_{\rm standard} + \mathcal{Z}_{\rm supplémentaire})\,. \tag{3.80}$$

alors que pour la théorie de type II c'est (3.69). La fonction de partition $\mathcal{Z}_{\rm supplémentaire}$ est absente dans ce cas ci. Le terme $\mathcal{Z}_{\rm supplémentaire}$ est en général négligeable si $R_d \approx 1$, où une extension du groupe de jauge $U(1) \to SU(2)$ se produit. La contribution de $\mathcal{Z}_{\rm standard}$ pour des valeurs standard de R_d peut être donnée sous deux formes (correspondant à $\Delta = 1$ et $\Delta = 0$ dans les notations ci-dessus), reliées l'une et

l'autre par resommation de Poisson. Nous définissons la température T et l'échelle de brisure de la supersymétrie M (définies dans le repère d'Einstein) comme

$$T = \frac{1}{2\pi R_0\, e^{-\frac{2\phi_{\rm dil}}{d-2}}}\,, \qquad M = \frac{1}{2\pi R_9\, e^{-\frac{2\phi_{\rm dil}}{d-2}}} \equiv \frac{e^{\sqrt{\frac{d-1}{d-2}}\Phi}}{2\pi}. \tag{3.81}$$

En terme de $\{T, z, \eta, \zeta\}$, la pression P et la densité d'énergie ρ prennent la forme

$$P(T, z, \eta, \zeta) \equiv T^d\, p(z, \eta, \zeta), \qquad \rho(T, z, \eta, \zeta) \equiv T^d\, r(z, \eta, \zeta)\,, \tag{3.82}$$

avec ζ et η définies à l'équation (3.72) et $r = d\,p - p_z$. La fonction p peut être écrite sous l'une des deux formes équivalentes

$$\begin{aligned} p(z, \eta, \zeta) &= n_T \left[\hat{f}_T^{(d)}(z) + k_T^{(d)}(z, \eta - |\zeta|)\right] + n_V \left[\hat{f}_V^{(d)}(z) + k_V^{(d)}(z, \eta - |\zeta|)\right] \\ &\quad + \tilde{n}_T\, g_T^{(d)}(z, \eta, |\zeta|) + \tilde{n}_V\, g_V^{(d)}(z, \eta, |\zeta|) \\ &= e^{|\zeta| - \eta - z} \left[n_T\, f_T^{(d+1)}(z, \eta - |\zeta|) + n_V\, f_V^{(d+1)}(z, \eta - |\zeta|)\right] \\ &\quad + \tilde{n}_T\, g_T^{(d)}(z, \eta, |\zeta|) + \tilde{n}_V\, g_V^{(d)}(z, \eta, |\zeta|)\,, \end{aligned} \tag{3.83}$$

correspondant à $\Delta = 1$ et $\Delta = 0$ respectivement dans l'équation Eq. (3.65). Pour les modèles de type II, nous prenons simplement $\tilde{n}_T = \tilde{n}_V = 0$. Notons de plus que p est une fonction paire de ζ, comme l'impose la T-dualité $R_d \to 1/R_d$. Dans cette expression, n_T est le nombre d'états de masse nulle pour une valeur standard de R_d, alors que $\tilde{n}_T$ est le nombre d'états de masse nulle additionnels au point où le groupe de jauge est étendu. Nous pouvons aussi remarquer que p ne dépend que de z et $y = |\zeta| - \eta$. Les fonctions $k_{T,V}^{(d)}$ ne sont non-négligeables uniquement dans la phase de décompactification (voir plus bas). De façon similaire, les fonctions $g_{T,V}^{(d)}$ sont dominantes au point où le groupe de jauge s'étend et sont négligeables hors de cette très petite région. La valeur de n_V est donnée par la somme sur les états de masse nulle avec chaque état pondéré par un signe. Les valeurs précises de ces signes dépendent de la configuration précise de brisure de supersymétrie, n_V pouvant être négatif pour certaines configurations.

Plus concrètement, nous avons $\mathcal{M} = T^{8-d}$,

$$n_T = \frac{2^4}{2}\, D_0\,, \qquad -1 \leq \frac{n_V}{n_T} \leq 1\,, \qquad \frac{\tilde{n}_T}{n_T} = \frac{2}{D_0}\,, \qquad \tilde{n}_V = \tilde{n}_T\,. \tag{3.84}$$

Les définitions des diverses fonctions apparaissant dans l'équation (3.83) sont données par

$$\hat{f}_T^{(d)}(z) = \frac{\Gamma\left(\frac{d+1}{2}\right)}{\pi^{\frac{d+1}{2}}} \sum_{\tilde{k}_0,\tilde{k}_9} \frac{e^{dz}}{\left[e^{2z}(2\tilde{k}_0+1)^2+(2\tilde{k}_9)^2\right]^{\frac{d+1}{2}}},$$

$$k_T^{(d)}(z,\eta-|\zeta|) = {\sum_{m_d}}' |m_d|^{\frac{d+1}{2}} e^{\frac{d+1}{2}(\eta-|\zeta|)} e^{dz} \sum_{\tilde{k}_0,\tilde{k}_9} \frac{2K_{\frac{d+1}{2}}\left(2\pi|m_d|e^{\eta-|\zeta|}\sqrt{e^{2z}(2\tilde{k}_0+1)^2+(2\tilde{k}_9)^2}\right)}{\left[e^{2z}(2\tilde{k}_0+1)^2+(2\tilde{k}_9)^2\right]^{\frac{d+1}{4}}},$$

$$g_T^{(d)}(z,\eta,|\zeta|) = \left(e^{2|\zeta|}-1\right)^{\frac{d+1}{2}} e^{\frac{d+1}{2}(\eta-|\zeta|)} e^{dz} \sum_{\tilde{k}_0,\tilde{k}_9} \frac{2K_{\frac{d+1}{2}}\left(2\pi(e^{2|\zeta|}-1)e^{\eta-|\zeta|}\sqrt{e^{2z}(2\tilde{k}_0+1)^2+(2\tilde{k}_9)^2}\right)}{\left[e^{2z}(2\tilde{k}_0+1)^2+(2\tilde{k}_9)^2\right]^{\frac{d+1}{4}}}$$

$$f_T^{(d+1)}(z,\eta-|\zeta|) = \frac{\Gamma\left(\frac{d}{2}+1\right)}{\pi^{\frac{d}{2}+1}} \sum_{\tilde{k}_0,\tilde{k}_9,\tilde{m}_d} \frac{e^{(d+1)z}}{\left[e^{2z}(2\tilde{k}_0+1)^2+(2\tilde{k}_9)^2+e^{-2(\eta-|\zeta|)}\tilde{m}_d^2\right]^{\frac{d}{2}+1}}, \tag{3.85}$$

ainsi que les fonctions résultantes données par

$$\hat{f}_V^{(d)}(z) = e^{(d-1)z}\hat{f}_T^{(d)}(-z),\ k_V^{(d)}(z,\eta-|\zeta|) = e^{(d-1)z}k_T^{(d)}(-z,\eta-|\zeta|-z), \tag{3.86}$$

$$g_V^{(d)}(z,\eta,|\zeta|) = e^{(d-1)z}g_T^{(d)}(-z,\eta-z,|\zeta|),\ f_V^{(d+1)}(z,\eta-|\zeta|) = e^{dz}f_T^{(d+1)}(-z,\eta-|\zeta|-z). \tag{3.87}$$

Etude des diverses phases

Cas hétérotique Dans le cas hétérotique montré sur la figure 3.4, il y a cinq différents régimes à considérer. Pour z grand et négatif, $z \ll -1$, nous obtenons le comportement montré sur la figure Fig. 3.4 avec 5 différentes phases. Pour $z \geq -1$, cinq phases doivent aussi être considérées, mais la phase de décompactification est différente, comme montré sur la figure Fig. 3.5. En fait, la phase de décompactification est un peu plus compliquée que ce qui est décrit ici, mais nous n'entrerons pas dans les détails. Une évolution du nombre de phases en fonction de z n'apparaît que si $n_V < 0$. Si $n_V > 0$, nous avons seulement la figure Fig. 3.4. Pour $n_V < 0$, les deux comportements globaux sont connectés car z évolue quand le temps passe. Par exemple, la phase $z \gg 1$ n'existe pas pour longtemps car dans ce régime, le potentiel pour z est très pentu et très rapidement nous atteignons $z \simeq 1$. Nous notons $R_{0,9}$ le maximum de R_0 et R_9. Dans la suite nous discutons les différentes phases.

- I : $|R_d - R_d^{-1}| < 1/R_{0,9}$

  En particulier, nous avons à l'origine, $\zeta = 0$, le comportement

  $$p(z,\eta,0) = (n_T+\tilde{n}_T)\,\hat{f}_T^{(d)}(z) + (n_V+\tilde{n}_V)\,\hat{f}_V^{(d)}(z) := \tilde{p}(z)\,. \tag{3.88}$$

  C'est précisément la forme obtenue quand la dynamique de R_d peut être ignorée *i.e.* $R_d \simeq 1$ est stabilisé. Dans l'équation (3.88), les contributions de n_T et $\tilde{n}_T$ sont de la même forme car elles viennent des états sans masse au point $\zeta = 0$. Étant donné que $\tilde{n}_T$ et $\tilde{n}_V$ sont positifs, l'extremum de $-P$ en $\zeta = 0$ est toujours un minimum.

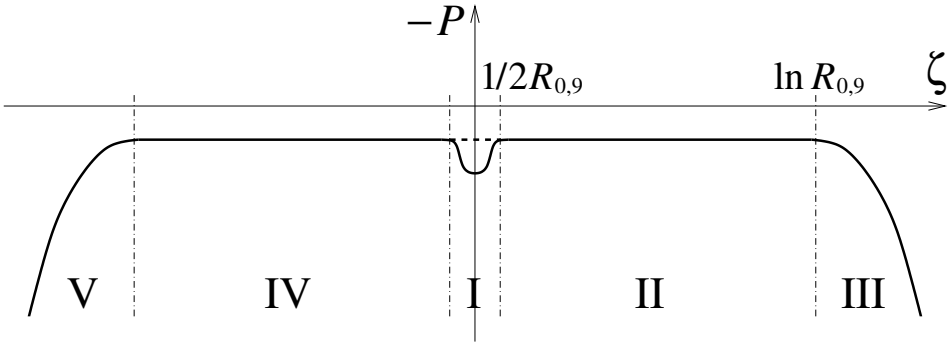

FIG. 3.4 – $P(\zeta)$ varie quand $n_V > 0$. Si $n_V < 0$, c'est uniquement possible si $z \ll -1$.

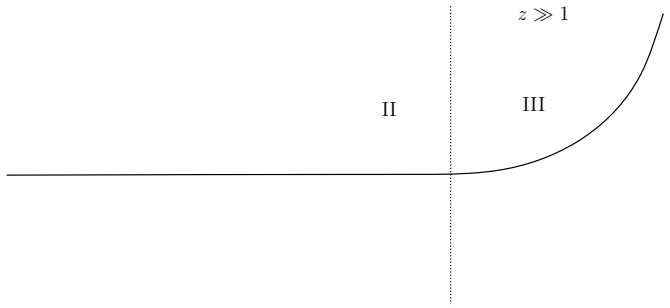

FIG. 3.5 – Phase III pour $z \gg 1$ et $n_V < 0$. Une telle phase n'existe pas pour $n_V > 0$. La phase V est T-duale.

- II : $R_d - R_d^{-1} > 1/R_{0,9}$ et $R_d < R_{0,9}$
  P est constant tout le long du plateau défini par les inégalités ci-dessus. Dans ce cas, la pression reproduit le résultat en d dimensions pour n_T états sans masse. Physiquement, nous sommes éloignés du point d'extension de la symétrie de jauge, par conséquent les états de masse nulle supplémentaires propres à ce point n'existent plus. Concrètement nous avons

$$p(z,\eta,\zeta) \simeq n_T\, \hat{f}_T^{(d)}(z) + n_V\, \hat{f}_V^{(d)}(z) := \hat{p}(z)\,. \tag{3.89}$$

  Les deux signes sont autorisés quand $n_V < 0$.

$$\begin{aligned} -P &\underset{z\to-\infty}{\sim} -T^d\, n_T\, e^{-z}\, S^o_{d+1} \underset{z\to-\infty}{\to} -\infty\,, \\ &\underset{z\to+\infty}{\sim} -T^d\, n_V\, e^{dz}\, S^o_{d+1} \underset{z\to+\infty}{\to} \mathrm{sign}(-n_V)\infty\,, \end{aligned} \tag{3.90}$$

  où S^o_d (et S^e_d pour un usage ultérieur) sont des constantes,

$$S^o_d = \frac{\Gamma\left(\frac{d}{2}\right)}{\pi^{\frac{d}{2}}} \sum_m \frac{1}{|2m+1|^d}\,, \qquad S^e_d = \frac{\Gamma\left(\frac{d}{2}\right)}{\pi^{\frac{d}{2}}} \sum_m{}' \frac{1}{|2m|^d}\,. \tag{3.91}$$

- III : $R_d > R_{0,9}$
  Nous avons

$$p(z,\eta,\zeta) \simeq e^{|\zeta|-\eta-z} \left(n_T\, \hat{f}_T^{(d+1)}(z) + n_V\, \hat{f}_V^{(d+1)}(z) \right)\,, \tag{3.92}$$

montrant qu'il est plus naturel de considérer le système en $d+1$ dimensions. C'est le cas car, dans cette limite, le cercle de rayon R_d est décompactifié. La croissance exponentielle de $-P$ quand $\zeta \to \pm\infty$ peut être des deux signes quand $n_V < 0$. Pour $z \gg 1$, nous avons $-P \to \infty$ alors que $z \ll 1$, $-P \to -\infty$. Si $n_V > 0$, la seconde possibilité existe uniquement.

- IV : $e^{-\zeta} - e^{\zeta} > \mathcal{O}[\min(e^{-\eta}, e^{-\eta-z})]$ et $-\zeta < \mathcal{O}[\max(\eta, \eta+z)]$
  i.e. $R_d^{-1} - R_d > 1/R_{0,9}$ and $R_d^{-1} < R_{0,9}$
  C'est la phase $T-$duale de la phase II et a le même comportement quand $\zeta \to -\zeta$.
- V : $-\zeta > \mathcal{O}[\max(\eta, \eta+z)]$ *i.e.* $R_d^{-1} > R_{0,9}$
  Cette phase est $T-$duale de la phase III et a le même comportement avec $\zeta \to -\zeta$. Dans ce cas, la direction d est compactifiée si initialement R_d est suffisamment grand ou bien elle reste petite si initialement R_d est trop faible. Dans le second cas, le plateau rattrape la décompactification Dans la théorie effective, ces modes de masse nulle sont naturellement considérés comme des excitations d'un système $d+1$ dimensionnel, théorie $T-$ duale de la théorie effective de la phase III.

Chaque région contient soit un extremum du potentiel soit une région plate, entrainant à chaque fois l'existence d'un UDR (Univers dominé par le rayonnement). Chacun de ces UDR est stable pour des petites fluctuations et est localement un attracteur pour des conditions initiales standard. Pour R_d fixé, il a été montré dans [32] qu'un UDR est un attracteur global.

Théorie de type II

Le cas de la théorie de type II peut être obtenu à partir de celui de la corde hétérotique en prenant $\tilde{n}_T = \tilde{n}_V = 0$. Le minimum local de $-P$ en $\zeta = 0$ n'est plus présent et nous obtenons simplement un plateau. Il y a désormais trois différents régimes à considérer : le plateau, la phase de décompactification et le maximum local pour $z \simeq 0$. Ces phases ont exactement la même description que pour la théorie hétérotique. Étant donné qu'il n'y a plus d'extension du groupe de jauge $U(1) \to SU(2)$ dans ce cas, la phase $SU(2)$, I, n'existe pas perturbativement pour les théories de type II. Cependant, par dualité hétérotique-type II, nous nous attendons à ce que non-perturbativement, la phase I existe pour les théories de type II. Un candidat naturel à cet effet consiste à introduire une paire de D-branes dont la séparation est associée à un module spectateur R_d. Quand R_d est au point self-dual dans la théorie hétérotique, nous prédisons que dans les théories de type II cela aura pour effet de stabiliser les D-branes au dessus l'une de l'autre, produisant une extension du groupe de jauge $U(1) \to SU(2)$. Lorsque nous augmentons la séparation des D-branes, nous nous éloignons du point d'extension du groupe de jauge.

5 Conclusions et perspectives

5.1 Résumé

Dans ce chapitre, nous avons détaillé les résultats obtenus dans les publications 1 et 2. La publication 3 est un résumé plus qualitatif de ce chapitre. Les travaux évoqués ici sont novateurs et nécessitent encore beaucoup d'approfondissements.

Notre but était de montrer qu'en partant de la théorie des cordes, en considérant un gaz de cordes dans un espace-temps présentant certaines caractéristiques, nous pouvions trouver dans la limite où le gaz est faiblement couplé les quantités fondamentales décrivant ce gaz : sa pression et sa densité dans un espace isotrope ou bien son énergie libre et sa densité dans un espace anisotrope. Une fois cette étape validée, il est *facile* de coupler ce gaz de cordes à l'action effective du modèle pour analyser les interactions entre ce gaz et l'espace-temps. Bien entendu, ces interactions engendrent l'évolution de l'Univers, c'est à dire son histoire cosmologique. Il est ensuite possible d'analyser avec certains détails cette cosmologie.

Nous avons obtenu que cette dernière est très souvent caractérisée par un univers dominé par le rayonnement (UDR), du moins après un temps suffisamment long. On vérifie que dans tous les cas ces UDR sont stables pour les petites et grandes fluctuations[7].

Au fur et à mesure de notre étude, les modèles étudiés ont gagné en complexité et en richesse. Nous avons augmenté le nombre de dimensions brisant la supersymétrie d'une part, et nous avons introduit des dimensions internes dynamiques d'autre part. Dans les deux cas, les calculs se compliquent sérieusement, mais l'intérêt de la théorie des cordes est évident. En effet, une approche du type de la théorie des champs nous donnerait plusieurs théories des champs non connectées ; au contraire, nous obtenons un réseau de théories des champs bien connectées entre elles à un niveau plus fondamental : celui de la théorie des cordes. L'étude d'une dimension interne dynamique est menée avec beaucoup de détails et il est montré, à un niveau perturbatif, comment la corde hétérotique et la corde de type II diffèrent.

5.2 Extensions

Il reste beaucoup de notions à approfondir dans l'approche présentée ici. D'une part, certains travaux théoriques méritent d'être faits pour mieux comprendre les modèles étudiés, d'autre part des travaux plus phénoménologiques sont également utiles pour vérifier si les prédictions des modèles étudiés pourraient, ou non, s'accorder avec l'expérience.

L'inclusion de la matière et l'obtention d'un scénario cosmologique plus abouti font partie de la première classe de travaux. La relaxation de l'hypothèse d'adiabaticité de l'évolution cosmique, l'étude des perturbations cosmologiques, une analyse

[7]Strictement parlant, nous ne l'avons vérifié que pour le premier modèle de la section 3, mais il est naturel d'étendre ce résultat aux autres modèles.

numérique du modèle évoqué à la fin de la section 4 et l'étude de la possible surproduction de gravitinos pendant l'ère de rayonnement sont des exemples de travaux plus phénoménologiques.

Chapitre 4

Flots géométriques et instantons gravitationnels

Dans ce chapitre et le suivant nous étudions en détail une correspondance très précise entre instantons gravitationnels et flots géométriques. On supposera dans ces deux chapitres que l'espace-temps a quatre dimensions, soit trois dimensions d'espace. Les espace-temps considérés auront tous la structure d'une foliation d'un espace-tridimensionnel sur lequel agit de manière simplement transitive[1] un groupe de Bianchi. Ce chapitre introductif débute par une présentation des groupes de Bianchi ainsi que des instantons gravitationnels, puis quelques éléments sur les flots géométriques et en particulier le flot de Ricci sont donnés. L'annexe B, présentant les différentes algèbres issues de la classification de Bianchi, offre plus de détails.

1 Espaces homogènes et groupes de Bianchi

Cette section a pour but d'introduire un ensemble bien précis de variétés tridimensionnelles : les espaces homogènes de dimension 3 vus comme variétés de groupes agissant de façon simplement transitive sur la variété. On débute par une introduction aux espaces homogènes puis une discussion de la classification de Bianchi est présentée.

1.1 Espaces homogènes

Un espace homogène pour un groupe G est une variété non-vide, ou un espace topologique, X, sur lequel G agit continument comme groupe de symétries de façon transitive. Dans ce travail de thèse nous nous sommes restreints aux actions simplement transitives. Pour cette raison entre autre, nous devons nous limiter au

[1] Une action de groupe est dite *simplement transitive* si, en tant qu' application, elle est **injective** et **transitive**. Un groupe G agit transitivement sur un ensemble S si pour tous $(x, y) \in S$, il existe $g \in G$ tel que $g \cdot x = y$.

cas tridimensionnel. Si X est un espace homogène et H_o le stabilisateur[2] d'un point $o \in X$, les points de X sont alors ceux du quotient gauche

$$\frac{G}{H_o}. \tag{4.1}$$

Différents quotients par rapport à différents point o_i sont reliés entre eux par conjugaisons. Deux types d'espaces homogènes X existent : les espaces compacts et non-compacts. Les seconds étant beaucoup plus difficiles à étudier (voir [33, 34] pour un résumé remarquable) et moins familiers, nous nous limiterons aux premiers. Par espace compact, nous entendons toute variété dont au moins un quotient est compact. Une **géométrie** est une variété X simplement connexe, lisse, munie d'une action transitive d'un groupe de Lie G avec des stabilisateurs compacts. Pour reformuler, une géométrie est un espace homogène compact, lisse et simplement connexe. L'utilité de cette notion réside dans un remarquable théorème stipulant que toute géométrie, localement homogène associée à un groupe de Lie simplement connexe G est également homogène globalement. Par conséquent, l'étude des variétés homogènes globales se ramène à celle des géométries sur des groupes simplement connexes. Thurston [35] a classifié l'ensemble de ces *géométries* en 8 classes. Cinq de ces classes ont ainsi pu être associées à des variétés de groupes de la classe A de Bianchi : les groupes unimodulaires[3]. Deux autres classes peuvent être associées à deux groupes de la classe B de Bianchi alors que la dernière géométrie ne possède pas la structure de variété de groupe. Le flot de Ricci normalisé (voir plus bas) sur l'ensemble de ces géométries a été étudié par [36].

1.2 Groupes de Bianchi

L. Bianchi classifia en 1897 l'ensemble des algèbres en trois dimensions [37]. Ces algèbres caractérisent, localement, l'ensemble des groupes en trois dimensions. Cela ne fournit pas la classification globale des groupes en trois dimensions, car des propriétés topologiques globales peuvent par exemple ne pas se décrire par un isomorphisme local. L'exemple le plus frappant étant certainement le groupe $SO(3)$, non-simplement connexe, mais d'algèbre de Lie $\mathfrak{so}(3)$ isomorphe à celle de $SU(2)$ qui lui est simplement connexe. Cette classification est donnée en annexe B avec d'autres détails.

Chacun des groupes de Bianchi possède des **formes invariantes à gauche**, c'est à dire invariantes par action d'éléments des groupes à gauche. Des formes invariantes à droite existent aussi, mais si le groupe n'est pas unimodulaire, ces formes ne sont pas les mêmes. Travailler avec les unes ou les autres de ces formes est équivalent. Dans ce rapport nous utilisons des formes invariantes à gauche σ^i, dont le nombre est égal au rang du groupe qu'elles décrivent. Ces formes satisfont à l'algèbre

$$d\sigma^i = \frac{c^i_{jk}}{2}\sigma^j \wedge \sigma^k. \tag{4.2}$$

[2]Le stabilisateur G_x d'un point x est l'ensemble des éléments $g \in G$ laissant invariant x.
[3]Une des géométries peut être reliée à deux groupes de Bianchi.

Notons e_i les vecteurs duaux de ces formes, au sens $\sigma^i(e_j) = \delta^i_j$, ces vecteurs satisfont alors naturellement à l'algèbre

$$[e_i, e_j] = -c^i_{jk} e_k. \tag{4.3}$$

Les groupes considérés sont des groupes de symétrie de variétés de dimension égale au rang du groupe. Soit un tel groupe G, il possède ainsi des vecteurs de Killing ξ_j vérifiant l'algèbre

$$[\xi_i, \xi_j] = c^i_{jk} \xi_k. \tag{4.4}$$

Parmi les neuf classes d'algèbres de Bianchi, Bianchi $I, II, VI_{-1}, VII_0, VIII$ et IX sont unimodulaires alors que les autres ne le sont pas. En écrivant les constantes de structure sous la forme (n étant une matrice et a un vecteur)

$$c^i_{jk} = \epsilon_{jks} n^{si} + \delta^i_k a_j - \delta^i_j a_k, \tag{4.5}$$

nous pouvons identifier les algèbres unimodulaires comme celles vérifiant $a_i = 0$ alors que les non-unimodulaires vérifient $\overrightarrow{a} \neq \overrightarrow{0}$. De plus, pour les algèbres unimodulaires il est possible avec un choix de base approprié d'obtenir une matrice n diagonale. C'est ce choix qui est fait en annexe B, il est différent du choix de [38].

On peut noter l'existence d'une classification similaire à celle de Bianchi en dimension 4, alors qu'il n'en existe pas pour des dimensions plus élevées.

Les algèbres unimodulaires ont la remarquable propriété de définir des variétés que l'on peut munir de métriques diagonales, préservées sous flot géométrique, dont le flot de Ricci.

2 Instantons gravitationnels

Rappels Un instanton gravitationnel d'un espace homogène en D dimensions muni d'une métrique

$$ds^2 = g_{\mu\nu} dx^\mu dx^\nu, \tag{4.6}$$

est une solution des équations d'Einstein dans le vide dans le cas où la métrique g est de signature Euclidienne[4]. Il est pratique de rappeler ici quelques notions sur le formalisme de Cartan en géométrie différentielle.

Considérons une variété M munie de coordonnées x^μ. Munissons là d'une métrique g (les σ^μ définissent un repère) :

$$ds^2 = g_{\mu\nu} \sigma^\mu \sigma^\nu, \tag{4.7}$$

et définissons un nouveau repère $\theta^a = \theta^a_\mu \sigma^\mu$ tel que

$$ds^2 = \delta_{ab} \theta^a \theta^b = \underbrace{\delta_{ab} \theta^a_\mu \theta^b_\nu}_{g_{\mu\nu}} \sigma^\mu \sigma^\nu. \tag{4.8}$$

[4]L'étude des solutions des équations d'Einstein dans le vide pour une signature $(--++)$ serait également intéressante.

Les variétés M considérées sont homogènes, c'est à dire que dans (4.7) les composantes de la métrique $g_{ij}(T)$ dépendent uniquement de la coordonnée T jouant le rôle d'un temps euclidien. Cette coordonnée T intervient dans la définition de la $1-$forme $\sigma^0 = dT$. De plus, on se restreint à la classe de variétés en D dimensions obtenue par foliations de variétée en $D-1$ dimensions. Dans la suite, pour toute fonction $F(T)$ nous noterons $\dot{F} = \frac{\partial F}{\partial T}$.

Introduisons ensuite la relation de définition de la connexion de spin ω_{ab} (ou nous supposons que la torsion est nulle et nous imposons la condition $\omega_{ab} = -\omega_{ba}$) :

$$d\theta^a = -\omega^a_b \theta^b, \tag{4.9}$$

la $2-$forme de courbure est alors donnée par

$$\mathcal{R}^a_b = d\omega^a_b + \omega^a_c \wedge \omega^c_b = \frac{1}{2} R^a_{bcd} \theta^c \wedge \theta^d, \tag{4.10}$$

où R^a_{bcd} est le tenseur de Riemann qui donne par contraction le tenseur de Ricci $R^a_{bad} = R_{bd}$ puis le scalaire de courbure $\mathcal{R} = R^a_a$.

Développons ensuite la connexion de spin sur l'ancienne base dx^μ, $\omega^a_b = \omega^a_{b\mu} dx^\mu$, nous pouvons alors obtenir les composantes de la $2-$forme de courbure :

$$\mathcal{R}_{0a} = \dot{\omega}_{0a\mu} dt \wedge \theta^\mu + \frac{1}{2} \omega_{0a\mu} c^\mu_{\nu\rho} \theta^\nu \wedge \theta^\rho - \omega_{0b\mu} \omega^b_{a0} dt \wedge \theta^\mu + \omega_{0b\beta} \omega^b_{a\gamma} \theta^\beta \wedge \theta^\gamma \tag{4.11}$$

et

$$\begin{aligned} \mathcal{R}_{ab} &= \dot{\omega}_{ab\alpha} dt \wedge \theta^\alpha + \frac{1}{2} \omega_{ab\alpha} c^\alpha_{\beta\gamma} \theta^\beta \theta^\gamma + \omega_{a0\alpha} \omega^0_{b\beta} \theta^\alpha \wedge \theta^\beta \\ &+ \omega_{ac0} \omega^c_{b\alpha} dt \wedge \theta^\alpha - \omega_{ac\alpha} \omega^c_{b0} dt \wedge \theta^\alpha + \omega_{ac\alpha} \omega^c_{b\beta} \theta^\alpha \wedge \theta^\beta. \end{aligned} \tag{4.12}$$

Il est commode de décomposer la $2-$forme de courbure en partie auto-duale (s) et partie anti-auto duale (a) :

$$\mathcal{R}_{ab} = \mathcal{R}^{(s)}_{ab} + \mathcal{R}^{(a)}_{ab}. \tag{4.13}$$

Par définition nous avons

$$\mathcal{R}^{(a,s)}_{ab} = \pm \frac{1}{2} \epsilon_{ab}{}^{cd} \mathcal{R}^{(a,s)}_{cd}, \tag{4.14}$$

où $\pm = +, -$ respectivement pour $\mathcal{R}^{(s)}_{ab}$ et $\mathcal{R}^{(a)}_{ab}$. Nous pouvons donc écrire

$$2\mathcal{R}^{(a)}_{0b} = [\dot{I}_{b\alpha} - I_{c\alpha} \omega^c_{b0}] dt \wedge \theta^\alpha + \frac{1}{2} [I_{b\alpha} c^\alpha_{\beta\gamma} + \epsilon^{ac}_b I_{a\beta} I_{c\gamma}] \theta^\beta \wedge \theta^\gamma \tag{4.15}$$

où

$$I_{i\alpha} = \omega_{0i\alpha} - \frac{1}{2} \epsilon_i{}^{jk} \omega_{jk\alpha}. \tag{4.16}$$

Avant de poursuivre sur cette décomposition, mentionnons que la distinction entre anti auto-dualité et auto-dualité est arbitraire et histoire de conventions. Dans cette thèse nous avons pris la convention d'imposer l'auto-dualité et non l'anti auto-dualité, avec les conventions que cela impose. Il est possible de montrer que toute

courbure duale vérifie les équations d'Einstein dans le vide $R_{ab} = 0$. La relation clé de cette démonstration est l'identité cyclique[5]

$$R^a_{[bcd]} = 0. \tag{4.17}$$

Les instantons gravitationnels ont beaucoup été étudiés dans la littérature, notamment ceux obtenus par foliation d'un espace tri-dimensionnel M_3 de symétrie $SU(2)$. Dans ce cas ci, les solutions des équations d'auto-dualité portent les noms d'Eguchi-Hanson, Taub-NUT et Belinski. Quelques commentaires à leur sujet sont donnés ci-après.

Nous n'avons pour l'instant parlé que de l'auto-dualité de la 2−forme de courbure, on peut de la même façon définir l'auto-dualité de la connexion de spin, nous écrivons ainsi

$$\omega_{bd} = \omega^{(s)}_{bd} + \omega^{(a)}_{bd}. \tag{4.18}$$

Une connexion auto-duale implique automatiquement une courbure auto-duale, mais la réciproque n'est pas exacte. On peut cependant montrer que lorsque l'on a une courbure auto-duale alors que la connexion ne l'est pas, un changement de base permet de se ramener à une connexion auto-duale. On peut parler de transformation *de jauge* pour passer d'une connexion à l'autre. En effet, ce type de transformations ne transporte aucune information fondamentale sur la variété.

Les instantons gravitationnels peuvent aussi se généraliser à nombre de situations. Un cas classique[6] réside en l'incorporation de la constante cosmologique Λ. Les équations d'auto-dualité sont des équations du premier ordre, alors que les équations d'Einstein sont du second ordre. Les équations de l'auto-dualité sont des intégrales premières de celles d'Einstein dans l'euclidien. De plus, elles sont composées de deux groupes d'équations : 3 équations d'évolution du premier ordre, et 3 contraintes. Une intégrale première I sera caractérisée par $\dot{I} = 0$. Nous voyons donc qu'une intégrale première est $I_{i\alpha}$. La condition nécessaire et suffisante pour que ce soit le cas est

$$\omega_{ik0} = 0 \Longleftrightarrow \dot{\theta}_{i\alpha} = -g_{\alpha\beta}\dot{\theta}^{\beta}_{i}. \tag{4.19}$$

On peut toujours satisfaire à cette condition. En effet si on a une solution $\theta_{i\alpha}$, nous pouvons considérer

$$\tilde{\theta}_{i\alpha} = O_a{}^b(t)\theta_{b\alpha},\ O_a{}^b(t) \in O(3), \tag{4.20}$$

qui remplira la condition (4.19) si et seulement si

$$\dot{O}_a{}^b(t) = \frac{1}{2}O_a{}^c(t)\left(\theta^{\alpha}_c\dot{\theta}^b_{\alpha} - \dot{\theta}_{c\alpha}\theta^{\alpha b}\right). \tag{4.21}$$

Il est toujours possible de satisfaire cette équation. Cinématiquement, cela revient à déterminer une succession de rotations connaissant la vitesse angulaire. Les intégrales premières correspondent donc aux équations

$$\dot{\theta}_{i\alpha} = \theta_{i\gamma}\left[(n^{\gamma\mu} - a_\rho\epsilon^{\rho\gamma\mu})g_{\mu\alpha} - \frac{1}{2}\delta^{\gamma}_{\alpha}n^{\mu}_{\mu}\right] - I_{i\alpha}\sqrt{\det(g_{\alpha\beta})}. \tag{4.22}$$

[5]Voir l'annexe B pour des rappels sur la formalisme de Cartan en géométrie différentielle.
[6]c'est d'ailleurs ce cas-ci que les mathématiciens utilisent pour parler de courbure auto-duale

De (4.15), on écrit les équations de contraintes accompagnant celles d'évolution

$$I_{i\alpha}c^{\alpha}_{\beta\gamma} = -\epsilon^{jk}_{i} I_{j\beta} I_{k\gamma}. \tag{4.23}$$

Ainsi, tout le problème de trouver des courbures auto-duales non singulières et réelles réside dans la résolution simultanée de (4.19) et (4.23). Cela sera effectué dans le chapitre suivant.

Pour clore cette courte introduction aux instantons gravitationnels, il est intéressant de mentionner les plus connus, résultant de l'analyse de Bianchi IX.

Instantons gravitationnels de Bianchi IX Considérons la variété de groupe $SU(2)$ et munissons là d'une métrique invariante à gauche

$$ds^2 = (\gamma_1\gamma_2\gamma_3)^2 dT^2 + \sum_i \gamma_i^2 \sigma_i^2, \tag{4.24}$$

où σ_i sont les formes de Maurer-Cartan introduites en annexe C. Les instantons gravitationnels de ce modèle sont bien connus. Ils sont partagés en deux classes : les instantons *axisymétriques* et *anisotropes*. Chaque classe est composée de deux sous-classes. La raison de cette division vient, comme on le verra plus en détail dans le chapitre suivant, de la différence entre l'auto-dualité de la connexion et celle de la courbure. Exiger l'auto dualité de la courbure n'est pas équivalent dans le cas de SU(2) à exiger celle de la connexion. Les équations d'auto-dualité de la connexion diffèrent des intégrales premières de l'auto-dualité de la courbure par l'absence d'un triplet de paramètres $\lambda_i = 0, 1$. Lorsque $\lambda_i = 0$ nous avons équivalence entre les deux auto-dualités, on parle alors de la branche de *Lagrange*, alors que quand $\lambda_i = 1$ nous obtenons la branche *d'Halphen*.

Instantons axisymétriques L'auto-dualité de la connexion entraine la solution d'Eguchi-Hanson[7].

$$ds^2 = \frac{dr^2}{1-\left(\frac{a}{r}\right)^4} + r^2\left(\sigma_1^2 + \sigma_2^2 + \left(1 - \left(\frac{a}{r}\right)^4\right)\sigma_3^2\right). \tag{4.25}$$

L'auto-dualité de la 2−forme de courbure implique outre la solution d'Eguchi-Hanson, la présence d'une seconde solution, dite de Taub-NUT

$$ds^2 = \frac{1}{4}\frac{r+m}{r-m}dt^2 + (r^2 - m^2)(\sigma_1^2 + \sigma_2^2) + 4m^2\frac{r-m}{r+m}\sigma_3^2. \tag{4.26}$$

Étudions plus en détail ces deux instantons au travers de leurs propriétés géométriques à l'approche des singularités et asymptotiquement.

L'instanton d'Eguchi-Hanson ressemble à celui de Belavin dans dans la théorie de Yang-Mills [39]. Pour décrire avec plus de précsions les propriétés des instantons

[7] La solution présentée est dite de type II, alors qu'une autre solution dite de type I existe également. Je ne ferai que l'évoquer sans la détailler car cela est inutile.

évoqués, rappelons le concept de **bolt** et de **nut**. Pour cela, nous suivons la présentation de [40], [41] et considérons la métrique diagonale la plus générale pour Bianchi IX :

$$ds^2 = d\tau^2 + a(\tau)^2\sigma_1^2 + b(\tau)^2\sigma_2^2 + c(\tau)^2\sigma_3^2. \tag{4.27}$$

La variété décrite par ces coordonnées est régulière, par opposition à *singulière*, quand les fonctions a, b, c sont finies, non singulières à distance τ finie. Cependant, il peut parfois apparaître des singularités dans la métrique, mais ces singularités peuvent être éliminées par changement de coordonnées (telle que la métrique de Schwarzschild et sa singularité au rayon de Schwarzschild) et la métrique rester régulière. Nous classifions dans la suite les comportements de la métrique lorsque $\tau \to 0$ et $\tau \to \infty$. On dira qu'une métrique a une singularité de type *nut* éliminable en $\tau = 0$ si au voisinage de $\tau = 0$:

$$a^2 = b^2 = c^2 = \tau^2. \tag{4.28}$$

Cette singularité n'est pas physique et peut être éliminée en reparamétrant la variété avec des coordonnées cartésiennes proches du point $\tau = 0$ car la métrique résultante n'est autre que celle du plan en coordonnées polaires. Une métrique a une singularité de type *bolt* jetable proche de $\tau = 0$ si

$$\begin{aligned} a^2,\ b^2 \qquad & \text{sont finis,} \\ c^2 = n^2\tau^2, \qquad & n \in \mathbb{Z}. \end{aligned} \tag{4.29}$$

La métrique ainsi obtenue, dans le cas de Bianchi IX avec la paramétrisation donnée en annexe B au moyen des angles d'Euler, est

$$ds^2 = d\tau^2 + \frac{n^2\tau^2}{4}d\psi^2 + \underbrace{d\theta^2 + \sin(\theta)^2 d\phi^2}_{S^2}. \tag{4.30}$$

En choisissant ψ tel que $\frac{n\psi}{2} \in [0, 2\pi[$, la singularité est une fois de plus une singularité de coordonnées du plan $\mathbb{R}^2$ à l'origine. En choisissant des coordonnées cartésiennes on peut éliminer cette singularité.

En ce qui concerne l'étude asymptotique $\tau \to \infty$, on distingue trois cas : *l'infini Euclidien*, *l'infini Taubien*, et *l'infini en cône*. Ces trois possibilités sont données respectivement par

$$\begin{aligned} a, b, c, \to \frac{\xi}{2}, \quad & \xi \to \infty, \quad 0 \leq \psi \leq 4\pi, \\ a, b, \to \xi, \quad & \xi \to \infty, \quad c \to \text{const.}4\pi, \\ a, b, c, \to \frac{\xi}{2}, \quad & \xi \to \infty, \quad 0 \leq \psi \leq 2\pi. \end{aligned} \tag{4.31}$$

Dans la métrique (4.26), posant $t = m + \epsilon$, nous obtenons au voisinage de $t = m$

$$ds^2 = d\tau^2 + \tau^2(\sigma_1^2 + \sigma_2^2 + \sigma_3^3),\ \tau = \sqrt{2m\epsilon}. \tag{4.32}$$

Cette singularité est donc une singularité de type *nut* éliminable. De même, pour la métrique (4.25), nous avons pour $t \approx a$ avec θ et ϕ fixés

$$ds^2 = \frac{1}{4}\left[du^2 + u^2 d\psi^2\right], \; u^2 = t^2\left[1 - \left(\frac{a}{t}\right)^4\right], \tag{4.33}$$

qui est un *bolt* si l'on choisit le domaine de variation standard pour ψ : $\psi \in [0, 2\pi[$.

On peut également trouver des instantons axisymétriques à plusieurs centres (plusieurs singularités apparentes). Un exemple est donné par ([42])

$$ds^2 = V^{-1}(\mathbf{x})(d\tau + \omega \cdot d\mathbf{x})^2 + V(\mathbf{x})d\mathbf{x} \cdot d\mathbf{x}, \; \nabla V = \pm \nabla \times \omega, \; V = \epsilon + 2m \sum_{i=1}^{k} \frac{1}{|\mathbf{x} - \mathbf{x}_i|}. \tag{4.34}$$

Le cas $\epsilon = k = 1$ est la métrique (4.26) dans un système de coordonnées différent alors que pour $\epsilon = 1$ et k général nous obtenons la métrique multi Taub-NUT. De manière générale, cette solution multi-centres possède k *nuts* à l'origine.

Instantons anisotropes Ces instantons sont plus compliqués à trouver. En effet, l'ansatz axisymétrique simplifie beaucoup le système d'équations à résoudre. La plupart du temps, les solutions des équations d'auto-dualité ont des singularités, c'est pourquoi on fera attention de ne pas les appeler *instantons*. Le cas le plus simple *a priori* est la branche de Lagrange, qui correspond comme on va le voir à la solution de Belinski et al[8]. La branche d'Halphen donne des solutions variées et plus complexes comme on va le voir.

La solution de Belinski est la métrique (analytiquement simple)

$$ds^2 = \frac{1}{\sqrt{F_1(r)F_2(r)F_3(r)}}\left[dr^2 + \frac{r^2}{4}\left\{F_2(r)F_3(r)\sigma_1^2 + F_1(r)F_3(r)\sigma_2^2 + F_1(r)F_2(r)\sigma_3^2\right\}\right], \tag{4.35}$$

où $F_i(r) = 1 - \frac{16x_i}{r^4}$, $i = 1, 2, 3$ et $x_i \in \mathbb{R}$. Cette métrique est asymptotiquement euclidienne, mais lorsque nous nous approchons des x_i, des singularités apparaissent rendant la solution incomplète. Pour que la solution décrivent un espace anisotrope, il faut que $x_i \neq x_j$ pour $i \neq j$.

Si cela n'est pas le cas ; soit $x_1 = x_2 = x_3$ et nous retrouvons le cas de l'espace plat, soit deux seulement des x_i sont égaux. Supposons alors que les x_i satisfont $x_1 \geq x_2 \geq x_3$, deux cas sont à considérer

- $x_1 = x_2$, nous obtenons la métrique d'Eguchi-Hanson de type II,
- $x_2 = x_3$, nous obtenons la métrique d'Eguchi-Hanson de type I.

Les structures globales des métriques I et II ne sont pas les mêmes. Premièrement, bien que dans le cas général la courbure diverge en un des x_i, ces divergences s'annulent lorsque deux x_i sont égaux. La métrique de type I ressemble au cas général et est incomplète. D'un autre côté, la métrique de type II peut être complétée [44] en une solution sans singularités mais nous n'irons pas plus loin dans cette direction. La solution de la branche d'Halphen est quand à elle bien plus compliquée et a été

[8]que nous appelons *solution de Belinski* pour simplifier

décrite pour la première fois récemment dans [43]. Les résultats présentés dans cette section sont donc partiellement nouveaux.

Les équations régissant cette solution sont données par le système, après transformations[9],

$$\left\{\begin{array}{lcl} \dot{\Omega}_1 & = & \Omega_2\Omega_3 - \Omega_1(\Omega_2+\Omega_3), \\ \dot{\Omega}_2 & = & \Omega_1\Omega_3 - \Omega_2(\Omega_1+\Omega_3), \\ \dot{\Omega}_3 & = & \Omega_1\Omega_2 - \Omega_3(\Omega_1+\Omega_2), \end{array}\right. \tag{4.38}$$

où $\Omega_i = \gamma_j\gamma_k$, $\epsilon_{ijk} = 1$. Ce système d'équations est le système d'Halphen tel qu'étudié au 19ème siècle. Ce système fut d'abord découvert par Darboux [45] dans son étude des surfaces triplement orthogonales puis étudié et résolu par Halphen, [46, 47]. Ce système d'équations est apparu à de nombreuses reprises depuis en physique. En introduisant $Y = -2(\Omega_1+\Omega_2+\Omega_3)$ nous obtenons l'équation

$$\dddot{Y} = 2Y\ddot{Y} - 3\dot{Y}^2, \tag{4.39}$$

connue sous le nom **d'équation de Chazy**.

Ces équations (Halphen, Chazy), mais aussi bien d'autres issues de la théorie des systèmes intégrables, ont la particularité d'intervenir dans l'étude des solutions auto-duales de la théorie de Yang-Mills[10]. De plus ces équations ont des propriétés remarquables facilitant la recherche de leur solution la plus générale. En particulier, si $\omega_\alpha(z)$ est une solution du système d'Halphen pour $z \in \mathbb{C}$, alors

$$\tilde{\omega}_\alpha(z) = \frac{1}{(cz+d)^2}\omega_\alpha\left(\frac{az+b}{cz+d}\right) + \frac{c}{cz+d} \tag{4.40}$$

est aussi solution, avec $\begin{pmatrix} a & b \\ c & d \end{pmatrix} \in PSL(2,\mathbb{C}) = \frac{SL(2,\mathbb{C})}{\mathbb{Z}_2}$. Une solution particulière est donnée par

$$\omega_\alpha(z) = -\frac{1}{2}\frac{d}{dz}\log E_\alpha(z) \tag{4.41}$$

où E_α forme un triplet de formes modulaires de poids 2, c'est à dire se transformant comme

$$z \to -\frac{1}{z} : \begin{pmatrix} E_1 \\ E_2 \\ E_3 \end{pmatrix} \to z^2 \begin{pmatrix} E_2 \\ E_1 \\ -E_3 \end{pmatrix} \tag{4.42}$$

[9] Ces équations sont celles obtenues par le flot de Ricci de la métrique

$$ds^2 = \gamma_i\sigma_i^2 \tag{4.36}$$

et par l'auto-dualité de la métrique

$$ds^2 = (\gamma_1\gamma_2\gamma_3)^2 dT^2 + \gamma_i(T)^2\sigma_i^2. \tag{4.37}$$

[10] à tel point que des conjectures stipulant que chaque système intégrable doit être une réduction des équations de Yang-Mills auto-duales ont vu le jour. Aucune preuve n'existe à ce jour et cette conjecture cesse d'être vraie en dimension supèrieure à 3.

et

$$z \to z+1 : \begin{pmatrix} E_1 \\ E_2 \\ E_3 \end{pmatrix} \to - \begin{pmatrix} E_3 \\ E_2 \\ E_1 \end{pmatrix}. \tag{4.43}$$

Notons que cette étude n'est valable que lorsque les ω_α sont tous différents, or c'est précisément la situation qui nous intéresse le plus. Un exemple de triplet de formes modulaires est donné par

$$E_1 = \frac{\frac{d\lambda}{dz}}{\lambda},\ E_2 = \frac{\frac{d\lambda}{dz}}{\lambda - 1},\ E_3 = \frac{\frac{d\lambda}{dz}}{\lambda(\lambda-1)}, \tag{4.44}$$

où λ est solution de l'équation de Schwartz

$$\frac{d^3\lambda/dz^3}{d\lambda/dz} - \frac{3}{2}\left(\frac{d^2\lambda/dz^2}{d\lambda/dz}\right)^2 = -\frac{1}{2}\left(\frac{1}{\lambda^2} + \frac{1}{(\lambda-1)^2} - \frac{1}{\lambda(\lambda-1)}\right)\left(\frac{d\lambda}{dz}\right)^2. \tag{4.45}$$

Une solution particulièrement connue de l'équation de Schwartz est données par la fonction modulaire elliptique $\lambda = \frac{\theta_2^4}{\theta_3^4}$. Bien que les résultats présentés soient en terme de fonctions $\omega_\alpha(z)$ complexes, les résultats physiques que l'on cherche doivent être réels. Nous introduisons alors le temps réel T de telle sorte que les solutions $\Omega_\alpha(T)$ soient données par

$$\Omega_\alpha(T) = -\frac{1}{2}\frac{d}{dT}\log E_\alpha(iT). \tag{4.46}$$

On montre que pour des conditions initiales positives telles que

$$0 < \Omega_{10} < \Omega_{20} < \Omega_{30}, \tag{4.47}$$

nous avons

$$0 < \Omega_1(T) < \Omega_2(T) < \Omega_3(T),\ \forall T. \tag{4.48}$$

Ce résultat est très intéressant dans l'optique de l'analyse du flot de Ricci (dont nous parlerons dans un moment) et de la connexion entre flot de Ricci et instantons gravitationnels étudiée dans le chapitre suivant. Le comportement numérique d'une solution est donné par la figure 4.1.

Si Ω_{i0} est fini alors $\Omega_i = \frac{1}{T} + o\left(\frac{1}{T}\right)$, $T \to \infty$. La conséquence naturelle pour la solution obtenue est une singularité de type *nut*. Une autre solution existe avec $\Omega_1 < 0 < \Omega_3 < \Omega_2$ et est définie pour $T > 0$ et caractérisée par

$$\Omega_1 \approx -\frac{\pi}{2T^2},\ \Omega_{2,3} \approx \frac{1}{T},\ T \to 0 \tag{4.49}$$

et

$$\Omega_{1,3} \approx \mp 4\pi e^{-\pi T},\ \Omega_2 \approx \frac{\pi}{2} + 4\pi e^{-2\pi T},\ T \to \infty. \tag{4.50}$$

Les transformations (4.40) peuvent néanmoins bouger le pôle $\Omega_1 = 0$ en $T_0 \neq 0$ et restaurer la positivité de Ω_1. Pour cela il nous suffit de prendre a, c tels que $\frac{a}{c} > 0$ et tels que la géométrie en $T \to \infty$ soit donnée par un *nut* avec $\Omega_i(T) \approx \frac{1}{T}$. Cette

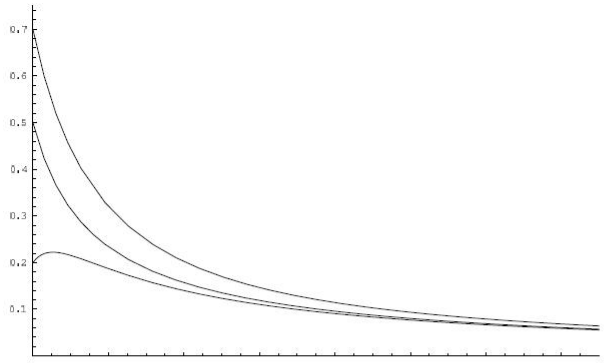

FIG. 4.1 – Comportement de la solution anisotrope avec $\Omega_1(0) < \Omega_2(0) < \Omega_3(0)$. De haut en bas nous avons $\Omega_3(T)$, $\Omega_2(T)$ et $\Omega_1(T)$.

solution a deux pôles, en $T_0 = -\frac{b}{a}$ et $T_\infty = -\frac{d}{c}$ avec $T_0 > T_\infty$. En approchant T_0 nous avons

$$\Omega_1 \approx -\frac{\pi}{2a^2}\frac{1}{(T-T_0)^2},\ \Omega_{2,3} \approx \frac{1}{T-T_0}. \tag{4.51}$$

Les fonctions $\Omega_i(T)$ sont définies pour $T > T_0$ et $T < T_\infty$ avec des comportements miroirs l'un de l'autre. Nous pouvons donc étudier sans perdre de généralités le cas $T > T_0$ uniquement. Il est alors facile de montrer qu'il existe T_* tel que $T_0 < T_* < \infty$ et pour $T \geq T_*$ on ait $\Omega_1(T) \geq 0$. L'ordre de départ : $\Omega_1 < \Omega_3 < \Omega_2$ est alors préservé. Comme pour la solution de Belinski, un Nut est présent en $T \to \infty$, mais T_0 (*l'infini* pour notre solution) est protégé par une singularité de courbure en $T_* > T_0$. Lorsque nous passons du cas anisotrope au cas axisymétrique, il est facile de constater l'absence de singularités de courbures.

On peut cependant obtenir une solution régulière des équations d'auto-dualité dans le cas anisotrope : l'instanton d'Atiyah-Hitchin [48]. Cet instanton est donné par

$$\begin{aligned}
\Omega_1^H &= \frac{\pi}{6i}\left(\bar{E}_2 - \theta_2^4 - \theta_3^4\right) \\
\Omega_2^H &= \frac{\pi}{6i}\left(\bar{E}_2 + \theta_3^4 + \theta_4^4\right) \\
\Omega_3^H &= \frac{\pi}{6i}\left(\bar{E}_2 + \theta_2^4 - \theta_4^4\right) \qquad (4.52)
\end{aligned}$$

$$(4.53)$$

où $\bar{E}_2(z) = \frac{12}{i\pi}\frac{d}{dz}\log\eta$.

Continuons ce chapitre par quelques rappels sur les flots géométriques.

3 Flots géométriques

Considérons une variété non pathologique $\mathcal{M}$, nous pouvons munir cette variété de coordonnées, définir des outils de géométrie différentielle, calculer différents

estimateurs de la courbure de cette variété,$\cdots$. Supposons que nous voulions étudier la déformation de cette variété sous un flot géométrique quelconque, c'est à dire sa déformation dictée par l'équation

$$\frac{\partial R_c}{\partial t}|_{P\in\mathcal{M}} = \mathcal{F}(\mathcal{M})_{P\in\mathcal{M}}, \tag{4.54}$$

où $R_c(p)$ est un rayon caractéristique de la variété en P, t un paramètre d'évolution arbitraire, P un point arbitraire de $\mathcal{M}$ et $\mathcal{F}(\mathcal{M})$ une fonction de la courbure de $\mathcal{M}$. La courbure d'une variété[11] dicte son évolution. Un endroit de courbure nulle ne subira aucune déformation, alors que les lieux de courbure maximale seront les plus modifiés. Un point fixe naturel de ces équations de flot est donc l'ensemble des variétés sans courbure. La conjecture naïve que l'on peut faire est que sous un flot géométrique, les variétés tendent à ne plus avoir de courbure. Cette conjecture est plus puissante qu'il n'y parait.

Pour une variété en dimensions D il existe différentes notions de courbure. La courbure moyenne, la courbure de Gauss, la courbure de Riemann, celle induite par le tenseur de Cotton ($D = 3$), par le tenseur de Weyl ($D > 3$) $\cdots$. Ces différents tenseurs sont détaillés dans l'annexe B. Dans cette thèse nous nous sommes concentrés avec mes collaborateurs sur les trois derniers tenseurs nommés, ceux de Riemann, Cotton et Weyl.

Par convention nous dirons qu'une variété est *plate*, ou *de courbure nulle*, si son tenseur de Riemann s'annule. En dimension $D > 3$, le tenseur de Weyl est très utile pour étudier les variétés plates à une transformation conforme près car il s'annule pour ces dernières. En dimension 4 ce tenseur peut se dériver du tenseur de Bach alors qu'en dimension 3 le tenseur de Weyl n'est plus défini, c'est le tenseur de Cotton qui l'est et lui est équivalent dans son principe. Dans cette section nous nous contentons de définitions et résultats standards concernant les flots géométriques. Les résultats nouveaux obtenus pendant cette thèse sont reportés au chapitre suivant.

Le flot de Ricci est certainement *le* plus connu des flots géométriques. Il consiste en l'équation

$$\frac{\partial g_{\mu\nu}}{\partial T} = -R_{\mu\nu}, \tag{4.55}$$

où $R_{\mu\nu}$ est le tenseur de Ricci. Cette équation ressemble, comme on peut le montrer, à une équation de la chaleur. Le flot de Ricci peut *a priori* être étudié en dimension arbitraire, mais le cas tridimensionnel est particulier par sa simplicité et son intérêt physique et mathématique. Le flot de Ricci a beaucoup été utilisé pour étudier la conjecture de Thurston, définie ci dessous, qui pour la première fois a été exprimée en dimension 3.

La plupart des flots géométriques ont des propriétés similaires, notamment la ressemblance avec une équation de la chaleur.

[11] ceci est un abus de langage, il s'agit en fait de la courbure de la connexion dont est munie la variété

Bref Historique Le flot de Ricci est apparu en 1982 dans le travail de R. Hamilton sur les variétés tridimensionnelles avec courbure de Ricci positive. Ce travail avait pour but la preuve de la **Conjecture de Géométrisation** au travers du flot de Ricci. Introduite par W. Thurston, cette conjecture stipule grossièrement que chaque variété de dimension 3, fermée, admet une décomposition géométrique, soit une décomposition en briques élémentaires admettant des métriques localement homogènes. L'idée derrière cette conjecture est de pouvoir approximer une variété très compliquée par une succession de sous-variétés plus simples. Différentes versions, affaiblies, de la conjecture de géométrisation, ont été proposées et prouvées dans la littérature. Récemment, les travaux de G. Perelman [49] ont apporté des avancées considérables dans le domaine. Il est depuis admis qu'au travers du flot de Ricci, ce dernier a réussi à prouver la conjecture de Thurston. Ce travail monumental utilise pleinement le flot de Ricci et la théorie des déformations qui lui est associé. En effet, certaines parties de variétés peuvent tendre vers des singularités, des pincements, sous le flot de Ricci, il convient donc de zoomer ces zones de manière appropriée pour pouvoir les étudier. Bien que cet explication heuristique soit très facile à comprendre, la technique derrière tout ceci est autrement plus compliquée et nous n'avons pas eu besoin de l'utiliser pendant cette thèse.

Extensions du Flot de Ricci Il est possible d'étendre le flot de Ricci et de définir de nouveaux flots. Dans cette thèse nous avons étudié des flots géométriques de la forme

$$\frac{\partial g_{ij}}{\partial T} = -\alpha R_{ij} + \beta R g_{ij} + \gamma g_{ij} + \delta C_{ij}. \tag{4.56}$$

Par Renormalisation du temps T nous pouvons bien entendu poser $\alpha = 1$, néanmoins laissant α arbitraire permet de décomposer ce flot très général en différents flots étudiés dans la littérature.

- $\beta = \gamma = \delta = 0$: flot de Ricci,
- $\alpha = \gamma = \delta = 0$: flot de Yamabe,
- $\beta = \alpha = \delta = 0$: flot de constante cosmologique,
- $\beta = \gamma = \alpha = 0$: flot de Cotton,
- $\gamma = \delta = 0,\ \beta = \frac{\alpha}{3}$: flot de Ricci normalisé.

Outre le flot de Ricci, une attention particulière a été apportée dans cette thèse au flot de Ricci normalisé auquel on ajoute le terme de Cotton, soit $\gamma = 0$. Le flot de Ricci normalisé possède la particularité que le volume de la variété est conservé sous le flot, tout comme le flot de Cotton, d'où le mélange naturel des deux. En revanche, excepté des ajustements très fins de conditions initiales et/ou paramètres, le flot de Ricci non normalisé, le flot de constante cosmologique et le flot de Yamabe ne préservent pas le volume de la variété.

Flot géométrique et algèbres de Bianchi Une remarque fondamentale doit être apportée sur le flot géométrique agissant sur une variété de groupe de Bianchi. Si l'algèbre de Bianchi sous-jacente est unimodulaire, la métrique sur la variété peut être prise diagonale et le restera sous l'évolution du flot. Si par contre l'algèbre est non-unimodulaire, il n'existe pas de preuve permettant de diagonaliser la métrique

et considérer ce cas comme le plus général. Pour les cas Bianchi IV et $VII_{h\neq 0}$, nous pouvons même observer qu'une métrique diagonale n'est pas préservée par flot de Ricci et/ou flot de Ricci normalisé.

En 1992, [36] étudia les propriétés des huit géométries de Thurston, donc entre autre des variétés de groupes de la classe A de Bianchi et deux variétés de groupes de la classe B, sous le flot de Ricci normalisé. A titre de travail non publié, nous avons également fait cette étude pour le flot de Ricci quelconque (non normalisé, incluant donc le flot de Yamabe) pour l'ensemble des algèbres de Bianchi en supposant la métrique la plus générale à chaque fois. [50] retrace le même type d'étude concernant le flot de Cotton cette fois ci. Les techniques utilisées sont assez simples et standard, en effet ces études portant principalement sur des métriques diagonales, deux cas se dégagent : le cas axisymétrique et le cas totalement anisotrope. Le premier est plus simple à résoudre que le second et peut en général se résoudre analytiquement. Le cas anisotrope nécessite souvent des techniques numériques, bien que des estimations de convergences puissent être obtenues analytiquement.

Chapitre 5

Flots géométriques et systèmes gravitationnels

Ce chapitre est l'avant dernier de ce rapport, et le dernier à présenter des résultats nouveaux développés durant cette thèse.

La première partie fournit une présentation assez détaillée d'une application des flots géométriques à la physique : comment le flot de Ricci peut aider à décrire des espaces auto-duaux. Ce sujet a fait l'objet des publications 4 et 5. Dans la section 1 nous détaillerons le travail de la publication 5 où nous avons étudié une classe d'espaces homogènes auto-duaux de dimension quatre vus comme des foliations d'espaces de dimension trois avec des algèbres tridimensionnelles y agissant librement. Ensuite nous montrerons dans la section 2 que certaines de ces solutions s'obtiennent également par des flots géométriques bien précis, nous établirons les notations et traiterons le cas de l'algèbre tridimensionnelle de Bianchi IX. Nous mentionnerons également des résultats obtenus pour les autres algèbres de la classification.

Le reste de ce chapitre sera consacré à l'étude d'un flot géométrique de la forme

$$\frac{dg_{\mu\nu}}{dt} = -R_{\mu\nu} + \beta C_{\mu\nu} + \Lambda, \tag{5.1}$$

où $R_{\mu\nu}$ est le tenseur de Ricci de la métrique g, $C_{\mu\nu}$ son tenseur de Cotton, Λ une constante et β une constante. Ce flot intervient dans la théorie non relativiste de la gravitation d'Horăva-Lifshitz. Le mélange des flots de Ricci et de Cotton est étudié dans la section 3 avant de mentionner quelques résultats quand nous avons en plus $\Lambda \neq 0$. Ces résultats sont basés sur les publications 6 et 7. Les résultats concernant les flots non normalisés et la recherche d'attracteurs non triviaux ont nécessité beaucoup de travail numérique, et moins de travail analytique. Néanmoins, *tous les résultats analytiques utilisant des approximations/hypothèses obtenues numériquement ont été vérifiés plusieurs fois et sont en parfaite adéquation avec les observations numériques.* Les codes informatiques utilisés ici sont des algorithmes standard de résolution d'équations différentielles couplées. La méthode de Runge-Kutta avec un pas adaptatif a été choisie, et adaptée de [51].

1 Espaces auto-duaux en quatre dimensions

Dans cette section on reporte les résultats majeurs obtenus dans la publication 5 où nous avons étudié les espaces homogènes quadri-dimensionnels auto-duaux avec un groupe de symétrie de dimension trois agissant librement sur un feuillet tridimensionnel associé.

Bien que de prime abord réductrice, cette étude est en faite très puissante et très générale car elle permet de classifier les espaces auto-duaux d'une importante et large gamme d'espaces homogènes. Cette étude a été commencée dans le passé, notamment dans [52] mais aussi dans beaucoup d'autres travaux. Cependant il y a dans tous ces travaux un manque certain de généralité qui implique la nécessité d'aller au delà de ce qui a été fait et de proposer une classification exhaustive des espaces auto-duaux, et rigoureuse, pour cette large gamme de variétés homogènes. Le travail [52], bien qu'incomplet, est cependant le plus complet à ce jour sur le sujet. L'objectif de la publication 5 était de retrouver les résultats de [52] tout en présentant ceux qui manquaient, et ceci dans un cadre rigoureux et exhaustif. Cette section reprend une large partie de la publication 5.

1.1 Rappels du chapitre 4

Considérons une variété de groupe M munie de coordonnées x^μ. Munissons là d'une métrique (les formes de Maurer-Cartan de la variété sont notées σ^μ)

$$ds^2 = g_{\mu\nu}\sigma^\mu\sigma^\nu, \tag{5.2}$$

et définissons des formes $\theta^a = \theta^a_\mu\sigma^\mu$ telles que

$$ds^2 = \delta_{ab}\theta^a\theta^b = \underbrace{\delta_{ab}\theta^a_\mu\theta^b_\nu}_{g_{\mu\nu}}\sigma^\mu\sigma^\nu. \tag{5.3}$$

On a vu que la condition nécessaire et suffisante pour avoir des équations d'auto-dualité du premier ordre est

$$\dot{\theta}_{i\alpha} = -g_{\alpha\beta}\dot{\theta}^\beta_i. \tag{5.4}$$

On montre alors que les équations d'auto-dualité s'écrivent

$$\dot{\theta}_{i\alpha} = \theta_{i\gamma}\left[(n^{\gamma\mu} - a_\rho\epsilon^{\rho\gamma\mu})g_{\mu\alpha} - \frac{1}{2}\delta^\gamma_\alpha n^\mu_\mu\right] - I_{i\alpha}\sqrt{\det(g_{\alpha\beta})}, \tag{5.5}$$

où les $I_{i\alpha}$ sont des constantes vérifiant deux contraintes.

Première contrainte. D'abord nous avons des contraintes sur les $I_{i\alpha}$ eux mêmes

$$I_{i\alpha}c^\alpha_{\beta\gamma} = -\epsilon^{jk}_i I_{j\beta}I_{k\gamma}. \tag{5.6}$$

Nous avons introduis ci dessus les constantes de structure $c^\alpha_{\beta\gamma}$ issues de la relation

$$d\sigma^\alpha = \frac{1}{2}c^\alpha_{\beta\gamma}\,\sigma^\beta \wedge \sigma^\gamma \tag{5.7}$$

et qui s'écrivent également, en introduisant une matrice symétrique n et un vecteur a :

$$c^{\alpha}{}_{\beta\gamma}\epsilon^{\beta\gamma\mu} = 2(n^{\alpha\mu} + \epsilon^{\alpha\mu\beta}a_{\beta}). \tag{5.8}$$

D'après la relation (5.6), on peut interpréter $I_{i\alpha}$ comme un homomorphisme entre l'algèbre de Lie du groupe d'isométrie de la variété M, $\mathfrak{g}_{hom}$, et l'algèbre $\mathfrak{so}(3)$:

$$I \ : \mathfrak{g}_{hom} \to \mathfrak{so}(3). \tag{5.9}$$

En fonction du rang de cette application on a différentes solutions auto-duales, et le but de la publication 5 était de classifier ces solutions. Les algèbres admettant des espaces homogènes auto-duaux sont alors données par

- **rang 3** (maximal) type IX ,
- **rang 2** impossible,
- **rang 1** types $I, II, III, IV, V, VI, VII$,
- **rang 0** toutes les algèbres de Bianchi.

Seconde contrainte. La seconde contrainte sur les $I_{i\alpha}$ vient de l'existence même d'équations du premier ordre, elle est d'ailleurs plus une contrainte sur les composantes de la matrice θ^{α}_{k} impliquant notamment que certaines s'annulent,

$$I_{i\alpha}\theta^{\alpha}_{j} - I_{j\alpha}\theta^{\alpha}_{i} = -2\, a_{\rho}\, \theta^{\rho k}\epsilon_{kij}. \tag{5.10}$$

Dans la suite nous donnons la classification complète des solutions auto-duales. Pour la plupart des cas la matrice θ et la métrique $\theta^T\theta$ peuvent être prises diagonales en considérant les libertés de transformations dues aux transformations de rotations et de $Gl(3,\mathbb{R})$. Uniquement dans le cas de Bianchi III au rang 1 nous devons considérer une métrique plus générale.

1.2 Classification

Rang de l'application I Si le rang est nul, alors $I_{i\alpha} = 0$ de sorte qu'il est possible de montrer (voir publication 5) que le cas le plus général est une métrique diagonale. Dans le cas où le rang vaut 3, on montre que seule Bianchi IX fonctionne et que la métrique peut encore être prise diagonale. Enfin, dans le cas de rang 1, le plus compliqué, pour Bianchi I, II, VI_{-1}, et VII_0 nous pouvons nous ramener à une métrique diagonale alors que pour Bianchi III nous avons une solution non-diagonale qui ne peut se ramener au cas diagonal. Cette dernière solution pour une algèbre non unimodulaire est nouvelle.

Liste des solutions

Bianchi I La solution est

$$ds^2 = e^{-2\,\epsilon\,t}\, dt^2 + e^{-2\,\epsilon\,t}\,(\sigma^1)^2 + (\sigma^2)^2 + (\sigma^3)^2 \tag{5.11}$$

et décrit un espace plat pour les solutions de rang ϵ ($\epsilon = 0, 1$).

Bianchi II La solution générale, où le rang ϵ apparaît, est

$$ds^2 = \frac{t\, e^{2\,\epsilon\, t/b_0}}{b_0^2\, c_0^2} dt^2 + \frac{1}{t}(\sigma^1)^2 + \frac{t}{b_0^2}(\sigma^2)^2 + \frac{t\, e^{2\,\epsilon\, t/b_0}}{c_0^2}(\sigma^3)^2. \tag{5.12}$$

Bianchi III Les solutions auto-duales pour Bianchi III sont forcément de rang 1. Si $a \neq r$ alors la solution est donnée par

$$\begin{aligned} ds^2 &= \frac{F(t)}{32\, c_0^4\, \cosh^4\big(t - t_*\big)} dt^2 + \frac{\big(K\, t - 1\big)\tanh\big(t - t_*\big) - K}{c_0^2}(\sigma^3)^2 \\ &\quad + \frac{g_1(t)}{F(t)}(\sigma^1)^2 + \frac{g_2(t)}{F(t)}(\sigma^2)^2 + 2\,\frac{g_3(t)}{F(t)}\,\sigma^1\,\sigma^2, \end{aligned} \tag{5.13}$$

où nous avons introduis les fonctions $F(t)$, $g_1(t)$, $g_2(t)$ et $g_3(t)$ données par

$$\begin{aligned} F(t) &= 8\, c_0^2\, \cosh\big(t - t_*\big)\Big[\big(K\, t - 1\big)\sinh\big(t - t_*\big) - K\, \cosh\big(t - t_*\big)\Big], \\ g_1(t) &= (K^2 + 1)\cosh\big(2(t - t_*)\big) + 2\, K\, \sinh\big(2(t - t_*)\big) + 2K^2\, t^2 + K^2 - 1, \\ g_2(t) &= (K^2 + 1)\cosh\big(2(t - t_*)\big) - 2\, K\, \sinh\big(2(t - t_*)\big) \\ &\quad + 2K^2\, t^2 - 8\, K\, t + K^2 + 7, \\ g_3(t) &= (K^2 - 1)\cosh\big(2(t - t_*)\big) + 2\, K^2\, t^2 - 4\, K\, t + K^2 + 1. \end{aligned} \tag{5.14}$$

La solution avec $a = r$ est donnée par

$$\begin{aligned} ds^2 &= \frac{L\,(B-1)}{4}\frac{\tanh(t)}{\cosh^2(t)}\, dt^2 + L\,(B-1)\,\tanh(t)\,\big(\sigma^3\big)^2 \\ &\quad + \frac{L}{4\,(B-1)}\Big\{\big[2\, B^2\, \mathrm{csch}(2\, t) + \tanh(t)\big]\,\big(\sigma^1\big)^2 + \\ &\quad -2\,[\tanh(t) - 2\, B\,(B-2)\mathrm{csch}(2\, t)]\,\sigma^1\,\sigma^2 \\ &\quad \big[\mathrm{csch}(2\, t)(\cosh(2\, t) + 2\,(B-2)^2 - 1\big]\,\big(\sigma^2\big)^2\Big\}. \end{aligned} \tag{5.15}$$

Bianchi VI$_0$ La métrique générale de rang ϵ, auto-duale, est donnée par :

$$ds^2 = \sin(2\, t)\,\frac{e^{2\,\epsilon\, Z\, t}}{c_0^2}\Big(dt^2 + \big(\sigma^3\big)^2\Big) + \tan(t)\,\big(\sigma^1\big)^2 + \cot(t)\,\big(\sigma^2\big)^2, \tag{5.16}$$

où $t \in [0, \pi/2]$.

Bianchi VII$_0$ La métrique générale de rang ϵ, auto-duale, est donnée par :

$$ds^2 = \sinh(2\, t)\,\frac{e^{2\,\epsilon\, Z\, t}}{c_0^2}\Big(dt^2 + \big(\sigma^3\big)^2\Big) + \tanh(t)\,\big(\sigma^1\big)^2 + \coth(t)\,\big(\sigma^2\big)^2 \tag{5.17}$$

On observe également que la limite à grand t de la solution de rang 1 donne une autre solution des équations d'auto-dualité donnée par

$$ds^2 = c_0^2\, e^{2(1+Z)t}\Big(dt^2 + \big(\sigma^3\big)^2\Big) + \big(\sigma^1\big)^2 + \big(\sigma^2\big)^2. \tag{5.18}$$

Bianchi VIII Il n'y a que la solution de rang 0 :

$$ds^2 = \frac{P^{-1/2}}{4}dx^2 + P^{1/2}\left(\frac{(\sigma^1)^2}{x_1 - x} + \frac{(\sigma^2)^2}{x_2 - x} + \frac{(\sigma^3)^2}{x}\right) \tag{5.19}$$

avec $P = (x_1 - x)(x_2 - x)x$ où x_1, x_2 sont positifs et $0 \leq x \leq \min\{x_1, x_2\}$.

Bianchi IX Nous avons des solutions à la fois de rang 0 (équations de *Lagrange*) et de rang 3 (équations de *Darboux-Halphen*). Ces solutions ont été présentées et étudiées avec de nombreux détails dans le chapitre précédent.

Dans la publication 5 nous donnons toutes les étapes de cette classification. nous n'avons pas souhaité les introduire ici pour alléger le débat. Une extension naturelle de ce travail serait de considérer des espaces homogènes plus généraux ou bien d'inclure la constante cosmologique. Une extension triviale serait de considérer une métrique de signature $(--++)$ où Bianchi VIII jouerait alors un rôle analogue à celui de Bianchi IX dans notre cas.

Les espaces homogènes auto-duaux obtenus ci-dessus sont des foliations d'espaces de dimension 3 et vérifient des équations d'auto-dualité bien précises. On peut écrire un de ces espaces de la forme $\mathbb{R} \times M_3$. Dans la section suivante, on montre qu'en général, on peut associer simplement à toute variété M_3 une autre variété, $N_3(M_3)$, telles que les équations du flot de Rici (éventuellement légèrement modifié) de la variété $N_3(M_3)$ redonnent les équations d'auto-dualité de l'espace $\mathbb{R} \times M_3$. Nous montrons, qu'à une exception près, nous pouvons réinterpréter les solutions auto-duales ci-dessus à l'aide de flots de Ricci.

2 Espaces homogènes auto-duaux et flots de Ricci

2.1 Posons le problème...

Nous avons décris dans le chapitre précédent différents espaces homogènes auto-duaux. Ils ont tous la particularité d'être obtenus pour une variété quadridimensionnelle, homogène, et associée à l'algèbre de Bianchi IX. Un espace auto-dual, solution des équations d'Einstein dans le vide dans l'euclidien, est une solution réelle (par opposition à complexe) mais parfois très compliquée à trouver. En effet, les équations d'Einstein sous-jacentes sont du second ordre. Pour simplifier, il est possible d'imposer des symétries supplémentaires afin de réduire le nombre de degrés de libertés, c'est pourquoi les solutions axisymétriques d'Eguchi-Hanson et Taub-Nut ont été trouvées avant les solutions anisotropes. Nous allons voir dans ce chapitre qu'il est possible de décrire certains espaces auto-duaux par des équations bien connues des mathématiciens car obtenues à partir de flots géométriques.

Nous supposerons que l'espace-temps euclidien est en quatre dimensions, et obtenu par foliation d'un espace de dimension trois. Les différentes copies de cet espace de dimension trois lorsque le temps évolue sont appelées des *feuillets d'espace*. Sur chaque feuillet, un groupe de symétrie de dimension au moins 3 est supposé agir

transitivement : nous imposons alors *l'homogénéité*. Nous ne requérons aucune hypothèse de symétrie supplémentaire. L'extension de l'étude menée dans les publications 4 et 5 aux espaces inhomogènes est un projet intéressant qui mérite développements.

Les espaces qui nous intéressent peuvent se construire à partir des algèbres tridimensionnelles qui ont été classifiées par Bianchi dans [37] et revus (en rendant la présentation plus moderne) par Taub [53]. De nombreux résultats, obtenus par exemple par [54] et [36], ont été obtenus concernant les propriétés de ces variétés homogènes le long de flots géométriques comme le flot de Ricci

$$\frac{\mathrm{d}g_{ij}}{\mathrm{d}t} = -R_{ij}. \tag{5.20}$$

Dans ce projet, nous avons été amené à modifier légèrement ce flot pour rendre notre classification plus aboutie. Cette modification, comme on le verra, consiste à ajouter un terme de connexion de jauge au tenseur de Ricci.

Nous allons chercher à comprendre comment le comportement des espaces homogènes en trois dimensions étudiés ici, sous des flots géométriques, est relié au comportement des espaces auto-duaux en quatre dimensions obtenus en foliant simplement les variétés homogènes de dimension trois précédentes. On peut tenter de justifier cette approche de plusieurs façons.

- Tout d'abord, il y a dans la notion d'espace auto-dual celle d'évolution d'une solution euclidienne des équations d'Einstein par rapport à une variable temporelle : le temps euclidien t_E. Dans la notion de flot géométrique, il y a aussi la notion d'évolution d'une variété sous l'effet d'un paramètre, le paramètre d'évolution du flot T_f. Parfois les flots géométriques sont des approximations de flots de renormalisation (d'échelle de renormalisation μ). Nos résultats peuvent permettre de mieux comprendre le lien entre les deux échelles t_E et μ, et plus généralement entre les paramètres t_E et T_f.
- Il y a ensuite cette théorie non relativiste de la gravitation d'Horăva [17]. Nous donnerons plus de détails sur cette théorie dans la section 4 de ce chapitre. L'idée de base est de considérer notre espace-temps quadri-dimensionnel comme ayant une direction temporelle privilégiée et possédant la forme d'une foliation de surfaces en trois dimensions (hypothèses similaires aux espaces auto-duaux considérés ici). La dynamique de ces feuillets d'espace est décrite par un flot géométrique mélangeant les tenseurs de Ricci et de Cotton. Ce type de flot est étudié avec beaucoup de détails dans les publications 6 et 7.

Avant de partir dans un exposé moins qualitatif, mentionnons que dans la publication 4 nous avons également entrevu le cas d'une constante cosmologique non nulle, $\Lambda \neq 0$; mais pour des raisons diverses nous n'avons pas souhaité inclure pleinement ce cas dans ce rapport. Globalement on peut dire que toute l'étude faite dans cette section et la suivante peut s'étendre avec beaucoup de problèmes supplémentaires au cas de l'auto-dualité de la deux-forme de Weyl et non plus celle de Riemann. On donnera de temps en temps quelques remarques sur le cas $\Lambda = 0$, sans toutefois trop entrer dans le vif du sujet[1].

[1] Les résultats obtenus sont d'ailleurs préliminaires.

Notons également que nous avons le choix de travailler avec des formes auto-duales ou anti auto-duales. Un tel choix n'est que pure convention évidemment et nous choisissons de travailler avec la convention d'auto-dualité qui sur une deux-forme X_{ab} s'énonce

$$*X_{ab} = \frac{1}{2}\epsilon_{ab}{}^{cd}X_{cd} = X_{ab}. \tag{5.21}$$

Le groupe d'homéomorphismes de la variété de dimension trois, foliée par le temps dans le cas de l'espace auto-dual, ou évoluant sous l'effet d'un flot géométrique dans le cas éponyme, est noté G_{hom}.

Lorsque la courbure de Riemann est auto-duale, il en va de même pour la connexion de spin à une transformation de repère locale près à valeur dans $SU(2) \subset SO(4) \cong SU(2)_{\text{sd}} \otimes SU(2)_{\text{asd}}$, compatible avec la foliation.[2]. L'ensemble des transformations locales agissant sur la connexion de spin est donné par les plongements non équivalents de G_{hom} dans $SU(2)$. Ces transformations ont la remarquable propriété de ne pas être dépendantes du temps, contrairement au cas où $\Lambda \neq 0$. C'est cette absence de dépendance en le temps qui rend le problème globalement plus facile. Afin d'illustrer cette histoire de *plongements de groupes*, utilisons le chapitre précédent pour le cas de Bianchi IX et remarquons que les deux solutions axisymétriques, Eguchi-Hanson et Taub-Nut, correspondent aux deux façons évidentes de plonger $G_{\text{hom}} = SU(2)$ dans $SO(4) \approx SU(2) \times SU(2)$ (respectivement le plongement non-trivial et le plongement trivial).

Le principe même de foliation permet de mettre en valeur la décomposition $SU(2)_{\text{sd}} \otimes SU(2)_{\text{asd}}$ de $SO(4)$ qui est à la base du succès de notre entreprise. Les équations du premier ordre résultant de l'auto-dualité de la connexion de spin sont les équations d'un flot géométrique très simple mélangeant le flot de Ricci et une connexion $SU(2)$. Cette combinaison que l'on va voir dans la suite permet de créer le gradient qui transporte l'information du flot de la métrique tri-dimensionnelle. Quand cette connexion $SU(2)$ s'identifie avec la connexion de spin, le flot n'est pas de Ricci, mais presque (voir la suite), alors que quand le plongement de départ est trivial (annulation de la connexion $SU(2)$), le flot est de Ricci. Bien que la discussion paraisse simple, il n'est pas évident que tous les groupes de Bianchi amènent à des variétés de dimension trois permettant toute cette gymnastique. Nous montrons dans la suite que les seuls groupes de Bianchi qui permettent de plonger G_{hom} partiellement ou totalement dans $SU(2)_{\text{(a)sd}} \subset SO(4)$ sont les groupes de Bianchi I, II, $\text{VII}_{h=0}$et IX.

Nous présentons la classification dans la suite de cette section et analysons les résultats obtenus pour Bianchi IX avant de présenter les autres cas qui fonctionnent dans la section suivante. Nous verrons également des subtilités supplémentaires pour les algèbres Bianchi VI_{-1} et VIII. L'extension de cette classification au cas non-unimodulaire est un problème intéressant mais qui apparaît difficile.

[2]Pourquoi $SO(4)$ au lieu de $O(4)$? voir la publication 4.

2.2 Notre classification

Nous considérons des espaces-temps quadri-dimensionnels admettant des sections spatiales homogènes. Pour simplifier la discussion nous considérons une métrique diagonale (pour les algèbres de Bianchi considérées ici, il existe toujours une base où cette approximation est consistante, [38]. La métrique est alors prise de la forme

$$\mathrm{d}s^2 = \mathrm{d}t^2 + \sum_i \left(\gamma_i \sigma^i\right)^2 \tag{5.22}$$

où les $\gamma_i(t)$ sont des fonctions à déterminer et les $\{\sigma^i, i = 1, 2, 3\}$ sont les formes de Maurer-Cartan de G_{hom}. Ces formes obéissent à

$$\mathrm{d}\sigma^i = \frac{1}{2} C^i{}_{jk} \sigma^j \wedge \sigma^k, \tag{5.23}$$

où les vecteurs duaux e_i ($\sigma^i(e_j) = \delta^i_j$) forment une algèbre avec les relations de commutation

$$[e_i, e_j] = -C^i{}_{jk} e_k. \tag{5.24}$$

Les vecteurs de Killing ξ_i génèrent le groupe d'isométrie G_{hom} et satisfont à

$$[\xi_i, \xi_j] = C^i{}_{jk} \xi_k. \tag{5.25}$$

Nous utilisons un repère orthonormal en quatre dimensions $\{\theta^a, a = 0, \ldots, 3\}$ où

$$\mathrm{d}s^2 = \delta_{ab} \theta^a \theta^b = g_{ij} \sigma^i \sigma^j. \tag{5.26}$$

Les équations de structure de Cartan pour une métrique et une connexion sans torsion $\omega^a{}_b$ sont

$$\omega_{ab} = -\omega_{ba}, \quad \mathrm{d}\theta^a + \omega^a{}_b \wedge \theta^b = 0, \tag{5.27}$$

alors que la deux-forme de Riemann s'écrit

$$\mathcal{R}^a{}_b = \mathrm{d}\omega^a{}_b + \omega^a{}_c \wedge \omega^c{}_b \equiv \frac{1}{2} R^a{}_{bcd} \theta^c \wedge \theta^d, \tag{5.28}$$

et satisfait à l'identité de Bianchi

$$\mathcal{R}^a{}_b \wedge \theta^b = 0. \tag{5.29}$$

La un-forme de Ricci est quand à elle donnée par

$$\mathcal{R}_b = \mathcal{R}^a{}_b \left(e^a\right) = R_{bc} \theta^c, \tag{5.30}$$

où R_{bc} sont les composantes du tenseur de Ricci. Pour les espaces considérés (métrique (5.22)), la base orthonormale naturelle est $\theta^0 = \mathrm{d}t$ et $\theta^i = \gamma_i \sigma^i$, donnant lieu à

$$\mathrm{d}\theta^0 = 0, \quad \mathrm{d}\theta^i = \frac{\dot{\gamma}_i}{\gamma_i} \theta^0 \wedge \theta^i + \frac{1}{2} \frac{\gamma_i}{\gamma_j \gamma_k} c^i{}_{jk} \theta^j \wedge \theta^k. \tag{5.31}$$

La un-forme de connexion a pour composantes

$$\omega^i{}_0 = \frac{\dot{\gamma}_i}{\gamma_i} \theta^i \tag{5.32}$$

et

$$\omega^i{}_j = \frac{1}{2\gamma_1\gamma_2\gamma_3}\left[\left(\gamma_i^2 C^i{}_{jk} - \gamma_k^2 C^k{}_{ij} - \gamma_j^2 C^j{}_{ik})\right)\theta^k + 2\gamma^i\gamma^k C^i{}_{ji}\theta^i - 2\gamma^j\gamma^k C^j{}_{ij}\theta^j\right] \tag{5.33}$$

où l'indice k n'est pas sommé et les indices i, j et k prennent des valeurs différentes. L'action d'Hilbert-Einstein peut être exprimée comme

$$S = -\frac{1}{32\pi G}\int_{\mathcal{M}_4} \epsilon_{abcd}\left(\mathcal{R}^{ab} - \frac{\Lambda}{6}\theta^a\wedge\theta^b\right)\wedge\theta^c\wedge\theta^d, \tag{5.34}$$

où Λ est la constante cosmologique. Cette action est un extremum quand

$$\left(\mathcal{R}^{ab} - \frac{\Lambda}{3}\theta^a\wedge\theta^b\right)\wedge\theta^c\epsilon_{abcd} = 0. \tag{5.35}$$

Nous pouvons alors introduire la deux-forme de Weyl, on-shell,

$$\mathcal{W}^{ab} = \mathcal{R}^{ab} - \frac{\Lambda}{3}\theta^a\wedge\theta^b \equiv \frac{1}{2}W^{ab}{}_{cd}\theta^c\wedge\theta^d \tag{5.36}$$

et sa forme duale

$$\tilde{\mathcal{W}}^{ab} = \frac{1}{2}\epsilon^{ab}{}_{cd}\mathcal{W}^{cd}. \tag{5.37}$$

Les équations du mouvement (5.35) donnent alors

$$\tilde{\mathcal{W}}^c{}_d\wedge\theta^d = 0. \tag{5.38}$$

Une condition suffisante pour que (5.38) soit vérifiée est

$$\tilde{\mathcal{W}}^{ab} = \pm\mathcal{W}^{ab}, \tag{5.39}$$

comme conséquence de l'identité de Bianchi (5.29). Les équations (5.39) sont du second ordre, mais des équations du premier ordre peuvent être obtenues en considérant la connexion de spin. Cette connexion de spin et la forme de courbure appartiennent à la représentation antisymétrique **6** de $SO(4)$. Sous une rotation locale de $SO(4)$ du repère orthonormal

$$\theta^{a\prime} = \Lambda^{-1\,a}{}_b\theta^b, \tag{5.40}$$

elles se transforment selon

$$\mathcal{R}^{a\prime}{}_b = \Lambda^{-1\,a}{}_c\mathcal{R}^c{}_d\Lambda^d{}_b, \tag{5.41}$$

$$\mathcal{W}^{a\prime}{}_b = \Lambda^{-1\,a}{}_c\mathcal{W}^c{}_d\Lambda^d{}_b \tag{5.42}$$

et

$$\omega^{a\prime}{}_b = \Lambda^{-1\,a}{}_c\omega^c{}_d\Lambda^d{}_b + \Lambda^{-1\,a}{}_c\mathrm{d}\Lambda^c{}_b. \tag{5.43}$$

En décomposant $SO(4)$ comme $SU(2)_{\mathrm{sd}}\otimes SU(2)_{\mathrm{asd}}$, les formes ci dessus à valeurs dans $SO(4)$ peuvent se décomposer en parties à valeurs dans $SU(2)_{(\mathrm{a})\mathrm{sd}}$. Nous avons aussi ($\mathbf{6} = (\mathbf{3}_{\mathrm{sd}}, \mathbf{3}_{\mathrm{asd}})$) :

$$\varpi^a{}_b|_{(\mathrm{a})\mathrm{sd}} = \frac{1}{2}\left(\varpi^a{}_b \pm \tilde{\varpi}^a{}_b\right) \tag{5.44}$$

où

$$\tilde{\varpi}^{ab} = \frac{1}{2}\epsilon^{ab}{}_{cd}\varpi^{cd}; \tag{5.45}$$

ϖ signifie ω, $\mathcal{R}$ ou $\mathcal{W}$ et le signe $+$ est associé à la représentation auto-duale. En utilisant cette décomposition, nous pouvons décomposer la dynamique sur deux unformes, vecteurs de $SU(2)_{\text{(a)sd}}$: $\omega^a{}_b|_{\text{sd}}$ et $\omega^a{}_b|_{\text{asd}}$. Nous les notons comme

$$\begin{array}{lllllllll} \omega^0{}_1\Big|_{\text{asd}} & = & \omega^3{}_2\Big|_{\text{asd}} & = & A_1, & \omega^1{}_0\Big|_{\text{sd}} & = & \omega^3{}_2\Big|_{\text{sd}} & = & \Sigma^1, \\ \omega^0{}_2\Big|_{\text{asd}} & = & \omega^1{}_3\Big|_{\text{asd}} & = & A_2, & \omega^2{}_0\Big|_{\text{sd}} & = & \omega^1{}_3\Big|_{\text{sd}} & = & \Sigma^2, \\ \omega^0{}_3\Big|_{\text{asd}} & = & \omega^2{}_1\Big|_{\text{asd}} & = & A_3, & \omega^3{}_0\Big|_{\text{sd}} & = & \omega^2{}_1\Big|_{\text{sd}} & = & \Sigma^3. \end{array} \tag{5.46}$$

Jusqu'à la fin de cette section nous travaillons principalement avec l'auto-dualité de la 2-forme de Riemann[3]. Nous pouvons toujours nous ramener localement à $A_i \to 0$ ou $\Sigma^i \to 0$, et la loi de transformation de la forme A définie en (5.46), sous $SU(2)_{\text{asd}} \subset SO(4)$, est donnée par (5.43). Une connexion anti auto-duale de pure jauge est nécessairement de la forme $-\mathrm{d}\Lambda\Lambda^{-1}$. Elle définie alors un triplet de générateurs de $SU(2)$ réalisés par les formes σ^i apparaissant dans (5.22, 5.23) :

$$A_i = \frac{1}{2}\lambda_i\sigma^i, \quad i = 1, 2, 3. \tag{5.47}$$

Nous avons introduit un lot de paramètres λ_i pouvant prendre les valeurs 0, 1 ; dépendant des formes de Maurer-Cartan de $SU(2)_{\text{asd}}$, si elles peuvent se réaliser en les σ^i ($\lambda_i = 1$) ou non ($\lambda_i = 0$). La solution $\lambda_1 = \lambda_2 = \lambda_3 = 0$ revient à imposer l'auto-dualité dans le repère considéré, alors que dans les autres cas, l'auto-dualité est obtenue après une transformation de $SU(2)_{\text{asd}}$ appropriée. Comme mentionné plus haut, les valeurs des paramètres λ_i dépendent du plongement de G_{hom} dans $SU(2)$. Si aucun plongement n'est possible, comme pour le cas de Bianchi VIII, alors seule la solution $\lambda_i = 0$ est autorisée. Du point de vue de l'espace auto-dual, les λ_i sont des constantes d'intégration venant du passage des équations d'auto-dualité du second ordre aux intégrales premières du premier ordre. Les relations que doivent satisfaire ces constantes sont données par les trois équations de contraintes associées.

Si nous avions une constante cosmologique non nulle, il suffirait alors de remplacer la connexion A_i par

$$A_i = \frac{1}{2}\lambda_i(t)\sigma^i, \quad i = 1, 2, 3. \tag{5.48}$$

Dans ce cas ci, nous aurions un couplage des fonctions γ_i aux fonctions λ_j, et notre solution auto-duale pour la deux-forme de Weyl serait donnée par les nouvelles équations (en plus des équations du premier ordre sur les γ_j standard)

$$\dot{\lambda}_i + \frac{\Lambda_{\text{c}}}{3}\gamma_i = 0, \quad i = 1, 2, 3 \tag{5.49}$$

et

$$\lambda_i C^i{}_{jk} + \lambda_j\lambda_k + \frac{\Lambda_{\text{c}}}{3}\gamma_j\gamma_k = 0 \tag{5.50}$$

(i, j, k permutation cyclique de $1, 2, 3$, pas de sommation sur i).

[3] La classification des algèbres de Bianchi avec tous les outils nécessaires est donnée dans l'annexe B.

Liens avec les flots géométriques

Nous considérons les mêmes espaces-temps en quatre dimensions que ceux étudiés plus haut, et nous nous intéressons plus particulièrement à leurs feuillets tri-dimensionnels décris par la métrique

$$ds^2_{3D} = \sum_i \gamma_i^2 (\sigma^i)^2 = \sum_{\alpha,\beta=1}^{3} g_{\alpha\beta}\sigma^\alpha\sigma^\beta. \tag{5.51}$$

Cette métrique est celle d'un espace de dimension trois, M_3. A cet espace associons la variété $N_3(M_3)$ dont la métrique est

$$ds^2_{3D,N_3} = \sum_i \tilde{\gamma}_i (\sigma^i)^2 = \sum_{\alpha,\beta=1}^{3} \tilde{g}_{\alpha\beta}\sigma^\alpha\sigma^\beta. \tag{5.52}$$

Nous utilisons ensuite un flot de Ricci modifié donné par

$$\frac{d\tilde{g}_{\alpha\beta}}{dt} = \tilde{R}_{\alpha\beta}[\tilde{g}] + A_\alpha A_\beta \tag{5.53}$$

ou pour le cas diagonal considéré ici :

$$\frac{d\tilde{\gamma}_i}{dt} = \tilde{R}_{ii}[\tilde{g}] + A_i^2. \tag{5.54}$$

La connexion A est une pure jauge et ses composantes λ_i sont des constantes et satisfont les contraintes (5.58). Avec nos conventions en annexe B, les constantes de structure des algèbres unimodulaires ont la propriété $C^i{}_{jk} = 0$ quand $i = j$ ou $i = k$. Par conséquent, les équations de flot obtenues de (5.54) peuvent s'écrire comme

$$\begin{aligned} \frac{\dot{\tilde{\gamma}}_i}{\tilde{\gamma}_i} &= -\sum_{j,k=1}^{3} \frac{1}{4\tilde{\gamma}_1\tilde{\gamma}_2\tilde{\gamma}_3}\left[C^{i2}{}_{jk}\tilde{\gamma}_i^2 - 2C^{j2}{}_{ki}\tilde{\gamma}_j^2 + 2C^j{}_{ki}C^k{}_{ij}\tilde{\gamma}_j\tilde{\gamma}_k\right] + \frac{1}{2}\epsilon_{ijk}\tilde{\gamma}_j\tilde{\gamma}_k A_i^2, \\ \epsilon_{ijk} = 1 & \quad . \end{aligned} \tag{5.55}$$

De façon similaire, les équations d'auto-dualité associées à l'espace M_3 de métrique (5.51) (avec constante cosmologique Λ) peuvent s'écrire comme

$$\frac{\dot{\gamma}_i}{\gamma_i} = \sum_{j,k=1}^{3} \frac{\epsilon_{ijk}}{2\gamma_1\gamma_2\gamma_3}\left[-\frac{C^i{}_{jk}}{2}\gamma_i^2 + \frac{1}{2}(C^j{}_{ki}\gamma_j^2 + C^k{}_{ij}\gamma_k^2) + \lambda_i\gamma_j\gamma_k\right], \quad \epsilon_{ijk} = 1, \tag{5.56}$$

$$\dot{\lambda}_i = -\frac{\Lambda}{3}\gamma_i, \ i = 1,2,3 \tag{5.57}$$

avec les contraintes

$$\lambda_i C^i_{jk} = -\lambda_j\lambda_k - \frac{\Lambda}{3}\gamma_j\gamma_k, \ \epsilon_{ijk} = 1. \tag{5.58}$$

Dans le cas où $\Lambda = 0$, en utilisant l'annexe B, les équations (5.55) et (5.56) sont les mêmes pour les algèbres de Bianchi I, II, VII_0 et IX. Pour les algèbres de Bianchi VI_{-1} et VIII, les équations d'auto-dualité de la métrique (5.22) sont les mêmes que

celles du flot de Ricci associées à la métrique (5.52) de la variété N_3, où $\tilde{\gamma}_j = \epsilon\gamma_j$ et $\epsilon = \pm 1$ dépendant de j et des conventions.[4]. Pour les algèbres de Bianchi I, II, VII_0 et IX, (5.55) montre que le flot de Ricci pur ($A_i = 0$) sélectionne la branche non triviale de l'espace auto-dual correspondant (i.e. $(\lambda_1, \lambda_2, \lambda_3) \neq (0,0,0)$) quand

$$\exists\, j \neq k \neq i \neq j \text{ tel que } C^i_{jk} C^k_{ij} \neq 0, \tag{5.59}$$

soit pour les algèbres VII_0 et IX. Pour les deux autres cas, le flot de Ricci pure sélectionne la branche triviale. Dans chaque cas, les autres branches sont facilement obtenues en jouant sur la connexion de pure jauge A_i. Dans le paragraphe suivant nous donnons l'exemple de Bianchi IX avant de traiter les autres algèbres unimodulaires dans la section suivante.

Cas de $SU(2)$

Nous avons $G_{\mathrm{hom}} = SU(2)$. Les équations de l'auto-dualité, (5.48,5.49,5.50) donnent

$$\begin{aligned}
\dot{\gamma}_1 &= \frac{(\gamma_2-\gamma_3)^2-\gamma_1^2}{2\gamma_2\gamma_3} - \lambda_1 + 1, \quad \dot{\lambda}_1 = -\frac{\Lambda}{3}\gamma_1, \\
\dot{\gamma}_2 &= \frac{(\gamma_3-\gamma_1)^2-\gamma_2^2}{2\gamma_3\gamma_1} - \lambda_2 + 1, \quad \dot{\lambda}_2 = -\frac{\Lambda}{3}\gamma_2, \\
\dot{\gamma}_3 &= \frac{(\gamma_1-\gamma_2)^2-\gamma_3^2}{2\gamma_1\gamma_2} - \lambda_3 + 1, \quad \dot{\lambda}_3 = -\frac{\Lambda}{3}\gamma_3,
\end{aligned} \tag{5.60}$$

et

$$\lambda_i = \lambda_j\lambda_k + \frac{\Lambda}{3}\gamma_j\gamma_k \tag{5.61}$$

(i, j, k permutation cyclique de $1, 2, 3$). Nous posons $\Lambda = 0$. Deux branches différentes existent alors dans les équations ci-dessus. La première est obtenue avec $\lambda_i = 0$ (annulation de la partie anti auto-duale de la connexion de spin). Les équations (5.60) peuvent être résolues et donnent les solutions axisymétriques ($\gamma_1 \neq \gamma_2 = \gamma_3$), Eguchi–Hanson I et II [55, 56]. Une solution totalement anisotrope est également possible et donnée par [44]. La seconde branche correspond à $\lambda_i = 1$ (seule solution possible par symétrie). Ici, la partie anti auto-duale de la connexion de spin est une pure jauge et reflète le fait que $G_{\mathrm{hom}} \equiv SU(2)$ avec un unique plongement dans $SU(2)_{\mathrm{asd}}$. Une fois de plus, le système est intégrable et donne la solution de Taub-Nut et celle d'Halphen–Atiyah–Hitchin [46, 47] (solution régulière). Plus de détails sur ces deux solutions peuvent être trouvés dans le chapitre introductif précédent.

Le point le plus remarquable de notre travail est que les équations (5.60) et (5.61), décrivent aussi l'évolution d'une famille de surfaces de Bianchi IX sous flot géométrique. Considérons une telle famille avec la métrique (5.52) où les γ_i sont fonctions d'un paramètre t (qui n'a plus rien d'une coordonnée, c'est le paramètre d'évolution le long du flot). Comme annoncé plus haut *la solution euclidienne auto-duale est équivalente à celle donnée par le flot de Ricci pur*. Ceci est vrai lorsque la

[4] Il est immédiat de voir, pour des raisons dimensionnelles, pourquoi la métrique du feuillet tri-dimensionnel doit être la racine carrée de celle de l'espace-temps en quatre dimensions

connexion de spin anti auto-duale de l'espace auto-dual est une pure jauge, $\lambda_i = 1$, soit dans le cas de Taub-Nut. Pour tout autre cas, le flot géométrique décrivant l'évolution de la surface tri-dimensionnelle correspondante n'est pas le flot de Ricci pur, un champ de jauge $SU(2)$ étant couplé au système :

$$A^i = -\sigma^i. \tag{5.62}$$

2.3 Les autres algèbres unimodulaires de la classification

On donne les résultats sans commentaires particuliers, l'intérêt de cette partie est de montrer que Bianchi IX n'est pas un cas isolé, mais que l'on peut avoir des phénomènes similaires pour d'autres algèbres de Bianchi. Pour les expressions explicites des formes de Maurer-Cartan et des constantes de structure, voir l'annexe B.

Bianchi I Dans ce cas G_{hom} est isomorphe au groupe des translations en dimension 3, T_3. Les équations d'auto-dualité sont données par

$$\begin{aligned}
\dot{\gamma}_1 &= -\lambda_1 + 1, \quad \dot{\lambda}_1 = -\frac{\Lambda}{3}\gamma_1, \\
\dot{\gamma}_2 &= -\lambda_2 + 1, \quad \dot{\lambda}_2 = -\frac{\Lambda}{3}\gamma_2, \\
\dot{\gamma}_3 &= -\lambda_3 + 1, \quad \dot{\lambda}_3 = -\frac{\Lambda}{3}\gamma_3,
\end{aligned}$$

et

$$\lambda_j \lambda_k = -\frac{\Lambda}{3}\gamma_j \gamma_k \tag{5.63}$$

(ijk permutation cyclique de $1, 2, 3$). Si $\Lambda = 0$, la solution triviale $\lambda_i = 0$ implique $\dot{\gamma}_i = 0$, qui est aussi l'équation triviale de flot de Ricci de Bianchi I. La branche non triviale

$$\exists! j, \ \lambda_j \neq 0 \text{ et } \lambda_{k \neq j} = 0 \tag{5.64}$$

peut être obtenue avec une connexion de jauge $SU(2)$ appropriée.

Bianchi II C'est l'algèbre d'Heisenberg. Les équations d'auto-dualité sont

$$\begin{aligned}
\dot{\gamma}_1 &= \frac{-\gamma_1^2}{2\gamma_2\gamma_3} - \lambda_1 + 1, \quad \dot{\lambda}_1 = -\frac{\Lambda}{3}\gamma_1, \\
\dot{\gamma}_2 &= \frac{\gamma_1^2}{2\gamma_3\gamma_1} - \lambda_2 + 1, \quad \dot{\lambda}_2 = -\frac{\Lambda}{3}\gamma_2, \\
\dot{\gamma}_3 &= \frac{\gamma_1^2}{2\gamma_1\gamma_2} - \lambda_3 + 1, \quad \dot{\lambda}_3 = -\frac{\Lambda}{3}\gamma_3,
\end{aligned}$$

et

$$\begin{aligned}
\lambda_1\lambda_2 &= -\frac{\Lambda}{3}\gamma_1\gamma_2, \\
\lambda_1\lambda_3 &= -\frac{\Lambda}{3}\gamma_1\gamma_3, \\
\lambda_1 &= \lambda_2\lambda_3 + \frac{\Lambda}{3}\gamma_2\gamma_3.
\end{aligned} \tag{5.65}$$

Si $\Lambda = 0$, (5.65) implique qu'outre la solution triviale $\lambda_i = 0$, il existe une solution non triviale donnée par

$$\exists j \neq 1,\ \lambda_j \neq 0 \text{ et } \lambda_{k\neq j} = 0. \tag{5.66}$$

Dans ce cas, le flot de Ricci donne les équations correspondant au cas trivial $\lambda_i = 0$. Les branches non triviales décrites par $\lambda_{i_0} \neq 0, \lambda_{i\neq i_0} = 0$ pour $i_0 = 2, 3$, peuvent être obtenues à partir d'un flot de Ricci modifié comme pour Bianchi I.

Bianchi VII$_0$ C'est l'algèbre de Lie du groupe de symétries du plan. Les équations d'auto-dualité sont données par

$$\begin{aligned}
\dot\gamma_1 &= \frac{\gamma_1^2 - \gamma_2^2}{2\gamma_2\gamma_3} - \lambda_1 + 1, & \dot\lambda_1 &= -\frac{\Lambda}{3}\gamma_1, \\
\dot\gamma_2 &= \frac{\gamma_2^2 - \gamma_1^2}{2\gamma_3\gamma_1} - \lambda_2 + 1, & \dot\lambda_2 &= -\frac{\Lambda}{3}\gamma_2, \\
\dot\gamma_3 &= -\frac{(\gamma_1+\gamma_2)^2}{2\gamma_1\gamma_2} - \lambda_3 + 1, & \dot\lambda_3 &= -\frac{\Lambda}{3}\gamma_3,
\end{aligned} \tag{5.67}$$

et

$$\begin{aligned}
\lambda_1 &= -\lambda_2\lambda_3 - \frac{\Lambda}{3}\gamma_2\gamma_3, \\
\lambda_2 &= -\lambda_1\lambda_3 - \frac{\Lambda}{3}\gamma_1\gamma_3, \\
\lambda_1\lambda_2 &= -\frac{\Lambda}{3}\gamma_1\gamma_2.
\end{aligned} \tag{5.68}$$

Quand $\Lambda = 0$ nous avons la solution triviale $\lambda_i = 0$ alors qu'il existe une solution non triviale donnée par

$$\lambda_3 \neq 0,\ \lambda_{1,2} = 0. \tag{5.69}$$

C'est cette branche non triviale qui est sélectionnée par le flot de Ricci. La branche triviale est obtenue par le flot de Ricci modifié standard ici.

Nous avons obtenu bien d'autres résultats, en commençant par la généralisation de cette étude au cas $\Lambda \neq 0$. Pour plus de détails, voir les publications 4 et 5.

Dans la suite nous parlons d'une autre utilisation des flots géométriques en physique : l'étude de la théorie d'Horăva-Lifshitz. Nous avons étudié cette théorie en long et en large dans le cas où la condition de balance détaillée est imposée. Nous verrons dans la section suivante que de nombreux résultats nouveaux tant sur la physique de la théorie que sur les mathématiques des flots géométriques induits, peuvent être obtenus.

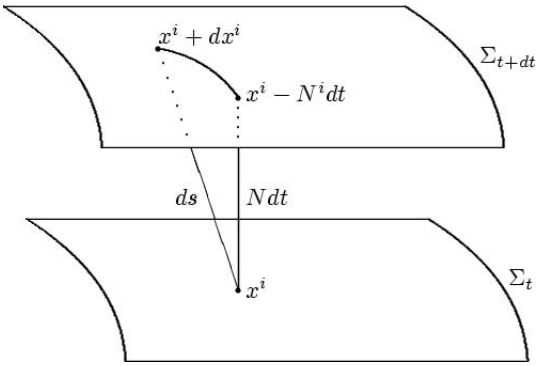

FIG. 5.1 – Principe de la décomposition ADM. On peut voir cette dernière comme une généralisation du théorème de Pythagore, et on comprend mieux le sens physique des différents termes de cette décomposition.

3 Théorie d'Hořava et flots géométriques

La théorie d'Horăva est une théorie non relativiste de la gravitation, complète dans l'UV. Ce dernier point est un grand succès de la théorie. La théorie des cordes avait d'ailleurs pour but lors de son introduction et du début de son étude, de produire une théorie de la gravitation qui soit régulière dans l'UV. La raison principale étant la nature étendue des cordes qui était censée éliminer les divergences UV qui gênent considérablement toute approche de théorie des champs. La théorie d'Horăva se distingue de la RG par le fait qu'elle n'est pas invariante sous le groupe des difféomorphismes complet, mais au contraire sous un groupe réduit correspondant à la décomposition ADM d'une métrique.

Décomposition ADM La figure 5.1 illustre mes propos. Elle est tirée de [57]. La décomposition est la suivante :

$$ds^2 = -N(t,x)^2 dt^2 + g_{ij}(dx^i + N^i dt)(dx^j + N^j dt). \tag{5.70}$$

Dans cette décomposition nous avons introduit les fonctions $N(t,x)$ et $N^i(t,x)$. L'action d'Hilbert Einstein d'espace-temps,

$$S = \int d^4x \sqrt{-g} R, \tag{5.71}$$

se réécrit alors comme

$$S_3 = \int dt \int_\Sigma d^3x \left(\pi^{ij} \dot{g}_{ij} - N^i H_i - NH \right), \tag{5.72}$$

où nous avons introduit les variables

$$\pi^{ij} = \sqrt{g}(K^{ij} - g^{ij}K),\ H_i = -2\nabla_j \pi_i^j,\ H = \frac{1}{\sqrt{g}} g_{ij} g_{kl} (\pi^{ik}\pi^{jl} - \pi^{ij}\pi^{kl}) - \sqrt{g}R. \tag{5.73}$$

Cette décomposition permet entre autre d'interpréter dans certains cas l'évolution de l'Univers comme le mouvement d'une particule dans un potentiel. L'étude de ce potentiel révèle des propriétés parfois très intrigantes sur l'Univers, ses conditions initiales, $\cdots$. De plus, on peut mettre l'action résultante sous la forme

$$S_3 = \int dt \int_\Sigma d^3x \left(\pi^{ij}\dot{g}_{ij} - \mathcal{H}(g_{ij}, \pi^{kl})\right), \tag{5.74}$$

où la fonction $\mathcal{H}(g_{ij}, \pi^{kl})$ fait office de densité hamiltonienne décrivant l'Univers. De façon tout à fait naturelle, les équations d'Hamilton tirées de cette densité hamiltonienne doivent être les équations du mouvement de notre système.

On paramètre ensuite la métrique du feuillet d'espace, g_{ij}, comme étant diagonale et donnée par

$$g_{11} = e^{\beta_+ + \sqrt{3}\beta_- + \Omega},\ g_{22} = e^{\beta_+ - \sqrt{3}\beta_- + \Omega} \text{ et } g_{33} = e^{-2\beta_+ + \Omega}. \tag{5.75}$$

On a alors $\det(g) = e^{3\Omega}$, le volume du feuillet d'espace. L'avantage de cette paramétrisation, par rapport à simplement $g_{ii} = \gamma_i$, est de mettre en valeur de nouveaux points fixes dans les coordonnées $(\beta_\pm, \Omega)$ qui ne sont pas présents dans les coordonnées γ_i. Bien sur, ces nouveaux points fixes correspondent à des solutions précises qui existent aussi avec la paramétrisation des γ_i ; mais dans ce cas ci les γ_i sont dépendant du temps et ne tendent plus vers des constantes mais vers des fonctions dépendant du temps et parfois compliquées.

Ces attracteurs n'apparaissent que lorsque le flot étudié n'est pas normalisé de sorte que le volume puisse évoluer. Ils sont très compliqués à déterminer, et il est très difficile de prétendre les avoir tous trouvés. Néanmoins, dans le cas où la constante cosmologique Λ est nulle et pour une métrique axisymétrique, on prétend les avoir tous trouvé tous ces attracteurs. D'après leur étude, il apparait que très souvent, une paramétrisation de la métrique autre que les γ_i les transcrit en termes de points fixes du flot, et non plus d'attracteurs compliqués.

Un avantage plus certain de la paramétrisation avec les $(\beta_\pm, \Omega)$ est l'étude de solutions à rebonds où le volume du feuillet d'espace diminue dans un premier temps puis augmente ensuite. Nous parlons ici de solutions avec rebonds dans le cas de la gravité d'Horăva pure, non pas dans le cas de la gravité d'Horăva avec la présence de matière en plus.

Si on étudie la cosmologie d'un espace homogène, alors nous pouvons poser $N = 1$ et $N^i = 0$. Dans ce cas la discussion est simplifiée et la densité hamiltonienne est la suivante :

$$H(p_\pm, \beta_\pm) = \sqrt{p_+^2 + p_-^2 + W(\beta_\pm)}, \tag{5.76}$$

où $\dot{\beta}_\pm = \frac{\partial H}{\partial p_\pm}$ et $\dot{p}_\pm = -\frac{\partial H}{\partial \beta_\pm}$.

Théorie d'HL Dans la théorie d'Horăva, sous une transformation de changement d'échelle, le temps ne se comporte plus comme une dimension d'espace, au contraire nous avons la transformation

$$t \to l^3 t,\ x \to lx. \tag{5.77}$$

C'est cette transformation particulière qui donne à la théorie son caractère non relativiste. La théorie d'Horăva utilise la décomposition ADM d'une métrique où les variables dynamiques sont N, N_i et g_{ij}.

$$ds^2 = -N(t,x)^2 dt^2 + g_{ij}(dx^i + N^i dt)(dx^j + N^j dt). \tag{5.78}$$

Sans entrer dans les détails, cette théorie qui est finie dans l'UV (donc renormalisable, ceci est du à la présence de termes impliquant le tenseur de Cotton) donne la Relativité Générale dans l'IR. On a donc un moyen de modifier la RG pour la rendre finie dans l'UV (la RG n'est maitrisée que dans l'IR, tout parait ainsi consistent). Dans cette thèse nous n'avons pas cherché à vérifier si oui ou non la théorie d'Horăva s'accorde avec l'expérience. De nombreux travaux ([58] par exemple) ont montré que l'absence de symétries aussi nombreuses qu'en RG entraine des problèmes avec la théorie d'Horăva. Il existe un mode physique supplémentaire par exemple. On ne retrouve également pas la solution de Schwarzschild.

L'action de la théorie d'Horăva est la somme d'un terme cinétique et d'un terme de potentiel : $S = S_K + S_V$ où

$$S_K = \frac{2}{\kappa^2} \int dt d^3x \sqrt{g} N (K_{ij} K^{ij} - \lambda K^2), \tag{5.79}$$

avec $K_{ij} = \frac{1}{2N}(\dot{g}_{ij} - \nabla_i N_j - \nabla_j N_i)$ la courbure extrinsèque et $K = g^{ij} K_{ij}$. La Relativité Générale est retrouvée dans cette théorie pour $\lambda = 1$. Pour l'action S_V, Horăva a choisi une action obéissant à une condition de *balance détaillée*. Cette action est donnée par

$$S_V = \int dt d^3x \sqrt{g} N V \tag{5.80}$$

où (nous introduisons diverses constantes dans un souci de comparaison avec la littérature, mais la plupart de ces constantes vont être absorbées par exemple dans une redéfinition du temps)

$$\begin{aligned} V \;=\; & \frac{\kappa^2}{2w_{\mathrm{CS}}^2} C^{ij} C_{ij} - \frac{\kappa^2}{w_{\mathrm{CS}} \kappa_W^2} C^{ij} R_{ij} + \\ & \frac{\kappa^2}{2\kappa_W^4} \left(R^{ij} R_{ij} - \frac{4\lambda - 1}{4(3\lambda - 1)} R^2 \right) + \\ & \frac{\kappa^2 \Lambda_W}{2(3\lambda - 1)\kappa_W^4} \left(R - 3\Lambda_W \right). \end{aligned} \tag{5.81}$$

La super-métrique $\mathcal{G}^{ij;kl}$ dépend d'un paramètre *a priori* arbitraire λ, son inverse est donnée par

$$\mathcal{G}_{ij;kl} = \frac{1}{2} \left(g_{ik} g_{jl} + g_{il} g_{jk} \right) - \frac{\lambda}{3\lambda - 1} g_{ij} g_{kl}. \tag{5.82}$$

Une conséquence majeure de la présence de *la condition de balance détaillée* est que les équations du mouvement se réduisent à des équations du premier ordre donnant lieu à un flot géométrique :

$$\frac{1}{N} \partial_t g_{ij} = -\frac{\kappa^2}{\kappa_W^2} \left(R_{ij} - \frac{2\lambda - 1}{2(3\lambda - 1)} R g_{ij} + \frac{\Lambda_W}{1 - 3\lambda} g_{ij} \right) + \frac{\kappa^2}{w_{\mathrm{CS}}} C_{ij}. \tag{5.83}$$

Dans les publications 6 et 7 nous avons analysé ce flot compliqué sous beaucoup d'aspects. Ici, on se contentera de l'appliquer au cas de Bianchi IX. Après avoir rappelé des résultats standards pour le flot de Ricci normalisé ($\mu = \infty, \Lambda_W = 0, \lambda = \infty$), on parlera du flot de Cotton pur et du cas beaucoup plus intéressant quand $\Lambda_W = 0$ uniquement. On s'attardera sur ce cas ci en étudiant en partie le cas d'un flot non normalisé (c'est à dire ne maintenant pas le volume constant). Enfin, nous donnerons quelques résultats sur le cas $\Lambda_W \neq 0$, beaucoup plus compliqué bien entendu.

Le fait de pouvoir écrire des équations du mouvement du premier ordre indique des propriétés très particulières de la théorie d'Horăva, et même contradictoires ! En effet, on s'attendrait à obtenir des équations du second ordre, comme celles de la RG, mais moins bien déterminées que celles de la RG, car on a moins de symétries dans la théorie d'Horăva avec un groupe de difféomorphismes particulier comparé à la RG. Cependant c'est le contraire qui se passe, nous avons des équations mieux déterminées car du premier ordre ! On a besoin de moins de conditions initiales ! Ceci est évidemment dû à cette intrigante *condition de balance détaillée* qui n'est pas sans rappeler une condition d'auto-dualité en gravitation relativiste standard. Il faut cependant garder à l'esprit que la *condition de balance détaillée* donne des équations du premier ordre, solutions des équations du second ordre dans le Lorentzien, alors que l'auto-dualité donne des équations du premier ordre solutions de celles du second ordre dans l'euclidien.

Les différents travaux qui ont eu lieu sur la théorie d'Horăva ont montré que pour qu'elle soit plus proche de la vérité expérimentale, il fallait oublier cette *condition de balance détaillée*. Nous augmentons dans ce cas la complexité des équations du mouvement, mais nous ne traitons pas ce cas ici.

Lors de l'étude du flot géométrique (5.83), nous avons introduis, en suivant [50], une méthode graphique de visualisation des différents résultats assez intéressante. Cette méthode permet une étude plus complète et enrichissante.

Dans cette section, nous développons certains résultats obtenus dans la publication 7. Afin d'éviter un rapport trop long et trop catalogue, on omettra volontairement d'autres résultats. En particulier on ne dira quasiment rien à propos de l'approche canonique à la théorie d'HL, sujet de la publication 6, et nous ne mentionnerons que l'étude de Bianchi IX. Pour plus de détails, voir les publications 6 et 7.

3.1 Flot de Ricci+Cotton normalisé

Le flot le plus général intervenant dans la théorie d'HL peut dans le cas d'une métrique diagonale standard ($g_{00} = N^2, g_{ii} = \gamma_i$) être considéré de la forme[5]

$$\frac{d\gamma_i}{dt} = -R_{ii} + \underbrace{\left(\frac{\lambda - \frac{1}{2}}{3\lambda - 1}\right)}_{\beta} R\gamma_i + \frac{\Lambda_W}{3\lambda - 1}\gamma_i + \frac{1}{\mu}C_{ii}. \tag{5.84}$$

[5]Nous introduisons $\mu = \frac{w_{CS}}{\kappa_W^4}$ et redéfinissons le temps $dt \to dT = \frac{N\kappa^2}{\kappa_X^4}dt$.

La relation entre β et λ est illustrée par la figure 5.2 Dans ce paragraphe nous allons

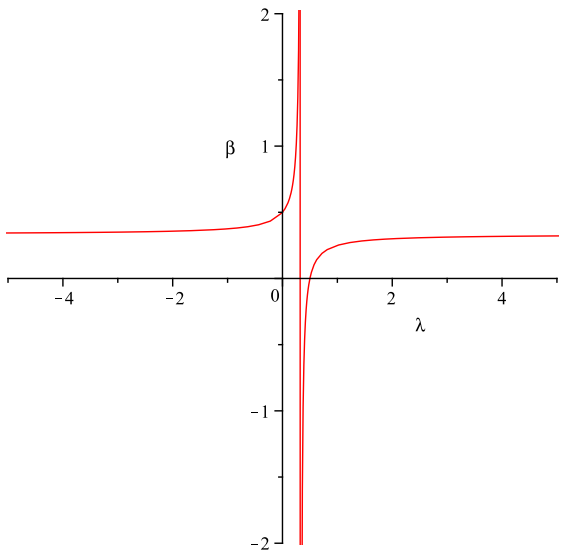

FIG. 5.2 – $\beta(\lambda)$

nous restreindre à $\Lambda_W = 0$ et $\beta = \frac{1}{3}$. Dans ce cas le flot préserve le volume car d'une part le tenseur de Cotton est sans trace (donc le flot de Cotton préserve le volume) et d'autre part la partie du flot impliquant le tenseur de Ricci est également sans trace lorsque $\beta = \frac{1}{3}$. L'avantage de ce type d'hypothèse est que l'on peut alors se limiter à deux fonctions indépendantes sur trois initialement, nous posons alors $\gamma_3 = \frac{L^6}{64\gamma_1\gamma_2}$ où L est une constante et $\gamma_{1,2}$ sont les deux variables indépendantes.

Nous considérons une variété de groupe de $SU(2)$ décrite par la métrique

$$ds^2 = Ndt^2 + \sum_i \gamma_i \sigma_i^2 \tag{5.85}$$

où les formes de Maurer-Cartan sont données en annexe B. Les composantes du tenseur de Riemann, de Cotton et le scalaire de courbure s'obtiennent par permutations circulaires à partir de

$$R = \frac{1}{2\gamma_1\gamma_2\gamma_3}\left[2\gamma_1\gamma_2 + 2\gamma_2\gamma_3 + 2\gamma_3\gamma_1 - \gamma_1^2 - \gamma_2^2 - \gamma_3^2\right], \tag{5.86}$$

$$R_{11} = \frac{1}{2\gamma_2\gamma_3}\left[\gamma_1^2 - (\gamma_2 - \gamma_3)^2\right], \tag{5.87}$$

$$C_{11} = -\frac{\gamma_1}{(\gamma_1\gamma_2\gamma_3)^{\frac{3}{2}}}\left[\gamma_1^2(2\gamma_1 - \gamma_2 - \gamma_3) - (\gamma_2 + \gamma_3)(\gamma_2 - \gamma_3)^2\right]. \tag{5.88}$$

Lorsque $\mu = \infty$ nous obtenons le flot de Ricci normalisé tel qu'étudié par [36] par exemple. Le flot de Cotton pure a lui aussi été étudié dans le cas de Bianchi IX, par [50]. Mettre les deux flots en compétition au sein d'un même et unique flot est très intéressant car de nouveaux phénomènes vont apparaître.

Il est commode de poser

$$\gamma_1 = \frac{xL^2}{4}, \quad \gamma_2 = \frac{yL^2}{4}, \quad \gamma_3 = \frac{L^2}{4xy} \ , \tag{5.89}$$

ainsi que

$$\tau = \frac{4}{L^2}T \ , \qquad \mu = \frac{w_{CS}L}{\kappa_W^2} \ . \tag{5.90}$$

Les équations à étudier dans le cas de Bianchi IX sont donc données par

$$\begin{aligned} \frac{\mathrm{d}x}{\mathrm{d}\tau} &= \frac{1}{\mu x^2 y^3}\Big\{ \left(1 + \frac{\mu}{3}xy + xy^2\right)\left(1 - xy^2\right)^2 \\ &\quad + \left(\frac{\mu}{3} + x\right)\left(1 + xy^2 - 2x^2y\right)x^3y^2 \Big\}, \end{aligned} \tag{5.91}$$

$$\begin{aligned} \frac{\mathrm{d}y}{\mathrm{d}\tau} &= \frac{1}{\mu x^3 y^2}\Big\{ \left(1 + \frac{\mu}{3}xy + x^2y\right)\left(1 - x^2y\right)^2 \\ &\quad + \left(\frac{\mu}{3} + y\right)\left(1 + x^2y - 2xy^2\right)x^2y^3 \Big\}. \end{aligned} \tag{5.92}$$

De manière générale nous ne savons pas intégrer ces équations en toute généralité. Ceci n'est possible que si $\mu = \infty$ ou bien $\gamma_1 = \gamma_2$ par exemple. Cependant l'étude du cas axisymétrique $\gamma_1 = \gamma_2$, bien qu'intéressante, est assez pédestre, et on renvoie le lecteur à la publication 7 pour tous les détails. En fait nous allons voir que l'on peut parfaitement étudier en grande partie le cas général de manière analytique. L'idée est d'utiliser la *théorie des systèmes dynamiques*.

Il existe des solutions simples aux équations du flot, les **points fixes**. Il peut y en avoir de trois types : isotrope, axisymétrique et anisotrope. Nous montrons dans la publication 7 qu'il n'en existe pas d'anisotrope, et nous classifions ces points fixes, ce qui est reporté ici.

On notera $(x, y) = (x_0, y_0)$ un point fixe, si nous linéarisons autour de ce point

$$x(t) = x_0(1 + \delta x(t)), \ y(t) = y_0(1 + \delta y(t)), \tag{5.93}$$

nous obtenons

$$\frac{\mathrm{d}}{\mathrm{d}\tau}\begin{pmatrix}\delta x \\ \delta y\end{pmatrix} = \begin{pmatrix} a & b \\ c & d\end{pmatrix}, \begin{pmatrix} x \\ y\end{pmatrix}, \tag{5.94}$$

où $b = c = 0$ et $a = d = -\left(1 + \frac{3}{\mu}\right)$. Le système linéarisé est automatiquement diagonalisé dans le sens où $b = c = 0$. La stabilité de ce point fixe dépend alors de μ :

- $1 + \frac{3}{\mu} > 0 \to \{\mu < -3 \text{ ou } \mu > 0\}$: le point fixe isotrope est stable,
- $1 + \frac{3}{\mu} < 0 \to \mu > -3$: le point fixe isotrope est instable,
- $\mu = -3$: les effets du tenseur de Ricci et de celui de Cotton se compensent, tous les points dans un voisinage du point fixe sont des points d'équilibre.

On peut retrouver ce résultat en regardant le temps caractéristique d'isotropisation τ dans le cas du flot de Ricci normalisé et dans celui du flot de Cotton, nous avons

$$\tau_R = \frac{1}{4},\ \tau_C = \frac{|\mu|}{12}. \tag{5.95}$$

Le point fixe isotrope est stable si et seulement si $\tau_R > \tau_C$ quand μ est négatif, autrement dis, si le flot de Ricci est suffisamment rapide pour rendre le système isotrope avant que le flot de Cotton n'impose l'anisotropie. On retrouve alors les mêmes résultats que ceux présentés plus haut.

Pour μ négatif, nous avons d'autres points fixes : des points fixes axisymétriques. Étant donné que nous avons trois choix possibles pour l'axisymétrie, il n'est pas curieux de trouver trois copies du même point fixe. Dans le plan (x, y) ces points fixes sont situés

- sur la diagonale $x = y$ avec $x_\star = \sqrt{\frac{-3}{\mu}}$,
- sur la branche $x^2 y = 1$ avec $x_\star = \sqrt{\frac{-3}{\mu}}$,
- sur la branche $xy^2 = 1$ avec $y_\star = \sqrt{\frac{-3}{\mu}}$.

Quand $\mu = -3$, ces points fixes se confondent avec le point fixe isotrope.

Pour déterminer la stabilité de ces points fixes, nous devons une nouvelle fois linéariser. Des propriétés de symétrie nous enseignent que nous pouvons nous limiter au premier, sur la diagonale $x = y$. La linéarisation autour de ce dernier est alors donnée par

$$\frac{\mathrm{d}}{\mathrm{d}\tau}\begin{pmatrix}\delta x\\ \delta y\end{pmatrix} = \frac{1}{2}\begin{pmatrix}\zeta_1+\zeta_2 & \zeta_1-\zeta_2\\ \zeta_1-\zeta_2 & \zeta_1+\zeta_2\end{pmatrix}\begin{pmatrix}\delta x\\ \delta y\end{pmatrix} \tag{5.96}$$

où

$$\zeta_1 = \frac{2}{3}\sqrt{-\frac{\mu}{3}}\left[\left(-\frac{\mu}{3}\right)^{\frac{3}{2}} - 1\right], \tag{5.97}$$

$$\zeta_2 = \frac{2}{3}\sqrt{-\frac{\mu}{3}}\left[\left(-\frac{3}{\mu}\right)^{\frac{3}{2}} - 1\right]\left[4\left(-\frac{3}{\mu}\right)^{\frac{3}{2}} - 1\right]. \tag{5.98}$$

Les deux ζ_i s'annulent quand $\mu = -3$ alors que ζ_2 a une autre racine pour $\mu = -6\sqrt[3]{2} \approx -7.56$. Par conséquent

- si $\mu < -6\sqrt[3]{2}$: $0 < \zeta_i$,
- si $-6\sqrt[3]{2} < \mu < -3$: $\zeta_2 < 0 < \zeta_1$,
- si $-3 < \mu < 0$: $\zeta_1 < 0 < \zeta_2$.

On constate ainsi que les trois points fixes axisymétriques ne sont jamais stables : ils sont instables pour $\mu < -6\sqrt[3]{2}$ et point selle autrement.

Résumé Pour $\mu > 0$ il y a un unique point fixe, qui plus est isotrope et stable, qui attire toutes les trajectoires en son voisinage (voir Fig. 5.3).

Pour $\mu < 0$ nous avons des points fixes axisymétriques ainsi qu'un point fixe isotrope. Leurs propriétés de stabilité ont été étudiées et pour $\mu = -3$ tous les

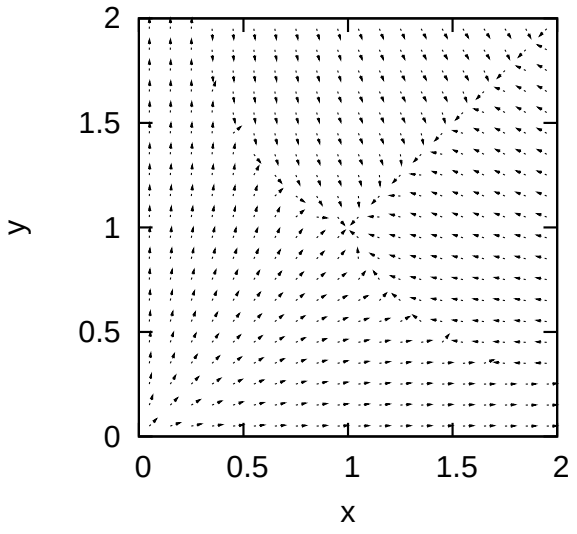

FIG. 5.3 – Point fixe isotrope pour $\mu > 0$ ($\mu = 2$ ici).

points fixes coalescent. Les figures 5.4,5.5,5.6 illustrent les propriétés de ces points fixes pour diverses valeurs de μ. On trouvera également dans la publication 7 des détails concernant un point fixe complètement anisotrope quand $\mu < -6 \cdot 2^{1/3}$.

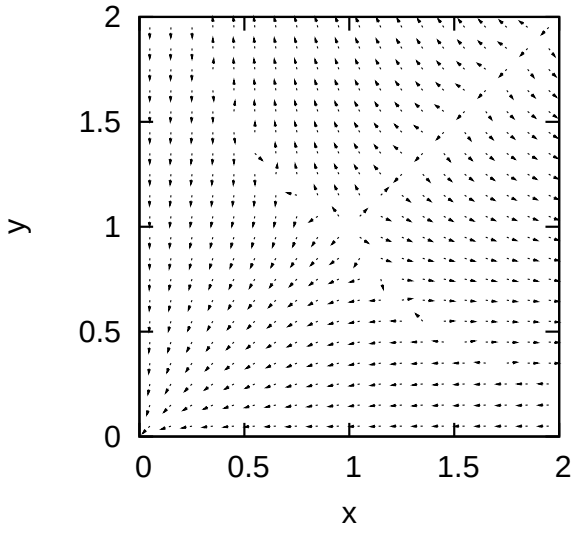

FIG. 5.4 – Points fixes pour $-3 < \mu < 0$ (ici $\mu = -2$).

Pour plus de détails concernant le flot de Ricci+Cotton normalisé, voir la publication 7.

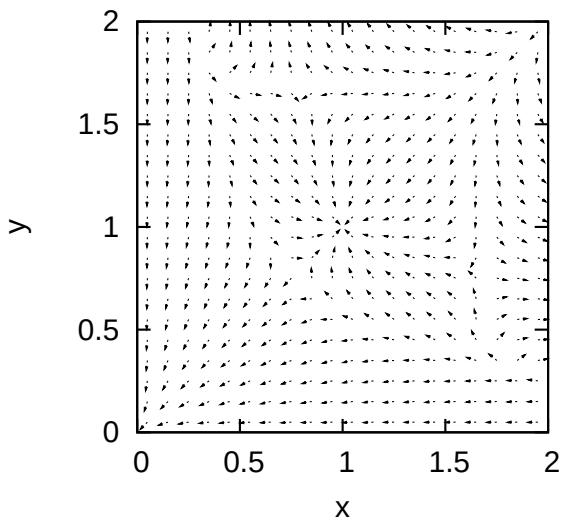

FIG. 5.5 – Points fixes pour $-6 \cdot 2^{1/3} < \mu < -3$ (ici $\mu = -5$).

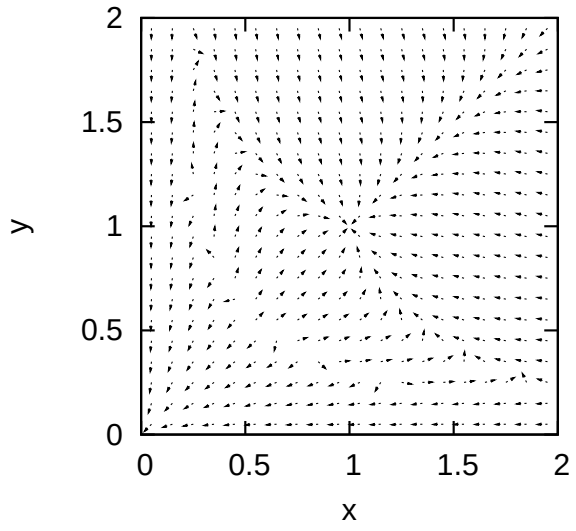

FIG. 5.6 – Points fixes pour $\mu < -6\,2^{1/3}$ (ici $\mu = -10$).

3.2 Flot de Ricci+Cotton non normalisé

Dans le paragraphe précédent nous avons pu constater que malgré l'hypothèse de volume préservé, le flot global était relativement compliqué à décrire, il est facile de comprendre que c'est encore plus le cas quand on relaxe l'hypothèse de conservation du volume. Dans ce cas ci, l'hypothèse simplificatrice qu'il convient de faire est l'axisymétrie : $\gamma_2 = \gamma_3$. Des résultats sur le cas complètement anisotrope ont été obtenus, mais nous n'en parlons pas ici.

Il y a deux types de flots non normalises que l'on peut construire avec le flot

de Ricci et celui de Cotton, correspondant aux deux choix de paramètres

$$(\mu = \infty, \beta \neq \frac{1}{3}),\ (\mu \neq \infty, \beta \neq 0). \tag{5.99}$$

Curieusement, le premier type de flot n'a pas été étudié dans la littérature. C'est pourtant un exemple très simple de flot non normalisé qui permet de poser les conventions. On remarque ainsi que ce flot, dans le cas de Bianchi IX, entraine toujours l'isotropie, avec le volume qui diverge pour $\beta > \frac{1}{3}$ et qui tend vers 0 pour $\beta < \frac{1}{3}$. On ne peut pas avoir axisymétrie uniquement avec ce flot, il faut un flot plus compliqué.

Si on considère le second type de flot il est alors possible d'obtenir une variété de phénomènes plus vaste. Comme le volume n'est plus conservé, les points fixes ne sont plus qu'une partie des solutions possibles, d'autres **attracteurs** existent. Afin d'éviter toute ambiguïté de terminologie, on dira qu'un **attracteur** est une classe de solutions présentant des similitudes. Les points fixes sont des attracteurs au même titre que des solutions ne tendant pas vers des constantes. Par exemple on verra que la solution isotrope est un attracteur qui soit diverge soit tend vers 0 quand t augmente.

Nous allons présenter les différents attracteurs obtenus pour le cas axisymétrique en insistant sur le fait que nous ne proposons pas ici de classification. Une telle classification reviendrait à dire que suivant telles valeurs de β et μ, telles valeurs des conditions initiales, nous avons telle solution. Nous ne sommes pas loin d'un tel résultat et laissons ceci pour un travail ultérieur.

Point fixe Demander $\dot{\gamma}_i = 0$ implique d'une part

$$\mu < 0, \tag{5.100}$$

et d'autre part

$$\gamma_1 = \frac{36}{\mu^2} = 4\gamma_2 = \gamma_1^0. \tag{5.101}$$

L'axisymétrie de ce point fixe est en accord avec le fait que $\mu < 0$. On pose ensuite (où les $\tilde{\gamma}_i$ sont des petites perturbations) $\tilde{\gamma}_1 = \frac{\delta x}{\gamma_1^0}$ et $\tilde{\gamma}_2 = \frac{\delta y}{\gamma_2^0}$ et

$$\gamma_1(t) = \gamma_1^0 \left(1 + \tilde{\gamma}_1(t)\right), \quad \gamma_2(t) = \frac{\gamma_1^0}{4} \left(1 + \tilde{\gamma}_2(t)\right). \tag{5.102}$$

Les équations linéarisées donnent

$$\begin{pmatrix} \dot{\tilde{\gamma}}_1 \\ \dot{\tilde{\gamma}}_2 \end{pmatrix} = M \begin{pmatrix} \tilde{\gamma}_1 \\ \tilde{\gamma}_2 \end{pmatrix} \tag{5.103}$$

avec

$$M = \begin{pmatrix} \frac{4(5-6\beta)}{3\gamma_1^0} & \frac{4(-8+6\beta)}{3\gamma_1^0} \\ \frac{2(1-12\beta)}{3\gamma_1^0} & \frac{2(2+12\beta)}{3\gamma_1^0} \end{pmatrix}. \tag{5.104}$$

Les valeurs propres de M sont réelles pour $\beta > 0$ et complexes pour $\beta < 0$. Elles sont données par

$$\zeta_\pm = \frac{1 \pm \sqrt{3\beta}}{36}\mu^2, \quad \zeta_\pm = \frac{1 \pm i\sqrt{-3\beta}}{36}\mu^2, \tag{5.105}$$

respectivement.

La stabilité de ce point fixe est alors facile à étudier
- $\beta < 0 \Rightarrow \mathrm{Re}(\zeta_\pm) > 0$: il est instable ;
- $\beta > 0$: il est instable si $0 < \beta < \frac{1}{3}$ et point selle si $\beta > \frac{1}{3}$.

On constate que ce point fixe n'est jamais complètement stable, ce qui est cohérent avec le fait que $\mu < 0$ et ce que l'on a vu plus haut.

Il est évident qu'il existe d'autres solutions que ce point fixe qui n'est jamais stable. Dans la suite nous présentons les quatre solutions différentes que nous avons obtenu dans la publication 7. On tient à préciser que beaucoup de travail numérique a été nécessaire.

Autres attracteurs Nous avons trouvé un point fixe quand $\mu < 0$, mais que se passe-t-il pour $\mu > 0$? De même, que se passe-t-il quand le point fixe n'est pas stable (c'est à dire tout le temps) ? Le flot tend alors vers un attracteur dépendant explicitement du temps.

Attracteurs isotrope et quasi-isotrope Pour commencer supposons l'isotropie : $\gamma_i(t) = \gamma_0(t)$. Nous obtenons alors la solution (valable même pour le cas $\mu = \infty$)

$$\gamma_0(t) = \frac{3\beta - 1}{2}t + \tilde{\gamma}_0. \tag{5.106}$$

Les composantes de la métrique s'annulent pour $t = t_v = \frac{4\tilde{\gamma}_0}{1-3\beta}$. Quand $\beta > \frac{1}{3}$, le flot est défini pour $t > t_v$ et le volume croît de zéro en t_v à l'infini pour des temps plus longs. Au contraire, si $t < t_v$, le flot est défini pour $t < t_v$ et le volume tend vers 0 en t_v.

Nous pouvons ensuite linéariser les équations autour de cet attracteur en posant

$$\gamma_i(t) = \gamma_0(t) + \delta\gamma_i(t) = \gamma_0(t)\left(1 + \tilde{\gamma}_i(t)\right). \tag{5.107}$$

Une nuance doit cependant être précisée. En effet on étudie dans la suite des attracteurs dépendant explicitement du temps, et une analyse perturbative de telles solutions est relativement ambigüe. On se contentera du fait que les solutions présentées peuvent être obtenues comme de simples points fixes dans d'autres choix de paramétrisation, et que la dépendance temporelle dans notre problème n'en est pas un. Pour faciliter la discussion et éviter une multiplication des notations nous avons choisi de ne pas parler des différentes paramétrisations donnant lieu à des points fixes.

– $\beta > \frac{1}{3}$.
Après suffisamment longtemps, nous pouvons négliger $\tilde{\gamma}_0$, obtenant ainsi la matrice simplifiée

$$M(t) = \frac{1}{\gamma_0(t)} \begin{pmatrix} -\frac{1+\beta}{2} & 1-\beta \\ \frac{1-\beta}{2} & -\beta \end{pmatrix}. \tag{5.108}$$

Dans cette approximation, on notera que M dépend seulement de β. Les valeurs propres de M sont alors données par

$$\zeta_1 = -\frac{1}{2\gamma_0(t)} \quad \text{et} \quad \zeta_2 = \frac{1-3\beta}{4\gamma_0(t)}, \tag{5.109}$$

qui sont toutes les deux négatives pour $\beta > \frac{1}{3}$. Les signes des valeurs propres ne sont pas affectés car leurs dépendances temporelles sont factorisées et de signes constants. L'attracteur isotrope apparaît donc comme stable pour des petites fluctuations. Il est important cependant de mettre en exergue le côté local de notre étude. En effet on peut montrer numériquement qu'il existe des exemples de solutions stables localement mais pas globalement. Il y a encore une autre subtilité, tout aussi importante. En effet on montre que dans une large classe de paramètres, $\tilde{\gamma}_i(t) \ll 1$, mais on ne dis rien sur $\tilde{\gamma}_i(t)\gamma_0(t)$, qui peut croître ou décroître. Nous pouvons alors obtenir

$$\tilde{\gamma}_i(t) \propto t^{\tilde{\alpha}_i}, \quad \tilde{\alpha}_1 = \frac{2}{1-3\beta}, \ \tilde{\alpha}_2 = -1. \tag{5.110}$$

Par conséquent

$$\delta\gamma_i(t) = \gamma_0(t)\tilde{\gamma}_i(t) \propto t^{\alpha_i}, \quad \alpha_1 = \frac{3-3\beta}{1-3\beta}, \ \alpha_2 = 0. \tag{5.111}$$

Comme nous supposons ici $\beta > \frac{1}{3}$ alors $\alpha_1 < 1$. On peut alors voir simplement que si $\beta < 1$, la différence $\gamma_1(t) - \gamma_2(t)$ tend vers 0 et le système est vraiment isotrope, alors que pour $\beta > 1$ cette différence diverge et l'on obtient un attracteur quasi-isotrope. Il est isotrope dans le sens où $\frac{\gamma_1}{\gamma_2} \to 1$ mais axisymétrique dans le sens où $\gamma_1 - \gamma_2 \to \infty$. Pour distinguer ces deux solutions on parlera d'attracteur isotrope dans le cas strictement isotrope $\beta < 1$ et d'attracteur de type I pour l'attracteur quasi-isotrope. Notons également que l'on pourrait définir un attracteur de type *Ibis* pour $\beta = 1$ où il est facile de montrer que $\gamma_1(t) - \gamma_2(t) \to$ cst..

– $\beta < \frac{1}{3}$.
La solution isotrope asymptotique (5.106) est maintenant limitée au domaine de définition $t < t_v = \frac{2\tilde{\gamma}_0}{1-3\beta}$. Autour de ce point particulier les équations de perturbations peuvent se linéariser et nous obtenons $\tilde{\gamma}_2 = -\frac{\tilde{\gamma}_1}{2} + C_0$ et $\dot{\gamma}_1 \propto -\frac{1}{\mu}$. Maintenant c'est μ qui apparaît dans la linéarisation, sans β. Pour $\mu > 0$ (5.106) est stable alors que pour $\mu < 0$ c'est instable.

L'analyse ci dessus montre que si $\beta < \frac{1}{3}$ l'attracteur isotrope apparaît si $0 < \mu$, alors que pour $\frac{1}{3} < \beta$, quelque soit μ, l'attracteur isotrope est stable jusqu'à $\beta = 1$, où l'attracteur de type I semble prendre le relais pour $1 < \beta$.

Jusqu'à présent nous n'avons découvert que deux types d'attracteurs, et notamment aucun attracteur axisymétrique non bizarre. Dans la suite de cette partie nous présentons les deux autres attracteurs que nous avons découvert, et qui eux sont totalement axisymétriques.

Attracteurs axisymétriques Les deux attracteurs que nous présentons ici ont été trouvés numériquement avant de vérifier analytiquement certaines de leurs propriétés. Il n'y a aucun doute sur leur existence et leur véracité. Cependant nous ne comprenons toujours pas dans quelles gammes de conditions initiales, paramètres, ces attracteurs apparaissent. Nous ne pouvons également pas certifier que les quatre attracteurs et le point fixe présentés ici et dans la publication 7 sont les seuls. S'il est certain qu'il n'y a pas d'autres points fixes, nous ne pouvons pas affirmer qu'il n'existe pas d'autres attracteurs. Cependant, des calculs et des simulations numériques assez poussées nous indiquent que nous avons très probablement une classification exhaustive. Nous présentons maintenant les deux attracteurs axisymétriques.

- Tout d'abord nous avons l'attracteur

$$\gamma_2(t) \approx \left(3\frac{\gamma_0^{\frac{3}{2}}}{\mu}t + \gamma_2^0\right)^{1/6}, \quad \gamma_1(t) \approx \frac{\gamma_0}{\gamma_2(t)^2}, \tag{5.112}$$

  (γ_0 est une constante) nommé attracteur de type II. Dans ce cas, le temps est borné supérieurement par $t_v = \frac{-\gamma_2^0\mu}{3\gamma_0^{\frac{3}{2}}}$ et $\gamma_{2,3}$ tendent vers 0 alors que γ_1 diverge. Le volume asymptotique, par contre, tend lui vers une constante : $V \to 16\pi^2\sqrt{\gamma_0}$.
- L'autre attracteur, nommé attracteur de type III, est donné par

$$\gamma_1(t) \approx \left(\gamma_1^0 - \omega t\right)^2, \quad \frac{\gamma_1(t)}{\gamma_2^2(t)} \approx \gamma_0. \tag{5.113}$$

  L'ansatz (5.113) résout les équations asymptotiquement si

$$\gamma_0 = \mu^2\left(\frac{\beta-1}{2}\right)^2 \text{ et } \omega = \sqrt{\gamma_0}(1-3\beta). \tag{5.114}$$

  Une nouvelle fois le temps est borné supérieurement par $t_v = \frac{\gamma_1^0}{\omega}$. Dans ce cas le flot se traduit par le fait que tous les γ_i s'annulent mais à des taux différents.

Pour plus de détails concernant le flot avec $\Lambda_W = 0$, consulter la publication 7.

3.3 Quelques résultats quand $\Lambda_W \neq 0$

Dans ce cas il est quasiment impossible de trouver l'ensemble des attracteurs. Par contre il est possible, dans l'hypothèse d'axisymétrie, de trouver l'ensemble des points fixes.

Point fixe isotrope Si on suppose $\gamma_2 = \gamma_3$ les équations du flot deviennent alors

$$\frac{1}{\gamma_1}\frac{\mathrm{d}\gamma_1}{\mathrm{d}t} = -\frac{\sqrt{\gamma_1}}{\mu\,\gamma_2^3}(\gamma_1-\gamma_2) - \frac{8\lambda-3}{4(3\lambda-1)}\frac{\gamma_1}{\gamma_2^2} + \frac{2\lambda-1}{3\lambda-1}\frac{1}{\gamma_2} + \frac{\Lambda_W}{3\lambda-1}, \quad (5.115)$$

$$\frac{1}{\gamma_2}\frac{\mathrm{d}\gamma_2}{\mathrm{d}t} = \frac{\sqrt{\gamma_1}}{2\mu\,\gamma_2^3}(\gamma_1-\gamma_2) + \frac{4\lambda-1}{4(3\lambda-1)}\frac{\gamma_1}{\gamma_2^2} - \frac{\lambda}{3\lambda-1}\frac{1}{\gamma_2} + \frac{\Lambda_W}{3\lambda-1}. \quad (5.116)$$

L'existence et la nature du point fixe dépendent de manière cruciale de Λ_W, μ et λ. En particulier, $\Lambda_W > 0$ permet un point fixe isotrope et un point fixe axisymétrique alors que $\Lambda_W < 0$ ne permet qu'un point fixe axisymétrique. Dans le cas $\Lambda_W = 0$ nous avons trouvé un point fixe axisymétrique dans le paragraphe précédent.

Indépendamment de μ nous avons un point fixe isotrope si $\Lambda_W > 0$, correspondant à une sphère S^3 de rayon $2\sqrt{\Lambda_W}$:

$$\gamma_1 = \gamma_2 = \gamma_3 = \frac{1}{4\Lambda_W}. \quad (5.117)$$

En linéarisant autour de ce point fixe

$$\gamma_1(t) = \frac{1}{4\Lambda_W}\,(1+\tilde{\gamma}_1(t))\,, \quad \gamma_2(t) = \frac{1}{4\Lambda_W}\,(1+\tilde{\gamma}_2(t))\,, \quad (5.118)$$

Il est alors facile de montrer que pour $\mu > 0$ et $\mu < -6\cdot 2^{1/3}$ ce point fixe est absolument stable, alors que sinon il est point selle. En particulier, il n'est jamais complètement instable.

Il existe ainsi des valeurs critiques $\lambda = 1/3$ et $\mu^2 = 36\Lambda_W$ où ζ_1 et ζ_2 s'annulent et séparent la stabilité de l'instabilité. Ces deux valeurs critiques sont très importantes dans la théorie d'HL. Par exemple, il a été montré que la cette théorie n'est bien définie quantiquement parlant que si $\lambda < \frac{1}{3}$.

Point fixe axisymétrique Quand $\Lambda_W > 0$ et $\mu < 0$ il y a un autre point fixe, axisymétrique

$$\gamma_1 = \frac{36\mu^2}{(\mu^2+27\Lambda_W)^2}, \quad \gamma_2 = \gamma_3 = \frac{9}{\mu^2+27\Lambda_W}. \quad (5.119)$$

Si $\Lambda_W < 0$ et $\mu < 0$ le même point fixe existe mais avec la restriction $\mu^2 > -27\Lambda_W$. On remarquera que ce point fixe axisymétrique redonne celui que l'on a trouvé pour $\lambda = 0$ quand on remplace Λ_W par 0 dans (5.119). Nous pouvons étudier les petites fluctuations autour de la position d'équilibre en linéarisant selon

$$\gamma_1(t) = \frac{36\mu^2}{(\mu^2+27\Lambda_W)^2}\,(1+\tilde{\gamma}_1(t))\,, \quad \gamma_2(t) = \frac{9}{\mu^2+27\Lambda_W}\,(1+\tilde{\gamma}_2(t))\,, \quad (5.120)$$

ce qui donne les équations $\dot{\tilde{\gamma}}_i = M_i^j\tilde{\gamma}_j$ avec

$$M = \frac{1}{27(3\lambda-1)}\begin{pmatrix} (9\lambda-2)\mu^2 - 36\Lambda_W(3\lambda-1) & -(18\lambda-5)\mu^2 + 36\Lambda(6\lambda-1) \\ -\frac{1}{2}(9\lambda-5)\mu^2 + \frac{27}{2}\Lambda_W(3\lambda-1) & (9\lambda-4)\mu^2 - 36\Lambda_W(3\lambda-2) \end{pmatrix}. \quad (5.121)$$

Les valeurs propres de M sont alors

$$\zeta_{\pm} = \frac{1}{18(3\lambda-1)}\left[2(3\lambda-1)\mu^2 - 27\Lambda_W(2\lambda-1) \pm \sqrt{\Delta}\right], \tag{5.122}$$

où

$$\Delta = 6(3\lambda-1)(2\lambda-1)\mu^4 - 72\Lambda_W\mu^2(3\lambda-1)^2 + 243\Lambda_W^2(12\lambda^2-6\lambda+1). \tag{5.123}$$

Dans la publication 7 nous montrons que ce point fixe n'est stable que si $-6\cdot 2^{1/3} < \mu < 0$. De manière générale, une des conclusions de la publication 7 est qu'il est très difficile pour un point fixe axisymétrique d'être stable, plus que pour un point fixe isotrope.

3.4 Approche canonique de la théorie d'HL

Dans la publication 6 nous étudions la théorie d'HL sur le modèle de l'Univers Mixmaster introduis dans [59]. Cette étude revient à considérer l'action de la théorie d'HL en utilisant le formalisme hamiltonien de la gravitation. On peut ainsi mettre en exergue la présence d'un hamiltonien décrivant le modèle de gravitation considéré. Cet hamiltonien peut ensuite être considéré comme celui d'une particule se déplaçant dans un potentiel, inclus dans l'hamiltonien. L'étude de ce potentiel permet ainsi d'étudier les propriétés de chaoticité de cette théorie de la gravitation. Nous n'en dirons pas plus ici, voir pour cela la publication 6.

Chapitre 6

Conclusions et ouvertures

Dans cette conclusion on ne présentera pas de résumé des chapitres précédents. En effet dans chacun d'eux on a pris soins de mentionner les différentes ouvertures et pistes de réflexion futures associées.

Ce très court chapitre est l'occasion de parler de pistes de recherches à venir qui feraient suite à [11]. MOND est une phénoménologie de la gravitation introduite par Milgrom [60] dans les années 1980. Elle suppose que l'équation fondamentale de la dynamique de Newton est remplacée par la relation plus générale

$$\mu\left(\frac{a}{a_0}\right)\overrightarrow{a} = -\overrightarrow{\nabla}\phi_N \tag{6.1}$$

où a_0 est une constante qui doit être fixée par les observations (de l'ordre de $10^{-10} m.s^{-2}$) et ϕ_N est le potentiel de gravitation Newtonien. La fonction μ est laissée arbitraire, sauf aux limites de grande et petite accélération :

$$\begin{aligned} a \ll a_0 \quad &\rightarrow \quad \mu(x) \approx x, \\ a \gg a_0 \quad &\rightarrow \quad \mu(x) \approx 1. \end{aligned} \tag{6.2}$$

TeVeS est une tentative pour rendre MOND relativiste introduite par Bekenstein [61] en 2004 et qui repose sur l'action générale

$$S = \int d^4x\sqrt{|g|}L + \int d^4x\sqrt{|\hat{g}|}\hat{L} \tag{6.3}$$

où g est la métrique géométrique, $\hat{g}$ la métrique physique, L le Lagrangien de la théorie et $\hat{L}$ le lagrangien de matière. Nous avons $L = L_g + L_s + L_v$ où

$$L_g = -\frac{1}{16\pi G}R,\ L_s = -\frac{1}{2}\left[\sigma^2 h^{\alpha\beta}\partial_\alpha\phi\partial_\beta\phi + \frac{G}{2l^2}\sigma^4 F(kG\sigma^2)\right], \tag{6.4}$$

$$L_v = -\frac{K}{32\pi G}\left[g^{\alpha\beta}g^{\mu\nu}(B_{\alpha\mu}B_{\beta\nu}) + \frac{2\lambda}{K}(g^{\mu\nu}u_\mu u_\nu - 1)\right]. \tag{6.5}$$

Nous avons introduis le tenseur $h^{\alpha\beta} = g^{\alpha\beta} - u^\alpha u^\beta$ où u_α est un champ vectoriel, les constantes l, k, K, les champs scalaires ϕ et σ, une fonction indéterminée F et un champ $B_{\alpha\beta} = \partial u_\alpha - \partial u_\beta$. Le lien entre les deux métriques est alors donné par

$$\hat{g}^{\mu\nu} = e^{2\phi}g^{\mu\nu} - 2u^\mu u^\nu \sinh(2\phi). \tag{6.6}$$

Certes cette action est compliquée et présente un certain nombre de paramètres arbitraires, mais il est remarquable de pouvoir obtenir une version relativiste de MOND.

Dans [11], bien avant cette thèse, nous nous sommes intéressés avec P. Ferreira, D. Motta et C. Skordis aux prédictions de TeVeS, une théorie relativiste de la gravitation obtenant MOND et Newton dans sa limite non relativiste, à la cosmologie. Nous avions montré que par exemple les différents champs introduis dans TeVeS pouvaient engendrer une constante cosmologique et permettre à l'Univers d'accélérer après la domination par la matière. L'intérêt de TeVeS pour la physique était alors des plus évidents : expliquer à la fois la matière noire et la constante cosmologique dans l'Univers.

Soucieux de vérifier certaines prédictions de MOND et TeVeS, de nombreux expérimentateurs ont cherché à étudier les prédictions de TeVeS pour la quantité et la distribution de matière noire dans les amas de galaxies. Des résultats concernant le *Bullet Cluster* [62] ont montré que TeVeS ne pouvait pas expliquer tous les phénomènes dus à la matière noire. Dés lors beaucoup de voix se sont levées pour critiquer une théorie qui avait seulement trois ou quatre ans d'âge : TeVeS.

De nombreux travaux, notamment dus à P. Ferreira et son équipe, voir [63] par exemple, ont permis de montrer que TeVeS n'était qu'un exemple de théorie relativiste généralisant MOND. Il est possible de construire ainsi des modèles plus simples que TeVeS et présentant moins de degrés de liberté. Il convient de préciser que toutes les expériences qui ont pu à un moment ou à un autre obtenir des résultats contradictoires à ceux prévus par TeVeS sont des critiques de TeVeS, et non MOND. L'objet de recherches futures devrait ainsi être l'obtention d'une théorie relativitse de la gravitation incluant MOND et Newton, et ne possédant pas les problèmes de TeVeS.

De très récents travaux dus à Milgrom [64] ont notamment illustré de telles théories. Cependant ces théories présentent tellement d'arbitraire qu'il est très difficile d'en tirer des prédictions. Il serait peut être plus judicieux de regarder du côté des modifications de la description géométrique de l'espace-temps plutôt que du côté de la modification du contenu en champs de l'espace-temps.

Annexe A

Savoir utiliser les fonctions modulaires

Les résultats de cette annexe sont tirés de [**?**, 30] et ne présentent en aucune façon un contenu exhaustif des fonctions modulaires de Dedekind et Jacobi entre autre. Pour plus d'informations, se référer à [?, 30]. On a volontairement choisi de présenter plus de résultats et détails que nécessaire.

1 Fonctions θ

Pour $a, b \in \mathbb{R}$ nous introduisons la **fonction elliptique de Jacobi**

$$\theta[^a_b](\nu|\tau) = \sum_{n\in\mathbb{Z}} q^{\frac{(n-a/2)^2}{2}} e^{2i\pi(\nu-b/2)(n-a/2)}, \tag{A.1}$$

où $q = e^{2i\pi\tau}$. Il est fréquent en théorie des cordes d'utiliser ces fonctions évaluées en $\nu = 0$, nous introduisons alors les notations de Jacobi/Erderlyi

$$\theta_1(\tau) = \theta[^1_1](0|\tau), \theta_2(\tau) = \theta[^1_0](0|\tau), \theta_3(\tau) = \theta[^0_0](0|\tau), \theta_4(\tau) = \theta[^0_1](0|\tau), \tag{A.2}$$

Cette annexe est ici pour présenter des résultats fondamentaux sur ces fonctions ainsi que celle de Dedekind qui leur est intimement reliée. Sous les transformations modulaires, dont deux générateurs sont

$$T(\tau) = \tau + 1,\ S(\tau) = -\frac{1}{\tau}, \tag{A.3}$$

les fonctions $\theta[^a_b](0, \tau)$ se transforment selon

$$\theta[^a_b](\nu, \tau + 1) = e^{-\frac{i\pi}{4}a(a-2)}\theta[^a_{a+b-1}](\nu, \tau) \tag{A.4}$$

$$\theta[^a_b](\frac{\nu}{\tau}, -\frac{1}{\tau}) = \sqrt{-i\tau}e^{\frac{i\pi}{12}ab+i\pi\frac{\nu^2}{\tau}}\theta[^b_{-a}](\nu, \tau). \tag{A.5}$$

La définition (A.1) faisant intervenir une somme, il est également possible d'obtenir une expression en terme de produits. Cette dernière peut parfois être plus appropriée :

- nous avons souvent besoin de tronquer ces fonctions en ne gardant que le terme principal, et seule un développement en produit permet d'isoler ce terme,
- Parfois les fonctions θ apparaissent dans des logarithmes, une formulation en produit est dans ce cas plus agréable.

Nous avons les développements

$$\theta_1(\nu|\tau) = 2q^{\frac{1}{8}}\sin(\pi\nu)\prod_{n=1}^{\infty}(1-q^n)(1-q^n e^{2\pi i\nu})(1-q^n e^{-2\pi i\nu}) \Rightarrow \theta_1(0|\tau)=0, \tag{A.6}$$

$$\theta_2(\nu|\tau) = 2q^{\frac{1}{8}}\cos(\pi\nu)\prod_{n=1}^{\infty}(1-q^n)(1+q^n e^{2\pi i\nu})(1+q^n e^{-2\pi i\nu}), \tag{A.7}$$

$$\theta_3(\nu|\tau) = \prod_{n=1}^{\infty}(1-q^n)(1+q^{n-1/2} e^{2\pi i\nu})(1+q^{n-1/2} e^{-2\pi i\nu}), \tag{A.8}$$

$$\theta_4(\nu|\tau) = \prod_{n=1}^{\infty}(1-q^n)(1-q^{n-1/2} e^{2\pi i\nu})(1-q^{n-1/2} e^{-2\pi i\nu}). \tag{A.9}$$

Définissons maintenant la fonction de Dedekind η :

$$\eta(\tau) = q^{1/24}\prod_{n=1}^{\infty}(1-q^n), \tag{A.10}$$

reliée aux fonctions θ par $\frac{\partial\theta_1}{\partial\nu}(\nu)|_{\nu=0} = 2\pi\eta^3(\tau)$. Sous les transformations modulaires, nous avons

$$\eta(\tau+1) = e^{\frac{i\pi}{12}}\eta(\tau) \quad \eta\left(-\frac{1}{\tau}\right) = \sqrt{-i\tau}\eta(\tau). \tag{A.11}$$

Les fonctions modulaires jouissent en général de propriétés de périodicités remarquables. Ces propriétés impliquent qu'il est inutile de parcourir l'ensemble des valeurs de leur domaine de définition, un sous-espace suffit. On a accès à l'ensemble des paramètres par une succession d'applications de transformations modulaires. Ceci est illustré sur la figure A.1 Un exemple de propriétés de périodicité est

$$\theta\left[{a \atop b}\right](\nu+\frac{\epsilon_1}{2}\tau+\frac{\epsilon_2}{2}|\tau) = e^{(-i\pi\tau/4)\epsilon_1^2-(i\pi\epsilon_1/2)(2\nu-b)-\frac{i\pi}{2}\epsilon_1\epsilon_2}\theta\left[{a-\epsilon_1 \atop b-\epsilon_2}\right](\nu|\tau). \tag{A.12}$$

Deux relations utiles peuvent être données par

$$\begin{aligned} 2\eta^3(\tau) &= \theta_2(\tau)\theta_3(\tau)\theta_4(\tau) \\ \theta_2^4(\nu|\tau)-\theta_1^4(\nu|\tau) &= \theta_3^4(\nu|\tau)-\theta_4^4(\nu|\tau). \end{aligned} \tag{A.13}$$

où la seconde est appelée *relation étrange de Jacobi*. Dans le cas d'orbifold, il est fréquent de devoir utiliser les relations

$$\theta_2(2\tau) = \sqrt{\frac{\theta_3^2(\tau)-\theta_4^2(\tau)}{2}} \quad \theta_3(2\tau) = \sqrt{\frac{\theta_3^2(\tau)+\theta_4^2(\tau)}{2}}, \tag{A.14}$$

$$\theta_4(2\tau) = \sqrt{\theta_3(\tau)\theta_4(\tau)} \quad \eta(2\tau) = \sqrt{\frac{\theta_2(\tau)\eta(\tau)}{2}}. \tag{A.15}$$

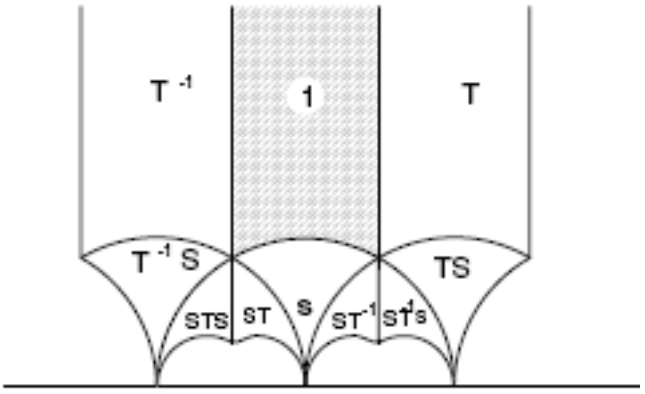

FIG. A.1 – Effets de transformations modulaires S et T successives sur le domaine fondamental en gris. L'ensemble des valeurs de τ_1, τ_2 peut ainsi être atteint. Tirée de [?].

Une autre relation importante est l'identité de Jacobi :

$$\frac{1}{2}\sum_{a,b=0}^{1}(-1)^{a+b+ab}\prod_{i=1}^{4}\theta^{[a]}_{b}](\nu_i) = -\prod_{i=1}^{4}\theta_1(\nu_i^{'}), \tag{A.16}$$

où $\nu_1^{'} = \frac{1}{2}(-\nu_1+\nu_2+\nu_3+\nu_4)$, $\nu_2^{'} = \frac{1}{2}(\nu_1-\nu_2+\nu_3+\nu_4)$, $\nu_3^{'} = \frac{1}{2}(\nu_1+\nu_2-\nu_3+\nu_4)$ et $\nu_1^{'} = \frac{1}{2}(\nu_1+\nu_2+\nu_3-\nu_4)$.
Nous donnons maintenant une série de résultats. On retiendra notamment l'équation (A.19) qui ressemble à une équation de la chaleur :

$$\frac{1}{2}\sum_{a,b=0}^{1}(-1)^{a+b+ab}\prod_{i=1}^{4}\theta^{[a+h_i]}_{b+g_i}](\nu_i) = -\prod_{i=1}^{4}\theta^{[1-h_i]}_{[1-g_i}](\nu_i^{'}), \tag{A.17}$$

$$\frac{1}{2}\sum_{a,b=0}^{1}(-1)^{a+b}\prod_{i=1}^{4}\theta^{[a]}_{b}](\nu_i) = -\prod_{i=1}^{4}\theta_1(\nu_i^{'}) + \prod_{i=1}^{4}\theta_1(\nu_i), \tag{A.18}$$

$$\left[\frac{1}{(2\pi i)^2}\frac{\partial^2}{\partial\nu^2} - \frac{1}{i\pi}\frac{\partial}{\partial\tau}\right]\theta^{[a]}_{b}](\nu|\tau), \tag{A.19}$$

$$\begin{aligned}
\frac{1}{4\pi i}\frac{\theta_2^{''}}{\theta_2} &= \partial_\tau \log\theta_2 = \frac{i\pi}{12}(E_2+\theta_3^4+\theta_4^4),\\
\frac{1}{4\pi i}\frac{\theta_3^{''}}{\theta_3} &= \partial_\tau \log\theta_3 = \frac{i\pi}{12}(E_2+\theta_2^4-\theta_4^4),\\
\frac{1}{4\pi i}\frac{\theta_4^{''}}{\theta_4} = \partial_\tau \log\theta_4 &= \frac{i\pi}{12}(E_2-\theta_2^4-\theta_3^4).
\end{aligned} \tag{A.20}$$

Les séries d'Eisenstein introduites dans (A.20) sont définies par

$$E_2 = \frac{12}{i\pi}\partial_\tau \log\eta = 1 - 24\sum_{n=1}^{\infty}\frac{nq^n}{1-q^n}, \tag{A.21}$$

$$E_4 = \frac{1}{2}(\theta_2^8 + \theta_3^8 + \theta_4^8) = 1 - 240 \sum_{n=1}^{\infty} \frac{n^3 q^n}{1-q^n}, \tag{A.22}$$

$$E_6 = \frac{1}{2}(\theta_2^4 + \theta_3^4)(\theta_4^4 + \theta_3^4)(\theta_4^4 - \theta_2^4) = 1 - 504 \sum_{n=1}^{\infty} \frac{n^5 q^n}{1-q^n}. \tag{A.23}$$

Pour obtenir un développement en série de ces fonctions, il est préférables d'utiliser les développements

$$\frac{1-E_2}{24} = \sum_{n=1}^{\infty} d_2(n) q^n \quad \frac{E_4 - 1}{240} = \sum_{n=1}^{\infty} d_4(n) q^n, \tag{A.24}$$

et

$$\frac{1-E_6}{504} = \sum_{n=1}^{\infty} d_6(n) q^n, \tag{A.25}$$

où nous avons défini

$$d_{2k}(N) = \sum_{n|N} n^{2k-1}, \ k = 1, 2, 3. \tag{A.26}$$

2 Resommation de Poisson

C'est un outil fondamental en théorie des cordes. Soit une fonction $f(x)$ dont la transformée de Fourier $\tilde{f}$ est $\tilde{f}(k) = \frac{1}{2\pi} \int_{-\infty}^{\infty} f(x) e^{ikx} dx$. La formule de resommation de Poisson stipule que

$$\sum_{n \in \mathbb{Z}} f(2\pi n) = \sum_{n \in \mathbb{Z}} \tilde{f}(n). \tag{A.27}$$

Si f est une gaussienne, nous avons alors

$$\sum_{n \in \mathbb{Z}} e^{-\pi a n^2 + \pi b n} = \frac{1}{\sqrt{a}} \sum_{n \in \mathbb{Z}} e^{-(\pi/a)(n+ib/2)^2}, \tag{A.28}$$

$$\sum_{n \in \mathbb{Z}} n e^{-\pi a n^2 + \pi b n} = -\frac{i}{\sqrt{a}} \sum_{n \in \mathbb{Z}} \frac{(n+ib/2)}{a} e^{-(\pi/a)(n+ib/2)^2} \tag{A.29}$$

et

$$\sum_{n \in \mathbb{Z}} n^2 e^{-\pi a n^2 + \pi b n} = \frac{1}{\sqrt{a}} \sum_{n \in \mathbb{Z}} \left[\frac{1}{2\pi a} - \frac{(n+ib/2)^2}{a^2} \right] e^{-(\pi/a)(n+ib/2)^2}. \tag{A.30}$$

La généralisation au cas multidimensionnel est

$$\sum_{m_i \in \mathbb{Z}} e^{-\pi m_i m_j A_{ij} + \pi B_i m_i} = \frac{1}{\sqrt{\det A}} \sum_{m_i \in \mathbb{Z}} e^{-\pi (m_k + iB_k/2)(A^{-1})_{kl}(m_l + iB_l/2)}. \tag{A.31}$$

Dans la section suivante nous expliquons comment certaines intégrales sur le domaine fondamental du tore peuvent se ramener à des intégrales plus simples, sur un domaine d'intégration semi-infini plus standard : demi plan ou rectangle. Cette technique est extrêmement utile pour calculer nombre d'intégrales et a été utilisée dans cette thèse.

3 Comment intégrer sur le domaine fondamental ?

Les bornes d'intégration du domaine fondamental sont données par $\tau_1 \in \left[-\frac{1}{2}, \frac{1}{2}\right]$ et $\tau_2 \in [\sqrt{1-\tau_1^2}, \infty[$. Cependant, dans un nombre important de cas physiquement intéressants, il est possible de simplifier ces bornes et calculer les intégrales explicitement. Ce paragraphe est adapté de [31]. Pour être très général, supposons que nous ayons

$$\sum_{A \in Mat(2\times 2,\mathbb{Z})} e^{-2i\pi T \det(A)} \frac{T_2}{\tau_2} e^{-\frac{\pi T_2}{\tau_2 U_2}|(1,U)A\binom{\tau}{1}|^2} \tag{A.32}$$

à intégrer sur le domaine fondamental. Considérons en plus de la matrice A, la matrice $A^{'}$ telle que $A^{'} = AV$ avec

$$V = \begin{pmatrix} a & b \\ c & d \end{pmatrix} \in SL(2,\mathbb{Z}). \tag{A.33}$$

Ces deux matrices donnent la même contribution à l'intégrale de (A.32), moyennant une transformation modulaire $\tau^{'} = \frac{a\tau+b}{c\tau+d}$. Ainsi, au lieu d'intégrer (A.32) avec $A^{'}$, ainsi que la mesure standard $\frac{d^2\tau}{\tau_2^2}$ sur le domaine fondamental ; nous intégrons (A.32) avec A dans l'action de V sur le domaine fondamental. Notre stratégie est par conséquent de partitionner toutes les matrices A en orbites du groupe modulaire, choisir un représentant de chaque orbite, A_0, et intégrer les contributions sur l'union des actions de V sur le domaine fondamental pour tous V dans le groupe modulaire donnant lieu à des matrices A_0V distinctes. Dans le groupe $GL(2,\mathbb{Z})$, le groupe modulaire a trois types d'orbites.

- L'orbite nulle, qui consiste en la matrice $A = 0$.
- Les orbites non-dégénérées, composées des matrices de déterminant non nul. Pour ces orbites, $V^{'} \neq V^{''}$ implique $A^{'} \neq A^{''}$. Par conséquent, le domaine fondamental devient
$$2 \times \{\tau \in \mathbb{C} : \tau_2 > 0\}. \tag{A.34}$$
Un représentant de cette orbite est donné par
$$a_0 = k, b_0 = j, c_0 = 0, d_0 = p, \tag{A.35}$$
avec $k > j \geq 0,\ p \neq 0$. Il y a une unique matrice de cette forme dans toute orbite non dégénérée.
- Les orbites dégénérées consistant en les matrices non nulles avec un déterminant nul. Elles peuvent toutes s'écrire sous la forme $A = \binom{j}{p} \times (c,d)$. Toutes les matrices dans la même orbite dégénérée ont les mêmes valeurs de j et p modulo un signe global. Par contre, (c,d) parcourent l'ensemble des paires d'entiers premiers entre eux. Un représentant de ce type d'orbite est donné par $c = 0$ et $d = 1$. Nous avons ainsi
$$A^{'} = A^{''} \Longleftrightarrow V^{'} = \begin{pmatrix} 1 & m \\ 0 & 1 \end{pmatrix} V^{''} \Longleftrightarrow \tau^{'} = \tau^{''} + m, \tag{A.36}$$
avec $m \in \mathbb{Z}$. La région d'intégration n'est donc plus le domaine fondamental mais la semi-bande
$$\left\{\tau \in \mathbb{C} : \tau_2 > 0, |\tau_1| < \frac{1}{2}\right\}. \tag{A.37}$$

Cependant il y a une subtilité dans ce calcul. Nous devons sommer uniquement sur les paires $(j,p) \neq (0,0)$ en tenant compte également que la paire $(-j,-p)$ donne la même contribution que la paire (j,p).
En guise de dernière remarque on peut mentionner la subtilité venant de l'inversion somme-intégrale lors du calcul de cette dernière. Nous avons à calculer l'intégrale d'une somme qui n'est pas la même chose que la somme d'une intégrale. Dans toutes les intégrales que nous avons eu à calculer, il était évident que l'inversion somme-intégrale sera bien définie. En effet, la présence d'exponentielles assurait toujours la possibilité de l'inversion.

Annexe B

Classification de Bianchi

Dans cette annexe nous donnons les informations essentielles concernant la classification des algèbres tridimensionnelles de Bianchi ainsi que les définitions des différents tenseurs utilisés dans cette thèse et le formalisme de Cartan en géométrie différentielle. La classification de Bianchi peut également être obtenue à partir de [38]. Pour toutes les algèbres nous donnons un lot de formes invariantes à gauche et l'algèbre qu'elles satisfont. Nous séparons les algèbres en deux classes, les *unimodulaires* (classe A), et les non unimodulaires (classe B).

1 Classification de Bianchi

Classe A

- Bianchi I : Dans une base de coordonnées cartésiennes $x^i,\ i = 1, 2, 3$ nous avons
$$\sigma^i = dx^i,\ d\sigma^i = 0. \tag{B.1}$$
- Bianchi II : Dans une base de coordonnées cartésiennes $x^i,\ i = 1, 2, 3$ nous avons
$$\begin{array}{rclrcl} \sigma^1 & = & dx^2 - x^1 dx^3, & d\sigma^1 & = & \sigma^2 \wedge \sigma^3, \\ \sigma^2 & = & dx^3, & d\sigma^2 & = & 0, \\ \sigma^3 & = & dx^1, & d\sigma^3 & = & 0. \end{array}$$
- Bianchi VI_{-1} : Dans une base de coordonnées cartésiennes $x^i,\ i = 1, 2, 3$ nous avons
$$\begin{array}{rclrcl} \sigma^1 & = & dx^1, & d\sigma^1 & = & 0, \\ \sigma^2 & = & e^{-x^1} dx^2 + e^{x^1} dx^3, & d\sigma^2 & = & \sigma^3 \wedge \sigma^1, \\ \sigma^3 & = & e^{-x^1} dx^2 - e^{x^1} dx^3, & d\sigma^3 & = & -\sigma^1 \wedge \sigma^2. \end{array}$$
- Bianchi VII_0 : Dans une base de coordonnées cartésiennes $x^i,\ i = 1, 2, 3$ nous avons
$$\begin{array}{rclrcl} \sigma^1 & = & C dx^2 - D dx^3, & d\sigma^1 & = & -\sigma^2 \wedge \sigma^3, \\ \sigma^2 & = & D dx^2 + D dx^3, & d\sigma^2 & = & \sigma^1 \wedge \sigma^3, \\ \sigma^3 & = & dx^1, & d\sigma^3 & = & 0. \end{array}$$

où

$$C = \cos x^1,\ D = -\sin x^1 \tag{B.2}$$

– Bianchi VIII : Dans une base de coordonnées cartésiennes $x^i,\ i = 1, 2, 3$ nous avons

$$\begin{array}{rclrcl} \sigma^1 & = & dx^1 + (1 + x^{1\ 2})dx^2 + (x^1 - x^2(1 + x^{1\ 2}))dx^3, & d\sigma^1 & = & -\sigma^2 \wedge \sigma^3, \\ \sigma^2 & = & 2x^1 dx^2 + (1 - 2x^1 x^2)dx^3, & d\sigma^2 & = & \sigma^3 \wedge \sigma^1, \\ \sigma^3 & = & dx^1 + (1 - x^{1\ 2})dx^2 + (x^1 + x^2 - x^{1\ 2}x^2)dx^3, & d\sigma^3 & = & \sigma^1 \wedge \sigma^2. \end{array}$$

– Bianchi IX : L'algèbre est

$$\begin{array}{rclrcl} \sigma^1 & = & \sin\vartheta \sin\psi\, \mathrm{d}\varphi + \cos\psi\, \mathrm{d}\vartheta, & d\sigma^1 & = & \sigma^2 \wedge \sigma^3, \\ \sigma^2 & = & \sin\vartheta \cos\psi\, \mathrm{d}\varphi - \sin\psi\, \mathrm{d}\vartheta, & d\sigma^2 & = & \sigma^3 \wedge \sigma^1, \\ \sigma^3 & = & \cos\vartheta\, \mathrm{d}\varphi + \mathrm{d}\psi, & d\sigma^3 & = & \sigma^1 \wedge \sigma^2 \end{array},$$

avec les angles d'Euler $0 \leq \vartheta \leq \pi, 0 \leq \varphi \leq 2\pi, 0 \leq \psi \leq 4\pi$.

Classe B

– Bianchi III : Dans une base de coordonnées cartésiennes $x^i,\ i = 1, 2, 3$ nous avons

$$\begin{array}{rclrcl} \sigma^1 & = & e^{-x^1}dx^2 & d\sigma^1, & = & \sigma^1 \wedge \sigma^2, \\ \sigma^2 & = & dx^3 & d\sigma^2, & = & 0, \\ \sigma^3 & = & dx^1 & d\sigma^3, & = & 0. \end{array}$$

– Bianchi IV : Dans une base de coordonnées cartésiennes $x^i,\ i = 1, 2, 3$ nous avons

$$\begin{array}{rclrcl} \sigma^1 & = & e^{-x^1}dx^2 - x^1 e^{-x^1}dx^3 & d\sigma^1, & = & \sigma^1 \wedge \sigma^3 + \sigma^2 \wedge \sigma^3, \\ \sigma^2 & = & e^{-x^1}dx^3 & d\sigma^2, & = & \sigma^2 \wedge \sigma^3, \\ \sigma^3 & = & dx^1, & d\sigma^3 & = & 0. \end{array}$$

– Bianchi V : Dans une base de coordonnées cartésiennes $x^i,\ i = 1, 2, 3$ nous avons

$$\begin{array}{rclrcl} \sigma^1 & = & e^{-x^1}dx^2 & d\sigma^1, & = & \sigma^1 \wedge \sigma^3, \\ \sigma^2 & = & e^{-x^1}dx^3 & d\sigma^2, & = & \sigma^2 \wedge \sigma^3, \\ \sigma^3 & = & dx^1, & d\sigma^3 & = & 0. \end{array}$$

– Bianchi $\mathrm{VI}_{h\neq -1}$: Dans une base de coordonnées cartésiennes $x^i,\ i = 1, 2, 3$ nous avons

$$\begin{array}{rclrcl} \sigma^1 & = & e^{-x^1}dx^2, & d\sigma^1 & = & \sigma^1 \wedge \sigma^3, \\ \sigma^2 & = & e^{-hx^1}dx^3, & d\sigma^2 & = & h\sigma^2 \wedge \sigma^3, \\ \sigma^3 & = & dx^1, & d\sigma^3 & = & 0. \end{array}$$

– Bianchi $\mathrm{VII}_{h\neq 0}$: Dans une base de coordonnées cartésiennes $x^i,\ i = 1, 2, 3$ nous avons

$$\begin{array}{rclrcl} \sigma^1 & = & (C - kD)dx^2 - Ddx^3, & d\sigma^1 & = & -\sigma^2 \wedge \sigma^3, \\ \sigma^2 & = & Ddx^2 + (C + kD)dx^3, & d\sigma^2 & = & \sigma^1 \wedge \sigma^3, \\ \sigma^3 & = & dx^1, & d\sigma^3 & = & 0. \end{array}$$

où

$$C = e^{-kx^1}\cos(ax^1),\ D = -\frac{1}{a}e^{-kx^1}\sin(ax^1),\ k = \frac{h}{2},\ a = \sqrt{(}1 - k^2) \tag{B.3}$$

2 Quelques tenseurs

Outre le tenseur de Riemann bien connu, nous avons utilisé dans cette thèse le tenseur de Weyl

$$W_{abcd} = R_{bacd} - \frac{2}{n-2}\left(g_{a[c}R_{d]b} - g_{b[c}R_{d]a}\right) + \frac{2}{(n-1)(n-2)}Rg_{a[c}g_{d]b}, \tag{B.4}$$

défini en dimension $n > 2$ et le tenseur de Cotton

$$C_{ijk} = \nabla_k R_{ij} - \nabla_j R_{ik} + \frac{1}{2(n-1)}\left(\nabla_j R g_{ik} - \nabla_k R g_{ij}\right). \tag{B.5}$$

Le tenseur de Weyl est invariant conforme pour $n \geq 4$, mais nul pour $n = 3$. C'est alors le tenseur de Cotton qui est bien défini en $n = 3$ et invariant conforme.

3 Formalisme de Cartan

Supposons que nous ayons une métrique dans l'euclidien donnée dans un repère quelconque :

$$ds^2 = g_{MN}dx^M dx^N, \tag{B.6}$$

nous pouvons introduire une base orthonormale $\theta^A = \theta^A_M dx^M$ telle que

$$ds^2 = \delta_{AB}\theta^A\theta^B. \tag{B.7}$$

La connexion de spin est alors donnée par l'équation de structure de Cartan

$$d\theta^A + \omega^A{}_B \wedge \theta^B = 0. \tag{B.8}$$

La 2−forme de courbure de Riemann est donnée par

$$\mathcal{R}^A_B = d\omega^A{}_B + \omega^A{}_C \wedge \omega^C{}_B = \frac{1}{2}R^A{}_{BCD}\theta^C \wedge \theta^D. \tag{B.9}$$

L'identité de Bianchi dans ce formalisme est

$$d\mathcal{R}^A_B + \omega^A{}_C \wedge \mathcal{R}^C_B - \mathcal{R}^A_C \wedge \omega^C{}_B = 0, \tag{B.10}$$

alors que l'identité cyclique est

$$\mathcal{R}^A_B \wedge \theta^B = 0. \tag{B.11}$$

Annexe C

Publication 1 : F. Bourliot, C. Kounnas and H. Partouche, "Attraction to a radiation-like era in early superstring cosmologies," Nucl. Phys. B 816 (2009) 227 [arXiv :0902.1892 [hep-th]].

Available online at www.sciencedirect.com
ScienceDirect
Nuclear Physics B 816 (2009) 227–255
NUCLEAR PHYSICS B
www.elsevier.com/locate/nuclphysb

Attraction to a radiation-like era in early superstring cosmologies ☆

François Bourliot [a,*], Costas Kounnas [b], Hervé Partouche [a]

[a] *Centre de Physique Théorique, Ecole Polytechnique,* [1] *F-91128 Palaiseau cedex, France*
[b] *Laboratoire de Physique Théorique, Ecole Normale Supérieure,* [2] *24 rue Lhomond, F-75231 Paris cedex 05, France*

Received 23 February 2009; accepted 3 March 2009

Available online 10 March 2009

Abstract

Starting from an initial classical four-dimensional flat background of the heterotic or type II superstrings, we are able to determine at the string one-loop level the quantum corrections to the effective potential due to the spontaneous breaking of supersymmetry by "geometrical fluxes". Furthermore, considering a gas of strings at finite temperature, the full "effective thermal potential" is determined, giving rise to an effective non-trivial pressure. The backreaction of the quantum and thermal corrections to the space–time metric as well as to the moduli fields induces a cosmological evolution that depends on the early time initial conditions and the number of spontaneously broken supersymmetries. We show that for a whole set of initial conditions, the cosmological solutions converge at late times to two qualitatively different trajectories: They are either attracted to (i) a thermal evolution similar to a radiation dominated cosmology, implemented by a coherent motion of some moduli fields, or to (ii) a "Big Crunch" non-thermal cosmological evolution dominated by the non-thermal part of the effective potential or the moduli kinetic energy. During the attraction to the radiation-like era, periods of accelerated cosmology can occur. However, they do not give rise to enough inflation (e-fold $\simeq 0.2$) for the models we consider, where $\mathcal{N} \geqslant 2$ supersymmetry is spontaneously broken to $\mathcal{N} = 0$.
© 2009 Elsevier B.V. All rights reserved.

☆ Research partially supported by the European ERC Advanced Grant 226371, ANR (CNRS-USAR) contract 05-BLAN-0079-02, and CNRS PICS contracts 3747 and 4172.

* Corresponding author.
E-mail addresses: francois.bourliot@cpht.polytechnique.fr (F. Bourliot), costas.kounnas@lpt.ens.fr (C. Kounnas), herve.partouche@cpht.polytechnique.fr (H. Partouche).

[1] Unité mixte du CNRS et de l'Ecole Polytechnique, UMR 7644.

[2] Unité mixte du CNRS et de l'Ecole Normale Supérieure associée à l'Université Pierre et Marie Curie (Paris 6), UMR 8549.

0550-3213/$ – see front matter © 2009 Elsevier B.V. All rights reserved.
doi:10.1016/j.nuclphysb.2009.03.006

1. Introduction

A sensible theoretical description of cosmology has certainly to take into account both the quantum and thermal effects. It is naturally the case for an early phase of the history, close to the Planck time, where quantum fluctuations are of same order of magnitude as the whole size of the universe and where the temperature is extremely high. It has to be the case as well at very late times, where the description of the cosmology should involve the electroweak phase transition and provide the missing link to the quantum particle physics of the standard model (or its supersymmetric stringy extension), account for realistic large scale structure formations, as well as describe correct temperature properties of the cosmic microwave background.

In the framework of strings, the theory of quantum gravity is well defined [1] (at least in certain cases) and can be considered at finite temperature as well [2–4]. Thus, in the stringy framework it is natural to attempt to describe the cosmological evolution of our universe. In the very early times and when the temperature approaches the so-called Hagedorn temperature [2–5], we are faced to non-trivial stringy singularities indicating a high temperature non-trivial phase transition. In the literature, there are many speculative proposals concerning the nature of this transition [2,4,6–8].

Conceptually, it is quite exotic to understand the early stringy phase utilizing the standard field theoretical geometrical notions [8–11]. Indeed, following for instance Refs. [9,11], the notions of geometry and even topology break down in this very early-time era. Only by considering stringy approaches based on 2-dimensional conformal field theory techniques, there is a hope to analyze further this phase. Actually, some conceptual progress in this direction has been achieved recently [11], but we are not yet in a position to give quantitative descriptions of our stringy universe at these very early times. This stringy-conceptual obstruction however is not an obstacle to the study of the cosmological evolution of our universe for much later times than the Hagedorn transition era, namely for late times such that $t \gg t_H$ [12–14].

A way to bypass the Hagedorn transition ambiguities consists in assuming the emergence of three large space-like directions for $t \gg t_H$, describing the three-dimensional space of our universe, and possibly some internal space directions of an intermediate size, characterizing the scale of the spontaneous breaking of supersymmetry, via geometrical fluxes, or even other (gauge or else) symmetry breaking scales [15]. Within this assumptions, the ambiguities of the "Hagedorn transition exit at t_E" can be parametrized, for $t \geqslant t_E$, in terms of initial boundary condition data at t_E. This is precisely the scope of the present work, were we focus on the intermediate cosmological era: $t_E \leqslant t \leqslant t_w$, namely, after the "Hagedorn transition exit" and before the electroweak symmetry breaking phase transition at t_w.

Modulo the initial boundary condition data at t_E, the stringy description of the intermediate cosmological era, turns out to be under control, at least for the string backgrounds where supersymmetry is spontaneously broken by "geometrical fluxes" [16,17]. These fluxes are implemented by a "stringy Scherk–Schwarz mechanism" involving n-internal compactified dimensions which are coupled non-trivially to some of the R-(super-)symmetric charges [8,13,14, 18–20]. Furthermore, the finite temperature effects are also implemented by a stringy Scherk–Schwarz compactification attached to the Euclidean time circle of radius $\beta = 1/T$ [2–4,8,13,14]. Here, the R-symmetry charge is just the helicity, so that space–time bosons are periodic while fermions are anti-periodic along the S^1 Euclidean time circle.

The breaking of supersymmetry and the quantum canonical ensemble at temperature T give rise to a non-trivial free energy at the one-loop string level. The latter is evaluated in a large regularized 3-space volume V_3. This amounts to considering the free energy of a gas of approximately

free strings,

$$F = -\frac{\ln Z}{\beta} \simeq -\frac{Z_{\text{1-loop}}^{(\text{string})}}{\beta}, \tag{1.1}$$

where $Z = \operatorname{Tr} e^{-\beta H}$ is the partition function at finite temperature and $Z_{\text{1-loop}}^{(\text{string})}$ is the one-loop connected graph i.e. genus one vacuum to vacuum string amplitude computed in the Euclidean background. In these equalities, we use the fact that the free energy of an infinite number of degrees of freedom can be found by a single string loop computation [12–14,21]. The pressure derived from the free energy, $P = -\partial F/\partial V_3$, has been computed for heterotic and type II models.[3] Supersymmetry is spontaneously broken by introducing geometrical fluxes *à la* Scherk–Schwarz involving n internal directions and by finite temperature effects. The pressure acts as a source occurring at 1-loop that backreacts on the original classical space–time metric and moduli fields background. In some cases, the perturbed equations of motion for the metric and moduli are shown to admit a cosmological evolution describing a radiation-like dominated era [12–14,23]. The latter is characterized by a time evolution where the temperature $T(t)$, the supersymmetry breaking scale $M(t)$ and the inverse scale factor $1/a(t)$ remain proportional [12–14,23]:

Radiation dominated solution:

$$T(t) \propto M(t) \propto 1/a(t) \quad \text{and} \quad H^2 \equiv \left(\frac{\dot{a}}{a}\right)^2 \propto \frac{1}{a^4}. \tag{1.2}$$

Very different time evolutions also exist when temperature effects are neglected [14]. In this case, the supersymmetry breaking scale evolves like:

Moduli dominated solution:

$$M(t) \propto 1/a(t)^{2+4/n} \quad \text{with } T(t) \ll M(t) \text{ and } H^2 \propto \frac{1}{a^{8(n+2)/n}}. \tag{1.3}$$

In this work we would like to examine the late time evolution of the universe in the intermediate cosmological era, $t_E \leqslant t \leqslant t_w$, in terms of initial boundary conditions (IBC) after the "Hagedorn transition exit at t_E". We show that the Radiation Dominated Solution (RDS) and the Moduli Dominated Solution (MDS) obtained for particular IBC are actually generic. For instance, for $n = 1$, there is a whole basin of IBC such that the resulting cosmological evolutions converge – depending on the model – either to the RDS or to the MDS. The first attractor corresponds to an expanding evolution controlled by a Friedmann equation $H^2 \propto 1/a^4$, where H is the Hubble parameter. The second one describes a Big Crunch behavior dominated by the non-thermal radiative corrections. In addition, all models admit a second basin of IBC that yields to another Big Crunch behavior, dominated by the moduli kinetic energy i.e. where $H^2 \propto 1/a^6$. Within the scope of our present work, the Big Crunch evolutions can be trusted as long as Hagedorn like singularities are not reached. Our analysis is also limited to the cases where the initial supersymmetry is higher or equal to two, $\mathcal{N} \geqslant 2$. Although the $\mathcal{N} = 1$ case is quite similar in some respects, it is much more involved in issues like the appearance of an effective cosmological term. It will be analyzed elsewhere.

Restricting to cases with $\mathcal{N} \geqslant 2$ initial supersymmetry, the attraction to the radiation era depends on the IBC: The convergence to the RDS is either exponential or via damping oscillations.

[3] Type I models realized as orientifolds of type IIB can also be considered. They can be dual to heterotic ones with an initially $\mathcal{N} = 4$, 2 or even 1 supersymmetry [22].

During this process, periods of accelerated expansion can occur. However, they are characterized by an e-fold number of order 0.2, which is too low to account for realistic astrophysical observations. It would be very interesting to extend our analysis to models with $\mathcal{N} = 1$ initial supersymmetry and see if the e-fold number is larger enough for an inflation era to occur.

In Section 2, the case of a supersymmetry breaking using a single internal direction (i.e. $n = 1$) is studied in details. We classify the models and find local basins of attraction. This analysis is completed by a more general exploration of the set of IBC by numerical simulations. In Section 3, the attraction mechanism to the RDS is extended to models where $n = 2$ internal directions participate in the supersymmetry breaking. We determine in Section 4 the e-fold number of the periods of acceleration. Our results, their limitations and our perspectives are summarized in Section 5.

2. Susy breaking involving $n = 1$ internal dimension

In this section, we summarize first the results and notations introduced in Ref. [13] and then we analyze the attractor mechanism. The starting background can be the heterotic, type I or type II superstring compactified on a 6-dimensional space $\mathcal{M}$ that can be either $S^1(R_4) \times T^5$ or $S^1(R_4) \times S^1 \times K3$. The sizes of T^5 and $S^1 \times K3$ are chosen to be of order the Planck length.[4] The supersymmetry breaking is introduced by "geometrical fluxes" via the coupling of the momentum and winding numbers of the Scherk–Schwarz circle $S^1(R_4)$ to an R-symmetry charge [3,13,14,18–20]. The radius of the circle R_4 controls the supersymmetry breaking scale M. In all applications, we will replace $K3$ by its orbifold limit, $K3 \sim T^4/\mathbb{Z}_2$.

In the heterotic and type I cases initially $\mathcal{N} = 4$ or $\mathcal{N} = 2$, the geometrical fluxes break spontaneously all the supersymmetries, $\mathcal{N} \to 0$. In type II, when the $S^1(R_4)$ coupling involves non-trivially left- and right-moving R-symmetry charges, all initial $\mathcal{N} = 8$, $\mathcal{N} = 4$, or $\mathcal{N} = 2$ supersymmetries are spontaneously broken. When the $S^1(R_4)$ coupling is left/right-"asymmetric" i.e. involves non-trivially a left- (or right-) moving R-symmetry charge only, half of the supersymmetries still survive: $\mathcal{N} \to \mathcal{N}/2$.

2.1. General setup, gravity-moduli equations

In all cases the computation of the free energy involves for the heterotic or type II superstring the background:

$$S^1(R_0) \times T^3 \times S^1(R_4) \times \mathcal{M}_5 \quad \text{with either } \mathcal{M}_5 = T^5 \text{ or } \mathcal{M}_5 = S^1 \times T^4/\mathbb{Z}_2. \tag{2.1}$$

The T^3 factor stands for the external space with regularized volume V_3 sent to infinity once the thermodynamical limit is taken. $S^1(R_0)$ is the Euclidean time circle of period $\beta = 2\pi R_0$ that defines the inverse temperature (in the string frame). In this direction, the Scherk–Schwarz circle amounts to coupling the momentum and winding numbers of the Euclidean time circle to the space–time fermion number [2–4,8,13,14]. The computation of the free energy density is well defined if the moduli R_0 and R_4 responsible for the spontaneous supersymmetry breaking are larger than the Hagedorn radius R_H, which is of order 1 in string units. At the Hagedorn radius, some winding modes become tachyonic so that the free energy develops a severe IR divergence [2–4,8,13,14]. If our goal is not to describe the phase transition that is occurring at

[4] We relax this hypothesis in Ref. [15].

the Hagedorn radius, we can suppose that in the intermediate cosmological era, R_0 and R_4 are large. In Refs. [13,14], it is shown that up to exponentially small terms of order $e^{-\pi R_0}$ or $e^{-\pi R_4}$, the pressure derived from the free energy density takes the following form [12–14,23],

$$P = T^4 p(z) \quad \text{where } e^z = \frac{M}{T}, \tag{2.2}$$

with the temperature T and supersymmetry breaking scale M defined as

$$T = \frac{1}{2\pi R_0 \sqrt{\operatorname{Re} S}}, \qquad M = \frac{1}{2\pi R_4 \sqrt{\operatorname{Re} S}}. \tag{2.3}$$

In these expressions, the factors involving the dilaton in 4 dimensions, $\operatorname{Re} S = e^{-2\phi_D}$, arise when we work in Einstein frame. In (2.2), p is a linear sum of functions of z with integer coefficients n_T and n_V [13,14],

$$p(z) = n_T f(z) + n_V \tilde{f}(z), \tag{2.4}$$

where

$$f(z) = \frac{\Gamma(5/2)}{\pi^{5/2}} \sum_{m_0, m_4} \frac{e^{4z}}{[(2m_0+1)^2 e^{2z} + (2m_4)^2]^{5/2}}, \qquad \tilde{f}(z) = e^{3z} f(-z), \tag{2.5}$$

and the sums are over the integers in $\mathbb{Z}$. n_T is the number of massless states of the model. If the Scherk–Schwarz circle $S^1(R_4)$ acts non-trivially on the left- and right-moving R-charges, n_V satisfies the inequality:

$$-1 \leqslant \frac{n_V}{n_T} \leqslant 1, \tag{2.6}$$

and depends on the choice of R-symmetries used to spontaneously break all the supersymmetries [13,14]. For an asymmetric $S^1(R_4)$ coupling i.e. trivial on the left- (or right-) moving R-symmetry charges, the supersymmetry breaking is partial and thus, there is no contribution $\tilde{f}$ to p. In that case, M is the mass of the $\mathcal{N}/2$ massive gravitini. In the following, we treat both kinds of models keeping in mind that $n_V = 0$ for asymmetric R-symmetry coupling to the momenta and windings of the 4th internal direction.

From a low energy effective field theory point of view, the pressure P is minus the effective potential at finite temperature. It is a source for the quantum fields, namely the dilaton ϕ_D and the modulus R_4, coupled to gravity [12–14,23]. It also introduces the "thermal field" R_0 to which there is no associated quantum fluctuation, as can be seen from the string model in light-cone gauge where oscillator modes in the direction 0 are gauged away. The source P is a 1-loop correction that backreacts on the classical 4-dimensional Lorentzian background, via the effective field theory action,

$$S = \int d^4x \sqrt{-g} \left[\frac{1}{2} R - g^{\mu\nu} \left(\partial_\mu \phi_D \partial_\nu \phi_D + \frac{1}{2} \frac{\partial_\mu R_4 \partial_\nu R_4}{R_4^2} \right) + P \right], \tag{2.7}$$

where we write explicitly the fields with non-trivial backgrounds only. Note that computing the 1-loop correction to the kinetic terms is not needed. Indeed, the wave function renormalization of the moduli (to recast the kinetic terms at 1-loop in a canonical form), would introduce an additional correction to the pressure at second order only. Thus, the full low energy dynamics at first order in string perturbation theory is described by the above action (2.7).

Before writing the equations of motion, it is useful to redefine the fields,

$$\phi := \sqrt{\frac{2}{3}}(\phi_D - \ln R_4), \qquad \phi_\perp := \frac{1}{\sqrt{3}}(2\phi_D + \ln R_4), \tag{2.8}$$

so that the action becomes:

$$S = \int d^4x \sqrt{-g}\left[\frac{1}{2}R - \frac{1}{2}\big((\partial\phi)^2 + (\partial\phi_\perp)^2\big) + P\right], \tag{2.9}$$

where the pressure and the supersymmetry breaking scale M take the form,

$$P = M^4 e^{-4z} p(z), \quad e^z = \frac{M}{T}, \quad M = \frac{e^{\alpha\phi}}{2\pi} \quad \text{with } \alpha = \sqrt{\frac{3}{2}}. \tag{2.10}$$

This shows that in the 2-dimensional moduli space (ϕ_D, R_4), the effective potential lifts the "no-scale modulus" ϕ, while keeping flat the orthogonal direction $\phi_\perp$. Assuming an homogeneous and isotropic cosmological metric with a flat 3-dimensional subspace,

$$ds^2 = -N(t)^2 dt^2 + a(t)^2\big(dx_1^2 + dx_2^2 + dx_3^2\big), \tag{2.11}$$

the Friedmann equation in the $N(t) = 1$ gauge takes the form,

$$3H^2 = \frac{1}{2}\dot\phi^2 + \frac{1}{2}\dot\phi_\perp^2 + \rho, \tag{2.12}$$

where the energy density ρ is defined by the identity,

$$\rho + P = T\frac{\partial P}{\partial T}, \tag{2.13}$$

and P is understood as a function of the independent variables T and M. As shown in Ref. [14], the expression of ρ follows from the variational principle applied to a gauge choice of the function $N = 1/T$. It is fundamental to stress here that the energy density defined by the variational principle is identical to the one derived from the second law of thermodynamics. From Eqs. (2.2) and (2.13), it follows that:

$$\rho = T^4 r(z) \quad \text{where } r = 3p - p_z, \tag{2.14}$$

where z-indices stand for derivatives with respect to $z = \ln(M/T)$. Varying the action with respect to the scale factor a or the scalar fields ϕ and $\phi_\perp$, we obtain:

$$2\dot H + 3H^2 = -\frac{1}{2}\dot\phi^2 - \frac{1}{2}\dot\phi_\perp^2 - P, \tag{2.15}$$

$$\ddot\phi + 3H\dot\phi = \frac{\partial P}{\partial\phi} \equiv \alpha(3P - \rho), \tag{2.16}$$

$$\ddot\phi_\perp + 3H\dot\phi_\perp = 0 \implies \dot\phi_\perp = \sqrt{2}\frac{c_\perp}{a^3}, \tag{2.17}$$

where $c_\perp$ is an arbitrary integration constant. Note that the last identity in Eq. (2.16) is a consequence of the fact that P is a dimension four object, $(M\partial_M + T\partial_T)P \equiv 4P$, and from the definitions (2.10) and (2.13). The conservation of the total energy–momentum tensor follows from the Einstein equations (2.12) and (2.15):

$$\frac{d}{dt}\left(\frac{1}{r2}\dot\phi^2 + \frac{1}{2}\dot\phi_\perp^2 + \rho\right) + 3H\big(\dot\phi^2 + \dot\phi_\perp^2 + \rho + P\big) = 0. \tag{2.18}$$

Using further the equations of the fields ϕ and $\phi_\perp$, we obtain from Eq. (2.18) that the $\{\rho, P\}$-system is not isolated but is coupled non-trivially to the "no-scale modulus field", ϕ [24,25]:

$$\dot{\rho} + 3H(\rho + P) + \alpha\dot{\phi}(3P - \rho) = 0. \tag{2.19}$$

2.2. Classification of the models, effective potential approach

Our aim is to analyze the time behavior of the system described above. For this purpose, one can choose four independent non-linear equations, for instance: Eqs. (2.12), (2.16), (2.17) and (2.19), any other choice being equivalent. Furthermore, we find convenient to express the dependence in time in terms of a dependence in the logarithm of scale factor $a(t)$:

$$\lambda := \ln a(t) \implies \dot{y} \equiv \frac{dy}{dt} = H\frac{dy}{d\lambda} \equiv H\overset{\circ}{y}, \tag{2.20}$$

for any function y. In particular, the definition $z = \alpha\phi - \ln(2\pi T)$ implies $\dot{T}/T = H(\alpha\overset{\circ}{\phi} - \overset{\circ}{z})$ that can be used to write

$$\dot{\rho} = HT^4\big(4r\alpha\overset{\circ}{\phi} + (r_z - 4r)\overset{\circ}{z}\big). \tag{2.21}$$

This equality is useful to express the conservation of energy–momentum (2.19) into a relation giving $\overset{\circ}{\phi}$ in terms of z and $\overset{\circ}{z}$,

$$\alpha\overset{\circ}{\phi} = \mathcal{A}_z(z)\overset{\circ}{z} - 1 \quad \text{where } \mathcal{A}_z(z) = \frac{4r - r_z}{3(r + p)}. \tag{2.22}$$

Integrating, one obtains

$$M = \frac{e^{\mathcal{A}(z)}}{a}, \tag{2.23}$$

where $\mathcal{A}(z)$ involves an integration constant. Using the above relations, the Friedmann equation (2.12) becomes

$$3H^2 = \frac{3}{8}H^2\big(\big(\mathcal{A}_z(z)\overset{\circ}{z} - 1\big)^2 - 1\big) + \frac{9}{8}\frac{e^{4(\mathcal{A}(z)-z)}}{a^4}r(z) + \frac{9}{8}\frac{c_\perp^2}{a^6}, \tag{2.24}$$

or

$$H^2 = T^4\frac{r(z)}{3 - \mathcal{K}(z, \overset{\circ}{z}, \overset{\circ}{\phi}_\perp)} \quad \text{with } \mathcal{K} = \frac{1}{2\alpha^2}\big(\mathcal{A}_z(z)\overset{\circ}{z} - 1\big)^2 + \frac{1}{2}\overset{\circ}{\phi}{}_\perp^2. \tag{2.25}$$

The equations for ϕ and $\phi_\perp$, (2.16) and (2.17), take the form,

$$\begin{cases} \frac{r(z)}{3-\mathcal{K}(z,\overset{\circ}{z},\overset{\circ}{\phi}_\perp)}(\mathcal{A}_z(z)\overset{\circ\circ}{z} + \mathcal{A}_{zz}(z)\overset{\circ}{z}{}^2) + \frac{r(z)-p(z)}{2}\mathcal{A}_z(z)\overset{\circ}{z} + V_z(z) = 0, \\ \frac{r(z)}{3-\mathcal{K}(z,\overset{\circ}{z},\overset{\circ}{\phi}_\perp)}\overset{\circ\circ}{\phi}_\perp + \frac{r(z)-p(z)}{2}\overset{\circ}{\phi}_\perp = 0. \end{cases} \tag{2.26}$$

For the derivation of the above equations, we used the relation $\ddot{y} = \dot{H}\overset{\circ}{y} + H^2\overset{\circ\circ}{y}$ for $y = \phi$ or $\phi_\perp$ as well as Eqs. (2.22), (2.25) and the linear sum of (2.12) and (2.15). As in Ref. [23], we have introduced the notion of an effective potential $V(z)$, defined by its derivative (and using

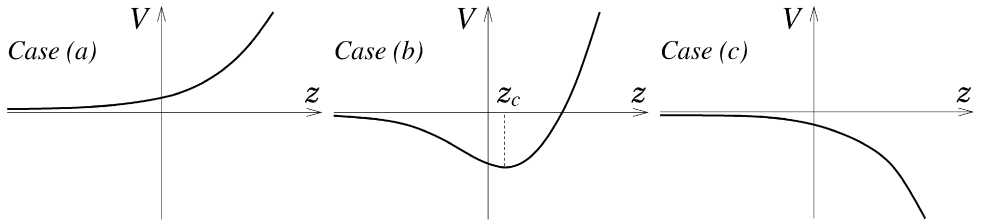

Fig. 1. The shape of the potential $V(z)$ in Eq. (2.26) depends on the ratio n_V/n_T. The Cases (a), (b) and (c) correspond to $-1 \leqslant n_V/n_T \leqslant -1/15$, $-1/15 < n_V/n_T < 0$ and $0 \leqslant n_V/n_T \leqslant 1$, respectively.

$\alpha^2 = 3/2$):

$$V_z(z) = r(z) - 4p(z). \tag{2.27}$$

We are going to see in the following section that any solution of the system with constant z, i.e. $z \equiv z_c$ where z_c is an extremum of $V(z)$, is giving rise to a particular RDS. The existence of such a critical point depends drastically on the shape of the potential $V(z)$, which is determined by its asymptotic behaviors for $z \to \pm\infty$. It is obvious from Eq. (2.4) and the definition (2.13) of ρ that $V(z)$ depends only on two parameters, namely, n_T and n_V. The asymptotic behavior $z \to \pm\infty$ can be easily derived:

- $(n_V/n_T) \neq 0$,

$$V(z) \sim_{z\to+\infty} -e^{4z}\left(\frac{n_V}{n_T}\right)\left(\frac{5}{4}n_T c_5^o\right), \quad \text{with } c_5^o = \frac{\Gamma(5/2)}{\pi^{5/2}}\sum_m \frac{1}{|2m+1|^5}, \tag{2.28}$$

- $(n_V/n_T) \neq -1/15 \equiv -(\sum'_m \frac{1}{(2m)^4})/(\sum_m \frac{1}{(2m+1)^4})$,

$$V(z) \sim_{z\to-\infty} -e^{3z}\left(\frac{n_V}{n_T} + \frac{1}{15}\right)\left(\frac{4}{3}n_T c_4^o\right), \quad \text{with } c_4^o = \frac{\Gamma(5/2)}{\pi^{5/2}}\frac{2}{3}\sum_m \frac{1}{(2m+1)^4}. \tag{2.29}$$

According to the ratio n_V/n_T, three distinct cases can actually arise (see Fig. 1),

- *Case* (a): $-1 \leqslant (n_V/n_T) \leqslant -1/15$
  $V(z)$ increases monotonically from 0 to $+\infty$.
- *Case* (b): $-1/15 < (n_V/n_T) < 0$
  $V(z)$ admits a unique minimum z_c, with $p(z_c)$ positive. When $(n_V/n_T) \to 0_-$ the critical value z_c goes to $+\infty$; when $(n_V/n_T) \to (-1/15)_+$ the critical value $z_c \to -\infty$.
- *Case* (c): $0 \leqslant (n_V/n_T) \leqslant 1$
  $V(z)$ decreases monotonically from 0 to $-\infty$.

Qualitatively, one can expect that the system represented by z can slide along its potential. It may run away in *Case* (a), $z(t) \to -\infty$, be stabilized in *Case* (b), $z(t) \to z_c$, and run away in *Case* (c), $z(t) \to +\infty$. Moreover, these behaviors should imply new ones by time reversal. In particular, other run away behaviors are expected: $z(t) \to +\infty$ in *Case* (a), $z(t) \to \pm\infty$ in *Case* (b), and $z(t) \to -\infty$ in *Case* (c). However, the study of the run away $z \to -\infty$ is out of the scope of the present work. This is due to the fact that this limit amounts to $R_4 \gg R_0 > 1$, so that the thermal

system should be studied in 5 dimensions. In the following, we will only consider the other behaviors, namely the stabilization of z and the run away $z \to +\infty$. Since the latter amounts to $R_0 \gg R_4 > 1$, it is consistent with our analysis in four dimensions but with negligible thermal effects.

2.3. Local attraction to the RDS

Clearly, the first equation in (2.26) admits a constant z solution whenever V has an extremum, i.e. in *Case* (b). It follows from Eq. (2.23) that M, T and $1/a$ are proportional during the evolution,

$$M(t) = e^{z_c} T(t) = \frac{e^{\mathcal{A}(z_c)}}{a(t)}. \tag{2.30}$$

The time dependence of the scale factor is dictated by the Friedmann equation (2.24) that simplifies to:

$$3H^2 = \frac{c_r^2}{a^4} + \frac{c_m^2}{a^6} \quad \text{where } c_r^2 = \frac{9}{2} e^{4(\mathcal{A}(z_c)-z_c)} p(z_c),\ c_m^2 = \frac{9}{8} c_\perp^2. \tag{2.31}$$

Integrating, t can be expressed in terms of the scale factor,

$$t(a) = t_0 \int_0^{a/a_0} \frac{x^2\,dx}{\sqrt{1+x^2}}, \quad t_0 = \sqrt{3}\frac{c_m^2}{|c_r|^3},\ a_0 = \left|\frac{c_m}{c_r}\right|,\ \forall a \geqslant 0, \tag{2.32}$$

up to an overall sign. There are thus two monotonic solutions mapped to one another by time reversal. For the expanding one, the universe life starts in a "moduli kinetic energy dominated era" characterized by a total energy density $\simeq c_m^2/a^6$, followed by a "radiation dominated era" with total energy density $\simeq c_r^2/a^4$. For large enough times, the evolution always enters in the radiation era: It is asymptotic to the critical solution $z \equiv z_c$, $c_m = 0$ i.e. (2.30) where

$$a(t) = \sqrt{t} \times \left(\frac{4}{3} c_r^2\right)^{1/4}, \qquad \dot{\phi}_\perp = 0. \tag{2.33}$$

To study the stability of this solution, we analyze its behavior under small perturbations. In terms of the variable $\lambda = \ln a$, we define

$$z(\lambda) = z_c + \varepsilon(\lambda), \qquad \overset{\circ}{\phi}_\perp(\lambda) = \overset{\circ}{\varepsilon}_\perp(\lambda), \tag{2.34}$$

for small ε and $\overset{\circ}{\varepsilon}_\perp$. At first order, the system (2.26) becomes

$$\begin{cases} \overset{\circ\circ}{\varepsilon} + \overset{\circ}{\varepsilon} + \xi\varepsilon = 0 \quad \text{where } \xi = 10\frac{p-p_{zz}}{19p+p_{zz}}|_{z_c}, \\ \overset{\circ\circ}{\varepsilon}_\perp + \overset{\circ}{\varepsilon}_\perp = 0. \end{cases} \tag{2.35}$$

The coefficient ξ is actually a function of the model dependent parameter n_V/n_T, since the latter appears explicitly in the definition of p and implicitly via z_c. Numerically, one finds that ξ is always positive. It increases from 0 to $+\infty$ when n_V/n_T varies from $-1/15$ to 0. The solution of the system (2.35) is

$$\overset{\circ}{\varepsilon}_\perp(\lambda) = c_3 e^{-\lambda},$$

$$\varepsilon(\lambda) = \begin{cases} c_1 e^{-\lambda(1+\sqrt{1-4\xi})/2} + c_2 e^{-\lambda(1-\sqrt{1-4\xi})/2} & \text{if } 0 < \xi < 1/4, \\ e^{-\lambda/2}(c_1 + c_2\lambda) & \text{if } \xi = 1/4, \\ e^{-\lambda/2}(c_1 \cos(\lambda\sqrt{\xi - 1/4}) + c_2 \sin(\lambda\sqrt{\xi - 1/4})) & \text{if } \xi > 1/4, \end{cases} \tag{2.36}$$

where $c_{1,2,3}$ are integration constants determined by the IBC. Since $\varepsilon(\lambda)$ and $\overset{\circ}{\varepsilon}_\perp(\lambda)$ converge to 0 for large λ in all cases, the critical solution is stable under small perturbations. In other words, the solution arising for arbitrary IBC such that $\varepsilon(0)$, $\overset{\circ}{\varepsilon}(0)$ and $\overset{\circ}{\varepsilon}_\perp(0)$ are small is attracted toward the critical one, $z \equiv z_c$, $\dot{\phi}_\perp \equiv 0$. The behavior of $\varepsilon(\lambda)$ is oscillating with damping when $0 < \xi < 1/4$, and exponentially convergent when $\xi \geqslant 1/4$. The special value $\xi = 1/4$ corresponds to $n_V/n_T \simeq -0.0246$.

2.4. Global attraction to the RDS

Since we have shown the existence of a local basin of attraction around the critical solution given in Eqs. (2.30) and (2.33), we want to know if this property is valid for more generic IBC. Actually, any initial values $(z_0, \overset{\circ}{z}_0, \overset{\circ}{\phi}_{\perp 0})$ at $\lambda = 0$ are allowed, as long as the positivity of the right-hand side of the Friedmann equation (2.25) is guaranteed,[5] i.e.

$$\frac{r(z_0)}{3 - \mathcal{K}(z_0, \overset{\circ}{z}_0, \overset{\circ}{\phi}_{\perp 0})} \geqslant 0. \tag{2.37}$$

We have studied numerically the system (2.26) for generic IBC satisfying the previous bound. Implementing in the code a positive increment for $\lambda = \ln a$ simulates the phases of the evolutions where the scale factor increases. We observe that the right-hand side of (2.25) never changes of sign. This means that the scale factor $a(t)$ is monotonic.[6] We always find that the solutions satisfy $z(\lambda) \to z_c$ and $\overset{\circ}{\phi}_\perp(\lambda) \to 0$ as $\lambda \to +\infty$, after possible oscillations. To illustrate the convergent behavior for large oscillations, we present a numerical example on Fig. 2. It is obtained for $n_V/n_T = -0.02$ that corresponds to $z_c \simeq 0.272$, with IC $(z_0, \overset{\circ}{z}_0, \overset{\circ}{\phi}_{\perp 0}) = (0.4, 0.8, 0.5)$. We conclude that for generic IBC, the expanding evolutions are attracted by the RDS that satisfies $z \equiv z_c$, $\dot{\phi}_\perp \equiv 0$ i.e. $3H^2 = c_r^2/a^4$ in Eq. (2.30).

The local behavior (2.36) also shows that the trajectory $z \equiv z_c$, $\dot{\phi}_\perp \equiv 0$ is repulsive, when λ decreases i.e. for evolutions where the scale factor is contracting. The Big Crunch solution obtained by time reversal on (2.33) is thus only formal, since it is highly unstable under small fluctuations. What we observe by numerical simulations is that for generic IBC, when we choose a negative increment for λ, then either $z \to +\infty$, or z oscillates with a greater and greater amplitude. To understand better the dynamics of the contracting evolutions, we are thus led to analyze carefully the system in the regime $z \gg 1$.

[5] IBC such that the right-hand side of (2.25) is negative correspond to solutions in Euclidean time.

[6] In general, a change of sign in the Friedmann equation during a simulation would be a numerical artifact meaning that H actually vanishes when the scale factor reaches an extremum.

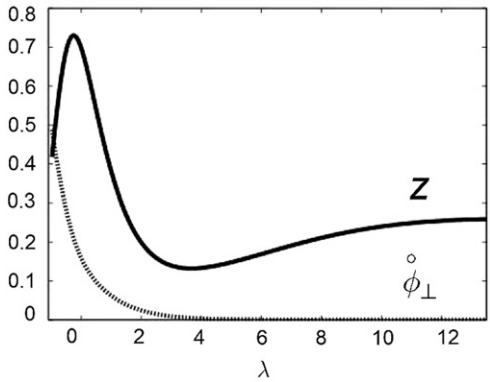

Fig. 2. Examples of damping oscillations of $z(\lambda)$ (solid curve) and convergence to zero of $\overset{\circ}{\phi}_\perp(\lambda)$ (dotted curve) illustrating the dynamical attraction toward the critical solution $z \equiv z_c \simeq 0.272$, $\dot{\phi}_\perp \equiv 0$, obtained for $n_V/n_T = -0.02$. The initial conditions are $(z_0, \overset{\circ}{z}_0, \overset{\circ}{\phi}_{\perp 0}) = (0.4, 0.8, 0.5)$.

2.5. Attraction to Big Crunch eras

We have seen that when the potential (2.27) admits a minimum z_c (*Case* (b)), the expanding cosmological evolutions for arbitrary IBC satisfy $z(t) \to z_c$. The shape of the potential in *Case* (c) of Fig. 1 suggests that when $n_V \geqslant 0$, the dynamics could admit a run away behavior $z(t) \to +\infty$. We also noticed at the end of the previous subsection that the contracting evolutions in *Case* (b) involve the large and positive value regime of z. For these reasons, we need to study the system for $z \gg 1$. In this limit the thermal effects $\mathcal{O}(T^4)$ are sub-dominant compare to the supersymmetry breaking effects $\mathcal{O}(M^4)$. The expansion of $p(z)$ contains two monomials in e^z,

$$p(z) = n_V e^{4z} c_5^o + \left(n_T c_4^o + n_V c_4^e\right) + \cdots \quad \text{where } c_4^e = \frac{\Gamma(5/2)}{\pi^{5/2}} \frac{2}{3} \sum_m{}' \frac{1}{(2m)^4}, \tag{2.38}$$

and c_5^o, c_4^o are defined in Eqs. (2.28) and (2.29). The dots stand for exponentially suppressed terms $\mathcal{O}(e^{-e^z})$. It follows that $\mathcal{A}_z(z) \simeq 1$ and the conservation of the energy–momentum Eq. (2.22) becomes

$$\overset{\circ}{z} = \overset{\circ}{M}/M + 1 \implies \frac{\dot{T}}{T} = -H \quad \text{i.e. } aT = a_0 T_0, \tag{2.39}$$

where $a_0 T_0$ is a positive constant depending on the IBC. From the expansion of $p(z)$ for large z in Eq. (2.38), it is clear that the behavior of the system is drastically different when $n_V \neq 0$ and when $n_V = 0$.

- $n_V \neq 0$, $z \gg 1$:

We have $\rho \simeq -P \simeq -M^4 n_V c_5^o$. The Friedmann equation (2.12) and the linear sum of Eqs. (2.12) and (2.15), together with the matter field equations (2.16) and (2.17), become

$$3H^2 = \frac{1}{2}\dot{\phi}^2 + \frac{1}{2}\dot{\phi}_\perp^2 - M^4 n_V c_5^o, \tag{2.40}$$

$$\dot{H} + 3H^2 = -M^4 n_V c_5^o, \tag{2.41}$$

$$\alpha\ddot{\phi} + 3H\alpha\dot{\phi} = 4\alpha^2 M^4 n_V c_5^o, \qquad \ddot{\phi}_\perp + 3H\dot{\phi}_\perp = 0. \tag{2.42}$$

The above equations would also arise if we had considered the system at zero temperature. This is due to the fact that when temperature effects are not taken into account, the sources of Einstein gravity always satisfy $\rho = -P$ equal to minus the effective potential (see Eq. (2.13)). However, this does not mean that in our case we shall find that $T(t) \to 0$. Actually, the regime $z \gg 1$ i.e. $M \gg T$ corresponds to thermal effects screened by radiative corrections, even if the temperature can be large. Combining Eqs. (2.41) and (2.42) one determines the scalar fields in terms of the scale factor (with $\alpha = \sqrt{3/2}$),

$$\alpha\dot{\phi} = -4\alpha^2 H + \frac{c_\phi}{a^3} \implies M = \frac{e^{c_\phi \int^t \frac{dt'}{a(t')^3}}}{a^6} \quad \text{and} \quad \dot{\phi}_\perp = \sqrt{2}\frac{c_\perp}{a^3}, \tag{2.43}$$

where c_ϕ and $c_\perp$ are constants depending on the IBC. The Friedmann equation (2.40) takes then the form

$$3H^2 = \frac{1}{3}\left(6H - \frac{c_\phi}{a^3}\right)^2 + \frac{c_\perp^2}{a^6} - M^4 n_V c_5^o. \tag{2.44}$$

We will consider separately the cases $c_\phi = 0$ and $c_\phi \neq 0$.

(i) $c_\phi = 0$:

$$M = M_0\left(\frac{a_0}{a}\right)^6, \qquad 3H^2 = -\frac{c_m^2}{a^6} + \frac{c_M^2}{a^{24}}, \quad \text{with } c_m = \frac{c_\perp^2}{3},\ c_M^2 = \frac{n_V}{3} M_0^4 c_5^o a_0^{24}, \tag{2.45}$$

where $M_0 a_0^6$ is a positive constant. This solution exists only for $n_V > 0$. If we also have $c_\perp = 0$, up to time reversal, the evolution describes a Big Crunch occurring at a finite time t_{BC},

$$a(t) = a_0(t_{\mathrm{BC}} - t)^{1/12} \times \left(16 M_0^4 n_V c_5^o\right)^{1/24}, \quad t < t_{\mathrm{BC}}. \tag{2.46}$$

Since $a \sim 1/T$, it follows that $e^z \propto aM \propto 1/a^5$, which is large if $t \lesssim t_{\mathrm{BC}}$ and implies a run away of z, consistently with our hypothesis $z \gg 1$. However, close to the Big Crunch, the scale M (as well as T, even if $T \ll M$) is formally diverging. This implies that the present analysis has to be restricted to the regime where $M < M_H$ i.e. $z < (5/6)\ln M_H$, where M_H is the supersymmetry breaking scale above which a Hagedorn-like transition occurs. To bypass this limit, one could try to extend our study to Hagedorn singularity free models [8].

For $c_\perp \neq 0$, the time can be expressed as a function of the scale factor,

$$t(a) = \pm t_{\mathrm{BC}} \int_{a/a_{\max}}^{1} \frac{x^{11}\,dx}{\sqrt{1 - x^{18}}} \quad \text{where } t_{\mathrm{BC}} = \frac{\sqrt{3}}{|c_M|} a_{\max}^{12},\ \forall a \leqslant a_{\max} = \left|\frac{c_M}{c_m}\right|^{1/9}. \tag{2.47}$$

Formally, this solution describes a Big Bang at $t = -t_{\mathrm{BC}}$ that initiates an expansion era. The latter stops when the scale factor reaches its maximum $a_{\max}$ at $t = 0$. The universe then contracts till $t = t_{\mathrm{BC}}$, where a Big Crunch occurs. As before, the last era of this evolution can be trusted for $t \lesssim t_{\mathrm{BC}}$, where the solution (2.47) is asymptotic to (2.46). Thus, we have shown that for IBC such that $z_0 \gg 1$ and $c_\phi = 0$, the dynamics is attracted to the MDS described by the Big Crunch solution of Eq. (2.46) with $c_\phi = c_\perp = 0$ and $3H^2 = c_M/a^{24}$.

(ii) $c_\phi \neq 0$:

We consider IBC such that $z_0 \gg 1$, with generic $c_\phi \neq 0$. The sign of $n_V \neq 0$ is arbitrary and we want again to find the basins of attraction of the dynamics. Instead of Eq. (2.40), it is more convenient to use the combination of Eqs. (2.40) and (2.41),

$$\dot{H} = -\frac{1}{2}\dot{\phi}^2 - \frac{1}{2}\dot{\phi}_\perp^2, \tag{2.48}$$

that becomes, utilizing the expressions (2.43) for $\dot{\phi}$ and $\dot{\phi}_\perp$:

$$\dot{H} = -\frac{1}{3}\left(6H - \frac{c_\phi}{a^3}\right)^2 - \frac{c_\perp^2}{a^6}. \tag{2.49}$$

Introducing the quantity σ,

$$\sigma = \frac{9}{4c_\phi}a^2\dot{a} = \frac{3}{4c_\phi}\left(a^3\right)^{\cdot} = \frac{9}{4c_\phi}a^3 H, \tag{2.50}$$

Eq. (2.49) takes the form:

$$\frac{\sigma\, d\sigma}{\sigma^2 - \sigma + \frac{3}{16}(1 + 3(c_\perp/c_\phi)^2)} = -9\frac{da}{a}, \tag{2.51}$$

valid in the $z \gg 1$ limit. In the same limit the field equations become:

$$\begin{cases} \frac{1}{\frac{1}{3}(\mathring{M}/M)^2 + \frac{1}{2}\mathring{\phi}_\perp^2 - 3}(\mathring{M}/M)^\circ - \mathring{M}/M - 6 = 0, \\ \frac{1}{\frac{1}{3}(\mathring{M}/M)^2 + \frac{1}{2}\mathring{\phi}_\perp^2 - 3}\mathring{\mathring{\phi}}_\perp - \mathring{\phi}_\perp = 0. \end{cases} \tag{2.52}$$

where the signs of n_V and the fractions in front of the second derivatives must be the same, so that the right-hand side of Eq. (2.25) is positive. This condition is required to study the evolutions in real time (and not Euclidean). This differential system is easily shown to be equivalent to

$$\begin{cases} 3(\mathring{M}/M)^\circ = (\mathring{M}/M + 6)\mathcal{P}(\mathring{M}/M), \\ \mathring{\phi}_\perp = \sqrt{2}\frac{c_\perp}{c_\phi}(\mathring{M}/M + 6) \end{cases} \tag{2.53}$$

where $c_\perp/c_\phi$ is an arbitrary constant denoted this way to make contact with the conventions of Eq. (2.43), and the polynomial

$$\begin{aligned} \mathcal{P}(x) = {} & \left[1 + 3(c_\perp/c_\phi)^2\right]x^2 + 36(c_\perp/c_\phi)^2 x \\ & + 9\left[12(c_\perp/c_\phi)^2 - 1\right] \text{ is of the sign of } n_V. \end{aligned} \tag{2.54}$$

Using the first equation in (2.43), one obtains

$$\sigma = \frac{9}{4}\frac{1}{\mathring{M}/M + 6}, \tag{2.55}$$

that can be used to identify consistently (2.51) with the first equation of (2.53). By the way, the real time condition translates to the condition that n_V and the denominator of the left-hand side of (2.51) have a common sign. We are going to solve this equation separately for $n_V > 0$ and $n_V < 0$.

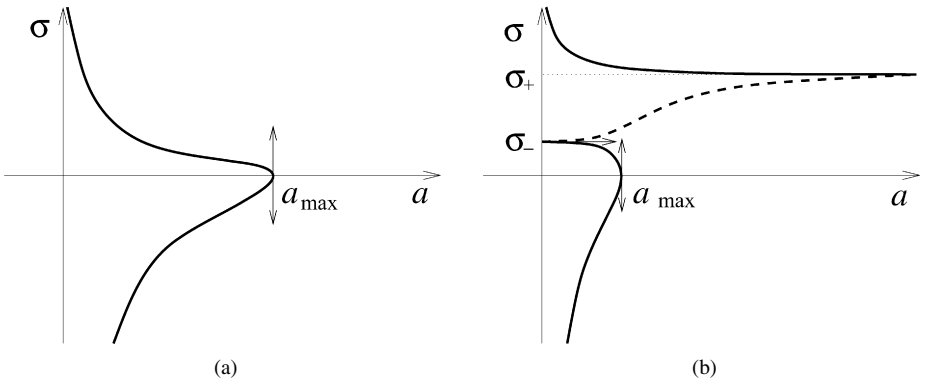

Fig. 3. σ, defined in Eq. (2.50) versus the scale factor a. (a) corresponds to $(c_\perp/c_\phi)^2 > 1/9$ and (b) corresponds to $(c_\perp/c_\phi)^2 \leqslant 1/9$. The solid lines are associated to the case $n_V > 0$, while the dashed one is associated to the case $n_V < 0$.

– For $n_V > 0$:

(i) When $(c_\perp/c_\phi)^2 > 1/9$, the denominator of (2.51) has no real root. Integrating, one obtains

$$\frac{a}{a_0} = \frac{\exp(-\frac{2}{9\sqrt{9(c_\perp/c_\phi)^2-1}}\tan^{-1}(\frac{4\sigma-2}{\sqrt{9(c_\perp/c_\phi)^2-1}}))}{(\sigma^2-\sigma+\frac{3}{16}(1+3(c_\perp/c_\phi)^2))^{1/18}}, \tag{2.56}$$

that is used to draw σ versus a on Fig. 3(a). Suppose $c_\phi > 0$. If at some time $\sigma > 0$, the definition of σ in Eq. (2.50) implies that a increases. Thus, the scale factor reaches a maximum $a_{\max}$ where σ vanishes. We then pass into the $\sigma < 0$ lower half plane where a decreases and converges to 0. Since $\sigma \to -\infty$ and $a \to 0$, one has $\dot{a} \to -\infty$, which is interpreted as a Big Crunch occurring at a finite time t_{BC}. Similar arguments apply when $c_\phi < 0$: If $\sigma < 0$, the scale factor increases up to $a_{\max}$ before converging to 0. This corresponds to a Big Crunch occurring at some finite time t_{BC}. To summarize, when the IBC are such that $c_\phi > 0$ ($c_\phi < 0$), the system follows the curve on Fig. 3(a) from up to down (down to up). The universe starts from a Big Bang, reaches a maximum size, and ends with a Big Crunch. Of course, only the parts of this evolution consistent with the hypothesis $z \gg 1$ can be trusted. In particular, when we approach t_{BC}, one has $\sigma \to -s\infty$, where $s = \mathrm{sign}(c_\phi)$, and Eq. (2.56) implies,

$$a(t) \simeq (t_{\mathrm{BC}} - t)^{1/12} \times \left((16/3)|c_\phi| a_0^9 e^{s9\pi/2}\right)^{1/12}, \quad t \lesssim t_{\mathrm{BC}}. \tag{2.57}$$

This result can be used to show that the integral in M in Eqs. (2.43) is bounded when $t \to t_{\mathrm{BC}}$ so that a consistent run away $e^z \propto 1/a^5 \to +\infty$ is found. An important remark then follows. The behavior (2.57) implies that c_ϕ/a^3 is dominated by H in Eq. (2.43), showing that the dynamics for $(c_\perp/c_\phi)^2 > 1/9$ is always attracted by the solution for $c_\phi = c_\perp = 0$.

(ii) When $(c_\perp/c_\phi)^2 \leqslant 1/9$, the left-hand side of Eq. (2.51) has two real roots. Integrating, one has

$$\text{for } \left(\frac{c_\perp}{c_\phi}\right)^2 < \frac{1}{9}: \quad \frac{a}{a_0} = \frac{|\sigma-\sigma_-|^{\frac{\sigma_-}{9(\sigma_+-\sigma_-)}}}{|\sigma-\sigma_+|^{\frac{\sigma_+}{9(\sigma_+-\sigma_-)}}}, \quad \sigma_\pm = \frac{1}{2} \pm \pm\frac{1}{4}\sqrt{1-9(c_\perp/c_\phi)^2}, \tag{2.58}$$

$$\text{for } \left(\frac{c_\perp}{c_\phi}\right)^2 = \frac{1}{9}: \quad \frac{a}{a_0} = \frac{e^{\frac{1}{18(\sigma-1/2)}}}{|\sigma - \frac{1}{2}|^{1/9}}, \quad \sigma_\pm = \frac{1}{2}, \tag{2.59}$$

where $\sigma_- < \sigma < \sigma_+$. Fig. 3(b) shows σ as a function of a.[7] When $c_\phi > 0$, the arguments used in case (i) apply on the branch $\sigma < \sigma_-$, where the system evolves from up to down. The scale factor grows up to $a_{\max}$ before converging to 0. Similarly, when $c_\phi < 0$ and the system follows the branch $\sigma > \sigma_+$, the scale factor converges to 0. In both cases, a Big Crunch occurs at t_{BC} and the behavior (2.57), with $s = 0$, is valid. The dynamics is again attracted by the solution associated to $c_\phi = c_\perp = 0$.

Some new features occur for $c_\phi < 0$, when $\sigma < \sigma_-$ (see Fig. 3(b)). The scale factor increases up to its maximum $a_{\max}$ before converging to 0, while $\sigma \to \sigma_-$, implying $\dot{a} \to -\infty$. A Big Crunch at a finite time t_{BC} occurs but since $\sigma \to \sigma_-$, one has

$$a(t) \simeq (t_{\mathrm{BC}} - t)^{1/3} \times \left((4/3)|c_\phi|\sigma_-\right)^{1/3}, \quad t \lesssim t_{\mathrm{BC}}. \tag{2.60}$$

However, this behavior can be trusted as long as $e^z \propto aM \propto |t_{\mathrm{BC}} - t|^{\frac{3}{4\sigma_-} - \frac{5}{3}} \to +\infty$. This condition implies that the scaling $(t_{\mathrm{BC}} - t)^{1/3}$ exists when

$$c_\phi < 0 \quad \text{and} \quad \frac{1}{9}(1 - 1/25) < \left(\frac{c_\perp}{c_\phi}\right)^2 \leqslant \frac{1}{9}. \tag{2.61}$$

In this case, the evolution is not attracted by the solution $c_\phi = c_\perp = 0$. Actually, Eq. (2.43) can be rewritten as

$$\alpha\phi \simeq -\left(2 - \frac{3}{4\sigma_-}\right) \ln|t_{\mathrm{BC}} - t| + c \to +\infty \quad \text{when } t \to t_{\mathrm{BC}}, \tag{2.62}$$

so that the integration constant c is negligible. There is thus a new basin of attraction, to the solution (2.60) with $c = 0$ i.e. such that

$$3H^2 \simeq \frac{c_m^2}{a^6} \quad \text{where } c_m = \frac{1}{27} c_\phi^2 \sigma_-^2, \ c = 0. \tag{2.63}$$

As for the previous Big Crunch behavior, the divergence of M (and T) is only formal since the present analysis supposes $M < M_H$, where a Hagedorn-like transition occurs. On the contrary, for $(c_\perp/c_\phi)^2$ smaller than the lower bound of the range (2.61), we formally have $e^z \propto |t_{\mathrm{BC}} - t|^{\frac{3}{4\sigma_-} - \frac{5}{3}} \to 0$, which shows that the system actually exits from the regime $z \gg 1$ we started with. Similarly, if $c_\phi > 0$ and the system evolves along the branch $\sigma > \sigma_+$ of Fig. 3(b), one has $a \to +\infty$ and $\sigma \to \sigma_+$. This implies $a \simeq t^{1/3} \times ((4/3)c_\phi\sigma_+)^{1/3}$ and $t \to +\infty$. However, for large positive z, this implies $e^z \propto aM \propto t^{\frac{3}{4\sigma_+} - \frac{5}{3}} \to 0$, which shows that the system actually exits in the regime $z \gg 1$.

Summary for $n_V > 0$:

We have shown analytically that when $z_0 \gg 1$, either $z \to +\infty$ or z quits the regime $z \gg 1$. To study the dynamics at finite z, we use again a code that implements Eqs. (2.26). The phases of expansion are simulated when a positive increment for λ is chosen. For generic IBC, we observe that the right-hand side of the Friedmann equation (2.25) changes sign at some finite $a = a_{\max}$.

[7] To be precise, the slope at the point $(a, \sigma) = (0, \sigma_-)$ is infinite when $(1 - 4/361)/9 < (c_\perp/c_\phi)^2 \leqslant 1/9$, finite when $(c_\perp/c_\phi)^2 = (1 - 4/361)/9$ and vanishing when $(c_\perp/c_\phi)^2 < (1 - 4/361)/9$.

This actually means that the scale factor has reached a maximum (the Hubble parameter H vanishes), and that the evolution enters into a phase of contraction. Such eras are simulated by choosing a negative increment for λ and we observe that for generic IBC, z ends by running away. As a conclusion, the generic IBC admit two basins of attraction to MDS. The evolutions converge either to the solution where $c_\phi = c_\perp = 0$ i.e. such that $3H^2 = c_M^2/a^{24}$, or to the solution with $c = 0$ and $3H^2 = c_m^2/a^6$.

– *For* $n_V < 0$:

For IBC such that $z_0 \gg 1$, the real time condition translates to $\sigma_- < \sigma < \sigma_+$ (see Fig. 3(b)). If $c_\phi > 0$, the definition of σ in Eq. (2.51) reaches $\dot{a} > 0$. It follows that $a \to +\infty$ and $\sigma \to \sigma_+$. Thus, $a \simeq t^{1/3} \times ((4/3)c_\phi \sigma_+)^{1/3}$ where $t \to +\infty$, and $e^z \propto aM \propto t^{\frac{3}{4\sigma_+} - \frac{5}{3}} \to 0$. We conclude that the system exits the regime $z \gg 1$. When $-1/15 < n_V/n_T < 0$ (*Case* (b)), this result is compatible with Section 2.3, where we found that the expanding evolutions satisfy $z \to z_c$.

If on the contrary $c_\phi < 0$, one has $\dot{a} < 0$. It follows from Fig. 3(b) that $a \to 0$ and $\sigma \to \sigma_-$, so that $\dot{a} \to -\infty$. The dynamics is attracted by the Big Crunch solution (2.60) i.e. (2.63) that can be trusted when the conditions (2.61) are satisfied. For smaller values of $(c_\perp/c_\phi)^2$, the system exits the regime $z \gg 1$. These conclusions are compatible with the numerical simulations of the contracting evolutions described at the end of Section 2.4, for generic IBC in *Case* (b). We found there that either $z \to +\infty$, as expected from the existence of the Big Crunch solution (2.60), or z oscillates with a larger and larger amplitude, implying that when z is large and positive, it can exit the regime $z \gg 1$.

- $n_V = 0$, $z \gg 1$:

We argued in Section 2.3 that when $-1/15 < n_V/n_T < 0$, the expanding evolutions are such that z is attracted by a critical value z_c. Since $z_c \to +\infty$ when $n_V/n_T \to 0_-$, we expect the expanding solutions for $n_V = 0$ to satisfy $z(t) \to +\infty$. Actually, this run away may be natural since the potential in Eq. (2.27) decreases linearly for large positive z, $V \sim -z n_T c_4^o$. In fact, a numerical study of the differential system (2.26) with $n_V = 0$ confirms that for generic IBC, z enters the regime $z \gg 1$ when we simulate the expanding solutions. On the other hand, for the evolutions where the scale factor decreases, we find either $z \to +\infty$ or z oscillates with a larger and larger amplitude. In all these cases, we are thus invited to consider analytically the system in the regime $z \gg 1$.

In this limit, the thermal effective potential for ϕ in Eq. (2.16) vanishes (up to exponentially small terms in z). Both ϕ and $\phi_\perp$ are flat directions, and their kinetic energies involve two constants c_ϕ, $c_\perp$, determined by the IBC,

$$\alpha\dot{\phi} = \frac{c_\phi}{a^3}, \qquad \dot{\phi}_\perp = \sqrt{2}\frac{c_\perp}{a^3}. \tag{2.64}$$

The energy density in the Friedmann equation (2.12) is $\rho \simeq 3T^4 n_T c_4^o$ and, using (2.39), one has

$$3H^2 = \frac{c_r^2}{a^4} + \frac{c_m^2}{a^6} \quad \text{where } c_r^2 = 3n_T c_4^o (a_0 T_0)^4,\ c_m^2 = c_\perp^2 + \frac{c_\phi^2}{3}. \tag{2.65}$$

This equation admits two monotonic solutions (see Eq. (2.32)), mapped to one another under time reversal. However, one can only trust them as long as $z \gg 1$.

– For the expanding evolutions, since $a(t) \to +\infty$ when $t \to +\infty$, Eq. (2.64) implies that $M(t)$ converges to a constant M_0. It follows that $e^z = M/T \propto a \to +\infty$, showing the validity of the solution for large enough time. We conclude that for generic IBC, the expanding evolutions are attracted to the RDS, Eq. (2.33), with $M = M_0$.
– For the contracting evolutions, depending on c_ϕ and $c_\perp$, we have

$$a(t) \simeq (t_{\mathrm{BC}} - t)^{1/3} \times \left(3c_m^2\right)^{1/6},$$
$$M \simeq M_0\left(1 - \frac{t}{t_{\mathrm{BC}}}\right)^{-\frac{1}{[1+3(c_\perp/c_\phi)^2]^{1/2}}}, \quad t \lesssim t_{\mathrm{BC}}, \tag{2.66}$$

if the constraints

$$c_\phi > 0 \quad \text{and} \quad \left(\frac{c_\perp}{c_\phi}\right)^2 < \frac{8}{3} \tag{2.67}$$

are satisfied (so that $z \to +\infty$ when $t \to t_{\mathrm{BC}}$). Alternatively, if $c_\phi = c_\perp = 0$, the solution

$$a(t) \simeq \sqrt{t_{\mathrm{BC}} - t} \times \left(\frac{4}{3}c_r^2\right)^{1/4}, \qquad M \simeq M_0 \tag{2.68}$$

is also consistent with a run away of z. For all other values of c_ϕ and $c_\perp$, z exits the regime $z \gg 1$. Our conclusions for the contracting evolutions are that there are two sets of generic IBC. The first gives rise to a run away of z that corresponds to the Big Crunch solutions (2.66) or (2.68). The second yields an oscillation regime in z, with larger and larger amplitude.

3. Susy breaking involving $n = 2$ internal directions

In this section we extend our analysis to models where the supersymmetry breaking is induced by $n = 2$ Scherk–Schwarz circles $S^1(R_4) \times S^1(R_5)$ in the 4th and 5th internal dimensions as in Ref. [14]. Thus, we are considering the heterotic or type II superstrings on

$$S^1(R_0) \times T^3 \times S^1(R_4) \times S^1(R_5) \times \mathcal{M}_4, \tag{3.1}$$

where $\mathcal{M}_4$ is either T^4 or $K3 \sim T^4/\mathbb{Z}_2$. As shown in [14], such models allow cosmological evolutions that describe radiation dominated eras, with stabilized complex structure modulus R_5/R_4 [14]. The present analysis could certainly be extended to the other classes of models described in [14], where asymmetric Scherk–Schwarz compactifications in the directions 4 and/or 5 are considered. These models would involve run away solutions in the spirit of the *Cases* (c) and (a) for $n = 1$.

R_0, R_4, R_5 are restricted to be large enough in order to avoid Hagedorn-like phase transitions. In this regime, the free energy and pressure are computed in Ref. [14]:

$$P = T^4 p(z, Z) \quad \text{where } e^z = \frac{M}{T},\ T = \frac{1}{2\pi R_0\sqrt{\mathrm{Re}\, S}},$$
$$M = \frac{1}{2\pi\sqrt{R_4 R_5}\sqrt{\mathrm{Re}\, S}},\ e^Z = \frac{R_5}{R_4}. \tag{3.2}$$

T is the temperature in the Einstein frame, M is the supersymmetry breaking scale which is given in terms of the geometric mean of the moduli R_4 and R_5, and Z parametrizes the complex structure modulus R_5/R_4. The quantity $p(z, Z)$ is a linear sum of functions, with model-dependent

integer coefficients,

$$p(z,Z) = n_T\, p_{100}(z,Z) + n_{010}\, p_{010}(z,Z) + n_{001}\, p_{001}(z,Z) + n_{111}\, p_{111}(z,Z), \tag{3.3}$$

where n_T is again the number of massless states and

$$p_{\tilde{g}_0\tilde{g}_4\tilde{g}_5} = \frac{2}{\pi^3} \sum_{\tilde{m}_0,\tilde{m}_4,\tilde{m}_5} \frac{e^{4z}}{[(2\tilde{m}_0+\tilde{g}_0)^2 e^{2z} + (2\tilde{m}_4+\tilde{g}_4)^2 e^{-Z} + (2\tilde{m}_5+\tilde{g}_5)^2 e^{Z}]^3}. \tag{3.4}$$

3.1. Gravitational and moduli equations

The low energy effective action (2.7) with the kinetic term of R_5 taken into account can be written in terms of redefined fields as:

$$S = \int d^4x \sqrt{-g}\left[\frac{1}{2}R - \frac{1}{2}\left((\partial\phi)^2 + (\partial\phi_\perp)^2 + \frac{1}{2}(\partial Z)^2\right) + P\right], \tag{3.5}$$

where

$$\begin{aligned} &\phi := \phi_D - \ln\sqrt{R_4 R_5}, \qquad \phi_\perp := \phi_D + \ln\sqrt{R_4 R_5}, \\ &P = M^4 e^{-4z} p(z,Z), \qquad M = \frac{e^{\phi}}{2\pi}. \end{aligned} \tag{3.6}$$

For evolutions satisfying the metric ansatz (2.11), the Friedmann equation is

$$3H^2 = \frac{1}{2}\dot{\phi}^2 + \frac{1}{4}\dot{Z}^2 + \frac{1}{2}\dot{\phi}_\perp^2 + T^4 r \quad \text{where } r(z,Z) = 3p - p_z, \tag{3.7}$$

while the equation for the scale factor,

$$2\dot{H} + 3H^2 = -\frac{1}{2}\dot{\phi}^2 - \frac{1}{4}\dot{Z}^2 - \frac{1}{2}\dot{\phi}_\perp^2 - T^4 p, \tag{3.8}$$

can be replaced by the conservation of the energy–momentum in a form similar to Eq. (2.19),

$$\dot{\rho} + 3H(\rho + P) + \dot{\phi}T^4(3p - r) + \dot{Z}T^4 p_Z = 0. \tag{3.9}$$

For the scalar fields, one has

$$\ddot{\phi} + 3H\dot{\phi} = T^4(3p - r), \tag{3.10}$$

$$\ddot{Z} + 3H\dot{Z} = T^4 2 p_Z, \tag{3.11}$$

$$\ddot{\phi}_\perp + 3H\dot{\phi}_\perp = 0 \implies \dot{\phi}_\perp = \sqrt{2}\frac{c_\perp}{a^3}. \tag{3.12}$$

We proceed by introducing the variable λ of (2.20) as in Section 2.2 to express

$$\begin{aligned} &\mathring{\phi} = \mathcal{A}(z,Z)\mathring{z} + \mathcal{B}(z,Z)\mathring{Z} - 1 \\ &\quad \text{where } \mathcal{A}(z,Z) = \frac{4r - r_z}{3(r+p)},\ \mathcal{B}(z,Z) = -\frac{r_Z + p_Z}{3(r+p)}, \end{aligned} \tag{3.13}$$

that reaches, by integration,

$$M = \frac{e^{\mathcal{F}(\ln a)}}{a} \quad \text{where } \mathring{\mathcal{F}}(\lambda) := \mathcal{A}(z,Z)\mathring{z} + \mathcal{B}(z,Z)\mathring{Z}. \tag{3.14}$$

This result can be used to rewrite the Friedmann equation (3.7) in either of the following forms,

$$3H^2 = \frac{3}{5}H^2\left((\mathcal{A}\overset{\circ}{z} + \mathcal{B}\overset{\circ}{Z} - 1)^2 + \frac{1}{2}\overset{\circ}{Z} - 1\right)^2 + \frac{6}{5}\frac{e^{4[\mathcal{F}(\ln a)-z]}}{a^4}r(z,Z) + \frac{6}{5}\frac{c_\perp^2}{a^6}, \tag{3.15}$$

or

$$H^2 = T^4\frac{r(z,Z)}{3-\mathcal{K}(z,\overset{\circ}{z},Z,\overset{\circ}{Z},\overset{\circ}{\phi}_\perp)}$$
$$\text{where } \mathcal{K} = \frac{1}{2}\left(\mathcal{A}(z,Z)\overset{\circ}{z} + \mathcal{B}(z,Z)\overset{\circ}{Z} - 1\right)^2 + \frac{1}{4}\overset{\circ}{Z}{}^2 + \frac{1}{2}\overset{\circ}{\phi}{}_\perp^2, \tag{3.16}$$

while the equations for the scalars become

$$\begin{cases} \frac{r}{3-\mathcal{K}}(\mathcal{A}\overset{\circ\circ}{z} + \mathcal{B}\overset{\circ\circ}{Z} + \mathcal{A}_z\overset{\circ}{z}{}^2 + (\mathcal{A}_Z + \mathcal{B}_z)\overset{\circ}{z}\overset{\circ}{Z} + \mathcal{B}_Z\overset{\circ}{Z}{}^2) + \frac{r-p}{2}(\mathcal{A}\overset{\circ}{z} + \mathcal{B}\overset{\circ}{Z}) + V_z^{(z)} = 0, \\ \frac{r}{3-\mathcal{K}}\overset{\circ\circ}{Z} + \frac{r-p}{2}\overset{\circ}{Z} + V_Z^{(Z)} = 0, \\ \frac{r}{3-\mathcal{K}}\overset{\circ\circ}{\phi}_\perp + \frac{r-p}{2}\overset{\circ}{\phi}_\perp = 0 \end{cases} \tag{3.17}$$

where we have defined

$$V_z^{(z)}(z,Z) = \frac{r-5p}{2} \quad \text{and} \quad V_Z^{(Z)}(z,Z) = -2p_Z. \tag{3.18}$$

3.2. Attraction to the RDS

A wide range of behaviors can emerge from this system of differential equations. However, in the spirit of Section 2.3, we choose to look for cosmological solutions with stabilized complex structures $e^z = R_0/\sqrt{R_4R_5}$ and $e^Z = R_5/R_4$ i.e. satisfying $(z,Z) \equiv (z_c, Z_c)$. From the system (3.17), such solutions exist if the following conditions are simultaneously satisfied,

$$V_z^{(z)}(z_c,Z_c) = 0 \quad \text{i.e. } 2p(z_c,Z_c) + p_z(z_c,Z_c) = 0, \tag{3.19}$$

$$V_Z^{(Z)}(z_c,Z_c) = 0 \quad \text{i.e. } p_Z(z_c,Z_c) = 0. \tag{3.20}$$

These equations define two sets of curves in the (z,Z)-plane, whose intersections determine the critical points (z_c, Z_c). Supposing such a solution exists, the corresponding cosmological evolution is characterized by $\overset{\circ}{\mathcal{F}} = 0$ in Eq. (3.14) and thus

$$M(t) = e^{z_c}T(t) = \frac{e^{\mathcal{F}}}{a(t)} \quad \text{where } \mathcal{F} = \text{cst.},\ R_5(t) = e^{Z_c}R_4(t), \tag{3.21}$$

together with the Friedmann equation (3.15),

$$3H^2 = \frac{c_r^2}{a^4} + \frac{c_m^2}{a^6} \quad \text{where } c_r^2 = 6e^{4(\mathcal{F}-z_c)}p(z_c,Z_c),\ c_m^2 = \frac{6}{5}c_\perp^2. \tag{3.22}$$

The latter is qualitatively identical to the one found for $n = 1$ in *Case* (b). The evolution with expanding scale factor is asymptotic to the critical solution $(z,Z) \equiv (z_c, Z_c)$, $c_m = 0$, where $a(t)$ is given in (2.33).

To study the local stability around a critical solution with $c_m = 0$, we define small perturbations around it,

$$z(\lambda) = z_c + \varepsilon(\lambda), \qquad Z(\lambda) = Z_c + E(\lambda), \qquad \overset{\circ}{\phi}_\perp(\lambda) = \overset{\circ}{\varepsilon}_\perp(\lambda), \tag{3.23}$$

and consider the system (3.17) at first order in ε, E and $\overset{\circ}{\varepsilon}_\perp$. The latter can be brought into the form

$$\begin{cases} \overset{\circ\circ}{\varepsilon} + \overset{\circ}{\varepsilon} + \xi\varepsilon + \omega E = 0 & \text{where } \xi = \frac{9p(4p-p_{zz})+2p_{zZ}^2}{2p(26p+p_{zz})}|_{(z_c,Z_c)},\ \omega = \frac{p_{zZ}(2p_{ZZ}-9p)}{2p(26p+p_{zz})}|_{(z_c,Z_c)}, \\ \overset{\circ\circ}{E} + \overset{\circ}{E} + \Xi E + \Omega\varepsilon = 0 & \text{where } \Xi = -\frac{p_{ZZ}}{p}|_{(z_c,Z_c)},\ \Omega = -\frac{p_{zZ}}{p}|_{(z_c,Z_c)}, \\ \overset{\circ\circ}{\varepsilon}_\perp + \overset{\circ}{\varepsilon}_\perp = 0. \end{cases} \tag{3.24}$$

To proceed, we specialize on the set of models whose R-symmetry charges coupled to the winding and momentum numbers in the directions 4 and 5 are identical. For this set, it is shown in [14] that the function p in Eq. (3.3) takes the form,

$$p(z,Z) = n_T[p_{100}+p_{111}] + n_V[p_{010}+p_{001}], \quad -1 \leqslant \frac{n_V}{n_T} \leqslant 1, \tag{3.25}$$

and that the range of n_V/n_T can be divided in four phases whose frontiers are given by $\{-0.215, -1/31, 0\}$ [14].

- For $n_V/n_T \lesssim -0.215$, the constraint (3.19) has no solution.
- For $-0.215 \lesssim n_V/n_T < -1/31$, the constraint (3.19) defines a non-trivial curve, while the condition (3.20) is satisfied on the axis $Z = 0$. The two loci intersect at a point $(z_c, 0)$.
- For $-1/31 < n_V/n_T < 0$, the constraint (3.19) defines a non-trivial curve, while the condition (3.20) corresponds to 3 curves, one of which being the axis $Z = 0$. There is a unique intersection point $(z_c, 0)$.
- For $0 < n_V/n_T$, the constraint (3.19) has no solution.

Thus, a solution to the equations of motion with constant complex structures (z_c, Z_c) exists when $-0.215 \lesssim n_V/n_T < 0$.

The class of models we consider have a symmetry $R_4 \leftrightarrow R_5$ that translates to $Z \leftrightarrow -Z$. This implies $p_{zZ}(z_c, 0) = 0$ and

$$\xi = \frac{9}{2}\frac{4p-p_{zz}}{26p+p_{zz}}\bigg|_{(z_c,Z_c)}, \qquad \omega = 0, \qquad \Xi = -\frac{p_{ZZ}}{p}\bigg|_{(z_c,Z_c)}, \qquad \Omega = 0. \tag{3.26}$$

As in the $n = 1$ case, one finds numerically that ξ and Ξ are always positive. They increase from 0 to $+\infty$ when n_T/n_V varies from $\simeq -0.215$ to 0, which shows that $\varepsilon(\lambda)$, $E(\lambda)$ (and $\overset{\circ}{\varepsilon}_\perp(\lambda)$) are always converging to zero. This means that in the class of models under investigation, when a solution (z_c, Z_c) exists, it is stable under small perturbations.

A numerical study of the exact system (3.17) shows that for generic IBC $(z_0, \overset{\circ}{z}_0, Z_0, \overset{\circ}{Z}_0, \overset{\circ}{\phi}_{\perp 0})$ such that the right-hand side of Eq. (3.16) is positive, the expanding cosmological solutions satisfy $(z(\lambda), Z(\lambda)) \to (z_c, Z_c)$ when $\lambda \to +\infty$. We conclude that the dynamics of the expanding evolutions is attracted by the RDS described by the critical solution $(z, Z) \equiv (z_c, Z_c)$, $\dot{\phi}_\perp \equiv 0$ i.e. $3H^2 = c_r^2/a^4$ (Eq. (3.21)).

4. An inflation era?

We have described how cosmological evolutions can be determined by the R-charges of the massless spectrum. In particular, we found that the dynamics can be attracted to a radiation era, with stabilized complex structures. In standard cosmology, such an era follows a period of inflation introduced to explain the observed flatness and homogeneity of our universe, or solve

the topological defect problem. It is thus important to analyze if our attraction mechanism admits periods of accelerated cosmology.

Using the Einstein equations, the inflation condition $\ddot{a} > 0$ or $\dot{H} + H^2 > 0$ can be translated into an inequality between the thermal sources ρ, P and the scalar kinetic energies (take $\dot{Z} = 0$ for $n = 1$),

$$\frac{1}{2}\left(P + \frac{1}{3}\rho\right) < -\frac{1}{3}\left(\dot{\phi}^2 + \frac{1}{2}\dot{Z}^2 + \dot{\phi}_\perp^2\right). \tag{4.1}$$

Using the variable λ and Eq. (2.25) (or (3.16)), we obtain

$$p - \frac{1}{6}p_z < -2\left(p - \frac{1}{3}p_z\right)\frac{1}{\frac{3}{\mathcal{K}} - 1} \leqslant 0, \tag{4.2}$$

where there are two conditions in one: First, $p - p_z/6$ has to be negative, and second it has to be negative enough compared to the right-hand side that depends on the kinetic energies.

For the classes of models we considered for $n = 1$ (see Eq. (2.4)) and $n = 2$ (see Eq. (3.25)), one can show that a necessary condition to have $p - p_z/6 < 0$ is $n_V < 0$. We thus carry on our discussion in this case. It then follows that the quantity $p - p_z/3$ in (4.2) is always positive. Altogether, a necessary and sufficient condition for an accelerated cosmology is:

$$n_V < 0 \quad \text{and} \quad \mathcal{K} < \mathcal{I} \quad \text{where } \mathcal{I} = -\frac{3p - \frac{1}{2}p_z}{p - \frac{1}{2}p_z}. \tag{4.3}$$

Actually, when deriving (4.3) from (4.2), one also finds that $\mathcal{I} \leqslant 3$. However, this is an empty constraint since the function $\mathcal{I}$ satisfies $\mathcal{I} \leqslant 1$.

For a susy breaking with $n = 1$

From (4.3), in order to have solutions, we need $\mathcal{I}(n_V/n_T, z) > 0$. This condition defines a domain in the $(n_V/n_T, z)$-plan where, by definition, $\mathcal{I} = 0$ on the boundary. However, it happens that $\mathcal{I} \lesssim 1$ in the interior, as can be seen on Fig. 4(a). We can thus estimate the e-fold number by considering z large and positive. In particular, when $-1/15 < n_V/n_T < 0$, the z's allowing periods of accelerated cosmology are always larger than z_c. When $z \gg 1$, the condition (4.3) simplifies to

$$\mathcal{K} \simeq \frac{1}{3}(\mathring{M}/M)^2 + (c_\perp/c_\phi)^2(\mathring{M}/M + 6)^2 \lesssim 1, \tag{4.4}$$

where we have used the second equation of (2.53). An era of acceleration exists if $(c_\perp/c_\phi)^2 < 1/33$. It begins and ends at most when $\mathring{M}/M$ saturates the inequality (4.4) i.e. equals

$$l_{b,e} = \frac{-18(c_\perp/c_\phi)^2 \pm \sqrt{3[1 - 33(c_\perp/c_\phi)^2]}}{1 + 3(c_\perp/c_\phi)^2}. \tag{4.5}$$

To find the scale factors a_b and a_e when this arises, we integrate the first equation of (2.53),

$$\begin{aligned} \ln\left(\frac{a}{a_0}\right) &\equiv \lambda - \lambda_0 \\ &= \gamma \ln|\mathring{M}/M + 6| + \gamma_+ \ln|\mathring{M}/M - l_+| + \gamma_- \ln|\mathring{M}/M - l_-|, \end{aligned} \tag{4.6}$$

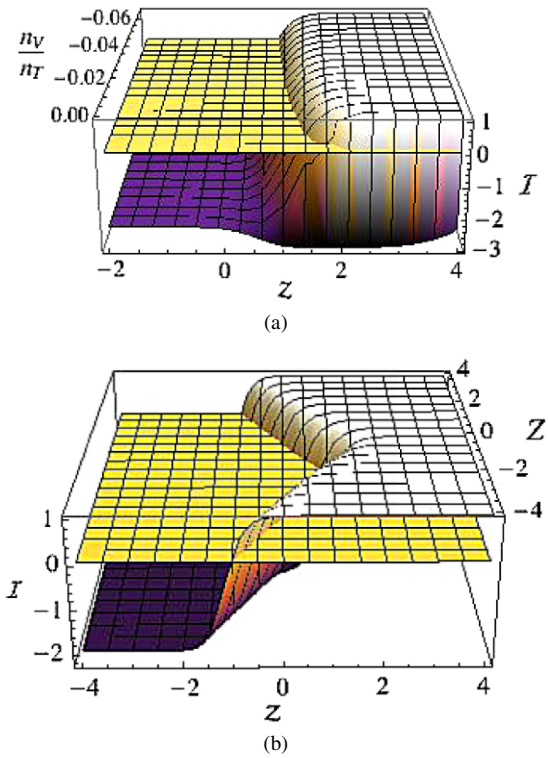

Fig. 4. For one modulus z, (a): In the domain $\mathcal{I} > 0$ of the $(n_V/n_T, z)$-plane $(-1/15 < n_V/n_T < 0)$, $\mathcal{I}$ can be approximated by 1, its value for $z \gg 1$. For two moduli (z, Z), (b): For any fixed $-0.215 \lesssim n_V/n_T < 0$, in the domain $\mathcal{I} > 0$ of the (z, Z)-plane, $\mathcal{I}$ can be approximated by 1, its asymptotic value in the sectors II, III, IV, V defined in Eq. (4.9). (b) is drawn for $n_V/n_T = -1/63$.

where

$$
\begin{aligned}
l_\pm &= \frac{-18(c_\perp/c_\phi)^2 \pm 3\sqrt{1-9(c_\perp/c_\phi)^2}}{1+3(c_\perp/c_\phi)^2}, \\
\gamma &= \frac{3}{1+3(c_\perp/c_\phi)^2}\frac{1}{(l_+ + 6)(l_- + 6)}, \\
\gamma_\pm &= \pm\frac{3}{1+3(c_\perp/c_\phi)^2}\frac{1}{(l_\pm + 6)(l_+ - l_-)}.
\end{aligned}
\tag{4.7}
$$

Inserting the particular values (4.5) in (4.6), the maximum e-fold number is found to be

$$
e(c_\perp/c_\phi) = \ln\frac{a_e}{a_b} = \gamma \ln\left|\frac{l_e+6}{l_b+6}\right| + \gamma_+ \ln\left|\frac{l_e-l_+}{l_b-l_+}\right| + \gamma_- \ln\left|\frac{l_e-l_-}{l_b-l_-}\right|, \tag{4.8}
$$

that satisfies $e(c_\perp/c_\phi) \leqslant e(0) \simeq 0.227$. Thus, even if periods of accelerated scale factor are allowed, they do not give rise to inflationary eras.

For a susy breaking with $n = 2$

For any fixed $n_V/n_T < 0$, the condition $\mathcal{I}(n_V/n_T, z, Z) > 0$ defines a domain in the (z, Z)-plan, as shown on Fig. 4(b). Using the notations of [14], this zone spans four asymptotic sectors defined as follows,

$$\begin{aligned}
&\text{II:}\quad Z \to -\infty,\ z \sim \eta Z,\ |\eta| < \frac{1}{2}, \qquad \text{III:}\quad Z \sim \eta z \to -\infty,\ -2 < \eta < 0,\\
&\text{IV:}\quad Z \sim \eta z \to +\infty,\ 0 < \eta < 2, \qquad \text{V:}\quad Z \to +\infty,\ z \sim \eta Z,\ |\eta| < \frac{1}{2},
\end{aligned} \tag{4.9}$$

inside of which $\mathcal{I} \lesssim 1$. We will evaluate the e-fold number by approximating $p(z, Z)$ by its asymptotic expansions, which are well defined in each sectors [14]:

$$\begin{aligned}
p^{\mathrm{II}} &= e^{4z}e^{-3Z}n_V S_6^o + e^{-z}e^{-Z/2}\big(n_T S_5^o + n_V S_5^e\big) + e^{3z}e^{3Z/2}(n_T + n_V)\big(S_4^o + S_4^e\big) + \cdots,\\
p^{\mathrm{III}} &= e^{4z}e^{-3Z}n_V S_6^o + e^{4z}e^{2Z}n_V\big(S_5^o + S_5^e\big) + 2\big(n_T S_4^o + n_V S_4^e\big) + \cdots,\\
p^{\mathrm{IV}} &= e^{4z}e^{3Z}n_V S_6^o + e^{4z}e^{-2Z}n_V\big(S_5^o + S_5^e\big) + 2\big(n_T S_4^o + n_V S_4^e\big) + \cdots,\\
p^{\mathrm{V}} &= e^{4z}e^{3Z}n_V S_6^o + e^{-z}e^{Z/2}\big(n_T S_5^o + n_V S_5^e\big) + e^{3z}e^{-3Z/2}(n_T + n_V)\big(S_4^o + S_4^e\big) + \cdots
\end{aligned} \tag{4.10}$$

where the dots stand for exponentially suppressed terms and the coefficients $S_{4,5,6}^{o,e}$ are constants.[8]

It is interesting to note that the behavior of the temperature depends drastically on the location of the representative point of the system in the (z, Z)-plan. In sectors III and IV, one finds $\mathcal{A} \simeq 1$, $\mathcal{B} \simeq 0$ as in the 1 modulus case, while in sectors II (or V), one has $\mathcal{A} \simeq 4/3$, $\mathcal{B} \simeq 1/6$ (or $-1/6$). Using the energy–momentum conservation in the form of Eq. (3.13), this reaches

$$\text{II:}\quad \frac{M^2 e^Z}{a^6 T^8} = \text{cst.}, \qquad \text{III} \cup \text{IV:}\quad aT = \text{cst.}, \qquad \text{V:}\quad \frac{M^2 e^{-Z}}{a^6 T^8} = \text{cst.} \tag{4.11}$$

However, the equations of motion for the scalar fields are identical in all these asymptotic sectors,

$$\begin{cases}
\dfrac{1}{\frac{1}{2}(\mathring{M}/M)^2 + \frac{1}{4}\dot{Z}^2 + \frac{1}{2}\mathring{\phi}_\perp{}^2 - 3}(\mathring{M}/M)^\circ - \mathring{M}/M - 4 = 0,\\
\dfrac{1}{\frac{1}{2}(\mathring{M}/M)^2 + \frac{1}{4}\dot{Z}^2 + \frac{1}{2}\mathring{\phi}_\perp^2 - 3}\mathring{\mathring{Z}} - \mathring{Z} + 6 = 0,\\
\dfrac{1}{\frac{1}{2}(\mathring{M}/M)^2 + \frac{1}{4}\dot{Z}^2 + \frac{1}{2}\mathring{\phi}_\perp^2 - 3}\mathring{\mathring{\phi}}_\perp - \mathring{\phi}_\perp = 0
\end{cases} \tag{4.12}$$

where the fractions in front of the second derivatives must have the sign of n_V i.e. negative. When $\mathring{M}/M + 4 \neq 0$, it is easy to show that there exist constants $c_\phi \neq 0$, c_Z, $c_\perp$ such that

$$\begin{cases}
2(\mathring{M}/M)^\circ = (\mathring{M}/M + 4)\mathcal{P}(\mathring{M}/M),\\
\mathring{Z} - 6 = 2\frac{c_Z}{c_\phi}(\mathring{M}/M + 4),\\
\mathring{\phi}_\perp = \sqrt{2}\frac{c_\perp}{c_\phi}(\mathring{M}/M + 4)
\end{cases} \tag{4.13}$$

[8] Their precise values are not needed in the following but can be found in the appendix of [14].

where

$$\mathcal{P}(x) = \left[1 + 2(c_Z/c_\phi)^2 + 2(c_\perp/c_\phi)^2\right]x^2 + 4\left[4(c_Z/c_\phi)^2 + 3c_Z/c_\phi + 4(c_\perp/c_\phi)^2\right]x + 4\left[8(c_Z/c_\phi)^2 + 12c_Z/c_\phi + 8(c_\perp/c_\phi)^2 + 3\right] \text{ is of the sign of } n_V. \tag{4.14}$$

The condition (4.3) is also identical in all asymptotic sectors II, ..., V,

$$\mathcal{K} \simeq \frac{1}{2}(\mathring{M}/M)^2 + \left[(c_Z/c_\phi)(\mathring{M}/M) + 3\right]^2 + (c_\perp/c_\phi)^2(\mathring{M}/M + 4)^2 \lesssim 1, \tag{4.15}$$

where we have used the second and third equations of (4.13). A period of accelerated cosmology exists if

$$(c_\perp/c_\phi)^2 < \frac{1}{14}, \quad c_- < c_Z/c_\phi < c_+ \quad \text{where } c_\pm = \frac{-6 \pm 2\sqrt{2[1 - 14(c_\perp/c_\phi)^2]}}{7}. \tag{4.16}$$

It begins and ends at most when $\mathring{M}/M$ saturates the inequality (4.15) i.e. equals

$$l_{b,e} = \frac{-2[4(c_Z/c_\phi)^2 + 3c_Z/c_\phi + 4(c_\perp/c_\phi)^2] \pm \sqrt{14(c_+ - c_Z/c_\phi)(c_Z/c_\phi - c_-)}}{1 + 2(c_Z/c_\phi)^2 + 2(c_\perp/c_\phi)^2}. \tag{4.17}$$

To find the corresponding scale factors a_b, a_e, we integrate the first equation of (4.13),

$$\ln\left(\frac{a}{a_0}\right) \equiv \lambda - \lambda_0 = \gamma \ln|\mathring{M}/M + 4| + \gamma_+ \ln|\mathring{M}/M - l_+| + \gamma_- \ln|\mathring{M}/M - l_-|, \tag{4.18}$$

where

$$l_\pm = \frac{-2[4(c_Z/c_\phi)^2 + 3c_Z/c_\phi + 4(c_\perp/c_\phi)^2] \pm \sqrt{10(C_+ - c_Z/c_\phi)(c_Z/c_\phi - C_-)}}{1 + 2(c_Z/c_\phi)^2 + 2(c_\perp/c_\phi)^2},$$

$$\text{with } C_\pm = \frac{-6 \pm \sqrt{7[3 - 10(c_\perp/c_\phi)^2]}}{5},$$

$$\gamma = \frac{2}{1 + 2(c_Z/c_\phi)^2 + 2(c_\perp/c_\phi)^2}\frac{1}{(l_+ + 4)(l_- + 4)},$$

$$\gamma_\pm = \pm\frac{2}{1 + 2(c_Z/c_\phi)^2 + 2(c_\perp/c_\phi)^2}\frac{1}{(l_\pm + 4)(l_+ - l_-)}. \tag{4.19}$$

Inserting (4.17) in (4.18), the maximum e-fold number is found to be

$$e(c_Z/c_\phi, c_\perp/c_\phi) = \ln\frac{a_e}{a_b} = \gamma \ln\left|\frac{l_e + 4}{l_b + 4}\right| + \gamma_+ \ln\left|\frac{l_e - l_+}{l_b - l_+}\right| + \gamma_- \ln\left|\frac{l_e - l_-}{l_b - l_-}\right|, \tag{4.20}$$

that satisfies $e(c_Z/c_\phi, c_\perp/c_\phi) \leqslant e(-3/2, 0) \simeq 0.189$. The order of magnitude of the e-fold number for $n = 1$ and $n = 2$ is thus the same. They cannot account for the astrophysical observations.

5. Summary, limitations and perspectives

The present work focuses on an intermediate cosmological era, $t_E \leqslant t \leqslant t_w$. The time t_E corresponds to the exit of an Hagedorn phase i.e. after the notion of topology and geometry emerge, with 3 large space-like dimensions and possibly internal directions of intermediate scales. The characteristic time t_w is associated to the electroweak phase transition, occurring before large scale structure formations in the universe.

To describe the intermediate era, we consider flat classical 4-dimensional space–times within the context of superstring theory, where $\mathcal{N} = 8, 4, 2$ supersymmetry is spontaneously broken. Our aim is to determine the different cosmological behaviors that can be induced when three kinds of effects are taken into account. Namely,

– statistical physics effects at temperature T,
– radiative corrections of magnitude M, the spontaneous supersymmetry breaking scale,
– the presence of moduli fields, whose kinetic energies scale as $1/a^6$.

We determine the low energy effective action at the one-loop level and parametrize data at the exit t_E of the Hagedorn phase by a set of IBC.

To be specific, when $n = 1$ internal radius is involved in the supersymmetry breaking, we show that, depending on the R-symmetry charges of the massless spectra, the models can be grouped in different *Cases* (a), (b) or (c). For each, there exists a partition of the set of IBC, whose classes yield cosmological evolutions that share a common behavior.

- In *Case* (a), one class of IBC seems to induce a spontaneous decompactification of the internal direction involved in the breaking of supersymmetry. It is out of the scope of the present paper.
- In *Case* (b), the evolutions of the scale factor are monotonic. The expanding solutions belong to the same class and are attracted to a radiation dominated era. Asymptotically, one has $3H^2 \propto 1/a^4 \propto T^4 \propto M^4$, where $a(t) \propto \sqrt{t}$.
- In *Case* (c), a class of IBC reaches solutions attracted to a Big Crunch era dominated by the radiative corrections to the initially vanishing vacuum energy. Asymptotically, one has $3H^2 \propto M^4 \propto 1/a^{24} \propto T^{24}$, where $a(t) \propto (t_{\mathrm{BC}} - t)^{1/12}$.
- In all cases, a class of IBC reaches solutions attracted to a Big Crunch era dominated by the classical moduli kinetic energy. Asymptotically, one has $3H^2 \propto 1/a^6 \propto T^6 \propto M^{1/(1-3/(8\sigma_-))}$, where σ_- is given in Eq. (2.57) and $a(t) \propto (t_{\mathrm{BC}} - t)^{1/3}$.

Our analysis has some limitations. First of all, we have supposed that the radii involved in the spontaneous breaking of supersymmetry and the radius of the Euclidean time are large enough to avoid Hagedorn like singularities in the partition functions. Since we found Big Crunch behaviors where $T \ll M$ are formally diverging, these evolutions must be restricted to M lower than a maximum Hagedorn bound. It would be interesting to relax this constraint by considering models free of such singularities [8].

Also, we have studied the thermal and quantum corrections at the one-loop level in flat backgrounds where moduli have some kinetic energy. This means that the induced sources P, ρ and their backreactions on the "cold" classical backgrounds we start with must be small. Thus, we need afterwords to check the consistency of our approach.

– For the RDS, we have

$$P(t) \propto \rho(t) \propto \frac{1}{a(t)^4} \propto \frac{1}{t^2} \longrightarrow 0, \tag{5.1}$$

which shows its validity.

– For the Big Crunch attractor $a(t) \propto (t_{\mathrm{BC}} - t)^{1/12}$ of the MDS, both the thermal/quantum sources and the classical moduli kinetic energy are diverging. Formally, one has

$$P(t) = -\rho(t) \propto M^4 \propto \frac{1}{a(t)^{24}} \propto \frac{1}{(t_{\mathrm{BC}} - t)^2} \gg \frac{1}{a^6} \propto \frac{1}{\sqrt{t_{\mathrm{BC}} - t}}, \tag{5.2}$$

which shows that this solution has to be restricted to times where P and ρ do not exceed too much the classical kinetic energy.

– This limitation does not exist for the Big Crunch behavior $a(t) \propto (t_{\mathrm{BC}} - t)^{1/3}$. Even if the thermal/quantum sources and the classical moduli kinetic energy are diverging, one has

$$P(t) = -\rho(t) \propto M^4 \propto \frac{1}{a(t)^{24-9/\sigma_-}} \propto \frac{1}{(t_{\mathrm{BC}} - t)^{8-3/\sigma_-}} \ll \frac{1}{a^6} \propto \frac{1}{(t_{\mathrm{BC}} - t)^2}, \tag{5.3}$$

since $\sigma_- < 1/2$. Thus, the backreaction on the classical background is always small. The dynamical attraction to this solution is only limited by the Hagedorn transitions mentioned previously.

To go beyond the constraint that the thermal/quantum corrections must be small, one can try to compute the higher string loop corrections and, if possible, use string–string dualities to find the non-perturbative corrections to the effective action. For the models under consideration in this work, the extended supersymmetry is only broken spontaneously, at the scale M and/or by thermal effects at the scale T. This means that the UV behavior of the theories is not affected by these soft breaking and that the renormalization theorems for extended supersymmetries should persist. To find the cosmological evolutions beyond the first order in perturbation theory, both the thermal effective potential and the corrections to the kinetic terms have to be computed.

The attraction phenomena we found can be generalized to models where n internal radii are involved in the spontaneous breaking of supersymmetry. In particular, we have shown that for $n = 2$, the attraction to the radiation era persists. In the process, the complex structure modulus associated to the ratio of the two radii converges to a constant i.e. is dynamically stabilized.

During the convergence to the radiation dominated era, the ratio M/T reaches its critical value exponentially or with damping oscillations. Periods of accelerated expansions are also allowed. However, the e-fold number seems to depend weakly on n and, at least for $n = 1, 2$, does not give rise to enough periods of inflation (e-fold $\leqslant 0.2$). Since we have considered models with $\mathcal{N} = 8, 4, 2$ initial supersymmetry (i.e. before spontaneous breaking), it would be interesting to extend our work to $\mathcal{N} = 1$ models and see if the order of magnitude of the e-fold is higher.

Acknowledgements

We are grateful to I. Antoniadis, J. Estes and N. Toumbas for useful discussions. H.P. thanks the Ecole Normale Superieure for hospitality. F.B. thanks M. Petropoulos and I. Florakis for fruitful and stimulating discussions.

This work is partially supported by the ANR (CNRS-USAR) contract 05-BLAN-0079-02. The work of F.B. and H.P. is also supported by the European ERC Advanced Grant 226371, and CNRS PICS contracts 3747 and 4172.

References

[1] M.B. Green, J.H. Schwarz, E. Witten, Superstring Theory, vol. 1. Introduction, Cambridge Monographs on Mathematical Physics, Cambridge Univ. Press, Cambridge, UK, 1987, 469 p.;

M.B. Green, J.H. Schwarz, E. Witten, Superstring Theory, vol. 2. Loop Amplitudes, Anomalies and Phenomenology, Cambridge Monographs on Mathematical Physics, Cambridge Univ. Press, Cambridge, UK, 1987, 596 p.;
J. Polchinski, String Theory, vol. 1. An Introduction to the Bosonic String, Cambridge Univ. Press, Cambridge, UK, 1998, 402 p.;
J. Polchinski, String Theory, vol. 2. Superstring Theory and Beyond, Cambridge Univ. Press, Cambridge, UK, 1998, 531 p.;
E. Kiritsis, Introduction to superstring theory, Leuven notes in mathematical and theoretical physics, hep-th/9709062;
E. Kiritsis, String Theory in a Nutshell, Princeton Univ. Press, Princeton, USA, 2007, 588 p.

[2] J. Atick, E. Witten, The Hagedorn transition and the number of degrees of freedom of string theory, Nucl. Phys. B 310 (1988) 291.

[3] C. Kounnas, B. Rostand, Coordinate dependent compactifications and discrete symmetries, Nucl. Phys. B 341 (1990) 641.

[4] I. Antoniadis, C. Kounnas, Superstring phase transition at high temperature, Phys. Lett. B 261 (1991) 369;
I. Antoniadis, J.P. Derendinger, C. Kounnas, Non-perturbative supersymmetry breaking and finite temperature instabilities in $N = 4$ superstrings, hep-th/9908137;
C. Kounnas, Universal thermal instabilities and the high-temperature phase of the $N = 4$ superstrings, hep-th/9902072.

[5] R. Hagedorn, Statistical thermodynamics of strong interactions at high-energies, Nuovo Cimento Suppl. 3 (1965) 147;
S. Fubini, G. Veneziano, Level structure of dual-resonance models, Nuovo Cimento A 64 (1969) 811;
K. Bardakci, S. Mandelstam, Analytic solution of the linear-trajectory bootstrap, Phys. Rev. 184 (1969) 1640;
K. Huang, S. Weinberg, Ultimate temperature and the early universe, Phys. Rev. Lett. 25 (1970) 895;
B. Sathiapalan, Vortices on the string world sheet and constraints on toral compactification, Phys. Rev. D 35 (1987) 3277;
Y.I. Kogan, Vortices on the world sheet and string's critical dynamics, JETP Lett. 45 (1987) 709, Pis'ma Zh. Eksp. Teor. Fiz. 45 (1987) 556;
M. Axenides, S.D. Ellis, C. Kounnas, Universal behavior of D-dimensional superstring models, Phys. Rev. D 37 (1988) 2964;
D. Kutasov, N. Seiberg, Number of degrees of freedom, density of states and tachyons in string theory and CFT, Nucl. Phys. B 358 (1991) 600;
D. Israel, V. Niarchos, Tree-level stability without spacetime fermions: Novel examples in string theory, JHEP 0707 (2007) 065, arXiv:0705.2140 [hep-th].

[6] M. Gasperini, G. Veneziano, Pre-big bang in string cosmology, Astropart. Phys. 1 (1993) 317, hep-th/9211021;
M. Gasperini, M. Maggiore, G. Veneziano, Towards a non-singular pre-big bang cosmology, Nucl. Phys. B 494 (1997) 315, hep-th/9611039.

[7] N. Matsuo, Superstring thermodynamics and its application to cosmology, Z. Phys. C 36 (1987) 289;
R.H. Brandenberger, String gas cosmology and structure formation: A brief review, hep-th/0702001;
R.H. Brandenberger, C. Vafa, Superstrings in the early universe, Nucl. Phys. B 316 (1989) 391;
A. Tseytlin, C. Vafa, Elements of string cosmology, Nucl. Phys. B 372 (1992) 443, hep-th/9109048;
B.A. Bassett, M. Borunda, M. Serone, S. Tsujikawa, Aspects of string-gas cosmology at finite temperature, Phys. Rev. D 67 (2003) 123506, hep-th/0301180;
M. Borunda, L. Boubekeur, The effect of α' corrections in string gas cosmology, JCAP 0610 (2006) 002, hep-th/0604085.

[8] C. Angelantonj, C. Kounnas, H. Partouche, N. Toumbas, Resolution of Hagedorn singularity in superstrings with gravito-magnetic fluxes, Nucl. Phys. B 809 (2009) 291, arXiv:0808.1357 [hep-th].

[9] E. Kiritsis, C. Kounnas, Dynamical topology change, compactification and waves in a stringy early universe, hep-th/9407005;
E. Kiritsis, C. Kounnas, Dynamical topology change in string theory, Phys. Lett. B 331 (1994) 51, hep-th/9404092;
E. Kiritsis, C. Kounnas, Dynamical topology change, compactification and waves in string cosmology, Nucl. Phys. B (Proc. Suppl.) 41 (1995) 311, gr-qc/9701005;
E. Kiritsis, C. Kounnas, String gravity and cosmology: Some new ideas, gr-qc/9509017.

[10] C. Kounnas, N. Toumbas, J. Troost, A wave-function for stringy universes, JHEP 0708 (2007) 018, arXiv:0704.1996 [hep-th].

[11] C. Kounnas, Massive boson–fermion degeneracy and the early structure of the universe, Fortschr. Phys. 56 (2008) 1143, arXiv:0808.1340 [hep-th];

I. Florakis, C. Kounnas, Orbifold symmetry reductions of massive boson–fermion degeneracy, arXiv:0901.3055 [hep-th].

[12] C. Kounnas, H. Partouche, Inflationary de Sitter solutions from superstrings, Nucl. Phys. B 795 (2008) 334, arXiv: 0706.0728 [hep-th].

[13] T. Catelin-Jullien, C. Kounnas, H. Partouche, N. Toumbas, Thermal/quantum effects and induced superstring cosmologies, Nucl. Phys. B 797 (2008) 137, arXiv:0710.3895 [hep-th];
T. Catelin-Jullien, C. Kounnas, H. Partouche, N. Toumbas, Thermal and quantum superstring cosmologies, Fortschr. Phys. 56 (2008) 792, arXiv:0803.2674 [hep-th].

[14] T. Catelin-Jullien, C. Kounnas, H. Partouche, N. Toumbas, Induced superstring cosmologies and moduli stabilization, arXiv:0901.0259 [hep-th].

[15] F. Bourliot, J. Estes, C. Kounnas, H. Partouche, in preparation.

[16] J.P. Derendinger, C. Kounnas, P.M. Petropoulos, F. Zwirner, Superpotentials in IIA compactifications with general fluxes, Nucl. Phys. B 715 (2005) 211, hep-th/0411276;
J.P. Derendinger, C. Kounnas, P.M. Petropoulos, F. Zwirner, Fluxes and gaugings: $N = 1$ effective superpotentials, Fortschr. Phys. 53 (2005) 926, hep-th/0503229;
G. Villadoro, F. Zwirner, $N = 1$ effective potential from dual type-IIA D6/O6 orientifolds with general fluxes, JHEP 0506 (2005) 047, hep-th/0503169;
G. Villadoro, F. Zwirner, D terms from D-branes, gauge invariance and moduli stabilization in flux compactifications, JHEP 0603 (2006) 087, hep-th/0602120;
L. Andrianopoli, M.A. Lledo, M. Trigiante, The Scherk–Schwarz mechanism as a flux compactification with internal torsion, JHEP 0505 (2005) 051, hep-th/0502083;
G. Dall'Agata, N. Prezas, Scherk–Schwarz reduction of M-theory on G_2-manifolds with fluxes, JHEP 0510 (2005) 103, hep-th/0509052;
J.P. Derendinger, P.M. Petropoulos, N. Prezas, Axionic symmetry gaugings in $N = 4$ supergravities and their higher-dimensional origin, Nucl. Phys. B 785 (2007) 115, arXiv:0705.0008 [hep-th];
G. Curio, A. Klemm, D. Lust, S. Theisen, On the vacuum structure of type II string compactifications on Calabi–Yau spaces with H-fluxes, Nucl. Phys. B 609 (2001) 3, hep-th/0012213.

[17] C. Angelantonj, S. Ferrara, M. Trigiante, New $D = 4$ gauged supergravities from $N = 4$ orientifolds with fluxes, JHEP 0310 (2003) 015, hep-th/0306185;
C. Angelantonj, R. D'Auria, S. Ferrara, M. Trigiante, $K3 \times T^2/\mathbb{Z}_2$ orientifolds with fluxes, open string moduli and critical points, Phys. Lett. B 583 (2004) 331, hep-th/0312019;
C. Angelantonj, S. Ferrara, M. Trigiante, Unusual gauged supergravities from type IIA and type IIB orientifolds, Phys. Lett. B 582 (2004) 263, hep-th/0310136;
C. Angelantonj, R. D'Auria, S. Ferrara, M. Trigiante, $K3 \times T^2/Z_2$ orientifolds with fluxes, open string moduli and critical points, Phys. Lett. B 583 (2004) 331, hep-th/0312019;
C. Angelantonj, M. Cardella, N. Irges, An alternative for moduli stabilisation, Phys. Lett. B 641 (2006) 474, hep-th/0608022.

[18] J. Scherk, J.H. Schwarz, Spontaneous breaking of supersymmetry through dimensional reduction, Phys. Lett. B 82 (1979) 60.

[19] R. Rohm, Spontaneous supersymmetry breaking in supersymmetric string theories, Nucl. Phys. B 237 (1984) 553.

[20] C. Kounnas, M. Porrati, Spontaneous supersymmetry breaking in string theory, Nucl. Phys. B 310 (1988) 355;
S. Ferrara, C. Kounnas, M. Porrati, F. Zwirner, Superstrings with spontaneously broken supersymmetry and their effective theories, Nucl. Phys. B 318 (1989) 75.

[21] P. Ditsas, E.G. Floratos, Finite temperature closed bosonic string in a finite volume, Phys. Lett. B 201 (1988) 49.

[22] I. Antoniadis, C. Bachas, C. Fabre, H. Partouche, T.R. Taylor, Aspects of type I–type II–heterotic triality in four dimensions, Nucl. Phys. B 489 (1997) 160, hep-th/9608012;
I. Antoniadis, H. Partouche, T.R. Taylor, Duality of $N = 2$ heterotic–type I compactifications in four dimensions, Nucl. Phys. B 499 (1997) 29, hep-th/9703076;
I. Antoniadis, H. Partouche, T.R. Taylor, Lectures on heterotic–type I duality, Nucl. Phys. B (Proc. Suppl.) 61 (1998) 58, Nucl. Phys. B (Proc. Suppl.) 67 (1998) 3, hep-th/9706211.

[23] I. Antoniadis, C. Kounnas, The dilaton classical solution and the supersymmetry breaking evolution in an expanding universe, Nucl. Phys. B 284 (1987) 729.

[24] E. Cremmer, S. Ferrara, C. Kounnas, D.V. Nanopoulos, Naturally vanishing cosmological constant in $N = 1$ supergravity, Phys. Lett. B 133 (1983) 61;
J.R. Ellis, C. Kounnas, D.V. Nanopoulos, No scale supersymmetric GUTs, Nucl. Phys. B 247 (1984) 373;
J.R. Ellis, C. Kounnas, D.V. Nanopoulos, Phenomenological $SU(1, 1)$ supergravity, Nucl. Phys. B 241 (1984) 406;

J.R. Ellis, A.B. Lahanas, D.V. Nanopoulos, K. Tamvakis, No-scale supersymmetric standard model, Phys. Lett. B 134 (1984) 429.

[25] E. Witten, Dimensional reduction of superstring models, Phys. Lett. B 155 (1985) 151;
S. Ferrara, C. Kounnas, M. Porrati, General dimensional reduction of ten-dimensional supergravity and superstring, Phys. Lett. B 181 (1986) 263;
M. Cvetic, J. Louis, B.A. Ovrut, A string calculation of the Kähler potentials for moduli of $\mathbb{Z}_N$ orbifolds, Phys. Lett. B 206 (1988) 227;
L.J. Dixon, V. Kaplunovsky, J. Louis, On effective field theories describing (2, 2) vacua of the heterotic string, Nucl. Phys. B 329 (1990) 27;
M. Cvetic, J. Molera, B.A. Ovrut, Kähler potentials for matter scalars and moduli of $\mathbb{Z}_N$ orbifolds, Phys. Rev. D 40 (1989) 1140.

Annexe D

Publication 2 : F. Bourliot, J. Estes, C. Kounnas and H. Partouche, "Cosmological Phases of the String Thermal Effective Potential," Nucl. Phys. B 830 (2010) 330 [arXiv :0908.1881 [hep-th]].

Available online at www.sciencedirect.com
ScienceDirect
Nuclear Physics B 830 (2010) 330–373
NUCLEAR PHYSICS B
www.elsevier.com/locate/nuclphysb

Cosmological phases of the string thermal effective potential ☆

F. Bourliot [a], J. Estes [a,*], C. Kounnas [b], H. Partouche [a]

[a] *Centre de Physique Théorique, Ecole Polytechnique,* [1] *F-91128 Palaiseau cedex, France*
[b] *Laboratoire de Physique Théorique, Ecole Normale Supérieure,* [2] *24 rue Lhomond, F-75231 Paris cedex 05, France*

Received 24 September 2009; received in revised form 14 December 2009; accepted 7 January 2010

Available online 14 January 2010

Abstract

In a superstring framework, the free energy density $\mathcal{F}$ can be determined unambiguously at the full string level once supersymmetry is spontaneously broken via geometrical fluxes. We show explicitly that only the moduli associated to the supersymmetry breaking may give relevant contributions. All other spectator moduli μ_I give exponentially suppressed contributions for relatively *small* (as compared to the string scale) temperature T and supersymmetry breaking scale M. More concisely, for $\mu_I > T$ and M, $\mathcal{F}$ takes the form

$$\mathcal{F}(T, M; \mu_I) = \mathcal{F}(T, M) + \mathcal{O}\left[\exp\left(-\frac{\mu_I}{T}\right), \exp\left(-\frac{\mu_I}{M}\right)\right].$$

We study the cosmological regime where T and M are below the Hagedorn temperature scale T_H. In this regime, $\mathcal{F}$ remains finite for any values of the spectator moduli μ_I. We investigate extensively the case of one spectator modulus μ_d corresponding to R_d, the radius-modulus field of an internal compactified dimension. We show that its thermal effective potential $V(T, M; \mu) = \mathcal{F}(T, M; \mu)$ admits five phases, each of which can be described by a distinct but different effective field theory. For late cosmological times, the Universe is attracted to a "Radiation-like evolution" with $M(t) \propto T(t) \propto 1/a(t) \propto t^{-2/d}$. The spectator modulus $\mu(t)$ is stabilized either to the stringy enhanced symmetry point where $R_d = 1$, or fixed at an

☆ Research partially supported by the ERC Advanced Grant 226371, ANR contract 05-BLAN-0079-02, CNRS PICS contracts 3747 and 4172, and the Groupement d'Intérêt Scientifique P2I.

* Corresponding author.
E-mail addresses: Francois.Bourliot@cpht.polytechnique.fr (F. Bourliot), John.Estes@cpth.polytechnique.fr (J. Estes), Costas.Kounnas@lpt.ens.fr (C. Kounnas), Herve.Partouche@cpht.polytechnique.fr (H. Partouche).

[1] Unité mixte du CNRS et de l'Ecole Polytechnique, UMR 7644.

[2] Unité mixte du CNRS et de l'Ecole Normale Supérieure associée à l'Université Pierre et Marie Curie (Paris 6), UMR 8549.

0550-3213/$ – see front matter © 2010 Published by Elsevier B.V.
doi:10.1016/j.nuclphysb.2010.01.004

arbitrary constant $\mu_0 > T, M$. For arbitrary boundary conditions at some initial time, t_E, $\mu(t)$ may pass through more than one effective field theory phase before its final attraction.
© 2010 Published by Elsevier B.V.

1. Introduction

String theory provides a framework to obtain a sensible theoretical description of the cosmological evolution of our Universe. Nowadays, it is the only known framework in which the quantum gravity effects are under control [1], at least for certain physically relevant cases. Following the stringy cosmological approach developed recently in Refs. [2–4], the classical string vacuum is taken to be supersymmetric with a fixed amount of supersymmetries defined in flat space–time.

This initial choice does not give rise to any cosmological evolution. In the presence of supersymmetry, the quantum corrections to the gravitational background would lead to a flat space–time, or would modify it at most to Anti-de Sitter, domain walls or gravitational wave backgrounds respecting a time-like or light-like killing symmetry. The above cosmological obstructions are however physically irrelevant for two fundamental reasons:

- Firstly, supersymmetry is broken in the real world (at least spontaneously and not explicitly), at a characteristic supersymmetry breaking scale M.
- Secondly, in the case of thermal cosmologies, the supersymmetry is effectively (spontaneously) broken at the temperature scale T.

Both the M and T supersymmetry breaking scales induce at the quantum level a non-trivial free energy density $\mathcal{F}(T, M)$, which plays the role of an effective thermal potential $V(T, M) = \mathcal{F}(T, M)$ that modifies the gravitational and field equations, giving rise to non-trivial cosmological solutions, as has been explicitly shown in Refs. [2,3,5]. Both the supersymmetry breaking and finite temperature phenomena can be implemented in the framework of superstrings [6–8] by introducing non-trivial "fluxes" in the initially supersymmetric vacua. Furthermore, in the case where supersymmetry is spontaneously broken by "geometrical fluxes" [9,10], the free energy $\mathcal{F}(T, M)$ is under control and is calculable at the *full* string level, free of any infrared and ultraviolet ambiguities [2,3]. This is true, provided T and M are below a critical value close to the string mass scale, the so-called Hagedorn temperature T_H [6–8,11]. In the framework of stringy-thermal cosmologies, $T \simeq T_H$ corresponds to very early times when we are facing non-trivial stringy singularities indicating a non-trivial phase transition at high temperatures [6,8,12,13,15] at time t_H. In the literature, there are many speculative proposals concerning the nature of this transition [6,8,12–16].

A way to bypass the Hagedorn transition ambiguities was proposed in Ref. [4]. It consists of assuming the emergence of $(d-1)$ large space-like directions for times $t \gg t_H$, describing the $(d-1)$-dimensional space of the Universe, and possibly some internal space directions of an intermediate size characterizing the scale M of the spontaneous breaking of supersymmetry via geometrical fluxes [9,10]. Within these assumptions, the ambiguities of the "Hagedorn transition exit at t_E" can be parameterized, for $t \geqslant t_E$, in terms of initial boundary condition data at $t_E \geqslant t_H$. In this way, the intermediate cosmological era $t_E \leqslant t \leqslant t_W$, *i.e.* after the "Hagedorn transition exit" and before the electroweak symmetry breaking phase transition at t_W, was extensively studied in Ref. [4] in the case of $d = 4$. An output of the present analysis is that the cosmological

"radiation-like" evolution found in Refs. [2,3,5,17] generalizes to a "Radiation-like Dominated Solution" (RDS) in d-dimensional space–time,

$$\mathrm{RDS}^d: \quad M(t) \propto T(t) \propto 1/a(t) \propto t^{-2/d}, \quad \text{for } t_E \leqslant t \leqslant t_W, \tag{1.1}$$

and is unique at late times in certain physically relevant supersymmetry breaking schemes. As a necessary and sufficient consistency requirement, we note that in this intermediate cosmological regime $T_H \gg T$, $M \gg T_W$, the smallness of the space–time curvature scales, $H^2 = (\dot{a}/a)^2$ and $\dot{H}$, the dilaton and the evolving radii scales, $\dot{\phi}^2_{\mathrm{dil}}$, $\ddot{\phi}_{\mathrm{dil}}$, $(\dot{R}_I/R_I)^2$, $\ddot{R}_I/R_I$, are guaranteed to be small ($\leqslant \mathcal{O}(T^d, M^d)$), thanks to the "attractor mechanism" towards the RDS in late cosmological times. In particular, they are all decreasing at late cosmological times and so our quasi-static approximation becomes better and better as time passes. In addition, our perturbative approximation becomes better and better as time progress due to the falling of the dilaton.

We point out that the evolution is radiation-like in the sense that the external space–time's evolution is identical to that of a radiation dominated universe. However, in our case the expansion is driven not only by radiation, but also by the coherent motion of the supersymmetry breaking modulus M. We would also like to stress that a key result of [4] was that the RDS^4 is actually an attractor of the dynamics. The important consequence of this attractor, is to wash out the dependence of the cosmological evolution on the choice of initial boundary conditions, which were used to parameterize our ignorance of the physics involved in the Hagedorn transition. In this paper we show that the attractor naturally extends to the higher-dimensional RDS^d.

Although this analysis was done in the framework of initial vacua with $\mathcal{N}_4 = 2$ supersymmetry, the claim is that it will still be valid in more realistic models with initial $\mathcal{N}_4 = 1$ supersymmetry [18]. We would like to stress here that the limitation $t \leqslant t_W$ in the infrared regime follows from the appearance in the low energy effective field theory of a new scale, namely the "infrared renormalization group invariant transmutation scale Q", at which the supersymmetric standard model Higgs (mass)^2 becomes negative (no-scale radiative breaking of $SU(2) \times U(1) \to U(1)_{\mathrm{em}}$ [19,20]). Q is irrelevant as long as $M, T \gg Q$; however it becomes relevant and stops the $M(t)$ evolution when $T \simeq Q$ at $t \simeq t_W$ *i.e.* when the electroweak breaking phase transition takes place. Although the physics for $t \gg t_W$ is of main importance in particle physics and in inflationary cosmology at t_W, it will not be examined in this work. The main reason for us is its strong dependence on the initial vacuum data which screens interesting universality properties. *We therefore work in the intermediate cosmological era $t_E \leqslant t \leqslant t_W$ or $T_H \gg T \gg Q$, i.e. after the Hagedorn phase transition and before the electroweak one*. In this regime the transmutation scale Q can be consistently neglected and, furthermore, the Hagedorn transition ambiguities are taken into account in terms of initial boundary conditions (IBC) after the "Hagedorn transition exit" at t_E. This scenario gives a dynamical explanation of the smallness of the supersymmetry breaking scale as compared to the string or Planck scales. Indeed, extrapolating the $\mathrm{RDS}^{d=4}$ up to the low energy regime where $T = \mathcal{O}(1\ \mathrm{TeV})$ one finds (thanks to the attractor mechanism), that the natural value of the supersymmetry breaking scale $M(t)$ is naturally small and around the electroweak phase transition, independently of its initial value at early cosmological times.

The only known supersymmetry breaking mechanism that can be unambiguously adapted at the string perturbative level, is the one we consider here where supersymmetry is spontaneously broken via "geometrical fluxes". This choice implies the existence of at least one relatively large compact dimension (the one which is associated to supersymmetry breaking). This is by far not in contradiction with experimental results both in particle physics and cosmology. For several years, the possibility of "large extra dimensions" has attracted the attention of the particle physics community; the future data analysis at the LHC and elsewhere includes searches for sig-

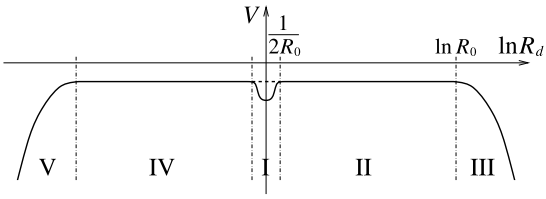

Fig. 1. Qualitative shape of the effective potential V versus $\ln R_d$, with T, M (and the dilaton in Einstein frame) fixed. When $\ln R_d$ varies, five distinct phases can arise in the heterotic case. i) The Higgs phase I, ii) the flat potential phases II, IV and iii) the higher-dimensional phases III, V. The phases IV and V are T-dual to II and III. In the type II case, the phase I does not exist and the plateaux II and IV are connected. The plot is valid for $T > M$, for $T < M$ one simply replaces R_0 with R_9.

nals indicating the existence of large extra dimensions at scales $1/R \sim \mathcal{O}(1\ \text{TeV})$, which is the characteristic prediction of supersymmetry breaking via geometrical fluxes.

Many other choices for supersymmetry breaking exist. However in most cases it is not well known, in our days, the precise stringy corrections to all orders in α' that are necessary in order to study the intermediate cosmological regime. In all other supersymmetry breaking mechanisms we are forced to work in the effective supergravity framework. Our results may help to make more general stringy approaches possible in the future. There are indications that our results can be converted to other string vacua, utilizing string/string and M-theory dualities. In particular the geometrical fluxes are mapped to other types of fluxes, for instance the three form R–R and NS–NS fluxes in type IIB — orientifolds. In this respect, the exact stringy approach in the intermediate cosmological regime gives us profound (non-perturbative) information via M-theory and string dualities.

In addition to generalizing the results of [4] to arbitrary dimension, we analyze the time behavior of *the spectator moduli not participating in the breaking of supersymmetry*. Following Refs. [2,3,5], one can show that only the supersymmetry breaking moduli $M(t)$ and $T(t)$ can give a relevant contribution to the free energy density $\mathcal{F}$. Intuitively, all other moduli μ_I are either attracted and stabilized to the "stringy" extended gauge symmetry points, close to the string scale $\mu_I \sim M_{\text{string}}$, or are effectively frozen to an arbitrary value such that $\mu_I \gg T$ and M, giving rise to exponentially suppressed contributions:

$$\mathcal{F}(T, M; \mu_I) = \mathcal{F}(T, M) + \mathcal{O}\left[\exp\left(-\frac{\mu_I}{T}\right), \exp\left(-\frac{\mu_I}{M}\right)\right]. \tag{1.2}$$

One point of the present paper is to explicitly verify this intuition for the moduli coming from the spectator tori. Indeed, the supersymmetry breaking moduli generate a non-trivial potential for the spectator moduli and freeze them as expected. Considering the effect on a single spectator modulus ($\mu \propto 1/R_d$) in the case of the heterotic string, the thermal effective potential $V(T, M; \mu)$ admits five distinct phases, each of which can be described by a different effective field theory. The interesting result is that by using a string theory framework and working at the *full* string level, we are able to link together, within a single framework, the different effective field theories. Furthermore, the main result of this paper is to derive at the string perturbative level (however exact in α'), the full string free energy $\mathcal{F}(T, M; \mu_I)$ as a functional of the supersymmetry breaking moduli T, M, the string coupling constant modulus dil and "spectator moduli" μ_I, for a certain class of string vacua where the spontaneous breaking of supersymmetry is induced by geometrical fluxes.

The form of the potential is sketched in Fig. 1 and the phases are summarized as follows ($T \propto 1/R_0$, $M \propto 1/R_9$):

I. Higgs phase: With $|R_d - \frac{1}{R_d}| < \frac{1}{R_0}$ and/or $\frac{1}{R_9}$.
This phase contains the stringy extended symmetry point at the self-dual point $R_d = 1$. The appropriate effective field theory description of this phase is in terms of a d-dimensional theory of gravity coupled to an $SU(2)$ gauge theory. R_d is dynamically stabilized at this point. Such a notion of moduli stabilization, has been studied in the literature before [21,22,13]. Here we demonstrate such moduli stabilization in the context of the heterotic superstring by an explicit computation of the effective potential.

II. Flat potential phase: With $\frac{1}{R_0}$ and $\frac{1}{R_9} < R_d - \frac{1}{R_d} < R_0$ and R_9.
Here, the appropriate effective field theory description is in terms of a d-dimensional theory of gravity coupled to an $U(1)$ gauge field.

III. Higher-dimensional phase: With R_0 and/or $R_9 < R_d$.
For macroscopic values of the spectator modulus R_d, the appropriate effective field theory description is the $(d+1)$-dimensional theory of gravity. The modulus R_d becomes the $\hat{g}_{dd}$ component of the metric, $\hat{g}_{dd} = (2\pi R_d)^2$ and the evolution is attracted to that of an RDS in $d+1$ dimensions.
One may also consider the case in which the radius R_d is still internal. For large enough values of R_d so that we can neglect terms of order $(R_0/R_d)^d$ and $(R_9/R_d)^d$, the evolution is attracted to an RDS^{d+1} for a long period of time. However, at late times R_0 and R_9 always catch R_d and the solution is ultimately attracted to the RDS^d of phase II.

IV. Dual flat potential phase: With $\frac{1}{R_0}$ and $\frac{1}{R_9} < \frac{1}{R_d} - R_d < R_0$ and R_9.
The effective theory description is T-dual to that of phase II. The light degrees of freedom are the winding modes instead of the Kaluza–Klein momenta of phase II.

V. Dual higher-dimensional phase: With R_0 and/or $R_9 < \frac{1}{R_d}$.
This phase is T-dual to phase III. Its properties are derived from the ones of phase III under the replacement $R_d \to 1/R_d$ and phase II $\to$ IV. In particular, the dual effective field theory is a $(d+1)$-dimensional theory of gravity, with $\hat{g}_{dd} = (2\pi/R_d)^2$.

The above different phases of a common string setting *cannot be described in the context of a single field theory*. This is due to the necessary presence of the string winding modes. In a field theory framework, only the phases II and III (or IV and V) can be described by a common field theory. The winding modes are particularly important for the stabilization of the modulus in phase I at the extended symmetry point, and furthermore for the description of the T-dual phases IV and V. In contrast to field theory, string theory naturally interpolates between these various phases, due to the generation of an effective potential in the presence of temperature and spontaneous supersymmetry breaking.

For each phase, there exists an RDS as in (1.1). We show that these solutions are stable against small perturbations and that for arbitrary IBC close to an RDS, the cosmological evolution is attracted to this RDS. In [4], the spectator moduli were taken to be frozen and it was shown that under this hypothesis the RDS is a global attractor. Taking into account the existence of gravitational friction for an expanding universe, we expect in the present work with dynamical spectator moduli such as R_d, the results of [4] to generalize so that the evolution is always attracted to the RDS of one of the five phases.

In the case of type II strings, the phase I does not exist perturbatively, so that the phases II and IV combine into a single plateau. This is due to the lack of massless states necessary to enhance the $U(1)$ to $SU(2)$. However, by heterotic-type II duality, we expect such an enhancement to exist non-perturbatively, so that all five phases should exist at the non-perturbative level. The effects correspond to the addition of branes whose separation is governed by the spectator moduli.

The organization of the paper is as follows. In Section 2, we discuss in more details the specific setup analyzed in this paper. The thermal effective potential is given and it is shown to have the five phases discussed above. In Section 3, we show that an RDS solution exists in each phase. In addition, we show the stability of the solutions against small perturbations. In Section 4, we briefly discuss the role of non-perturbative objects in the type II string theory. In Section 5, we summarize our results and discuss further avenues of research. In Appendix A, the thermal partition functions for the heterotic and type II strings are presented, together with their asymptotic properties to be used in the different phases. The gravity and field equations are given for each effective field theory phase in Appendix B.

2. Effective thermal potential in superstrings with spontaneously broken supersymmetry

In the presence of temperature, the one-loop partition function of both the heterotic and type II superstrings is non-vanishing and yields the one-loop effective potential at finite temperature. In addition, spontaneous supersymmetry breaking is induced by the presence of geometrical fluxes [2,3] along the internal cycles of the background manifold. We introduce these fluxes via the generalization to the context of string theory of Scherk–Schwarz [23] compactifications in field theory [24,25]. They induce further contributions to the one-loop partition function, which persist even at zero temperature [2,3]. Due to various ways of introducing the fluxes, there are multiple supersymmetry breaking configurations for the same initially supersymmetric background. In [2,3], such one-loop thermal effective potentials were derived in the limit of small temperature T and small supersymmetry breaking scale M for the heterotic and type II superstrings compactified on T^6 and $T^2 \times \frac{T^4}{\mathbb{Z}_2}$ orbifolds. The partition functions were calculated for small but otherwise arbitrary temperature and supersymmetry breaking scale, while the remaining moduli were taken to be frozen close to the string scale.

We want to relax the latter hypothesis and examine the behavior of the spectator moduli in the presence of temperature and supersymmetry breaking. In Appendix A, we compute the partition functions for the heterotic (A.16) and type II (A.21) cases. The background manifold is of the form $S^1_E \times T^D \times T^n$ (or $S^1_E \times T^D \times \frac{T^4}{\mathbb{Z}_2} \times T^n$ in the orbifold models), where S^1_E is the compact Euclidean time circle and the T^n torus involves the geometrical fluxes which generate the breaking of supersymmetry. The T^D spectator moduli are not participating in the breaking of supersymmetry. We take both the temperature and supersymmetry breaking scales to be small, while allowing the T^D spectator moduli to remain arbitrary. This enables us to study the resulting effects of the effective thermal potential on the T^D moduli.

For simplicity, we specialize to the following 10-dimensional Euclidean background that contains:

- The Euclidean time direction, with radius R_0 which determines the temperature T.
- The $1, \ldots, d-1$ directions, which are taken to be very large and form, together with the time, a d-dimensional space–time.
- The circle $S^1(R_d)$, with arbitrary radius. For small R_d, $S^1(R_d)$ is considered as part of the internal compactified space. For macroscopic R_d, however, $S^1(R_d)$ becomes part of a space–time of dimension $d+1$. By macroscopic we mean that we can probe it with current experiments. R_d is the only "spectator" radius whose dynamics is taken into account.
- The $n = 1$ circle involved in the spontaneous breaking of supersymmetry. We take it to be along the compact direction 9, with radius R_9.

- The remaining compact directions, with radii $R_{d+1}, \ldots, R_8$. They are taken to be fixed close to the string scale. (In the orbifold models, the $\frac{T^4}{\mathbb{Z}_2}$ factor spans the directions $5, \ldots, 8$. Its dynamics are consider in the companion paper [18].)

Utilizing the general expressions associated with the heterotic and type II partition functions given in Appendix A, we can easily obtain the ones associated to the background chosen above, namely

$$S^1(R_0) \times T^{d-1} \times S^1(R_d) \times \mathcal{M} \times S^1(R_9), \tag{2.1}$$

where $\mathcal{M} = T^{8-d}$ or $T^{4-d} \times \frac{T^4}{\mathbb{Z}_2}$. The heterotic (type II) models admit a supersymmetry characterized by 16 or 8 (32 or 16) supercharges, which are spontaneously broken by the "stringy Scherk–Schwarz compactifications" in the directions 9 and 0 [2,3]. The scales of supersymmetry breaking M and temperature T are characterized by $1/R_9$ and $1/R_0$, respectively. We take R_0 and R_9 to be large, but still much smaller than the radii of the T^{d-1} torus so that we have the following inequality

$$R_1, \ldots, R_{d-1} \gg R_0, R_9 \gg 1. \tag{2.2}$$

As long as R_d is smaller than the size of the external space T^{d-1}, it is more convenient to express the effective field theory action S in terms of fields, which have a natural interpretation in d dimensions. We are interested in isotropic and homogeneous backgrounds. More specifically, we take the gauge fields to be pure gauge and the remaining scalar fields and the space–time metric to depend only on time. This will have the advantage that after such a reduction, the different effective field theories will be describable within a single framework. The backgrounds we will consider are non-trivial for the d-dimensional metric $g_{\mu\nu}$, the d-dimensional dilaton ϕ_{dil}, and the moduli fields. However, since we allow R_d to vary arbitrarily in size, it may become of the order of the external T^{d-1} radii, so that $S^1(R_d)$ should be considered as a part of a $(d+1)$-dimensional space–time. In this case the effective action S is naturally expressed in terms of redefined fields and space–time metric in $d+1$ dimensions.

In Appendix B, the dimensional reduction from 10 dimensions to d dimensions is carried out explicitly and the resulting action in Einstein frame is given in (B.7). The case we are considering here has $n = 1$, $\Delta = 9 - A - d$ (where $A = 0$ in the toroidal models and $A = 4$ in the orbifold ones) and $\mathcal{D} = d$. The resulting action is

$$S = \int d^d x \sqrt{-g} \left(\frac{R}{2} - \frac{1}{2}(\partial\Phi)^2 - \frac{1}{2}(\partial\phi_\perp)^2 - \frac{1}{2}(\partial\zeta)^2 + P \right), \tag{2.3}$$

where we have defined the normalized fields,

$$\Phi := \frac{2}{\sqrt{(d-2)(d-1)}}\phi_{\text{dil}} - \sqrt{\frac{d-2}{d-1}}\eta, \qquad \phi_\perp := \frac{2}{\sqrt{d-1}}\phi_{\text{dil}} + \frac{1}{\sqrt{d-1}}\eta \tag{2.4}$$

along with

$$\zeta := \ln R_d, \qquad \eta := \ln R_9. \tag{2.5}$$

The remaining moduli are taken to be fixed close to the string scale.

The source P is a pressure equal to $-\mathcal{F}$, the free energy density (see Eq. (B.12)). It is the opposite of the one-loop effective potential at finite temperature and is related to the one-loop partition function as,

$$P = e^{\frac{2d}{d-2}\phi_{\text{dil}}} \frac{Z}{V_{0,\ldots,d-1}}, \tag{2.6}$$

where $V_{0,\ldots,d-1}$ is the d-dimensional Euclidean volume (in string frame) and Z is the partition function computed in Appendix A. In the next sub-section we shall give the exact form of P in terms of a convenient set of variables.

2.1. Specific form of the effective thermal potential

For the heterotic case, the partition function is given in Eq. (A.16) which can be re-written in the following convenient form

$$Z = \left(\prod_{i=0}^{d-1} R_i\right) R_9 \frac{2^4}{2} \sum_{\tilde{g}_0+\tilde{g}_9=1} (\mathcal{Z}_{\text{generic}} + \mathcal{Z}_{\text{enhanced}}). \tag{2.7}$$

For the type II case, Eq. (A.21), there is no contribution $\mathcal{Z}_{\text{enhanced}}$.

In the heterotic case, $\mathcal{Z}_{\text{enhanced}}$ is generically suppressed except when R_d is close to its self-dual point, where an enhancement of the gauge group $U(1) \to SU(2)$ occurs. The contribution $\mathcal{Z}_{\text{generic}}$ for generic R_d can be written in two equivalent forms,[3] related to one another by a Poisson resummation of the momentum lattice index m_d of the circle $S^1(R_d)$.

In the Einstein frame, the temperature T and supersymmetry breaking scale M are dressed by the dilaton field ϕ_{dil} and are given by Eqs. (B.10) and (B.5):

$$T = \frac{e^{\frac{2\phi_{\text{dil}}}{d-2}}}{2\pi R_0}, \qquad M = \frac{e^{\frac{2\phi_{\text{dil}}}{d-2}}}{2\pi R_9} \equiv \frac{e^{\sqrt{\frac{d-1}{d-2}}\Phi}}{2\pi}. \tag{2.8}$$

Observe that in the ratio $\frac{M}{T} = \frac{R_0}{R_9}$, the ϕ_{dil} dependence drops out. The expression for P gets simplified drastically once it is written in terms of the complex structure modulus z,

$$z := \ln \frac{M}{T} = \ln \frac{R_0}{R_9}. \tag{2.9}$$

In terms of the independent variables $\{T, z, \eta, \zeta\}$, the pressure P takes the factorized form

$$P(T, z, \eta, \zeta) \equiv T^d p(z, \eta, \zeta), \tag{2.10}$$

with ζ and η defined in (2.5). Furthermore, p can be written in terms of functions with natural interpretations either in d or $d+1$ dimensions. (In Eq. (A.16), the first case corresponds to $\Delta = 9 - A - d$ and the second to $\Delta = 8 - A - d$.) In the heterotic case, the two equivalent forms for p are:

$$\begin{aligned} p(z, \eta, \zeta) &= n_T\big[\hat{f}_T^{(d)}(z) + k_T^{(d)}\big(z, \eta - |\zeta|\big)\big] + n_V\big[\hat{f}_V^{(d)}(z) + k_V^{(d)}\big(z, \eta - |\zeta|\big)\big] \\ &\quad + \tilde{n}_T g_T^{(d)}\big(z, \eta, |\zeta|\big) + \tilde{n}_V g_V^{(d)}\big(z, \eta, |\zeta|\big) \\ &= e^{|\zeta|-\eta-z}\big[n_T f_T^{(d+1)}\big(z, \eta - |\zeta|\big) + n_V f_V^{(d+1)}\big(z, \eta - |\zeta|\big)\big] \\ &\quad + \tilde{n}_T g_T^{(d)}\big(z, \eta, |\zeta|\big) + \tilde{n}_V g_V^{(d)}\big(z, \eta, |\zeta|\big), \end{aligned} \tag{2.11}$$

with the functions defined below. For the type II case, one simply takes $\tilde{n}_T = \tilde{n}_V = 0$. Note that p is an even function of ζ, as follows from T-duality $R_d \to 1/R_d$. In this expression, n_T is the number of massless boson/fermion pairs of states in the originally supersymmetric background,

[3] In the notations of Appendix A, these two forms correspond to $\Delta = 9 - A - d$ and $\Delta = 8 - A - d$, where $A = 0$ for the toroidal models and $A = 4$ for the orbifold ones.

for generic R_d. $\tilde{n}_T$ is the number of additional ones at the enhanced gauge symmetry point. The value of n_V is given by the sum over the n_T pairs, with each pair weighted by a sign. The distribution of signs depends on the specific supersymmetry breaking configuration and can yield a negative n_V. For the heterotic models we consider, one has

$$n_T = \frac{2^4}{2} D_0, \qquad -1 \leqslant \frac{n_V}{n_T} \leqslant 1, \qquad \frac{\tilde{n}_T}{n_T} = \frac{2}{D_0}, \qquad \tilde{n}_V = \tilde{n}_T. \tag{2.12}$$

The definitions of the various functions appearing in Eq. (2.11) are given by

$$\begin{aligned}
\hat{f}_T^{(d)}(z) &= \frac{\Gamma(\frac{d+1}{2})}{\pi^{\frac{d+1}{2}}} \sum_{\tilde{k}_0,\tilde{k}_9} \frac{e^{dz}}{[e^{2z}(2\tilde{k}_0+1)^2 + (2\tilde{k}_9)^2]^{\frac{d+1}{2}}}, \\
k_T^{(d)}\big(z, \eta - |\zeta|\big) &= \sum_{m_d}{}' |m_d|^{\frac{d+1}{2}} e^{\frac{d+1}{2}(\eta - |\zeta|)} e^{dz} \\
&\quad \times \sum_{\tilde{k}_0,\tilde{k}_9} \frac{2K_{\frac{d+1}{2}}(2\pi |m_d| e^{\eta-|\zeta|}\sqrt{e^{2z}(2\tilde{k}_0+1)^2 + (2\tilde{k}_9)^2})}{[e^{2z}(2\tilde{k}_0+1)^2 + (2\tilde{k}_9)^2]^{\frac{d+1}{4}}}, \\
g_T^{(d)}\big(z, \eta, |\zeta|\big) &= \big(e^{2|\zeta|} - 1\big)^{\frac{d+1}{2}} e^{\frac{d+1}{2}(\eta - |\zeta|)} e^{dz} \\
&\quad \times \sum_{\tilde{k}_0,\tilde{k}_9} \frac{2K_{\frac{d+1}{2}}(2\pi (e^{2|\zeta|}-1) e^{\eta-|\zeta|}\sqrt{e^{2z}(2\tilde{k}_0+1)^2 + (2\tilde{k}_9)^2})}{[e^{2z}(2\tilde{k}_0+1)^2 + (2\tilde{k}_9)^2]^{\frac{d+1}{4}}}, \\
f_T^{(d+1)}\big(z, \eta - |\zeta|\big) &= \frac{\Gamma(\frac{d}{2}+1)}{\pi^{\frac{d}{2}+1}} \sum_{\tilde{k}_0,\tilde{k}_9,\tilde{m}_d} \frac{e^{(d+1)z}}{[e^{2z}(2\tilde{k}_0+1)^2 + (2\tilde{k}_9)^2 + e^{-2(\eta-|\zeta|)}\tilde{m}_d^2]^{\frac{d}{2}+1}},
\end{aligned} \tag{2.13}$$

where $K_\alpha(z)$ are modified Bessel functions of the second kind. The remaining functions with lower index V are related to those with lower index T by $M \leftrightarrow T$ duality transformations ($z \leftrightarrow -z$):

$$\begin{aligned}
\hat{f}_V^{(d)}(z) &= e^{(d-1)z} \hat{f}_T^{(d)}(-z), \\
k_V^{(d)}\big(z, \eta - |\zeta|\big) &= e^{(d-1)z} k_T^{(d)}\big(-z, \eta - |\zeta| + z\big), \\
g_V^{(d)}\big(z, \eta, |\zeta|\big) &= e^{(d-1)z} g_T^{(d)}\big(-z, \eta + z, |\zeta|\big), \\
f_V^{(d+1)}\big(z, \eta - |\zeta|\big) &= e^{dz} f_T^{(d+1)}\big(-z, \eta - |\zeta| + z\big).
\end{aligned} \tag{2.14}$$

We will first focus on the dynamics of the modulus R_d, and so we consider the behavior of $-P = -T^d p(z, \eta, \zeta)$ at fixed T, z and η. Note that when the functions $g_T^{(d)}$ and $g_V^{(d)}$ can be neglected, the pressure only depends on two quantities, z and $\eta - |\zeta|$.

2.2. *The five heterotic effective field theory phases*

Considering the effect on a single spectator modulus R_d in the case of the heterotic string, the thermal effective potential $-P$ admits five distinct phases corresponding to different effective field theories. The form of the potential is sketched in Fig. 1 and the phases are summarized as follows:

- **I: Higgs phase**

$$\left|R_d - \frac{1}{R_d}\right| < \frac{1}{R_0} \quad \text{and/or} \quad \frac{1}{R_9}. \tag{2.15}$$

This phase contains the stringy extended symmetry point at the self-dual point $R_d = 1$. The appropriate effective field theory description is in terms of a d-dimensional theory of gravity coupled to an $SU(2)$ gauge field. We will see that the modulus R_d can be stabilized at the self-dual point which turns out to be the minimum of the effective thermal potential. Indeed, considering the expression of p in (2.11), the functions $g_T^{(d)}$ and/or $g_V^{(d)}$ are of the same order as $\hat{f}_T^{(d)}$ and $\hat{f}_V^{(d)}$, while $k_T^{(d)}$ and $k_V^{(d)}$ are exponentially small due to the behavior of the modified Bessel functions $K_{\frac{d+1}{2}}$. In particular, one has at the origin $\zeta = \ln R_d = 0$ the following behavior,

$$p(z, \eta, \zeta = 0) = (n_T + \tilde{n}_T)\hat{f}_T^{(d)}(z) + (n_V + \tilde{n}_V)\hat{f}_V^{(d)}(z) := \tilde{p}(z). \tag{2.16}$$

This is precisely the form obtained in [2], when the dynamics of R_d was ignored *i.e.* R_d was taken to be stabilized close to the string scale. In Eq. (2.16), the contribution of n_T and $\tilde{n}_T$ is of the same form since both contributions come from massless states when ζ is at the enhanced gauge symmetry point $\zeta = 0$. Due to the fact that $\tilde{n}_T$ and $\tilde{n}_V$ are positive, the extremum of $-P$ at $\zeta = 0$ is always a minimum.

- **II: The flat potential phase**

$$\frac{1}{R_0} \quad \text{and} \quad \frac{1}{R_9} < R_d - \frac{1}{R_d}, \quad \text{and} \quad R_d < R_0 \quad \text{and} \quad R_9. \tag{2.17}$$

For this range of the modulus, there exists a description in terms of a d-dimensional theory of gravity coupled to a $U(1)$ gauge field. Note that the range of this region grows as R_0 and R_9 increase. Modulo exponentially suppressed terms $\mathcal{O}[\exp(-\frac{\mu}{T}), \exp(-\frac{\mu}{M})]$, the potential for the modulus is flat. We will see that for certain IBC, the modulus R_d may be frozen to an arbitrary value on this plateau, due to the gravitational friction of the expanding universe. The exponentially suppressed terms are irrelevant in this phase and cannot modify this behavior. In this range (2.17), the contributions of $k_T^{(d)}$ and $k_V^{(d)}$, as well as $g_T^{(d)}$ and $g_V^{(d)}$ are exponentially small compared to $f_T^{(d)}$ and $f_V^{(d)}$, so that $-P$ is independent of $\zeta = \ln R_d$. The pressure reproduces the result in d dimensions for n_T massless boson/fermion pairs in the originally supersymmetric model (as opposed to phase I which has $n_T + \tilde{n}_T$ massless pairs). Physically, we are away from the enhanced symmetry point and so the previous $SU(2)$ states are no longer massless. More concretely, along the plateau we have

$$p(z, \eta, \zeta) \simeq n_T \hat{f}_T^{(d)}(z) + n_V \hat{f}_V^{(d)}(z) := \hat{p}(z). \tag{2.18}$$

Either sign of this quantity is allowed when $n_V < 0$. Indeed, considering the large $|z|$ behavior, (2.18) implies

$$\begin{aligned} -P &\underset{z\to-\infty}{\sim} -T^d n_T e^{-z} S_{d+1}^o \underset{z\to-\infty}{\to} -\infty, \\ &\underset{z\to+\infty}{\sim} -T^d n_V e^{dz} S_{d+1}^o \underset{z\to+\infty}{\to} \operatorname{sign}(-n_V)\infty, \end{aligned} \tag{2.19}$$

where S_d^o (and S_d^{oe} for later use) is a constant,

$$S_d^o = \frac{\Gamma(\frac{d}{2})}{\pi^{\frac{d}{2}}} \sum_m \frac{1}{|2m+1|^d}, \qquad S_d^{oe} = \frac{\Gamma(\frac{d}{2})}{\pi^{\frac{d}{2}}} \sum_m{}' \frac{1}{|m|^d}, \tag{2.20}$$

and we see that $-P$ may take any value.

- **III: Higher-dimensional phase**

$$R_0 \quad \text{and/or} \quad R_9 < R_d. \tag{2.21}$$

For large values of the spectator modulus R_d, the appropriate effective field theory description is the $(d+1)$-dimensional theory of gravity. The modulus R_d becomes the $\hat{g}_{dd}$ component of the string frame metric, $\hat{g}_{dd} = (2\pi R_d)^2$.

All contributions of $|m_d|$ in $k_T^{(d)}$ and/or $k_V^{(d)}$ are substantial, and the behavior of p is better understood in terms of its second expression in (2.11). In addition, $g_T^{(d)}$ and $g_V^{(d)}$ are exponentially small. In particular, for $R_d^\epsilon \gg R_9$ and R_0 (which are both $\gg 1$),[4] one has

$$p(z,\eta,\zeta) \simeq e^{|\zeta|-\eta-z}\left(n_T \hat{f}_T^{(d+1)}(z) + n_V \hat{f}_V^{(d+1)}(z) + e^{d(z+\eta-|\zeta|)}(n_T+n_V)\frac{S_d^{oe}}{4}\right), \tag{2.22}$$

where the term $e^{d(z+\eta-|\zeta|)} \equiv (R_0/R_d^\epsilon)^d$ is power-like subdominant. In this expression, we neglect terms that are exponentially small in (R_d^ϵ/R_0) or (R_d^ϵ/R_9). The appearance of the functions $\hat{f}_T^{(d+1)}$ and $\hat{f}_V^{(d+1)}$ confirms that it is more natural to consider the system in $d+1$ dimensions. This is the case since, in this limit, the circle of radius R_d is very large. In Fig. 1, the exponential growth of $-P$ when $\zeta \to +\infty$ is decreasing. This is always the case when $n_V > 0$ but for $n_V < 0$ is only true when z *i.e.* M/T is small enough. This can be seen by considering the large $|z|$ limit of (2.22),

$$\begin{aligned} -P &\underset{z\to-\infty}{\sim} -T^d e^{|\zeta|-\eta} n_T e^{-2z} S_{d+2}^o \underset{z\to-\infty}{\to} -\infty, \\ &\underset{z\to+\infty}{\sim} -T^d e^{|\zeta|-\eta} n_V e^{dz} S_{d+2}^o \underset{z\to+\infty}{\to} \operatorname{sign}(-n_V)\infty, \end{aligned} \tag{2.23}$$

where S_{d+2}^o is defined in (2.20). We will see that the attraction to the RDS^{d+1} implies z to evolve such that the potential for ζ ends by being exponentially decreasing. The RDS^{d+1} will then correspond to a run away behavior $R_d(t) \to +\infty$. The RDS^{d+1} is stable only when the subdominant term $(R_0/R_d^\epsilon)^d$ can be neglected. This is always true when R_d is macroscopic, since we restrict our study to temperatures above the electroweak scale *i.e.* R_0 not very large compared to the internal space and R_9 in particular.

If R_d is internal and the subdominant term is not negligible, we will find that the universe is attracted back to phase II, where R_d becomes static and the evolution becomes that of an RDS^d. Finally we note that at early times, where T and M are well above the electroweak scale, it is possible to have R_d internal while keeping $(R_0/R_d^\epsilon)^d$ negligible for a large amount of time. In this case at early times the evolution is initially attracted to an RDS^{d+1}. However, at late times $(R_0/R_d^\epsilon)^d$ will always become relevant and the evolution always ends in an RDS^d.

- **IV: T-dual flat potential phase**

$$\frac{1}{R_0} \quad \text{and} \quad \frac{1}{R_9} < \frac{1}{R_d} - R_d, \quad \text{and} \quad \frac{1}{R_d} < R_0 \quad \text{and} \quad R_9. \tag{2.24}$$

The effective theory description is T-dual to the phase II where the light degrees of freedom are the winding modes instead of the Kaluza–Klein momentum modes of the phase II.

[4] We introduce $\epsilon = \operatorname{sign}(\zeta)$ which is 1 in phase III and -1 in the T-dual phase V.

- **V: T-dual higher-dimensional phase**

$$R_0 \quad \text{and/or} \quad R_9 < \frac{1}{R_d}. \tag{2.25}$$

This phase is the T-dual of phase III. The light degrees of freedom are the winding modes. $-P$ has the same form as in case III, after one transforms $\zeta \to -\zeta$. The effective field theory is naturally described in $d+1$ space–time dimensions, with $\hat{g}_{dd} = (2\pi/R_d)^2$ in string frame.

We have to stress here that the above phases arise from a common string setting but *cannot be described in the context of a single field theory*, due to the lack of the string winding modes. In field theory, only the phases II and III (or their T-dual IV and V) can be described by a single field theory. In phase I, the string winding modes play a particularly important role for the stabilization of the radius R_d at the extended symmetry point, as shown in Section 3.1. In contrast to field theory, string theory naturally interpolates between these various phases.

2.3. *The type II field theory phases*

The perturbative type II structure of $-P$ can be derived from the heterotic one by taking $\tilde{n}_T = \tilde{n}_V = 0$, so that phase I is now equivalent to phases II and III. The local minimum of $-P$ at $\zeta = 0$ is not present anymore and there is a single plateau I $\cup$ II $\cup$ IV (see Fig. 1). In phase III (or V), when $R_d^\epsilon \gg R_9$ and R_0 (which are both $\gg 1$), the function p in type II is identical to the heterotic one given in Eq. (2.22). Thus, in type II, the field ζ admits flat potential phases II and IV in d-dimensions, and the higher-dimensional phases III and V in $d+1$ dimensions. Again the higher-dimensional phases III and V are stable only to the extent that we can neglect the $(R_0/R_d^\epsilon)^d$ contribution in Eq. (2.22), which is always valid for macroscopic values of R_d^ϵ. However, when R_d^ϵ is internal, the final evolution is always attracted to the RDS^d of phase II or IV. In addition, during the times for which $(R_0/R_d)^d$ may be ignored, the universe admits an earlier evolution well approximated by an RDS^{d+1}. Since there is no enhancement of $U(1) \to SU(2)$, the "$SU(2)$ Higgs phase" does not exist perturbatively for type II theories. However, by heterotic-type II duality, we expect non-perturbative effects which may enhance the $U(1) \to SU(2)$ and imply an "$SU(2)$ phase" I. The non-perturbative effects can correspond to the addition of branes whose separation is governed by the spectator modulus. This will be discussed in more details in Section 4. Alternatively, branes wrapped on a vanishing cycle whose size is fixed by the spectator modulus provide another dual type II set up.

3. Radiation-like dominated solutions (RDS) of the Universe and stabilization of the spectator moduli

In Section 2.2, five distinct phases for the thermal effective potential $-P$ were identified for the heterotic string. Here, we analyze in detail the behavior of the system in the first three phases. The behavior of phases IV and V is found from that of phases II and III by T-duality $R_d \to 1/R_d$ and we do not consider them explicitly. We show that the radius R_d can be constant, either at the minimum of the potential in phase I or at any value along the flat region II. In phase III, R_d initially increases along with the expansion of the space–time. When the quantities $(R_0/R_d)^d$ and $(R_9/R_d)^d$ can be neglected, this evolution continues and is well described by an RDS^{d+1}. For values of R_d which are internal, R_d is always caught by R_0 and R_9 and after which the

evolution is attracted back to phase II. A distinct RDS^d exists in regions I, II and IV, while in region III and V there exists an RDS^{d+1} for macroscopic values of R_d^ϵ.

Next we show that these cosmological evolutions are stable against small perturbations. In particular, for phase I, the spectator modulus R_d is stabilized at the self-dual point, while for phases III (and V) it becomes part of the space–time metric. For phases II (and IV) the spectator modulus is weakly stabilized due to the presence of gravitational friction arising from the expansion of the universe. From these results, one expects in general that when the dynamics of all spectator moduli are taken into account, the radii that are not dynamically decompactified are (weakly) stabilized at scales smaller than the ones characterizing the temperature and supersymmetry breaking.

For the type II string case described in Section 2.3, there is no phase I, due to the absence of the heterotic $U(1) \to SU(2)$ enhancement at the self dual point. The remaining type II phases are identical to the heterotic ones.

3.1. Case I: Higgs phase

In this case, the radius R_d is naturally interpreted as a scalar Higgs field for an $SU(2)$ gauge group coupled to gravity in d dimensions. As mentioned before, our analysis is restricted to field configurations which are isotropic and homogeneous. We thus look for extrema of the action (2.3) whose metric, temperature and scalars satisfy the ansatz

$$ds^2 = -dt^2 + a(t)^2\big((dx^1)^2 + \cdots + (dx^{d-1})^2\big), \quad T(t), \quad z(t), \quad \phi_\perp(t), \quad \zeta(t). \tag{3.1}$$

The Einstein equations involve a thermal energy–momentum tensor whose components are the energy density ρ and pressure P. Using (2.10) and (B.11), the energy density ρ takes a factorized form

$$\rho = T^d r(z, \eta, \zeta) \quad \text{with } r = (d-1)p - p_z, \tag{3.2}$$

where p_z denotes the partial derivative with respect to z. Given solutions to the scalar equations of motion, we may always find corresponding solutions to the Einstein equations. We therefore focus first on solving the scalar equations. Their reduction on the ansatz (3.1) is given in Eqs. (B.35), (B.38) and (B.39) and summarized here as

$$h\mathcal{F}(\overset{\circ\circ}{z}, \overset{\circ\circ}{\phi}_\perp, \overset{\circ\circ}{\zeta}, \overset{\circ}{z}, \overset{\circ}{\phi}_\perp, \overset{\circ}{\zeta}) + V_z = 0, \tag{3.3}$$

$$h\overset{\circ\circ}{\phi}_\perp + \frac{1}{d-2}(r-p)\overset{\circ}{\phi}_\perp - \frac{1}{\sqrt{d-1}}p_\eta = 0, \tag{3.4}$$

$$h\overset{\circ\circ}{\zeta} + \frac{1}{d-2}(r-p)\overset{\circ}{\zeta} - p_\zeta = 0, \tag{3.5}$$

where h is defined in Eq. (B.33) and $\mathcal{F}(\overset{\circ\circ}{z}, \overset{\circ\circ}{\phi}_\perp, \overset{\circ\circ}{\zeta}, \overset{\circ}{z}, \overset{\circ}{\phi}_\perp, \overset{\circ}{\zeta})$ is a function which vanishes when all of its arguments vanish. We have reparameterized our fields in terms of the scale factor $\ln a$ so that time-derivatives have been replaced with $(\ln a)$-derivatives denoted as $\overset{\circ}{f}$.

3.1.1. Radiation-like dominated solution

To start off, we note that the fact the model is invariant under the T-duality $R_d \to 1/R_d$ implies $p(z, \eta, \zeta)$ is an even function of ζ, so that the first derivative of p with respect to ζ vanishes at $\zeta = 0$. Thus, $\zeta \equiv 0$ is a solution to Eq. (3.5). Next, from Eq. (2.16), the source P is independent

of η at $\zeta = 0$, so that $p_\eta(z, \eta, 0) \equiv 0$. As a consequence, Eq. (3.4) is solved for any constant $\phi_\perp \equiv \phi_{\perp 0}$, and we find that $\phi_\perp$ remains a modulus.

It is convenient to introduce the quantities $\tilde{p}(z)$ and $\tilde{r}(z)$, which are related to the pressure P and energy density ρ at $\zeta = 0$ as

$$P(z, \eta, 0) = T^d p(z, \eta, 0) = T^d \tilde{p}(z), \qquad \rho(z, \eta, 0) = T^d r(z, \eta, 0) = T^d \tilde{r}(z). \tag{3.6}$$

Eq. (3.3) implies the complex structure z can be a constant, $z \equiv \tilde{z}_c$, as long as $\tilde{z}_c$ is a root of V_z. As in Eq. (B.40), here V_z takes the simple form

$$\tilde{V}_z(z) := V_z(z, \eta, 0) = \sqrt{\frac{d-2}{d-1}}(\tilde{r} - d\tilde{p}). \tag{3.7}$$

The shape of $\tilde{V}(z)$ depends drastically on the model dependent parameter $\frac{n_V + \tilde{n}_V}{n_T + \tilde{n}_T} \in [-1, 1]$ and can be inferred from the behavior for large positive or large negative z,

$$\begin{aligned} \tilde{V}(z) &\underset{z \to -\infty}{\sim} -e^{(d-1)z}\left(\frac{1}{2^d - 1} + \frac{n_V + \tilde{n}_V}{n_T + \tilde{n}_T}\right) \times (n_T + \tilde{n}_T)\frac{d}{2(d-1)}\sqrt{\frac{d-2}{d-1}}S_d^o, \\ &\underset{z \to +\infty}{\sim} -e^{dz}(n_V + \tilde{n}_V) \times \left(1 + \frac{1}{d}\right)\sqrt{\frac{d-2}{d-1}}S_{d+1}^o, \end{aligned} \tag{3.8}$$

with S_d^o defined in Eq. (2.20). Three cases arise:

- *Case* ($\tilde{a}$): For $\frac{n_V + \tilde{n}_V}{n_T + \tilde{n}_T} < -\frac{1}{2^d - 1}$, $\tilde{V}$ increases monotonically.
- *Case* ($\tilde{b}$): For $-\frac{1}{2^d - 1} < \frac{n_V + \tilde{n}_V}{n_T + \tilde{n}_T} < 0$, $\tilde{V}$ has a unique minimum $\tilde{z}_c$, and $\tilde{p}(\tilde{z}_c) > 0$.
- *Case* ($\tilde{c}$): For $0 < \frac{n_V + \tilde{n}_V}{n_T + \tilde{n}_T}$, $\tilde{V}$ decreases monotonically.

We choose to concentrate on models where z can be stabilized. This corresponds to the *Case* ($\tilde{b}$) [4],[5] so that

$$\textit{Case } (\tilde{b}): \quad -\frac{1}{2^d - 1} < \frac{n_V + \tilde{n}_V}{n_T + \tilde{n}_T} < 0, \tag{3.9}$$

which guarantees the possibility to fix z at the critical value $\tilde{z}_c$ such that (see Eq. (3.7)),

$$\tilde{r}(\tilde{z}_c) = d\tilde{p}(\tilde{z}_c). \tag{3.10}$$

This is the state equation for radiation in $d + 1$ dimensions.[6] The scalar equations of motion have now been satisfied and the remaining Einstein equations are easily solved. The overall dependence on time is determined from the Friedmann equation (B.33) which takes the form

$$\frac{1}{2}(d-2)(d-1)H^2 = \frac{\tilde{c}_r}{a^d} \quad \text{where } \tilde{c}_r = \frac{(d-1)^2}{d(d-2)}\tilde{r}(\tilde{z}_c)e^{-d\tilde{z}_c}(\tilde{a}_0\tilde{M}_0)^d, \tag{3.11}$$

[5] The models in *Case* ($\tilde{c}$) admit a so-called "Moduli Dominated Solution" corresponding to a contracting Universe (where $z(t) \to +\infty$ is running away) [4]. The models in *Case* ($\tilde{a}$) are analyzed in [18] and admit an RDS in $d + 1$ dimensions, after dynamical decompactification of the internal radius R_9 involved in the supersymmetry breaking (*i.e.* $z \ll -1$).

[6] As explained in [2,3], once taking into account the kinetic energy density of the scalar Φ, one recovers the state equation for radiation in d dimensions, as expected for an RDS^d.

and is easily integrated. Here, $\tilde{a}_0$ and $\tilde{M}_0$ are integration constants. Using the remaining Eq. (B.28), the full solution we find is,

$$a(t) = \left(\frac{t}{\tilde{t}_0}\right)^{2/d} \tilde{a}_0 \quad \text{where } \frac{\tilde{a}_0}{\tilde{t}_0^{2/d}} = \left(\frac{d^2 \tilde{c}_r}{2(d-2)(d-1)}\right)^{1/d},$$
$$T(t) = M(t) e^{-\tilde{z}_c} = \frac{1}{a(t)} e^{-\tilde{z}_c} \tilde{a}_0 \tilde{M}_0, \qquad \phi_\perp(t) = \phi_{\perp 0}, \qquad \zeta(t) = 0, \tag{3.12}$$

where Φ is related to M by the definition (2.8). This particular evolution is characterized by a temperature T, a spontaneous supersymmetry breaking scale M, and an inverse scale factor that are proportional for all times. From the form of the Friedmann equation, Eq. (3.11), this solution is to be interpreted as a radiation-like era in d dimensions, with frozen internal radius $R_d \equiv 1$ and a modulus $\phi_\perp$. In the next sub-section, our aim is to analyze the stability of this heterotic solution and show that it is an attractor of the dynamics for an open set of generic initial boundary conditions.

3.1.2. Attraction to the radiation-like era and spectator modulus stabilization

To analyze the stability of the radiation-like era (3.12), we consider small fluctuations around it,

$$z = \tilde{z}_c + \varepsilon_{(z)}, \qquad \phi_\perp = \phi_{\perp 0} + \varepsilon_{(\phi_\perp)}, \qquad \zeta = 0 + \varepsilon_{(\zeta)}, \tag{3.13}$$

where $|\varepsilon_{(z)}|$, $|\varepsilon_{(\phi_\perp)}|$ and $|\varepsilon_{(\zeta)}|$ are $\ll 1$. The equations of motion for the scalars given in Eqs. (B.35), (B.38) and (B.39) become at first order,

$$\ddot{\varepsilon}_{(z)} + \frac{1}{2}(d-2)\dot{\varepsilon}_{(z)} + \tilde{C}\varepsilon_{(z)} = 0 \quad \text{where } \tilde{C} = \frac{1}{2}(d-2)^2(d+1)\left.\frac{\tilde{r}_z - d\tilde{p}_z}{d\tilde{r} - \tilde{r}_z}\right|_{\tilde{z}_c}, \tag{3.14}$$

$$\ddot{\varepsilon}_{(\phi_\perp)} + \frac{1}{2}(d-2)\dot{\varepsilon}_{(\phi_\perp)} = 0, \tag{3.15}$$

$$\ddot{\varepsilon}_{(\zeta)} + \frac{1}{2}(d-2)\dot{\varepsilon}_{(\zeta)} + \tilde{E}(\eta)\varepsilon_{(\zeta)} = 0 \quad \text{where } \tilde{E}(\eta) = -\frac{(d-2)^2}{2(d-1)} \frac{p_{\zeta\zeta}(\tilde{z}_c, \eta, 0)}{\tilde{p}(\tilde{z}_c)}. \tag{3.16}$$

It is important to note that even if p_ζ vanishes and p is independent of η when $\zeta = 0$, this is not the case for $p_{\zeta\zeta}$, and indeed we find

$$p_{\zeta\zeta}(z, \eta, 0) = 32\pi^2 e^{2(\eta+z)} \big(\tilde{n}_T \hat{f}_T^{(d-2)}(z) + \tilde{n}_V \hat{f}_V^{(d-2)}(z)\big). \tag{3.17}$$

Due to the friction term $\frac{1}{2}(d-2)$, the solutions of Eq. (3.14) for arbitrary IBC converge to 0 as $t \to +\infty$ (with eventually damped oscillations), if and only if $\tilde{C} > 0$. This is precisely the case when the condition (3.9) is satisfied. Similarly, all solutions to Eq. (3.15) also converge to 0. Finally, the generic solution of Eq. (3.16) is

$$\varepsilon_{(\zeta)} = \left(\frac{a_1}{a}\right)^{\frac{d-2}{4}} \left[c_+ J_{\frac{d-1}{4}}\left(\frac{d-1}{d-2}\left(\frac{a}{a_1}\right)^{\frac{d-2}{d-1}}\right) + c_- J_{-\frac{d-1}{4}}\left(\frac{d-1}{d-2}\left(\frac{a}{a_1}\right)^{\frac{d-2}{d-1}}\right)\right], \tag{3.18}$$

where J_α are Bessel functions of the first kind, while c_+, c_- (and a_1) are constants determined by the IBC. As $t \to +\infty$ or equivalently $a \to +\infty$, the above solution converges to 0 with damped oscillations, due to the behavior of the Bessel functions. We thus conclude that the spectator modulus is stabilized at the self-dual point and that the radiation-like era (3.12) is a local attractor.

3.2. Case II: Flat potential phase

We now analyze the phase II. In this case, ζ is a flat direction of the thermal effective potential $-P$ which takes the simple form given in Eq. (2.18). There is no enhancement of the gauge group to $SU(2)$ and the spectator modulus R_d is simply a flat direction. Although there is no potential for ζ in this phase, fluctuations in ζ are still suppressed due to the gravitational friction caused by the expansion of the universe. In addition, we are going to see that depending on the IBC, even if the evolution starts in phase II, it may exit from it and enter either phase I or phase III. This result is non-trivial due to the fact that as the universe expands, so does the size of the plateau of the flat potential phase.

As in Section 3.1, we restrict our analysis to isotropic and homogeneous d-dimensional universes. We take the same ansatz as in (3.1), and consequently all of the equations of motion of Appendix B.1 are valid in the case considered here. On the plateau, $p(z,\eta,\zeta)$ is equal to $\hat{p}(z)$ given in Eq. (2.18), where the dependencies on η and ζ are exponentially small in R_0 or R_9 and are thus neglected. As a consequence, $p_\zeta(z,\eta,\zeta_0) \simeq p_\eta(z,\eta,\zeta_0) \simeq 0$, for any ζ_0 on the plateau.

3.2.1. Radiation-like dominated solution

Up to the replacement $\zeta(t) \equiv 0 \to \zeta(t) \equiv \zeta_0$, the vanishing of $p_\zeta(z,\eta,\zeta_0)$ and $p_\eta(z,\eta,\zeta_0)$ were the only ingredients used at the beginning of Section 3.1 to derive the radiation-like dominated solution in d dimensions (3.12). Thus, in the present case a similar solution exists. It is obtained by defining $\hat{p}$ and $\hat{r}$ as $\tilde{p}$ and $\tilde{r}$, but with $\tilde{n}_T$ and $\tilde{n}_V$ set to zero

$$\hat{p} = \tilde{p}|_{\tilde{n}_T=\tilde{n}_V=0}, \qquad \hat{r} = \tilde{r}|_{\tilde{n}_T=\tilde{n}_V=0}. \tag{3.19}$$

The condition similar to (3.9) for the existence of a solution with stabilized z is now,

$$\textit{Case } (\hat{b}): \quad -\frac{1}{2^d-1} < \frac{n_V}{n_T} < 0, \tag{3.20}$$

in which case there is a unique $\hat{z}_c$ satisfying

$$\hat{r}(\hat{z}_c) = d\,\hat{p}(\hat{z}_c). \tag{3.21}$$

In phase II, the radiation-like era can be written as

$$\begin{aligned} a(t) &= \left(\frac{t}{\hat{t}_0}\right)^{2/d} \hat{a}_0 \quad \text{where } \frac{\hat{a}_0}{\hat{t}_0^{2/d}} = \left(\frac{d^2\hat{c}_r}{2(d-2)(d-1)}\right)^{1/d}, \\ T(t) &= M(t)e^{-\hat{z}_c} = \frac{1}{a(t)} e^{-\hat{z}_c}\hat{a}_0\hat{M}_0, \qquad \phi_\perp(t) = \phi_{\perp 0}, \qquad \zeta(t) = \zeta_0, \end{aligned} \tag{3.22}$$

where $\hat{a}_0$ and $\hat{M}_0$ are integration constants, $\hat{c}_r$ is defined as in Eq. (3.11) but with "hat" quantities and Φ is related to M by the definition (2.8).

3.2.2. Attraction to the radiation-like era with R_d constant

The study of the stability given in Section 3.1.2 can also be applied in the present case. More explicitly, the equations of motion for the perturbations of the scalars become

$$\overset{\circ\circ}{\varepsilon}_{(z)} + \frac{1}{2}(d-2)\overset{\circ}{\varepsilon}_{(z)} + \hat{C}\varepsilon_{(z)} = 0 \quad \text{where } \hat{C} = \frac{1}{2}(d-2)^2(d+1)\left.\frac{\hat{r}_z - d\,\hat{p}_z}{d\hat{r} - \hat{r}_z}\right|_{\hat{z}_c}, \tag{3.23}$$

$$\overset{\circ\circ}{\varepsilon}_{(\phi_\perp)} + \frac{1}{2}(d-2)\overset{\circ}{\varepsilon}_{(\phi_\perp)} = 0, \tag{3.24}$$

$$\overset{\circ\circ}{\varepsilon}_{(\zeta)} + \frac{1}{2}(d-2)\overset{\circ}{\varepsilon}_{(\zeta)} = 0, \tag{3.25}$$

where the analogue of $\tilde{E}(\eta)$ in Eq. (3.16) vanishes, since $p_{\zeta\zeta}(\hat{z}_c, \eta, \zeta_0) \simeq 0$. The positivity of $\hat{C}$ is again guaranteed by the condition (3.20) and all perturbations $\varepsilon_{(z)}, \varepsilon_{(\phi_\perp)}, \varepsilon_{(\zeta)}$ converge to 0 as $t \to +\infty$.

We conclude that if ζ is initially in the range where its potential is flat, some generic IBC imply an attraction to a regime where ζ and $\phi_\perp$ are constant moduli. Even if the potential of the spectator modulus R_d and $\phi_\perp$ are flat, these fields are nevertheless "stabilized in a weak sense" since the expansion of the universe dilutes their kinetic energies which then vanish for late times. Physically, the friction terms proportional to H freeze them in place at late times. After this has occurred, $R_d(t)$ is a constant, while $R_9(t)$ and $R_0(t)$ behave as $a^{\frac{d-2}{d-1}}$ and are thus increasing such that the complex structure-like ratio $e^z = R_0(t)/R_9(t)$ is stabilized.

3.2.3. *Falling off the plateau*

We now show that despite the expansion of the plateau and the friction terms, for sufficiently large initial velocities, it is always possible for ζ to escape from the plateau and enter regions III or I. To show this, we will simply find particular IBC that yield this precise behavior.

Suppose ζ is somewhere along the plateau and choose, as in Section 3.2.1, $z \equiv \hat{z}_c$ and $\phi \equiv \phi_{\perp 0}$, which are trivial solutions to Eqs. (3.3) and (3.4). Eq. (B.30) gives $\overset{\circ}{\Phi} = -\sqrt{\frac{d-2}{d-1}}$, so that the definition (2.4) implies

$$\overset{\circ}{\eta} = (\overset{\circ}{\eta} + \overset{\circ}{z}) = \frac{d-2}{d-1}, \tag{3.26}$$

which is nothing but the "constant velocity" of the right edge of the plateau. This defines an escape velocity and we now wish to know if it is possible for $\overset{\circ}{\zeta}$ to be larger than this speed for a long enough time to reach the edge of the plateau. One can see that taking ζ as,

$$\zeta = \zeta_0 + (d-2)\sqrt{\frac{d}{d-1}}\ln a, \tag{3.27}$$

solves the ζ-equation of motion (3.5).[7] We see that ζ is rolling at approximately (see the previous footnote) "constant velocity" given by $\overset{\circ}{\zeta} \simeq (d-2)\sqrt{\frac{d}{d-1}}$, and in particular we have $\overset{\circ}{\zeta} > \overset{\circ}{\eta}$. As a result, for initial values ζ_{init}, η_{init} and a_{init}, there is always a scale factor a_{fall} where ζ reaches the right boundary of the plateau. It is defined by

$$\min(\eta_{\text{init}}, \eta_{\text{init}} + z_c) - \zeta_{\text{init}} = \left((d-2)\sqrt{\frac{d}{d-1}} - \frac{d-2}{d-1}\right)(\ln a_{\text{fall}} - \ln a_{\text{init}}) > 0. \tag{3.28}$$

Another solution with opposite velocity $\overset{\circ}{\zeta}$ is also allowed, so that ζ can roll and enter phase I.

3.3. *Case III: Higher-dimensional phase*

Here we analyze phase III of Section 2.2. When R_d is comparable to the size of T^{d-1}, it is natural to interpret the model in $d+1$ dimensions. The fields with non-trivial vacuum expectation

[7] One may worry that this solution yields a singular H. To remedy this, one can introduce a perturbation $\overset{\circ}{\varepsilon}_{(\zeta)} := ca^{d-2}$ to ζ, such that $|ca_{\text{fall}}^{d-2}| \ll 1$, where a_{fall} is defined in Eq. (3.28).

value are the Einstein frame metric $g'_{\mu\nu}$ and dilaton $\phi'_{\rm dil}$ in $d+1$ dimensions, coupled to the scalar η defined in (2.5). We use primes here to denote that the fields are now normalized in $d+1$ dimensions and are not the same as the fields appearing in the two previous sections. Note that $\zeta = \ln R_d$ is now one of the degrees of freedom of $g'_{\mu\nu}$. In the notations of Appendix B.2, we are now in the case $n=1$ and $\Delta = 8 - A - d$ (where $A=4$ for toroidal models and $A=4$ for orbifold ones), so that the effective space–time dimension is $\mathcal{D} = d+1$.

The action S in (2.3) can be written equivalently as

$$S = \int d^{d+1}x\,\sqrt{-g'}\left(\frac{R'}{2} - \frac{1}{2}\left(\partial\Phi'\right)^2 - \frac{1}{2}\left(\partial\phi'_\perp\right)^2 + P'\right), \tag{3.29}$$

where we have introduced the canonically normalized fields

$$\Phi' := \frac{2}{\sqrt{d(d-1)}}\phi'_{\rm dil} - \sqrt{\frac{d-1}{d}}\eta, \qquad \phi'_\perp := \frac{2}{\sqrt{d}}\phi'_{\rm dil} + \frac{1}{\sqrt{d}}\eta. \tag{3.30}$$

The pressure P' defined in $d+1$ dimensions is the free energy density $-\mathcal{F}'$ (see Eq. (B.12)). It is related to the partition function Z by,

$$P' = e^{\frac{2(d+1)}{d-1}\phi'_{\rm dil}}\frac{Z}{V_{0,\ldots,d}}, \tag{3.31}$$

where the partition function is given as before in Eq. (2.7). In $d+1$ dimensions, the temperature T' and supersymmetry breaking scale M' (both measured in Einstein frame, see Eqs. (B.10) and (B.5)) have different normalizations compared to their counterparts in Eqs. (2.8), but the complex structure z remains the same,

$$T' = \frac{e^{\frac{2\phi'_{\rm dil}}{d-1}}}{2\pi R_0}, \qquad M' = \frac{e^{\frac{2\phi'_{\rm dil}}{d-1}}}{2\pi R_9} \equiv \frac{e^{\sqrt{\frac{d}{d-1}}\Phi'}}{2\pi}, \qquad e^z := \frac{M'}{T'} = \frac{R_0}{R_9}. \tag{3.32}$$

We are interested in extrema of S that can be interpreted as homogeneous but anisotropic space–times with rotation group $SO(d-1)$. We consider the ansatz

$$\begin{aligned} &ds'^2 = -dt^2 + a'(t)^2\left(\left(dx^1\right)^2 + \cdots + \left(dx^{d-1}\right)^2\right) + b(t)^2\left(dx^d\right)^2, \\ &T'(t), \quad \Phi'(t), \quad \phi'_\perp(t), \end{aligned} \tag{3.33}$$

where the metric scale factor b along the direction d is related to ζ by[8]

$$b := e^{|\zeta| - \frac{2\phi'_{\rm dil}}{d-1}}. \tag{3.34}$$

The thermal part of the energy–momentum tensor involves an energy density ρ', the pressure P' (associated to the directions $1,\ldots,d-1$) and a pressure $P' + b(\partial P'/\partial b)$ in the direction d (see Eqs. (B.11)–(B.13)). They are more conveniently written as functions of $\{T', z, \eta, \zeta\}$ in terms of which they take a factorized form,

$$P' \equiv T'^{d+1}p'\left(z,\eta,|\zeta|\right), \qquad \rho' \equiv T'^{d+1}r'\left(z,\eta,|\zeta|\right). \tag{3.35}$$

The functions p' and r' are related to their counterparts in d dimensions p and r (Eqs. (2.10) and (3.2)) as,

[8] We introduce absolute values $|\zeta| \equiv \epsilon\zeta$ for our analysis to also be valid in the T-dual phase V.

$$p'(z,\eta,|\zeta|) = e^{\eta-|\zeta|+z}p(z,\eta,|\zeta|), \qquad r'(z,\eta,|\zeta|) = e^{\eta-|\zeta|+z}r(z,\eta,|\zeta|),$$
$$r' = dp' - p'_z. \tag{3.36}$$

The equations of motion reduced on the ansatz (3.33) are derived in Appendix B.2. There are three independent Einstein equations, coupled to two scalar equations. It is relevant to introduce a modulus ξ as

$$e^{\xi} := \frac{b}{a'}, \tag{3.37}$$

which is a "complex structure for the external space". Then, one can replace one of the Einstein equations by the equation for the scalar ξ. Effectively, we have three scalars, whose equations of motion (B.59), (B.61) and (B.62) can be solved, before considering the remaining Einstein equations. The scalar equations of motion are summarized here as

$$h'\mathcal{F}'(\overset{\circ\circ}{z}, \overset{\circ\circ}{\phi}{}'_\perp, \overset{\circ\circ}{\zeta}, \overset{\circ}{z}, \overset{\circ}{\phi}{}'_\perp, \overset{\circ}{\zeta}) + V'_z = 0, \tag{3.38}$$

$$h'\overset{\circ\circ}{\phi}{}'_\perp + \frac{1}{d-1}(r' - p' - p'_{|\zeta|})\overset{\circ}{\phi}{}'_\perp - \frac{1}{\sqrt{d}}(p'_\eta + p'_{|\zeta|}) = 0, \tag{3.39}$$

$$h'\overset{\circ\circ}{\xi} + \frac{1}{d-1}(r' - p' - p'_{|\zeta|})\overset{\circ}{\xi} - p'_{|\zeta|} = 0, \tag{3.40}$$

where h' is defined in Eq. (B.57) and $\mathcal{F}'(\overset{\circ\circ}{z}, \overset{\circ\circ}{\phi}{}'_\perp, \overset{\circ\circ}{\zeta}, \overset{\circ}{z}, \overset{\circ}{\phi}{}'_\perp, \overset{\circ}{\zeta})$ is a function which vanishes when all of its arguments vanish.

3.3.1. Radiation-like dominated solution in $d+1$ dimensions

Our aim is to study the dynamics when the characteristic size of the direction d is larger than the scale of the internal space. When $R_d \gg R_9$ and R_0, one observes from Eqs. (3.36) and (2.22) that if we neglect the subdominant term $e^{d(z+\eta-|\zeta|)} = (R_0/R_d^\epsilon)^d$, the pressure P' is independent of η and ζ

$$p'(z,\eta,|\zeta|) \simeq n_T \hat{f}_T^{(d+1)}(z) + n_V \hat{f}_V^{(d+1)}(z) := \hat{p}'(z) \quad \text{when } |\zeta| \gg \eta \text{ and } \eta + z. \tag{3.41}$$

In this regime, we define similarly $\hat{r}'(z) := r'$ and observe that since $p'_\eta \simeq p'_{|\zeta|} \simeq 0$, constant $\phi'_\perp \equiv \phi'_{\perp 0}$ and $\xi \equiv \xi_0$ solve trivially Eqs. (3.39) and (3.40). $\phi'_\perp$ and ξ are thus moduli in this limit. Note that neglecting the power-like term $(R_0/R_d^\epsilon)^d$ is justified if R_d is macroscopic, since we restrict our analysis to temperatures above the electroweak scale. In particular, if R_d takes values such that $(R_d/R_0)^d \gtrsim e^{2\pi R_0}$ and $(R_d/R_0)^d \gtrsim e^{2\pi R_9}$ it is of the order of terms which we have already dropped.

A constant $z \equiv \hat{z}'_c$ is allowed by Eq. (3.38) if $V'_z = 0$. In the regime we focus on with $R_d \gg R_9, R_0$, the definition (B.60) simplifies to

$$V'_z(z,\eta,|\zeta|) \simeq \sqrt{\frac{d-1}{d}}(\hat{r}' - (d+1)\hat{p}') := \hat{V}'_z(z), \tag{3.42}$$

which is identical to (3.7) in $d+1$ dimensions. $\hat{V}'(z)$ admits a critical point in what we call *Case* $(\hat{b}')$ (by analogy with (3.20)), defined by the condition

$$\textit{Case}\ (\hat{b}'): \quad -\frac{1}{2^{d+1}-1} < \frac{n_V}{n_T} < 0. \tag{3.43}$$

When this is satisfied, $\hat{z}'_c$ is the unique solution to

$$\hat{r}'(\hat{z}'_c) = (d+1)\hat{p}'(\hat{z}'_c), \tag{3.44}$$

which is the state equation of radiation in $d+2$ dimensions.[9]

The scalar equations of motion Eqs. (3.38), (3.39) and (3.40) have now been satisfied. The remaining Einstein equations are easily integrated. The overall time dependence is determined by the Friedmann equation (B.57), which becomes

$$\frac{1}{2}(d-1)\,dH'^2 = \frac{\hat{c}'_r}{a'^{d+1}} \quad \text{where } \hat{c}'_r = \frac{d^2}{(d+1)(d-1)}\hat{r}'(\hat{z}'_c)e^{-(d+1)\hat{z}'_c}\big(\hat{a}'_0\hat{M}'_0\big)^{d+1}. \tag{3.45}$$

The full solution we obtain is,

$$a'(t) = \left(\frac{t}{\hat{t}'_0}\right)^{\frac{2}{d+1}}\hat{a}'_0 \quad \text{where } \frac{\hat{a}'_0}{\hat{t}'^{\frac{2}{d+1}}_0} = \left(\frac{(d+1)^2\hat{c}'_r}{2(d-1)d}\right)^{\frac{1}{d+1}},$$

$$T'(t) = M'(t)e^{-\hat{z}'_c} = \frac{1}{a'(t)}e^{-\hat{z}'_c}\hat{a}'_0\hat{M}'_0 = \frac{1}{b(t)}e^{\xi_0-\hat{z}'_c}a'_0M'_0, \qquad \phi'_\perp(t) = \phi'_{\perp 0}, \tag{3.46}$$

where Φ' is related to M' by definition (3.32), and $\hat{a}'_0$, $\hat{M}'_0$, ξ_0 and $\phi'_{\perp 0}$ are arbitrary integration constants. For this particular evolution, it is useful to rescale the space coordinate x^d to bring the metric (3.33) in an isotropic form,

$$x'^d := e^{\xi_0}x^d \quad \Longrightarrow \quad ds'^2 = -dt^2 + a'(t)^2\big((dx^1)^2 + \cdots + (dx^{d-1})^2 + (dx'^d)^2\big). \tag{3.47}$$

This shows that there is an enhancement of the local rotation group, $SO(d-1) \to SO(d)$. We learn from the effective Friedmann equation (3.45) that this evolution of the universe can be interpreted as a radiation-like era in $d+1$ dimensions. The temperature T' and supersymmetry breaking scale M' are inversely proportional to the isotropic scale factor a', while $\phi'_\perp$ remains a modulus. Next, we study the stability and attraction properties of this solution.

3.3.2. Attraction to the radiation-like era in $d+1$ dimensions via decompactification of $S^1(R_d)$

To study the stability of the solution (3.46) (which is valid when the subdominant term $(R_0/R_d^\epsilon)^d$ is negligible in Eq. (2.22)), we analyze the behavior of the small fluctuations around it,

$$z = \hat{z}'_c + \varepsilon_{(z)}, \qquad \phi'_\perp = \phi'_{\perp 0} + \varepsilon_{(\phi'_\perp)}, \qquad \xi = \xi_0 + \varepsilon_{(\xi)}, \tag{3.48}$$

where $|\varepsilon_{(z)}|$, $|\varepsilon_{(\phi'_\perp)}|$ and $|\varepsilon_{(\xi)}|$ are $\ll 1$. The scalar equations of motion, Eqs. (B.59), (B.61) and (B.62), in this regime become

$$\overset{\circ\circ}{\varepsilon}_{(z)} + \frac{1}{2}(d-1)\overset{\circ}{\varepsilon}_{(z)} + \hat{C}'\varepsilon_{(z)} = 0, \tag{3.49}$$

$$\overset{\circ\circ}{\varepsilon}_{(\phi'_\perp)} + \frac{1}{2}(d-1)\overset{\circ}{\varepsilon}_{(\phi'_\perp)} = 0, \tag{3.50}$$

$$\overset{\circ\circ}{\varepsilon}_{(\xi)} + \frac{1}{2}(d-1)\overset{\circ}{\varepsilon}_{(\xi)} = 0, \tag{3.51}$$

[9] One has to take into account the classical kinetic energy part of the stress tensor to recover the equation of state for radiation in $d+1$ dimensions.

where

$$\hat{C}' = \frac{1}{2}(d-1)^2(d+2)\frac{\hat{r}'_z - (d+1)\hat{p}'_z}{(d+1)\hat{r}' - \hat{r}'_z}\bigg|_{\hat{z}'_c}. \tag{3.52}$$

We find that $\hat{C}'$ always satisfies $\hat{C}' > 0$ in *Case* $(\hat{b}')$ defined in (3.43). This implies that for arbitrary IBC, the solutions of Eq. (3.49) converge to 0 (with eventually damped oscillations) as $t \to +\infty$. In addition, all solutions to Eqs. (3.50) and (3.51) also converge to 0, when $t \to +\infty$.

Thus, the radiation-like era in $d+1$ dimensions (3.46) is stable under small fluctuations, when the subdominant term $(R_0/R_d^\epsilon)^d$ in Eq. (2.22) is neglected. There is an open set of IBC, in particular when R_d is initially macroscopic, such that the solutions are attracted by this evolution, which is characterized by an enhanced local rotation group. The Kähler modulus R_d is better understood in terms of the "external space complex structure" ratio $e^\xi = b/a = R_d/R$, where R is the radius of one of the $d-1$ space-like dimensions. This is similar to what is happening to the Kähler modulus R_9 that we consider through the complex structure-like ratio $e^z = M/T = R_0/R_9$. However, while z is dynamically stabilized to the value $\hat{z}'_c$, ξ is a modulus ξ_0. This last remark is due to the fact that we consider local equations of motion only. An additional choice of global boundary conditions on the relative sizes of the large external dimensions would specify ξ_0. Only astrophysical observations may be sensitive to moduli such as ξ_0, but not "local" experiments encountered in particle physics.

3.3.3. Residual force and attraction back to phase II

Here, we want to study the effect of the subdominant term in Eq. (2.22). We take it small compared to 1 but not negligible and in particular, we want to analyze how it perturbs the results of the previous subsection, namely the attraction to the RDS^{d+1}. We first introduce y as

$$e^y := e^{z+\eta-|\zeta|} = \left(\frac{R_0}{R_d^\epsilon}\right). \tag{3.53}$$

It will be convenient to express the conservation of the energy–momentum tensor (B.52) in the following form,

$$e^{dy} = e^{-(d-1)\xi}\left(r' + p'\right) \times \text{cst}. \tag{3.54}$$

Let us consider a generic perturbation around the RDS^{d+1},

$$z = \hat{z}'_c + \varepsilon_{(z)}, \qquad \phi'_\perp = \phi'_{\perp 0} + \varepsilon_{(\phi'_\perp)}, \qquad \xi = \xi_0 + \varepsilon_{(\xi)}, \qquad y = y_0 + \varepsilon_{(y)}, \tag{3.55}$$

where $|\varepsilon_{(z)}|$, $|\varepsilon_{(\phi'_\perp)}|$, $|\varepsilon_{(\xi)}|$, $|\varepsilon_{(y)}|$ and the constant e^{dy_0} are $\ll 1$. At order one, the equations for $\varepsilon_{(z)}$ and $\varepsilon_{(\phi'_\perp)}$ are identical to (3.49) and (3.50), when e^{dy_0} was neglected. However, the equation for $\varepsilon_{(\xi)}$ becomes

$$\overset{\circ\circ}{\varepsilon}_{(\xi)} + \frac{1}{2}(d-1)\left(\overset{\circ}{\varepsilon}_{(\xi)} + c_1 e^{dy_0}\right) = 0 \quad \text{where } c_1 = (n_T + n_V)\frac{(d-1)S_d^{oe}}{4\hat{p}'(\hat{z}'_c)} > 0, \tag{3.56}$$

while Eq. (3.54) gives

$$\overset{\circ}{\varepsilon}_{(y)} = -c_2\overset{\circ}{\varepsilon}_{(\xi)} + c_3\overset{\circ}{\varepsilon}_{(z)}$$
$$\text{where } c_2 = \frac{1-\frac{1}{d}}{1 - e^{-(d-1)\xi_0}(n_T+n_V)\frac{S^{oe}}{4}\cdot\text{cst}} > 0, \; c_3 = \frac{\hat{r}'_z + \hat{p}'_z}{\hat{r}'_z + \hat{p}'_z}\bigg|_{\hat{z}'_c}. \tag{3.57}$$

This implies that $\overset{\circ}{\varepsilon}_{(z)}$ and $\overset{\circ}{\varepsilon}_{(\phi'_\perp)}$ are converging to zero when the scale factor $a'(t)$ is expanding. However, $\overset{\circ}{\varepsilon}_{(\xi)} \to -c_1 e^{dy_0}$ and $\overset{\circ}{\varepsilon}_{(y)} \to c_1 c_2 e^{dy_0}$. We conclude that $e^y = R_0/R_d^\epsilon$ and $e^{y-z} = R_9/R_d^\epsilon$ are slowly increasing *i.e.* the distance between R_d^ϵ and the plateau decreases. The interpretation of the evolution in terms of RDS^{d+1} remains valid until e^{dy} and $e^{d(y-z)}$ cease to be $\ll 1$. As said in the previous subsection, this cannot happen if R_d is initially macroscopic and we are interested in temperature and supersymmetry breaking scales larger than the electroweak scale.[10] However, if initially R_d^ϵ is larger than R_0 and R_9 but still microscopic, the above analysis suggests that it will be "caught by the plateau" and the cosmology is attracted back to phase II *i.e.* the RDS^d.

4. Non-perturbative cosmologies in type II

As discussed in Section 2.3, the thermal effective potential in type II theories does not give rise to a Higgs phase I as in the heterotic string. The reason for this difference is that at the self-dual point, there is no enhancement $U(1) \to SU(2)$ and thus no growth of the number of massless degrees of freedom. However, we expect by heterotic-type II duality that such a phase should be possible in type II at the non-perturbative level. A natural candidate setup to produce this effect in type II is to introduce a pair of D-branes, whose separation is related to the spectator modulus R_d. The stabilization of R_d at the self-dual point in the heterotic case suggests in the dual type II picture that the effect of the thermal effective potential is to fix the D-branes on top of each other, thus producing an $U(1) \to SU(2)$ enhancement. This attractive force between the D-branes will only be local, in the sense that if we separate the D-branes from each other so that R_d is in the range of phase II of Section 2.2, the thermal effective potential should allow stable finite distances between the D-branes. If we further increase the separation, we expect to reach a point where the thermal effective potential induces a repulsive force that pushes the D-branes away from each other and we are entering phase III. However, $R_0(t)$ and $R_9(t)$ are increasing faster than $R_d(t)$. When they catch it, the force between the D-branes vanishes and the distance between them becomes static and we are back in phase II. On the contrary, if the distance between the D-branes is macroscopic, the effective potential induces a repulsive force that pushes the D-branes away from each other and we are in the higher-dimensional phase III.

Another set up dual to the heterotic gauge group enhancement can be considered in terms of singularities in the internal space. For instance, a type IIA D2-brane wrapped on a vanishing $\mathbb{CP}^1$ cycle of radius dual to R_d can give rise to an $SU(2)$ gauge theory and admits a mirror description in type IIB [26]. The equivalence between the brane-world and geometrical singularity pictures can be analyzed along the lines of Ref. [27].

5. Conclusion and discussion

In this work, we have considered string theory models in flat space, where geometrical fluxes induce a spontaneous breaking of supersymmetry and finite temperature. We have computed the 1-loop free energy density, which is nothing but the effective potential at finite temperature and first order in perturbation theory. It depends on the temperature T, the supersymmetry breaking

[10] In non-realistic models (such as the ones considered in this work) where no new physics arises at the electroweak scale, considering macroscopic but finite R_0 and R_9 catching R_d would correspond to a phase of the universe in $d+2$ dimensions with the temperature effectively zero.

scale M and "spectator moduli" that characterize the internal space but *are not* involved in the breaking of supersymmetry. Our aim was to analyze the dynamics of these spectator moduli in the presence of both temperature and supersymmetry breaking.

We have analyzed in many details heterotic and type IIB models where the dynamics of only one of the spectator radii, R_d, is taken into account. More precisely, we have considered Euclidean backgrounds which are of the form $S^1(R_0) \times T^{d-1} \times S^1(R_d) \times \mathcal{M} \times S^1(R_9)$, where $S^1(R_0)$ and $S^1(R_9)$ both contain fluxes. The flux along the Euclidean time cycle $S^1(R_0)$ introduces temperature $T \propto 1/R_0$ and the flux along $S^1(R_9)$ implies the spontaneous breaking of supersymmetry at a scale $M \propto 1/R_9$. The torus T^{d-1} is very large, while the internal manifold $\mathcal{M}$ is either T^{8-d} or $T^{4-d} \times \frac{T^4}{\mathbb{Z}_2}$, with fixed radii close to the string length.

In heterotic models, we found five distinct phases of the thermal effective potential (see Fig. 1). In phase I, the potential plays a role in confining the spectator modulus by giving it an effective mass in addition to the gravitational friction effects. R_d plays the role of a Higgs field stabilized at the enhanced gauge symmetry point $R_d = 1$, where $U(1) \to SU(2)$. In phase II (or IV), R_d converges to an arbitrary constant. This is simply due to the gravitational friction arising from the expansion of the universe. Thus, while the modulus may take any value, its excitations always die off as the universe expands. In phase III (or V), if R_d (or $1/R_d$) is macroscopic, meaning that we may always neglect the sub-dominant term in the effective potential (2.22), then R_d increases proportionally to the expansion of the universe. In this case, the dynamics of the modulus is better understood in terms of a complex structure characterizing the anisotropy of a $(d+1)$-dimensional universe. As in phases II and IV, the excitations of this complex structure die off due to gravitational friction. If instead R_d is internal, it always enters phase II (or IV).

The analysis of the type IIB case is qualitatively the same, up to an important difference. The heterotic Higgs phase does not exist, since there is no gauge symmetry enhancement at $R_d = 1$ in type II superstrings, at least in a perturbative approach. However, we expect by heterotic-type II duality that such a gauge theory enhancement should occur once taking into account non-perturbative effects in type II superstrings. In particular, the modulus governing the distance between D-branes or the size of some cycle on which a brane is wrapped could play the dual role of the heterotic radius R_d.

The heterotic picture of phase I naturally generalizes to the case where all spectator moduli are allowed to vary. Although we did not consider this case explicitly, one may analyze models with non-diagonal tori. We expect the existence of local minima of the thermal effective potential at each enhanced symmetry point, as a consequence of the increase in the number of light states. The lowest such point should be given by the most symmetric point.

For the backgrounds $S^1(R_0) \times T^{d-1} \times S^1(R_d) \times \mathcal{M} \times S^1(R_9)$, the thermal effective potential has a universal form, up to model-dependent integer parameters (n_T, n_V). n_T is the number of massless boson/fermions pairs in the original supersymmetric model *i.e.* before the fluxes are switched on. n_V depends on the precise prescription chosen to break supersymmetry. In the heterotic phase I, (n_T, n_V) has to be replaced by $(n_T + \tilde{n}_T, n_V + \tilde{n}_V)$ to account for the additional massless states arising at the enhanced symmetry point. Depending on the IBC, we found that the dynamics of the Universe can be attracted to either of the five Radiation-like Dominated Solutions associated to the five phases, provided the following conditions are fulfilled:

$$\text{phase I:} \quad -\frac{1}{2^d - 1} < \frac{n_V + \tilde{n}_V}{n_T + \tilde{n}_T} < 0,$$

$$\text{phases II} \cup \text{IV:} \quad -\frac{1}{2^d - 1} < \frac{n_V}{n_T} < 0,$$

$$\text{phases III} \cup \text{V}: \quad -\frac{1}{2^{d+1}-1} < \frac{n_V}{n_T} < 0. \tag{5.1}$$

When some (or all) of these conditions are not satisfied, different histories of the Universe are possible. For instance, suppose a model satisfies the second of the above conditions, but not the third, with R_d macroscopic and thus initially in phase III. Depending on the remaining initial boundary data, we conjecture at least three different late time behaviors to arise, which again correspond to Radiation-like Dominated Solutions:

- A dynamical compactification of the spectator radius R_d to enter phases II, I, or IV. The attractor is an RDS^d, where $M \propto 1/R_9$.
- A dynamical decompactification of the radius R_9 that participates in the spontaneous breaking of supersymmetry. This mechanism was conjectured in [4] and is shown in an explicit example in [18]. The attractor solution is an RDS^{d+2}, where supersymmetry is spontaneously broken by thermal effects only (no M).
- A (non-perturbative) connection to a cousin model with flux in some of the previously spectator directions. For instance, for $d+1=4$ and flux in two internal directions, say 8 and 9, the constraint $-\frac{1}{15} < \frac{n_V}{n_T} < 0$ is replaced by the less restrictive one $-0.215 < \frac{n_V}{n_T} < 0$ (see [3]). The attractor solution is an RDS^{d+1}, where $M \propto 1/\sqrt{R_8 R_9}$. The interesting point here is that the solution is stabilized by the spontaneous generation of topological flux.

In this work, we restricted our discussion of orbifold models to cases where $\frac{T^4}{\mathbb{Z}_2}$ did not contain flux and had its radii fixed close to the string scale. In the companion paper [18], we fill this gap and extend the analysis to cases where an orbifold action is non-trivial on dynamical circles and whose radii are either participating in the breaking of supersymmetry or are spectators.

We would like to conclude by giving a summary of the results which have been made in studying the intermediate cosmological regime within the framework of string theory, as developed in [2–5] as well as the current paper:

- The first result is the discovery of the Radiation-like Cosmological Solutions (RDS^d). These RDS^d solutions are not the "usual" radiation solutions defined by $\rho_{\text{thermal}} = (d-1)P_{\text{thermal}}$, but instead satisfy $\rho_{\text{total}} = (d-1)P_{\text{total}}$ only after the contribution from the coherent evolution of the supersymmetry breaking modulus is included. These solutions, are also consistent in that the evolution of the space–time curvature scales, $H^2 = (\dot{a}/a)^2$ and $\dot{H}$, the dilaton and the evolving radii scales, $\dot{\phi}^2_{\text{dil}}$, $\ddot{\phi}_{\text{dil}}$, $(\dot{R}_I/R_I)^2$, $\ddot{R}_I/R_I$, is such that they decrease as time progresses. Thus if one starts with small curvature and small coupling, at later times one is guaranteed to remain within the regime of small curvature and small coupling.
- The second result is the discovery of the "attractor mechanism" which is valid in the intermediate cosmological regime (after the Hagedorn transition or alternatively the inflation era but before electro-weak symmetry breaking); within this era the RDS^d cosmological solutions are not only stable under small fluctuations but also are the only solutions ("attractors") at late cosmological times. Furthermore, thanks to this attractor mechanism, most of the Hagedorn exit ambiguities are washed out in later cosmological times.
- The third result, is the fact that it is possible to derive at the string perturbative level (however exact in α'), the full string free energy $\mathcal{F}(T, M; \mu_I)$ as a functional of all moduli (including the SUSY breaking moduli T, M, the string coupling constant modulus dil as well as the "spectator moduli" μ_I), at least for a certain class of string vacua where the spontaneous breaking of supersymmetry is induced by geometrical fluxes.

There are two main directions in going further with this approach. First, one may carry out our analysis with four-dimensional heterotic models, whose internal space $\frac{T^6}{\mathbb{Z}_2\times\mathbb{Z}_2}$ in the presence of fluxes breaks spontaneously $\mathcal{N}_4 = 1$ supersymmetry. Depending on the details of the internal space and spontaneous supersymmetry breaking configuration, it is possible for an additional scale Q to appear at very late cosmological times. Q is the "infrared renormalisation group invariant transmutation scale" induced at the quantum level by the radiative corrections of the soft supersymmetry breaking terms at low energies [19,20]. When $T(t) \leqslant Q$, the electroweak phase transition takes place, $SU(2) \times U(1) \to U(1)_{\mathrm{em}}$. This starts to be the case at a time t_W and, for $t > t_W$, the supersymmetry breaking scale M is stabilized at a value close to Q. In earlier cosmological times where $M(t), T(t) \gg Q$, the transmutation scale is irrelevant and does not modify our analysis. An important consequence of this scenario, is a dynamical explanation of the supersymmetry breaking scale. Indeed, extrapolating the $\mathrm{RDS}^{d=4}$ up to the low energy regime where $T = \mathcal{O}(1\ \mathrm{TeV})$ one finds (thanks to the attractor mechanism), that the natural value of the supersymmetry breaking scale $M(t)$ is naturally small and around the electroweak phase transition, independently of its initial value at early cosmological times.

The above statement is absolutely correct, if one assumes that there are no other mass scales created in the infrared, like for instance the various "infrared renormalization group invariant scales Q" associated with: (i) Λ_G of hidden gauge group(s), or (ii) the transmutation scale(s) Q_H (induced in the infrared), by the renormalized structure of the "supersymmetry breaking terms". The existence of non-trivial dynamical scale(s) Q modify the very late cosmological evolution, namely after the electroweak phase transition around $T = T_W \sim Q_H \sim \mathcal{O}(1\ \mathrm{TeV})$. Due to this, the intermediate cosmological regime which we study in this paper is defined by: $T_E \gg T(t), M(t) \gg T_W$.

Obviously, the physics for $t \gg t_W$ is of main importance in (astro)particle physics and late time cosmology. Unfortunately, the infrared phase at $t \gg t_W$ depends strongly on the specific choice of four-dimensional $\mathcal{N}_4 = 1$ superstring vacuum and the way of spontaneously breaking supersymmetry. A lot of work is necessary to determine the initial superstring vacua that leads in late-times to the precise structure of our Universe. On the other hand, we would like to stress here that the qualitative infrared behavior of the effective stringy "no-scale" field theory [20,28] strongly suggests that we are in an interesting string evolutionary scenario after the "Hagedorn-transition exit", $t > t_E$, connecting cosmology to particle physics.

Secondly, in the regime close to or at the Hagendorn transition, the conventional notions of General Relativity such as geometry and topology are well defined only in the low energy and/or small curvature approximations of a string theory setup [29]. In the very early times of the Universe, $t < t_E$, purely stringy phenomena at very small distances and strong curvature scales imply that the physics could be quite different from what one might expect from a "naive" field theory point of view [29]. In this early epoch, classical gravity is no longer valid and has to be replaced by a more fundamental singularity-free theory such as (super-)string theory [16]. Thus, the main obstruction in such a stringy cosmological framework is the Hagedorn temperature limitation $T < T_H$. Actually, this is not a pathology but rather the signal that a phase transition from a previous vacuum is taking place. The Hagedorn-like singularities have to be resolved either by a stringy phase transition [6,8,12,13] or by choosing Hagedorn-free string vacua in the early stage of the universe [16,15].

In this work, we have bypassed the Hagedorn transition ambiguities by considering arbitrary initial boundary conditions (IBC) at t_E, the "Hagedorn transition exit time". Thanks to the attraction to "Radiation-like Universes" in late times, most of the ambiguities are washed out. It is however of fundamental interest to investigate further the early non-geometric era of our universe

and to show that the induced IBC at t_E solve naturally the "flatness" and "entropy" problem in late cosmological times. This stringy scenario would be an alternative (or at least complementary) to the conventional inflationary scenarios proposed in field theory.

Acknowledgements

We are grateful to R. Brandenberger and N. Toumbas for useful discussions. H.P. thanks the Ecole Normale Supérieure for hospitality.

This work is partially supported by the ANR (CNRS-USAR) contract 05-BLAN-0079-02. The work of F.B., J.E. and H.P. is also supported by the European ERC Advanced Grant 226371 and CNRS PICS contracts 3747 and 4172. J.E. acknowledges financial support from the Groupement d'Intérêt Scientifique P2I.

Appendix A. Partition function

A.1. Heterotic string on tori

We first focus on the heterotic string compactified on a Euclidean toroidal space, while heterotic and type IIB orbifolds will be considered in Appendix A.2. Our starting point is the heterotic string in a background $S^1_E \times T^D \times T^n$ $(n = 9 - D)$, where $S^1_E(R_0)$ is the Euclidean time compactified on a circle of radius R_0. For simplicity, we choose the tori T^D and T^{9-D} to be products of circles $\prod_{p=1}^{D} S^1(R_p)$ and $\prod_{i=D+1}^{9} S^1(R_i)$. The partition function vanishes, due to supersymmetry:

$$Z = \int_F \frac{d\tau_1\, d\tau_2}{2\tau_2} \frac{1}{2} \sum_{a,b} (-1)^{a+b+ab} \vartheta^4 \left[\begin{smallmatrix} a \\ b \end{smallmatrix}\right] \frac{\Gamma_{(0,16)}}{\eta^{12}\bar{\eta}^{24}} \times \Gamma_{(1,1)}(R_0) \times \prod_{p=1}^{D} \Gamma_{(1,1)}(R_p) \times \prod_{i=D+1}^{9} \Gamma_{(1,1)}(R_i). \tag{A.1}$$

To implement finite temperature, we deform the $\Gamma_{(1,1)}(R_0)$ lattice by coupling the space–time fermion number $Q_F \equiv a$ to the momentum along $S^1_E(R_0)$. We also introduce a spontaneous supersymmetry breaking by coupling R-symmetry charges $a + Q_i$ $(i = D + 1, \ldots, 9)$ to the momenta along the T^n directions. Spin statistics and modular invariance then determines the precise replacement of the lattices as

$$\forall i \in I_b = \{0, D+1, \ldots, 9\},$$
$$\Gamma_{(1,1)}(R_i) \to \frac{R_i}{\sqrt{\tau_2}} \sum_{\tilde{m},n} e^{-\pi \frac{R_i^2}{\tau_2} |\tilde{m}_i + n_i \tau|^2} (-1)^{\tilde{m}_i(a+Q_i) + n_i(b+L_i) + \varepsilon_i \tilde{m}_i n_i}. \tag{A.2}$$

I_b is the set of labels associated to directions with fluxes that break spontaneously supersymmetry. In practice, the Q_i's $(i \in I_b)$ are linear combinations of charges of the $E_8 \times E_8'$ lattice, for which ε_i is determined to be 0 or 1. In our notations, $Q_0 = L_0 \equiv 0$ and $\varepsilon_0 = 1$. A convenient rewriting of the phases in Eq. (A.2) is done by defining $\tilde{m}_i = 2\tilde{k}_i + \tilde{g}_i$, $n_i = 2l_i + h_i$ and summing over $\tilde{g}_i, h_i \in \{0, 1\}$ and $\tilde{k}_i, l_i$ over all integers. We may evaluate the sum over the spin structures a and b by redefining $a = \hat{a} + \sum_{i \in I_b} \tilde{h}_i$ and $b = \hat{b} + \sum_{i \in I_b} \tilde{g}_i$. The phases from (A.1) and (A.2) combine to give

$$a+b+ab+\sum_{i\in I_b}\big(\tilde{g}_i(a+Q_i)+h_i(b+L_i)+\varepsilon_i\tilde{g}_i\tilde{h}_i\big)$$
$$=\hat{a}+\hat{b}+\hat{a}\hat{b}+\sum_{i\in I_b}\tilde{g}_i(1+Q_i)+P(\vec{\tilde{g}},\vec{h},\vec{Q},\vec{L},\vec{\varepsilon}) \tag{A.3}$$

where $P(\vec{\tilde{g}},\vec{h},\vec{Q},\vec{L},\vec{\varepsilon})$ consists of terms which vanish when $h_i=0$ ($\forall i\in I_b$). We may now make use of the Jacobi identity

$$\frac{1}{2}\sum_{\hat{a},\hat{b}}(-1)^{\hat{a}+\hat{b}+\hat{a}\hat{b}}\vartheta^4\left[\begin{smallmatrix}\hat{a}+\sum_i h_i\\ \hat{b}+\sum_i\tilde{g}_i\end{smallmatrix}\right]=-\vartheta^4\left[\begin{smallmatrix}1+\sum_i h_i\\ 1+\sum_i\tilde{g}_i\end{smallmatrix}\right] \tag{A.4}$$

to obtain the result

$$Z=-\int_F\frac{d\tau_1\,d\tau_2}{2\tau_2}\sum_{\tilde{g}_j,h_j(j\in I_b)}(-1)^{\sum_k\tilde{g}_k(1+Q_k)}(-1)^{P(\vec{\tilde{g}},\vec{h},\vec{Q},\vec{L},\vec{\varepsilon})}\vartheta^4\left[\begin{smallmatrix}1+\sum_q h_q\\ 1+\sum_q\tilde{g}_q\end{smallmatrix}\right]$$
$$\times\prod_{i\in I_b}\Gamma_{(1,1)}\left[\begin{smallmatrix}h_i\\ \tilde{g}_i\end{smallmatrix}\right](R_i)\times\prod_{p=1}^{D}\Gamma_{(1,1)}(R_p)\times\frac{\Gamma_{(0,16)}}{\eta^{12}\bar{\eta}^{24}}, \tag{A.5}$$

where we have introduced the shifted lattices

$$\Gamma_{(1,1)}\left[\begin{smallmatrix}h_i\\ \tilde{g}_i\end{smallmatrix}\right](R_i)=\frac{R_i}{\sqrt{\tau_2}}\sum_{\tilde{k}_i,l_i}e^{-\pi\frac{R_i^2}{\tau_2}|2\tilde{k}_i+\tilde{g}_i+(2l_i+h_i)\tau|^2}. \tag{A.6}$$

Important simplifications can be made, using the fact that $R_i\gg 1$ ($i\in I_b$):

- When $2l_i+h_i\neq 0$ in Eq. (A.6), the integrand in the partition function (A.5) contains a factor $e^{-\pi R_i^2(2l_i+h_i)\tau_2}$ implying an exponentially suppressed contribution after integration. We thus restrict to the sectors with $l_i=h_i=0$ ($i\in I_b$).
- The sectors $\sum_i h_i=\sum_i\tilde{g}_i=0$ mod 2 are supersymmetric and therefore do not contribute, as can be seen from the presence of a $\vartheta^4\left[\begin{smallmatrix}1\\ 1\end{smallmatrix}\right]$ factor in (A.5). We thus only keep the sectors $h_i=0$ ($i\in I_b$), $\sum_i\tilde{g}_i=1$ mod 2.
- All of them, have at least one $i\in I_b$ such that $\tilde{g}_i=1$, so that the integrand in (A.5) contains a factor $e^{-\pi\frac{R_i^2}{\tau_2}}$. This implies that we can extend the integral over the fundamental domain, to an integral over the full upper half strip. The error introduced this way is exponentially suppressed.[11]

Altogether, the partition function reduces to

[11] Note that if the model before introducing temperature and internal fluxes was not supersymmetric, the sector $h_i=\tilde{g}_i=0$ ($\forall i\in I_b$) would not vanish. Its integral over the fundamental domain would not be suppressed by any $e^{-\pi\frac{R_i^2}{\tau_2}}$ ($i\in I_b$) factor and could not be replaced by the integral over the strip. The result would imply a very large (but finite) contribution to the vacuum energy, proportional to the number of massless bosons minus the number of massless fermions.

$$Z = \left(\prod_{k\in I_b} R_k\right) \int_{-\frac{1}{2}}^{\frac{1}{2}} d\tau_1 \int_0^{+\infty} \frac{d\tau_2}{2\tau_2^{\frac{n+3}{2}}} \sum_{\substack{\tilde{k}_j,\tilde{g}_j\,(j\in I_b)\\ \sum_j \tilde{g}_j = 1 \bmod 2}} e^{-\frac{\pi}{\tau_2}\sum_i R_i^2(2\tilde{k}_i+\tilde{g}_i)^2}$$
$$\times (-1)^{\sum_k \tilde{g}_k Q_k} \frac{\vartheta^4\left[\begin{smallmatrix}1\\0\end{smallmatrix}\right]}{\eta^{12}\bar{\eta}^{24}} \Gamma_{(0,16)} \times \prod_{p=1}^{D} \Gamma_{(1,1)}(R_p). \tag{A.7}$$

In this expression, the low lying contributions from the oscillators and right moving lattice $\Gamma_{(0,16)}$ are

$$(-1)^{\sum_{k\in I_b} \tilde{g}_k Q_k} \frac{\vartheta^4\left[\begin{smallmatrix}1\\0\end{smallmatrix}\right]}{\eta^{12}\bar{\eta}^{24}} \Gamma_{(0,16)} = 2^4\left(\frac{1}{\bar{q}} + D_0(\vec{\tilde{g}}, \vec{Q}) + \mathcal{O}(q,\bar{q})\right), \tag{A.8}$$

where $q = e^{2i\pi\tau}$ and $D_0(\vec{\tilde{g}}, \vec{Q})$ is the sum over massless degrees of freedom with each mode weighted by the factor $(-1)^{\sum_k \tilde{g}_k Q_k}$. Defining $I_s = \{1,\dots,D\}$ the set of "spectator" directions *i.e.* that do not break supersymmetry, the lattice of T^D can also be expanded as

$$\prod_{p=1}^{D} \Gamma_{(1,1)}(R_p) = \sum_{m_q,n_q\,(q\in I_s)} e^{-\pi\tau_2 \sum_p ((\frac{m_p}{R_p})^2 + (n_p R_p)^2)} e^{-2i\pi\tau_1 \sum_p m_p n_p}. \tag{A.9}$$

The change of variable $\tau_2 = x\pi(\sum_{i\in I_b} R_i^2(2\tilde{k}_i + \tilde{g}_i))$ in the τ_2-integration shows that the massive contributions in Eqs. (A.8) and (A.9) are exponentially suppressed, compared to the massless ones. We thus concentrate our attention on the light degrees of freedom. Because we have been able to replace the fundamental domain with the half strip, the integration over τ_1 now simply enforces the level matching condition. The constant term in the r.h.s. of Eq. (A.8) combined with Eq. (A.9) implies that it is enough to keep for each $p \in I_s$,

$$\begin{cases} n_p = 0 & \text{if } R_p \gg \max\limits_{i\in I_b} R_i, \\ m_p = 0 & \text{if } R_p \ll \dfrac{1}{\max_{i\in I_b} R_i}, \\ m_p = n_p = 0 & \text{else.} \end{cases} \tag{A.10}$$

Similarly, the $\bar{q}^{-1}$ term in Eq. (A.8) combined with Eq. (A.9) implies that it is enough to keep for each $q \in I_s$,

$$m_q = n_q = \pm 1 \quad \text{if } R_q \simeq 1 \quad \text{with } m_p, n_p \text{ given in Eq. (A.10)}, \forall p \in I_s,\ p \neq q. \tag{A.11}$$

Physically, the above two winding modes are responsible for the gauge symmetry enhancement $U(1) \to SU(2)$ at $R_q = 1$. Away from the self dual point, they are massive: Their contribution to Z becomes exponentially negligible, while the $SU(2)$ is Higgsed. The enhancement of the symmetry will play an important role in stabilizing R_q around one. The following reduced expression for the partition function when $R_p \geqslant 1$ ($\forall p \in I_s$) is then obtained,

$$Z = \left(\prod_{k\in I_b} R_k\right) \frac{2^4}{2} \sum_{\substack{\tilde{k}_j,\tilde{g}_j\,(j\in I_b)\\ \sum_j \tilde{g}_j = 1 \bmod 2}} \frac{2^4}{2} \int_0^{+\infty} \frac{d\tau_2}{\tau_2^{\frac{n+3}{2}}} \exp\left(-\frac{\pi}{\tau_2}\sum_{i\in I_b} R_i^2(2\tilde{k}_i + \tilde{g}_i)^2\right)$$

$$\times \left\{ D_0(\vec{\tilde{g}}, \vec{Q}) \sum_{m_r (r \in I_s)} \exp\left(-\pi \tau_2 \sum_{p \in I_s} \left(\frac{m_p}{R_p} \right)^2 \right) \right.$$
$$+ 2 \sum_{q \in I_s} \exp\left(-\pi \tau_2 \left(\frac{1}{R_q^2} + R_q^2 - 2 \right) \right)$$
$$\left. \times \sum_{m_r (r \in I_s, r \neq q)} \exp\left(-\pi \tau_2 \sum_{p \in I_s, p \neq q} \left(\frac{m_p}{R_p} \right)^2 \right) \right\}. \tag{A.12}$$

The companion expressions when any $R_p \leqslant 1$ $(p \in I_s)$ is obtained by replacing $R_p \to \frac{1}{R_p}$.

The above result can be rewritten in various forms. We introduce an integer parameter Δ and split the T^D torus as $T^{D-\Delta} \times T^{\Delta}$. Correspondingly, the "spectator" indices I_s are divided in two sets,

$$I_s^l = \{1, \ldots, D - \Delta\}, \qquad I_s^s = \{D - \Delta + 1, \ldots, D\}, \tag{A.13}$$

and we perform a Poisson resummation on the $T^{D-\Delta}$ zero mode lattice. The reason for that is that when some R_p $(p \in I_s)$ is "small" *i.e.* $R_p \ll \inf_{i \in I_b} R_i$, the Hamiltonian formulation of Eq. (A.12) is relevant, while when some R_p $(p \in I_s)$ is "large" *i.e.* $R_p \gg \max_{i \in I_b} R_i$, the Lagrangian formulation is more convenient. The alternative forms for arbitrary Δ are:

$$Z = \left(\prod_{k \in I_b} R_k \right) \left(\prod_{s' \in I_s^l} R_{s'} \right) \sum_{\substack{\tilde{k}_j, \tilde{g}_j (j \in I_b) \\ \sum_j \tilde{g}_j = 1 \bmod 2}} \frac{2^4}{2} \int_0^{+\infty} \frac{d\tau_2}{\tau_2^{\frac{D-\Delta+n+3}{2}}} \exp\left(-\frac{\pi}{\tau_2} \sum_{i \in I_b} R_i^2 (2\tilde{k}_i + \tilde{g}_i)^2 \right)$$
$$\times \left\{ D_0(\vec{\tilde{g}}, \vec{Q}) \sum_{\substack{\tilde{m}_{r'} (r' \in I_s^l) \\ m_r (r \in I_s^s)}} \exp\left(-\frac{\pi}{\tau_2} \sum_{p' \in I_s^l} (\tilde{m}_{p'} R_{p'})^2 - \pi \tau_2 \sum_{p \in I_s^s} \left(\frac{m_p}{R_p} \right)^2 \right) \right.$$
$$+ 2 \sum_{q \in I_s^s} \exp\left(-\pi \tau_2 \left(\frac{1}{R_q^2} + R_q^2 - 2 \right) \right)$$
$$\times \sum_{\substack{\tilde{m}_{r'} (r' \in I_s^l) \\ m_r (r \in I_s^s, r \neq q)}} \exp\left(-\frac{\pi}{\tau_2} \sum_{p' \in I_s^l} (\tilde{m}_{p'} R_{p'})^2 - \pi \tau_2 \sum_{p \in I_s^s, p \neq q} \left(\frac{m_p}{R_p} \right)^2 \right)$$
$$+ 2 \sum_{q' \in I_s^s} \frac{\sqrt{\tau_2}}{R_{q'}} \exp\left(-\pi \tau_2 \left(\frac{1}{R_{q'}^2} + R_{q'}^2 - 2 \right) \right)$$
$$\left. \times \sum_{\substack{\tilde{m}_{r'} (r' \in I_s^l, r' \neq q') \\ m_r (r \in I_s^s)}} \exp\left(-\frac{\pi}{\tau_2} \sum_{p' \in I_s^l, p' \neq q'} (\tilde{m}_{p'} R_{p'})^2 - \pi \tau_2 \sum_{p \in I_s^s} \left(\frac{m_p}{R_p} \right)^2 \right) \right\}. \tag{A.14}$$

Using the integral form of the modified Bessel function of the second kind $K_\alpha(z)$,

$$\int_0^{+\infty} \frac{d\tau_2}{\tau_2^\alpha} \exp\left(-\frac{\pi}{\tau_2} F \right) \exp(-\pi \tau_2 G) = \left(\frac{G}{F} \right)^{\frac{(\alpha-1)}{2}} 2 K_{\alpha-1}(2\pi \sqrt{FG}), \tag{A.15}$$

one obtains

$$
\begin{aligned}
Z = {} & \left(\prod_{k\in I_b} R_k\right)\left(\prod_{s'\in I_s^l} R_{s'}\right)\frac{2^4}{2}\sum_{\substack{\tilde{k}_j,\tilde{g}_j\,(j\in I_b)\\ \sum_j \tilde{g}_j = 1 \bmod 2}} \Bigg\{ D_0(\vec{\tilde{g}},\vec{Q}) \sum_{\tilde{m}_{r'}(r'\in I_s^l)} \Bigg[\frac{\Gamma(\frac{D-\Delta+n+1}{2})}{(\pi F_1)^{\frac{D-\Delta+n+1}{2}}} \\
& + {\sum_{m_r(r\in I_s^s)}}' \left(\frac{G_1}{F_1}\right)^{\frac{D-\Delta+n+1}{4}} 2K_{\frac{D-\Delta+n+1}{2}}(2\pi\sqrt{F_1G_1})\Bigg] \\
& + 2\sum_{q\in I_s^s} \sum_{\substack{\tilde{m}_{r'}(r'\in I_s^l)\\ m_r(r\in I_s^s, r\neq q)}} \left(\frac{G_2}{F_1}\right)^{\frac{D-\Delta+n+1}{4}} 2K_{\frac{D-\Delta+n+1}{2}}(2\pi\sqrt{F_1G_2}) \\
& + 2\sum_{q'\in I_s^l} \sum_{\substack{\tilde{m}_{r'}(r'\in I_s^l, r'\neq q')\\ m_r(r\in I_s^s)}} \frac{1}{R_{q'}}\left(\frac{G_3}{F_3}\right)^{\frac{D-\Delta+n}{4}} 2K_{\frac{D-\Delta+n}{2}}(2\pi\sqrt{F_3G_3})\Bigg\},
\end{aligned}
\tag{A.16}
$$

where we have defined

$$
\begin{aligned}
F_1 &= \sum_{i\in I_b} R_i^2(2\tilde{k}_i+\tilde{g}_i)^2 + \sum_{p'\in I_s^l}(\tilde{m}_{p'}R_{p'})^2, \\
G_1 &= \sum_{p\in I_s^s}\left(\frac{m_p}{R_p}\right)^2, \qquad G_2 = \left(\frac{1}{R_q}-R_q\right)^2 + \sum_{p\in I_s^s,\, p\neq q}\left(\frac{m_p}{R_p}\right)^2, \\
F_3 &= \sum_{i\in I_b} R_i^2(2\tilde{k}_i+\tilde{g}_i)^2 + \sum_{p'\in I_s^l,\, p'\neq q'}(\tilde{m}_{p'}R_{p'})^2, \\
G_3 &= \left(\frac{1}{R_{q'}}-R_{q'}\right)^2 + \sum_{p\in I_s^s}\left(\frac{m_p}{R_p}\right)^2.
\end{aligned}
\tag{A.17}
$$

In the second line of Eq. (A.16), the "primed" sum in the brackets means that $m_r = 0$ ($\forall r \in I_s^s$) is excluded. We remind the reader that Eq. (A.16) is valid when $R_p \geqslant 1$ ($\forall p \in I_s^l \cup I_s^s$). The expressions with some R_q's such that $R_q \leqslant 1$ is obtained by T-duality *i.e.* by exchanging them with their inverses, $R_q \to \frac{1}{R_q}$, in Eqs. (A.16) and (A.17).

It will be convenient to have the rules for decompactifying directions of $T^{D-\Delta}$ as well as the rules for freezing one of the T^{Δ} radii.

- For decompactifying a radius $R_{s'}$ ($s' \in I_s^l$), one simply keeps only the terms with $\tilde{m}_{s'} = 0$ in (A.16). In the last line, one also discards the term with $q' = s'$. The net result is a remaining overall factor of $R_{s'}$ in the first line.
- In order to freeze a radius R_s ($s \in I_s^s$) at the self dual point $R_s = 1$, one keeps only the terms with $m_s = 0$ in (A.16). In addition, one discards the term with $q = s$ in the third line and shifts $D_0 \to D_0 + 2$.
- In order to freeze a radius R_s ($s \in I_s^s$) at an arbitrary value such that $1/R_s$ and $R_s \ll \inf_{i\in I_b} R_i$, one keeps only the terms with $m_s = 0$ in (A.16). In addition, one discards the term with $q = s$ in the third line.

A.2. Heterotic and type IIB orbifolds

We next consider the heterotic string on $S^1_E \times T^D \times \frac{T^4}{\mathbb{Z}_2} \times T^n$ ($n = 5 - D$). The partition function vanishes, due to the 8 conserved space–time supercharges,

$$Z = \int_F \frac{d\tau_1\, d\tau_2}{2\tau_2} \frac{1}{2} \sum_{H,G} \frac{1}{2} \sum_{a,b} (-1)^{a+b+ab} \vartheta^2 \left[\begin{smallmatrix} a \\ b \end{smallmatrix}\right] \vartheta \left[\begin{smallmatrix} a+H \\ b+G \end{smallmatrix}\right] \vartheta \left[\begin{smallmatrix} a-H \\ b-G \end{smallmatrix}\right] Z_{(4,4)} \left[\begin{smallmatrix} H \\ G \end{smallmatrix}\right] \frac{\Gamma_{(0,16)} \left[\begin{smallmatrix} H \\ G \end{smallmatrix}\right]}{\eta^8 \bar{\eta}^{20}}$$
$$\times \Gamma_{(1,1)}(R_0) \times \prod_{p=1}^{D} \Gamma_{(1,1)}(R_p) \times \prod_{i=D+5}^{9} \Gamma_{(1,1)}(R_i), \tag{A.18}$$

where H, G are equal to 0 or 1. $Z_{(4,4)}[\begin{smallmatrix} H \\ G \end{smallmatrix}]$ is the block that accounts for the $\frac{T^4}{\mathbb{Z}_2}$ part of the background and the right moving $\Gamma_{(0,16)}[\begin{smallmatrix} H \\ G \end{smallmatrix}]$ lattice is consistently $\mathbb{Z}_2$-twisted to guarantee modular invariance, thereby breaking part of the initial gauge group. Temperature and supersymmetry breaking are again introduced by modifying the lattice sums along S^1_E and T^n as in (A.2). However, the left moving charges Q_i may now also involve the "orbifold twist number" H.

The analysis of the toroidal case can be applied the same way. Defining $I_b = \{0, D+5, \ldots, 9\}$, any sector with some $h_i \neq 0$ ($i \in I_b$) is exponentially suppressed and the sectors with $\sum_{i \in I_b} h_i = 0$ and $\sum_{i \in I_b} \tilde{g}_i = 0$ vanish due to supersymmetry. We may again replace the fundamental domain with the full upper half strip. We treat $\frac{T^4}{\mathbb{Z}_2}$ as part of the internal sector, with frozen moduli much smaller than $\inf_{i \in I_b} R_i$. As before, the non-exponentially suppressed contributions to the partition function arise from the massless modes (and their light towers of KK (or winding) states). For explicit examples, see [2]. The net result is that the partition function is of the same form as in (A.16) except that the numbers $D_0(\vec{\tilde{g}}, \vec{Q})$ are different.

The type IIB partition function on $S^1_E \times T^D \times \frac{T^4}{\mathbb{Z}_2} \times T^n$ ($n = 5 - D$) takes the form

$$Z = \int_F \frac{d\tau_1\, d\tau_2}{2\tau_2} \frac{1}{2} \sum_{H,G} \frac{1}{2} \sum_{a,b} (-1)^{a+b+ab} \vartheta^2 \left[\begin{smallmatrix} a \\ b \end{smallmatrix}\right] \vartheta \left[\begin{smallmatrix} a+H \\ b+G \end{smallmatrix}\right] \vartheta \left[\begin{smallmatrix} a-H \\ b-G \end{smallmatrix}\right]$$
$$\times \frac{1}{2} \sum_{\bar{a},\bar{b}} (-1)^{\bar{a}+\bar{b}+\bar{a}\bar{b}} \bar{\vartheta}^2 \left[\begin{smallmatrix} \bar{a} \\ \bar{b} \end{smallmatrix}\right] \bar{\vartheta} \left[\begin{smallmatrix} \bar{a}+H \\ \bar{b}+G \end{smallmatrix}\right] \bar{\vartheta} \left[\begin{smallmatrix} \bar{a}-H \\ \bar{b}-G \end{smallmatrix}\right]$$
$$\times \frac{Z_{(4,4)}}{\eta^{12} \bar{\eta}^{12}} \times \Gamma_{(1,1)}(R_0) \times \prod_{p=1}^{D} \Gamma_{(1,1)}(R_p) \times \prod_{i=D+5}^{9} \Gamma_{(1,1)}(R_i). \tag{A.19}$$

Temperature and supersymmetry breaking are again introduced by modifying the lattice sums along S^1_E and T^n. However, in the type IIB case, we may introduce phases similar to Eq. (A.2) but involving either left moving R-charges $a + Q_i$ ($i \in I_b$), or right moving ones $\bar{a} + \bar{Q}_i$, or both. In the present paper, we consider cases where both left and right charges are non-trivial. Some models in this class where shown to allow critical cosmological evolutions corresponding to radiation-like eras [3,4].

For $R_i \gg 1$ ($\forall i \in I_b$), the manipulations used in the heterotic case can be applied similarly, up to an important difference. In the sector $\left[\begin{smallmatrix} H \\ G \end{smallmatrix}\right] = \left[\begin{smallmatrix} 0 \\ 0 \end{smallmatrix}\right]$, the analogue of the heterotic contribution given in Eq. (A.8) is in type IIB,

$$(-1)^{\sum_{k\in I_b} \tilde{g}_k (Q_k+\tilde{Q}_k)} \frac{\vartheta^4\left[\begin{smallmatrix} 1 \\ 0 \end{smallmatrix}\right]\bar{\vartheta}^4\left[\begin{smallmatrix} 1 \\ 0 \end{smallmatrix}\right]}{\eta^{12}\bar{\eta}^{12}} = 2^4\big(1+\mathcal{O}(q,\bar{q})\big). \tag{A.20}$$

Consequently, there is no massless winding mode arising when some $R_q = 1$ ($q \in I_s$), as opposed to the heterotic states given in (A.11). The final form of the partition function is then formally identical to the two first lines of the heterotic one (A.16), with coefficient $D_0(\vec{\tilde{g}}, \vec{Q}, \vec{\tilde{Q}})$,

$$Z = \left(\prod_{k\in I_b} R_k\right)\left(\prod_{s'\in I_s^l} R_{s'}\right)\frac{2^4}{2} \sum_{\substack{\tilde{k}_j, \tilde{g}_j (j\in I_b) \\ \sum_j \tilde{g}_j = 1 \bmod 2}} \left\{ D_0(\vec{\tilde{g}}, \vec{Q}, \vec{\tilde{Q}}) \sum_{\tilde{m}_{r'}(r'\in I_s^l)} \left[\frac{\Gamma(\frac{D-\Delta+n+1}{2})}{(\pi F_1)^{\frac{D-\Delta+n+1}{2}}} \right.\right.$$
$$\left.\left. + \sum_{m_r (r\in I_s^s)}{}' \left(\frac{G_1}{F_1}\right)^{\frac{D-\Delta+n+1}{4}} 2K_{\frac{D-\Delta+n+1}{2}}(2\pi\sqrt{F_1 G_1}) \right]\right\}, \tag{A.21}$$

where F_1, G_1 are defined in Eq. (A.17).

Appendix B. Equations of motion

In this appendix, we derive the equations of motion in our thermal backgrounds. The 9 space-like directions are $T^D \times T^n$ in the toroidal models and $T^D \times \frac{T^4}{\mathbb{Z}_2} \times T^n$ in the orbifold ones. To unify the two cases, we define $n = 9 - A - D$, where $A = 0$ in toroidal compactifications and $A = 4$ in orbifold ones. Geometrical fluxes in the T^n torus break spontaneously supersymmetry. A T^{d-1} sub-torus of T^D is taken to be isotropic and very large, to be interpreted as part of the spatial directions of the space–time. In practice, this means that the radii of T^{d-1} are proportional for all time t and that the associated KK states are continuous, implying the convergence of the partition function. The remaining T^{D-d+1} sub-torus is allowed to have arbitrary radii. When they are all small, we interpret them as internal and the space–time dimension is d. When only Δ of the T^{D-d+1} radii ($D-(d-1) \geqslant \Delta \geqslant 0$) are small, the space–time dimension is then $\mathcal{D} \equiv D+1-\Delta$. However, this space–time with enhanced dimension is anisotropic since only part of its space-like radii are evolving proportionally.

Our starting point is the standard 10-dimensional dilaton-gravity theory,

$$S = \frac{1}{2}\int d^{10}x\,\sqrt{-\hat{g}_{10}}e^{-2\phi_{\mathrm{dil}\,10}}\big[\hat{R}_{10} + 4\partial_\mu\phi_{\mathrm{dil}\,10}\partial^\mu\phi_{\mathrm{dil}\,10}\big] - \int d^{10}x\,\sqrt{-g_{10}}\hat{\mathcal{F}}_{10}. \tag{B.1}$$

The hats denote that we are in string frame and the numerical subscripts, here 10, indicate the space–time dimension. $\phi_{\mathrm{dil}\,10}$ and $\hat{\mathcal{F}}_{10}$ are the dilaton and free energy density in 10 dimensions. The latter is related to the partition function by $\hat{\mathcal{F}}_{10} = -\frac{Z}{V_{10}}$, where V_{10} is the 10-dimensional volume of the Euclidean background in which we computed Z. We split the T^D torus as $T^{\mathcal{D}-1} \times T^\Delta$ and dimensionally reduce on T^Δ and T^n (or $\frac{T^4}{\mathbb{Z}_2} \times T^n$ in the orbifold models). The action becomes

$$S = \frac{1}{2}\int d^{\mathcal{D}}x\,\sqrt{-\hat{g}_{\mathcal{D}}}\,e^{-2\phi_{\mathrm{dil}\,\mathcal{D}}}\Big[\hat{R}_{\mathcal{D}} + 4\partial_\mu\phi_{\mathrm{dil}\,\mathcal{D}}\partial^\mu\phi_{\mathrm{dil}\,\mathcal{D}}$$

$$- \sum_{p=D-\Delta+1}^{D} \frac{\partial_\mu R_p \partial^\mu R_p}{R_p^2} - \sum_{i=D+1}^{9} \frac{\partial_\mu R_i \partial^\mu R_i}{R_i^2} \Bigg] - \int d^{\mathcal{D}} x \sqrt{-\hat{g}_{\mathcal{D}}} \hat{\mathcal{F}}_{\mathcal{D}}, \tag{B.2}$$

where the dilaton in $\mathcal{D}$-dimensions is $\phi_{\mathrm{dil}\,\mathcal{D}} = \phi_{\mathrm{dil}\,10} - \frac{1}{2}\sum_{\gamma=D-\Delta+1}^{9} \ln 2\pi R_\gamma$ and $\hat{\mathcal{F}}_{\mathcal{D}} = -\frac{Z}{V_{\mathcal{D}}}$. In some instances, we will suppose for simplicity that some internal radii are frozen. This will be the case for some radii of T^Δ, and the radii of $\frac{T^4}{\mathbb{Z}_2}$ in the orbifold models. Then, the corresponding kinetic terms would simply disappear from the action (B.2). Performing the conformal transformation $g_{\mathcal{D}} = \exp(-\frac{4}{\mathcal{D}-2}\phi_{\mathrm{dil}\,\mathcal{D}})\hat{g}_{\mathcal{D}}$ brings us to Einstein frame and the action becomes

$$S = \frac{1}{2}\int d^{\mathcal{D}} x \sqrt{-g_{\mathcal{D}}} \Bigg[R_{\mathcal{D}} - \frac{4}{\mathcal{D}-2}\partial_\mu \phi_{\mathrm{dil}\,\mathcal{D}} \partial^\mu \phi_{\mathrm{dil}\,\mathcal{D}} - \sum_{p=D-\Delta+1}^{D} \frac{\partial_\mu R_p \partial^\mu R_p}{R_p^2}$$
$$- \sum_{i=D+1}^{9} \frac{\partial_\mu R_i \partial^\mu R_i}{R_i^2} \Bigg] - \int d^{\mathcal{D}} x \sqrt{-g_{\mathcal{D}}} \mathcal{F}_{\mathcal{D}}, \tag{B.3}$$

where $\mathcal{F}_{\mathcal{D}} = \exp(\frac{2\mathcal{D}}{\mathcal{D}-2}\phi_{\mathrm{dil}\,\mathcal{D}})\hat{\mathcal{F}}_{\mathcal{D}}$. The supersymmetry breaking scale measured in Einstein frame, $M_{\mathcal{D}}$, is given by the inverse volume of T^n,

$$M_{\mathcal{D}} = e^{\frac{2\phi_{\mathrm{dil}\,\mathcal{D}}}{\mathcal{D}-2}} \prod_{i=D+A+1}^{9} \frac{1}{(2\pi R_i)^{1/n}} = \frac{1}{2\pi} \exp\left(\frac{2\phi_{\mathrm{dil}\,\mathcal{D}}}{\mathcal{D}-2} - \frac{1}{n} \sum_{i=D+A+1}^{9} \ln R_i \right). \tag{B.4}$$

It is convenient to introduce an explicit field notation, $\Phi_{\mathcal{D}}$, for the supersymmetry breaking scale as

$$M_{\mathcal{D}} = \frac{e^{\alpha \Phi_{\mathcal{D}}}}{2\pi} \quad \text{where } \alpha^2 = \frac{1}{\mathcal{D}-2} + \frac{1}{n}. \tag{B.5}$$

The coefficient α is chosen so that $\Phi_{\mathcal{D}}$ has a canonically normalized kinetic term. We can introduce other fields, $\phi_{\perp\mathcal{D}}$ and φ_i $(i = 1, \ldots, n-1)$, to describe the remaining degrees of freedom among the dilaton and radii of T^n. The explicit transformation law is given as

$$\begin{pmatrix} \Phi_{\mathcal{D}} \\ \phi_{\perp\mathcal{D}} \\ \varphi_{n-1} \\ \vdots \\ \varphi_1 \end{pmatrix} = \begin{pmatrix} \frac{1}{\alpha\sqrt{\mathcal{D}-2}} & -\frac{1}{\alpha n} & -\frac{1}{\alpha n} & \cdots & -\frac{1}{\alpha n} \\ \sqrt{\frac{\mathcal{D}-2}{\mathcal{D}+n-2}} & \frac{1}{\sqrt{\mathcal{D}+n-2}} & \frac{1}{\sqrt{\mathcal{D}+n-2}} & \cdots & \frac{1}{\sqrt{\mathcal{D}+n-2}} \\ 0 & \frac{n-1}{\sqrt{n(n-1)}} & -\frac{1}{\sqrt{n(n-1)}} & \cdots & -\frac{1}{\sqrt{n(n-1)}} \\ \vdots & & \ddots & & \vdots \\ 0 & \cdots & 0 & -\frac{1}{\sqrt{2}} & -\frac{1}{\sqrt{2}} \end{pmatrix} \begin{pmatrix} \frac{2}{\sqrt{\mathcal{D}-2}}\phi_{\mathrm{dil}\,\mathcal{D}} \\ \ln R_9 \\ \ln R_8 \\ \vdots \\ \ln R_{D+A+1} \end{pmatrix}. \tag{B.6}$$

Finally, we denote the Δ degrees of freedom of T^Δ as $\zeta_p = \ln R_{D-\Delta+p}$ $(p = 1, \ldots, \Delta)$. In terms of these fields, the action takes the canonical form[12]

$$S = \int d^{\mathcal{D}} x \sqrt{-g_{\mathcal{D}}} \Bigg[\frac{R_{\mathcal{D}}}{2} - \frac{1}{2}\partial_\mu \phi_{\perp\mathcal{D}} \partial^\mu \phi_{\perp\mathcal{D}} - \frac{1}{2}\partial_\mu \Phi_{\mathcal{D}} \partial^\mu \Phi_{\mathcal{D}} - \frac{1}{2}\sum_{i=1}^{n-1} \partial_\mu \varphi_i \partial^\mu \varphi_i$$

[12] One could also introduce $A = 4$ more scalars associated to the radii of $T^4/\mathbb{Z}_2$ in the orbifold models. However, as announced before, we consider from now on these radii to be internal and constant.

$$-\frac{1}{2}\sum_{p=1}^{\Delta}\partial_\mu\zeta_p\partial^\mu\zeta_p\Bigg]-\int d^{\mathcal{D}}x\,\sqrt{-g_{\mathcal{D}}}\mathcal{F}_{\mathcal{D}}. \tag{B.7}$$

The metric variation gives the standard Einstein equation in terms of the stress energy tensor. It is convenient to single out the terms coming from the thermal corrections and so we define the thermal energy–momentum tensor as

$$T_{\mathcal{D}\mu\nu}=-g_{\mathcal{D}\mu\nu}\mathcal{F}_{\mathcal{D}}+2\frac{\partial\mathcal{F}_{\mathcal{D}}}{\partial(g_{\mathcal{D}})^{\mu\nu}}. \tag{B.8}$$

We are interested in space–times which are homogeneous but anisotropic, since the radii of $T^{\mathcal{D}-d}$ are allowed to vary independently of the radii of the very large T^{d-1}. In this case, the fields are only allowed to vary with time and we take the metric to be of the form

$$ds^2_{\mathcal{D}}=-dt^2+a(t)^2\sum_{l=1}^{d-1}dx_l^2+\sum_{k=1}^{\mathcal{D}-d}b_k(t)^2\,dx^2_{d-1+k}. \tag{B.9}$$

The b_k are the scale factors of the $T^{\mathcal{D}-d}$ torus in Einstein frame and are related to the radii in string frame by $b_k=e^{\frac{-2}{\mathcal{D}-2}\phi_{\mathrm{dil}\,\mathcal{D}}}2\pi R_k$ if $R_k\gg 1$ (exchange $R_k\to 1/R_k$ if $R_k\ll 1$). It is also convenient to introduce the temperature related to the radius of the Euclidean time used in the computation of Z as

$$T_{\mathcal{D}}\equiv\frac{e^{\frac{2}{\mathcal{D}-2}\phi_{\mathrm{dil}\,\mathcal{D}}}}{2\pi R_0} \tag{B.10}$$

(not to be confused with the stress energy tensor). Defining the thermal energy density $\rho_{\mathcal{D}}\equiv T_{\mathcal{D}00}$ and pressure $P_{\mathcal{D}}\equiv a^{-2}T_{\mathcal{D}ll}$ (no sum on $l=1,\dots,d-1$), the thermal energy–momentum tensor can be expressed as[13]

$$T_{\mathcal{D}00}=\mathcal{F}_{\mathcal{D}}+2T_{\mathcal{D}}^2\frac{\partial\mathcal{F}_{\mathcal{D}}}{\partial T_{\mathcal{D}}^2}=\left(T_{\mathcal{D}}\frac{\partial P_{\mathcal{D}}}{\partial T_{\mathcal{D}}}-P_{\mathcal{D}}\right), \tag{B.11}$$

$$T_{\mathcal{D}ll}=-a^2\mathcal{F}_{\mathcal{D}}=a^2P_{\mathcal{D}}, \tag{B.12}$$

$$T_{\mathcal{D}d+k,d+k}=-b_k^2\mathcal{F}_{\mathcal{D}}+2\frac{\partial\mathcal{F}_{\mathcal{D}}}{\partial b_k^{-2}}=b_k^2\left(P_{\mathcal{D}}+b_k\frac{\partial P_{\mathcal{D}}}{\partial b_k}\right). \tag{B.13}$$

Note that the thermal energy density $\rho_{\mathcal{D}}$ satisfies the thermodynamical identity $\rho_{\mathcal{D}}=T_{\mathcal{D}}\frac{\partial P_{\mathcal{D}}}{\partial T_{\mathcal{D}}}-P_{\mathcal{D}}$. The Ricci tensor can be expressed in terms of $H\equiv\frac{\dot a}{a}$ and $K_k\equiv\frac{\dot b_k}{b_k}$ $(k=1,\dots,\mathcal{D}-d)$. The off-diagonal elements automatically vanish, as well as those of the thermal energy–momentum tensor (B.11). The remaining diagonal Einstein equations become

$$0=(d-1)\big(\dot H+H^2\big)+\sum_{k=1}^{\mathcal{D}-d}\big(\dot K_k+K_k^2\big)+\dot\phi^2_{\perp\mathcal{D}}+\dot\Phi^2_{\mathcal{D}}+\sum_{i=1}^{n-1}\dot\varphi_i^2+\sum_{i=1}^{\Delta}\dot\zeta_i^2$$

[13] The extra temperature factor of $T_{\mathcal{D}}^2$ in the second term of the first equation in (B.11) can be seen as follows. The variation of the free energy density can be taken when the coordinates are such that the metric is just the analytic continuation of the Euclidean background, $ds^2_{\mathcal{D}}=-T_{\mathcal{D}}^{-2}\,dt^2+a(t)^2\sum_l ds_l^2+\sum_k b_k(t)^2\,dx^2_{d-1+k}$. The factor of $T_{\mathcal{D}}^2$ then comes from changing the metric coordinates to have (B.9).

$$+\frac{\mathcal{D}-3}{\mathcal{D}-2}\rho_{\mathcal{D}}+\frac{d-1}{\mathcal{D}-2}P_{\mathcal{D}}+\frac{1}{\mathcal{D}-2}\sum_{k=1}^{\mathcal{D}-d}\left(P_{\mathcal{D}}+b_k\frac{\partial P_{\mathcal{D}}}{\partial b_k}\right), \tag{B.14}$$

$$0=(d-1)H^2+\dot{H}+H\sum_{k=1}^{\mathcal{D}-d}K_k-\frac{1}{\mathcal{D}-2}\rho_{\mathcal{D}}-\frac{\mathcal{D}-d-1}{\mathcal{D}-2}P_{\mathcal{D}}$$
$$+\frac{1}{\mathcal{D}-2}\sum_{k=1}^{\mathcal{D}-d}\left(P_{\mathcal{D}}+b_k\frac{\partial P_{\mathcal{D}}}{\partial b_k}\right), \tag{B.15}$$

$$0=\dot{K}_k+K_k^2+(d-1)K_kH+K_k\sum_{j=1(j\neq k)}^{\mathcal{D}-d}K_j-\frac{1}{\mathcal{D}-2}\rho_{\mathcal{D}}-\frac{\mathcal{D}-3}{\mathcal{D}-2}\left(P_{\mathcal{D}}+b_k\frac{\partial P_{\mathcal{D}}}{\partial b_k}\right)$$
$$+\frac{d-1}{\mathcal{D}-2}P_{\mathcal{D}}+\frac{1}{\mathcal{D}-2}\sum_{j=1(j\neq k)}^{\mathcal{D}-d}\left(P_{\mathcal{D}}+b_j\frac{\partial P_{\mathcal{D}}}{\partial b_j}\right)\quad(k=1,\dots,\mathcal{D}-d), \tag{B.16}$$

where $\mathcal{D}=D+1-\Delta$. The equations of motion for the scalars reduce to

$$\ddot{\Phi}_{\mathcal{D}}+(d-1)H\dot{\Phi}_{\mathcal{D}}+\sum_{k=1}^{\mathcal{D}-d}K_k\dot{\Phi}_{\mathcal{D}}=\frac{\partial P_{\mathcal{D}}}{\partial\Phi_{\mathcal{D}}}, \tag{B.17}$$

$$\ddot{\phi}_{\perp\mathcal{D}}+(d-1)H\dot{\phi}_{\perp\mathcal{D}}+\sum_{k=1}^{\mathcal{D}-d}K_k\dot{\phi}_{\perp\mathcal{D}}=\frac{\partial P_{\mathcal{D}}}{\partial\phi_{\perp\mathcal{D}}}, \tag{B.18}$$

$$\ddot{\zeta}_p+(d-1)H\dot{\zeta}_p+\sum_{k=1}^{\mathcal{D}-d}K_k\dot{\zeta}_p=\frac{\partial P_{\mathcal{D}}}{\partial\zeta_p}\quad(p=1,\dots,\Delta), \tag{B.19}$$

$$\ddot{\varphi}_i+(d-1)H\dot{\varphi}_i+\sum_{k=1}^{\mathcal{D}-d}K_k\dot{\varphi}_i=\frac{\partial P_{\mathcal{D}}}{\partial\varphi_i}\quad(i=1,\dots,n-1). \tag{B.20}$$

B.1. Reduced equations of motion for phases I and II

Here, we apply the above results to the background of Sections 3.1 and 3.2. We have $n=1$ internal direction that breaks supersymmetry and $D=8-A$ "spectator" directions ($A=0$ for the toroidal models and $A=4$ for the orbifold ones). We split $T^D\equiv T^{d-1}\times(S^1(R_d)\times T^{D-d})$, where T^{d-1} is very large, the radii of T^{D-d} are small and frozen, and we are interested in the regime where R_d and $1/R_d$ are smaller than $\inf_{i\in I_b}R_i$. We thus choose $\Delta=9-A-d$ and find an effective space–time dimension $\mathcal{D}=d$. Beside the temperature T_d, the independent fields are the scale factor a and the scalars Φ_d, $\phi_{\perp d}$ and $\zeta_1=\ln R_d$, whose expressions follow from Eq. (B.6), with $\alpha=\sqrt{(d-1)/(d-2)}$,

$$\Phi_d\equiv\frac{2}{\sqrt{(d-2)(d-1)}}\phi_{\mathrm{dil}\,d}-\sqrt{\frac{d-2}{d-1}}\ln R_9,$$
$$\phi_{\perp d}\equiv\frac{2}{\sqrt{d-1}}\phi_{\mathrm{dil}\,d}+\frac{1}{\sqrt{d-1}}\ln R_9,$$
$$\zeta_1\equiv\ln R_d. \tag{B.21}$$

To simplify the notations, we will denote the fields as T, a, Φ, $\phi_\perp$, ζ and the thermal energy density and pressure as ρ, P.

The two Einstein equations (B.14) and (B.15) simplify and can be replaced by the Friedmann equation and an equation expressing the conservation of energy,

$$\frac{1}{2}(d-2)(d-1)H^2 = \frac{1}{2}\left(\dot{\Phi}^2 + \dot{\phi}_\perp^2 + \dot{\zeta}^2\right) + \rho, \tag{B.22}$$

$$\dot{\rho} + (d-1)H(\rho + P) + \dot{\Phi}\frac{\partial P}{\partial \Phi} + \dot{\phi}_\perp \frac{\partial P}{\partial \phi_\perp} + \dot{\zeta}\frac{\partial P}{\partial \zeta} = 0, \tag{B.23}$$

where the sources P, ρ satisfy (see Section 2.1)

$$P = T^d p(z,\eta,\zeta), \qquad \rho = T\frac{\partial P}{\partial T} - P$$
$$\Longrightarrow \quad \rho = T^d r(z,\eta,\zeta) \quad \text{with } r = (d-1)p - p_z, \tag{B.24}$$

where $\eta = \ln R_9$ and e^z is the ratio of temperature to supersymmetry breaking *i.e.* $z = \sqrt{\frac{d-1}{d-2}}\Phi - \ln(2\pi T)$.[14] The scalar field equations (B.17)–(B.19) reduce to

$$\ddot{\Phi} + (d-1)H\dot{\Phi} = \frac{\partial P}{\partial \Phi} = T^d\left(\sqrt{\frac{d-1}{d-2}}p_z - \sqrt{\frac{d-2}{d-1}}p_\eta\right), \tag{B.25}$$

$$\ddot{\phi}_\perp + (d-1)H\dot{\phi}_\perp = \frac{\partial P}{\partial \phi_\perp} = \frac{T^d}{\sqrt{d-1}}p_\eta, \tag{B.26}$$

$$\ddot{\zeta} + (d-1)H\dot{\zeta} = \frac{\partial P}{\partial \zeta} = T^d p_\zeta. \tag{B.27}$$

Note that Eq. (B.23) can easily be integrated. Writing $\dot{P} = \dot{\Phi}\frac{\partial P}{\partial \Phi} + \dot{\phi}_\perp \frac{\partial P}{\partial \phi_\perp} + \dot{\zeta}\frac{\partial P}{\partial \zeta} + \dot{T}\frac{\partial P}{\partial T}$, one derives from Eq. (B.23) and the relation between ρ and P in Eq. (B.24),

$$\dot{\rho} + \dot{P} + (d-1)H(\rho + P) = \frac{\dot{T}}{T}(\rho + P) \quad \Longrightarrow \quad (aT)^{d-1}\left(r(z,\eta,\zeta) + p(z,\eta,\zeta)\right) = \text{cst}. \tag{B.28}$$

It is useful to parameterize our functions in terms of $\ln a$ and thereby replace time-derivatives by $(\ln a)$-derivatives, in which case we have

$$\dot{f} = H\frac{df}{d\ln a} := H\overset{\circ}{f}, \tag{B.29}$$

for any function f. Critical solutions do not have constant Φ but rather constant z and so it is relevant to change variables from Φ to z in Eq. (B.25). Physically, this corresponds to the fact that for stable solutions the ratio of the supersymmetry breaking scale to the temperature scale must be a constant. In order to proceed, we first express the derivative of the energy density ρ in T, z, η and ζ variables as $\dot{\rho} = T^d H(dr\overset{\circ}{T}/T + r_z\overset{\circ}{z} + r_\eta\overset{\circ}{\eta} + r_\zeta\overset{\circ}{\zeta})$ and note from the definition of z that $\overset{\circ}{T}/T = \sqrt{(d-1)/(d-2)}\overset{\circ}{\Phi} - \overset{\circ}{z}$. Using these two expressions, Eq. (B.23) can be reexpressed as

$$\overset{\circ}{\Phi} = \mathcal{A}_{(z)}\overset{\circ}{z} + \mathcal{A}_{(\phi_\perp)}\overset{\circ}{\phi}_\perp + \mathcal{A}_{(\zeta)}\overset{\circ}{\zeta} + \mathcal{B}, \tag{B.30}$$

[14] In this section, it is understood that partial derivatives of p are with respect to z, η or ζ with the remaining variables held constant.

where

$$\mathcal{A}_{(z)}(z,\eta,\zeta)=\frac{dr-r_z}{\mathcal{E}},\qquad \mathcal{A}_{(\phi_\perp)}(z,\eta,\zeta)=-\frac{1}{\sqrt{d-1}}\frac{r_\eta+p_\eta}{\mathcal{E}},$$
$$\mathcal{A}_{(\zeta)}(z,\eta,\zeta)=-\frac{r_\zeta+p_\zeta}{\mathcal{E}},\qquad \mathcal{B}(z,\eta,\zeta)=-(d-1)\frac{r+p}{\mathcal{E}},\tag{B.31}$$

and

$$\mathcal{E}=\sqrt{\frac{d-1}{d-2}}(dr+p_z)-\sqrt{\frac{d-2}{d-1}}(r_\eta+p_\eta).\tag{B.32}$$

Eq. (B.30) can now be used to eliminate Φ from the equations. We first use it to write the Friedmann Eq. (B.22) in the form,

$$H^2=hT^d\quad \text{where } h(z,\eta,\zeta;\mathring{z},\mathring{\phi}_\perp,\mathring{\zeta})=\frac{r}{\frac{1}{2}(d-2)(d-1)-\mathcal{K}}\tag{B.33}$$

and

$$\mathcal{K}=\frac{1}{2}\big[(\mathcal{A}_{(z)}\mathring{z}+\mathcal{A}_{(\phi_\perp)}\mathring{\phi}_\perp+\mathcal{A}_{(\zeta)}\mathring{\zeta}+\mathcal{B})^2+\mathring{\phi}_\perp^2+\mathring{\zeta}^2\big].\tag{B.34}$$

Next, noting that $\ddot{\Phi}=\dot{H}\mathring{\Phi}+H^2\mathring{\mathring{\Phi}}$, one can express $\dot{H}$ in terms of H, ρ, P using Einstein's equations and bring (B.25) into the form,

$$\begin{aligned}
&h\left[\mathcal{A}_{(z)}\mathring{\mathring{z}}+\mathcal{A}_{(\phi_\perp)}\mathring{\mathring{\phi}}_\perp+\mathcal{A}_{(\zeta)}\mathring{\mathring{\zeta}}+(\mathring{z},\mathring{\phi}_\perp,\mathring{\zeta})\mathcal{C}\begin{pmatrix}\mathring{z}\\ \mathring{\phi}_\perp\\ \mathring{\zeta}\end{pmatrix}\right]\\
&\quad+\left[h\left(\mathcal{B}_z-\sqrt{\frac{d-2}{d-1}}(\mathcal{A}_{(z)}\mathcal{B})_\eta\right)+\frac{1}{d-2}(r-p)\mathcal{A}_{(z)}\right]\mathring{z}\\
&\quad+\left[h\left(\frac{1}{\sqrt{d-1}}\mathcal{B}_\eta-\sqrt{\frac{d-2}{d-1}}(\mathcal{A}_{(\phi_\perp)}\mathcal{B})_\eta\right)+\frac{1}{d-2}(r-p)\mathcal{A}_{(\phi_\perp)}\right]\mathring{\phi}_\perp\\
&\quad+\left[h\left(\mathcal{B}_\zeta-\sqrt{\frac{d-2}{d-1}}(\mathcal{A}_{(\zeta)}\mathcal{B})_\eta\right)+\frac{1}{d-2}(r-p)\mathcal{A}_{(\zeta)}\right]\mathring{\zeta}+V_z=0,
\end{aligned}\tag{B.35}$$

where the matrix $\mathcal{C}$ is

$$\begin{pmatrix}
\mathcal{A}_{(z)z}-\sqrt{\frac{d-2}{d-1}}\mathcal{A}_{(z)}\mathcal{A}_{(z)\eta} & \mathcal{A}_{(z)\eta}(\frac{1}{\sqrt{d-1}}-\sqrt{\frac{d-2}{d-1}}\mathcal{A}_{(\phi_\perp)}) & \mathcal{A}_{(z)\zeta}-\sqrt{\frac{d-2}{d-1}}\mathcal{A}_{(\zeta)}\mathcal{A}_{(z)\eta}\\
\mathcal{A}_{(\phi_\perp)z}-\sqrt{\frac{d-2}{d-1}}\mathcal{A}_{(z)}\mathcal{A}_{(\phi_\perp)\eta} & \mathcal{A}_{(\phi_\perp)\eta}(\frac{1}{\sqrt{d-1}}-\sqrt{\frac{d-2}{d-1}}\mathcal{A}_{(\phi_\perp)}) & \mathcal{A}_{(\phi_\perp)\zeta}-\sqrt{\frac{d-2}{d-1}}\mathcal{A}_{(\zeta)}\mathcal{A}_{(\phi_\perp)\eta}\\
\mathcal{A}_{(\zeta)z}-\sqrt{\frac{d-2}{d-1}}\mathcal{A}_{(z)}\mathcal{A}_{(\zeta)\eta} & \mathcal{A}_{(\zeta)\eta}(\frac{1}{\sqrt{d-1}}-\sqrt{\frac{d-2}{d-1}}\mathcal{A}_{(\phi_\perp)}) & \mathcal{A}_{(\zeta)\zeta}-\sqrt{\frac{d-2}{d-1}}\mathcal{A}_{(\zeta)}\mathcal{A}_{(\zeta)\eta}
\end{pmatrix}\tag{B.36}$$

and we have introduced $V(z,\eta,\zeta;\mathring{z},\mathring{\phi}_\perp,\mathring{\zeta})$, whose derivative with respect to z is

$$V_z=-\sqrt{\frac{d-1}{d-2}}p_z+\sqrt{\frac{d-2}{d-1}}p_\eta+\frac{1}{d-2}(r-p)\mathcal{B}-\sqrt{\frac{d-1}{d-2}}h\mathcal{B}_\eta\mathcal{B}.\tag{B.37}$$

Similarly, Eqs. (B.26), (B.27) for $\phi_\perp$ and ζ become,

$$h\overset{\circ\circ}{\phi}_\perp + \frac{1}{d-2}(r-p)\overset{\circ}{\phi}_\perp - \frac{1}{\sqrt{d-1}}p_\eta = 0, \tag{B.38}$$

$$h\overset{\circ\circ}{\zeta} + \frac{1}{d-2}(r-p)\overset{\circ}{\zeta} - p_\zeta = 0. \tag{B.39}$$

Finally, note that for $\zeta = 0$, V_z defined in (B.37) does not depend on velocities anymore,

$$V_z|_{\zeta=0} = \sqrt{\frac{d-2}{d-1}}\big(r(z,\eta,0) - dp(z,\eta,0)\big). \tag{B.40}$$

B.2. Reduced equations of motion for phase III

We want to write the fields and equations of motions in the regime of Section 3.3. Again, $n = 1$ and $D = 8 - A$. We split T^D as $(T^{d-1} \times S^1(R_d)) \times T^{D-d}$, where T^{d-1} is very large, the radii of T^{D-d} are small and frozen, and we are interested in the regime where R_d (or its inverse) is large. We thus take $\Delta = 8 - A - d$, which implies an effective space–time dimension $\mathcal{D} = d + 1$. The independent fields are the temperature T_{d+1}, the scale factor associated to the torus T^{d-1}, the scale factor b_1 of the spatial circle $S^1(R_d)$ and Φ_{d+1}, $\phi_{\perp d+1}$. The definitions of the scalars is derived from Eq. (B.6), with $\alpha = \sqrt{d/(d-1)}$,

$$\begin{aligned}
\Phi_{d+1} &\equiv \frac{2}{\sqrt{d(d-1)}}\phi_{\mathrm{dil}\,d+1} - \sqrt{\frac{d-1}{d}}\ln R_9,\\
\phi_{\perp d+1} &\equiv \frac{2}{\sqrt{d}}\phi_{\mathrm{dil}\,d+1} + \frac{1}{\sqrt{d}}\ln R_9.
\end{aligned} \tag{B.41}$$

We introduce simpler notations for the fields in $d + 1$ dimensions, T', a', b, Φ', $\phi'_\perp$, and for the thermal energy density and pressure, ρ', P'.

There are three Einstein equations (B.14)–(B.16) which simplify as,

$$-(d-1)\big(\dot{H}' + H'^2\big) - \big(\dot{K} + K^2\big) = \dot{\Phi}'^2 + \dot{\phi}'^2_\perp + \frac{1}{d-1}\left((d-2)\rho' + dP' + b\frac{\partial P'}{\partial b}\right), \tag{B.42}$$

$$\dot{H}' + (d-1)H'^2 + H'K = \frac{1}{d-1}\left(\rho' - P' - b\frac{\partial P'}{\partial b}\right), \tag{B.43}$$

$$\dot{K} + (d-1)H'K + K^2 = \frac{1}{d-1}\left(\rho' - P' + (d-2)b\frac{\partial P'}{\partial b}\right), \tag{B.44}$$

where $H' = \frac{\dot{a}'}{a'}$ and $K = \frac{\dot{b}}{b}$. The dependencies of the thermal sources P' and ρ' are as follows (see Section 3.3),

$$\begin{aligned}
&P' = T'^{d+1}p'\big(z,\eta,|\zeta|\big), \qquad \rho' = T'\frac{\partial P'}{\partial T'} - P'\\
&\quad\Longrightarrow\quad \rho' = T'^{d+1}r'\big(z,\eta,|\zeta|\big) \quad \text{with } r' = dp' - p'_z,
\end{aligned} \tag{B.45}$$

where $\eta = \ln R_9$, $\zeta = \ln R_d$ is related to the definition of b via $|\zeta| = \ln b + \frac{1}{\sqrt{d(d-1)}}\Phi' + \frac{1}{\sqrt{d}}\phi'_\perp$ and e^z is the ratio of temperature to supersymmetry breaking *i.e.* $z = \sqrt{\frac{d}{d-1}}\Phi' - \ln(2\pi T')$.[15] The scalar equations of motion given in (B.17) and (B.18) become in the present case,

$$\ddot{\Phi}' + \big((d-1)H' + K\big)\dot{\Phi}' = \frac{\partial P'}{\partial \Phi'} = T'^{d+1}\left(\sqrt{\frac{d}{d-1}}p'_z - \sqrt{\frac{d-1}{d}}p'_\eta + \frac{1}{\sqrt{(d-1)d}}p'_{|\zeta|}\right), \tag{B.46}$$

$$\ddot{\phi}'_\perp + \big((d-1)H' + K\big)\dot{\phi}'_\perp = \frac{\partial P'}{\partial \phi'_\perp} = \frac{T'^{d+1}}{\sqrt{d}}\big(p'_\eta + p'_{|\zeta|}\big). \tag{B.47}$$

Again, it is convenient to derive from Eqs. (B.42)–(B.47) the Friedmann equation and the conservation of the energy–momentum tensor,

$$\frac{1}{2}(d-1)\big((d-2)H'^2 + 2HK\big) = \frac{1}{2}\big(\dot{\Phi}'^2 + \dot{\phi}'^2_\perp\big) + \rho', \tag{B.48}$$

$$\dot{\rho}' + \big((d-1)H' + K\big)\big(\rho' + P'\big) + \dot{\Phi}'\frac{\partial P'}{\partial \Phi'} + \dot{\phi}'_\perp\frac{\partial P'}{\partial \phi'_\perp} + \dot{b}\frac{\partial P'}{\partial b} = 0. \tag{B.49}$$

To obtain a useful form for the remaining independent equations, we first define

$$e^\xi := \frac{b}{a'} \quad \Longrightarrow \quad K \equiv H' + \dot{\xi}, \tag{B.50}$$

and then subtract Eq. (B.43) from (B.44) to obtain,

$$\ddot{\xi} + \big((d-1)H' + K\big)\dot{\xi} = b\frac{\partial P'}{\partial b} = T'^{d+1}p'_{|\zeta|}. \tag{B.51}$$

Eq. (B.49) can be integrated by writing $\dot{P}' = \dot{\Phi}'\frac{\partial P'}{\partial \Phi'} + \dot{\phi}'_\perp\frac{\partial P'}{\partial \phi'_\perp} + \dot{b}\frac{\partial P'}{\partial b} + \dot{T}'\frac{\partial P'}{\partial T'}$ to obtain,

$$\dot{\rho}' + \dot{P}' + \big(dH' + \dot{\xi}\big)\big(\rho' + P'\big) = \frac{\dot{T}'}{T'}\big(\rho' + P'\big)$$
$$\Longrightarrow \quad \big(a'T'\big)^d e^\xi\big(r'\big(z,\eta,|\zeta|\big) + p'\big(z,\eta,|\zeta|\big)\big) = \text{cst}. \tag{B.52}$$

As in Appendix B.1, we introduce $(\ln a')$-derivatives, where for any function f,

$$\dot{f} = H'\frac{df}{d\ln a'} := H'\overset{\circ}{f}. \tag{B.53}$$

Proceeding in an analogous manner as the derivation of (B.30), Eq. (B.49) can also be rewritten as

$$\overset{\circ}{\Phi}' = \mathcal{A}'_{(z)}\overset{\circ}{z} + \mathcal{A}'_{(\phi'_\perp)}\overset{\circ}{\phi}'_\perp + \mathcal{A}'_{(\xi)}\overset{\circ}{\xi} + \mathcal{B}', \tag{B.54}$$

where

[15] In this section, it is understood that partial derivatives of p' with respect to z, η or $|\zeta|$ are with the two other variables held constant.

$$\mathcal{A}'_{(z)}\big(z,\eta,|\zeta|\big)=\frac{(d+1)r'-r'_z}{\mathcal{E}'},\qquad \mathcal{A}'_{(\phi'_\perp)}\big(z,\eta,|\zeta|\big)=-\frac{1}{\sqrt{d}}\frac{r'_\eta+p'_\eta}{\mathcal{E}'},$$
$$\mathcal{A}'_{(\xi)}\big(z,\eta,|\zeta|\big)=-\frac{r'+p'+r'_{|\zeta|}+p'_{|\zeta|}}{\mathcal{E}'},\qquad \mathcal{B}'(z,\eta,\zeta)=-\frac{d(r'+p')+r'_{|\zeta|}+p'_{|\zeta|}}{\mathcal{E}'},\tag{B.55}$$

and

$$\mathcal{E}'=\sqrt{\frac{d}{d-1}}\big((d+1)r'+p'_z\big)-\sqrt{\frac{d-1}{d}}\big(r'_\eta+p'_\eta\big)+\frac{1}{\sqrt{(d-1)d}}\big(r'_{|\zeta|}+p'_{|\zeta|}\big).\tag{B.56}$$

Eq. (B.54) can be used to recast the Friedmann equation (B.48) in the form,

$$H'^2=h'T'^{d+1}\quad\text{where } h'\big(z,\eta,|\zeta|;\mathring{z},\mathring{\phi}_\perp,\mathring{\xi}\big)=\frac{r'}{\frac{1}{2}(d-1)d-\mathcal{K}'},\tag{B.57}$$

where

$$\mathcal{K}'=\frac{1}{2}\big[\big(\mathcal{A}'_{(z)}\mathring{z}+\mathcal{A}'_{(\phi'_\perp)}\mathring{\phi}'^2_\perp+\mathcal{A}'_{(\xi)}\mathring{\xi}+\mathcal{B}'\big)^2+\mathring{\phi}'^2_\perp-(d-1)\mathring{\xi}^2\big].\tag{B.58}$$

For the scalar Φ', its equation becomes

$$\begin{aligned}
&h'\left[\mathcal{A}'_{(z)}\mathring{\mathring{z}}+\mathcal{A}'_{(\phi'_\perp)}\mathring{\mathring{\phi}}'_\perp+\mathcal{A}'_{(\xi)}\mathring{\mathring{\xi}}+\big(\mathring{z},\mathring{\phi}'_\perp,\mathring{\xi}\big)\mathcal{C}'\begin{pmatrix}\mathring{z}\\ \mathring{\phi}'_\perp\\ \mathring{\xi}\end{pmatrix}\right]\\
&\quad+\left[h'\left(\mathcal{B}'_z-\sqrt{\frac{d-1}{d}}\big(\mathcal{A}'_{(z)}\mathcal{B}'\big)_\eta+\frac{1}{\sqrt{(d-1)d}}\big(\mathcal{A}'_{(z)}\mathcal{B}'\big)_{|\zeta|}+\mathcal{A}'_{(z)|\zeta|}\right)\right.\\
&\quad\left.+\frac{(r'-p'-p'_{|\zeta|})}{d-1}\mathcal{A}_{(z)}\right]\mathring{z}\\
&\quad+\left[h'\left(\frac{1}{\sqrt{d}}\big(\mathcal{B}'_\eta+\mathcal{B}'_{|\zeta|}\big)-\sqrt{\frac{d-1}{d}}\big(\mathcal{A}'_{(\phi'_\perp)}\mathcal{B}'\big)_\eta+\frac{1}{\sqrt{(d-1)d}}\big(\mathcal{A}'_{(\phi'_\perp)}\mathcal{B}'\big)_{|\zeta|}+\mathcal{A}'_{(\phi'_\perp)|\zeta|}\right)\right.\\
&\quad\left.+\frac{(r'-p'-p'_{|\zeta|})}{d-1}\mathcal{A}'_{(\phi'_\perp)}\right]\mathring{\phi}'_\perp\\
&\quad+\left[h'\left(\mathcal{B}'_{|\zeta|}-\sqrt{\frac{d-1}{d}}\big(\mathcal{A}'_{(\xi)}\mathcal{B}'\big)_\eta+\frac{1}{\sqrt{(d-1)d}}\big(\mathcal{A}'_{(\xi)}\mathcal{B}'\big)_{|\zeta|}+\mathcal{A}'_{(\xi)|\zeta|}\right)\right.\\
&\quad\left.+\frac{(r'-p'-p'_{|\zeta|})}{d-1}\mathcal{A}'_{(\xi)}\right]\mathring{\xi}+V'_z=0,
\end{aligned}\tag{B.59}$$

where the components of the matrix $\mathcal{C}'$ are collected below, in Eqs. (B.63)–(B.65) and $V'(z,\eta,|\zeta|;\mathring{z},\mathring{\phi}_\perp,\mathring{\zeta})$ is defined by

$$\begin{aligned}
V'_z=&-\sqrt{\frac{d}{d-1}}p'_z+\sqrt{\frac{d-1}{d}}p'_\eta-\frac{1}{\sqrt{(d-1)d}}p'_{|\zeta|}\\
&+\frac{1}{d-1}(r'-p'-p'_{|\zeta|})\mathcal{B}'+h'\left[\mathcal{B}'_{|\zeta|}\left(\frac{1}{\sqrt{(d-1)d}}\mathcal{B}'+1\right)-\sqrt{\frac{d-1}{d}}\mathcal{B}'_\eta\mathcal{B}'\right].
\end{aligned}\tag{B.60}$$

The remaining equations (B.47) for $\phi'_\perp$ and (B.51) for ξ take the form

$$h' \overset{\circ\circ}{\phi}{}'_\perp + \frac{1}{d-1}\left(r' - p' - p'_{|\zeta|}\right)\overset{\circ}{\phi}{}'_\perp - \frac{1}{\sqrt{d}}\left(p'_\eta + p'_{|\zeta|}\right) = 0, \tag{B.61}$$

$$h' \overset{\circ\circ}{\xi} + \frac{1}{d-1}\left(r' - p' - p'_{|\zeta|}\right)\overset{\circ}{\xi} - p'_{|\zeta|} = 0. \tag{B.62}$$

For completeness, we collect all entries of the matrix $\mathcal{C}'$ that appears in Eq. (B.59):

$$\begin{aligned}
\mathcal{C}'_{zz} &= \mathcal{A}'_{(z)z} - \mathcal{A}'_{(z)}\left(\sqrt{\frac{d-1}{d}}\mathcal{A}'_{(z)\eta} - \frac{1}{\sqrt{(d-1)d}}\mathcal{A}'_{(z)|\zeta|}\right),\\
\mathcal{C}'_{\phi'_\perp z} &= \mathcal{A}'_{(\phi'_\perp)z} - \mathcal{A}'_{(z)}\left(\sqrt{\frac{d-1}{d}}\mathcal{A}'_{(\phi'_\perp)\eta} - \frac{1}{\sqrt{(d-1)d}}\mathcal{A}'_{(\phi'_\perp)|\zeta|}\right),\\
\mathcal{C}'_{\xi z} &= \mathcal{A}'_{(\xi)z} - \mathcal{A}'_{(z)}\left(\sqrt{\frac{d-1}{d}}\mathcal{A}'_{(\xi)\eta} - \frac{1}{\sqrt{(d-1)d}}\mathcal{A}'_{(\xi)|\zeta|}\right),
\end{aligned} \tag{B.63}$$

$$\begin{aligned}
\mathcal{C}'_{z\phi'_\perp} &= \frac{\mathcal{A}'_{(z)\eta} + \mathcal{A}'_{(z)|\zeta|}}{\sqrt{d}} - \mathcal{A}'_{(\phi'_\perp)}\left(\sqrt{\frac{d-1}{d}}\mathcal{A}'_{(z)\eta} - \frac{1}{\sqrt{(d-1)d}}\mathcal{A}'_{(z)|\zeta|}\right),\\
\mathcal{C}'_{\phi'_\perp\phi'_\perp} &= \frac{\mathcal{A}'_{(\phi'_\perp)\eta} + \mathcal{A}'_{(\phi'_\perp)|\zeta|}}{\sqrt{d}} - \mathcal{A}'_{(\phi'_\perp)}\left(\sqrt{\frac{d-1}{d}}\mathcal{A}'_{(\phi'_\perp)\eta} - \frac{1}{\sqrt{(d-1)d}}\mathcal{A}'_{(\phi'_\perp)|\zeta|}\right),\\
\mathcal{C}'_{\xi\phi'_\perp} &= \frac{\mathcal{A}'_{(\xi)\eta} + \mathcal{A}'_{(\xi)|\zeta|}}{\sqrt{d}} - \mathcal{A}'_{(\phi'_\perp)}\left(\sqrt{\frac{d-1}{d}}\mathcal{A}'_{(\xi)\eta} - \frac{1}{\sqrt{(d-1)d}}\mathcal{A}'_{(\xi)|\zeta|}\right),
\end{aligned} \tag{B.64}$$

$$\begin{aligned}
\mathcal{C}'_{z\xi} &= \mathcal{A}'_{(z)|\zeta|} - \mathcal{A}'_{(\xi)}\left(\sqrt{\frac{d-1}{d}}\mathcal{A}'_{(z)\eta} - \frac{1}{\sqrt{(d-1)d}}\mathcal{A}'_{(z)|\zeta|}\right),\\
\mathcal{C}'_{\phi'_\perp\xi} &= \mathcal{A}'_{(\phi'_\perp)|\zeta|} - \mathcal{A}'_{(\xi)}\left(\sqrt{\frac{d-1}{d}}\mathcal{A}'_{(\phi'_\perp)\eta} - \frac{1}{\sqrt{(d-1)d}}\mathcal{A}'_{(\phi'_\perp)|\zeta|}\right),\\
\mathcal{C}'_{\xi\xi} &= \mathcal{A}'_{(\xi)|\zeta|} - \mathcal{A}'_{(\xi)}\left(\sqrt{\frac{d-1}{d}}\mathcal{A}'_{(\xi)\eta} - \frac{1}{\sqrt{(d-1)d}}\mathcal{A}'_{(\xi)|\zeta|}\right).
\end{aligned} \tag{B.65}$$

References

[1] M.B. Green, J.H. Schwarz, E. Witten, Superstring Theory, vol. 1, Introduction, Cambridge Monographs On Mathematical Physics, Cambridge Univ. Press, Cambridge, UK, 1987, p. 469;
M.B. Green, J.H. Schwarz, E. Witten, Superstring Theory, vol. 2, Loop Amplitudes, Anomalies and Phenomenology, Cambridge Monographs On Mathematical Physics, Cambridge Univ. Press, Cambridge, UK, 1987, p. 596;
J. Polchinski, String Theory, vol. 1, An Introduction to the Bosonic String, Cambridge Univ. Press, Cambridge, UK, 1998, p. 402;
J. Polchinski, String Theory, vol. 2, Superstring Theory and Beyond, Cambridge Univ. Press, Cambridge, UK, 1998, p. 531;
E. Kiritsis, String Theory in a Nutshell, Princeton Univ. Press, Princeton, USA, 2007, p. 588.

[2] T. Catelin-Jullien, C. Kounnas, H. Partouche, N. Toumbas, Thermal/quantum effects and induced superstring cosmologies, Nucl. Phys. B 797 (2008) 137, arXiv:0710.3895 [hep-th];
T. Catelin-Jullien, C. Kounnas, H. Partouche, N. Toumbas, Thermal and quantum superstring cosmologies, Fortschr. Phys. 56 (2008) 792, arXiv:0803.2674 [hep-th].

[3] T. Catelin-Jullien, C. Kounnas, H. Partouche, N. Toumbas, Induced superstring cosmologies and moduli stabilization, arXiv:0901.0259 [hep-th].

[4] F. Bourliot, C. Kounnas, H. Partouche, Attraction to a radiation-like era in early superstring cosmologies, Nucl. Phys. B 816 (2009) 227, arXiv:0902.1892 [hep-th].
[5] C. Kounnas, H. Partouche, Inflationary de Sitter solutions from superstrings, Nucl. Phys. B 795 (2008) 334, arXiv:0706.0728 [hep-th].
[6] J. Atick, E. Witten, The Hagedorn transition and the number of degrees of freedom of string theory, Nucl. Phys. B 310 (1988) 291.
[7] C. Kounnas, B. Rostand, Coordinate dependent compactifications and discrete symmetries, Nucl. Phys. B 341 (1990) 641.
[8] I. Antoniadis, C. Kounnas, Superstring phase transition at high temperature, Phys. Lett. B 261 (1991) 369;
I. Antoniadis, J.P. Derendinger, C. Kounnas, Non-perturbative supersymmetry breaking and finite temperature instabilities in $\mathcal{N}=4$ superstrings, arXiv:hep-th/9908137;
C. Kounnas, Universal thermal instabilities and the high-temperature phase of the $\mathcal{N}=4$ superstrings, arXiv:hep-th/9902072.
[9] J.P. Derendinger, C. Kounnas, P.M. Petropoulos, F. Zwirner, Superpotentials in IIA compactifications with general fluxes, Nucl. Phys. B 715 (2005) 211, arXiv:hep-th/0411276;
J.P. Derendinger, C. Kounnas, P.M. Petropoulos, F. Zwirner, Fluxes and gaugings: $\mathcal{N}=1$ effective superpotentials, Fortschr. Phys. 53 (2005) 926, arXiv:hep-th/0503229;
G. Villadoro, F. Zwirner, $\mathcal{N}=1$ effective potential from dual type-IIA D6/O6 orientifolds with general fluxes, JHEP 0506 (2005) 047, arXiv:hep-th/0503169;
G. Villadoro, F. Zwirner, D terms from D-branes, gauge invariance and moduli stabilization in flux compactifications, JHEP 0603 (2006) 087, arXiv:hep-th/0602120;
L. Andrianopoli, M.A. Lledo, M. Trigiante, The Scherk–Schwarz mechanism as a flux compactification with internal torsion, JHEP 0505 (2005) 051, arXiv:hep-th/0502083;
G. Dall'Agata, N. Prezas, Scherk–Schwarz reduction of M-theory on G_2-manifolds with fluxes, JHEP 0510 (2005) 103, arXiv:hep-th/0509052;
J.P. Derendinger, P.M. Petropoulos, N. Prezas, Axionic symmetry gaugings in $\mathcal{N}=4$ supergravities and their higher-dimensional origin, Nucl. Phys. B 785 (2007) 115, arXiv:0705.0008 [hep-th];
G. Curio, A. Klemm, D. Lust, S. Theisen, On the vacuum structure of type II string compactifications on Calabi–Yau spaces with H-fluxes, Nucl. Phys. B 609 (2001) 3, arXiv:hep-th/0012213.
[10] C. Angelantonj, S. Ferrara, M. Trigiante, New $D=4$ gauged supergravities from $\mathcal{N}=4$ orientifolds with fluxes, JHEP 0310 (2003) 015, arXiv:hep-th/0306185;
C. Angelantonj, R. D'Auria, S. Ferrara, M. Trigiante, $K3\times T^2/\mathcal{Z}_2$ orientifolds with fluxes, open string moduli and critical points, Phys. Lett. B 583 (2004) 331, arXiv:hep-th/0312019;
C. Angelantonj, S. Ferrara, M. Trigiante, Unusual gauged supergravities from type IIA and type IIB orientifolds, Phys. Lett. B 582 (2004) 263, arXiv:hep-th/0310136;
C. Angelantonj, M. Cardella, N. Irges, An alternative for moduli stabilisation, Phys. Lett. B 641 (2006) 474, arXiv:hep-th/0608022.
[11] R. Hagedorn, Statistical thermodynamics of strong interactions at high-energies, Nuovo Cim. Suppl. 3 (1965) 147;
S. Fubini, G. Veneziano, Level structure of dual-resonance models, Nuovo Cim. A 64 (1969) 811;
K. Bardakci, S. Mandelstam, Analytic solution of the linear-trajectory bootstrap, Phys. Rev. 184 (1969) 1640;
K. Huang, S. Weinberg, Ultimate temperature and the early universe, Phys. Rev. Lett. 25 (1970) 895;
B. Sathiapalan, Vortices on the string world sheet and constraints on toral compactification, Phys. Rev. D 35 (1987) 3277;
Y.I. Kogan, Vortices on the world sheet and string's critical dynamics, JETP Lett. 45 (1987) 709, Pisma Zh. Eksp. Teor. Fiz. 45 (1987) 556;
M. Axenides, S.D. Ellis, C. Kounnas, Universal behavior of D-dimensional superstring models, Phys. Rev. D 37 (1988) 2964;
D. Kutasov, N. Seiberg, Number of degrees of freedom, density of states and tachyons in string theory and CFT, Nucl. Phys. B 358 (1991) 600;
D. Israel, V. Niarchos, Tree-level stability without spacetime fermions: Novel examples in string theory, JHEP 0707 (2007) 065, arXiv:0705.2140 [hep-th].
[12] M. Gasperini, G. Veneziano, Pre-big bang in string cosmology, Astropart. Phys. 1 (1993) 317, arXiv:hep-th/9211021;
M. Gasperini, M. Maggiore, G. Veneziano, Towards a non-singular pre-big bang cosmology, Nucl. Phys. B 494 (1997) 315, arXiv:hep-th/9611039.
[13] N. Matsuo, Superstring thermodynamics and its application to cosmology, Z. Phys. C 36 (1987) 289;

J. Kripfganz, H. Perlt, Cosmological impact of winding strings, Class. Quant. Grav. 5 (1988) 453;
R.H. Brandenberger, C. Vafa, Superstrings in the early universe, Nucl. Phys. B 316 (1989) 391;
M.J. Bowick, S.B. Giddings, High temperature strings, Nucl. Phys. B 325 (1989) 631;
A. Tseytlin, C. Vafa, Elements of string cosmology, Nucl. Phys. B 372 (1992) 443, arXiv:hep-th/9109048;
R.H. Brandenberger, String gas cosmology, arXiv:0808.0746 [hep-th];
R.H. Brandenberger, T. Battefeld, S. Watson, String gas cosmology, Rev. Mod. Phys. 78 (2006) 435, arXiv:hep-th/0510022;
B.A. Bassett, M. Borunda, M. Serone, S. Tsujikawa, Aspects of string-gas cosmology at finite temperature, Phys. Rev. D 67 (2003) 123506, arXiv:hep-th/0301180;
M. Borunda, L. Boubekeur, The effect of α' corrections in string gas cosmology, JCAP 0610 (2006) 002, arXiv:hep-th/0604085.

[14] N. Kaloper, L. Kofman, A.D. Linde, V. Mukhanov, On the new string theory inspired mechanism of generation of cosmological perturbations, JCAP 0610 (2006) 006, arXiv:hep-th/0608200;
N. Kaloper, S. Watson, Geometric precipices in string cosmology, Phys. Rev. D 77 (2008) 066002, arXiv:0712.1820 [hep-th].

[15] C. Angelantonj, C. Kounnas, H. Partouche, N. Toumbas, Resolution of Hagedorn singularity in superstrings with gravito-magnetic fluxes, Nucl. Phys. B 809 (2009) 291, arXiv:0808.1357 [hep-th].

[16] C. Kounnas, Massive boson–fermion degeneracy and the early structure of the universe, Fortschr. Phys. 56 (2008) 1143, arXiv:0808.1340 [hep-th];
I. Florakis, C. Kounnas, Orbifold symmetry reductions of massive boson–fermion degeneracy, arXiv:0901.3055 [hep-th].

[17] I. Antoniadis, C. Kounnas, The dilaton classical solution and the supersymmetry breaking evolution in an expanding universe, Nucl. Phys. B 284 (1987) 729.

[18] J. Estes, C. Kounnas, H. Partouche, Superstring cosmology for $N_4 = 1 \to 0$ superstring vacua, in preparation.

[19] E. Cremmer, S. Ferrara, C. Kounnas, D.V. Nanopoulos, Naturally vanishing cosmological constant in $\mathcal{N} = 1$ supergravity, Phys. Lett. B 133 (1983) 61;
J.R. Ellis, C. Kounnas, D.V. Nanopoulos, No scale supersymmetric GUTs, Nucl. Phys. B 247 (1984) 373;
J.R. Ellis, C. Kounnas, D.V. Nanopoulos, Phenomenological $SU(1,1)$ supergravity, Nucl. Phys. B 241 (1984) 406;
J.R. Ellis, A.B. Lahanas, D.V. Nanopoulos, K. Tamvakis, No-scale supersymmetric standard model, Phys. Lett. B 134 (1984) 429.

[20] S. Ferrara, C. Kounnas, F. Zwirner, Mass formulae and natural hierarchy in string effective supergravities, Nucl. Phys. B 429 (1994) 589, arXiv:hep-th/9405188;
S. Ferrara, C. Kounnas, F. Zwirner, Nucl. Phys. B 433 (1995) 255, Erratum;
C. Kounnas, F. Zwirner, I. Pavel, Towards a dynamical determination of parameters in the minimal supersymmetric standard model, Phys. Lett. B 335 (1994) 403, arXiv:hep-ph/9406256;
C. Kounnas, I. Pavel, G. Ridolfi, F. Zwirner, Possible dynamical determination of m_t, m_b and m_τ, Phys. Lett. B 354 (1995) 322, arXiv:hep-ph/9502318.

[21] S. Watson, Moduli stabilization with the string Higgs effect, Phys. Rev. D 70 (2004) 066005, arXiv:hep-th/0404177.

[22] S.P. Patil, R. Brandenberger, Radion stabilization by stringy effects in general relativity and dilaton gravity, Phys. Rev. D 71 (2005) 103522, arXiv:hep-th/0401037.

[23] J. Scherk, J.H. Schwarz, Spontaneous breaking of supersymmetry through dimensional reduction, Phys. Lett. B 82 (1979) 60.

[24] R. Rohm, Spontaneous supersymmetry breaking in supersymmetric string theories, Nucl. Phys. B 237 (1984) 553.

[25] C. Kounnas, M. Porrati, Spontaneous supersymmetry breaking in string theory, Nucl. Phys. B 310 (1988) 355;
S. Ferrara, C. Kounnas, M. Porrati, F. Zwirner, Superstrings with spontaneously broken supersymmetry and their effective theories, Nucl. Phys. B 318 (1989) 75.

[26] A. Strominger, Massless black holes and conifolds in string theory, Nucl. Phys. B 451 (1995) 96, arXiv:hep-th/9504090;
S. Kachru, C. Vafa, Exact results for $\mathcal{N} = 2$ compactifications of heterotic strings, Nucl. Phys. B 450 (1995) 69, arXiv:hep-th/9505105;
S. Kachru, A. Klemm, W. Lerche, P. Mayr, C. Vafa, Nonperturbative results on the point particle limit of $\mathcal{N} = 2$ heterotic string compactifications, Nucl. Phys. B 459 (1996) 537, arXiv:hep-th/9508155;
I. Antoniadis, H. Partouche, Exact monodromy group of $\mathcal{N} = 2$ heterotic superstring, Nucl. Phys. B 460 (1996) 470, arXiv:hep-th/9509009;
H. Partouche, Non perturbative check of $\mathcal{N} = 2$, $D = 4$ heterotic/type II duality, Nucl. Phys. B (Proc. Suppl.) 55 (1997) 210, arXiv:hep-th/9610119.

[27] P. Kaste, H. Partouche, On the equivalence of $\mathcal{N} = 1$ brane worlds and geometric singularities with flux, JHEP 0411 (2004) 033, arXiv:hep-th/0409303.

[28] E. Witten, Dimensional reduction of superstring models, Phys. Lett. B 155 (1985) 151;
S. Ferrara, C. Kounnas, M. Porrati, General dimensional reduction of ten-dimensional supergravity and superstring, Phys. Lett. B 181 (1986) 263;
M. Cvetic, J. Louis, B.A. Ovrut, A string calculation of the Kähler potentials for moduli of $\mathcal{Z}_N$ orbifolds, Phys. Lett. B 206 (1988) 227;
L.J. Dixon, V. Kaplunovsky, J. Louis, On effective field theories describing (2, 2) vacua of the heterotic string, Nucl. Phys. B 329 (1990) 27;
M. Cvetic, J. Molera, B.A. Ovrut, Kähler potentials for matter scalars and moduli of $\mathcal{Z}_N$ orbifolds, Phys. Rev. D 40 (1989) 1140.

[29] E. Kiritsis, C. Kounnas, Dynamical topology change, compactification and waves in a stringy early universe, arXiv:hep-th/9407005;
E. Kiritsis, C. Kounnas, Dynamical topology change in string theory, Phys. Lett. B 331 (1994) 51, arXiv:hep-th/9404092;
E. Kiritsis, C. Kounnas, Dynamical topology change, compactification and waves in string cosmology, Nucl. Phys. B (Proc. Suppl.) 41 (1995) 311, arXiv:gr-qc/9701005;
E. Kiritsis, C. Kounnas, String gravity and cosmology: Some new ideas, arXiv:gr-qc/9509017.

Annexe E

Publication 3 : F. Bourliot, J. Estes, C. Kounnas and H. Partouche, "Thermal and quantum induced early superstring cosmology," arXiv :0910.2814 [hep-th], *accepted for publication by NOVA publishers.*

CPHT–L094.0909, LPTENS–09/31, October 2009

Thermal and quantum induced early superstring cosmology

F. Bourliot[1], J. Estes[1], C. Kounnas[2] and H. Partouche[1]

[1] Centre de Physique Théorique, Ecole Polytechnique,[†]
F–91128 Palaiseau cedex, France
Francois.Bourliot@cpht.polytechnique.fr
John.Estes@cpht.polytechnique.fr
Herve.Partouche@cpht.polytechnique.fr

[2] Laboratoire de Physique Théorique, Ecole Normale Supérieure,[‡]
24 rue Lhomond, F–75231 Paris cedex 05, France
Costas.Kounnas@lpt.ens.fr

arXiv:0910.2814v1 [hep-th] 15 Oct 2009

Abstract

In this work, we review the results of Refs [1] – [5] dedicated to the description of the early Universe cosmology induced by quantum and thermal effects in superstring theories. The present evolution of the Universe is described very accurately by the standard Λ-CDM scenario, while very little is known about the early cosmological eras. String theory provides a consistent microscopic theory to account for such missing epochs. In our framework, the Universe is a torus filled with a gas of superstrings. We first show how to describe the thermodynamical properties of this system, namely energy density and pressure, by introducing temperature and supersymmetry breaking effects at a fundamental level by appropriate boundary conditions.

We focus on the intermediate period of the history: After the very early "Hagedorn era" and before the late electroweak phase transition. We determine the back-reaction of the gas of strings on the initially static space-time, which then yields the induced cosmology. The consistency of our approach is guaranteed by checking the quasi-staticness of the evolution. It turns out that for arbitrary initial boundary conditions at the exit of the Hagedorn era, the quasi-static evolutions are universally attracted to radiation-dominated solutions. It is shown that at these attractor points, the temperature, the inverse scale factor of the Universe and the supersymmetry breaking scale evolve proportionally. There are two important effects which result from the underlying string description. First, initially small internal dimensions can be spontaneously decompactified during the attraction to a radiation dominated Universe. Second, the radii of internal dimensions can be stabilized.

[†] Unité mixte du CNRS et de l'Ecole Polytechnique, UMR 7644.

[‡] Unité mixte du CNRS et de l'Ecole Normale Supérieure associée à l'Université Pierre et Marie Curie (Paris 6), UMR 8549.

1 Why and how studying superstring cosmology?

We are aware of the existence of four interactions: Gravity, weak interaction, electromagnetism and strong interaction. Though gravity is the oldest known one, it is still the less well understood. In quantum field theory, electromagnetism and the weak interaction have successfully been embedded into the electroweak interaction [6], while the strong interaction is very well described by QCD. A common wisdom is that at very high energies, these three interactions combine into a Grand Unified Theory (GUT) based on a gauge group $G_{\rm GUT}$ containing at least the standard model group $SU(3)_{\rm strong} \times SU(2)_{\rm weak} \times U(1)_{\rm elec}$. As one lowers the energy/temperature, the interactions unified in $G_{\rm GUT}$ start to separate and the standard model emerges. In particular, the electroweak phase transition takes place at low energy and implies that electromagnetism and the weak interaction split. While theoretically promising, there is still no experimental evidence for the existence of such a GUT.

Though interesting for studying the last three interactions, the above GUT scenario has an important drawback: It does not include gravity. The oldest known interaction does not merge with the others in such a consistent quantum field theory. However, it is not currently possible to access experimentally domains of energies relevant for testing a quantum theory of gravity, except maybe through astrophysical and cosmological observations of phenomena involving very high energies. Consequently, the realm of quantum gravity has been, and is still, the one for theorists. Over the last thirty years, there has been various attempts to formulate a consistent quantum theory of gravity. Not all of them try to also embed gravity with the other three forces in a Quantum Theory Of Everything (QTOE). String Theory [7] is a candidate for a QTOE, and it is an important open problem to realize within it not only the standard model of particle physics but also the known cosmology of our Universe.

What we mean by "known cosmology" can be described by the Cosmological Standard Model, dubbed the Λ-CDM model (Cold Dark Matter). The latter proposes an history of our space-time and predicts its ultimate fate. Starting just after its birth, the Universe underwent a very fast period of acceleration, called *Inflation*. The latter diluted the primordial inhomogeneities, topological relics and rendered the space flat. At the end of inflation, the Universe undergoes a short period of "reheating" and an era of domination by radiation then appears. As the temperature lowers, symmetry breaking phase transitions occur (and in particular the electroweak breaking) and the fundamental particles acquire a mass via the

Higgs mechanism. As the Universe cools, hadrons such as the proton and neutron start to form. Progressively, matter appears as the results of thermonuclear reactions. Consequently, after some time, matter dominates and leads to structure formation. However, it no longer dominates today since there are observational evidences that our Universe is slightly accelerating [8]. This is implemented theoretically speaking, by introducing a tiny cosmological constant. For a wider discussion on standard cosmology and the history of our Universe, see [9].

General Relativity is the theory which best describes gravity in a classical setting. Supposing the Universe to be 4-dimensional with coordinates x^μ ($\mu = 0, \ldots, 3$), the Einstein equation takes the form

$$G_{\mu\nu} := R_{\mu\nu} - \frac{1}{2} R\, g_{\mu\nu} = T_{\mu\nu}, \tag{1.1}$$

in appropriate units such that $c = 1$ and $8\pi G = 1$. In (1.1), $R_{\mu\nu}$ is the Ricci tensor, while $T_{\mu\nu}$ is the stress-energy tensor. Due to inflation, the Λ-CDM model treats the Universe as homogeneous and isotropic at sufficiently large scales, and spatially flat. It is then possible to show [10] that the metric describing such a space-time is given by the following FLRW (Friedmann-Lemaître-Robertson-Walker) one:

$$ds^2 = -N(t)^2 dt^2 + a(t)^2 \sum_{\mu=1}^{3} (dx^\mu)^2, \tag{1.2}$$

where $a(t)$ is the *scale factor*. In a homogeneous and isotropic space-time, the stress-energy tensor takes, in the perfect fluid approximation, the form

$$T_{\mu\nu} = (P + \rho)\, u_\mu u_\nu + P g_{\mu\nu}, \tag{1.3}$$

where u^μ is the 4-speed of the cosmic fluid, satisfying $u^\mu u_\mu = -1$. ρ is the energy density and P the pressure. The Λ-CDM model describes phenomenologically the observed features of our Universe by coupling Einstein gravity to a matter sector whose field content, potentials and kinetic terms are constrained only by observations. These sources are described by perfect fluids of species $i = 1, 2, \ldots$ characterized by their densities ρ_i and pressures P_i related by equations of state $P_i = \omega_i\, \rho_i$, with parameter ω_i. To be concrete, the Λ-CDM model states that 97% of the energetic content of the Universe is described by dark matter (27%) and a cosmological constant Λ (70%) for dark vacuum energy. While there is much indirect experimental evidence for them, these two quantities still lack direct measurement

so that their exact nature is still unknown. Theoretically speaking, there is a wide diversity of scenarios with both dark matter and cosmological constant candidates (see [11, 12] for a cosmological scenario trying to explain both dark matter and cosmological constant). The remaining 3% of the content of the Universe is spanned between pressureless non-relativistic baryonic matter and radiation, the second being a tiny fraction of the first in our present epoch. Though very interesting, the phenomenological approach of the Λ-CDM model lacks an underlying microscopic derivation.

It is a challenge for String Theory to provide such a foundation. However, despite considerable efforts toward unraveling string cosmology over the last few years, still very little is known about the dynamics of strings in time-dependent settings. Indeed, it seems difficult to obtain time-dependent solutions in string theory at the classical level. After extensive studies in the framework of superstring compactifications, the obtained results appear to be unsuitable for cosmology. In most cases, the classical ground states correspond to static Anti-de Sitter like or flat backgrounds but not time-dependent ones. The same situation appears to be true in the effective supergravity theories. Naively, the results obtained in this direction may yield to the conclusion that cosmological backgrounds are unlikely to be found in superstring theory. However, quantum and thermal corrections are neglected in the classical string/supergravity regime. Actually, it turns out that in certain cases, the quantum and thermal corrections are under control [2]- [5] at the full string level and that cosmological evolutions at finite temperature can be generated dynamically at the quantum level. The purpose of the present work is to review them and show how some of the weak points of phenomenological approaches can be explored and analyzed concretely in a consistent theoretical framework. In particular, we will describe how one can find the energy density and pressure from microscopic arguments, by studying the canonical ensemble of a gas of strings.

In order to understand how cosmological solutions arise naturally in this context, we first consider classical supersymmetric flat backgrounds in 4 dimensions. They are obtained from the 10-dimensional space-time in which superstrings are living by compactifying 6 directions. The study of the thermodynamics of a gas of superstring states filling this background makes sense at the quantum level only (this is well known from Planck, when he introduced the notion of quanta to solve the UV catastrophe problem in black body physics). At finite

temperature, the quantum and thermal fluctuations produce a non-zero free energy density which is computable perturbatively at the full string level. Note that in this context, it can be determined order by order in the Riemann surface genus expansion without the UV ambiguities encountered in the analogous computation in quantum field theory. An energy density and pressure can be derived from the free energy. Their back-reaction on the space-time metric and moduli fields (the continuous parameters of the models) gives rise to specific cosmological evolutions. In this review, the above strategy is restricted to the domain of temperatures lower than the Hagedorn temperature and higher than the electroweak breaking scale to be specified in the next paragraphs. In this intermediate regime, the evolution of the Universe is found to converge to a radiation dominated era.

More interesting models are those where space-time supersymmetry is spontaneously broken at a scale M before finite temperature is switched on. With the supersymmetry breaking mechanism we consider, the stringy quantum corrections are under control in a way similar to the thermal ones [2] – [5]. In large classes of models, the back-reaction of the quantum and thermal corrections on the space-time metric and the moduli fields induces a cosmological evolution which is attracted to a radiation dominated era. The latter is characterized by a temperature and a supersymmetry breaking scale that evolve proportionally to the inverse of the scale factor, $T(t) \propto M(t) \propto 1/a(t)$.

In the context of string theory, we can study much higher energies than the ones tested so far. We are then limited by the appearance of a *Hagedorn phase transition* at ultra high temperature [13]. It is a consequence of the exponential growth of the number of states that can be thermalized at high temperature and implies a divergence of the canonical thermal partition function. The latter can be computed in Matsubara formalism *i.e.* in Euclidean time compactified on an circle of circumference β, the inverse temperature. The Hagedorn instability is signaled by string modes wrapping the Euclidean time circle that become tachyonic (*i.e.* with negative (mass)^2) when the temperature is above the Hagedorn temperature T_H [14,15]. The possible existence of an Hagedorn era in the very early Universe provides a possible alternative or at least a complementary point of view to inflation, as developed in [16]. However, we do not discuss this very high temperature regime here, and we will consider the physics at low enough temperatures compared to T_H to avoid the occurrence of a Hagedorn phase transition [17]. Note that models free of Hagedorn instabilities [18, 19]

and still under computational control can also be constructed. In the present review, we bypass the Hagedorn era ambiguities by assuming that 3 large spatial directions have emerged before t_E (the exit time of the Hagedorn era), along with internal space directions whose size characterizes the scale of spontaneous supersymmetry breaking. Within this assumption, we parameterize our ignorance of the detailed physics in the Hagedorn era by considering arbitrary initial boundary conditions (IBC) for the fields at t_E.

At late cosmological times, when the temperature of the Universe is low enough, it is possible for an additional scale Q to become relevant. Q is the infrared renormalisation group invariant transmutation scale induced at the quantum level by the radiative corrections of the soft supersymmetry breaking terms at low energies [20]. When $T(t) \sim Q$, the electroweak phase transition takes place, $SU(2) \times U(1) \to U(1)_{elec}$. This starts to be the case at a time t_W and, for $t > t_W$, the supersymmetry breaking scale M is stabilized at a value close to Q. In earlier cosmological times where $M(t) \sim T(t) > Q$, the transmutation scale Q is irrelevant and the Universe is in the radiation era. It turns out that the electroweak symmetry breaking transition is very sensitive to the specifics of the string background considered, while in the earlier radiation era the results are fairly robust. We restrict our analysis to the intermediate cosmological times:

$$t_E \ll t \ll t_W, \tag{1.4}$$

namely, after the exit of the Hagedorn era and before the electroweak symmetry breaking.

In section 2, we present the basics of our approach and apply it to the simplest examples where supersymmetry is spontaneously broken by temperature effects only. In this class of models, the moduli (radii) of the internal space are held fixed, close to the string scale. In section 3, we analyze models where supersymmetry is spontaneously broken even at zero temperature. We take into account the dynamics of the supersymmetry breaking scale M which is a field and keep frozen the other moduli. This is only in section 4 that we show the latter hypothesis is consistent by taking into account the dynamics of internal radii that are not participating in the breaking of supersymmetry. The last section is devoted to our conclusions.

2 Basics of our approach

2.1 Thermodynamics and variational principle

Let us first describe how thermodynamical results can be derived from general relativity. As a simple example, we consider the gas of a single bosonic state at temperature T in a 3-dimensional torus T^3, which is nothing but a box with periodic boundary conditions and large volume $V_{\rm box} = (2\pi R_{\rm box})^3$. The number of particles is not fixed and the canonical ensemble partition function $Z_{\rm th}$ is defined in terms of the Hamiltonian H and inverse temperature β. In second quantized formalism, $Z_{\rm th}$ can be expressed as a path integral

$$Z_{th} := \mathrm{Tr}\, e^{-\beta H} = \int \mathcal{D}\varphi\, e^{-S_E[\varphi]}, \tag{2.1}$$

where S_E is the Euclidean action of the quantum field φ and the Euclidean time is compact with period β. The boundary condition along the Euclidean circle of the bosonic field φ is periodic (while a fermionic field would be anti-periodic). The thermal partition function can be written in terms of an infinite sum of connected or disconnected Feynmann graphs. Supposing the gas to be (almost) perfect, the particles do not interact (much) with themselves and we can approximate the result at one loop. The free energy takes the form

$$F = -\frac{\ln Z_{\rm th}}{\beta} \simeq -\frac{Z_{1-\rm loop}}{\beta}, \tag{2.2}$$

where $Z_{1-\rm loop}$ is the unique connected graph at 1-loop, the *bubble diagram*, a single propagator whose two ends are identified. Then, one can derive from F the energy density and pressure using standard thermodynamics identities.

However, it is also possible to use the fact that $Z_{1-\rm loop}$ is, from a quantum field theory point of view, the 1-loop vacuum-to-vacuum amplitude *i.e.* vacuum energy inside the box. Viewing the whole space we are living in as the box itself, the classical Einstein action must be corrected at 1-loop by a contribution to the "cosmological constant",

$$S = \int d^4x \sqrt{-g}\, \left(\frac{R}{2} + \frac{Z_{1-\rm loop}}{\beta V_{\rm box}} \right). \tag{2.3}$$

Note that in the above action, we are back to real time *i.e.* *Lorentzian* signature, by analytic continuation on the time variable. The stress-energy tensor is found by varying with respect to the metric,

$$T_{\mu\nu} = -\frac{2}{\sqrt{-g}} \frac{\delta}{\delta g^{\mu\nu}} \left(\sqrt{-g}\, \frac{Z_{1-\rm loop}}{\beta V_{\rm box}} \right). \tag{2.4}$$

Originally, the classical background is homogeneous and locally flat Minkowski space. Its metric is of the form (1.2) with laps function $N = \beta$ and scale factor $a = 2\pi R_{\rm box}$, as follows from the analytic continuation of the Euclidean background in which the 1-loop vacuum-to-vacuum amplitude has been computed. With $Z_{1-\rm loop}$ a function of β and $V_{\rm box}$, the stress-energy tensor takes the form $T^\mu{}_\nu = {\rm diag}(-\rho, P, P, P)^\mu{}_\nu$, where

$$P = \frac{1}{\beta}\frac{\partial Z_{1-\rm loop}}{\partial V_{\rm box}} \equiv -\left(\frac{\partial F}{\partial V_{\rm box}}\right)_\beta \tag{2.5}$$

$$\rho = -\frac{1}{V_{\rm box}}\frac{\partial Z_{1-\rm loop}}{\partial \beta} \equiv \frac{1}{V_{\rm box}}\left(\frac{\partial(\beta F)}{\partial \beta}\right)_{V_{\rm box}}. \tag{2.6}$$

In these expressions, the right hand sides follow from Eq. (2.2) and reproduce the standard thermodynamical results. When $Z_{1-\rm loop}$ is proportional to $V_{\rm box}$ *i.e.* the free energy is extensive, these relations simplify to

$$P = -\mathcal{F} \qquad \text{and} \qquad \rho = T\frac{\partial P}{\partial T} - P, \tag{2.7}$$

where $\mathcal{F} := \dfrac{F}{V_{\rm box}}$ is the free energy density and the relation between ρ and P is the state equation.

The above approach has the advantage to allow to go farther than deducing the thermodynamical identities. As long as the 1-loop sources ρ and P are small perturbations of the classically homogeneous and isotropic static background, one can find their back-reaction on the space-time metric by solving the Einstein equation (1.1). In other words, a quasi-static evolution $\beta(t)$, $a(t)$ is found. This hypothesis amounts to supposing that the evolution is a sequence of thermodynamical equilibria *i.e.* that it is slow enough for the temperature to be remain homogenous.

We could have been satisfied by this quantum field theory approach in general relativity if an important difficulty would not arise: In most cases, $Z_{1-\rm loop}$ is actually divergent ! This is always the case for a single bosonic (or fermionic) field. However, suppose the gas contains two species of free particles, one bosonic of mass M_B and one fermionic of mass M_F. The 1-loop vacuum-to-vacuum amplitude is found to be

$$Z_{1-\rm loop} = \beta V_{\rm box}\int_0^{+\infty}\frac{dl}{2l}\frac{1}{(2\pi l)^2}\sum_{\tilde m_0}\left(e^{-\frac{l}{2}M_B^2} - (-)^{\tilde m_0}e^{-\frac{l}{2}M_F^2}\right)e^{-\frac{\beta^2\tilde m_0^2}{2l}}, \tag{2.8}$$

where l is a "Schwinger parameter", the proper time of each particle when it runs into a loop wrapped $\tilde m_0$ along the Euclidean time circle. If $M_B \neq M_F$ (that could arise from a

spontaneous breaking of supersymmetry), the contribution to this integral with $\tilde{m}_0 = 0$ is divergent in the UV, $l \to 0$. We conclude that only the exactly supersymmetric spectrum $M_B = M_F$ gives a well defined free energy.

As is well know, the amplitudes in string theory are free of UV divergences and one can expect that the above approach applied in this context will give a perfectly well established framework to describe thermodynamics in time-dependent backgrounds. Actually, we are going to see that string theory provides a rigorous microscopic derivation of the sources ρ and P and their equation of state.

2.2 Supersymmetric string models at finite T

We start to implement the ideas sketched at the end of the previous section on simple string theory models in 4-dimensional Minkowski space-time, where supersymmetry is spontaneously broken by thermal effects only. The case of models where supersymmetry is spontaneously broken even at zero temperature is addressed in the next section.

To be specific, we consider heterotic models but type II or type I ones can be treated similarly. To analyze the canonical ensemble of a gas of heterotic strings, we consider 10-dimensional backgrounds of the form

$$\underbrace{S^1(R_0)}_{\text{Euclidean time}} \times \underbrace{T^3(R_{\text{box}})}_{\text{space}} \times \underbrace{\mathcal{M}_6}_{\text{internal space}} , \tag{2.9}$$

where $S^1(R_0)$ is the Euclidean time circle of perimeter $\beta = 2\pi R_0$, $T^3(R_{\text{box}})$ denotes the spatial part which is taken to be flat and compact *i.e.* a very large torus, and $\mathcal{M}_6$ represents the remaining internal manifold.

Classically, the vacuum energy vanishes. This is clear from the fact that the genus-0 vacuum-to-vacuum string amplitude is computed on the Riemann sphere, which is simply connected and thus cannot wrap the Euclidean time. Consequently, it cannot probe the temperature effects that are responsible of the breaking of supersymmetry. However, the genus-1 Riemann surface which is nothing but a torus has two cycles that can wrap the Euclidean time so that a non-trivial 1-loop contribution to the vacuum-to-vacuum energy arises, $Z_{1-\text{loop}}$. To be specific, we focus on the simplest example where $\mathcal{M}_6 = T^6$, which means that at $T = 0$ the model is $\mathcal{N} = 4$ supersymmetric in 4 dimensions for the heterotic

case. Using world-sheet techniques, $Z_{1-\text{loop}}$ is given by [2]- [5]

$$Z_{1-\text{loop}} = \frac{\beta V_{\text{box}}}{(2\pi)^4} \int_{\mathcal{F}} \frac{d\tau d\bar{\tau}}{4(\text{Im}\,\tau)^3} \frac{1}{2} \sum_{a,b} (-1)^{a+b+ab} \frac{\vartheta^4[{a \atop b}]}{\eta^4} \frac{\Gamma_{(6,22)}}{\eta^8 \bar{\eta}^{24}} \sum_{\tilde{m}_0, n_0} e^{-\frac{\pi R_0^2}{\text{Im}\,\tau}|\tilde{m}_0 + n_0 \tau|^2} (-1)^{\tilde{m}_0 a + \tilde{n}_0 b + \tilde{m}_0 n_0}. \tag{2.10}$$

A few words might be helpful to understand this expression. On the 2-dimensional world-sheet of the heterotic string, there are left moving superstring waves and right moving bosonic ones. There are thus 10 left moving world-sheet fermions and bosons, and 26 right moving world-sheet bosons. However, ghosts cancel the contributions of two bosons (left and right) and two left fermions. The remaining fermions contribute the factor $\vartheta^4[{a \atop b}](\tau)/\eta^4(\tau)$ with an appropriate spin-statistic phase $(-1)^{a+b+ab}$ depending on the integers a, b modulo 2 associated to the boundary conditions of the fermions along the two circles of the world-sheet torus. The contributions of the left and right moving world-sheet bosons correspond to the $\Gamma_{(6,22)}(\tau, \bar{\tau})/\eta^8(\tau)/\bar{\eta}^{24}(\bar{\tau})$ factor. $\Gamma_{(6,22)}$ is a lattice that corresponds to the 0-modes of the 16 right moving bosons (without left partners) and the six internal left and right moving bosons that realize the coordinates of the internal space T^6. In field theory, the loop can wrap $\tilde{m}_0$ times around the Euclidean time. In string theory, the closed string itself can also be wrapped n_0 times around $S^1(R_0)$. This is why we have a double discrete sum on arbitrary integers $\tilde{m}_0, n_0$ and a generalized phase $(-1)^{\tilde{m}_0 a + \tilde{n}_0 b + \tilde{m}_0 n_0}$ that involves the winding number n_0, as compared to Eq. (2.8), where space-time bosons (fermions) correspond to $a = 0$ ($a = 1$).

Another important difference between the field and string theory amplitudes, Eqs (2.8) and (2.10), is that the integration over the Schwinger parameter from 0 to $+\infty$ is replaced by an integral over the *fundamental domain* of $SL(2, \mathbb{Z})$,

$$\mathcal{F} = \left\{ \tau \in \mathbb{C} \;\Big/\; |\text{Re}\,\tau| \leq \frac{1}{2}, \;\; \text{Im}\,\tau > 0, \;\; |\tau| \geq 1 \right\}, \tag{2.11}$$

which does not contain the line $\text{Im}\,\tau = 0$. Since the "Schwinger parameter" or proper time along the string world-sheet torus is $\text{Im}\,\tau$, there is no risk of any UV divergence. This property of the amplitude is only due to the extended nature of the string that provides a natural cut-off in the UV. Contrarily to the field theory case, the UV finiteness of the amplitude is guaranteed in all models, even when the spectrum at zero temperature is not supersymmetric (see section 3). However, both in field and string theory, the amplitude is finite in the IR (l and $\text{Im}\,\tau \to +\infty$) as long as there is no tachyon in the spectrum (*i.e.*

no particle with $(\text{mass})^2 < 0$). A careful analysis shows that string states winding around the Euclidean time circle become tachyonic when $1/R_H < R_0 < R_H$, where $R_H = \dfrac{1+\sqrt{2}}{2}$ in $\sqrt{\alpha'}$ units [14] – [17], the string length we have set to 1 in Eq. (2.10) and now on for notational simplicity. R_H determines the Hagedorn temperature at which a phase transition occurs. As announced in section 1, we restrict ourselves to the study of epochs in the history of the Universe that follow the Hagedorn era and thus consider only regimes where $R_0 \gg 1$.

In the amplitude (2.10) (or (2.8) in field theory), the dominant contributions arise from the lightest states. The pure Kaluza-Klein (KK) states associated to the Euclidean time circle have masses of order $1/R_0$. Strings with non-trivial winding number n_0 around $S^1(R_0)$ get a contribution to their mass proportional to the length of the circle *i.e.* R_0. Similarly, the KK and winding states associated to the internal space $\mathcal{M}_6$ have masses contributions of order $1/R_I$ and R_I, where R_I denotes some generic radius (modulus) characterizing the size of $\mathcal{M}_6$. Finally, each string that oscillates has a contribution of order 1 to its mass. For simplicity in this section, we suppose that all radii R_I are satisfying the constraint

$$\frac{1}{R_0} \ll R_I \ll R_0 \tag{2.12}$$

that will be justified in section 4.[1] It follows that the towers of pure KK states along the Euclidean time are much lighter than any other states in the spectrum. Given that, the partition function (2.10) can be written as

$$Z_{1-\text{loop}} = \beta V_{\text{box}} \frac{1}{(2\pi R_0)^4}\, n_T\, c_4 + \cdots \qquad \text{where} \qquad c_4 = \frac{1}{\pi^2} \sum_{\tilde{m}_0} \frac{1}{|2\tilde{m}_0 + 1|^4} = \frac{\pi^2}{48} \tag{2.13}$$

and the dots stand for contributions of order $\mathcal{O}(e^{-2\pi R_0})$ for the oscillating states, $\mathcal{O}(e^{-2\pi R_0/R_I})$ and $\mathcal{O}(e^{-2\pi R_0 R_I})$ for the KK and the winding states of $\mathcal{M}_6$, and $\mathcal{O}(e^{-2\pi R_0^2})$ for winding states around $S^1(R_0)$. These terms are all exponentially suppressed, compared to the dominant contribution. In Eq. (2.13), n_T is the number of massless boson-fermion pairs in the supersymmetric model when the temperature is not switched on. The constant c_4 is a dressing that accounts for the full towers of KK states along $S^1(R_0)$.

Let us determine the back-reaction of the non-trivial 1-loop vacuum energy on the originally static background. At order one in string perturbation theory, the low energy effective

[1] It will be shown that for arbitrary I.B.C. at the exit of the Hagedorn era, R_I is dynamically attracted to the interval $1/R_0 < R_I < R_0$ and then converges to a constant.

action at finite temperature is

$$S = \int d^4x \sqrt{-g_{st}} \left[e^{-2\phi} \left(\frac{R_{st}}{2} + 2(\partial\phi)^2 \right) + \frac{Z_{1-\text{loop}}}{\beta V_{box}} \right], \tag{2.14}$$

where ϕ is the dilaton in four dimensions. Compared to the general relativity case Eq. (2.3), the string "coupling constant" is actually the field $e^{2\phi}$. The choice in the definition of the metric tensor that gives rise to the above mixing of the dilaton and the Ricci curvature is referred as the string frame metric. In (2.14), we have kept constant the over massless fields of the string spectrum since the 1-loop source does not involve them in the present case (see the next sections for more general models). Their kinetic terms are thus vanishing.

The action may be converted to a more convenient "Einstein frame" by rescaling the metric as $g_{st\mu\nu} = e^{2\phi}\, g_{\mu\nu}$,

$$S = \int d^4x \sqrt{-g} \left[\frac{R}{2} - (\partial\phi)^2 - \mathcal{F} \right], \tag{2.15}$$

where

$$\mathcal{F} = -T^4\, n_T\, c_4 \qquad \text{and} \qquad T = \frac{1}{2\pi R_0\, e^{-\phi}}. \tag{2.16}$$

$\mathcal{F}$ and T which contain a dilaton dressing are the free energy density and temperature when they are measured in Einstein frame. Supposing that the back-reaction of the thermal sources induce a quasi-static evolution of the homogeneous and isotropic background, dilaton and temperature, we consider an ansatz

$$\begin{aligned} & ds^2 = -N(x^0)^2 (dx^0)^2 + a(x^0)^2 \left[(dx^1)^2 + (dx^2)^2 + (dx^3)^2 \right], \qquad \phi(x^0), \\ & \text{where} \qquad N(x^0) \equiv 2\pi R_0\, e^{-\phi} \equiv \frac{1}{T(x^0)}, \qquad a(x^0) \equiv 2\pi R_{box}\, e^{-\phi}. \end{aligned} \tag{2.17}$$

The derivation of the stress-energy tensor reaches

$$\rho = 3P \qquad \text{where} \qquad P = T^4\, n_T\, c_4, \tag{2.18}$$

which is nothing but Stefan's law for radiation. This was expected since under the hypothesis (2.12), all non-zero masses are of order 1 which is also the scale of T_H. Since we consider temperatures far below the Hagedorn one, only the massless states can be thermalized. The massive ones remain "cold" *i.e.* decoupled from the thermal system.

The equations of motion are easily solved. In terms of cosmological time such that $N dx^0 = dt$, the velocity of the dilaton, $\dot{\phi} \propto 1/a^3$, goes to zero when the Universe expands.

The evolution is thus attracted to the particular solution where ϕ is constant *i.e.* the cosmology of a Universe filled by a radiation fluid:

$$a(t) = \sqrt{t} \times a_0 T_0 (n_T c_4)^{1/4} = \frac{1}{T(t)} \times a_0 T_0 \ , \qquad \phi = cst., \tag{2.19}$$

where a_0, T_0 are integration constants. We shall refer to such an attractor as a Radiation Dominated Solution (RDS).

Though we started with the huge machinery of string theory, we finally ended with standard results when the Universe is filled with radiation, after we consider the dominant contribution of massless modes. The reader could be skeptical about the need to require such heavy tools to describe such simple physics. However, we remind that our approach gives a rigorous microscopic derivation of these results that will be generalized in sections 3 and 4 to models whose free energies are UV divergent in field theory. In addition, we are going to see that when the dynamics of other scalar fields is taken into account, the underlying string theory provides a connection between naively disconnected theories as seen from a field theory point of view. This string theoretic effect marks the novelty of our approach.

3 Non-supersymmetric string models at finite T

The aim of the previous section was to present the basic ideas of a string theory framework able to provide a microscopic origin for source terms for the gravitational (and moduli) fields. We considered a model $\mathcal{N} = 4$ supersymmetric when temperature is not switched on. In order to recover a non-supersymmetric physics at very low temperature *i.e.* late time from a cosmological point of view, we need to consider models whose spectra are not supersymmetric, even at $T = 0$. From a phenomenological point of view, we are particularly interested in models with $\mathcal{N} = 1$ spontaneously broken supersymmetry.

To switch on finite temperature, we have introduced periodic or antiperiodic boundary conditions on the Euclidean time circle for the string states, depending on their fermionic number ($a = 0$ for bosons and $a = 1$ for fermions in Eq. (2.10)). In a similar way, a spontaneous breaking of supersymmetry can be generated by non-trivial boundary conditions on internal circles $S^1(R_i)$ $(i = 4, \ldots, 3 + n)$, using R-symmetry charges $a + Q_i$. Both finite temperature and supersymmetry breaking implemented this way can be thought as a string theoretic generalizations of Scherk-Schwarz compactifications [21]. Physically speaking, this

can be thought as introducing non-trivial background fluxes along the cycles. Two mass scales then appear and are *a priori* time-dependent: The temperature $T \propto \frac{1}{2\pi R_0}$ and the supersymmetry breaking scale $M \propto \frac{1}{2\pi(\prod_i R_i)^{1/n}}$. The initially degenerate mass levels of bosons and fermions split by amounts proportional to T and/or M. This mass splitting is the signal of supersymmetry breaking and gives rise to a non-trivial free energy density at 1-loop. Note that in the pure thermal case, each originally degenerate boson-fermion pair gives a positive contribution to $Z_{1-\text{loop}}$ since it is always the fermion that is getting a mass shift (their momenta along $S^1(R_0)$ are half integer). However, when introducing supersymmetry breaking, bosons can have non-trivial R-symmetry charges and acquire masses bigger than the ones for fermions. Consequently, negative contributions to the vacuum energy can arise. This will play an important role for RDS to exist. In the following, we first consider simple examples of models with $n = 1$ before sketching some cases with $n = 2$ to observe how ratios of radii (commonly referred as "complex structure moduli") can be stabilized.

3.1 Supersymmetry breaking involving $n = 1$ internal dimension

We want to study the canonical ensemble of a gas of heterotic strings, where supersymmetry is spontaneously broken by non-trivial boundary conditions along the internal direction 4. To be specific, we focus on two kinds of backgrounds (2.9), with internal space

$$\text{(I)} \ : \quad \mathcal{M}_6 = S^1(R_4) \times S^1 \times \frac{T^4}{\mathbb{Z}_2} \qquad \text{or} \qquad \text{(II)} \ : \quad \mathcal{M}_6 = \frac{S^1(R_4) \times T^3}{\mathbb{Z}_2} \times T^2. \tag{3.1}$$

$\mathbb{Z}_2$ acts as $x^I \to -x^I$, where $I = 6, 7, 8, 9$ in case (I) and $I = 4, 5, 6, 7$ in case (II), and breaks explicitly half of the supersymmetries. Thus, the above models have spectra where $\mathcal{N} = 2$ supersymmetry is spontaneously broken to zero by the internal flux around $S^1(R_4)$ and the temperature effects. Models with $\mathcal{N} = 1 \to 0$ can also be analyzed by considering $\mathcal{M}_6 = \dfrac{S^1(R_4) \times T^5}{\mathbb{Z}_2 \times \mathbb{Z}_2}$. They share similar cosmological properties with the models in case (II).

As in the pure thermal case of section 2, tachyonic instabilities arise when R_0 or R_4 approach R_H. In order for the canonical ensemble to be well defined, we will restrict our analysis to regimes where $R_0 \gg 1$ and $R_4 \gg 1$. We also suppose that all internal radii that are not participating in the spontaneous breaking of supersymmetry satisfy

$$\frac{1}{R_0} \ll R_I \ll R_0 \qquad \text{and} \qquad \frac{1}{R_4} \ll R_I \ll R_4 \qquad (I \neq 4), \tag{3.2}$$

and remind the reader that section 4 is devoted to the justification that this is consistent with the dynamics of the R_I's. Under these hypothesis, the 1-loop partition function of the pure thermal case (2.13) is generalized to

$$Z_{1-\text{loop}} = \beta V_{\text{box}} \left(\frac{1}{(2\pi R_0)^4}\, n_T\, \hat{f}_T^{(4)}(z) + \frac{1}{(2\pi R_4)^4}\, n_V\, e^{-z}\, \hat{f}_T^{(4)}(-z) + \frac{1}{(2\pi R_0)^4}\, n'_T\, c_4 + \cdots \right), \tag{3.3}$$

where

$$\hat{f}_T^{(4)}(z) = \frac{\Gamma(5/2)}{\pi^{5/2}} \sum_{\tilde{k}_0, \tilde{k}_4 \in \mathbb{Z}} \frac{e^{4z}}{[(2\tilde{k}_0+1)^2 e^{2z} + (2\tilde{k}_4)^2]^{5/2}}\,, \qquad e^z = \frac{R_0}{R_4}. \tag{3.4}$$

In Eq. (3.3), R_0 and R_4 being large, the modes which are KK excitations along both $S^1(R_0)$ and $S^1(R_4)$ give dominant contributions corresponding to the two first terms in the parenthesis. In other words, while R_i/R_I and $R_i R_I$ ($i = 0, 4$ and $I \neq 4$) are very large and give exponentially suppressed contributions we neglect, it is not necessary the case for R_0/R_4. As a consequence, the dimension full factors $1/R_0^4$ and $1/R_4^4$ are dressed with non-trivial functions of the "complex structure" ratio $e^z = R_0/R_4$. In case (I), n_T is the number of massless states (before we switch on finite temperature). n_V is the number of massless bosons minus the number of massless fermions (before we switch on finite temperature) and depends on the choice of R-symmetry charge $a+Q_4$ used to break spontaneously supersymmetry. Both n_T and n_V contain contributions arising from the untwisted and twisted sectors of the $\mathbb{Z}_2$-orbifold, while $n'_T = 0$. In case (II), n_T and n_V are defined similarly, but contain contributions from the untwisted sector only. On the contrary, the mass spectrum in the $\mathbb{Z}_2$-twisted sector does not depend on R_4 and supersymmetry between the associated states is spontaneously broken by thermal effects only. n'_T is then the number of massless boson/fermion pairs in the twisted sector (before we switch on finite temperature). To summarize, we have

$$n_T > 0\,, \qquad -1 \leq \frac{n_V}{n_T} \leq 1\,, \qquad n'_T = 0 \ \text{ in case (I)}\,, \qquad n'_T > 0 \ \text{ in case (II)}. \tag{3.5}$$

As before, $Z_{1-\text{loop}}$ backreacts on the classical 4-dimensional Lorentzian background, via the effective field theory action,

$$S = \int d^4x \sqrt{-g_{st}} \left[e^{-2\phi} \left(\frac{R_{st}}{2} + 2(\partial\phi)^2 + \frac{1}{2}(\partial \ln R_4)^2 \right) + \frac{Z_{1-\text{loop}}}{\beta V_{\text{box}}} \right], \tag{3.6}$$

where the scalar kinetic term of R_4 is included since there is a non-trivial source at 1-loop for it. Before writing the equations of motion, it is useful to redefine the scalar fields as,

$$\Phi := \sqrt{\frac{2}{3}}\,(\phi - \ln R_4)\,, \qquad \phi_\perp := \frac{1}{\sqrt{3}}\,(2\phi + \ln R_4)\,, \tag{3.7}$$

and switch from string to Einstein frame metric. The action becomes

$$S = \int d^4x\sqrt{-g}\left[\frac{R}{2} - \frac{1}{2}\left((\partial\phi)^2 + (\partial\phi_\perp)^2\right) - \mathcal{F}\right], \tag{3.8}$$

where $\mathcal{F}$ is the free energy density,

$$\mathcal{F} = -T^4\left(n_T\,\hat{f}_T^{(4)}(z) + n_V\,e^{3z}\hat{f}_T^{(4)}(-z) + n'_T\,c_4\right) := -T^4\,p(z), \tag{3.9}$$

and z can be expressed in terms of the temperature and supersymmetry breaking scales as,

$$e^z = \frac{M}{T}\,, \qquad T = \frac{1}{2\pi\,R_0 e^{-\phi}}\,, \qquad M = \frac{1}{2\pi R_4\,e^{-\phi}} \equiv \frac{e^{\sqrt{\frac{3}{2}}\,\Phi}}{2\pi}. \tag{3.10}$$

Assuming an homogeneous and isotropic Universe with a flat 3-dimensional subspace as in Eq. (2.17), the 1-loop components of the stress-tensor are found to be:

$$P = T^4\,p(z) \qquad \text{and} \qquad \rho = T^4\left(3p(z) - p_z(z)\right) := T^4\,r(z)\,, \tag{3.11}$$

where p_z stands for a derivation with respect to z, $p_z = \frac{\partial}{\partial z}p$. The fields are only time-dependent and their equations of motion are:

$$3H^2 = \frac{1}{2}\dot{\Phi}^2 + \frac{1}{2}\dot{\phi}_\perp^2 + \rho\,, \tag{3.12}$$

$$\dot{\rho} + 3H(\rho + P) + \sqrt{\frac{3}{2}}\,\dot{\Phi}\,(3P - \rho) = 0\,, \tag{3.13}$$

$$\ddot{\Phi} + 3H\dot{\Phi} = \frac{\partial P}{\partial \Phi} \equiv \sqrt{\frac{3}{2}}\,(3P - \rho)\,, \tag{3.14}$$

$$\ddot{\phi}_\perp + 3H\dot{\phi}_\perp = 0 \qquad \Longrightarrow \qquad \dot{\phi}_\perp = \sqrt{2}\,\frac{c_\perp}{a^3}\,, \tag{3.15}$$

where $c_\perp$ is an integration constant. Denoting $\overset{\circ}{f} \equiv \dfrac{df}{d\ln a}$, we can first obtain the relation $\overset{\circ}{z} = \sqrt{\frac{3}{2}}\,\overset{\circ}{\Phi} - \frac{\overset{\circ}{T}}{T}$. Differentiating this identity and using the equations of motion, we can substitute Eq. (3.14) with an equation for z of the form

$$h(z, \overset{\circ}{z}, \overset{\circ}{\phi}_\perp)\left(\mathcal{A}(z)\overset{\circ\circ}{z} + \mathcal{B}(z)\overset{\circ}{z}^2\right) + \mathcal{C}(z)\overset{\circ}{z} + V_z(z) = 0, \tag{3.16}$$

where we introduce the notion of an effective potential V:

$$V_z(z) = r - 4\,p\,. \tag{3.17}$$

The explicit expressions for $h(z, \overset{\circ}{z}, \overset{\circ}{\phi}_\perp)$, $\mathcal{A}(z)$, $\mathcal{B}(z)$ and $\mathcal{C}(z)$ can be found in Ref. [4]. Eq. (3.16) admits a static solution $z \equiv z_c$, $\phi_\perp \equiv cst.$ when the potential $V(z)$ admits a critical point z_c. It happens that the shape of $V(z)$ depends drastically on the parameters n_V/n_T and n'_T:

- In case (I), $n_T' = 0$ and three behaviors can arise, as depicted on Fig. 1:
  - Case (Ia): For $\dfrac{n_V}{n_T} < -\dfrac{1}{15}$, $V(z)$ increases.
  - Case (Ib): For $-\dfrac{1}{15} < \dfrac{n_V}{n_T} < 0$, $V(z)$ has a unique minimum z_c, and $p(z_c) > 0$.
  - Case (Ic): For $0 < \dfrac{n_V}{n_T}$, $V(z)$ decreases.
- In case (II), $n_T' > 0$. In the three above ranges, the behaviors differ from case (I) for large negative z, where the potentials are linearly decreasing (see Fig. 1):
  - Case (IIa) & (IIb): For $n_V < 0$, $V(z)$ has a unique minimum z_c, and $p(z_c) > 0$.
  - Case (IIc): For $0 < n_V$, $V(z)$ decreases.

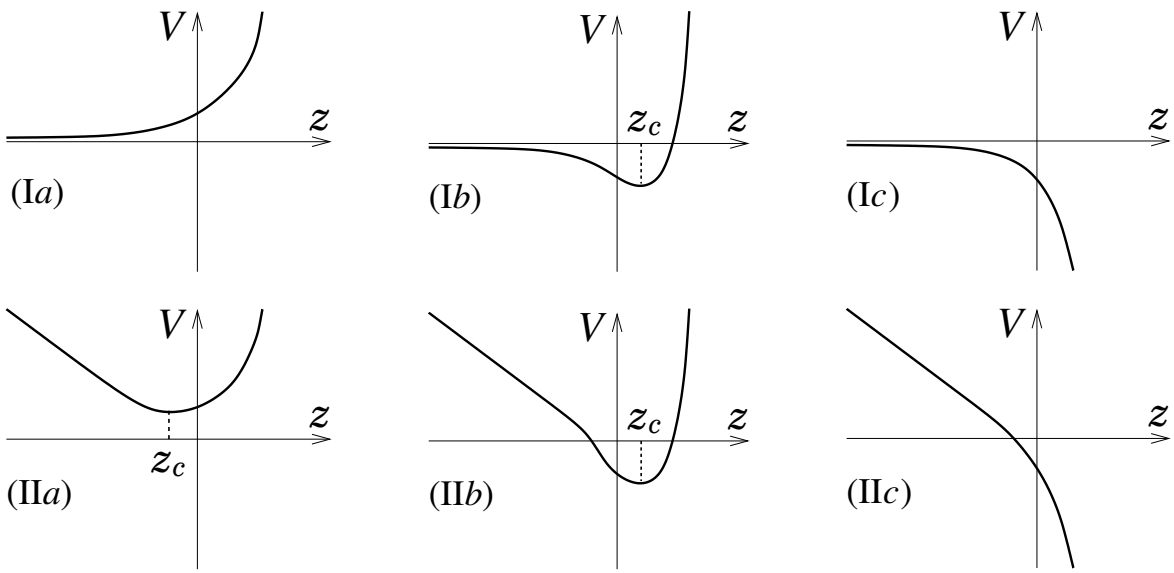

Figure 1: *Different qualitative behaviors of $V(z)$. The cases (a), (b) and (c) correspond to $-1 < n_V/n_T < -1/15$, $-1/15 < n_V/n_T < 0$ and $0 < n_V/n_T < 1$. For models of type* (I)*, an extremum exists in case (b) only. For models of type* (II)*, an extremum occurs in cases (a) and (b) i.e. $n_V < 0$.*

Thus, the cases (Ib), (IIb) and (IIa) admit a very particular solution where both scalars are constants *i.e.* $z \equiv z_c$ and $c_\perp = 0$. The conservation of the stress-tensor (3.13) and the Friedmann equation (3.12) gives then:

$$M(t) = T(t)\, e^{z_c} = \frac{1}{a(t)} \times a_0 M_0 \qquad \text{with} \qquad a(t) = \sqrt{\frac{t}{t_0}} \times a_0 \ , \quad \phi_\perp = cst. \tag{3.18}$$

where a_0, M_0, t_0 are constants. This evolution is characterized by a temperature T, a spontaneous supersymmetry breaking scale M and an inverse scale factor that are proportional for all times, with $H^2 \propto 1/a^4$ and $\phi_\perp$ a modulus. It is thus an RDS.

Using the positivity properties of $h(z, \overset{\circ}{z}, \overset{\circ}{\phi}_\perp)$, $\mathcal{A}(z)$, $\mathcal{B}(z)$ and $\mathcal{C}(z)$, it is easy to check analytically that this RDS is stable for small perturbations, implying that it is a local attractor of the dynamics [4]. Global attraction is also true, but numerics are required to yield to this conclusion. Fig. 2 gives an example of convergence to the RDS obtained for a generic choice of I.B.C..

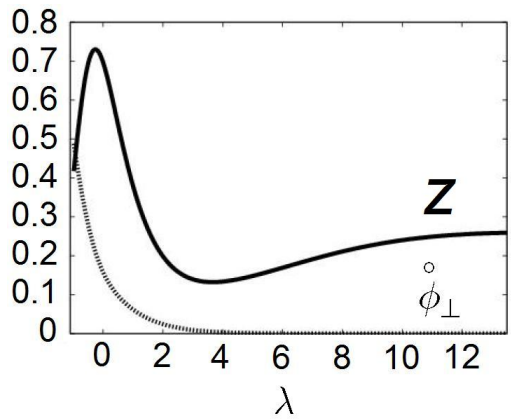

Figure 2: *Example of damping oscillations of $z(\lambda)$ where $\lambda \equiv \ln a$ (solid curve) and convergence to zero of $\overset{\circ}{\phi}_\perp(\lambda)$ (dotted curve) illustrating the dynamical attraction towards the critical solution $z \equiv z_c \simeq 0.272$, $\dot{\phi}_\perp \equiv 0$. It correspond to $\frac{n_V}{n_T} = -0.02$, $n'_T = 0$ i.e. some case* (I*b*)*. The initial conditions are* $(z_0, \overset{\circ}{z}_0, \overset{\circ}{\phi}_{\perp 0}) = (0.4, 0.8, 0.5)$.

In case (Ia), one can show analytically that when $z \ll -1$ and $|\overset{\circ}{z}| \ll 1$, the friction due to the expansion of the Universe implies $\overset{\circ}{z}$ to converge to 0. In other words, z is attracted to an arbitrary constant along the flat region of $V(z)$. The cosmological evolution is thus converging to the RDS (3.18), where $z_c \ll -1$ is a modulus whose value is now determined by the I.B.C.. A numerical study shows that for arbitrary I.B.C., z ends by sliding along its potential and enters the regime $z \ll -1$, $|\overset{\circ}{z}| \ll 1$ that yields to the above conclusions. It follows that the evolution is always attracted to the RDS. However, since $e^z = R_0/R_4 \ll 1$ with $R_0 \gg 1$, it is more natural to interpret the RDS from a 5-dimensional point of view *i.e.* to consider $S^1(R_4)$ as part of the space-time itself. In that case, R_4 does not appear in the definition of a scalar field M (or Φ), but is interpreted as a fifth component of the metric, $g_{st44} = (2\pi R_4)^2$. The attractor (3.18) is then rewritten as an RDS in 5 dimensions, where

supersymmetry is spontaneously broken by thermal effects only: The scale factor $a'(t)$ of the directions 1, 2, 3, the scale factor $b(t)$ of the direction 4 and the temperature T' of the 5-dimensional Universe evolve proportionally for all times and one has $H'^2 \propto 1/a'^5$. The mechanism described in case (Ia) thus corresponds to the *dynamical decompactification* of an internal direction involved in the spontaneous breaking of supersymmetry.

Finally, in cases (Ic) and (IIc), one can show that the scale factor ends by decreasing (eventually after a turning point where $\dot{a} = 0$) and that ρ and P are formally diverging at late times [4, 5]. This implies that our underlying hypothesis of quasi-staticness of the evolution breaks down at some time, since the perturbations of the background are very large. Thermodynamics out of equilibrium should then be applied and is out of the scope of the present work.

As a conclusion, the originally static models based on internal backgrounds $\mathcal{M}_6$ given in Eq. (3.1) or of the form $\dfrac{S^1(R_4) \times T^5}{\mathbb{Z}_2 \times \mathbb{Z}_2}$ are giving rise to cosmological evolutions attracted to RDS if and only if the partition function $\mathbb{Z}_{1-\text{loop}}$ contains a negative contribution, $n_V \leq 0$.[2] In addition, the space-time dimension of the late time evolution is determined dynamically in case (I). It is important to mention that during the attraction to the RDS, there is no substantial period of accelerated expansion for the Universe *i.e.* this intermediate era cannot account for inflation. Moreover, it is easy to see numerically that the time needed to reach the RDS can exceed the age of our real Universe, especially in case (I). To avoid this problem, one can start with I.B.C. close enough to the radiation era or restrict to models in case (II), due to the replacement of the plateau for $z \ll -1$ by a steeper potential. Note that the more realistic models where $\mathcal{N} = 1$ is spontaneously broken belong precisely to this class.

3.2 $n = 2$ models and complex structure stabilization

New phenomena can occur when the results of the previous section are extended to models with non-trivial boundary conditions along $n = 2$ internal directions, say 4 and 5. To be specific, let us analyze 4-dimensional Euclidean backgrounds with internal space

$$\mathcal{M}_6 = S^1(R_4) \times S^1(R_5) \times \mathcal{M}_4, \tag{3.19}$$

[2]The limit case $n_V = 0$ can be seen to yield an RDS in 4 dimensions [4].

where $R_0, R_4, R_5 \gg 1$ to avoid any risk of Hagedorn-like phase transition. Again, we restrict ourselves to radii R_I of the space $\mathcal{M}_4$ satisfying

$$\frac{1}{R_i} \ll R_I \ll R_i \qquad (i = 0, 4, 5\,; \quad I \neq 4, 5). \tag{3.20}$$

As before, the dominant contribution to the 1-loop partition function $Z_{1-\text{loop}}$ arises from the pure KK excitations along the circles $S^1(R_i)$ $(i = 0, 4, 5)$, while the other modes give exponentially damped terms that can be safely neglected. By analogy with Eq. (3.4), $Z_{1-\text{loop}}$ can be expressed in terms of triple discrete sums involving two ratios of radii *i.e.* two "complex structures". A convenient choice for them is,

$$e^z := \frac{R_0}{\sqrt{R_4 R_5}}\,, \qquad e^Z := \frac{R_5}{R_4}\,. \tag{3.21}$$

In terms of the temperature T and the supersymmetry breaking scale M, the free energy density is found to take the following form,

$$\mathcal{F} = -T^4\, p(z, Z) \qquad \text{where} \qquad e^z = \frac{M}{T}\,, \quad T = \frac{1}{2\pi\, R_0 e^{-\phi}}\,, \quad M = \frac{1}{2\pi\sqrt{R_4 R_5}\, e^{-\phi}}. \tag{3.22}$$

Depending on the precise way to break supersymmetry along the internal directions 4 and 5, different cosmological behaviors are found. In some cases one or the other of the directions 4 and 5 is spontaneously decompactified and we are back to a case already treated in the previous subsection (generalized in higher dimensions). In other cases, (z, Z) is found to converge to a critical point (z_c, Z_c) corresponding again to an RDS in 4 dimensions, where $T(t) \propto M(t) \propto 1/a(t)$. The new phenomenon encountered in such simple models is the dynamical stabilization of the complex structure $e^Z = R_5/R_4$.

4 Stabilization of Kähler structures

In the previous sections, we have supposed that the internal radii-moduli R_I that are not participating in the spontaneous breaking of supersymmetry are bounded by the radii (and their inverses) that do participate in the breaking (see Eqs (2.12) and (3.2)). This hypothesis was fundamental to ague that the R_I's appear in the 1-loop free energy through exponentially suppressed terms only. Here, we would like to justify this assumption is consistent by analyzing the dynamics of theR_I's, the so-called "Kähler moduli", for arbitrary initial values and velocities.

Since R_I can *a priori* be large, the associated $S^1(R_I)$ may be treated as a space-time direction rather than an internal one. We therefore consider the framework of the previous sections with arbitrary number $d-1$ of large spatial directions and, for simplicity, we consider the dynamics of a single internal circle, $S^1(R_d)$. As an example, we introduce a spontaneous breaking of supersymmetry that involves $n = 1$ internal circle, say in the direction 9, $S^1(R_9)$. Temperature is implemented as usually with non-trivial boundary conditions along the Euclidean time $S^1(R_0)$. Altogether, we consider the following 10-dimensional background in heterotic or type II superstring,

$$S^1(R_0) \times T^{d-1}(R_{\rm box}) \times S^1(R_d) \times \mathcal{M}_{10-d-2} \times S^1(R_9), \tag{4.1}$$

where $R_0 \gg 1$ and $R_9 \gg 1$, while the remaining radii R_I of the internal manifold $\mathcal{M}_{10-d-2}$ satisfy

$$\frac{1}{R_0} \ll R_I \ll R_0 \qquad \text{and} \qquad \frac{1}{R_9} \ll R_I \ll R_9 \qquad (I \neq d). \tag{4.2}$$

Since we do not consider a $\mathbb{Z}_2$ orbifold action on $S^1(R_9)$, we are actually considering models in case (I), in the notations of section 3 (see [5] for other cases).

Due to the T-duality on $S^1(R_d)$, $Z_{1-\rm loop}$ admits a symmetry $R_d \to 1/R_d$ that relates the regime $R_d \geq 1$ to $R_d \leq 1$. When $R_d \gg 1$, the light states are the KK modes along the directions $S^1(R_0)$, $S^1(R_9)$ and $S^1(R_d)$. As in section 3.2, their contribution to $Z_{1-\rm loop}$ involves two complex structures, say R_0/R_9 and R_9/R_d. On the contrary, when R_d approaches 1 from above, not only the winding but also the KK modes along $S^1(R_4)$ cease to contribute substantially, since their mass is 1 (in $\sqrt{\alpha'}$ units), up to a numerical factor. However, in heterotic string theory, this numerical factor happens to be 0 for the particular modes whose winding and momentum numbers are $\tilde{m}_d = n_d = \pm 1$ (the extended gauge symmetry point $U(1) \to SU(2)$ at $R_d = 1$). In other words, while these specific states are super massive for generic values of R_d, their KK towers along $S^1(R_0)$, $S^1(R_9)$ do contribute when $R_d \simeq 1$. Defining

$$e^z := \frac{R_0}{R_9}\,, \qquad e^\eta := R_9\,, \qquad e^\zeta := R_d, \tag{4.3}$$

and dropping terms that are exponentially suppressed in any regime of R_d, the string partition is found to be

$$Z_{1-\rm loop} = \beta V_{\rm box}\, \frac{1}{(2\pi R_0)^d}\, p(z,\eta,\zeta), \tag{4.4}$$

where p can be expressed in one way or another as,

$$
\begin{aligned}
p(z,\eta,\zeta) &= n_T\,\left[\hat{f}_T^{(d)}(z)+k_T^{(d)}(z,\eta-|\zeta|)\right]+n_V\,\left[\hat{f}_V^{(d)}(z)+k_V^{(d)}(z,\eta-|\zeta|)\right] \\
&\quad+\tilde{n}_T\,g_T^{(d)}(z,\eta,|\zeta|)+\tilde{n}_V\,g_V^{(d)}(z,\eta,|\zeta|) \\
&= e^{|\zeta|-\eta-z}\left[n_T\,f_T^{(d+1)}(z,\eta-|\zeta|)+n_V\,f_V^{(d+1)}(z,\eta-|\zeta|)\right] \\
&\quad+\tilde{n}_T\,g_T^{(d)}(z,\eta,|\zeta|)+\tilde{n}_V\,g_V^{(d)}(z,\eta,|\zeta|).
\end{aligned}
\tag{4.5}
$$

Note that p is an even function of ζ, as follows from T-duality $R_d \to 1/R_d$. n_T is the number of massless states for generic R_d, while n_V is the difference between the numbers of bosons and fermions which are massless. $\tilde{n}_T$ is the number of additional massless states at the self-dual point $R_d = 1$ and $\tilde{n}_V = \tilde{n}_T$ because these modes are bosons. Physically, the KK reduction of the 10-dimensional metric tensor along $S^1(R_d)$ provides generically an $U(1)$ gauge theory, which is enhanced to $SU(2)$ when $(R_d - 1/R_d)$, interpreted as a Higgs VEV, vanishes. The properties of the functions $g_T^{(d)}$ and $g_V^{(d)}$ is precisely to interpolate between the different massless spectra ($U(1)$ *versus* $SU(2)$). They are not functions of two complex structures z and $\eta-|\zeta|$ only, since the string scale $\sqrt{\alpha'}$ is entering the game. The definitions of the various functions appearing in Eq. (4.5) are

$$
\begin{aligned}
\hat{f}_T^{(d)}(z) &= \frac{\Gamma\left(\frac{d+1}{2}\right)}{\pi^{\frac{d+1}{2}}}\sum_{\tilde{k}_0,\tilde{k}_9}\frac{e^{dz}}{\left[e^{2z}(2\tilde{k}_0+1)^2+(2\tilde{k}_9)^2\right]^{\frac{d+1}{2}}}\,, \\
k_T^{(d)}(z,\eta-|\zeta|) &= {\sum_{m_d}}'|m_d|^{\frac{d+1}{2}}e^{\frac{d+1}{2}(\eta-|\zeta|)}e^{dz}\sum_{\tilde{k}_0,\tilde{k}_9}\frac{2K_{\frac{d+1}{2}}\left(2\pi|m_d|e^{\eta-|\zeta|}\sqrt{e^{2z}(2\tilde{k}_0+1)^2+(2\tilde{k}_9)^2}\right)}{\left[e^{2z}(2\tilde{k}_0+1)^2+(2\tilde{k}_9)^2\right]^{\frac{d+1}{4}}}\,, \\
g_T^{(d)}(z,\eta,|\zeta|) &= \left(e^{2|\zeta|}-1\right)^{\frac{d+1}{2}}e^{\frac{d+1}{2}(\eta-|\zeta|)}e^{dz}\sum_{\tilde{k}_0,\tilde{k}_9}\frac{2K_{\frac{d+1}{2}}\left(2\pi(e^{2|\zeta|}-1)e^{\eta-|\zeta|}\sqrt{e^{2z}(2\tilde{k}_0+1)^2+(2\tilde{k}_9)^2}\right)}{\left[e^{2z}(2\tilde{k}_0+1)^2+(2\tilde{k}_9)^2\right]^{\frac{d+1}{4}}}\,, \\
f_T^{(d+1)}(z,\eta-|\zeta|) &= \frac{\Gamma\left(\frac{d}{2}+1\right)}{\pi^{\frac{d}{2}+1}}\sum_{\tilde{k}_0,\tilde{k}_9,\tilde{m}_d}\frac{e^{(d+1)z}}{\left[e^{2z}(2\tilde{k}_0+1)^2+(2\tilde{k}_9)^2+e^{-2(\eta-|\zeta|)}\tilde{m}_d^2\right]^{\frac{d}{2}+1}}\,,
\end{aligned}
\tag{4.6}
$$

with the remaining ones given as

$$\hat{f}_V^{(d)}(z) = e^{(d-1)z}\,\hat{f}_T^{(d)}(-z), \qquad k_V^{(d)}(z,\eta-|\zeta|) = e^{(d-1)z}\,k_T^{(d)}(-z,\eta-|\zeta|+z),$$
$$g_V^{(d)}(z,\eta,|\zeta|) = e^{(d-1)z}\,g_T^{(d)}(-z,\eta+z,|\zeta|), \quad f_V^{(d+1)}(z,\eta-|\zeta|) = e^{dz}\,f_T^{(d+1)}(-z,\eta-|\zeta|+z). \tag{4.7}$$

In the type II case, the partition function takes formally the form of the heterotic one, with $\tilde{n}_T = \tilde{n}_V = 0$. This is due to the fact that in type II, there is no enhancement of symmetry at $R_d = 1$.

Treating the circle $S^1(R_d)$ as an internal direction, the dimensional reduction from 10 to d dimensions involves the metric and dilaton field ϕ_d in d dimensions, together with the scalars η and ζ,

$$S = \int d^dx\sqrt{-g}\left(\frac{R}{2} - \frac{1}{2}(\partial\Phi)^2 - \frac{1}{2}(\partial\phi_\perp)^2 - \frac{1}{2}(\partial\zeta)^2 - \mathcal{F}\right), \tag{4.8}$$

where we have defined the normalized fields

$$\Phi := \frac{2}{\sqrt{(d-2)(d-1)}}\,\phi_d - \sqrt{\frac{d-2}{d-1}}\,\eta\,, \qquad \phi_\perp := \frac{2}{\sqrt{d-1}}\,\phi_d + \frac{1}{\sqrt{d-1}}\,\eta\,. \tag{4.9}$$

The 1-loop free energy density $\mathcal{F} = -Z_{1-\text{loop}}/(\beta V_{\text{box}})$ depends on the temperature T, the supersymmetry breaking scale M (*i.e.* Φ), ζ and implicitly on $\phi_\perp$ via η,

$$\mathcal{F} = -T^d\,p(z,\eta,\zeta)\,, \qquad e^z = \frac{M}{T}\,, \qquad T = \frac{e^{\frac{2\phi_d}{d-2}}}{2\pi R_0}\,, \qquad M = \frac{e^{\frac{2\phi_d}{d-2}}}{2\pi R_9} \equiv \frac{e^{\sqrt{\frac{d-1}{d-2}}\Phi}}{2\pi}. \tag{4.10}$$

As usually, a FLRW ansatz for the metric and time-dependent scalars yields a stress-tensor whose thermal energy density and pressure are

$$P = T^d\,p(z,\eta,\zeta) \qquad \text{and} \qquad \rho = T^d\,r(z,\eta,\zeta)\,, \quad r = (d-1)p - p_z. \tag{4.11}$$

Among the five independent equations of motions, we are particularly interested in the equation for ζ,

$$\ddot{\zeta} + (d-1)H\dot{\zeta} - \frac{\partial P}{\partial\zeta} = 0, \tag{4.12}$$

whose potential $-P$, as a function of ζ (the over fields held fixed), is shown on Fig. 3 (when $z < 0$ *i.e.* $R_0 < R_9$). In the heterotic case, the profile of $-P$ can be divided in five phases, while in type II models the range I is reduced to a single point. The behavior in phase III (phase V) is exponentially decreasing (increasing), while when $z > 0$ and large enough, it is exponentially increasing (decreasing).

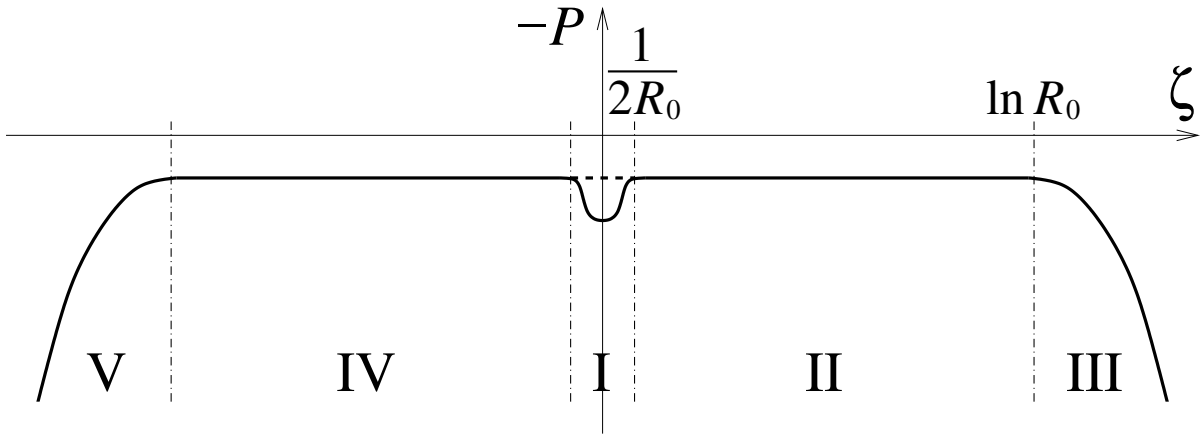

Figure 3: *Qualitative shape of the thermal effective potential $-P$ of $\zeta = \ln R_d$ (the other variables held fixed, with $z < 0$). There are five phases in the heterotic models, while the range* I *is reduced to a single point in type II. When $z > 0$, one has to replace R_0 by R_9 in the boundaries of the ranges and if z is large enough, phase* III *(*V*) is increasing (decreasing).*

heterotic models

- **I : Higgs phase,** $\left|R_d - \frac{1}{R_d}\right| < \frac{1}{R_0}$ and/or $\frac{1}{R_9}$.

  The functions $k_T^{(d)}$ and $k_V^{(d)}$ in the first expression of Eq. (4.5) are exponentially suppressed and can be neglected. Since p is an even function of ζ, we have at the origin $p_\zeta = 0$ so that $\zeta(t) \equiv 0$ is a solution to (4.12). It follows that the pressure is drastically simplified, since

  $$p(z, \eta, 0) = (n_T + \tilde{n}_T)\, \hat{f}_T^{(d)}(z) + (n_V + \tilde{n}_V)\, \hat{f}_V^{(d)}(z) := \tilde{p}(z)\,, \tag{4.13}$$

  i.e. does not depend on η. Thus, the analysis of the particular solution $\zeta \equiv 0$ brings us back to the study of section 3.1, once generalized in d dimensions. We conclude that when

  $$-\frac{1}{2^d - 1} < \frac{n_V + \tilde{n}_V}{n_T + \tilde{n}_T} < 0, \tag{4.14}$$

  there exists an RDS^d (Radiation Dominated Solution in d dimensions). The behavior of the first order fluctuations around this solution are found to be exponentially damped. As a result, the RDS^d is a local attractor of the dynamics and R_d is stabilized at the self-dual point of enhanced symmetry.

- **II : Flat potential phase,** $\frac{1}{R_0}$ and $\frac{1}{R_9} < R_d - \frac{1}{R_d} < R_0$ and R_9.

As in phase I, $k_T^{(d)}$ and $k_V^{(d)}$ in Eq. (4.5) can be neglected. Indeed, by definition, phase II starts when the functions $g_T^{(d)}$ and $g_V^{(d)}$ responsible for the interpolation between the generic and the enhanced massless spectra are exponentially suppressed as well. It follows that p is independent of η and ζ,

$$p(z,\eta,\zeta) \simeq n_T\, \hat{f}_T^{(d)}(z) + n_V\, \hat{f}_V^{(d)}(z) := \hat{p}(z)\,. \tag{4.15}$$

Consequently, any $\zeta(t) \equiv \zeta_0$ when ζ is in the range II solves Eq. (4.12). For any given ζ_0, we are back again to the analysis of section 3.1 and a particular RDS^d exists when

$$-\frac{1}{2^d-1} < \frac{n_V}{n_T} < 0. \tag{4.16}$$

Small perturbations around such an RDS^d are found to the damped, even if the potential for ζ is flat. Actually, the fluctuations of ζ around any ζ_0 are suppressed due to the presence of "gravitational friction" in (4.12). In this sense, one can conclude that ζ is marginally stabilized.

- **III : Higher dimensional phase,** R_0 and/or $R_9 < R_d$.

As in phase II, $g_T^{(d)}$ and $g_V^{(d)}$ in Eq. (4.5) can be neglected. However, by definition, phase III starts when the functions $k_T^{(d)}$ and/or $k_V^{(d)}$ cease to be exponentially suppressed. In particular, when $R_d \gg R_0$ and R_9, one finds, using the second form of Eq. (4.5),

$$p(z,\eta,\zeta) \simeq e^{|\zeta|-\eta-z}\left(n_T\, \hat{f}_T^{(d+1)}(z) + n_V\, \hat{f}_V^{(d+1)}(z) + e^{d(z+\eta-|\zeta|)}(n_T+n_V)\frac{S_d^{oe}}{4}\right)\,, \tag{4.17}$$

where $S_d^{oe} = \frac{\Gamma\left(\frac{d}{2}\right)}{\pi^{\frac{d}{2}}}\sum_m{}' \frac{1}{|m|^d}$. The term $e^{d(z+\eta-|\zeta|)} = (R_0/R_d)^d$ is power-like subdominant and exponentially small terms have been ignored.

Neglecting the small contribution $(R_0/R_d)^d$, the appearance of the functions $\hat{f}_T^{(d+1)}$ and $\hat{f}_V^{(d+1)}$ in p indicate that it is more natural to reconsider the system from a $(d+1)$-dimensional point of view. Regarding $S^1(R_4)$ as part of the space-time, R_4 is no longer an internal modulus but a component of the metric, $g_{st,dd} = (2\pi R_d)^2$. Denoting with primes all quantities in $d+1$ dimensions, the vacuum-to-vacuum energy density in the effective action in higher dimension, $Z_{1-\text{loop}}/(\beta V_{\text{box}} 2\pi R_d)$, is giving rise to can a pressure $P' = T'^{(d+1)}\, p'(z,\eta,\zeta)$, where

$$p'(z,\eta,\zeta) \simeq n_T\, \hat{f}_T^{(d+1)}(z) + n_V\, \hat{f}_V^{(d+1)}(z) := \hat{p}'(z)\,. \tag{4.18}$$

One more time, one concludes from the analysis of section 3.1 that an RDS^{d+1} with isotropic metric exists if

$$-\frac{1}{2^{d+1}-1} < \frac{n_V}{n_T} < 0. \tag{4.19}$$

By isotropic metric, we mean that

$$e^{\xi} := b/a' = R_d/R_{\rm box}, \tag{4.20}$$

where a' is the scale factor in the directions $1, \ldots, d-1$ and b is the scale factor in the direction d, satisfies $\xi(t) \equiv \xi_0$, a constant determined by the I.B.C.. Small perturbations around such a solution are shown to converge to zero. Since $\xi(t)$ measures the anisotropy of the local metric, one concludes that the attracting RDS^{d+1} is characterized by an enhanced spatial rotation group $SO(d-1) \to SO(d)$. The ratio e^{ξ_0} is interpreted as a "complex structure" of the "external space" we live in.

On the contrary, whenever the contribution $(R_0/R_d)^d$ in Eq. (4.17) is not negligible, we find it yields a "residual force" such that even though $\zeta(t)$ *i.e.* $R_d(t)$ is increasing, it is always caught by $R_9(t)$ and $R_0(t)$. Thus, the dynamics exits phase III and the system enters into region II, where the solution is attracted to an RDS^d.

- **IV : Dual flat potential phase,** $\frac{1}{R_0}$ and $\frac{1}{R_9} < \frac{1}{R_d} - R_d < R_0$ and R_9.

  This region is the T-dual of phase II and has the same behavior, with $\zeta \to -\zeta$. The light states that contribute to $\mathbb{Z}_{1-\rm loop}$ are the windings modes along $S^1(R_d)$ instead of the KK excitations.

- **V : Dual higher dimensional phase,** R_0 and/or $R_9 < \frac{1}{R_d}$.

  This region is the T-dual of phase III and has the same behavior, with $\zeta \to -\zeta$.

To summarize, when the Kähler modulus $R_d(t)$ is internal, it is attracted to the intersection of the ranges $1/R_i(t) < R_d(t) < R_i(t)$ $(i = 0, 9)$ and ends by being marginally stabilized or stabilized at $R_d = 1$. On the contrary, when $R_d(t)$ is large enough, the Universe is $(d+1)$-dimensional and R_d expands and runs away, with $R_d(t) \propto R_{\rm box}(t)$. It is then better understood in terms of the complex structure $R_d/R_{\rm box}$, which is marginally stabilized.

type II superstring models

As said before, there is no enhanced symmetry point at $R_d = 1$ in the type II superstring models. Thus, their analysis can be derived from the heterotic one by taking $\tilde{n}_T = \tilde{n}_V = 0$. Since the local minimum of $-P$ at $\zeta = 0$ is not present anymore, the plateaux II and IV on Fig. 3 are connected.

However, we expect by heterotic-type II duality that an Higgs phase I should exist in type II superstring at the non-perturbative level. A possible setup to describe this effect is to consider a pair of D-branes, whose distance is dual to the modulus R_d. In this context, our Universe is a "brane-world", whose spatial directions are parallel to the D-branes. The stabilization of R_d at the self-dual point on the heterotic side should imply the non-perturbative thermal effective potential in type II to force the D-branes to stay on top of each other, thus producing an $U(1) \to SU(2)$ enhancement. However, this attraction between the D-branes should only be local, since if they are separated enough so that the dual modulus R_d enters phase II, the thermal effective potential should allow stable finite distances between the D-branes. If the distance between the D-branes is very large, the force between them will be repulsive and the expanding Universe develops one more dimension.

An alternative non-perturbative type II set up realizing a gauge group enhancement involves singularities in the internal space. For example, a type IIA D2-brane wrapped on a vanishing 2-sphere whose radius is dual to R_d produces an $SU(2)$ gauge theory. It also admits a mirror description in type IIB [22]. The equivalence between the brane-world and geometrical singularity pictures can be analyzed along the lines of Ref. [23].

5 Conclusions and Perspectives

In this review, we describe some basics of early Universe cosmology in the framework of string theory. We first place the $(d-1)$-dimensional space in a very large box, while much smaller compactified directions span an internal space. To introduce temperature, we consider the Euclidean version of the background, where appropriate boundary conditions are imposed along the Euclidean time circle. Supersymmetry breaking is implemented in a similar way by choosing non-trivial boundary conditions along internal compact directions. In four dimensions, we analyze models where $\mathcal{N} = 4, 2, 1$ supersymmetry is spontaneously broken. The advantage of string theory is to cure all UV diverges encountered in field theory.

In this work, we restrict our study to the intermediate times $t_E \ll t \ll t_W$ *i.e.* after the end of the Hagedorn era and before the electroweak phase transition. The pressure and energy density of the gas of strings are computed from a microscopic point of view, using the 1-loop Euclidean string partition function. We then study the solutions of the low energy effective action and find that the quasi-static evolutions are attracted to Radiation Dominated Solutions. During the convergence to an RDS, there is no inflation (or a very tiny amount). However, interesting effects can occur. Internal radii that are participating into the spontanoues breaking of supersymmetry can be decompactified dynamically and lead to a change in the dimension of space-time. Moreover, the internal radii that are not participating in the spontaneous breaking of supersymmetry are stabilized. In general, the Universe tends to increase spontaneously its symmetries: The gauge symmetries or the local isotropy. Usually, the field theory description of the full evolution is in term of a succession of *different* field theories. The underlying string theory is required to connect them.

To go further, lots of work is still needed to unravel some experimental predictions from our framework. In four dimensions, models with spontaneously broken $\mathcal{N} = 1$ supersymmetry are particularly interesting, since they can include chiral matter. Dealing with them is under progress, in order to go beyond t_W. To do that, one needs to compute the radiative corrections to the different fields entering the action. Only after this full work is accomplished, it becomes possible to discuss what happens in the matter dominated era, and observe if a late time inflation era can exist. There are strong beliefs that $\mathcal{N} = 1$ models will produce a non zero cosmological constant.

Another direction of work concerns the relaxation of the homogeneity assumption. We could thus deal with the issues of entropy production and adiabaticity. On simpler grounds, it could be interesting to show that small initial homogeneities disappear and that the standard FLRW ansatz is an attractor in the space of backgrounds.

Finally, an important issue to examine is the existence of *a mechanism alternative to inflation* during the Hagedorn era. There are already some proposals in this direction in Ref. [16]. Preliminary results by some of the authors indicate that such a mechanism is plausible for non-pathological sting vacua, where the Hagedorn transition is resolved [18, 19].

Acknowledgements

The authors would like to thank NOVA publishers for giving us the opportunity to write this review. We are grateful to N. Toumbas for useful discussions. H.P. thanks the Ecole Normale Supérieure for hospitality.
This work is partially supported by the ANR (CNRS-USAR) contract 05-BLAN-0079. The work of F.B, J.E. and H.P is supported by the European contracts PITN-GA-2009-237920, ERC-2008-AdG 20080228, the CNRS PICS contracts 3747, 4172 and the INTAS grant 03-51-6346. J.E. acknowledges financial support from the Groupement d'Intérêt Scientifique P2I.

References

[1] C. Kounnas and H. Partouche, "Instanton transition in thermal and moduli deformed de Sitter cosmology," Nucl. Phys. B **793** (2008) 131 [arXiv:0705.3206 [hep-th]];

C. Kounnas and H. Partouche, "Inflationary de Sitter solutions from superstrings," Nucl. Phys. B **795** (2008) 334 [arXiv:0706.0728 [hep-th]].

[2] T. Catelin-Jullien, C. Kounnas, H. Partouche and N. Toumbas, "Thermal/quantum effects and induced superstring cosmologies," Nucl. Phys. B **797** (2008) 137 arXiv:0710.3895 [hep-th];

T. Catelin-Jullien, C. Kounnas, H. Partouche and N. Toumbas, "Thermal and quantum superstring cosmologies," Fortsch. Phys. **56** (2008) 792 [arXiv:0803.2674 [hep-th]].

[3] T. Catelin-Jullien, C. Kounnas, H. Partouche and N. Toumbas, "Induced superstring cosmologies and moduli stabilization," arXiv:0901.0259 [hep-th].

[4] F. Bourliot, C. Kounnas and H. Partouche, "Attraction to a radiation-like era in early superstring cosmologies," Nucl. Phys. B **816** (2009) 227 [arXiv:0902.1892 [hep-th]];

F. Bourliot, J. Estes, C. Kounnas and H. Partouche, "Cosmological Phases of the String Thermal Effective Potential," arXiv:0908.1881 [hep-th].

[5] J. Estes, C. Kounnas and H. Partouche, "Superstring cosmology for $\mathcal{N}_4 = 1 \to 0$ superstring vacua," LPTENS–09/32, CPHT–RR080.0709 in print.

[6] T. Morii, C.S. Lim, S.N. Mukherjee, "The physics of the standard model and beyond," (World Scientific, 2004).

[7] J. Polchinski, "String Theory," **Vol. 1** & **2**, (Cambridge University press, 2001).

[8] S. Perlmutter, "A study of 42 type Ia supernovae and a resulting measurement of Omega(M) and Omega(Lambda)," Physics Reports-Review section of Physics Letters **307 (1-4)**: 325-331 (1998).

[9] P.J.E. Peebles, "Principles of Physical Cosmology," (Princeton series in Physics, 1993).

[10] R.M. Wald, "General Relativity," (The University of Chicago Press, 1984).

[11] F. Bourliot, P. G. Ferreira, D. F. Mota and C. Skordis, "The cosmological behavior of Bekenstein's modified theory of gravity," Phys. Rev. D **75** (2007) 063508 [arXiv:astro-ph/0611255].

[12] H. Zhao, "Constraining TeVeS gravity as effective dark matter and dark energy," Int. J. Mod. Phys. D **16** (2008) 2055 [arXiv:astro-ph/0610056].

[13] R. Hagedorn, "Statistical thermodynamics of strong interactions at high-energies," Nuovo Cim. Suppl. **3**, 147 (1965);

K. Huang and S. Weinberg, "Ultimate temperature and the early universe," Phys. Rev. Lett. **25**, 895 (1970);

B. Sathiapalan, "Vortices on the string world sheet and constraints on toral compactification," Phys. Rev. D **35**, 3277 (1987);

Y. I. Kogan, "Vortices on the world sheet and string's critical dynamics," JETP Lett. **45**, 709 (1987) [Pisma Zh. Eksp. Teor. Fiz. **45**, 556 (1987)];

M. Axenides, S. D. Ellis and C. Kounnas, "Universal behavior of D-dimensional superstring models," Phys. Rev. D **37**, 2964 (1988);

D. Kutasov and N. Seiberg, "Number of degrees of freedom, density of states and tachyons in string theory and CFT," Nucl. Phys. B **358** (1991) 600.

[14] J. Atick and E. Witten, "The Hagedorn transition and the number of degrees of freedom of string theory," Nucl. Phys. B **310**, 291 (1988).

[15] C. Kounnas and B. Rostand, "Coordinate dependent compactifications and discrete symmetries," Nucl. Phys. B **341** (1990) 641.

[16] A. Nayeri, R. H. Brandenberger and C. Vafa, "Producing a scale-invariant spectrum of perturbations in a Hagedorn phase of string cosmology,' Phys. Rev. Lett. **97**, 021302 (2006) [arXiv:hep-th/0511140];

R. H. Brandenberger, A. Nayeri, S. P. Patil and C. Vafa, "Tensor modes from a primordial Hagedorn phase of string cosmology," Phys. Rev. Lett. **98**, 231302 (2007) [arXiv:hep-th/0604126];

R. H. Brandenberger, A. Nayeri, S. P. Patil and C. Vafa, "String gas cosmology and structure formation," Int. J. Mod. Phys. A **22**, 3621 (2007) [arXiv:hep-th/0608121];

R. H. Brandenberger, "Alternatives to cosmological inflation," arXiv:0902.4731 [hep-th].

[17] I. Antoniadis and C. Kounnas, "Superstring phase transition at high temperature," Phys. Lett. B **261** (1991) 369;

I. Antoniadis, J. P. Derendinger and C. Kounnas, "Non-perturbative supersymmetry breaking and finite temperature instabilities in $\mathcal{N} = 4$ superstrings," arXiv:hep-th/9908137;

C. Kounnas, "Universal thermal instabilities and the high-temperature phase of the $\mathcal{N} = 4$ superstrings," arXiv:hep-th/9902072.

[18] C. Angelantonj, C. Kounnas, H. Partouche and N. Toumbas, "Resolution of Hagedorn singularity in superstrings with gravito-magnetic fluxes," Nucl. Phys. B **809** (2009) 291 [arXiv:0808.1357 [hep-th]].

[19] C. Kounnas, "Massive boson–fermion degeneracy and the early structure of the universe," Fortsch. Phys. **56** (2008) 1143 [arXiv:0808.1340 [hep-th]];

I. Florakis and C. Kounnas, "Orbifold symmetry reductions of massive boson-fermion degeneracy," Nucl. Phys. B **820** (2009) 237 [arXiv:0901.3055 [hep-th]].

[20] J. R. Ellis, C. Kounnas and D. V. Nanopoulos, "No scale supersymmetric GUTs," Nucl. Phys. B **247** (1984) 373;

J. R. Ellis, C. Kounnas and D. V. Nanopoulos, "Phenomenological $SU(1,1)$ supergravity," Nucl. Phys. B **241** (1984) 406;

J. R. Ellis, A. B. Lahanas, D. V. Nanopoulos and K. Tamvakis, "No-scale supersymmetric standard model," Phys. Lett. B **134**, 429 (1984).

[21] J. Scherk and J. H. Schwarz, "Spontaneous breaking of supersymmetry through dimensional reduction," Phys. Lett. B **82** (1979) 60;

R. Rohm, "Spontaneous supersymmetry breaking in supersymmetric string theories," Nucl. Phys. B **237** (1984) 553;

C. Kounnas and M. Porrati, "Spontaneous supersymmetry breaking in string theory," Nucl. Phys. B **310** (1988) 355;

S. Ferrara, C. Kounnas, M. Porrati and F. Zwirner, "Superstrings with spontaneously broken supersymmetry and their effective theories," Nucl. Phys. B **318** (1989) 75.

[22] A. Strominger, "Massless black holes and conifolds in string theory," Nucl. Phys. B **451** (1995) 96 [arXiv:hep-th/9504090];

S. Kachru and C. Vafa, "Exact results for $\mathcal{N} = 2$ compactifications of heterotic strings," Nucl. Phys. B **450** (1995) 69 [arXiv:hep-th/9505105];

I. Antoniadis and H. Partouche, "Exact monodromy group of $\mathcal{N} = 2$ heterotic superstring," Nucl. Phys. B **460** (1996) 470 [arXiv:hep-th/9509009];

H. Partouche, "Non perturbative check of $\mathcal{N} = 2$, $D = 4$ heterotic/type II duality," Nucl. Phys. Proc. Suppl. **55B** (1997) 210 [arXiv:hep-th/9610119].

[23] P. Kaste and H. Partouche, "On the equivalence of $\mathcal{N} = 1$ brane worlds and geometric singularities with flux," JHEP **0411** (2004) 033 [arXiv:hep-th/0409303].

Annexe F

Publication 4 : F. Bourliot, J. Estes, P. M. Petropoulos and Ph. Spindel, "Gravitational instantons, self-duality and geometric flows," Phys. Rev. D 81 (2010) 104001 [arXiv :0906.4558 [hep-th]].

PHYSICAL REVIEW D **81,** 104001 (2010)

Gravitational instantons, self-duality, and geometric flows

F. Bourliot, J. Estes, and P. M. Petropoulos
Centre de Physique Théorique, CNRS–UMR 7644, Ecole Polytechnique, 91128 Palaiseau Cedex, France

Ph. Spindel
Service de Mécanique et Gravitation, Université de Mons–Hainaut, 20 Place du Parc, 7000 Mons, Belgium
(Received 12 September 2009; published 3 May 2010)

We discuss four-dimensional "spatially homogeneous" gravitational instantons. These are self-dual solutions of Euclidean vacuum Einstein equations. They are endowed with a product structure $\mathbb{R} \times \mathcal{M}_3$ leading to a foliation into three-dimensional subspaces evolving in Euclidean time. For a large class of homogeneous subspaces, the dynamics coincides with a geometric flow on the three-dimensional slice, driven by the Ricci tensor plus an $\mathfrak{so}(3)$ gauge connection. The flowing metric is related to the vielbein of the subspace, while the gauge field is inherited from the anti-self-dual component of the four-dimensional Levi-Civita connection.

DOI: 10.1103/PhysRevD.81.104001 PACS numbers: 04.20.−q, 02.40.−k

The aim of the present paper is to report on an intriguing and potentially important relationship between four-dimensional self-dual gravitational instantons and three-dimensional geometric flows. The framework is that of four-dimensional Euclidean geometry $\mathcal{M}_4$, which is topologically $\mathbb{R} \times \mathcal{M}_3$ with leaves $\mathcal{M}_3$ assumed to be homogeneous spaces of Bianchi type.

Gravitational instantons are classical solutions of general relativity and potential tools to handle quantum transitions; they are also important ingredients of strings and branes, entering in various symmetry-breaking schemes. Many solutions of Einstein's equations were made available in the late 1970's (see e.g. [1–5]); however, no criterion has ever been presented that allows one to foresee, according to an elegant, unified and comprehensive pattern, the expected classes of Bianchi solutions. In this paper we present such a criterion, with possible applications to more general situations.

On the other side, geometric flows of three-dimensional homogeneous spaces are interesting in their own right; they turned out to play a role in Hamilton's program for proving Poincaré's and Thurston's conjectures. A relevant question is to ask whether and how this flow behavior of one-parameter families of three-dimensional spaces is related to the Euclidean-time evolution inside a gravitational instanton, where the homogeneous spaces appear as the leaves of the foliation. This question is motivated by several facts.

First, Ricci-flow equations are renormalization-group equations for two-dimensional sigma models, with $t \propto -\log\mu$ the renormalization-group time [6–9]. Setting a relation between the latter and the Euclidean time of a gravitational instanton would be one more indication in favor of the dynamical generation of time in string theory—similar in spirit to the role of the Liouville field in noncritical strings. Second, it was noticed, but overlooked as a coincidence in [10,11], that some Ricci-flow interpretation may exist for a particular class of Bianchi IX metrics. Geometric-flow first-order equations also emerge as classical equations of motion in modified Einstein gravity [12] as a consequence of a Bogomol'nyi-Prasad-Sommerfield–like condition (the detailed balance). It is thus legitimate to ask whether a self-duality condition could have a similar effect, on more general grounds, under appropriate homogeneity and foliation assumptions. Lastly, the governing of gravitational behavior by a first order equation is reminiscent of holographic situations. Along the lines of [13], we hope that the first order flow equations can ultimately be used to reconstruct the bulk fields from the boundary data.

The achievements we will exhibit are twofold. On the one hand, we show that real, nondegenerate, self-dual solutions exist only for unimodular Bianchi groups or for the one of type III, and are classified in terms of the homomorphisms of $\mathfrak{g} \to \mathfrak{so}(3)$, where $\mathfrak{g}$ is the real Lie algebra of the Bianchi group under consideration and $SO(3)$ the anti-self-dual factor of the group $SO(4)$. On the other hand, we observe that the self-duality requirement leads to first-order equations, which turn out to describe a geometric flow for three-dimensional Bianchi manifolds, driven by the Ricci tensor combined with a flat $SO(3)$ gauge field (tildes refer to three-dimensional tensors):

$$\frac{d\tilde{g}_{ij}}{dt} = -\tilde{R}_{ij} - \frac{1}{2}\,\mathrm{tr}(\tilde{A}_i\tilde{A}_j). \tag{1}$$

As already stated, we seek Euclidean four-dimensional spaces of the type $\mathcal{M}_4 = \mathcal{M}_3 \times \mathbb{R}$ with homogeneous spatial sections $\mathcal{M}_3$. The latter are assumed to be of Bianchi type: a three-dimensional group G acts simply transitively on the leaves, which are therefore endowed with the structure of a group manifold (hence we exclude H_3, $H_2 \times S^1$ or $S^2 \times S^1$). Unimodular groups are referred to as Bianchi A and consist of the Abelian three-

 © 2010 The American Physical Society

dimensional translation group, the Heisenberg group, $E(1,1)$, $E(2)$, $SL(2,\mathbb{R})$, and $SU(2)$. The metric for $\mathcal{M}_4$ can always be of the form

$$ds^2 = N^2 dT^2 + g_{ij}\sigma^i\sigma^j, \tag{2}$$

where $g_{ij}(T)$ are functions to be determined and σ^i are G-invariant forms. It is convenient to introduce an orthonormal frame $\{\theta^a, a = 0, 1, 2, 3 = \{0, \alpha\}\}$,

$$ds^2 = \delta_{ab}\theta^a\theta^b, \tag{3}$$

by setting

$$\theta^0 = NdT, \qquad \theta^\alpha = \Theta^\alpha{}_j\sigma^j \quad \text{with} \quad g_{ij} = \delta_{\alpha\beta}\Theta^\alpha{}_i\Theta^\beta{}_j, \tag{4}$$

where $\alpha, \beta, \ldots$ label orthonormal space indices. We will make the convenient gauge choice $N = \Theta = \sqrt{\det g_{ij}}$, and later use another "time" t defined as $dt = \Theta dT$.

Euclidean solutions to vacuum Einstein equations can be obtained by imposing (anti-)self-duality of the Riemann curvature twoform. This is a well-studied topic, and for reasons that will become clear, we would first like to elaborate. Spin connection and curvature forms belong to the antisymmetric **6** representation of $SO(4)$. In four dimensions, this group of local frame rotations factorizes as $SO(3)_{\rm sd} \otimes SO(3)_{\rm asd}$, and the connection ω_{ab} and curvature $\mathcal{R}_{ab}$ $SO(4)$-valued forms can be reduced with respect to the $SO(3)_{(a)sd}$ as $\mathbf{6} = (\mathbf{3}_{\rm sd}, \mathbf{3}_{\rm asd})$ [14]:

$$\begin{aligned} \Sigma_\alpha &= \frac{1}{2}\left(\omega_{0\alpha} + \frac{\epsilon_{\alpha\beta\gamma}}{2}\omega^{\beta\gamma}\right), \\ A_\alpha &= \frac{1}{2}\left(\omega_{0\alpha} - \frac{\epsilon_{\alpha\beta\gamma}}{2}\omega^{\beta\gamma}\right) \end{aligned} \tag{5}$$

for the connection, and similarly for the curvature which now reads

$$\begin{aligned} \mathcal{S}_\alpha &= d\Sigma_\alpha - \epsilon_{\alpha\beta\gamma}\Sigma^\beta \wedge \Sigma^\gamma, \\ \mathcal{A}_\alpha &= dA_\alpha + \epsilon_{\alpha\beta\gamma}A^\beta \wedge A^\gamma. \end{aligned} \tag{6}$$

The $\{\mathcal{S}_\alpha, \Sigma_\alpha\}$ are vectors of $SO(3)_{\rm sd}$ and singlets of $SO(3)_{\rm asd}$ and vice versa for $\{\mathcal{A}_\alpha, A_\alpha\}$.

Imposing that $\mathcal{S}_\alpha$ or $\mathcal{A}_\alpha$ be zero is sufficient to solve vacuum Einstein equations. We will focus here on the self-dual solutions; anti-self-dual solutions are obtained by $O(4)$ parity or time-reversal transformations.

First-order equations can be obtained by taking the spin connection A_α in (6) to be

$$A_\alpha = 0. \tag{7}$$

This first integral raises two questions: (i) does $A_\alpha = 0$ lead to *consistent* vacuum solutions, and (ii) is this unique? Concerning the second question, it is known that, barring global issues, if $\mathcal{A}_\alpha = 0$ one can always find an $SO(3)_{\rm asd}$ local transformation (see e.g. [2]) such that (7) holds in the rotated frame, which is no longer invariant though. This property opens a practical issue: if we insist on keeping the original invariant frame, we must allow for flat anti-self-dual parts in the connection. Listing all nonequivalent connections of this type will provide a classification of all possible spatially homogeneous self-dual instantons.

Both questions can be answered accurately. First, we can prove that Eq. (7) admits nondegenerate solutions, except at isolated points where the metric determinant may vanish, for the Bianchi A class and Bianchi III only. Second, we show that there are as many nonequivalent G-invariant connections A with vanishing anti-self-dual curvature $\mathcal{A}$ as homomorphisms of $\mathfrak{g} \to \mathfrak{so}(3)$. We will refer to them as *branches* of solutions, even though this distinction is to some extent bound to our requirement of invariant frame [16]. It will turn out that in every case there are two such branches. We define general $I_{\alpha i}$ such that $A_\alpha = \frac{1}{2}I_{\alpha i}\sigma^i$ and introduce this ansatz in $\mathcal{A}_\alpha = 0$ together with (2) and (4). The equations we obtain are [17]

$$\dot{\Theta}_{\alpha i} = \Theta_{\alpha j}[(n^{j\ell} - a_k\epsilon^{kj\ell})g_{\ell i} - \tfrac{1}{2}\delta^j_i n^{k\ell}g_{k\ell}] - \Theta I_{\alpha i} \tag{8}$$

(where the dot stands for a derivative with respect to T) plus a constraint on the constants of motion $I_{\alpha i}$,

$$I_{\alpha\ell}c^\ell{}_{jk} + \epsilon_{\alpha\beta\gamma}I^\beta{}_j I^\gamma{}_k = 0. \tag{9}$$

This constraint defines a homomorphism of $\mathfrak{g} \to \mathfrak{so}(3)$ and its solutions are classified in terms of these homomorphisms. By using appropriate transformations, one can bring the $I_{\alpha\ell}$ into a diagonal form with entries $\{\lambda_1, \lambda_2, \lambda_3\}$ taking the values 0 or 1.

To make contact with existing literature [5], we note that Eq. (9) can lead to imaginary solutions. These are related to homomorphisms of $\mathfrak{g}$ into real subalgebras of $\mathfrak{su}(2,\mathbb{C})$, which provide more freedom but *are not* genuine instantons. We summarize the various possibilities as follows:

Bianchi Class A.—The rank-zero homomorphism which maps $\mathfrak{g}$ to the null generator of $\mathfrak{so}(3)$ with $\lambda_i = 0$ is always available and leads to consistent solutions. There is always a second homomorphism (unique up to trivial algebra automorphisms), which is rank one in types I, II, VI_{-1}, and VII_0, where it maps one generator of $\mathfrak{g}$ onto one of $\mathfrak{so}(3)$ with a single nonvanishing λ_i; and rank three in type IX, where it is the isomorphism of $\mathfrak{g} \equiv \mathfrak{so}(3)$ to itself with all $\lambda_i = 1$. The case of VIII exhibits a rank-three homomorphism in $\mathbb{C}$—$\lambda_1 = 1$, $\lambda_2 = \lambda_3 = -i$—and corresponds to a real solution in a space with signature $(-,-,+,+)$. The case VI_{-1} similarly admits a rank-one homomorphism in $\mathbb{C}$: $\lambda_1 = i$, $\lambda_2 = \lambda_3 = 0$. These cases turn out to be necessary in setting the advertised relation with the Ricci flow of three-dimensional Bianchi spaces.

Bianchi Class B.—Only rank-zero and rank-one homomorphisms are *a priori* possible. However, they generally lead to singular metrics, except for a special case in Bianchi III, which requires a nondiagonal metric.

We now focus on the Bianchi A class, where we may always assume a diagonal coframe without restriction:

$\Theta_{\alpha i} = \gamma_i \delta_{\alpha i}$. With this simplification, we can turn to the interpretation of the Euclidean-time evolution in the above gravitational instantons as a geometric flow of a family of three-dimensional homogeneous spaces. For concreteness we carry out first a well-studied case, that of Bianchi IX [4]. We take $I_{\alpha i} = (1 - \tilde{\lambda})\delta_{\alpha i}$, with $\tilde{\lambda} = 0$ (isomorphism) corresponding to the Taub-NUT branch and $\tilde{\lambda} = 1$ (trivial homomorphism) to the Eguchi-Hanson branch. The self-duality equations (8) read [(i, j, k) are circular permutations of (1, 2, 3)]

$$2\frac{\dot{\gamma}_i}{\gamma_i} = (\gamma_j - \gamma_k)^2 - \gamma_i^2 + 2\tilde{\lambda}\gamma_j\gamma_k. \tag{10}$$

For the Taub-NUT branch ($\tilde{\lambda} = 0$) the observation (already made in [10,11]) is that Eqs. (10) are *Ricci-flow equations* for three-dimensional Bianchi IX geometries

$$d\tilde{s}^2 = \tilde{g}_{ij}\sigma^i\sigma^j = \delta_{\alpha\beta}\tilde{\theta}^\alpha\tilde{\theta}^\beta, \tag{11}$$

which are also of the diagonal type: $\tilde{g}_{ij}(t) = \delta_{ij}\gamma_i(t)$.

For the Eguchi-Hanson branch ($\tilde{\lambda} = 1$), the flowing three-dimensional geometries are again Bianchi IX with (11). Examining the self-duality equations (10), we now find in addition to the Ricci tensor an $\mathfrak{so}(3)$ gauge field $\tilde{A}$ on the flowing three-spheres. It originates from the Levi-Civita anti-self-dual connection A and reads

$$\tilde{A} = \tilde{A}_i\sigma^i = -\tilde{\lambda}\delta_{\alpha i}T^\alpha\sigma^i, \tag{12}$$

where T^α are the generators of $\mathfrak{so}(3)$ in the adjoint, satisfying $\mathrm{tr}(T^\alpha T^\beta) = -2\delta^{\alpha\beta}$. This $\mathfrak{so}(3)$ gauge field vanishes for the Taub-NUT case but is nonzero for the Eguchi-Hanson case. In both cases, however, its field strength is zero. With this field, Eq. (10) is recast as announced in the beginning:

$$\frac{d\tilde{g}_{ij}}{dt} = -\tilde{R}_{ij} - \frac{1}{2}\,\mathrm{tr}(\tilde{A}_i\tilde{A}_j). \tag{13}$$

The flow equation (13) follows directly from (8) with an $\mathfrak{so}(3)$ gauge field

$$\tilde{A} = -\tilde{I}_{\alpha i}T^\alpha\sigma^i. \tag{14}$$

As a consequence of (9), the $\tilde{I}_{\alpha i}$'s are subject to

$$\tilde{I}_{\alpha\ell}c^\ell{}_{jk} + \epsilon_{\alpha\beta\gamma}\tilde{I}^\beta{}_j\tilde{I}^\gamma{}_k = 0, \tag{15}$$

which is a flatness condition for $\tilde{A}$: $\tilde{F} = d\tilde{A} + [\tilde{A}, \tilde{A}] \equiv 0$. The gauge field is a *flat background field*: it does not flow ($\dot{\tilde{A}} = 0$) but contributes to the flow of the metric.

The above developments set a correspondence between the time evolution in self-dual gravitational instantons foliated with homogeneous leaves and the flow (parametric in time) evolution of homogeneous Bianchi IX spaces, valid for branches labeled by flat $\mathfrak{so}(3)$ connections over G. We now proceed to show that this correspondence holds for all Bianchi A classes. We illustrate this correspondence explicitly for the remaining Bianchi I, II, VI_{-1}, VII_0, and VIII classes. Hence, the corresponding three-manifolds $\mathcal{M}_3$ are endowed with a metric (11), where

$$\tilde{g}_{ij}(t) = \delta_{ij}\tilde{\gamma}_i(t). \tag{16}$$

Note that the correspondence does not take the three-dimensional part of the four-dimensional metric to be equal to the three-dimensional metric. Similarly, in the diagonal ansatz, we take (14) as an $\mathfrak{so}(3)$ gauge field with

$$\tilde{I}_{\alpha i} = \tilde{\lambda}_i\delta_{\alpha i}, \tag{17}$$

where $\tilde{\lambda}_i$ are subject to the constraints (15), recast as

$$\tilde{\lambda}_i c^i{}_{jk} + \epsilon_{ijk}\tilde{\lambda}_j\tilde{\lambda}_k = 0 \tag{18}$$

(no summation on i, j, k). Consequently, the geometric-flow equations obtained from (13) can be written as

$$\frac{\dot{\tilde{\gamma}}_i}{\tilde{\gamma}_i} = -\sum_{j,k=1}^{3}\frac{1}{4}[(c^i{}_{jk})^2\tilde{\gamma}_i^2 - 2(c^j{}_{ki})^2\tilde{\gamma}_j^2 + 2c^j{}_{ki}c^k{}_{ij}\tilde{\gamma}_j\tilde{\gamma}_k] + \tilde{\lambda}_i^2\frac{\tilde{\gamma}_1\tilde{\gamma}_2\tilde{\gamma}_3}{\tilde{\gamma}_i}, \tag{19}$$

where the dot stands for $\tilde{\gamma}_1\tilde{\gamma}_2\tilde{\gamma}_3\ d/dt$. Correspondingly, the self-duality equations (8) read

$$\frac{\dot{\gamma}_i}{\gamma_i} = \sum_{j,k=1}^{3}\frac{\epsilon_{ijk}}{2}\left[-\frac{c^i{}_{jk}}{2}\gamma_i^2 + \frac{1}{2}(c^j{}_{ki}\gamma_j^2 + c^k{}_{ij}\gamma_k^2)\right] + \lambda_i\frac{\gamma_1\gamma_2\gamma_3}{\gamma_i} \tag{20}$$

(as already quoted, here the dot stands for $\gamma_1\gamma_2\gamma_3\ d/dt$).

Each of the above equations has two branches. From the self-dual four-dimensional side, this is determined by each of the two nonequivalent homomorphisms of $\mathfrak{g} \to \mathfrak{so}(3)$, as a consequence of the flatness of the anti-self-dual Levi-Civita connection A. From the three-dimensional viewpoint, this corresponds to the two nonequivalent flat $\mathfrak{so}(3)$—G-invariant—connections $\tilde{A}$ over the group manifold G. This holds over the real numbers for Bianchi I, II, VII_0, and IX, whereas Bianchi VI_{-1} and VIII require us to pass to the complex i.e. change signature. In all Bianchi A spaces, the advertised correspondence holds as one-to-one for each class and each branch. It goes as follows: in cases I, II, VII_0, IX, we must set for the metric $\tilde{\gamma}_i = \gamma_i, \quad \forall\ i$, whereas there is a fine structure for the gauge field: $\tilde{\lambda}_i = \lambda_i \quad \forall\ i$ for I and II, and $\tilde{\lambda}_i = 1 - \lambda_i \quad \forall\ i$ for VII_0 and IX [18].

For VI_{-1} we find the correspondence $\{\tilde{\gamma}_1, \tilde{\gamma}_2, \tilde{\gamma}_3\} = \{i\gamma_1, i\gamma_2, \gamma_3\}$ for the metric coefficients, while for the connection, the coefficients $\{\lambda_i\}$ and $\{\tilde{\lambda}_i\}$ are interchanged as $\{0, 0, 0\} \leftrightarrow \{i, 0, 0\}$. Similarly, for VIII we find the correspondence $\{\tilde{\gamma}_1, \tilde{\gamma}_2, \tilde{\gamma}_3\} = \{\gamma_1, -i\gamma_2, -i\gamma_3\}$ with $\{\lambda_i\}$ and $\{\tilde{\lambda}_i\}$ interchanged as $\{0, 0, 0\} \leftrightarrow \{0, -i, -i\}$.

Because of their complex nature, the classes VI_{-1} and VIII are not interesting for gravitational instantons. They are nevertheless useful for setting the correspondence on universal grounds and may play a more physical role in the

search of self-dual solutions in a four-dimensional setting with signature $(-,-,++)$.

The correspondence described here, involving in three dimensions the "square root" of the four-dimensional metric, has a genuine intrinsic geometrical meaning, related to a remarkable scaling property of the Riemann tensor in three-dimensional homogeneous spaces [19]. It has, furthermore, some immediate consequences. For example, there is a potential application of the integrability properties of self-duality equations to tackle Ricci or related flows beyond the usual asymptotic analysis [20]. Another, more fundamental result is the appearance of a new and yet unravelled kind of flow, namely, Ricci flow in the presence of a gauge field. As it stands, this flow exhibits two intriguing features: the absence of evolution for $\tilde{A}$ and its flatness, both resulting from the flatness of the anti-self-dual four-dimensional Levi-Civita connection which in turn follows from the self-duality requirement.

More general flows with nonvanishing $\dot{\tilde{A}}$ and $\tilde{F}$ can be obtained by replacing the self-duality condition on the *Riemann* curvature with a milder one, still allowing a first-order time evolution without imposing that the anti-self-dual Levi-Civita connection be a pure gauge. This is possible by allowing for a *cosmological constant* in four dimensions. In this case, self-duality of the Riemann is traded for that of the Weyl tensor. The anti-self-dual part of the connection now explicitly depends on time, and the corresponding curvature is nonzero. This is illustrated in the celebrated solution of Fubini-Study for Bianchi IX. Translated in the three-dimensional side, the equation for the metric flow is still given by (13) but is now accompanied by a flow for $\tilde{A}$ and a constraint for $\tilde{F}$. The gauge field thus carries dynamics, which decouples when the cosmological constant is turned off.

As a conclusion we would like to make some final remarks and stress the role of each ingredient that we have used in setting the gravitational-instanton/geometric-flow correspondence. We worked in four dimensions, where the orthogonal group is factorized into two three-dimensional subgroups and all degrees of freedom are reduced as self-dual plus anti-self-dual. The foliation plus homogeneity assumption further introduces three-dimensional leaves and another three-dimensional group, G related to $SO(3)$ with nontrivial homomorphisms. Finally, the self-duality requirement effectively reduces the system to a three-dimensional one, whose dynamics turns out to be equivalent to a geometric flow on homogeneous three-manifolds endowed with an $\mathfrak{so}(3)$ gauge connection. Although the present scheme seems quite rigid, generalizations are possible in several ways. Self-duality can be directly implemented in seven dimensions and possibly generalized in higher dimensions in the sense of reducing degrees of freedom by trading second-order equations for first-order ones. Understanding the geometrical underpinnings of the correspondence, based on higher-dimensional flows, may give insight into such generalizations. Multi-instantons [15] provide another rich playground for extensions, although the absence of homogeneity may be an obstruction.

The authors would like to thank C. Bachas, I. Bakas, M. Berthelson, P. Bieliavsky, M. Carfora, D. Friedan, G. Gibbons, J. Isemberg, D. Lüst , A. Petkou, M.-T. Wang, and E. Woolgar for stimulating discussions. P. S. thanks the IHES and acknowledges financial support from IISN-Belgium (Convention No. 4.4511.06). J. E. acknowledges financial support from the GIS-P2I. This work was supported by the ANR Contract No. 05-BLAN-NT09-573739 and by CNRS-FNRS-CGRI-2009.

[1] E. T. Newman, L. Tamburino, and T. J. Unti, J. Math. Phys. (N.Y.) **4**, 915 (1963).
[2] T. Eguchi and A. J. Hanson, Ann. Phys. (N.Y.) **120**, 82 (1979).
[3] V. A. Belinsky, G. W. Gibbons, D. N. Page, and C. N. Pope, Phys. Lett. **76B**, 433 (1978).
[4] G. W. Gibbons and C. N. Pope, Commun. Math. Phys. **66**, 267 (1979).
[5] D. Lorenz, Acta Phys. Pol. **14**, 791 (1983).
[6] L. Alvarez-Gaumé, D. Z. Freedman, and S. Mukhi, Ann. Phys. (N.Y.) **134**, 85 (1981).
[7] E. Braaten, T. L. Curtright, and C. K. Zachos, Nucl. Phys. **B260**, 630 (1985).
[8] D. H. Friedan, Ann. Phys. (N.Y.) **163**, 318 (1985).
[9] H. Osborn, Ann. Phys. (N.Y.) **200**, 1 (1990).
[10] M. Cvetič, G. W. Gibbons, H. Lu, and C. N. Pope, Phys. Rev. D **65**, 106004 (2002).
[11] I. Bakas, D. Orlando, and P. M. Petropoulos, J. High Energy Phys. 01 (2007) 040.
[12] P. Horava, J. High Energy Phys. 03 (2009) 020.
[13] D. S. Mansi, A. C. Petkou, and G. Tagliabue, Classical Quantum Gravity **26**, 045008 (2009).
[14] The splitting into self-dual and anti-self-dual parts of the $SO(4)$ group acting on the tangent space spanned by the orthonormal vierbein is adapted to the slicing of $\mathcal{M}_4$ into the homogeneous space and the orthogonal direction. This choice is mandatory for revealing the geometric-flow interpretation (1). Metric representations other than (2) exist, such as the one used in [15], which are convenient for Bianchi IX generalizations like multicenter instantons, but not suitable for our purposes. We thank the referee for an interesting exchange on this issue.
[15] G. W. Gibbons and S. W. Hawking, Commun. Math. Phys. **66**, 291 (1979).

[16] For Bianchi IX, in the Gibbons-Hawking coordinates [15], the distinction between the Taub-NUT and Eguchi-Hanson solutions is less sharp because of the choice made of self-dual connections.

[17] The structure constants of Bianchi groups are given in terms of n^{ij} and a^i: $c^k{}_{ij} = \epsilon_{ij\ell} n^{\ell k} + \delta^k_j a_i - \delta^k_i a_j$. Here, we focus on unimodular groups, for which $a^i = 0$ and n^{ij} is diagonal: I (0, 0, 0), II (1, 0, 0), VI_{-1} (0, 1, −1), VII_0 (1, 1, 0), VIII (−1, 1, 1), and IX (1, 1, 1).

[18] Whenever $\exists i \neq j \neq k$ such that $c^i{}_{jk} c^k{}_{ij} \neq 0$, that is to say for Bianchi VII_0 and IX, as well as VI_{-1} and VIII, the branches are crossed.

[19] We plan to elaborate on this in a future communication.

[20] J. Isenberg and M. Jackson, J. Diff. Geom. **35**, 723 (1992).

Annexe G

Publication 5 : F. Bourliot, J. Estes, P. M. Petropoulos and Ph. Spindel, "G3-homogeneous gravitational instantons," Class. Quant. Grav. 27 (2010) 105007 [arXiv :0912.4848 [hep-th]].

Class. Quantum Grav. **27** (2010) 105007 (17pp) doi:10.1088/0264-9381/27/10/105007

$G3$-homogeneous gravitational instantons

F Bourliot[1], J Estes[2], P M Petropoulos[1] and Ph Spindel[3]

[1] Centre de Physique Théorique, CNRS–UMR 7644, Ecole Polytechnique, 91128 Palaiseau Cedex, France
[2] Laboratoire de Physique Théorique, CNRS–UMR 8549, Ecole Normale Supérieure, 24 rue Lhomond, F–75231 Paris cedex 05, France
[3] Service de Mécanique et Gravitation, Université de Mons, 20 Place du Parc, 7000 Mons, Belgique

E-mail: bourliot@cpht.polytechnique.fr, estes@cpht.polytechnique.fr, marios@cpht.polytechnique.fr and philippe.spindel@umons.ac.be

Received 24 December 2009, in final form 23 February 2010
Published 16 April 2010
Online at stacks.iop.org/CQG/27/105007

Abstract
We provide an exhaustive classification of self-dual four-dimensional gravitational instantons foliated with three-dimensional homogeneous spaces, i.e. homogeneous self-dual metrics on four-dimensional Euclidean spaces admitting a Bianchi simply transitive isometry group. The classification pattern is based on the algebra homomorphisms relating the Bianchi group and the duality group $SO(3)$. New and general solutions are found for Bianchi III.

PACS numbers: 02.40.Ky, 04.90.e

1. Introduction

Classical solutions of general relativity in diverse dimensions have been analyzed over the years from various perspectives. Instanton-like configurations have in particular attracted attention because of their potential role in the determination of transition amplitudes in quantum gravity. Similarly, their real-time counterpart turns out to be useful in the Hartle–Hawking formulation of quantum cosmology, even though general relativity would ultimately require a ultra-violet completion, possibly provided by strings. In fact, several classical solutions turn out to be embeddable in string theory, sometimes even as exact backgrounds, and instantons have certainly played a major role in addressing many issues, among which are those related to (super)symmetry breaking.

Following the paradigm of self-dual Yang–Mills instantons [1], self-duality has been successfully implemented in four-dimensional general relativity. In order to be operational, self-duality must be accompanied by some specific ansatz for the geometry $\mathcal{M}$. The usual ansatz is to assume $\mathcal{M}$ topologically $\mathbb{R} \times \Sigma_3$ and, further, the leaves Σ_3 to be homogeneous spaces, admitting at least a three-dimensional group of motions $G3$.

The first solution obtained according to the above pattern is due to Eguchi and Hanson [2, 3] under the assumption of Bianchi IX geometry, i.e. with $SU(2)$ isometry. This

gravitational instanton was an alternative to the earlier Taub–NUT metric, constructed from a different perspective though [4]. Both were self-dual and $SU(2)$-homogeneous, with isometry enhancement to $SU(2) \times U(1)$. General extensions of Eguchi–Hanson solution to strict $SU(2)$ were obtained soon after [5], observing that the equations were a special case of the Euler top—with some peculiar inertia momenta—known as the Lagrange system [6]. A similar achievement for the Taub-NUT instanton revealed far more, and a particular solution was finally obtained in [7]. The difficulty to solve in full generality the corresponding equations was later understood in terms of non-algebraic integrability properties, as it was realized [8] that the system at hand had already been set by Darboux [9], and solved extensively by Halphen [10, 11], more than a century before, in terms of modular forms[4].

The above account for the Bianchi IX group raises immediately two questions: do other Bianchi groups possess similar solutions and what is the classification principle behind the appearance of distinguished classes of equations such as Lagrange versus Darboux–Halphen systems? Despite the large amount of information accumulated so far (see e.g. [13, 14]) and the physical interest of some—even simple—solutions like Kasner's Bianchi I [15], a precise and definite answer to these questions was still missing. The aim of the present work is to tame the plethora of scattered results under a simple classification principle. Our analysis is performed along the lines announced in [16]. It is general and exhaustive, and makes no assumptions on the geometry, other than those already quoted above. In particular, the issue of the choice of a diagonal versus non-diagonal metric in a given $G3$-invariant frame is treated with care, as opposed to some former, more cavalier approaches for non-unimodular Bianchi groups. As a bonus, this enables us to discover a new solution for Bianchi III, completing thereby the existing landscape.

Let us summarize the method and the results. Self-dual vacuum solutions satisfy $\Omega = \tilde{\Omega}$ where Ω is the Riemann curvature 2-form[5]. These are second-order equations and are equivalent to the first-order set obtained with the connection 1-form: $\omega = \tilde{\omega} + A$. The 1-form A appears as a 'constant of motion' of the second-order system. It stands as the anti-self-dual $\mathfrak{so}(3)$ part of the Levi–Civita connection and must be flat. The program is thus cast as follows: (i) find all possible flat $\mathfrak{so}(3)$ connections over $G3$, and (ii) for each of them, write the corresponding first-order equations, and find the most general solution. The latter can represent a *bona fide* geometry, but in most cases it is spoiled by naked singularities, if not everywhere degenerate like in all non-unimodular groups, except for Bianchi III.

In section 2 we provide some technical tools, useful to set our philosophy for the subsequent developments. Section 3 contains the core of the classification principle (point (i) above), whereas the exhaustive solution search (point (ii)) is presented in section 4. A last section (5) is devoted to the subtle issue of rotating (locally) the frame where $\omega = \tilde{\omega} + A$ into a frame where the connection is genuinely self-dual. Conclusions follow and a summary of all $G3$-invariant metrics finally available is presented in the appendix.

2. Notations and general considerations

Inspired by applications to homogeneous cosmology, we consider Euclidean spaces admitting a $G3$ group of motion acting transitively[6] on three-dimensional invariant subspaces of the

[4] A translation of the general Halphen–Darboux solutions in terms of gravitational instantons can be found in [12]. They are all plagued with naked singularities, except, marginally, for the particular solution of Atiyah–Hitchin [7].

[5] Self-duality can be imposed alternatively on the Weyl tensor, and leads thus to solutions with a cosmological constant like Fubini–Study or Pedersen [17]. Note also that anti-self-solutions are obtained by parity or time reversal.

[6] The three-dimensional group $G3$ acts *simply* transitively on the leaves, endowed thus with the structure of a group manifold. Hence, we exclude H_3, $H_2 \times S^1$ or $S^2 \times S^1$, which are the alternatives to the nine Bianchi classes.

form $\mathcal{M} = \mathbb{R} \times \Sigma^3$. The metric on these spaces can always be locally written as (see for instance [18], p 516, for proof)

$$\mathrm{d}s^2 = N(t)^2\,\mathrm{d}t^2 + \delta_{ab}\Theta^a\Theta^b. \tag{1}$$

Let us introduce the co-frame defined by $\Theta^0 = N(t)\,\mathrm{d}t$ and $\Theta^a = \theta^a_\alpha(t)\sigma^\alpha$, where σ^α are invariant 1-forms:

$$\mathrm{d}\sigma^\alpha = \tfrac{1}{2}c^\alpha_{\beta\gamma}\sigma^\beta \wedge \sigma^\gamma. \tag{2}$$

From the latter we obtain

$$\mathrm{d}\Theta^a = \dot\theta^a_\alpha\,\mathrm{d}t \wedge \sigma^\alpha + \frac{1}{2}\theta^a_\alpha c^\alpha_{\beta\gamma}\sigma^\beta \wedge \sigma^\gamma \tag{3}$$

$$= \frac{1}{N}\dot\theta^a_\alpha\theta^\alpha_b\,\Theta^0 \wedge \Theta^b + \frac{1}{2}\theta^a_\alpha c^\alpha{}_{\beta\gamma}\theta^\beta_b\theta^\gamma_c\,\Theta^b \wedge \Theta^c \tag{4}$$

providing the non-vanishing structure coefficients:

$$\beta^a{}_{0b} = \frac{1}{N}\dot\theta^a_\alpha\theta^\alpha_b = -\beta^a{}_{b0}, \tag{5}$$

$$\beta^a{}_{bc} = \theta^a_\alpha c^\alpha{}_{\beta\gamma}\theta^\beta_b\theta^\gamma_c = -\beta^a{}_{cb}, \tag{6}$$

and connection coefficients

$$\gamma_{0ab} = \tfrac{1}{2}(\beta_{ab0} + \beta_{ba0}) = \gamma_{0ba}, \tag{7}$$

$$\gamma_{ab0} = \tfrac{1}{2}(\beta_{ab0} - \beta_{ba0}) = -\gamma_{ba0}, \tag{8}$$

$$\gamma_{abc} = \tfrac{1}{2}(\beta_{abc} + \beta_{bca} - \beta_{cab}) = -\gamma_{bac}. \tag{9}$$

With respect to the basis $\{\mathrm{d}t, \sigma^\alpha\}$ the metric components are $g_{00} = N(t)^2$, $g_{0\alpha} = 0$ and $g_{\alpha\beta} = \delta_{ab}\theta^a_\alpha\theta^b_\beta$. The Levi-Civita connection 1-forms are

$$\omega_{0i} = \varpi_{0i\alpha}\sigma^\alpha, \qquad \omega_{ij} = \varpi_{ij0}\,\mathrm{d}t + \varpi_{ij\alpha}\sigma^\alpha.$$

Finally, we need the expression of the curvature components, which are

$$\begin{aligned}\Omega_{0i} &= \mathrm{d}\omega_{0i} + \omega_{0k} \wedge \omega^k_i \\ &= \dot\varpi_{0i\alpha}\,\mathrm{d}t \wedge \sigma^\alpha + \tfrac{1}{2}\varpi_{0i\alpha}c^\alpha{}_{\beta\gamma}\sigma^\beta \wedge \sigma^\gamma \\ &\quad - \varpi_{0k\alpha}\varpi^k{}_{i0}\,\mathrm{d}t \wedge \sigma^\alpha + \varpi_{0k\beta}\varpi^k{}_{i\gamma}\sigma^\beta \wedge \sigma^\gamma,\end{aligned} \tag{10}$$

$$\begin{aligned}\Omega_{jk} &= \mathrm{d}\omega_{jk} + \omega_{j0} \wedge \omega^0{}_k + \omega_{jl} \wedge \omega^l{}_k \\ &= \dot\varpi_{jk\alpha}\,\mathrm{d}t \wedge \sigma^\alpha + \tfrac{1}{2}\varpi_{jk\alpha}c^\alpha{}_{\beta\gamma}\sigma^\beta \wedge \sigma^\gamma + \varpi_{j0\alpha}\varpi^0{}_{k\beta}\sigma^\alpha \wedge \sigma^\beta \\ &\quad + \varpi_{jl0}\varpi^l{}_{k\alpha}\,\mathrm{d}t \wedge \sigma^\alpha - \varpi_{jl\alpha}\varpi^l{}_{k0}\,\mathrm{d}t \wedge \sigma^\alpha + \varpi_{jl\alpha}\varpi^l{}_{k\beta}\sigma^\alpha \wedge \sigma^\beta.\end{aligned} \tag{11}$$

With respect to this basis, the anti-self dual components of the curvature 2-form read

$$\begin{aligned}\Omega_{0i} - \tfrac{1}{2}\epsilon_{ijk}\Omega^{jk} &= \big[\dot\varpi_{0i\alpha} - \varpi_{0k\alpha}\varpi^k_{i0} - \tfrac{1}{2}\epsilon_i{}^{jk}\left(\dot\varpi_{jk\alpha} + \varpi_{jl0}\varpi^l{}_{k\alpha} - \varpi_{jl\alpha}\varpi^l{}_{k0}\right)\big]\,\mathrm{d}t \wedge \sigma^\alpha \\ &\quad + \tfrac{1}{2}\big[\varpi_{0i\alpha}c^\alpha{}_{\beta\gamma} + \varpi_{0k\beta}\varpi^k{}_{i\gamma} - \varpi_{0k\gamma}\varpi^k{}_{i\beta} \\ &\quad - \epsilon_i{}^{jk}\left(\tfrac{1}{2}\varpi_{jk\alpha}c^\alpha{}_{\beta\gamma} + \varpi_{j0\beta}\varpi^0{}_{k\gamma} + \varpi_{jl\beta}\varpi^l{}_{k\gamma}\right)\big]\sigma^\beta \wedge \sigma^\gamma\end{aligned} \tag{12}$$

or introducing

$$\bar{I}_{i\alpha} := \varpi_{0i\alpha} - \tfrac{1}{2}\epsilon_i^{\ jk}\varpi_{jk\alpha}, \tag{13}$$

$$\Omega_{0i} - \tfrac{1}{2}\epsilon_{ijk}\Omega^{jk} = \left[\dot{\bar{I}}_{i\alpha} - \bar{I}_{l\alpha}\varpi^{l}_{\ i0}\right]\mathrm{d}t \wedge \sigma^\alpha + \tfrac{1}{2}\left[\bar{I}_{i\alpha}c^{\alpha}_{\ \beta\gamma} + \epsilon_i^{\ jk}\bar{I}_{j\beta}\bar{I}_{k\gamma}\right]\sigma^\beta \wedge \sigma^\gamma. \tag{14}$$

Let us emphasize however that the 1-forms θ^α_k are not completely fixed, but defined up to time-dependent $O(3)$ transformations and time-independent $GL(3,\mathbb{R})$ transformations, we have indeed not yet fixed the basis of invariant forms.

3. Self-duality equations

Self-duality requires that

$$\Omega_{0i} - \tfrac{1}{2}\epsilon_{ijk}\Omega^{jk} = 0. \tag{15}$$

We see that to trivially obtain first integrals from this equation a sufficient (and necessary) condition is to require that

$$\varpi_{ik0} = 0 \Leftrightarrow \dot{\theta}_{i\alpha}\theta^\alpha_k - \dot{\theta}_{k\alpha}\theta^\alpha_i = 0 \Leftrightarrow \dot{\theta}_{i\alpha} = -g_{\alpha\beta}\dot{\theta}^\beta_i, \tag{16}$$

after which (14) becomes equivalent to

$$\dot{\bar{I}}_{i\alpha} = 0 \qquad \bar{I}_{i\alpha}c^{\alpha}_{\ \beta\gamma} + \epsilon_i^{\ jk}\bar{I}_{j\beta}\bar{I}_{k\gamma} = 0. \tag{17}$$

The gauge freedom allows us to always satisfy this condition. Indeed if we have a solution $\theta_{a\alpha}$, using a time-dependent rotation we obtain $\tilde{\theta}_{a\alpha} := \mathcal{O}_a^{\ b}(t)\theta_{b\alpha}$ which will fulfill the symmetry condition if

$$\dot{\mathcal{O}}_a^{\ b} = \tfrac{1}{2}\mathcal{O}_a^{\ c}\left(\theta^\alpha_c\dot{\theta}^b_\alpha - \dot{\theta}_{c\alpha}\theta^{\alpha b}\right) \tag{18}$$

This is a kinematic problem aiming to determine a sequence of rotations knowing the angular velocity so that it always admits a solution. Then the only transformations still possible correspond to the choice of the initial conditions of the kinematical problem, denoted from now on by the matrix O^b_a, and of arbitrary $GL(3,\mathbb{R})$ time-independent transformations, denoted from now on by the matrix Λ^β_α,

$$\theta_{a\alpha} \mapsto O_a^{\ b}\theta_{b\beta}\Lambda^\beta_\alpha. \tag{19}$$

In the gauge defined by (16), the first integrals ($\bar{I}_{i\alpha} = \text{const.}$) furnish the first-order equations we need to solve

$$\frac{1}{N}\dot{\theta}_{i\alpha} - \theta^{-1}\theta_{i\gamma}\left[(n^{\gamma\mu} - a_\rho\epsilon^{\rho\gamma\mu})g_{\mu\alpha} - \frac{1}{2}\delta^\gamma_\alpha n^\mu_\mu\right] := -\bar{I}_{i\alpha} \tag{20}$$

where $\theta = \sqrt{\det(g_{\ \alpha\beta})}$ and the symmetric tensor density $n^{\gamma\mu} = n^{(\gamma\mu)}$ and vector a_ρ are defined by the relations

$$c^{\alpha}_{\ \beta\gamma}\epsilon^{\beta\gamma\mu} = 2(n^{\alpha\mu} + \epsilon^{\alpha\mu\beta}a_\beta). \tag{21}$$

In the following we shall call the t coordinate *time* and speak about *evolution*, to describe this flow, though the framework is Euclidean.

Using time reparameterizations, we may choose a specific N without loss of generality. Equations (20) strongly suggest to adopt, in a first step at least, the gauge $N = \theta$. Let us note that in order to preserve this gauge condition when we make a transformation (19) we have to simultaneously rescale t by a factor $1/\det\left(\Lambda^\beta_\alpha\right)$; then the time variable may still only be changed by a shift $t \mapsto t + t_0$. But before trying to integrate equations (20) it is mandatory to solve the constraint equations

$$\bar{I}_{i\alpha}c^{\alpha}_{\ \beta\gamma} + \epsilon_i^{\ jk}\bar{I}_{j\beta}\bar{I}_{k\gamma} = 0. \tag{22}$$

The solutions of these equations describe homomorphisms from the Lie algebra of the homogeneity group $\mathfrak{g}_3$ into the Lie algebra $\mathfrak{so}(3)$:

$$\bar{I} : \mathfrak{g}_3 \to \mathfrak{so}(3). \tag{23}$$

Depending on the subalgebra of $\mathfrak{so}(3)$ on which we project $\mathfrak{g}_3$ different simplifications can occur. Let us remind that the only subalgebras of $\mathfrak{so}(3)$ are the trivial ones: $\mathfrak{so}(3)$ and the null one $\{\mathbf{0}\}$ and the one-dimensional ones : $\mathbb{R}$ (all equivalent, i.e. linked by internal conjugation). Thus, if the constants of motion $\bar{I}_{i\alpha}$ are not identically zero (in which case we have the trivial homomorphism mapping $\mathfrak{g}_3$ onto $\{\mathbf{0}\}$) either $\mathfrak{g}_3 = \mathfrak{so}(3)$ or the algebra $\mathfrak{g}_3$ has a two-dimensional ideal.

These remarks lead to the following Bianchi types to be considered, according to the rank of the matrix $\bar{I}_{i\alpha}$:

- **rank 3** (maximal) type IX ,
- **rank 2** impossible,
- **rank 1** types I, II, III, IV, V,VI,VII,
- **rank 0** all Bianchi types.

But it remains to examine if all these cases can effectively be obtained, i.e. if there are no obstructions coming from (16). Let us note that using (20), condition (16) can be written as

$$\bar{I}_{i\alpha}\theta^{\alpha}_{j} - \bar{I}_{j\alpha}\theta^{\alpha}_{i} + 2\,a_{\rho}\theta^{\rho k}\epsilon_{kij} = 0. \tag{24}$$

From this equation we see that for rank 0, we must have $a_\rho = 0$, which is the statement that rank 0 solutions must be from Bianchi class A, i.e. types I, II, VI_0, VII_0, VIII and IX, see table 1 for our conventions. For the rank 1 cases, as shown in the next section, the only solutions whose metric determinant does not everywhere vanish are those of Bianchi class A and type III.[7] Thus, if we also require the metric determinant to not everywhere vanish, the above list is reduced to

- **rank 3** (maximal) type IX,
- **rank 2** impossible,
- **rank 1** types I, II, III, VI_0, VII_0,
- **rank 0** types I, II, VI_0, VII_0, VIII, XI.

Thus, according to the rank of the mapping $\bar{I}$ we obtain the classification of solutions in the next section.

4. All self-dual solutions

In this section, we obtain all the self-dual solutions categorized by the rank of $\bar{I}$. Some of them have been discussed in the past in [13, 14].[8] On a similar ground of simplicity, the only rank 3 solution coming from the type IX Bianchi algebra has also been studied in [13, 14] and various other places in the past. We finally deal with the new cases, solutions of rank 1. Thanks to residual symmetries and constraints coming from the self-duality requirement, we

[7] To see this, first decompose $\bar{I}_{i\alpha}$ as $\bar{I}_{i\alpha} = \lambda_i I_\alpha$ where I_α and λ_i are two triples. For all types of Bianchi class B, except type III, the only solution to the constraint (22) is to take I_α proportional to a_α. In this case, one may show that (24) requires the determinant of θ^α_i to vanish.

[8] However, in [13, 14] the metrics were assumed to be *a priori* diagonal, a technical assumption just introduced to facilitate the integration of the flow equations. Here we justify that they furnish the most general ones in case of rank 0 cases, and when necessary shall discuss the integration of the relevant non-diagonal metrics.

Table 1. Canonical structure constants for the different Bianchi groups

Type	a	n^1	n^2	n^3	Usual name
		Class A			
I	0	0	0	0	Translations
II	0	1	0	0	Galilean
VII_0	0	1	1	0	Euclidean
VI_0	0	1	-1	0	Poincaré
IX	0	1	1	1	Rotation
VIII	0	1	1	-1	Lorentz
		Class B			
V	1	0	0	0	
IV	1	1	0	0	
VII_h	$h > 0$	1	1	0	
$\mathrm{VI}_{h\neq 1}$	$h > 0$	1	-1	0	
$\mathrm{III} \equiv \mathrm{VI}_1$	1	1	-1	0	

simplify as most as possible the equations and present the most general solutions as well as some particular simplified solutions when available.

Rank 0. All $\bar{I}_{k\alpha}$ are zero. The Bianchi type must be of class A, ($a_\rho = 0$), i.e. types I, II, VI_0, VII_0, VIII and IX. Equations (20) imply that the symmetry condition is always satisfied:

$$\dot{\theta}_{i\,\alpha}\theta^\alpha_j = \theta_{i\,\gamma}\left(n^{\gamma\mu} - \tfrac{1}{2}n^\nu_\nu\, g^{\gamma\mu}\right)\theta_{j\,\mu} = \dot{\theta}_{j\,\alpha}\theta^\alpha_i. \tag{25}$$

At an initial time, one may simultaneously diagonalize $g_{\mu\nu}$ and put $n^{\mu\nu}$ in its canonical form (see table 1). Thus, at initial time the co-frame components $\theta_{i\,\gamma}$ may be chosen diagonal, and they remain so during their evolution. The explicit integration of the evolution equations has been described a long time ago in [13, 14]; here this class of self-dual spaces is presented in appendix A for completeness.

Rank 3. Of course only Bianchi IX is possible for this case of maximal rank. In an appropriate frame the matrix n is the identity matrix. The self-duality condition (22) can be reinterpreted as a relation between three three-dimensional Euclidean vectors:

$$\vec{I}_1 = \vec{I}_2 \times \vec{I}_3 \tag{26}$$

and two similar relations obtained by circular permutation of the indices 1, 2, 3. Thus, these three vectors are perpendicular to each other and actually define an orthonormal frame of E^3. Acting with an appropriate element of $O(3)$, on the flat indices i, we may assume that $-(\bar{I}_{i\alpha})$ is the identity matrix. The integration of (20), under these assumptions, was first discussed in [6, 9–11] and the solution is given in appendix A.

Rank 1. In that case there exists two triplets I_α and λ_i such that $\bar{I}_{i\alpha} = \lambda_i I_\alpha$. Condition (22) reduces to

$$I_\alpha c^\alpha_{\beta\gamma} = 0. \tag{27}$$

Bianchi class A. In this case, condition (27) is equivalent to

$$I_\alpha n^{\alpha\beta} = 0, \tag{28}$$

so the matrix $(n^{\alpha\beta})$ has to be singular. Consequently the Bianchi type has to be I, II, VI_0 or VII_0. The symmetry condition (24) then becomes

$$\lambda_i \rho_j - \lambda_j \rho_i = 0 \qquad \text{with} \quad \rho_k = \theta_k^\alpha I_\alpha. \tag{29}$$

It is easy to see that if the initial conditions satisfy this condition, then the equation will automatically be preserved throughout the evolution. This can be seen by computing the evolution of ρ_i using (20) to obtain

$$\dot{\rho}_i = \left(\tfrac{1}{2} n^{\mu\nu} g_{\mu\nu} + \lambda^k \rho_k\right) \rho_i. \tag{30}$$

Thus, we find no restrictions on the existence of solutions to our self-dual problem.

In order to find the rank 1 solutions for Bianchi class A, let us start with the most general expression of the matrix of frame components:

$$\left(\theta_i^\alpha\right) = \begin{pmatrix} a & p & q \\ r & b & s \\ u & v & c \end{pmatrix}. \tag{31}$$

It can be simplified by making use of the transformations (19). Using an $O(3)$ transformation we may assume $\lambda = (0, 0, 1)$ and, without altering the canonical value of the structure constants, using $GL(3, \mathbb{R})$ transformations set

- $I_\alpha = (0, 0, 1)$ for Bianchi I,II
- $I_\alpha = (0, 0, Z)$ for Bianchi VI_0, VII_0.

Moreover, for Bianchi type I, II, VI_0 and VII_0 (Bianchi type of class A), without loss of generality, we may also assume the matrix (31) diagonal. This can be done using the transformations (19), which now leave I_α and λ_i invariant as well as the canonical values of the structure constants. The integration of the resulting self-duality equations was given in [13, 14].

For illustrative purpose let us discuss the Bianchi type VI_0. The integration proceeds as follows. First we observe that (29) imposes $u = v = 0$. Equations (30) then ensure that if u, v are chosen zero at the initial time, they will remain null. Then we remark that the evolution equations imply that the functions q and s are proportional to c:

$$q(t) = Qc(t), \qquad s(t) = Sc(t) \tag{32}$$

and that the transformations (19) of the frame that preserves the canonical choice of the structure constants, of I_α and λ are given by

$$O = \begin{pmatrix} \pm\cos(\phi) & \sin(\phi) & 0 \\ \mp\sin(\phi) & \cos(\phi) & 0 \\ 0 & 0 & 1 \end{pmatrix} \qquad \text{and} \qquad \Lambda^{-1} = \begin{pmatrix} \alpha & \beta & \gamma \\ \beta & \alpha & \delta \\ 0 & 0 & 1 \end{pmatrix}. \tag{33}$$

Transformations (33) allow to simplify the frame components, without loss of generality. First we may put $Q = S = 0$, i.e. $q(t) = s(t) = 0$ by performing a transformation with $O = Id$ and $\alpha = 1, \beta = 0, \gamma = -Q$ and $\delta = -S$. Then we still have the freedom to make transformations (33) with $\gamma = \delta = 0$. Performing, at an arbitrary time t_0, a new transformation with still $O = Id$ and $\alpha = \rho\ \cos(\varphi)$, $\beta = \rho\ \sin(\varphi)$ where $\rho > 0$ is arbitrary and φ determined by[9]

$$\sin(2\varphi) = -\frac{2(a_0 r_0 + p_0 b_0)}{\left(a_0^2 + b_0^2 + p_0^2 + r_0^2\right)}, \tag{34}$$

[9] We use the subscript 0 to indicate the value of the corresponding function at the instant considered : $a(t_0) = a_0$, etc.

we obtain a new frame such that now $a_0\, r_0 + b_0\, p_0 = 0$. Let us note that (34) makes sense because from $(a_0 \pm r_0)^2 + (b_0 \pm p_0)^2 > 0$ we deduce that its right-hand side member is always between -1 and $+1$. Then choosing $\Lambda = Id$ and O with ϕ such that

$$\sin(\phi)\, p_0 + \sin(\phi)\, b_0 = 0 = -\sin(\phi)\, a_0 + \cos(\phi)\, r_0 \tag{35}$$

we have obtained a diagonal frame at time t_0.

It remains then five functions to be determined: a, b, r, p and c. These functions have to satisfy the equations

$$\dot{a} = \frac{a\,\Delta - 2\kappa\, b}{2\,\kappa^2}, \tag{36}$$

$$\dot{b} = \frac{b\,\Delta + 2\kappa\, a}{2\,\kappa^2}, \tag{37}$$

$$\dot{p} = \frac{p\,\Delta + 2\kappa\, r}{2\,\kappa^2}, \tag{38}$$

$$\dot{r} = \frac{r\,\Delta - 2\kappa\, p}{2\,\kappa^2}, \tag{39}$$

$$\dot{c} = c\frac{\Delta - 2\,Z\,\kappa}{2\,\kappa^2}, \tag{40}$$

with

$$\Delta = (b^2 + r^2) - (a^2 + p^2), \qquad \text{and} \qquad \kappa = a\,b - p\,r. \tag{41}$$

It is obvious from these equations that κ is a constant. Moreover, the fact that we may diagonalize the frame at $t = t_0$ implies that it remains diagonal during all of its evolution; thus $r(t) = p(t) = 0$.

By considering the combination $X = a + \mathrm{i}\, b$ the main equation to solve is

$$\dot{X} = -X(X^2 - 4\,\mathrm{i}\,\kappa)/(2\,\kappa^2); \tag{42}$$

after which we may finally obtain c thanks to (40). Solving both equations yields

$$X = (a + i\, b) = 2\, X_0\, \mathrm{e}^{\mathrm{i}t/\kappa} \left(\mathrm{i}\,\kappa \Big/ \left(X_0^2\, \mathrm{e}^{2\,\mathrm{i}t/\kappa} - \bar{X}_0^2\, \mathrm{e}^{-2\,\mathrm{i}t/\kappa}\right)\right)^{1/2}, \tag{43}$$

$$c^2 = c_0^2\, \mathrm{e}^{-2\,Zt/\kappa}/(X(t)\, \bar{X}(t)). \tag{44}$$

Moreover the remaining transformation with $\Lambda^{-1} = \mathrm{diag}(\rho, \rho, 1)$ allows us to fix $\kappa = 1$. After a final translation of the variable t, and if necessary a flip of sign we obtain

$$a = 1/b = \sqrt{\cot(t)}, \tag{45}$$

$$c = c_0 \frac{\mathrm{e}^{Zt}}{\sqrt{\sin(2t)}}. \tag{46}$$

Similar expressions can be obtained for Bianchi type VII_0, but they involve real exponentials of time.

Bianchi class B. In this case , condition (27) is equivalent to

$$I_\beta n^{\alpha\beta} = \epsilon^{\alpha\mu\nu} I_\mu\, a_\nu \qquad (\epsilon^{123} = 1). \tag{47}$$

For algebras of Bianchi types IV, VI_h (with $h \neq 0, 1$) and VII_h (with $h \neq 0$) we found that the only solution to equations (47) is $I_\alpha = \lambda\, a_\alpha$, but for type III $= \mathrm{VI}_1$, we obtain a two-parameter solution. This is a reflection of the fact that the derived algebra now is of rank 1 instead of two.

Equations (24) read

$$\lambda_i \rho_j - \lambda_j \rho_i = -2\,\alpha^k \epsilon_{kij} \qquad \text{with} \quad \alpha^k = a_\mu \theta^{\mu\, k}. \tag{48}$$

As we require a non-singular co-frame, they are only compatible with an algebra of Bianchi type III. By derivation, using (25) we obtain the system of equations:

$$\begin{aligned} \dot{\rho}_i &= \left(\tfrac{1}{2} n^{\mu\nu} g_{\mu\nu} + \theta\, \lambda^k \rho_k\right) \rho_i + 2\theta \epsilon_i{}^{jk} \alpha_j \rho_k, \\ \dot{\alpha}_i &= \tfrac{1}{2} n^{\mu\nu} g_{\mu\nu}\, \alpha_i + \theta\, \lambda^k\, \alpha_k \rho_i. \end{aligned} \tag{49}$$

To check the consistency of (48) with (20), let us rewrite them as relations between vectors of a three-dimensional Euclidean space:

$$2\vec{\alpha} = -\vec{\lambda} \times \vec{\rho}, \tag{50}$$

$$\dot{\vec{\rho}} = \frac{n}{2}\vec{\rho} + \theta(\vec{\lambda} \cdot \vec{\rho})\vec{\rho} + 2\,\theta \vec{\alpha} \times \vec{\rho}, \tag{51}$$

$$\dot{\vec{\alpha}} = \frac{n}{2}\vec{\alpha} + \theta(\vec{\lambda} \cdot \vec{\alpha})\vec{\rho}. \tag{52}$$

Taking the derivative of (50) and inserting in it (51) and (52), we obtain

$$\begin{aligned} 2\dot{\vec{\alpha}} + \vec{\lambda} \times \dot{\vec{\rho}} &= n\vec{\alpha} + 2\theta(\vec{\lambda} \cdot \vec{\alpha})\vec{\rho} + \frac{n}{2}\vec{\lambda} \times \vec{\rho} + \theta(\vec{\lambda} \cdot \vec{\rho})\vec{\lambda} \times \vec{\rho} + 2\theta \vec{\lambda} \times (\vec{\alpha} \times \vec{\rho}), \\ &= \left(\frac{n}{2}\vec{\alpha} + \theta(\vec{\lambda} \cdot \vec{\rho})\right)(2\vec{\alpha} + \vec{\lambda} \times \vec{\rho}). \end{aligned}$$

Thus, if $2\vec{\alpha} + \vec{\lambda} \times \vec{\rho} = 0$ at a period of time, it always vanishes. This insures that the solution obeying this condition constitutes a self-dual solution.

It was shown in [13, 14] that there does not exist any diagonal self-dual metrics with a Bianchi type III symmetry group. We provide in the following the most general solution of type III, without any *a priori* (non-geometrical) assumption on the co-frame, from which it is easy to see that diagonal metrics do not exist but non-diagonal ones do. As previously, assuming a non-singular frame, by using rotations and linear transformations we may put $\lambda = (1, 0, 0)$ and $I_\alpha = (1, 1, 0)$. Then (24) implies that the frame must be of the form

$$\left(\theta_i^\alpha\right) = \begin{pmatrix} a & 2c - b & -2\,v - s \\ r & b & s \\ 0 & v & c \end{pmatrix}. \tag{53}$$

This frame can still be transformed, without altering the canonical structure constants and constants of motion, by acting on the right-hand side with the $GL(3, \mathbb{R})$ matrix

$$\Lambda^{-1} = \begin{pmatrix} 1 - \mu & \mu & \nu \\ \mu & 1 - \mu & -\nu \\ 0 & 0 & 1 \end{pmatrix} \tag{54}$$

and on the left-hand side with a rotation that leaves λ invariant

$$O = \begin{pmatrix} 1 & 0 & 0 \\ 0 & \cos(\phi) & \sin(\phi) \\ 0 & -\sin(\phi) & \cos(\phi) \end{pmatrix}. \tag{55}$$

The self-duality equations imply that $v(t) = Vc(t)$. Thus, we may assume that $v(t) = 0$ after, if necessary, a rotation of angle ϕ such that $\tan(\phi) = V$. Moreover we then see that $s(t) = Sc(t)$ and that by choosing an appropriate value of ν we may also assume $s(t) = 0$. The remaining parameter μ can by fixed by requiring $b(0) = 0$.

So without loss of generality, the frame we have to consider reduces to

$$\theta_k^\alpha = \begin{pmatrix} a & 2c-b & 0 \\ r & b & 0 \\ 0 & 0 & c \end{pmatrix}. \tag{56}$$

In order to pursue the integration it will be useful to redefine the unknown functions as follows (using the fact that c cannot vanish as we only consider non-singular frames):

$$a(t) = \alpha(t)\,c(t), \quad b(t) = \beta(t)c(t), \quad r(t) = \rho(t)\,c(t). \tag{57}$$

Then the self-duality equations lead to

$$\dot{\alpha} = \frac{2+\alpha^2+\alpha\rho}{(2\rho-(\alpha+\rho)\beta)\,c^2}, \tag{58}$$

$$\dot{\beta} = \frac{\rho-\alpha}{(2\rho-(\alpha+\rho)\beta)\,c^2}, \tag{59}$$

$$\dot{\rho} = \frac{2+\rho^2+\alpha\rho}{(2\rho-(\alpha+\rho)\beta)\,c^2}, \tag{60}$$

$$\dot{c} = \frac{\rho^2-\alpha^2+4\beta-4}{2c\,(2\rho-(\alpha+\rho)\beta)^2}. \tag{61}$$

They imply

$$\frac{\mathrm{d}(\rho-\alpha)}{\mathrm{d}\beta} = (\rho+\alpha) \qquad \text{and} \qquad \frac{\mathrm{d}(\rho+\alpha)}{\mathrm{d}\beta} = \frac{4+(\rho+\alpha)^2}{\rho-\alpha}. \tag{62}$$

These equations are easy to solve and lead to

$$\alpha = \sinh\left(\frac{\beta-\beta_*}{K}\right) - K\cosh\left(\frac{\beta-\beta_*}{K}\right),$$
$$\rho = \sinh\left(\frac{\beta-\beta_*}{K}\right) + K\cosh\left(\frac{\beta-\beta_*}{K}\right).$$

Then we may express, by a quadrature, the function c as a function of β using the equation obtained from the ratio of $\dot{\beta}$ and $\dot{c}$:

$$c^2 = c_0^2 \frac{\cosh\left(\frac{\beta-\beta_*}{K}\right)}{(\beta-1)\sinh\left(\frac{\beta-\beta_*}{K}\right) - K\cosh\left(\frac{\beta-\beta_*}{K}\right)} \tag{63}$$

and finally express everything as functions of t by integrating equation (59) which leads to the surprisingly simple result (after a flip of the sign of t):

$$\beta = \frac{K}{c_0^2}t. \tag{64}$$

The solution we discussed is generic. It depends on two arbitrary constants, namely c_0, K and β_*; note that we have used a time translation to set $\beta = 0$ at time $t = 0$. Also note that we assumed that a is always different from r. If for a value of t we set $a = r$, then they become

identical for all times. In this special case, the derivative of β vanishes and we obtain that $b(t) = Bc(t)$ implying the remaining equations:

$$\frac{\dot{c}}{c} = \frac{R}{a^2}, \qquad \frac{\dot{a}}{a} = -2\frac{R}{c^2} - \frac{R}{a^2}. \tag{65}$$

with $R = \frac{1}{2(1-B)}$.

To solve equations (65) we use an auxiliary function $y(t) = \log|a(t)c(t)|$ and obtain, after elementary operations, the first integral:

$$\dot{y}^2 + 4R^2\,\mathrm{e}^{-2y} = L^2, \tag{66}$$

from which we deduce the expression of the product $a(t)c(t)$ and

$$c(t)^2 = \frac{2\,R}{L}\coth[Lt], \tag{67}$$

$$a(t)^2 = \frac{R}{L}\sinh[2\,Lt]. \tag{68}$$

Let us note that Rt has to be positive for the solution to be real. When $t = 0$ we encounter a curvature singularity.

5. Self-dual connections

In the conventions we have used, we naturally find solutions whose curvature is self-dual while the connection is not. However, as we will show below, we may always make a local $SO(4)$ rotation to make the connection self-dual. In fact, the vanishing of the anti-self-dual part of the connection can be related to the integrability condition, thereby ensuring the existence of a pure self dual-connection. We shall illustrate this point by evaluating, in general, the gauge transformations which map our canonical co-frame to one whose associated connection is self-dual.

As is well known, the two (families of) parallelisms on the three-sphere S^3 provide a way to decompose any $SO(4)$ rotation into the product of self-dual and anti-self-dual $SO(3)$ rotations. If u, x, y and z are the coordinates of a point of S^3 : $u^2 + x^2 + y^2 + z^2 = 1$, an anti-self-dual $SO(3)$ element can be written as

$$O_{ad} := \begin{pmatrix} u & -x & -y & -z \\ x & u & z & -y \\ y & -z & u & x \\ z & y & -x & u \end{pmatrix}. \tag{69}$$

The gauge transformation generated by such a rotation leaves invariant the self-dual part of the connection but transforms the anti-self-dual one. Accordingly, when the anti-self-dual part of the connection, given by the constants $\bar{I}_{i\alpha}$, is non-zero, such a gauge transformation may set it to zero thanks to a solution of the equation:

$$\mathrm{d}O = O\,\underset{a}{\omega}. \tag{70}$$

More explicitly we obtain (with $\bar{\mathbf{I}}_k := \bar{I}_{k\alpha}\sigma^\alpha$ and $x^i := (x, y, z)$)

$$\mathrm{d}u = \tfrac{1}{2}x^k\,\bar{\mathbf{I}}_k, \qquad \mathrm{d}x^i = \tfrac{1}{2}(-u\,\bar{\mathbf{I}}_i + \epsilon^{ijk}x_j\,\bar{\mathbf{I}}_k). \tag{71}$$

As a first immediate consequence we see that this gauge transformation has to be t independent. Moreover we also obtain from equation (22):

$$\mathrm{d}\bar{\mathbf{I}}_i = \tfrac{1}{2}\bar{I}_{i\alpha}c^\alpha{}_{\beta\gamma}\sigma^\beta \wedge \sigma^\gamma = -\tfrac{1}{2}\epsilon_i^{jk}\bar{\mathbf{I}}_j \wedge \bar{\mathbf{I}}_k, \tag{72}$$

which indeed ensures the integrability of equations (71). In the case of a rank 1 mapping, $\bar{I}_{k\alpha} = \lambda_k I_\alpha$ (normalized such that $\sum_k \lambda_k^2 = 1$), this equation implies that there exists a function χ such that $\mathrm{d}\chi = I_\alpha \sigma^\alpha$. Correspondingly, the gauge transformation (69) that leads to a frame which has vanishing anti-self-dual connection is given by

$$u = \sin(\chi/2), \qquad x^k = \lambda^k \cos(\chi/2). \tag{73}$$

In the case of rank 3, the only possibility is Bianchi type IX. As discussed above it can be taken diagonal, with the matrix $(\bar{I}_{i\alpha}) = -\delta_{i\alpha}$. Moreover, it is well known that the components of the invariant 1-forms also define parallel vector fields. Using the identities $u\,\mathrm{d}u + x\,\mathrm{d}x + y\,\mathrm{d}y + z\,\mathrm{d}z = 0$ and $u^2 + x^2 + y^2 + z^2 = 1$, it is easy to check that the invariant 1-forms may be expressed as

$$\sigma^1 = -2(x\,\mathrm{d}u - u\,\mathrm{d}x + z\,\mathrm{d}y - y\,\mathrm{d}z), \tag{74}$$

$$\sigma^2 = -2(y\,\mathrm{d}u - z\,\mathrm{d}x - u\,\mathrm{d}y + x\,\mathrm{d}z), \tag{75}$$

$$\sigma^3 = -2(z\,\mathrm{d}u + y\,\mathrm{d}x - x\,\mathrm{d}y - u\,\mathrm{d}z), \tag{76}$$

which satisfy the invariance relations: $\mathrm{d}\sigma^i = \epsilon^i_{jk}\sigma^j \wedge \sigma^k$ (71). In the case where the matrix $(\bar{I}_{i\alpha})$ is not diagonal, it must be (in order to satisfy equations (26)) of the form $(\bar{I}_{i\alpha}) = -(O_{i\alpha})$ with O an $SO(3)$ rotation matrix. It is elementary to verify that equations (71) are solved by similar functions involving variables u and $(x'^k) = (x', y', z')$ related to $(x^k) = (x, y, z)$ by the rotation O:

$$x'k = -I_{kl}x^l \tag{77}$$

as it must be.

6. Conclusion

In this note we have achieved a complete classification of all the self-dual Euclidean spaces admitting a $G3$ simply transitive homogeneity group. For each Bianchi group, there are as many classes of solutions as homomorphisms $\bar{I} : \mathfrak{g}_3 \to \mathfrak{so}(3)$. For each of these homomorphisms, labeled by its rank, the self-duality constraint is described by a specific set of equations—like Lagrange or Darboux–Halphen in Bianchi IX, leading to distinct solutions such as Eguchi–Hanson or Taub–NUT respectively. These equations have non-everywhere vanishing solutions for all class A Bianchi groups (I, II, VI_0, VII_0, VIII and IX), whereas in class B solutions exist only for Bianchi III. The latter solutions (equations (A.4), (A.6)) are *all* rank 1 and non-diagonal, contrary to the lore that it seamed 'very unlikely to construct non-diagonal self-dual solutions of Bianchi types I–IX' [13, 14]. This expectation was empty for Bianchi A because in the present formulation, the diagonal ansatz is the most general, but not for Bianchi B.

It is fair to stress that the above conclusions have been reached by adopting a metric representation, equation (1), such that the foliation of $\mathcal{M}$ as $\mathbb{R} \times \Sigma_3$ is manifest and adapted to the splitting of the group $SO(4)$ into self-dual and anti-self-dual factors. Other choices for the metric may exist, where the distinction between the various classes of self-dual solutions is less sharp. This happens e.g. for Bianchi IX, in the Gibbons–Hawking representation [19], where Eguchi–Hanson (rank 0) and Taub–NUT (rank 1) are indeed, to some extent, unified. This is possible, however, at the price of abandoning the $G3$-invariant frames that we use. Here, this choice has been instrumental, not only for providing the classification in terms of the rank of the $\mathfrak{g}_3 \to \mathfrak{so}(3)$ homomorphism, but also for scanning all possible solutions.

Our analysis can easily be adapted to the ultra-hyperbolic case (spacetime signature $(-,-,+,+)$), where the algebra of Bianchi type VIII will play a role analogous to the one of Bianchi IX here. It should however be emphasized that we will have to distinguish, in that case, among the inequivalent one-dimensional subalgebras of $\mathfrak{so}(2,1)$. Other extensions concern the addition of a cosmological constant (Weyl self-duality), or the implementation of the method to higher dimensional set-ups admitting self-duality, as e.g. in seven dimensions. Last but not least, the physical analysis of the new Bianchi III solutions remains to be completed. The large number of moduli in (A.4), (A.6) make such an analysis quite involved.

It would be interesting to discover if the techniques and classification presented in this paper can be generalized to cases where we have a more general set-up than vacuum Einstein equations. For example, the evolution of certain Bianchi spaces in the presence of a cosmological constant, as well as various matter such as a perfect fluid and/or scalar, spinor and electro-magnetic fields, has been studied recently in [22–24]. The authors have derived exact solutions in certain cases, some of which are singularity free, and a complete classification of solutions would be appreciated. In the case of Einstein's equations with a cosmological constant, it is well known that requiring self-duality of the Weyl tensor is sufficient to satisfy the equations of motion. However, in this case our technics have to be abandoned as we are generically confronted with a system of second-order differential equations.

We note that most of the Bianchi classes have solutions which necessarily have singularities. It would be interesting to discover if these singularities could be cured by the introduction of either a cosmological constant and/or additional matter fields. Examples have already been discussed in [22–24] as well as [25, 26].

Acknowledgments

The authors thank P Bieliavsky for stimulating discussions and a referee for having indicated to us the paper [22]. François Bourliot, J Estes and M Petropoulos would like to thank the Service de Physique Théorique de l'Université Libre de Bruxelles as well as the Service de Mécanique et Gravitation de l'Université de Mons–Hainaut for kind hospitality. Philippe Spindel thanks the IHES where the present collaboration was initiated and the CPHT of Ecole Polytechnique, and acknowledges financial support from IISN-Belgium (convention 4.4511.06). John Estes acknowledges financial support from the Groupement d'Intérêt Scientifique P2I. This research was partially supported by the French Agence Nationale pour la Recherche, contract 09-BLAN-NT09-573739 and by the CNRS-FNRS-CGRI-2009.

Appendix. G3 self-dual metrics

We summarize here all known (real) self-dual $G3$-homogeneous gravitational instantons, following the classification pattern we have developed in terms of homomorphisms $\mathfrak{g}_3 \to \mathfrak{so}(3)$. These can be of rank 0, 1 or 3. Whenever rank 0 and rank 1 solutions coexist (i.e. for Bianchi I, II, VI_0 and VII_0), they are both captured by a single expression with a two-valued parameter $\epsilon = 0, 1$. Bianchi IX is the only case which possess rank 0 and rank 3 solutions. Bianchi III is the most peculiar: contrary to the other classes, it requires a non-diagonal co-frame (31) (and consequently a non-diagonal metric (1)) and allows exclusively rank 1 solutions. These solutions are new.

In the following presentation, integration constants that can be reabsorbed by coordinate redefinitions have been discarded. Consequently, all remaining parameters are *genuine moduli* of the solutions.

Bianchi I. The solution reads

$$\mathrm{d}s^2 = \mathrm{e}^{-2\epsilon t}\,\mathrm{d}t^2 + \mathrm{e}^{-2\epsilon t}(\sigma^1)^2 + (\sigma^2)^2 + (\sigma^3)^2 \tag{A.1}$$

and describes flat geometry for both rank ϵ solutions ($\epsilon = 0, 1$). Note, however, that the rank 0 case appears naturally in Cartesian coordinates, whereas rank 1 emerges in a kind of mixed Cartesian/polar, Euclidean–Rindler-like coordinates.

Bianchi II. The rank ϵ solutions are given by

$$\mathrm{d}s^2 = \frac{t\mathrm{e}^{2\epsilon t/b_0}}{b_0^2 c_0^2}\,\mathrm{d}t^2 + \frac{1}{t}(\sigma^1)^2 + \frac{t}{b_0^2}(\sigma^2)^2 + \frac{t\mathrm{e}^{2\epsilon t/b_0}}{c_0^2}(\sigma^3)^2. \tag{A.2}$$

The Kretschmann scalar is given by

$$\mathcal{K} = R_{MNPQ}R^{MNPQ} = 8b_0^2c_0^4\mathrm{e}^{-4t\epsilon/b_0}\frac{(\epsilon t)^2 + 3b_0\epsilon t + 3b_0^2}{t^6} \tag{A.3}$$

from which we can see that at $t = 0$ the metric has a curvature singularity.

Bianchi III. The Bianchi-III self-dual metrics are all rank one. They are captured by two expressions, depending on whether $a \neq r$ (equation (A.4)), or $a = r$ (equation (A.6)), in the general co-frame (31) after a convenient rescaling of t by $t \to c_0^2 t$ we obtain

$$\begin{aligned}\mathrm{d}s^2 = {} & \frac{F(t)}{32c_0^4\cosh^4(t-t_*)}\,\mathrm{d}t^2 + \frac{(Kt-1)\tanh(t-t_*) - K}{c_0^2}(\sigma^3)^2 \\ & + \frac{g_1(t)}{F(t)}(\sigma^1)^2 + \frac{g_2(t)}{F(t)}(\sigma^2)^2 + 2\frac{g_3(t)}{F(t)}\sigma^1\sigma^2,\end{aligned} \tag{A.4}$$

where we have introduced the functions $F(t)$, $g_1(t)$, $g_2(t)$ and $g_3(t)$ given by

$$\begin{aligned} F(t) &= 8c_0^2\cosh\big(t-t_*\big)[(Kt-1)\sinh(t-t_*) - K\cosh(t-t_*)], \\ g_1(t) &= (K^2+1)\cosh(2(t-t_*)) + 2K\sinh(2(t-t_*)) + 2K^2t^2 + K^2 - 1, \\ g_2(t) &= (K^2+1)\cosh(2(t-t_*)) - 2K\sinh(2(t-t_*)) + 2K^2t^2 - 8Kt + K^2 + 7, \\ g_3(t) &= (K^2-1)\cosh(2(t-t_*)) + 2K^2t^2 - 4Kt + K^2 + 1. \end{aligned} \tag{A.5}$$

Denoting the zeros of $F(t)$ as t_i, we find that the Kretschmann scalar diverges as $(t-t_i)^6$ as $t \to t_i$, indicating a curvature singularity at each of the two zeros of $F(t)$. The second solution with $a = r$ is given by

$$\begin{aligned}\mathrm{d}s^2 = {} & \frac{L(B-1)}{4}\frac{\tanh(t)}{\cosh^2(t)}\,\mathrm{d}t^2 + L(B-1)\tanh(t)(\sigma^3)^2 \\ & + \frac{L}{4(B-1)}\{[2\,B^2\,\mathrm{csch}(2t) + \tanh(t)](\sigma^1)^2 \\ & - 2[\tanh(t) - 2\,B(B-2)\mathrm{csch}(2t)]\sigma^1\sigma^2 \\ & \times [\mathrm{csch}(2t)(\cosh(2t) + 2(B-2)^2 - 1](\sigma^2)^2\}.\end{aligned} \tag{A.6}$$

In this case, the Kretschmann scalar is given by

$$\mathcal{K} = \frac{384\coth^6(t)}{(B-1)^2L^2} \tag{A.7}$$

and we find at $t = 0$ the metric has a curvature singularity. The general analysis of these geometries is involved and provides interesting features, which deserve a separate study.

Bianchi VI$_0$. The general metric for rank ϵ solutions reads

$$\mathrm{d}s^2 = \sin(2t)\frac{\mathrm{e}^{2\epsilon Zt}}{c_0^2}(\mathrm{d}t^2 + (\sigma^3)^2) + \tan(t)(\sigma^1)^2 + \cot(t)(\sigma^2)^2, \tag{A.8}$$

where $t \in [0, \pi/2]$. A curvature singularity appears at the boundaries $t = 0$ and $t = \pi/2$. The Kretschmann scalar is given by

$$\mathcal{K} = 16c_0^4\mathrm{e}^{-4t\epsilon Z}\frac{6\epsilon Z\sin(4t) + [9 - (\epsilon Z)^2]\cos(4t) + (\epsilon Z)^2 + 15}{\sin^6(2t)}, \tag{A.9}$$

and we see that at $t = 0, \pi/2$ the metric has a curvature singularity.

Bianchi VII$_0$. The general metric for rank ϵ solutions reads

$$\mathrm{d}s^2 = \sinh(2t)\frac{\mathrm{e}^{2\epsilon Zt}}{c_0^2}(\mathrm{d}t^2 + (\sigma^3)^2) + \tanh(t)(\sigma^1)^2 + \coth(t)(\sigma^2)^2 \tag{A.10}$$

The Kretschmann scalar is given by

$$\mathcal{K} = 16c_0^4\,\mathrm{e}^{-4t\epsilon Z}\frac{6\epsilon Z\sinh(4t) + [9 + (\epsilon Z)^2]\cosh(4t) - (\epsilon Z)^2 + 15}{\sinh^6(2t)} \tag{A.11}$$

and we again find a curvature singularity at $t = 0$. In the rank 1 case, we may take the large-t limit of the above metric to obtain

$$\mathrm{d}s^2 = c_0^2\mathrm{e}^{2(1+Z)t}(\mathrm{d}t^2 + (\sigma^3)^2) + (\sigma^1)^2 + (\sigma^2)^2 \tag{A.12}$$

which also solves the self-duality equations but has a vanishing Kretschmann scalar and is actually flat.

Bianchi VIII. There is only the rank 0 solution whose simplest writing is

$$\mathrm{d}s^2 = \frac{P^{-1/2}}{4}\mathrm{d}x^2 + P^{1/2}\left(\frac{(\sigma^1)^2}{x_1 - x} + \frac{(\sigma^2)^2}{x_2 - x} + \frac{(\sigma^3)^2}{x}\right) \tag{A.13}$$

with $P = (x_1 - x)(x_2 - x)x$ where x_1, x_2 are positive and $0 \leqslant x \leqslant \min\{x_1, x_2\}$. The Krestschmann scalar blows up as $x^{-3}(x - x_1)^{-3}(x - x_2)^{-3}$, indicating that the singularity at the boundary of the domain of definition of x is a true one. Let us assume $x_1 = \alpha^2 > x_2 = \beta^2$. We may re-express the metric in the gauge $N = \theta$, using Jacobi elliptic functions of module β/α. Making the substitution $x = \beta^2\,\mathrm{sn}^2(\alpha t)$ we obtain

$$\begin{aligned}\mathrm{d}s^2 = {}& \alpha\beta^2\mathrm{sn}(\alpha t)\,\mathrm{cn}(\alpha t)\,\mathrm{dn}(\alpha t)\,\mathrm{d}t^2 + \frac{\beta^2\,\mathrm{sn}(\alpha t)\,\mathrm{cn}(\alpha t)}{\alpha\,\mathrm{dn}(\alpha t)}(\sigma^1)^2 \\ & + \frac{\alpha\,\mathrm{sn}(\alpha t)\,\mathrm{dn}(\alpha t)}{\mathrm{cn}(\alpha t)}(\sigma^2)^2 + \frac{\alpha\,\mathrm{cn}(\alpha t)\,\mathrm{dn}(\alpha t)}{\mathrm{sn}(\alpha t)}(\sigma^3)^2.\end{aligned} \tag{A.14}$$

The t variable belongs to the interval $[0, 2\,K(\beta/\alpha)/\alpha]$, $K(k)$ being the complete elliptic integral of the first kind of module k.

Bianchi IX. We have solutions in case of rank 0 (*Lagrange* system of equations) and of rank 3 (*Darboux-Halphen* system of equations).

The general rank 0 solution[10] was found by Belinsky *et al* in [5] as a strict $SU(2)$-symmetric generalization of the Eguchi–Hanson gravitational instanton. The latter has

[10] The metric can be chosen diagonal; the off-diagonal entries are consistently set to zero in this class.

enhanced $SU(2) \times U(1)$ isometry and is a solution of the Lagrange system. An algebraic expression of the solution, analogous in form to equation (A.13), is

$$\mathrm{d}s^2 = \frac{P^{-1/2}}{4}\,\mathrm{d}x^2 + P^{1/2}\left(\frac{(\sigma^1)^2}{x-x_1} + \frac{(\sigma^2)^2}{x-x_2} + \frac{(\sigma^3)^2}{x}\right) \tag{A.15}$$

with $P = (x-x_1)(x-x_2)x$ where x_1, x_2 are negative. The general strict $SU(2)$-symmetric solutions have curvature singularities. To obtain the Eguchi–Hanson gravitational instanton, one may take $x_1 = x_2 = x_0$ and by a translation in x set $x_3 = 0$.

Let us assume $x_1 = -\alpha^2 < x_2 = -\beta^2$. In the gauge $N = \theta$, the metric can still be expressed in terms of standard Jacobi elliptic functions but now of module $\sqrt{\alpha^2-\beta^2}/\alpha$; using $x = \beta^2 \mathrm{sn}^2(\alpha t)/\mathrm{cn}^2(\alpha t)$ with $t \in [0, K(\sqrt{\alpha^2-\beta^2}/\alpha)/\alpha]$ we obtain

$$\begin{aligned}\mathrm{d}s^2 = {}& \alpha\beta^2 \frac{\mathrm{sn}(\alpha t)\,\mathrm{dn}(\alpha t)}{\mathrm{cn}^3(\alpha t)}\mathrm{d}t^2 + \frac{\beta^2\,\mathrm{sn}(\alpha t)}{\alpha\,\mathrm{cn}(\alpha t)\,\mathrm{dn}(\alpha t)}(\sigma^1)^2 \\ & + \frac{\alpha\,\mathrm{sn}(\alpha t)\,\mathrm{dn}(\alpha t)}{\mathrm{cn}(\alpha t)}(\sigma^2)^2 + \frac{\alpha\,\mathrm{dn}(\alpha t)}{\mathrm{sn}(\alpha t)\,\mathrm{cn}(\alpha t)}(\sigma^3)^2.\end{aligned} \tag{A.16}$$

The issue of the rank 3 solution is more subtle. It is a generalization of Taub–NUT metric, with strict $SU(2)$ isometry, and solves the Darboux–Halphen system. As explained in [8], it requires the use of modular forms. For simplicity we trade a, b, c for Ω_α, $\alpha = 1, 2, 3$, where $\Omega_1 = \frac{1}{bc}$, $\Omega_2 = \frac{1}{ac}$, and $\Omega_3 = \frac{1}{ab}$, and introduce a triplet of weight-two modular forms of $\Gamma(2) \subset PSL(2,\mathbb{Z})$:

$$E_1 = \frac{\mathrm{d}\lambda/\mathrm{d}z}{\lambda}, \quad E_2 = \frac{\mathrm{d}\lambda/\mathrm{d}z}{\lambda-1}, \quad E_3 = \frac{\mathrm{d}\lambda/\mathrm{d}z}{\lambda(\lambda-1)}, \tag{A.17}$$

where λ is solution of Schwartz' equation

$$\frac{\mathrm{d}^3\lambda/\mathrm{d}z^3}{\mathrm{d}\lambda/\mathrm{d}z} - \frac{3}{2}\left(\frac{\mathrm{d}^2\lambda/\mathrm{d}z^2}{\mathrm{d}\lambda/\mathrm{d}z}\right)^2 = -\frac{1}{2}\left(\frac{1}{\lambda^2} + \frac{1}{(\lambda-1)^2} - \frac{1}{\lambda(\lambda-1)}\right)\left(\frac{\mathrm{d}\lambda}{\mathrm{d}z}\right)^2. \tag{A.18}$$

Any real solution of the Darboux–Halphen system reads

$$\Omega_\alpha(t) = -\frac{1}{2}\frac{\mathrm{d}}{\mathrm{d}t}\log E_\alpha(it), \quad \alpha = 1, 2, 3, \tag{A.19}$$

and generates a Bianchi-IX, rank 1 gravitational instanton (equations (1) and (31)). A generic curvature singularity is present in these geometries. This singularity can be pushed at infinity for one specific choice of $\lambda(z)$: $\lambda = \theta_2^4/\theta_3^4$, where $\theta_{2,3}$ are the standard Jacobi theta functions[11]. This case corresponds to the Atiyah–Hitchin solution [20, 21]. Similar to the rank 0 solution, in the case that two of the metric factors are equal the solutions has enhanced $SU(2) \times U(1)$ isometry and takes the form of the well-known Taub-NUT metric

$$\mathrm{d}s^2 = \frac{r^2}{4(1+kr^2)^2}((\sigma^1)^2 + (\sigma^2)^2) + \frac{r^2}{4}(\sigma^3)^2 + \frac{1}{(1+kr^2)^4}\,\mathrm{d}r^2. \tag{A.20}$$

[11] For concreteness ($q = \exp 2\mathrm{i}\pi z$)

$$\theta_2(z) = 2q^{\frac{1}{8}}\prod_{n=1}^{\infty}(1-q^{2n})(1+q^n), \quad \theta_3(z) = \prod_{n=1}^{\infty}(1-q^n)(1+q^{n-1/2})^2.$$

References

[1] Belavin A A, Polyakov A M, Shvarts A S and Tyupkin Yu S 1975 Pseudoparticle solutions of the Yang-Mills equations *Phys. Lett.* **59B** 85

[2] Eguchi T and Hanson A J 1978 Asymptotically flat self-dual solutions to Euclidean gravity *Phys. Lett.* **74B** 249

[3] Eguchi T and Hanson A J 1979 Selfdual solutions to Euclidean gravity *Ann. Phys.* **120** 82

[4] Newman E T, Tamburino L and Unti T J 1963 Empty-space generalization of the Schwarzschild metric *J. Math. Phys.* **4** 915

[5] Belinsky V A, Gibbons G W, Page D N and Pope C N 1978 Asymptotically Euclidean Bianchi IX metrics in quantum gravity *Phys. Lett.* **76B** 433

[6] Gibbons G W and Pope C N 1979 The positive action conjecture and asymptotically Euclidean metrics In quantum gravity *Commun. Math. Phys.* **66** 267

[7] Atiyah M F, Hitchin N J and Singer I M 1978 Self-duality in four-dimensional Riemannian geometry *Proc. R. Soc.* A **362** 425

[8] Takhtajan L A 1992 A simple example of modular forms as tau functions for integrable equations *Theor. Math. Phys.* **93** 1308

Takhtajan L A 1992 A simple example of modular forms as tau functions for integrable equations *Teor. Mat. Fiz.* **93** 330

[9] Darboux G 1878 Mémoire sur la théorie des coordonnées curvilignes et des systèmes orthogonaux *Ann. Ec. Normale Supér.* **7** 101

[10] Halphen G-H 1881 Sur un système d'équations différentielles *C. R. Acad. Sc. Paris* **92** 1001

[11] Halphen G-H 1881 Sur certains systèmes d'équations différentielles *C. R. Acad. Sc. Paris* **92** 1004

[12] Petropoulos P M http://wwwth.mppmu.mpg.de/members/strings/Ricci/ ricci_files/Talks/Petropoulos.pdf

[13] Lorenz D 1983 Gravitational instanton solutions for Bianchi types I–IX *Acta Phys. Pol.* **14** 791

[14] Lorenz-Petzold D 1989 Gravitational instanton solutions *Prog. Theor. Phys.* **81** 17

[15] Kasner E 1921 Geometrical theorems on Einstein's cosmological equations *Am. J. Math.* **43** 217

[16] Bourliot F, Estes J, Petropoulos P M and Spindel Ph 2009 Gravitational instantons, self-duality and geometric flows arXiv:0906.4558 [hep-th]

[17] Pedersen H 1986 Einstein metrics, spinning top motions and monopoles *Math. Ann.* **274** 35

[18] Spindel Ph 1985 Gravity before supergravity *Supersymmetry (NATO ASI Series, Series B: Physics* vol 125*)* ed K Dietz, R Flume, G v Gehlen and V Rittenberg (New York and London: Plenum)

[19] Gibbons G W and Hawking S W 1979 Classification of gravitational instanton symmetries *Commun. Math. Phys.* **66** 291

[20] Atiyah M F and Hitchin N J 1985 Low-energy scattering of non-Abelian magnetic monopoles *Phil. Trans. R. Soc.* A **315** 459

[21] Atiyah M F and Hitchin N J 1985 Low-energy scattering of non-Abelian monopoles *Phys. Lett.* **107A** 21

[22] Barrow J D, Gaspar Y and Saffin P M 2000 Some exact non-vacuum Bianchi VI(0) and VII(0) instantons *Class. Quantum Grav.* **17** 1435 (arXiv:gr-qc/9905100)

[23] Saha B 2007 Interacting spinor and scalar fields in Bianchi cosmology arXiv:gr-qc/0701059

[24] Saha B and Rikhvitsky V 2006 Bianchi type I universe with viscous fluid: a qualitative analysis *Physica* D **219** 168 (arXiv:gr-qc/0410056)

[25] Spokoiny B L 1982 The effect of the electromagnetic fields on the evolution of homogeneous cosmological models near the singularity *Gen. Rel. Grav.* **14** 279

[26] Fay S 2000 Sufficient conditions for curvature invariants to avoid divergences in hyperextended scalar tensor theory for Bianchi models *Class. Quantum Grav.* **17** 2663 (arXiv:gr-qc/0309087)

Annexe H

Publication 6 : I. Bakas, F. Bourliot, D. Lust and M. Petropoulos, "Mixmaster universe in Horava-Lifshitz gravity," Class. Quant. Grav. 27 (2010) 045013 [arXiv :0911.2665 [hep-th]].

CPHT-RR111.1109
LMU-ASC 48/09
MPP-2009-180

Mixmaster universe in Hořava-Lifshitz gravity

Ioannis Bakas[*1], **Francois Bourliot**[†2], **Dieter Lüst**[‡3,4] and **Marios Petropoulos**[§2]

[1] *Department of Physics, University of Patras*
26500 Patras, Greece

[2] *Centre de Physique Théorique, Ecole Polytechnique*
CNRS UMR 7644, 91128 Palaiseau Cedex, France

[3] *Max-Planck-Institut für Physik*
Föhringer Ring 6, 80805 München, Germany

[4] *Arnold-Sommerfeld-Center für Theoretische Physik*
Department für Physik, Ludwig-Maximilians-Universität München
Theresienstraße 37, 80333 München, Germany

arXiv:0911.2665v1 [hep-th] 13 Nov 2009

November 13, 2009

ABSTRACT

We consider spatially homogeneous (but generally non-isotropic) cosmologies in the recently proposed Hořava-Lifshitz gravity and compare them to those of general relativity using Hamiltonian methods. In all cases, the problem is described by an effective point particle moving in a potential well with exponentially steep walls. Focusing on the closed-space cosmological model (Bianchi type IX), the mixmaster dynamics is now completely dominated by the quadratic Cotton tensor potential term for very small volume of the universe. Unlike general relativity, where the evolution towards the initial singularity always exhibits chaotic behavior with alternating Kasner epochs, the anisotropic universe in Hořava-Lifshitz gravity (with parameter $\lambda > 1/3$) is described by a particle moving in a frozen potential well with fixed (but arbitrary) energy E. Alternating Kasner epochs still provide a good description of the early universe for very large E, but the evolution appears to be non-ergodic. For very small E there are harmonic oscillations around the fully isotropic model. The question of chaos remains open for intermediate energy levels.

[*]bakas@ajax.physics.upatras.gr
[†]bourliot@cpht.polytechnique.fr
[‡]dieter.luest@lmu.de
[§]marios@cpht.polytechnique.fr

1 Introduction

General relativity predicts the existence of space-time singularities under some general conditions, which in a cosmological context are space-like and correspond to the initial singularity of the universe, [1], [2]. Studying the asymptotic behavior of Einstein equations in the vicinity of space-like singularities provides the way that the initial state of the universe is reached classically. A broad framework for this purpose was developed in the seminal work of Belinskii, Khalatnikov and Lifshitz, [3], [4], [5], who found that the spatial points decouple leading to dimensional reduction of the field equations to one (time) coordinate. Then, the universe is described as a point particle moving in an effective potential well, and, remarkably, the dynamical equations are the same as in spatially homogeneous (but generally non-isotropic) cosmological models, in particular Bianchi IX for having a closed universe with spherical topology. Thus, in this context, it becomes important to investigate the main features of the homogeneous and anisotropic cosmologies in the small volume limit of the universe, where the matter sources are ignored.

The dynamics of Bianchi IX model in vacuum (also known as mixmaster universe) has been thoroughly analyzed in the literature by Belinskii, Khalatnikov and Lifshitz, [3], [4], [5], and independently by Misner who used Hamiltonian methods, [6], [7], [8], [9], [10] (but see also the textbook [11] and the monograph [12]). The results can be summarized in a nut-shell by saying that the evolution consists of alternating Kasner epochs, acting as oscillations that permute the principal axes of the spherical spatial slices, as the universe is approaching the initial singularity. A good picture of the dynamics close to the singularity is then provided by a billiard motion in a finite region of Lobachevsky plane, which turns out to be chaotic. More general studies of the chaotic behavior of the mixmaster universe have been carried out in the literature over the years, [13], [14], [15], [16], and the whole subject is now well established and understood for general relativity in four space-time dimensions. Several generalizations have also been considered in detail, in particular in the context of higher dimensional Kaluza-Klein theories of gravity, [17], [18], where the billiard picture appears to be universal and the criteria for the appearance of chaos can be formulated in Lie algebraic terms that depend on the dimensionality of space-time, [19], [20], [21] (but see also [22] for a comprehensive review of these matters and references therein). In parallel, there have also been studies of the same problem in higher curvature generalizations of gravity, in particular in four dimensions, by adding R^2 (and possibly other) curvature terms to the gravitational action, where the chaotic behavior was found to be absent, [23], [24], [25]. Thus, the subject is quite rich and interesting in all generally covariant effective gravitational theories, including those that arise from string theory.

Recently, there has been a rather odd proposal in the literature to replace the rel-

ativistic theory of Einstein gravity by a non-relativistic field theory of Lifshitz type that is only applicable to the ultra-violet regime, [26], [27]. The resulting theory became known as Hořava-Lifshitz gravity and it is by construction a higher derivative modification of ordinary general relativity with anisotropic scaling in the space and time coordinates. As such, its field equations contain second derivatives in time and higher derivatives in space coordinates (actually up to six in four space-time dimensions where the present work will focus). This proposal aims to provide a renormalizable theory of quantum gravity at short distances that flows to ordinary general relativity in the infra-red domain of large distances. It is, however, quite different in nature from the (more conventional) higher derivative generalizations of Einstein gravity that have been considered so far, which remain fully covariant, whereas here the modification by higher curvature terms affects only the spatial dimensions.

It should be said straight from the beginning that there are no general theorems for the existence of singularities in Hořava-Lifshitz gravity, and under which conditions these may be valid, in particular for the existence of an initial space-like singularity in a cosmological context[1]. Furthermore, no analysis has been made so far on how these singularities, if present, will be approached asymptotically at very early times (one may phrase it by simply saying that the analysis "BKL for HL" is still lacking).

Remarkably, it can be seen that all spatially homogeneous (but generally anisotropic) cosmological space-times, including, in particular, the Bianchi IX model, provide consistent mini-superspace truncations of the field equations in Hořava-Lifshitz gravity, as in general relativity. In this paper we begin studying these models in detail, first because they are interesting in their own right, as they can provide a basis for comparing the two different theories of gravity in the classical and (hopefully in the future) in their quantum regime, and, second because they can also play a role in understanding the evolution of the universe close to the initial singularity, as in general relativity. In all cases, if the spatial points decouple close to the singularity, which is a reasonable expectation in general, the closed universe will be effectively described by mixmaster dynamics, viewed as point particle moving in a potential well whose structure depends on the theory. The framework that will be adopted throughout this study is that of Hamiltonian dynamics, since the action of Hořava-Lifshitz gravity is only defined through the $3+1$ ADM decomposition of the space-time metric.

The rest of this paper is organized as follows: Section 2 provides a brief overview

[1]The only case that has already been extensively studied in the literature is the analogue of Friedmann universe, which is an isotropic Bianchi IX model with suitable matter sources, and was found to exhibit a bounce - rather than a singularity - in the past under some technical but rather general conditions on the couplings of the theory, [28], [29], [30]. Such a bounce, however, might only be attributed to the particular model, since the addition of shearing components, due to anisotropies, could circumvent it and render it unstable. We will discuss more extensively this point later, in section 4, offering also some simple anisotropic models that do not exhibit a bounce.

of Hořava-Lifshitz gravity in $3+1$ dimensions and introduces the necessary notions in self-contained way. Section 3 explains why the homogeneous cosmologies are consistent models in Einstein gravity as well as in Hořava-Lifshitz gravity and describes mixmaster dynamics as an effective particle model moving in a potential well that is applicable to both theories. The effective potentials are derived in each case separately. Section 4 investigates the evolution of the universe close to the initial singularity, where the problem simplifies considerably, but it still exhibits rich structure. Unlike general relativity, where the potential vanishes for generic values of the anisotropy parameters and the evolution towards the initial singularity proceeds in an oscillatory fashion with alternating Kasner epochs, the universe in Hořava-Lifshitz gravity (with parameter $\lambda > 1/3$) is described by a particle moving in a frozen potential well with prescribed (but arbitrary) energy. The question of chaos in the corresponding motion is briefly addressed. Finally, section 5 contains our conclusions and discusses some open questions and directions for further research. Two appendices are also included at the end. The first contains useful formulas for the Bianchi IX model of three-geometries, collecting, in particular, the expressions for its Ricci curvature and Cotton tensors. The second contains a derivation of the bounce law from the exponentially steep walls of the potential well that will be used in mixmaster dynamics.

2 Hořava-Lifshitz gravity

General relativity as well as Hořava-Lifshitz gravity are formulated in a similar fashion using the ADM decomposition of the four-dimensional metric in space-time M_4, which is assumed to be topologically $R \times \Sigma_3$,

$$ds^2 = -N^2 dt^2 + \gamma_{ij}(dx^i + N^i dt)(dx^j + N^j dt) \ . \tag{2.1}$$

The three-dimensional slices Σ_3 have metric γ_{ij} and extrinsic curvature tensor

$$K_{ij} = \frac{1}{2N}\left(\frac{\partial \gamma_{ij}}{\partial t} - \nabla_i N_j - \nabla_j N_i\right) . \tag{2.2}$$

The space of all three-dimensional metrics γ_{ij}, which is known as Wheeler-DeWitt superspace, is very important in this study. It is endowed with a metric, often called DeWitt metric, [31], which is taken here to depend on a parameter λ in general. The metric in superspace, and its inverse, are defined as usual,

$$\mathcal{G}^{ijkl} = \frac{1}{2}\left(\gamma^{ik}\gamma^{jl} + \gamma^{il}\gamma^{jk}\right) - \lambda \gamma^{ij}\gamma^{kl} \ , \tag{2.3}$$

and

$$\mathcal{G}_{ijkl} = \frac{1}{2}\left(\gamma_{ik}\gamma_{jl} + \gamma_{il}\gamma_{jk}\right) - \frac{\lambda}{3\lambda - 1}\gamma_{ij}\gamma_{kl} \ , \tag{2.4}$$

so that

$$\mathcal{G}_{ijmn}\mathcal{G}^{mnkl} = \frac{1}{2}\left(\delta_i^k\delta_j^l + \delta_i^l\delta_j^k\right) \ . \tag{2.5}$$

The DeWitt metric is positive definite for $\lambda < 1/3$ and indefinite for $\lambda > 1/3$, which includes, in particular, the special value $\lambda = 1$ applicable to Einstein gravity.

The gravitational theories that will be considered in the sequel, using the ADM formalism (see, for instance, the textbook [11]), admit a four-dimensional action

$$S = S_{\mathrm{K}} - S_{\mathrm{V}} \ , \tag{2.6}$$

where S_{K} is the kinetic part of the action with universal form

$$S_{\mathrm{K}} = \frac{2}{\kappa^2}\int dt d^3x \sqrt{\det\gamma}\ N\ K_{ij}\mathcal{G}^{ijkl}K_{kl} \ . \tag{2.7}$$

The potential part of the action, S_{V}, is given by

$$S_{\mathrm{V}} = \int dt d^3x \sqrt{\det\gamma}\ N\ \mathcal{V} \ , \tag{2.8}$$

where $\mathcal{V}$ is chosen according to the theory.

Ordinary general relativity corresponds to $\lambda = 1$ and has potential term

$$\mathcal{V}_{\mathrm{GR}} = -\frac{2}{\kappa^2}(R - 2\Lambda) \tag{2.9}$$

that involves second derivatives in the space coordinates. Here, Λ is the cosmological constant in M_4, R is the Ricci scalar curvature of the three-dimensional metric γ_{ij} and $\kappa^2 = 32\pi G$ is expressed in terms of Newton's constant in four space-time dimensions. On the other hand, Hořava-Lifshitz gravity has a potential that involves higher order terms, thus breaking relativistic invariance of the four-dimensional theory, [26], [27]. These terms have a specific form, composed of several higher order (quadratic) curvature corrections, which are designed to smooth out the ultra-violet behavior of gravity. Also, the parameter λ is left undetermined in this context and may run with the energy scale in quantum theory.

A particularly simple choice of $\mathcal{V}$ in Hořava-Lifshitz gravity, though by no means unique, corresponds to the so called "detailed balance" condition, meaning

$$\mathcal{V}_{\mathrm{HL}} = \frac{\kappa^2}{2}E^{ij}\mathcal{G}_{ijkl}E^{kl} \ , \tag{2.10}$$

so that $\mathcal{V}$ is derived from a superpotential $\mathcal{W}$ in the sense

$$E^{ij} = \frac{1}{2\sqrt{\det\gamma}} \frac{\delta \mathcal{W}}{\delta \gamma_{ij}} \,. \tag{2.11}$$

In $3+1$ dimensions that will be considered here, the superpotential is taken to be the Euclidean action of three-dimensional topological gravity on Σ_3 with cosmological constant $\Lambda_{\rm w}$ (other than Λ),

$$\mathcal{W} = \frac{1}{w^2} \mathcal{W}_{\rm CS} + \mu \mathcal{W}_{\rm EH} \,, \tag{2.12}$$

where the first term refers to the gravitational Chern-Simons action, [32],

$$\mathcal{W}_{\rm CS} = \int_{\Sigma_3} d^3x \sqrt{\det\gamma}\, \epsilon^{ijk} \Gamma^l_{im} \left(\partial_j \Gamma^m_{kl} + \frac{2}{3} \Gamma^m_{jn} \Gamma^n_{kl} \right) , \tag{2.13}$$

with $\epsilon^{123} = 1$, and the second term is the corresponding three-dimensional Einstein-Hilbert action

$$\mathcal{W}_{\rm EH} = \int_{\Sigma_3} d^3x \sqrt{\det\gamma}\, \left(R - 2\Lambda_{\rm w} \right) . \tag{2.14}$$

Thus, $\mathcal{V}_{\rm HL}$ with "detailed balance" follows by computing E^{ij} varying the superpotential functional $\mathcal{W}$ with respect to the metric γ_{ij}. The result reads

$$E^{ij} = \frac{1}{w^2} C^{ij} - \frac{\mu}{2} G^{ij} \,, \tag{2.15}$$

where C_{ij} is the Cotton tensor of the metric γ_{ij} defined as follows,

$$C^{ij} = \frac{1}{2\sqrt{\det\gamma}} \frac{\delta \mathcal{W}_{\rm CS}}{\delta \gamma_{ij}} = \frac{1}{\sqrt{\det\gamma}} \epsilon^{ikl} \nabla_k \left(R^j{}_l - \frac{1}{4} \delta^j{}_l R \right) . \tag{2.16}$$

This is a symmetric and traceless tensor that vanishes if and only if the three-dimensional metric is conformally flat. The second term is the familiar Einstein tensor on Σ_3 with three-dimensional cosmological constant $\Lambda_{\rm w}$,

$$G^{ij} = -\frac{1}{\sqrt{\det\gamma}} \frac{\delta \mathcal{W}_{\rm EH}}{\delta \gamma_{ij}} = R^{ij} - \frac{1}{2} R \gamma^{ij} + \Lambda_{\rm w} \gamma^{ij} \,. \tag{2.17}$$

Putting all together, the potential terms of Hořava-Lifshitz gravity in $3+1$ dimensions satisfying the "detailed balance" condition are

$$\mathcal{V}_{\rm HL} = \alpha C_{ij} C^{ij} + \beta C_{ij} R^{ij} + \gamma R_{ij} R^{ij} + \delta R^2 + \epsilon R + \zeta \tag{2.18}$$

with coefficients

$$\alpha = \frac{\kappa^2}{2w^4}\,, \quad \beta = -\frac{\mu\kappa^2}{2w^2}\,, \quad \gamma = \frac{\mu^2\kappa^2}{8}\,, \quad \delta = -\frac{\mu^2\kappa^2(4\lambda-1)}{32(3\lambda-1)}\,,$$
$$\epsilon = \frac{\mu^2\kappa^2\Lambda_{\rm w}}{8(3\lambda-1)}\,, \quad \zeta = -\frac{3\mu^2\kappa^2\Lambda_{\rm w}^2}{8(3\lambda-1)}\,. \tag{2.19}$$

The last two terms are identical to the potential $\mathcal{V}_{\rm GR}$ of general relativity, with the appropriate identifications of the coefficients ϵ and ζ, whereas the remaining ones are higher order (quadratic) curvature corrections that apparently are suppressed in the infra-red limit of the theory.

More general choices of $\mathcal{V}_{\rm HL}$, other than "detailed balance", are also admissible and correspond to the sum (2.18) with arbitrary coefficients; they are only subject to the restriction that general relativity will emerge in the infra-red regime. The analysis that will be performed in the sequel applies equally well to all such general choices of potential in Hořava-Lifshitz gravity with or without "detailed balance".

Finally, it is important to note that the Hořava-Lifshitz theory of gravity is not invariant under general coordinate transformations in space-time; this should be contrasted with other higher order theories of gravity that remain relativistic. Since M_4 is topologically $R \times \Sigma_3$, it is only appropriate here to consider invariance of the action under the restricted class of foliation preserving diffeomorphisms,

$$\tilde{t} = \tilde{t}(t)\,, \qquad \tilde{x}^i = \tilde{x}^i(t,x)\,. \tag{2.20}$$

Thus, the lapse function N associated to the freedom of time reparametrization is restricted to be a function of t alone, whereas the shift vector N_i associated with diffeomorphisms of Σ_3 can depend on all space-time coordinates.

3 Mixmaster dynamics

The mixmaster universe arises as mini-superspace model of gravity assuming that the the three-dimensional slices Σ_3 are homogeneous geometries with the topology of S^3 and isometry group $SU(2)$. Thus, by employing the Bianchi IX ansatz, as explained in Appendix A, the four-dimensional metric is given in diagonal form[2] by

$$ds^2 = -N^2(t)dt^2 + \gamma_1(t)\sigma_1^2 + \gamma_2(t)\sigma_2^2 + \gamma_3(t)\sigma_3^2\,, \tag{3.1}$$

[2]More general non-diagonal metrics of the form $ds^2 = -N^2(t)dt^2 + \gamma_{ij}(t)\sigma_i\sigma_j$ are also legitimate for investigation, but they will not be considered at all in this paper.

using the invariant 1-forms σ_i of $SU(2)$. The metric coefficients are all taken to depend only on the time coordinate t. This class of metrics provides consistent reduction of vacuum Einstein equations to an autonomous system of ordinary non-linear differential equations for $\gamma_i(t)$ that has been studied extensively in the literature in the past fourty years. It provides a simple model of homogeneous, but generally anisotropic, universe, which proves valuable for studying the chaotic behavior of general relativity close to the initial singularity. The same ansatz also works consistently for the Hořava-Lifshitz gravity with or without "detailed balance" and gives rise to another - though more complicated - system of ordinary non-linear differential equations for the coefficients $\gamma_i(t)$.

The purpose of this section is to describe in detail the mini-superspace reduction of the field equations and transform them into an effective point particle model using Hamiltonian methods, as outlined by Misner, [6], [7], [8], [9], [10] (but see also the textbook [11] and the monograph [12]). Although our discussion is entirely confined to the Bianchi IX case, it should be noted here that all homogeneous spaces arising in the Bianchi classification of model three-geometries provide consistent reduction of general relativity as well as Hořava-Lifshitz gravity. The details for all other homogeneous cosmologies in Hořava-Lifshitz gravity will not be included here.

3.1 Effective particle model

Hamiltonian methods for homogeneous cosmologies are most appropriate to use in the ADM decomposition of space-time and they lead naturally to an effective point particle model with appropriately chosen external potential. The method is applicable to both general relativity and Hořava-Lifshitz gravity because the lapse function N is taken to depend only on t in such cases.

Recall that the canonical momenta conjugate to γ_{ij} are simply given by

$$\pi^{ij} = \frac{\delta S}{\delta(\partial\gamma_{ij}/\partial t)} = \frac{2}{\kappa^2}\sqrt{\det\gamma}\,\mathcal{G}^{ijkl}K_{kl} \tag{3.2}$$

given the dependence of the general gravitational action $S = S_{\mathrm{K}} - S_{\mathrm{V}}$ upon the extrinsic curvature, whereas the momenta conjugate to N and N_i vanish. Then, the Hamiltonian form of the action is

$$S = \int dt d^3x \left(\pi^{ij}\frac{\partial\gamma_{ij}}{\partial t} - N\mathcal{H} - N_i\mathcal{H}^i\right), \tag{3.3}$$

where

$$\mathcal{H} = \frac{\kappa^2}{2\sqrt{\det\gamma}}\pi^{ij}\mathcal{G}_{ijkl}\pi^{kl} + \sqrt{\det\gamma}\,\mathcal{V} \tag{3.4}$$

and

$$\mathcal{H}^i = -2\nabla_j \pi^{ij} \,. \tag{3.5}$$

In ordinary general relativity $\mathcal{H} = 0$ and $\mathcal{H}_i = 0$ are the constraints of the theory associated to general reparametrization invariance in the $3+1$ decomposition of the metric. In this context, N and N_i serve as Lagrange multipliers whose variation yields the constraints. On the other hand, the invariance of Hořava-Lifshitz gravity under the restricted class of foliation preserving diffeomorphisms leaves intact the momentum constraints $\mathcal{H}_i = 0$ and replaces the time constraint $\mathcal{H} = 0$ with the much weaker condition

$$\int d^3x \mathcal{H} = 0 \,. \tag{3.6}$$

For homogeneous cosmologies, $\mathcal{H}$ is only a function of t, and so is the lapse function N, and, therefore, there is no difference in the Hamiltonian description of the two theories other than the form of the potential. Also, in these cases, the momentum constraints are satisfied identically, since γ_{ij} and π^{ij} are functions of t only and the covariant derivative in $\mathcal{H}_i$ with respect to space coordinates reduces to an ordinary derivative. Thus, one may consistently choose $N_i = 0$ and forget altogether the momenta constraints.

Based on these observations, the Hamiltonian form of the gravitational action for homogeneous cosmologies takes the following form

$$S = 16\pi^2 \int dt \left(\pi^{ij} \frac{dg_{ij}}{dt} - N\mathcal{H} \right) \tag{3.7}$$

after performing the integration over space that accounts for the $16\pi^2$ factor. Here,

$$\mathcal{H} = \frac{\kappa^2}{2\sqrt{\det\gamma}} \left(\pi^{ij}\pi_{ij} - \frac{\lambda}{3\lambda - 1} (\pi^k{}_k)^2 \right) + \sqrt{\det\gamma}\, \mathcal{V} \tag{3.8}$$

depends only on t and it is constrained to vanish by varying S with respect to N.

At this point, one may employ the freedom of time reparametrizations $\tilde{t} = \tilde{t}(t)$ to eliminate N from the variational problem. Any choice of $N(t)$ inserted in equation (3.7) leaves the action in canonical Hamiltonian form, but the content of the gauge fixed action will be equivalent to the original one only if it is supplemented by the constraint $\mathcal{H} = 0$, which can no longer be derived from the variational principle. The most convenient choice is

$$N(t) = \frac{6}{\kappa^2} \sqrt{\det\gamma(t)} \,, \tag{3.9}$$

which will be adopted from now on. Thus, we arrive at an effective point particle Hamiltonian model for all homogeneous cosmologies; yet another formulation of this

point particle model will be mentioned shortly.

Further simplification occurs by introducing the volume and shape moduli of the three-geometry

$$\gamma_1 = e^{2\Omega+\beta_+ +\sqrt{3}\beta_-} \ , \quad \gamma_2 = e^{2\Omega+\beta_+ -\sqrt{3}\beta_-} \ , \quad \gamma_3 = e^{2\Omega-2\beta_+} \ , \tag{3.10}$$

as explained in Appendix A, so that $\sqrt{\det\gamma} = \sqrt{\gamma_1\gamma_2\gamma_3} = \exp(3\Omega)$. Then, it is appropriate to parametrize the components of the momenta matrix $\pi^i{}_j$, which is diagonal as is the metric matrix, as follows,

$$p_\Omega = 2\pi^k{}_k \ , \quad p^i{}_j = \pi^i{}_j - \frac{1}{3}\delta^i{}_j \pi^k{}_k \ , \tag{3.11}$$

and set

$$p^1{}_1 = \frac{1}{6}(p_+ + \sqrt{3}\, p_-) \ , \quad p^2{}_2 = \frac{1}{6}(p_+ - \sqrt{3}\, p_-) \ , \quad p^3{}_3 = -\frac{1}{3}p_+ \ . \tag{3.12}$$

It turns out that p_Ω is the conjugate momentum to the volume moduli Ω and $p_\pm$ are the conjugate momenta to the shape moduli $\beta_\pm$. In terms of these variables, the gauge fixed action S becomes

$$S = 16\pi^2 \int dt \left(p_\Omega \frac{d\Omega}{dt} + p_+ \frac{d\beta_+}{dt} + p_- \frac{d\beta_-}{dt} - H \right) , \tag{3.13}$$

where t denotes now the specific time coordinate following the choice (3.9) and

$$H = \frac{1}{2}\left(p_+^2 + p_-^2 - \frac{1}{2(3\lambda-1)} p_\Omega^2 \right) + V(\beta_+, \beta_-, \Omega) = 0 \ . \tag{3.14}$$

With the given choice of lapse, the effective potential of the model is

$$V = \frac{6}{\kappa^2} e^{6\Omega} \mathcal{V} \ . \tag{3.15}$$

This is the final form of the action that will be used to study the mixmaster universe in general relativity and Hořava-Lifshitz gravity and compare the results for the two theories. Note that in writing H above we left undetermined the parameter λ of the superspace metric in order to apply it to all cases of present interest.

Finally, as promised, we mention for completeness that there is an alternative formulation of the same effective point particle model based on the reduced ADM action. In this approach, which has been mostly used by Misner (and many others) in general relativity, one eliminates Ω by solving the Hamiltonian constraint for p_Ω and sets $t = \Omega$, choosing also N appropriately. The procedure is similar to going from the quadratic form of the action of a relativistic particle to its square-root form. Then,

the reduced variational problem corresponds to a point particle moving in two dimensions (provided by β_+ and β_- alone) under the influence of a time dependent potential well. The reduced ADM formulation is only adequate for $\lambda > 1/3$, but it will not be used here in any case.

Next, we will specialize the discussion to general relativity and Hořava-Lifshitz gravity and derive, in each case separately, the effective potential of the mixmaster universe that enters in the canonical Hamiltonian variational principle (3.13), (3.14). Hamilton's equations follow by varying Ω, $\beta_\pm$, p_Ω and $p_\pm$ and yield

$$\frac{d^2\beta_\pm}{dt^2} = -\frac{\partial V}{\partial \beta_\pm}\,, \qquad \frac{d^2\Omega}{dt^2} = \frac{1}{2(3\lambda-1)}\frac{\partial V}{\partial \Omega}\,. \tag{3.16}$$

We will not write down explicitly the resulting equations of motion - they cannot be solved in any case - but focus only on the qualitative features of mixmaster dynamics, following from the potential, which make it a valuable tool for exploring the behavior of the universe as it approaches the initial singularity[3].

3.2 General relativity

First, we consider the mixmaster dynamics in general relativity and present the form of the effective particle potential for comparison later with Hořava-Lifshitz gravity. It follows by expressing the three-dimensional Ricci scalar R, given in Appendix A, in terms of Ω and $\beta_\pm$ and reads, [6], [7], [8], [9], [10],

$$V_{\rm GR} = \frac{6}{\kappa^4}e^{4\Omega}\Big[2e^{2\beta_+}\Big(\cosh(2\sqrt{3}\beta_-)-1\Big) - 4e^{-\beta_+}\cosh(\sqrt{3}\beta_-) + e^{-4\beta_+}\Big] + \frac{24\Lambda}{\kappa^4}e^{6\Omega}\,. \tag{3.17}$$

The equations of motion that follow from the variational principle (setting also $\lambda = 1$) cannot be solved exactly. However, they have been studied extensively in the literature for many years and found to exhibit some very interesting qualitative features close to the initial singularity, where the volume of the universe vanishes as $\Omega \to -\infty$. These features will be discussed in some detail later. It will also be helpful in this context to have a good qualitative picture of the potential well.

The effective potential of mixmaster dynamics corresponds to a well shown in Fig.1 for fixed Ω. It has three canyon lines located at $\beta_- = 0$ and $\beta_- = \pm\sqrt{3}\beta_+$, where any

[3]In quantum cosmology one implements the Hamiltonian constraint by postulating the Wheeler-DeWitt equation $\hat{H}\Psi = 0$ for the "wave-function" of the universe with the appropriate factor ordering prescription. Some aspects of the problem have already been studied in the literature for the mixmaster model of ordinary quantum gravity, [33], [34], [35], and similar considerations can also be applied to the case of Hořava-Lifshitz canonical quantum gravity. We will postpone any further discussion of the quantum aspects of early time cosmology to future publication.

two γ_i's become equal. The potential is bounded from below and exhibits discrete Z_3 symmetry by permuting the principal axes of rotation of S^3. Thus, it has the shape of an equilateral triangle in the anisotropy space $(\beta_+,\ \beta_-)$ and exponentially steep walls far away from the origin. Very close to the origin the well is round, as can be seen by expanding $V_{\rm GR}$ up to quadratic order in $\beta_\pm$.

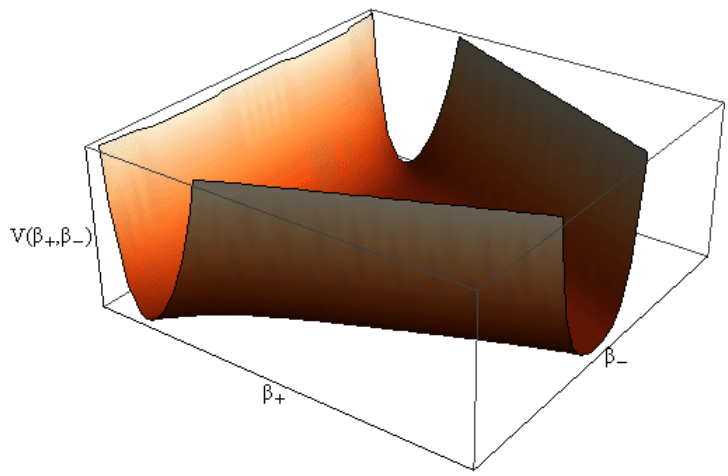

Figure 1: The potential well of mixmaster dynamics and its three canyons

Another useful representation of the effective potential is shown in Fig.2 below by drawing the equipotential curves.

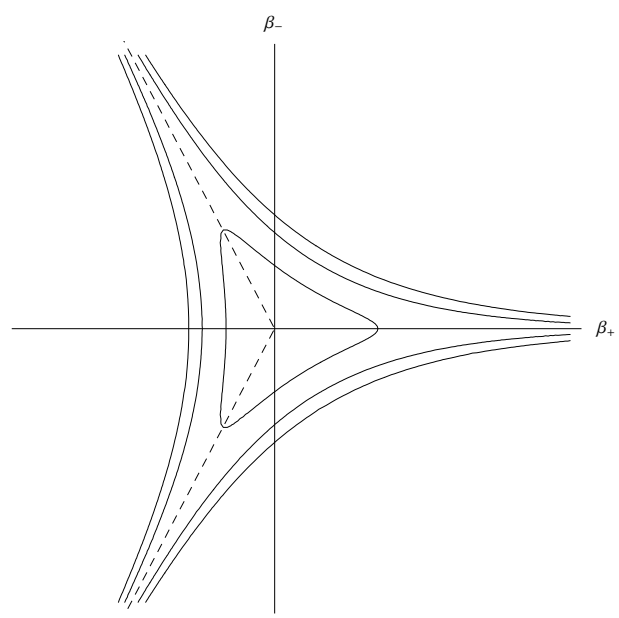

Figure 2: Equipotential lines of the effective potential $V_{\rm GR}(\beta_+, \beta_-)$

As can be seen, they extend symmetrically between the canyon lines $\beta_- = 0$ and $\beta_- = \pm\sqrt{3}\beta_+$, which correspond to a partially anisotropic universe with axial symmetry

(known as Taub space-time, [36]). The fully isotropic case corresponds to the origin $\beta_+ = 0 = \beta_-$, where the potential attains its minimum.

The asymptotic form of the potential for very large values of anisotropy is independent of the cosmological constant Λ and looks like

$$V_{\rm GR} \simeq \frac{6}{\kappa^4} e^{4\Omega} e^{-4\beta_+} \,, \qquad \text{as} \quad \beta_+ \to -\infty \tag{3.18}$$

and

$$V_{\rm GR} \simeq \frac{72}{\kappa^4} e^{4\Omega} \beta_-^2 e^{2\beta_+} \,, \qquad \text{as} \quad \beta_+ \to +\infty \,, \quad |\beta_-| << 1 \,. \tag{3.19}$$

Then, the asymptotic structure of the potential is completely characterized by combining these two relations with the triangular symmetry of the model.

The effective point particle can only escape to infinity along the canyon lines where the potential has the shape shown in Fig.3, keeping Ω fixed. The smallest deviation from axial symmetry will turn the particle against the infinitely steep walls.

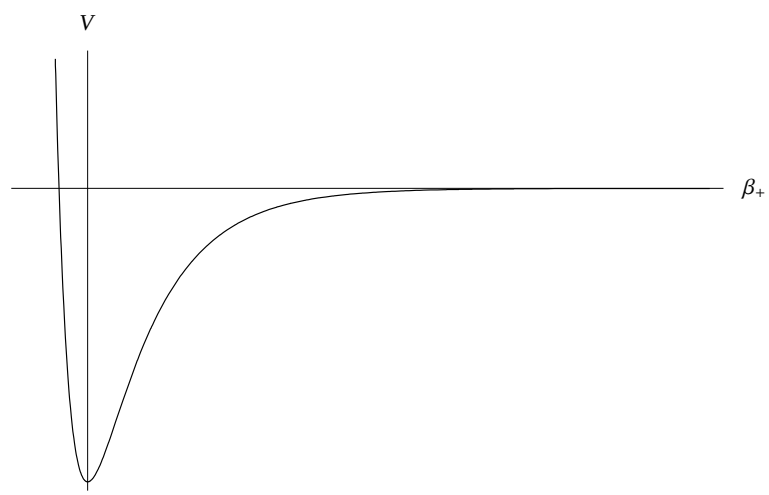

Figure 3: The form of the potential $V_{\rm GR}(\beta_+, \beta_-)$ along the canyon line $\beta_- = 0$

3.3 Hořava-Lifshitz gravity

Applying the same framework to Hořava-Lifshitz gravity, the effective point particle potential is described by

$$V_{\rm HL} = \frac{6}{\kappa^2} e^{6\Omega} \left(\alpha C_{ij} C^{ij} + \beta C_{ij} R^{ij} + \gamma R_{ij} R^{ij} + \delta R^2 + \epsilon R + \zeta \right) \,. \tag{3.20}$$

The coefficients are left arbitrary so that the discussion can be made as general possible without necessarily imposing the "detailed balance" condition. The only restriction we put here is $\alpha > 0$ for well-definiteness, so that $V_{\rm HL}(\beta_+, \beta_-)$ stays bounded from below.

Using the explicit expressions for C_{ij}, R_{ij} and R found in Appendix A and rewriting them in terms of the variables Ω and $\beta_\pm$, we obtain the following results for the individual terms entering in the effective potential of Bianchi IX cosmology:

$$\begin{aligned} C_{ij}C^{ij} &= \frac{1}{2}e^{-6\Omega}\Big[2e^{6\beta_+}\Big(3\cosh(6\sqrt{3}\beta_-) - 3\cosh(4\sqrt{3}\beta_-) + \cosh(2\sqrt{3}\beta_-) - 1\Big) - \\ & 2e^{3\beta_+}\Big(3\cosh(5\sqrt{3}\beta_-) - \cosh(3\sqrt{3}\beta_-) - 2\cosh(\sqrt{3}\beta_-)\Big) + \\ & 2\Big(\cosh(4\sqrt{3}\beta_-) + 2\cosh(2\sqrt{3}\beta_-) - 3\Big) - \\ & 4e^{-3\beta_+}\Big(\cosh(3\sqrt{3}\beta_-) - \cosh(\sqrt{3}\beta_-)\Big) + \\ & e^{-6\beta_+}\Big(2\cosh(2\sqrt{3}\beta_-) + 1\Big) - \\ & 6e^{-9\beta_+}\cosh(\sqrt{3}\beta_-) + 3e^{-12\beta_+}\Big], \end{aligned} \tag{3.21}$$

$$\begin{aligned} C_{ij}R^{ij} &= -e^{-5\Omega}\Big[2e^{5\beta_+}\Big(\cosh(5\sqrt{3}\beta_-) - \cosh(3\sqrt{3}\beta_-)\Big) \\ & -2e^{2\beta_+}\Big(\cosh(4\sqrt{3}\beta_-) - \cosh(2\sqrt{3}\beta_-)\Big) + e^{-4\beta_+} \\ & -2e^{-7\beta_+}\cosh(\sqrt{3}\beta_-) + e^{-10\beta_+}\Big], \end{aligned} \tag{3.22}$$

$$\begin{aligned} R_{ij}R^{ij} &= \frac{1}{4}e^{-4\Omega}\Big[2e^{4\beta_+}\Big(3\cosh(4\sqrt{3}\beta_-) - 4\cosh(2\sqrt{3}\beta_-) + 1\Big) - \\ & 8e^{\beta_+}\Big(\cosh(3\sqrt{3}\beta_-) - \cosh(\sqrt{3}\beta_-)\Big) + \\ & 4e^{-2\beta_+}\Big(\cosh(2\sqrt{3}\beta_-) + 1\Big) - \\ & 8e^{-5\beta_+}\cosh(\sqrt{3}\beta_-) + 3e^{-8\beta_+}\Big], \end{aligned} \tag{3.23}$$

$$\begin{aligned} R^2 &= \frac{1}{4}e^{-4\Omega}\Big[2e^{4\beta_+}\Big(\cosh(4\sqrt{3}\beta_-) - 4\cosh(2\sqrt{3}\beta_-) + 3\Big) - \\ & 8e^{\beta_+}\Big(\cosh(3\sqrt{3}\beta_-) - \cosh(\sqrt{3}\beta_-)\Big) + \\ & 4e^{-2\beta_+}\Big(3\cosh(2\sqrt{3}\beta_-) + 1\Big) - \\ & 8e^{-5\beta_+}\cosh(\sqrt{3}\beta_-) + e^{-8\beta_+}\Big] \end{aligned} \tag{3.24}$$

and

$$R = -\frac{1}{2}e^{-2\Omega}\left[2e^{2\beta_+}\left(\cosh(2\sqrt{3}\beta_-) - 1\right) - 4e^{-\beta_+}\cosh(\sqrt{3}\beta_-) + e^{-4\beta_+}\right] . \qquad (3.25)$$

The potential $V_{\rm HL}(\beta_+, \beta_-)$ also has the shape of an equilateral triangle with exponentially steep walls when $\alpha > 0$. Fig.1 and Fig.2 still provide a good qualitative picture of it far from the origin in (β_+, β_-) parameter space. Only the bottom area close to the origin has slightly different shape that depends on the relative coefficients of the individual terms of the potential. The equations of motion that follow from it provide the analogue of mixmaster dynamics in Hořava-Lifshitz gravity. We will not attempt to solve them here but rather confine ourselves to study some qualitative features that make the model useful for early time cosmology, as in general relativity.

For $\alpha > 0$, which will be assumed from now on, the asymptotic form of the potential $V_{\rm HL}$ for very large values of anisotropy is dominated completely by the quadratic Cotton tensor term, which happens to contain the steepest walls of all terms, and one has

$$V_{\rm HL} \simeq \frac{9}{\kappa^2}\alpha e^{-12\beta_+} , \qquad \text{as} \quad \beta_+ \to -\infty . \qquad (3.26)$$

Likewise, we have

$$V_{\rm HL} \simeq \frac{576}{\kappa^2}\alpha\beta_-^2 e^{6\beta_+} , \qquad \text{as} \quad \beta_+ \to +\infty , \quad |\beta_-| << 1 . \qquad (3.27)$$

Thus, unlike general relativity, we note that the asymptotic form of the potential is independent of Ω.

As before, the effective point particle can only escape to infinity along the canyon lines $\beta_- = 0$ and $\beta_- = \pm\sqrt{3}\beta_+$ which arise for general choices of $V_{\rm HL}$.

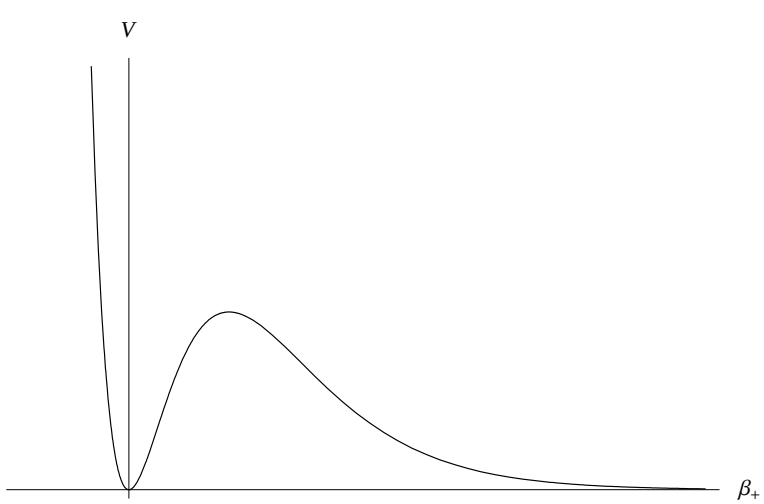

Figure 4: The form of the potential $V_{\rm Cotton}(\beta_+, \beta_-)$ along the canyon line $\beta_- = 0$

Fig.4 shows only the plot of the quadratic Cotton term of the potential, V_{Cotton}, along one of these lines, say $\beta_- = 0$; it exhibits a local maximum at $\beta_+ = (\log 2)/3$, where $\gamma_1 = \gamma_2 = 2\gamma_3$, and similar local maxima show up along the other two lines obtained by permuting γ_i. As will be seen later V_{Cotton} is the only relevant term of V_{HL} in early time cosmology.

4 Approach to the initial singularity

In this section we examine the dynamical behavior of the universe close to the initial singularity, where $\Omega \to -\infty$, using the Bianchi IX model in vacuum. In this context, it is important to have anisotropic models with general parameters $\beta_\pm$, since, otherwise, the universe will not be able close up to S^3 without radiation or matter sources. First, we will make some general - though crude - remarks about the existence of the initial singularity and then study the problem in question for the two different theories of gravitation.

4.1 General considerations

The isotropic Bianchi IX case in vacuum corresponds to a closed Robertson-Walker space-time

$$ds^2 = -N^2(t)dt^2 + e^{2\Omega(t)}d\Omega_3^2\,, \tag{4.1}$$

with $N(t) = (6/\kappa^2)\exp(3\Omega)$. Note, however, that this metric cannot remain isotropic more than instantaneously; consistency of the dynamics also requires the presence of some shearing components provided by space anisotropy in vacuum - beyond the pure dilation - or suitable sources and combinations thereof.

In general relativity, this follows from the form of the potential assuming $\beta_+ = 0 = \beta_-$ for all time. Since the potential

$$V_{\text{GR}}^{\text{isotropic}}(\Omega) = -\frac{6}{\kappa^4}\left[3e^{4\Omega} - 4\Lambda e^{6\Omega}\right] \tag{4.2}$$

is always negative for small volume, irrespective of Λ, it fails to satisfy the Hamiltonian constraint (setting $\lambda = 1$),

$$\frac{1}{8}p_\Omega^2 = 2\left(\frac{d\Omega}{dt}\right)^2 = V_{\text{GR}}^{\text{isotropic}}(\Omega)\,. \tag{4.3}$$

Adding sources, in the form of perfect fluid, remedies the situation and yields the Friedmann universe. Recall in this case that the potential density $\mathcal{V}_{\text{GR}}$ is modified by

adding the (positive) contribution of the energy density ρ of the fluid, so that[4]

$$2\left(\frac{d\Omega}{dt}\right)^2 = V_{\rm GR} + \mu\, e^{\nu\,\Omega}\,, \tag{4.4}$$

where the contribution of non-relativistic matter sources corresponds to $\nu = 3$ (since $\rho \sim V^{-1}$) and that of radiation to $\nu = 2$ (since $\rho \sim V^{-4/3}$) with $V = \exp(3\Omega)$. Clearly, the radiation term provides the dominant contribution in the small volume limit and one obtains an expanding isotropic and homogeneous universe with initial singularity at $T = 0$. If deviations from isotropy are subdominant in the small volume limit, compared to radiation, the initial singularity will persist in the presence of sources. This argument only applies to the anisotropy terms of the potential $V_{\rm GR}$ that depends on the volume as $\exp(4\Omega)$ via the curvature. The anisotropy, however, introduces additional (positive definite) terms in the Hamiltonian constraint, namely the kinetic energy of the anisotropy parameters $(d\beta_+/dt)^2 + (d\beta_-/dt)^2$ if one considers the Bianchi IX model, which completely dominate the evolution close to the initial singularity - essentially trying to "avoid" it by oscillations - as will be discussed later. In all cases, the universe can come to a singular state at $T = 0$ satisfying the field equations.

In Hořava-Lifshitz gravity, the isotropic potential does not receive contribution from the Cotton tensor, since C_{ij} vanishes identically. Thus, the potential given in general by equation (3.20), without necessarily assuming "detailed balance" condition, becomes

$$V_{\rm HL}^{\rm isotropic}(\Omega) = \frac{3}{2\kappa^2}\left[3(\gamma+3\delta)e^{2\Omega} + 6\epsilon e^{4\Omega} + 4\zeta e^{6\Omega}\right]. \tag{4.5}$$

The first term arises from the combined effect of $R_{ij}R^{ij}$ and R^2 and dominates the dynamics for small volume. The Hamiltonian constraint now reads

$$\frac{1}{4(3\lambda-1)}p_\Omega^2 = (3\lambda-1)\left(\frac{d\Omega}{dt}\right)^2 = V_{\rm HL}^{\rm isotropic}(\Omega) \tag{4.6}$$

and cannot be possibly fulfilled when

$$(3\lambda-1)(\gamma+3\delta) < 0\,. \tag{4.7}$$

This inequality, which is certainly satisfied for in the case of "detailed balance" condition (see the choice of coefficients (2.19)), means that the quadratic curvature terms correspond to "dark radiation" (since they effectively have "$\nu = 2$"), but with negative

[4]This is one of the Friedmann equation in standard cosmology with p_Ω being the Hubble parameter. Also, to compare with the more standard form of these equations, it is appropriate to use another time frame defined as $dT = N(t)dt$, where the Robertson-Walker metric takes the more familiar form $ds^2 = -dT^2 + a^2(T)d\Omega_3^2$ with $a = \exp\Omega$. Then, the initial singularity occurs at some finite past proper time, say $T = 0$, instead of $t = -\infty$.

energy density. It also implies that the universe cannot evolve isotropically in vacuum without turning on some shearing components, as in general relativity.

Adding sources, in the form of perfect fluid, leads to an interesting possibility when inequality (4.7) is fulfilled with $\lambda > 1/3$. In analogy with the previous analysis one obtains

$$(3\lambda - 1)\left(\frac{d\Omega}{dt}\right)^2 = V_{\rm HL} + \mu\, e^{\nu\,\Omega} \tag{4.8}$$

and the dominant contribution in the small volume limit is provided by the quadratic Ricci curvature terms and the matter sources with suitable ν. Then, isotropic evolution becomes possible, leading to a Friedmann universe in Hořava-Lifshitz gravity. When $\nu > 2$, there can be a bounce in Ω that replaces the initial singularity of the universe, [28], [29], [30], as can be easily seen by neglecting the contribution of the curvature R and the cosmological constant term. This is the only case for which the energy density of "dark radiation" can grow with respect to the regular matter energy[5]. Note, however, that possible deviations from isotropy will become dominant in the small volume limit, since the quadratic Cotton tensor term, which is independent of Ω, kicks in $V_{\rm HL}$ and washes away the effect of the previously thought relevant terms. The kinetic energy of the anisotropy parameters also contributes on equal footing. This indicates that the cosmological bounce is unstable against anisotropy, and, generically, the universe can come in a singular state at $T = 0$ satisfying the field equations. The validity or not of inequality (4.7) becomes irrelevant in the presence of anisotropy. Consistency also requires $\lambda > 1/3$, otherwise the Hamiltonian constraint cannot be possibly satisfied in the small volume limit in the presence of anisotropy; by the same token, the universe can only remain still in an isotropic state when $\lambda < 1/3$, and, therefore, this possibility will not be considered further.

Although the argument above does not provide a rigorous proof for the existence of an initial singularity in Hořava-Lifshitz cosmology, and under which general conditions this may be possible, it seems sufficient for the purposes of the present work[6]. Thus, in the following, we will use mixmaster cosmology to explore the approach to the initial singularity, as in general relativity.

[5]This condition by itself is quite restrictive since it rules out regular radiation before the bounce.

[6]Another example for having an initial singularity - rather than a bounce - is provided by the anisotropic Bianchi I model (also known as Kasner solution), although the reasoning is slightly different here. This is a common solution to general relativity and Hořava-Lifshitz gravity in vacuum because Σ_3 is a flat three-dimensional space and all components of the Ricci curvature and Cotton tensor vanish. In this case, the only contribution to the Hamiltonian constraint (neglecting the cosmological constant term for small volume) is provided by the kinetic energy of the anisotropy parameters and the universe can evolve towards the initial singularity without reaching a minimum volume. Thus, the bounce in the Friedmann model does not appear to be generic, in particular in the presence of anisotropy.

4.2 General relativity

The potential $V_{\rm GR}$ appears to vanish as one approaches the initial singularity. This is true for generic values of the anisotropy parameters $\beta_\pm$ implying Kasner behavior of the universe close to the singularity, which is taken to occur at the beginning of cosmic time, [3], [4], [5], [6], [7], [8], [9], [10]. In fact, since the Ricci scalar curvature of the homogeneous space Σ_3 vanishes in this limit, the space is effectively flat, as in Bianchi type-I cosmology, and it is more appropriate to use Cartesian dx, dy and dz instead of the 1-forms σ_i of $SU(2)$.

More precisely, when the potential vanishes, all momenta are constant satisfying $p_\Omega^2 = 4(p_+^2 + p_-^2)$ by the Hamiltonian constraint (with $\lambda = 1$). Then, it is convenient to introduce the following parametrization of the constant momenta,

$$n_1 = \frac{1}{3p_\Omega}\left(p_\Omega - 2p_+ - 2\sqrt{3}p_-\right) , \quad n_2 = \frac{1}{3p_\Omega}\left(p_\Omega - 2p_+ + 2\sqrt{3}p_-\right) ,$$
$$n_3 = \frac{1}{3p_\Omega}\left(p_\Omega + 4p_+\right) , \tag{4.9}$$

so that

$$n_1 + n_2 + n_3 = 1 = n_1^2 + n_2^2 + n_3^2 . \tag{4.10}$$

The remaining equations $d\beta_\pm/dt = p_\pm$ and $d\Omega/dt = -p_\Omega/4$ (so that $d\beta_\pm/d\Omega = -4p_\pm/p_\Omega$) can be easily solved to yield the metric coefficients $\gamma_i(t) = T^{2n_i}$ with respect to a time frame T defined by absorbing the lapse function as $dT = N(t)dt$. Then, the metric takes the familiar Kasner form

$$ds^2 = -dT^2 + T^{2n_1}dx^2 + T^{2n_2}dy^2 + T^{2n_3}dz^2 , \tag{4.11}$$

which describes an expanding flat universe with linearly varying volume element, $\sqrt{\det\gamma} = T$.

Thus, the mixmaster dynamics close to the initial singularity appears to follow the Kasner evolution with some fixed parameters (n_1, n_2, n_3). The Kasner universe is anisotropic as it always contains a direction, say z, along which distances contract rather than expand; this follows from the algebraic conditions (4.10), which imply that one of the n_i's, say n_3, is lying in the interval $-1/3 \leq n_3 \leq 0$. We may order the Kasner exponents as

$$-1/3 \leq n_3 \leq 0 \leq n_2 \leq 2/3 \leq n_1 \leq 1 \tag{4.12}$$

without loss of generality. The axially symmetric case corresponds to the choice of parameters $n_1 = n_2 = 2/3$ and $n_3 = -1/3$ (and permutations of the axes thereof).

This description is valid at generic points of (β_+, β_-) parameter space, but it can

break down far away from the origin when the effective point particle experiences the exponentially steep walls of the potential $V_{\rm GR}$. For example, when the particle approaches one of the triangular walls arising at $\beta_+ \to -\infty$, as it moves within the wedge $|\beta_-| < -\sqrt{3}\beta_+$, the dominant term of the potential is proportional to $\exp[4(\Omega - \beta_+)]$, as can be seen from the asymptotic behavior (3.18), and will become sufficiently large to influence the motion if $d\beta_+/d\Omega > 1$[7]. In the simplest case of axially symmetric evolution towards the wall, so that β_- stays zero along the trajectory and the Kasner exponents are $n_1 = n_2 = 2/3$ and $n_3 = -1/3$, it is clear from the Hamiltonian constraint $(d\beta_+/d\Omega)^2 + (d\beta_-/d\Omega)^2 = 4$ that $d\beta_+/d\Omega = 2$ and the inequality for having a bounce is satisfied. More generally, when the particle moves within the wedge $|\beta_-| < -\sqrt{3}\beta_+$ against the wall, we have

$$\frac{d\beta_+}{d\Omega} = 1 - 3n_3 \tag{4.13}$$

and the inequality $d\beta_+/d\Omega > 1$ is always satisfied since $n_3 < 0$. Similar considerations also apply to all other walls by the triangular symmetry of the model. Thus, the point particle will always bounce against the walls of the potential.

Summarizing, close to the initial singularity, the evolution of the universe is accurately described by Kasner dynamics until the particle hits the walls and enters into a new Kasner phase (with different parameters, in general) after the bounce[8]. The bounce repeats itself again and again, in general, leading to an oscillatory behavior of S^3 that alternates its three principal axes, while the universe is approaching the initial singularity, [3], [4], [5], [6], [7], [8], [9], [10]. It appears that almost all solutions obtained by successive bounces come arbitrarily close to the corners of the well associated to the special values of Misner parameter $s = 0$ or $s = \pm 3$ (by triangular symmetry). Then, the space-time metric comes close to $ds^2 = -dT^2 + dx^2 + dy^2 + T^2 dz^2$ (up

[7]The rate $d\beta_+/d\Omega$ is positive because β_+ decreases as Ω decreases while the particle is heading towards the wall in its descent towards the singularity.

[8]The bounce law for the Kasner parameters, $n_i \to n'_i$, has been worked out in the literature (but see also Appendix B). For a bounce against the wall at $\beta_+ \to -\infty$, it is most easily described as $s/3 \to 3/s$, using Misner's parametrization, [6],

$$n_1 = \frac{2s(s-3)}{3(s^2+3)}\,, \quad n_2 = \frac{2s(s+3)}{3(s^2+3)}\,, \quad n_3 = -\frac{(s-3)(s+3)}{3(s^2+3)}\,.$$

An alternative parametrization has been provided by Belinskii, Khalatnikov and Lifshitz, [3], [4], [5]. The axially symmetric case $n_1 = n_2 = 2/3$ and $n_3 = -1/3$ (corresponding to $s = \infty$) is special as the particle heads to the corner of the triangular well after the bounce, following the canyon line $\beta_- = 0$ with Kasner parameters $n'_1 = n'_2 = 0$ and $n'_3 = 1$ (corresponding to $s = 0$); this is also apparent from equations (4.9), since $p_- = 0$ all the time and p_+ only reverses sign relative to p_Ω after the bounce. The fixed points of the bounce law arise for $s = \pm 3$ and correspond to Kasner parameters $(1,0,0)$ and $(0,1,0)$ that describe the evolution of the particle along the canyon lines $\beta_- = \pm\sqrt{3}\beta_+$ without bounce. The bounce law from the other two walls follows by permutation of the axes, which is equivalent to replacing s by $(s \pm 3)/(s \mp 1)$, and amounts to $(s+3)/3(s-1) \to 3(s-1)/(s+3)$ or $(s-3)/3(s+1) \to 3(s+1)/(s-3)$ with fixed points $s = 0$ and 3 or $s = 0$ and -3 respectively.

to permutations of the axes), which is equivalent to the flat metric $ds^2 = -d\eta^2 + d\xi^2 + dx^2 + dy^2$ by the transformation $\xi = T\,\mathrm{sinh}z$ and $\eta = T\,\mathrm{cosh}z$. A new era of alternating Kasner epochs subsequently starts by permuting the axes, and so on. Actually, this motion can be formulated as billiard in a finite region of hyperbolic two-dimensional space, obtained by appropriate transformation of (β_+, β_-) parameter space, and, as such, it is chaotic (for an overview and history of the developments in the subject see, for instance, [10] and references therein); it also provides the origin of the chaotic behavior exhibited by mixmaster dynamics in general, [13], [14], [16].

The intuitive characterization of having chaos in early time cosmology is that when the universe starts with a well-defined state, it will evolve towards the singularity by going through almost all possible anisotropic stages by changing shape, as it does in general relativity.

4.3 Hořava-Lifshitz gravity

In this case, as one approaches the initial singularity, where $\Omega \to -\infty$, the potential does not vanish for generic values of $\beta_\pm$, contrary to what happens in general relativity. Instead, it is well approximated by

$$V_{\mathrm{HL}} = V_{\mathrm{Cotton}} \equiv \frac{6\alpha}{\kappa^2} e^{6\Omega} C_{ij} C^{ij}\,, \qquad \text{as} \quad \Omega \to -\infty\,. \tag{4.14}$$

This term can be alternatively written (in more compact form) as

$$V_{\mathrm{Cotton}} = \frac{\alpha}{\kappa^2}\Big[\left(\frac{\partial W}{\partial \beta_+}\right)^2 + \left(\frac{\partial W}{\partial \beta_-}\right)^2\Big]\,, \tag{4.15}$$

where the corresponding superpotential is

$$\begin{aligned} W \;=\; & e^{3\beta_+}\Big(\cosh(3\sqrt{3}\beta_-) - \cosh(\sqrt{3}\beta_-)\Big) - \cosh(2\sqrt{3}\beta_-) - \\ & e^{-3\beta_+}\cosh(\sqrt{3}\beta_-) + \frac{1}{2}e^{-6\beta_+}\,, \end{aligned} \tag{4.16}$$

and it is positive definite when $\alpha > 0$. Clearly, this applies to all models of Hořava-Lifshitz gravity, with or without "detailed balance". Consistency with the Hamiltonian constraint requires that $\lambda > 1/3$, which we assume in the following.

This is not surprising in retrospect because the quadratic Cotton tensor term is marginal in the gravitational action and it is expected to dominate in the ultra-violet regime of the theory. Furthermore, since V_{Cotton} is independent of Ω, the scale factor of the universe will evolve as a free particle with fixed (but arbitrary) momentum p_Ω, so that the volume of space diminishes linearly at early times (in the appropriate

time coordinate T). As for $\beta_\pm$ that determine the shape of the universe, they will keep changing all the time following the motion of a particle in a frozen (time-independent) well

$$E = \frac{1}{2}\left(\frac{d\beta_+}{dt}\right)^2 + \frac{1}{2}\left(\frac{d\beta_-}{dt}\right)^2 + V_{\text{Cotton}}(\beta_+, \beta_-) \tag{4.17}$$

with fixed energy level[9]

$$E = \frac{1}{4(3\lambda - 1)} p_\Omega^2 \,. \tag{4.18}$$

Thus, the dynamics appears more complicated now, compared to general relativity, and the universe will no be - in general - in a Kasner epoch before bouncing off the walls.

Solving this effective point particle problem is not an easy task, but one can examine some qualitative features of the motion depending on the energy E. When E is very large, the potential can be approximated by zero for generic values of $\beta_\pm$, since the particle looks insensitive to the small bumps at the bottom of the well[10]. Thus, only in this case, which resembles general relativity, the universe will be in a Kasner epoch far away from the walls (recall that the Kasner model is a common solution to the two theories and it is insensitive to the cosmological constant in the small volume limit). Note, however, that the bounce law is modified[11] compared to general relativity and resumes its standard form, as can be seen in Appendix B. But the qualitative picture remains the same: after the bounce the universe will enter into another Kasner epoch and so on, as in general relativity.

The picture of a billiard is also very useful here. For very large E we have a very

[9] We must require $E > 0$ so that the universe is anisotropic. Then, for small E, Ω diminishes slowly towards the initial singularity, whereas for large E it diminishes very fast.

[10] Actually, this is an assumption which can be safely made only for short time development of the system, based on intuition. In general, one should also prove that these bumps, no matter how small they are compared to E, do not influence much the long time development of the system after several iterations. Such non-perturbative results, which go back to Poincaré and fall within the classic theory of Kolmogorov, Arnol'd and Moser (KAM theory), [37] (but see also [38] and [39] for comprehensive exposition), are rather difficult to establish in classical mechanics and they will not be considered in detail in the present work. They should be properly investigated, however, as they might change the physical picture we are about to present after a very long time.

[11] A bounce against the steady wall occurring at $\beta_+ \to -\infty$, follows the rule of ordinary reflections, namely the incidence and reflection angles are equal. It is neatly described as $s/\sqrt{3} \to \sqrt{3}/s$, using the same parametrization of the Kasner parameters in terms of a single variable s as in general relativity. It should be compared to the bounce law $s/3 \to 3/s$ that governs the mixmaster universe in general relativity. In the present case, the fixed points arise at $s = \pm\sqrt{3}$ with associated Kasner exponents $n_1 = (1 \mp \sqrt{3})/3$, $n_2 = (1 \pm \sqrt{3})/3$ and $n_3 = 1/3$, respectively. As can be seen from the corresponding expressions in Appendix B, $p_+ = 0$ in this case and the point particle moves parallel to the wall (the two signs refer to the two directions of motion), until it hits the other walls. The bounce from the other two walls follows by permutation of the axes, as usual, which is equivalent to replacing s by $(s \pm 3)/(s \mp 1)$. Then, the bounce law yields the other fixed points $s = 3 \pm 2\sqrt{3}$ and $s = -3 \pm 2\sqrt{3}$ that describe a particle moving parallel to the other two walls in either direction. Clearly, one can have a closed orbit forming equilateral triangle, which does not seem possible in general relativity.

large region on the plane (β_+, β_-) bounded by an equilateral triangle inside which the particle moves freely with very large velocity. By simple rescaling, one can reformulate this problem as a particle moving freely inside an equilateral triangle of finite size with finite energy. The motion takes place on the plane following the standard rule of equal incidence and reflection angles. It is easy to prove that such a billiard is not ergodic. In fact, billiards in any triangular domain on the plane are non-ergodic when the angles of the triangle are rational multiples of 2π, since, then, all possible reflection angles along a given path of the particle assume only a finite set of values (see, for instance, [40]).

This should be contrasted with the ergodic behavior of the triangular billiard with moving walls that arises in general relativity, which can be viewed as a fixed triangular billiard with non-standard bounce law. The equivalent formulation of this problem in general relativity, as billiard in a compact domain of Lobachevsky plane with standard reflection rules, is another way of establishing ergodicity in that case, since the geodesic flow on surfaces with negative constant curvature is the prime example of ergodic behavior in Hamiltonian systems, [41] (but see also [40] for an overview).

In summary, for very large E, the motion of the effective point particle in Hořava-Lifshitz gravity is not chaotic, provided, of course, that the small bumps of the potential do not affect much the long time behavior of the system after many bounces. It is an immediate and important consequence of the KAM theory that small perturbations of non-degenerate Hamiltonian systems, like ours, are not ergodic[12]. Thus, in this case, if the universe starts with a well-defined state, it will evolve towards the singularity by changing shape but without passing through all possible anisotropic stages.

On the other hand, for intermediate E, the landscape of the bottom of the potential becomes visible to the particle and the bumps can no longer be ignored even for short time. Thus, the evolution between the walls becomes more complicated and (unfortunately) it cannot be described in simple terms. Also note that the canyon lines now exhibit a small bump, as shown in Fig.4, and, therefore, below a threshold,

$$E_\star = \frac{9\alpha}{16\kappa^2}\,, \tag{4.19}$$

the particle cannot exit the well and head towards its corners. For $E < E_\star$ the motion remains bounded, provided that the anisotropies are relatively small, and the particle oscillates around the origin (fully isotropic model). Thus, for intermediate E, the dy-

[12] At a given energy level, however, the invariant non-resonant (Kronecker) tori in phase space form a Cantor set, which has no interior points. Therefore, it is impossible to tell with finite precision whether a given initial position falls on an invariant torus or in a gap between such tori. In such cases, according to KAM theory, one can only make probabilistic statements for a chosen orbit to be on an invariant torus, and, hence, be stable.

namics of the universe close to the singularity is very different and complex and it is not yet clear if it remains non-ergodic. If a second integral of motion exists, the system will be integrable, but we have not been able to find such thing.

Finally, for very small values E and relatively small anistropies, the particle moves around the minimum of the potential as a two-dimensional isotropic oscillator,

$$E = \frac{1}{2}\left(\frac{d\beta_+}{dt}\right)^2 + \frac{1}{2}\left(\frac{d\beta_-}{dt}\right)^2 + \frac{81\alpha}{\kappa^2}(\beta_+^2 + \beta_-^2)\,, \tag{4.20}$$

which follows by expanding V_{Cotton} up to quadratic order around $\beta_+ = 0 = \beta_-$. In such case the motion is integrable and chaos is obviously absent. The universe still exhibits oscillatory behavior by changing shape in its descent towards the initial singularity, but the evolution is not Kasner-like. The universe passes through the isotropic model periodically with cyclic frequency $9\sqrt{2\alpha}/\kappa$.

The problem is certainly very rich and should be investigated in more detail, including numerical studies, in order to be able to make more conclusive and safe statements about chaos in the motion for general values of E. In fact, a Hamiltonian system like (4.17) can be ergodic at certain energy levels and non-ergodic at other levels. Here, there are also intermediate energies E separating into phases the behavior of mixmaster dynamics close to the initial singularity of the universe.

It is instructive to compare this behavior with the absence of chaos in fully covariant higher curvature generalizations of Einstein gravity, [23], [24], [25], where the reasoning is different. In the general context of $f(R)$ gravity in four space-time dimensions, there is a well known conformal relationship between the vacuum higher derivative theory and ordinary general relativity coupled to a scalar field

$$\varphi = \log f'(R) \tag{4.21}$$

with potential

$$V(\varphi) = \frac{1}{2f'^2}(Rf' - f)\,, \tag{4.22}$$

where prime denotes the derivative with respect to the four-dimensional scalar Ricci curvature. In the simplest case, the Einstein-Hilbert Lagrangian is replaced by $f(R) = R + \alpha R^2$, but $f(R)$ can also assume more general forms. The mixmaster universe provides a consistent mini-superspace model of $f(R)$ gravity, which is still described by a point particle that bounces off the walls of a triangular potential in the small volume limit. There is also an analogue of the Kasner solution in general relativity coupled to a scalar field, which is appropriate to use in this case. However, the effect of the scalar field φ is to slow down the speed of the point particle relative to the moving walls and the particle will bounce back only if it moves not too oblique relative to the walls; it

should be contrasted to general relativity without scalar field, where the point particle can hit the moving wall, say the one located at $\beta_+ \to -\infty$, from anywhere within the wedge $|\beta_-| < -\sqrt{3}\beta_+$. As a result, a few collisions are sufficient to make it so oblique that it will not bounce off another wall. So, the universe will enter quickly in a definite Kasner trajectory and stay there all the time in its approach to the singularity. Thus, the evolution is not chaotic in these theories.

5 Conclusions

We have shown that the homogeneous cosmologies provide consistent truncations of Hořava-Lifshitz gravity in vacuum and investigated them using Hamiltonian methods with emphasis on the closed space universe of Bianchi IX type. The field equations reduce to an autonomous system of ordinary differential equations describing the motion of a point particle in a potential well with Z_3 symmetry. In general, the potential depends on time, through the volume moduli, but when the universe approaches the initial singularity it freezes, as it becomes independent of time. Then, for $\lambda > 1/3$, the universe flows to the singularity by continuous changes of its shape, as in ordinary mixmaster cosmology, rolling like a particle in the well with fixed (but arbitrary) energy E. The main difference from general relativity is that the potential does not vanish for generic values of the anisotropy parameters, and, thus, the evolution of the early universe is not described by the Kasner solution away from the steep walls. The dynamics is more intricate now, but, still, the shape of the potential far away from the origin resembles that of general relativity and the particle can bounce off the walls. In a certain limit (large E), the motion appears to be non-ergodic, and, thus, chaos is absent. The same thing applies to very small values of the energy E, though for a different reason. However, it remains to be seen if the motion is chaotic for more general values of the parameter E, as in general relativity, and compare it further with mixmaster dynamics in fully covariant higher curvature generalizations of Einstein gravity. More work is certainly required in this direction and we hope to return to it elsewhere.

This work should be considered as the beginning of a more general investigation in Hořava-Lifshitz gravity. First, the most pressing open question is to revisit the singularity theorems of general relativity and examine under which general conditions they remain valid in theories with anisotropic scaling. In this context, we will also be able to see whether the matter bounce of the Friedmann model has more general value beyond the homogeneous and isotropic case. Assuming, however, that the occurrence of space-like singularities is generic in Hořava-Lifshitz gravity, it will be very important to examine how the singularity is approached by extending the standard analysis of

Belinskii, Khalatnikov and Lifshitz. If the spatial points decouple from the dynamics, which is a reasonable expectation even for theories with anisotropic scaling in space and time, then, the homogeneous cosmologies considered here will prove valuable tool for understanding the behavior of the universe near the initial singularity.

Second, it is interesting to consider the canonical quantization of Bianchi IX cosmology (or any other homogeneous model for that matter) as mini-superspace models to Hořava-Lifshitz gravity. This can provide a tractable way to compare it with Einstein gravity in the quantum regime. The Wheeler-DeWitt equation for the "wave-function" of the universe appears to be more manageable here because the walls of the effective potential are frozen in time in the domain of validity of quantum cosmology. On the contrary, in ordinary quantum gravity, the Bianchi IX model is more difficult to treat and interpret canonically because the corresponding potential is not inert to the evolution, but scales with time. We plan to address these issues in detail elsewhere.

Third, it should be noted that there is an intimate connection between the Euclidean version of Hořava-Lifshitz gravity with "detailed balance" and the theory of geometric flows. Namely, the gradient flow of the metric derived from the functional (superpotential) $\mathcal{W}$ yields a continuous deformation of the geometry on Σ_3 that is first order in time and trivially satisfies the higher order equations of motion of the theory. This was first pointed out in the original works, [26], [27], focussing, in particular, in $2+1$ dimensional gravity with anisotropic scaling and its connection to theory of Ricci flows on two-dimensional surfaces. In $3+1$ dimensions, the analogous deformation theory is provided by the so called Cotton flow of three-geometries, since the variation of the Chern-Simons term in the functional $\mathcal{W}$ is the Cotton tensor. This, then, provides the leading order term of the flow, which is third order in space, and it should also be augmented with the Ricci curvature terms that come about by varying the three-dimensional Einstein-Hilbert term in $\mathcal{W}$. Remarkably, the Cotton flow admits consistent truncation to an autonomous system of ordinary differential equations for all homogeneous three-geometries, [42], and the same thing applies to the Ricci flow, [43]. In a forthcoming paper we discuss solutions of the combined Cotton-Ricci flow for Bianchi IX geometries, which can be thought as gravitational instanton solutions in the $3+1$ Hořava-Lifshitz gravity, [44]. These configurations might also have important role in quantum gravity, in the spirit of the Hartle-Hawking proposal for the construction of the "wave-function" of the universe, using Euclidean path integrals. Thus, in this context, it is natural to expect that the theory of geometric flows will connect naturally to the problem of quantization of non-relativistic theories of gravitation, in general, and for the Bianchi IX mini-superspace model, in particular.

Finally, among other things, we mention the interesting possibility of higher dimensional generalizations. In such cases, the theory is still defined using the ADM

decomposition of the metric, as in $3+1$ dimensions, but the potential contains even higher curvature terms depending on the space dimension. For example, in $4+1$ dimensions, we can have spatial derivative terms up to order eight, which follow from a superpotential $\mathcal{W}$ that involves in its integrand the square of the Weyl tensor $C_{ijkl}C^{ijkl}$ and the square of Ricci curvature R^2, assuming the "detailed balance" condition, [27]; one can also add the corresponding Einstein-Hilbert term to $\mathcal{W}$, with cosmological constant, to insure that the theory flows to five-dimensional Einstein gravity at large scales . In such case, the Bach tensor of the four-dimensional spatial geometry, which is obtained by varying the square of the Weyl tensor in $\mathcal{W}$, replaces the Cotton tensor that was featuring earlier in the $3+1$ dimensional theory; if an R^2 term is also present in $\mathcal{W}$ one has to add its contribution, which scales in the same way. Then, the leading term of the potential $V_{\rm HL}$ (at least when the volume of the five-dimensional universe is very small) is provided by the square of the Bach tensor, plus possible additional contributions coming from R^2 in $\mathcal{W}$, and it is scale invariant. In analogy with the previous analysis, this term will dominate the cosmological evolution at early times and lead to a frozen potential well, irrespective "detailed balance", where the effective point particle rolls. Similar considerations apply to all higher dimensional cases. In view of the results obtained in the literature for higher dimensional homogeneous string cosmology models, [17], [18], [19], [20], [21], it is also important here to explore the universal features of dynamics close to the singularity and expose their dependence on space-time dimensionality.

Acknowledgements

This work was partially supported by the Cluster of Excellence "Origin and the Structure of the Universe" in Munich, Germany, the French Agence Nationale pour la Recherche programme "String Cosmology" under contract 05-BLAN-NT09-573739, the ERC Advanced Grant "Mass Hierarchy and Particle Physics at the TeV Scale" under contract 226371, the ITN programme "Unification in the LHC Era" under contract PITN-GA-2009-237920 and the bilateral programme GRC APIC PICS-Grèce for French-Greek scientific collaboration under contract 3747. The authors I.B., F.B. and M.P. are grateful to the hospitality extended to them at the Arnold Sommerfeld Center for Theoretical Physics in Munich during the early stages of this work. We also thank Anastasios Petkou and Marika Taylor for stimulating discussions during the GGI workshop "Perspectives in String Theory" that triggered parts of the present work as well as Elias Kiritsis, Hermann Nicolai and George Savvidy for fruitful exchanges. Finally, we thank Christos Sourdis for assistance in drawing the figures.

A Bianchi IX model geometry

The Bianchi IX model describes a homogeneous (but generally non-isotropic) three-dimensional geometry with the topology of S^3 and isometry group $SU(2)$. The line element is constructed using the corresponding left-invariant 1-forms σ_i,

$$\sigma_1 = \sin\psi\sin\theta d\phi + \cos\psi d\theta \,, \tag{A.1}$$

$$\sigma_2 = \cos\psi\sin\theta d\phi - \sin\psi d\theta \,, \tag{A.2}$$

$$\sigma_3 = \cos\theta d\phi + d\psi \tag{A.3}$$

and takes the form

$$ds^2 = \gamma_1\sigma_1^2 + \gamma_2\sigma_2^2 + \gamma_3\sigma_3^2 \,. \tag{A.4}$$

The 1-forms σ_i satisfy the defining $SU(2)$ relations

$$d\sigma_i + \frac{1}{2}\epsilon_{ijk}\sigma_j \wedge \sigma_k = 0 \,, \tag{A.5}$$

whereas the angles range as $0 \leq \theta \leq \pi$, $0 \leq \phi \leq 2\pi$ and $0 \leq \psi \leq 4\pi$, since ψ is extended to the double covering of the rotation group. The space integration is carried out using

$$\int \sigma_1 \wedge \sigma_2 \wedge \sigma_3 = \int \sin\theta \, d\theta \wedge d\phi \wedge d\psi = (4\pi)^2 \,. \tag{A.6}$$

Next, we present the expressions for the Ricci curvature and Cotton tensors of Bianchi IX metrics that will be used in the main text. Proper discussion requires the use of $e^i = \sqrt{\gamma_i}\,\sigma_i$ and the corresponding connection 1-forms $\omega^i{}_j$ satisfying the zero torsion relations $de^i + \omega^i{}_j \wedge e^j = 0$. Then, the curvature 2-forms are computed as

$$R^i{}_j = d\omega^i{}_j + \omega^i{}_k \wedge \omega^k{}_j \tag{A.7}$$

and the Ricci 1-forms are

$$(\mathrm{Ric})_i = i_k R^k{}_i \,. \tag{A.8}$$

The Ricci curvature scalar is $R = i_k(\mathrm{Ric})^k$. Also, the Cotton 2-form is given by

$$C^i = dY^i + \omega^i{}_j \wedge Y^j \,, \tag{A.9}$$

where Y^j are simply given by

$$Y^j = (\mathrm{Ric})^j - \frac{1}{4}Re^j \,. \tag{A.10}$$

With these explanations in mind, the non-vanishing components of the Ricci curvature tensor take the following form

$$R_{11} = \frac{1}{2\gamma_2\gamma_3}\left[\gamma_1^2 - (\gamma_2-\gamma_3)^2\right], \tag{A.11}$$

$$R_{22} = \frac{1}{2\gamma_1\gamma_3}\left[\gamma_2^2 - (\gamma_1-\gamma_3)^2\right], \tag{A.12}$$

$$R_{33} = \frac{1}{2\gamma_1\gamma_2}\left[\gamma_3^2 - (\gamma_1-\gamma_2)^2\right] \tag{A.13}$$

and, therefore, the Ricci scalar curvature is

$$R = -\frac{1}{2\gamma_1\gamma_2\gamma_3}\left(\gamma_1^2+\gamma_2^2+\gamma_3^2-2\gamma_1\gamma_2-2\gamma_2\gamma_3-2\gamma_1\gamma_3\right). \tag{A.14}$$

Also, the non-vanishing components of the Cotton tensor take the form

$$C_{11} = -\frac{\gamma_1}{2(\gamma_1\gamma_2\gamma_3)^{3/2}}\left[\gamma_1^2(2\gamma_1-\gamma_2-\gamma_3)-(\gamma_2+\gamma_3)(\gamma_2-\gamma_3)^2\right], \tag{A.15}$$

$$C_{22} = -\frac{\gamma_2}{2(\gamma_1\gamma_2\gamma_3)^{3/2}}\left[\gamma_2^2(2\gamma_2-\gamma_1-\gamma_3)-(\gamma_1+\gamma_3)(\gamma_1-\gamma_3)^2\right], \tag{A.16}$$

$$C_{33} = -\frac{\gamma_3}{2(\gamma_1\gamma_2\gamma_3)^{3/2}}\left[\gamma_3^2(2\gamma_3-\gamma_1-\gamma_2)-(\gamma_1+\gamma_2)(\gamma_1-\gamma_2)^2\right]. \tag{A.17}$$

It is convenient (and will be used throughout this paper) to parametrize the metric coefficients γ_i as follows,

$$\gamma_1 = e^{2\Omega+\beta_++\sqrt{3}\beta_-}, \tag{A.18}$$

$$\gamma_2 = e^{2\Omega+\beta_+-\sqrt{3}\beta_-}, \tag{A.19}$$

$$\gamma_3 = e^{2\Omega-2\beta_+}. \tag{A.20}$$

The volume of S^3 is parametrized by Ω, whereas β_+ and β_- measure the deviations from the isotropic metric that is associated to $\beta_+ = 0 = \beta_-$. Thus, for $\gamma_1 \neq \gamma_2 \neq \gamma_3$, the metric on S^3 is homogeneous, but not isotropic, having different circumference on great circles in each of the three mutually orthogonal principal directions. Axially symmetric non-isotropic metrics are obtained by choosing one of the deformation parameters equal to zero, say $\beta_- = 0$, in which case $\gamma_1 = \gamma_2 \neq \gamma_3$. Likewise, $\gamma_1 \neq \gamma_2 = \gamma_3$ requires $\beta_- = \sqrt{3}\,\beta_+$ and $\gamma_1 = \gamma_3 \neq \gamma_2$ requires $\beta_- = -\sqrt{3}\,\beta_+$.

Finally, note that the Cotton tensor vanishes in the isotropic case $\gamma_1 = \gamma_2 = \gamma_3$, since the metric of the round S^3 is conformally flat.

B The bounce law

In this appendix, we derive the bounce law of the effective point particle as it hits the wall located at $\beta \to -\infty$. Far away from the wall the potential is assumed to vanish and the particle moves freely, where this is applicable.

General relativity: In this case, the Hamiltonian is derived using the asymptotic form of the potential $V_{\rm GR}$, as $\Omega \to -\infty$, and becomes approximately

$$2H_{\rm GR} = p_+^2 + p_-^2 - \frac{1}{4}p_\Omega^2 + \frac{12}{\kappa^4}e^{4(\Omega-\beta_+)} \,. \tag{B.1}$$

The Ω-dependence of the potential can be easily transformed away by introducing new variables

$$\bar{\Omega} = \frac{1}{\sqrt{3}}\left(2\Omega - \frac{\beta_+}{2}\right) \,, \qquad \bar{\beta}_+ = \frac{1}{\sqrt{3}}(\beta_+ - \Omega) \tag{B.2}$$

and their conjugate momenta

$$\bar{p}_\Omega = \frac{2}{\sqrt{3}}(p_\Omega + p_+) \,, \qquad \bar{p}_+ = \frac{1}{\sqrt{3}}(p_\Omega + 4p_+) \,. \tag{B.3}$$

Then, the Hamiltonian takes the simpler form

$$2H_{\rm GR} = \frac{1}{4}\bar{p}_+^2 + p_-^2 - \frac{1}{4}\bar{p}_\Omega^2 + \frac{12}{\kappa^4}e^{-4\sqrt{3}\bar{\beta}_+} \,. \tag{B.4}$$

In terms of these variables, the potential is frozen in time and both $\bar{p}_\Omega$ and p_- are constants of motion. Dividing by parts, one obtains

$$\frac{\bar{p}_\Omega}{p_-} = \frac{2}{\sqrt{3}}\frac{1 + p_+/p_\Omega}{p_-/p_\Omega} = \text{constant} \tag{B.5}$$

relating the original momenta before and after the bounce.

At this point, it is useful to introduce Kasner exponents, which are applicable to the evolution of the universe well before and after the bounce,

$$\begin{aligned} n_1 &= \frac{1}{3p_\Omega}(p_\Omega - 2p_+ - 2\sqrt{3}p_-) \,, \qquad n_2 = \frac{1}{3p_\Omega}(p_\Omega - 2p_+ + 2\sqrt{3}p_-) \,, \\ n_3 &= \frac{1}{3p_\Omega}(p_\Omega + 4p_+) \,, \end{aligned} \tag{B.6}$$

and satisfy $n_1^2 + n_2^2 + n_3^2 = 1$ by virtue of the Hamiltonian constraint $p_\Omega^2 = 4(p_+^2 + p_-^2)$ far away from the wall. It is also convenient to parametrize the Kasner exponents in

terms of a single variable s, following Misner, [6],

$$n_1 = \frac{2s(s-3)}{3(s^2+3)}\,, \quad n_2 = \frac{2s(s+3)}{3(s^2+3)}\,, \quad n_3 = -\frac{(s-3)(s+3)}{3(s^2+3)}\,, \tag{B.7}$$

so that the constant of motion (B.5) takes the form

$$\frac{\bar{p}_\Omega}{p_-} = 2\frac{n_3+1}{n_2-n_1} = \frac{s}{3} + \frac{3}{s} = \text{constant}\,. \tag{B.8}$$

Thus, in general relativity, the bounce law against the wall $\beta_+ \to -\infty$ is simply described as

$$\frac{s}{3} \to \frac{3}{s}\,, \tag{B.9}$$

which leaves $\bar{p}_\Omega/p_-$ invariant and changes the Kasner exponents accordingly.

Hořava-Lifshitz gravity: The Hamiltonian is now derived using the asymptotic form of the potential $V_{\rm HL}$, which is independent of Ω when $\Omega \to -\infty$, and becomes approximately

$$2H_{\rm HL} = p_+^2 + p_-^2 - \frac{1}{2(3\lambda-1)}p_\Omega^2 + \frac{18\alpha}{\kappa^2}e^{-12\beta_+}\,. \tag{B.10}$$

The point particle moves freely before and after the bounce only when p_Ω is very large, in which case the Hamiltonian constraint simplifies to $p_\Omega^2 = 2(3\lambda-1)(p_+^2+p_-^2)$ for generic values of $\beta_\pm$. This will be implicitly assumed here and also that $\alpha > 0$ and $\lambda > 1/3$.

In the present case, there is no Ω-dependence on the wall located at $\beta_+ \to -\infty$ and it follows immediately that

$$\frac{p_\Omega}{p_-} = \text{constant}\,. \tag{B.11}$$

Then, this is an ordinary bounce from a steady wall following the standard rule that the incidence and reflection angles are equal asymptotically, namely p_+ flips sign and p_- remains unchanged. To compare with the previous case, it is convenient to describe the free motion of the particle well before and after the bounce using Kasner exponents, which are now defined as

$$\begin{aligned}
n_1 &= \frac{1}{3p_\Omega}\left(p_\Omega - \sqrt{2(3\lambda-1)}p_+ - \sqrt{6(3\lambda-1)}p_-\right)\,,\\
n_2 &= \frac{1}{3p_\Omega}\left(p_\Omega - \sqrt{2(3\lambda-1)}p_+ + \sqrt{6(3\lambda-1)}p_-\right)\,,\\
n_3 &= \frac{1}{3p_\Omega}\left(p_\Omega + 2\sqrt{2(3\lambda-1)}p_+\right)
\end{aligned} \tag{B.12}$$

and satisfy $n_1^2 + n_2^2 + n_3^2 = 1$ by virtue of the Hamiltonian constraint far away from the wall. By employing Misner's parametrization (B.7), as before, we obtain

$$\frac{p_\Omega}{p_-} = \sqrt{\frac{2(3\lambda - 1)}{3}} \frac{2}{n_2 - n_1} = \sqrt{\frac{3\lambda - 1}{2}} \left(\frac{s}{\sqrt{3}} + \frac{\sqrt{3}}{s} \right) = \text{constant} \,. \tag{B.13}$$

Thus, the bounce law against the wall at $\beta_+ \to -\infty$ is now described as

$$\frac{s}{\sqrt{3}} \to \frac{\sqrt{3}}{s} \,, \tag{B.14}$$

which leaves p_Ω / p_- invariant and changes the Kasner exponents accordingly. It has the same from as in general relativity, $s/3 \to 3/s$, setting

$$s_{\text{GR}} = \sqrt{3}\, s_{\text{HL}} \,. \tag{B.15}$$

Summarizing, the bounce in Hořava-Lifshitz gravity follows the standard reflection rule from a steady wall, whereas in general relativity this rule is modified by the moving walls and it is effectively described by inserting a factor of $\sqrt{3}$ in the corresponding Misner parameter. In general relativity, the standard rule of equal incidence and reflection angles only applies to the transformed Hamiltonian (B.4) from which the bounce law for the original momenta $p_\pm$ was derived.

References

[1] S.W. Hawking and R. Penrose, “The singularities of gravitational collapse and cosmology", Proc. Roy. Soc. Lond. A314 (1970) 529.

[2] S.W. Hawking and G.F.R. Ellis, *The large Scale Structure of Space-Time*, Cambridge University Press, Cambridge, 1975.

[3] V.A. Belinskii, I.M. Khalatnikov and E.M. Lifshitz, “Oscillatory approach to a singular point in the relativistic cosmology", Adv. Phys. 19 (1970) 525.

[4] V.A. Belinskii, I.M. Khalatnikov and E.M. Lifshitz, “Construction of a general cosmological solution of the Einstein equation with a time singularity", Sov. Phys. JETP 35 (1972) 838.

[5] V.A. Belinskii, I.M. Khalatnikov and E.M. Lifshitz, “A general solution of the Einstein equations with a time singularity", Adv. Phys. 31 (1982) 639.

[6] C.W. Misner, “Mixmaster universe", Phys. Rev. Lett. 22 (1969) 1071.

[7] C.W. Misner, “Quantum cosmology. I.", Phys. Rev. 186 (1969) 1319.

[8] C.W. Misner, “Classical and quantum dynamics of a closed universe", in *Relativity*, eds. M. Carmeli, S. Fickler and L. Witten, Plenum, New York, 1970.

[9] C.W. Misner, “Minisuperspace", in *Magic Without Magic - J.A. Wheeler 60th Anniversary Volume*, eds. J. Klauder, Freeman, San Francisco, 1972.

[10] C.W. Misner, “The mixmaster cosmological metrics", in *Deterministic Chaos in General Relativity*, eds. D. Hobill, A. Burd and A. Coley, Plenum, New York, 1994 [arXiv:gr-qc/9405068].

[11] C.W. Misner, K.S. Thorne and J.A. Wheeler, *Gravitation*, Freeman, San Francisco, 1973.

[12] M.P. Ryan, *Hamiltonian Cosmology*, Lecture Notes in Physics, Springer-Verlag, Berlin, 1972.

[13] J.D. Barrow, “Chaotic behaviour in general relativity", Phys. Repts. 85 (1982) 1.

[14] D.F. Chernoff and J.D. Barrow, “Chaos in the mixmaster universe", Phys. Rev. Lett. 50 (1983) 134.

[15] S.E. Rugh, “Chaos in the Einstein equations - characterization and importance", in *Deterministic Chaos in General Relativity*, eds. D. Hobill, A. Burd and A. Coley, Plenum, New York, 1994.

[16] N.J. Cornish and J.J. Levin, “The mixmaster universe is chaotic", Phys. Rev. Lett. 78 (1997) 998 [arXiv:gr-qc/9605029]; “Mixmaster universe: A chaotic Farey tale", Phys. Rev. D55 (1997) 7489 [arXiv:gr-qc/9612066].

[17] Y. Elskens and M. Henneaux, “Chaos in Kaluza-Klein models", Class. Quant. Grav. 4 (1987) L161; “Ergodic theory of the mixmaster universe in higher space-time dimensions", Nucl. Phys. B290 [FS20] (1987) 111; Y. Elskens, “Ergodic theory of the mixmaster universe in higher space-time dimensions. II", J. Stat. Phys. 48 (1987) 1269.

[18] J. Demaret, Y. de Rop and M. Henneaux, “Are Kaluza-Klein models of the universe chaotic?", Int. J. Theor. Phys. 28 (1989) 1067.

[19] T. Damour and M. Henneaux, “Chaos in superstring cosmology", Phys. Rev. Lett. 85 (2000) 920 [arXiv:hep-th/0003139]; “Oscillatory behaviour in homogeneous string cosmology models", Phys. Lett. B488 (2000) 108 [arXiv:hep-th/0006171]; “$E(10)$, $BE(10)$ and arithmetical chaos in string cosmology", Phys. Rev. Lett. 86 (2001) 4749 [arXiv:hep-th/0012172].

[20] T. Damour, M. Henneaux, B. Julia and H. Nicolai, “Hyperbolic Kac-Moody algebras and chaos in Kaluza-Klein models", Phys. Lett. B509 (2001) 323 [arXiv:hep-th/0103094].

[21] T. Damour, S. de Buyl, M. Henneaux and C. Schomblond, “Einstein billiards and overextensions of finite-dimensional simple Lie algebras", JHEP 0208 (2002) 030 [arXiv:hep-th/0206125].

[22] T. Damour, M. Henneaux and H. Nicolai, “Cosmological billiards", Class. Quant. Grav. 20 (2003) R145 [arXiv:hep-th/0212256].

[23] J.D. Barrow and H. Sirousse-Zia, “Mixmaster cosmological model in theories of gravity with a quadratic Lagrangian", Phys. Rev. D39 (1989) 2187.

[24] J.D. Barrow and S. Cotsakis, “Chaotic behaviour in higher-order gravity theories", Phys. Lett. B232 (1989) 172.

[25] S. Cotsakis, J. Demaret, Y. de Rop and L. Querella, “Mixmaster universe in fourth-order gravity theories", Phys. Rev. D48 (1993) 4595.

[26] P. Hořava, “Membranes at quantum criticality", JHEP 0903 (2009) 020 [arXiv:0812.4287].

[27] P. Hořava, “Quantum gravity at a Lifshitz point", Phys. Rev. D79 (2009) 084008 [arXiv:0901.3775].

[28] G. Calcagni, “Cosmology of the Lifshitz universe", JHEP 0909 (2009) 112 [arXiv:0904.0829].

[29] E. Kiritsis and G. Kofinas, “Hořava-Lifshitz cosmology", Nucl. Phys. B821 (2009) 467 [arXiv:0904.1334].

[30] R. Brandenberger, “Matter bounce in Hořava-Lifshitz cosmology", Phys. Rev. D80 (2009) 043516 [arXiv:0904.2835].

[31] B.S. DeWitt, “Quantum theory of gravity: 1. The canonical theory", Phys. Rev. 160 (1967) 1113.

[32] S. Deser, R. Jackiw and S. Templeton, “Topologically massive gauge theories", Ann. Phys. 140 (1982) 372; Erratum-ibid. 185 (1988) 406; “Three-dimensional massive gauge theories", Phys. Rev. Lett. 48 (1982) 975.

[33] S.W. Hawking and J.C. Luttrell, “The isotropy of the universe", Phys. Lett. B143 (1984) 83.

[34] H. Kodama, “Holomorphic wave function of the universe", Phys. Rev. D42 (1990) 2548.

[35] V. Moncrief and M.P. Ryan, “Amplitude-real-phase exact solutions for quantum mixmaster universe", Phys. Rev. D44 (1991) 2375.

[36] A.H. Taub, “Empty spacetimes admitting a three parameter group of motions", Ann. of Math. 53 (1951) 472.

[37] A.N. Kolmogorov, “On conservation of conditionally periodic motions for a small change in Hamilton’s function", Dokl. Akad. Nauk SSSR 98 (1954) 527; V.I. Arnol’d, “Proof of a theorem of A.N. Kolmogorov on the preservation of conditionally periodic motions under a small perturbation of the Hamiltonian", Russ. Math. Surv. 18 (1963) 9; J. Moser, “On invariant curves of area preserving mappings of an annulus", Nachr. Akad. Wiss. Gött. Math. Phys. Kl. II 1 (1962) 1.

[38] V.I. Arnol’d, *Mathematical Methods of Classical Mechanics*, second edition, Springer-Verlag, Berlin, 1989.

[39] J. Pöschel, “A lecture on the classical KAM theorem", Proc. Symp. Pure Math. 69 (2001) 707.

[40] Ya G. Sinai, *Introduction to Ergodic Theory*, Princeton University Press, Princeton, 1976.

[41] E. Hopf, “Fuchsian groups and ergodic theory", Trans. Am. Math. Soc. 39 (1936) 299; G.A. Hedlund, “The dynamics of geodesic flows", Bull. Am. Math. Soc. 45 (1939) 241.

[42] A.U.O. Kisisel, O. Sarioglu and B. Tekin, “Cotton flow", Class. Quant. Grav. 25 (2008) 165019 [arXiv:0803.1603].

[43] J. Isenberg and M. Jackson, “Ricci flow of locally homogeneous geometries on closed manifolds", J. Diff. Geom. 35 (1992) 723.

[44] I. Bakas, F. Bourliot, D. Lüst and M. Petropoulos, “Geometric flows in Hořava-Lifshitz gravity", in preparation.

Annexe I

Publication 7 : I. Bakas, F. Bourliot, D. Lust and M. Petropoulos, "Geometric flows in Horava-Lifshitz gravity," JHEP 1004 (2010) 131 [arXiv :1002.0062 [hep-th]].

CPHT-RR078.0709
MPP-2009-179
LMU-ASC 47/09

arXiv:1002.0062v3 [hep-th] 6 Apr 2010

GEOMETRIC FLOWS IN HOŘAVA–LIFSHITZ GRAVITY

Ioannis Bakas[*1], **François Bourliot**[†2], **Dieter Lüst**[‡3,4] and **Marios Petropoulos**[§2]

[1] *Department of Physics, University of Patras*
26500 Patras, Greece

[2] *Centre de Physique Théorique*
Ecole Polytechnique, CNRS UMR 7644
91128 Palaiseau Cedex, France

[3] *Max-Planck-Institut für Physik*
Föhringer Ring 6, 80805 München, Germany

[4] *Arnold-Sommerfeld-Center für Theoretische Physik*
Department für Physik, Ludwig-Maximilians-Universität München
Theresienstraße 37, 80333 München, Germany

April 7, 2010

ABSTRACT

We consider instanton solutions of Euclidean Hořava–Lifshitz gravity in four dimensions satisfying the detailed balance condition. They are described by geometric flows in three dimensions driven by certain combinations of the Cotton and Ricci tensors as well as the cosmological-constant term. The deformation curvature terms can have competing behavior leading to a variety of fixed points. The instantons interpolate between any two fixed points, which are vacua of topologically massive gravity with $\Lambda > 0$, and their action is finite. Special emphasis is placed on configurations with $SU(2)$ isometry associated with homogeneous but generally non-isotropic Bianchi IX model geometries. In this case, the combined Ricci–Cotton flow reduces to an autonomous system of ordinary differential equations whose properties are studied in detail for different couplings. The occurrence and stability of isotropic and anisotropic fixed points are investigated analytically and some exact solutions are obtained. The corresponding instantons are classified and they are all globally $\mathbb{R} \times S^3$ and complete spaces. Generalizations to higher-dimensional gravities are also briefly discussed.

[*]bakas@ajax.physics.upatras.gr
[†]bourliot@cpht.polytechnique.fr
[‡]dieter.luest@lmu.de
[§]marios@cpht.polytechnique.fr

Contents

1 Introduction **2**

2 Non-relativistic gravity, detailed balance and flows **6**

2.1 Non-relativistic gravity: a reminder 6

2.2 Euclidean action and flow equations 11

2.3 Entropy functional and action bound 14

3 Bianchi IX model geometry **16**

3.1 Some basic facts 16

3.2 Ricci flow 18

3.3 Cotton flow 20

4 Normalized Ricci–Cotton flow **23**

4.1 The general system of Bianchi IX equations 23

4.2 Classification of the fixed points 25

4.3 Phase portraits of the flow 30

4.4 Axisymmetric solutions 32

5 Ricci–Cotton flow with general couplings **36**

5.1 The axisymmetric Bianchi IX model 36

5.2 Classification of the fixed points 38

5.3 Phase portraits of the flow 41

5.4 The special case $\Lambda_W = 0$ 43

6 Space-time interpretation of the flow lines **45**

6.1 Global structure and completeness of the metrics 46

6.2 The action and moduli of $SU(2)$ instanton metrics 51

7 Generalization to higher dimensions **57**

7.1 Hořava–Lifshitz gravity in $4+1$ dimensions 57

7.2 Bach flow and its variants 58

1 Introduction

Based on ideas that were originally developed in condensed matter physics [1] and later applied to the description of aspects of particle interactions [2, 3, 4, 5], a modification of general relativity was recently proposed in [6, 7] and further studied under the name of Hořava–Lifshitz gravity. In this theory, which includes higher-order curvature terms on spatial slices, the diffeomorphism invariance of general relativity is broken explicitly setting a privileged time direction. This affects the ultra-violet behavior of the quantum theory, which, hence, looks power-counting renormalizable. Some efforts have been made to prove consistency of the quantum theory [8, 9], but the number of propagating degrees of freedom seems to invalidate the matching with Einstein's gravity in the infrared regime, and hence seems to disprove this theory as a viable alternative to general relativity [10, 11, 12, 13]. The investigation of these issues is still going on. Despite the difficulties and reservations, the Hořava–Lifshitz gravity still provides an interesting classical and quantum field theory framework, where one can address some interesting questions and explore several connections to ordinary gravity or string theory. These also include the appearance and relevance of geometric flows, which is the main subject of the present work.

Geometric flows, and, in particular, Ricci flows are interesting in their own right. In mathematics they turned out to play a crucial role in implementing Hamilton's program for proving Poincaré's and Thurston's conjectures [14, 15] (but see also [16] and [17] and references therein). In physics they originally appeared in off-critical string theory via the renormalization-group equations of two-dimensional non-linear sigma models, where the evolution of the metric under the Ricci flow equations provides the running of the bulk coupling to lowest order in perturbation theory (see [18] for the original result). In this context, the renormalization-group time is provided by the logarithmic length scale of the world-sheet, but in some cases it can also assume the role of genuine time, describing real-time evolution in string theory in regimes where the friction due to the motion of the dilaton effectively reduces the second-order evolution equations to the first-order renormalization-group flow equations [19, 20].

Ricci flow models also appear in the framework of four-dimensional gravitational instantons of general relativity. Solving Einstein's equations is, in general, an impossible task. It is substantially simplified under the assumption of self-duality as a sufficient condition to find vacuum solutions in the Euclidean sector of the theory. Homogeneity of spatial sections is often a further simplification to find explicit solutions. Although what we call space is somewhat arbitrary in Euclidean gravity, the latter

statement can be made precise by assuming a foliation in three-dimensional leaves that are invariant under an isometry group of motions. For these particular vacuum solutions, it turns out that the Euclidean time evolution of the homogeneous leaves inside the gravitational instanton can be recast as Ricci flow equations for the corresponding geometry on the homogeneous model spaces [21, 20, 22].

The modification of gravity proposed by Hořava in [6, 7] shares some features with the previous setting that allow to define the analogue of gravitational-instanton configurations. In particular, a foliation of the four-dimensional space is assumed from the very beginning with a privileged time direction at the level of the action. Furthermore, a condition called *detailed balance*, which is borrowed from non-equilibrium thermodynamics, requires that the dynamics follows from an appropriately chosen three-dimensional superpotential action. In the Euclidean version of the theory, this resembles the self-duality condition with similar consequences: for a class of configurations that minimize the action, the time evolution becomes first-order and describes a geometric flow on the leaves of the foliation. Unlike general relativity, where Ricci flow is equivalent to self-duality only for configurations with homogeneous leaves, the description of instanton-like solutions by geometric flows is generic in Hořava–Lifshitz gravity. The nature of the corresponding flow depends on the choice of the three-dimensional action used for detailed balance and it is driven, in general, by a certain combination of Ricci and Cotton tensors as well as the cosmological constant term. It is not our concern, and it will not be pursued here at all, to find whether such combinations of curvature tensors can also arise from the renormalization- group equations of some quantum field theory.

Our aim in this paper is to investigate aspects of the Euclidean dynamics of Hořava–Lifshitz gravity with detailed balance. Our motivations are diverse. First, classical instanton-like solutions are important for the determination of transition amplitudes in quantum gravity. They are also useful in the Hartle–Hawking formulation of quantum cosmology [23], even though classical cosmology per se requires the analysis of real-time equations. The geometric flows that emerge in this framework involve tensors with higher-order spatial derivatives terms, and, as such, they are new in the literature; they reduce to previously studied examples only for some special values of their parameters. Thus, it is instructive to formulate the flow equations in all generality, determine the nature of the fixed points and their stability properties, obtain explicit solutions, as well as study general questions such as the monotonicity of the evolution, the possible formation of singularities, the occurrence of bounces and so on. These questions arise naturally in the general theory of geometric flows and they are bound to be relevant for the space–time interpretation of the analogue of gravitational instantons in Hořava–Lifshitz theory.

The answer to these questions will be accomplished partially using some ansatz for the underlying three-dimensional spaces, leading to mini-superspace truncation of the flow equations. Otherwise, it does not be seem possible to draw general conclusions for the general system of equations, at least at the current level of our understanding of this problem. Still, the results that will be described are indicative of what should be expected in general. More systematic investigation of the infinite-dimensional dynamical system at hand requires substantial mathematical work that is not contained in this paper. Following the paradigm of gravitational instantons with isometry groups in Euclidean Einstein gravity, we will consider homogeneous geometries on the three-dimensional spatial slices of Hořava–Lifshitz gravity and focus, in particular, to the case of Bianchi IX geometry as a class of homogeneous but generally non-isotropic deformation of S^3; this model is often referred to as mixmaster universe in the Lorentzian (real-time) approach to cosmology [24, 25, 26], and was recently discussed in the framework of Hořava–Lifshitz gravity [27, 28]. Other Bianchi classes as well as more general inhomogeneous deformations of the three-sphere (under appropriate ansatz) can also be studied along similar lines, but they will not be discussed.

We set up the general problem using the Bianchi IX model geometry and study in detail some specific examples of the flow for different couplings in Hořava–Lifshitz gravity. Even in this case the resulting equations in mini-superspace are not easily tractable for generic values of the couplings. First, we will consider the Ricci flow and some of its variants that describe solutions of the modified theory of gravity with anisotropy scaling parameter $z = 2$ (see next section for this and other definitions) and compare them to instantons with $SU(2)$ isometry in ordinary gravity. We will also consider the Cotton flow, separately, and use it to construct solutions of Hořava–Lifshitz theory with anisotropy scaling parameter $z = 3$ by ignoring all Ricci curvature terms that become subdominant when the volume of S^3 is very small. We will also consider the combined Ricci–Cotton flow and explore the equations in detail first in the limit that the speed of light vanishes or equivalently Newton's constant becomes infinite (it is often called Carroll limit after [29]) . The normalized Ricci–Cotton flow and the unnormalized variant of it with vanishing cosmological constant provide the relevant equations in this limit. Finally, we will consider the general Ricci–Cotton flow with arbitrary couplings and obtain several qualitative results for its solutions.

In all cases it is assumed that the parameter of the superspace metric of the theory is restricted to values $\lambda < 1/3$ (in which case the cosmological constant will also be taken non-negative) so that the flow equations extremize the classical action, up to important boundary terms. Proper account of the boundary terms leads to the definition of instanton solutions as finite-action trajectories that interpolate between fixed points. Our analysis shows that the Ricci and the Cotton tensor terms can compete with each other, and, depending on the relative sign between the two, the flow equa-

tions can exhibit symmetric as well as anisotropic fixed points. The nature of these fixed points and their stability properties also have implications for the space–time interpretation of the corresponding gravitational instanton solutions. Axisymmetric solutions are associated with spaces with $SU(2) \times U(1)$ isometries, and, hence they are easier to describe in closed form.

Instanton solutions of Hořava–Lifshitz gravity, as they are defined, are rather special configurations that rely on the existence of multiple-degenerate vacua and correspond to special flow lines, which guarantee finiteness of their action. As it will turn out, they are also free of singularities and their space–time metrics are regular and complete. Note, however, that other flow lines, possibly with infinite action, also describe solutions of the second-order equations of motion, but they may have singularities. Although we are primarily interested in the class of instanton solutions, one should be open-minded for other more general possibilities too. For this reason, as well as for mathematical completeness, we will investigate the phase portraits of the flow equations in all generality. The selection of special trajectories that correspond to instantons will be made much later together with their space–time interpretation.

In section 2, we first briefly review the formulation of Hořava–Lifshitz gravity with detailed balance condition putting emphasis on the structure of the potential term and its associated superpotential. This analysis is then carried to the Euclidean regime where "zero-energy" (i.e., self-dual-like) configurations exist satisfying the flow equations. Restrictions on the parameter λ are also obtained together with an entropy functional that changes monotonically along the flow lines. The results are then used to define instanton solutions as in ordinary point particle systems. The Bianchi IX model geometry is introduced in section 3 where the truncation of the Ricci and Cotton flows are studied separately in detail. Section 4 is entirely devoted to the analysis of the normalized Ricci–Cotton flow and the explicit construction of its axisymmetric solutions. Section 5 discusses the case of unnormalized Ricci–Cotton flow obtained for general couplings. It contains the case study of positive and zero cosmological constant for axisymmetric configurations with $\lambda < 1/3$. Section 6 is devoted to the space–time interpretation of the flow line, as gravitational instantons, making comparisons with the analogous instanton solutions arising in general relativity. Complete classification of all gravitational-instanton metrics with $SU(2)$ isometry is also obtained. In section 7 we outline generalizations of the framework to higher-dimensional Hořava–Lifshitz gravities, which, for instance, in $4+1$ dimensions give rise to a new system of flow equations on four-manifolds driven by the Bach tensor. Finally, section 8 contains our conclusions and poses several questions for future work.

2 Non-relativistic gravity, detailed balance and flows

2.1 Non-relativistic gravity: a reminder

The theory of non-relativistic gravity developed in [6, 7] is valid for general space–time dimension $D+1$. It has three main features:

- Space-time is assumed to be topologically $\mathcal{M}_{D+1} = \mathbb{R} \times \mathcal{M}_D$, leading to a natural codimension-one foliation. Diffeormorphism invariance is broken down to the subgroup of foliation-preserving transformations. This breaking is controlled by a parameter λ.
- Scaling properties of space and time are different and captured by an integer z. Power counting renormalizability of the theory requires $z = D$.
- The interactions are determined by a detailed balance condition following from a Euclidean D-dimensional diffeomorphism-invariant action, which gives rise to marginal and relevant terms in $D+1$ dimensions.

The last item above is not generic in Hořava–Lifshitz gravity and it can be relaxed by allowing more arbitrary coefficients for the various marginal and relevant terms. However, it is a necessary ingredient in our study to connect it naturally with the theory of geometric flows. Thus, detailed balance will be assumed in the following.

Let us adopt the ADM (Arnowitt–Deser–Misner) decomposition of the metric (see, for instance, [30]), which is suitable for the $D+1$ foliation of space–time,

$$\mathrm{d}s^2 = -N^2 \mathrm{d}t^2 + g_{ij} \left(\mathrm{d}x^i + N^i \mathrm{d}t\right) \left(\mathrm{d}x^j + N^j \mathrm{d}t\right), \tag{2.1}$$

where N^i and N are the shift and lapse functions respectively. Here, $i, j, \ldots$ run in D dimensions and all tensors that will appear in the following are D-dimensional.

Using this decomposition, the Einstein–Hilbert action in $D+1$ dimensions (up to total derivative terms that may contribute in topologically non-trivial spaces) reads as follows,

$$S_{\mathrm{EH}} = \frac{1}{16\pi G_{\mathrm{N}}} \int \mathrm{d}^{D+1}x \, \sqrt{g} N \left(K_{ij}K^{ij} - K^2 + R - 2\Lambda\right), \tag{2.2}$$

where Λ is the genuine cosmological constant in $D+1$ dimensions. In this expression, K_{ij} is the second fundamental form that measures the extrinsic curvature of the leaves at constant t,

$$K_{ij} = \frac{1}{2N} \left(\partial_t g_{ij} - \nabla_i N_j - \nabla_j N_i\right), \tag{2.3}$$

and its trace $K = g^{ij}K_{ij}$ is the mean curvature. The first two terms in equation (2.2) provide the kinetic energy, since they include time derivatives of the field g_{ij}. Their specific combination can be recast in the form

$$K_{ij}G^{ijk\ell}_{\rm DW}K_{k\ell} = K_{ij}K^{ij} - K^2 \tag{2.4}$$

using the DeWitt metric in superspace

$$G^{ijk\ell}_{\rm DW} = \frac{1}{2}\left(g^{ik}g^{j\ell} + g^{i\ell}g^{jk}\right) - g^{ij}g^{k\ell}. \tag{2.5}$$

The potential term in Einstein gravity is provided by the three-dimensional Ricci scalar curvature R and the four-dimensional cosmological constant term Λ (when it is present), as shown in (2.2).

In non-relativistic gravity, space and time scale as $[t] = -z$, $[x] = -1$ and it is further assumed[1] that $[N_i] = z - 1$, $[N] = 0$ and $[g_{ij}] = 0$ so that $[K^2] = 2z$; it should be contrasted to general relativity where space and time scale the same with $z = 1$. This asymmetry is further implemented in the action, both in the kinetic and the potential terms by requiring foliation preserving covariance. The kinetic term is generalized as

$$S_{\rm K} = \frac{2}{\kappa^2}\int {\rm d}t\,{\rm d}^Dx\,\sqrt{g}NK_{ij}G^{ijk\ell}K_{k\ell} = \frac{2}{\kappa^2}\int {\rm d}t\,{\rm d}^Dx\,\sqrt{g}N\left(K_{ij}K^{ij} - \lambda K^2\right), \tag{2.6}$$

where $\left[\kappa^2\right] = z - D$ and λ is a dimensionless coupling measuring the breaking of the full diffeomorphism group. Here, $G^{ijk\ell}$ is the generalized metric in superspace

$$G^{ijk\ell} = \frac{1}{2}\left(g^{ik}g^{j\ell} + g^{i\ell}g^{jk}\right) - \lambda g^{ij}g^{k\ell}. \tag{2.7}$$

that coincides with the DeWitt metric when $\lambda = 1$. It is worth stressing that this metric can be positive-definite or indefinite depending on λ. Indeed, $g_{k\ell}$ is an "eigenvector",

$$G^{ijk\ell}g_{k\ell} = (1 - \lambda D)g^{ij}\,, \tag{2.8}$$

with eigenvalue $1 - \lambda D$. The sign of the latter changes at $\lambda = 1/D$ where the inverse no longer exists. Thus, for $\lambda < 1/D$ the metric is positive-definite and it becomes indefinite for all $\lambda > 1/D$ that include, in particular, $\lambda = 1$. This behavior and the fact that λ is ultimately an unprotected parameter of the theory, which, in principle can take any real value, should be kept in mind when considering quantum corrections.

[1] Proper restoration of the speed of light, which scales as $[c] = z - 1$, explains the various dimensions, as described in detail in the original works [6, 7].

The potential term of the theory has the general form

$$S_V = -\int \mathrm{d}t\, \mathrm{d}^D x\, \sqrt{g} N\, V[g] \tag{2.9}$$

and can also contribute in various ways to the breaking of diffeomorphism invariance. Note that $[V] = z + D$ and there is a large freedom to choose V so that it includes operators of dimension less than or equal to $z + D$ (called relevant and marginal operators, respectively). In order to reduce this freedom and take advantage of the renormalization properties of a D-dimensional system, it was proposed in [6, 7] to introduce a detailed balance condition that allows to express the potential in terms of a "superpotential" as follows:

$$V = \frac{\kappa^2}{2} E^{ij} \mathcal{G}_{ijk\ell} E^{k\ell}, \tag{2.10}$$

where

$$E^{ij} = -\frac{1}{2\sqrt{g}} \frac{\delta W[g]}{\delta g_{ij}} \tag{2.11}$$

and W a D-dimensional action so that $[E^{ij}] = D$. The tensor $\mathcal{G}_{ijk\ell}$ is defined as

$$\mathcal{G}_{ijk\ell} = \frac{1}{2}\left(g_{ik} g_{j\ell} + g_{i\ell} g_{jk}\right) - \frac{\lambda}{D\lambda - 1} g_{ij} g_{k\ell} \tag{2.12}$$

and coincides with the inverse of the metric in superspace with generic λ, i.e.,

$$G^{ijk\ell} \mathcal{G}_{k\ell mn} = \frac{1}{2}(\delta^i_m \delta^j_n + \delta^i_n \delta^j_m)\ . \tag{2.13}$$

The resulting theory is not invariant under general coordinate transformations of space–time. Indeed, since $\mathcal{M}_{D+1}$ is topologically $\mathbb{R} \times \mathcal{M}_D$, it is only appropriate to consider invariance of the action under the restricted class of foliation-preserving diffeomorphisms,

$$\tilde{t} = \tilde{t}(t)\ , \quad \tilde{x}^i = \tilde{x}^i(t, x)\ . \tag{2.14}$$

Then, the lapse function N associated with the freedom of time reparametrization is restricted to be a function of t alone, whereas the shift functions N_i associated with diffeomorphisms of $\mathcal{M}_D$ can depend on all space–time coordinates. This is often called the *projectable case* of Hořava–Lifshitz gravity and it will be assumed in the following. The non-projectable version of the theory leads to dynamical inconsistencies [31].

The choice of W depends on the dimension D. Here, we recall the choice for $D = 3$ with $z = 3$ that ensures power-counting renormalizability of the four-dimensional theory; generalization to higher dimensions will be discussed later in section 7. Then, the marginal operators in question are obtained from the three-dimensional gravitational

Chern–Simons action, which is familiar from topologically massive gravity [32],

$$W_{\rm CS} = \frac{1}{w_{\rm CS}} \int \omega_3(\omega) \,, \tag{2.15}$$

with density given in terms of the connection one-form ω by

$$\omega_3(\omega) = \frac{1}{2}{\rm Tr}\left(\omega \wedge {\rm d}\omega + \frac{2}{3}\omega \wedge \omega \wedge \omega\right). \tag{2.16}$$

The corresponding variation gives

$$E^{k\ell}_{\rm CS} = -\frac{1}{w_{\rm CS}} \frac{\varepsilon^{ijk}}{\sqrt{g}} \nabla_i \left(R^\ell_j - \frac{1}{4} R \delta^\ell_j\right) \equiv -\frac{1}{w_{\rm CS}} C^{k\ell}, \tag{2.17}$$

where $C^{k\ell}$ is the Cotton tensor and $\epsilon^{123} = 1$. The Cotton tensor is traceless, conserved and it vanishes identically for conformally flat metrics.

Relevant operators in four dimensions are generated by the Einstein–Hilbert three-dimensional action

$$W_{\rm EH} = \frac{2}{\kappa_W^2} \int {\rm d}^D x \sqrt{g} (R - 2\Lambda_W). \tag{2.18}$$

Note that neither κ_W^2 is the four-dimensional Newton's constant nor Λ_W is the four-dimensional cosmological constant, but they will be identified shortly. The variation of this action leads to

$$E^{k\ell}_{\rm EH} = \frac{1}{\kappa_W^2} \left(R^{k\ell} - \frac{R}{2} g^{k\ell} + \Lambda_W g^{k\ell}\right). \tag{2.19}$$

Combining the Chern–Simons and Einstein–Hilbert contributions to $E^{k\ell}$, with their respective couplings, the full potential of Hořava–Lifshitz gravity reads

$$\begin{aligned} V \;=\; & \frac{\kappa^2}{2w_{\rm CS}^2} C^{ij} C_{ij} - \frac{\kappa^2}{w_{\rm CS}\kappa_W^2} C^{ij} R_{ij} + \\ & \frac{\kappa^2}{2\kappa_W^4} \left(R^{ij} R_{ij} - \frac{4\lambda - 1}{4(3\lambda - 1)} R^2\right) + \\ & \frac{\kappa^2 \Lambda_W}{2(3\lambda - 1)\kappa_W^4} \left(R - 3\Lambda_W\right). \end{aligned} \tag{2.20}$$

The ultra-violet behavior of the resulting theory is dictated by the quadratic Cotton curvature term, which is marginal with dimension $2z = 6$, and corresponds to $z = 3$. It improves a lot the ultra-violet behavior of ordinary Einstein gravity at the expense of breaking general covariance of the theory at short distances. When the Cotton term

is absent, the resulting theory has a potential with quadratic Ricci curvature terms that become dominant in the ultra-violet regime and so $z = 2$. In either case, in the infrared limit one expects to flow by the most relevant operators (of dimension 2 and zero), which correspond to the last terms in equation (2.20), and recover general relativity provided that λ also flows to 1. However, no rigorous proof of any of these statements is yet available in the literature. Also, the counting of physical degrees of freedom of the theory, which is crucial for viewing it as viable modification of general relativity, is obscured by the outcome of local invariances and their potential restoration.

We also recall for completeness, using the relativistic coordinate $x^0 = ct$, that the effective speed of light for general λ is given by

$$c = \frac{\kappa^2}{2\kappa_W^2}\sqrt{\frac{\Lambda_W}{1-3\lambda}} \tag{2.21}$$

with $[c] = z - 1$. This shows that Λ_W must be negative when $\lambda > 1/3$ to ensure reality of c; likewise, Λ_W must be positive when $\lambda < 1/3$. Also, the four-dimensional effective cosmological constant is given by

$$\Lambda = \frac{3}{2}\Lambda_W \tag{2.22}$$

and, therefore, the range $\lambda > 1/3$ does not allow for de Sitter-like backgrounds in Hořava–Lifshitz gravity. These identifications are necessary in order to compare the infrared limit of the deformed theory to ordinary gravity so that the effective Newton constant reads as

$$G_N = \frac{\kappa^2}{32\pi c}\,. \tag{2.23}$$

Furthermore, λ should approach (flow to) 1 in the infrared limit in order to recover the full reparametrization invariance of general relativity, but this particular problem will not concern us at all here.

The search for classical solutions requires the use of the potential (2.20) and it is impossible to solve in full generality. Symmetry ansatz such as spatial homogeneity makes the problem more tractable, but still not exactly solvable. This includes, for example, the case of Bianchi IX geometry leading to the mixmaster universe model in four space–time dimensions with Lorentzian signature. We will not pursue this line of investigation here (see [27] for a detailed analysis and comparison with the mixmaster universe in general relativity [24, 25]), but elaborate on the Euclidean version of Hořava–Lifshitz gravity and then analyze its instanton solutions for Bianchi IX spatial geometries.

2.2 Euclidean action and flow equations

Besides the various physical motivations pertaining to the analysis of the Euclidean version of Hořava–Lifshitz theory, there is also a technical advantage for constructing solutions that satisfy first-order equations in time. This possibility is also encountered in general relativity when self-duality on the Riemann (and more generally on the Weyl) tensor is imposed leading to gravitational-instanton solutions in the Euclidean regime[2]. Although there is no direct analogue of self-duality in gravitational theories with anisotropic scaling, the detailed balance condition offers the appropriate replacement for defining instanton-like configurations. This is in fact possible in all dimensions unlike gravitational instantons of ordinary gravity that are only defined in four space–time dimensions.

The Euclidean action is obtained by setting $t \to -it$, $N^j \to iN^j$, whereas iS is traded for $-S$. Using equations (2.6) and (2.9) one obtains

$$S = \int \mathrm{d}t\, \mathrm{d}^D x\, \sqrt{g} N \left(\frac{2}{\kappa^2} \left(K_{ij} K^{ij} - \lambda K^2 \right) + V \right). \tag{2.24}$$

The expression for the potential (2.10) allows to rewrite the Euclidean action (2.24) in the form $S = S' + S''$, where

$$S' = \frac{2}{\kappa^2} \int \mathrm{d}t\, \mathrm{d}^D x\, \sqrt{g} N \left(K_{ij} \pm \frac{\kappa^2}{2} \mathcal{G}_{ijmn} E^{mn} \right) G^{ijk\ell} \left(K_{k\ell} \pm \frac{\kappa^2}{2} \mathcal{G}_{k\ell rs} E^{rs} \right) \tag{2.25}$$

and S'' is a total-derivative contribution to the action [6]. This boundary term will be considered later in detail (see equation (2.33)). The different signs correspond to the choice of time direction.

The action (2.25) is bounded below by zero provided that the superspace metric $G^{ijk\ell}$ is positive-definite. Then, configurations that obey the first-order differential equations

$$K_{ij} = \mp \frac{\kappa^2}{2} \mathcal{G}_{ijk\ell} E^{k\ell}, \tag{2.26}$$

are extrema of the action and as such they provide solutions of the Euclidean theory S'; the leaves of the corresponding space–time foliations have prescribed extrinsic curvature. This possibility arises only when $\lambda < 1/D$, in which case we must also demand that Λ_W is non-negative so that the speed of light in the Lorentzian version of the theory is real. Otherwise, for $\lambda > 1/D$, the action is non-bounded below by zero and

[2]Self-duality is best described in terms of the curvature two-form, as $\mathcal{R}_{ab} = \pm \tilde{\mathcal{R}}_{ab}$ in an orthonormal frame [33]. These equations are second-order in time, but they can be integrated once to yield first-order equations [34] that will be paralleled to the instanton solutions of Hořava–Lifshitz gravity; for further details see also [22], where this analogy is made even sharper for gravitational instantons with homogeneous spatial sections.

the first-order equations are not guaranteed to provide classical solutions. Thus, from now on, we restrict ourselves to $\lambda < 1/D$ and $\Lambda_W \geq 0$, where the first-order equations (2.26) provide extrema of S'. They are also extrema of the action S provided that the boundary term S'' is properly accounted. This problem will be treated carefully in section 2.3 and lead to the precise definition of instantons.

The solutions that we will investigate can be expressed in the form of geometric gradient flow equations for the metric g_{ij} modulo reparametrizations generated by the shift functions,

$$\partial_t g_{ij} = \mp\kappa^2 N \mathcal{G}_{ijk\ell} E^{k\ell} + \nabla_i N_j + \nabla_j N_i \,. \tag{2.27}$$

Since we are only considering the projectable case of Hořava–Lifshitz gravity, N is only a function of t and can be absorbed by redefining time, as $N(t)\mathrm{d}t \to \mathrm{d}t$. It is also natural to define vector fields with components $\xi_i = N_i/N$ that generally depend on space and time coordinates. Then, the geometric-flow equations assume the more standard form that will be used in the following,

$$\frac{1}{N(t)}\partial_t g_{ij} = \pm\frac{\kappa^2}{2\sqrt{g}}\mathcal{G}_{ijk\ell}\frac{\delta W[g]}{\delta g_{k\ell}} + \nabla_i \xi_j + \nabla_j \xi_i \,. \tag{2.28}$$

Specializing to $D = 3$, we write down explicitly the flow equations obtained by combining the variation of the Chern–Simons and Einstein–Hilbert actions,

$$\frac{1}{N}\partial_t g_{ij} = -\frac{\kappa^2}{\kappa_W^2}\left(R_{ij} - \frac{2\lambda - 1}{2(3\lambda - 1)}R g_{ij} + \frac{\Lambda_W}{1 - 3\lambda}g_{ij}\right) + \frac{\kappa^2}{w_{\mathrm{CS}}}C_{ij} + \nabla_i \xi_j + \nabla_j \xi_i \tag{2.29}$$

choosing for definiteness one of the two sign options; the other follows by time reversal. These equations describe the parametric evolution of a family of three-dimensional geometries

$$\mathrm{d}s_{\mathrm{t}}^2 = g_{ij}(x;t)\mathrm{d}x^i \mathrm{d}x^j \tag{2.30}$$

driven by the Ricci and Cotton tensors and the cosmological constant term, and, as such, they will be called *Ricci–Cotton flow* equations[3].

The fixed points are determined (modulo reparametrization terms) by the solutions of three-dimensional topologically massive gravity:

$$\frac{\kappa_W^2}{w_{\mathrm{CS}}}C_{ij} = R_{ij} - 2\Lambda_W g_{ij} \,, \quad \text{with } R = 6\Lambda_W \,. \tag{2.31}$$

[3]Perhaps a more appropriate name is Ricci–Yamabe–Cotton flow, since Rg_{ij} is the driving term of the so called Yamabe flow, $\partial_t g_{ij} = -Rg_{ij}$. The latter was introduced in the literature [35] to solve Yamabe's conjecture stating that any metric is conformally equivalent to a metric of constant curvature. Its effect is complementary to the Cotton term of the flow, which changes the conformal class of the metric. Thus, the combined flow equations we have obtained contain several competing deformations of the metric.

They include Einstein metrics with vanishing Cotton tensor, like the round sphere metric on S^3 (for $\Lambda_W > 0$), which is homogeneous and isotropic. There are other fixed points, however, with constant scalar curvature but with non-vanishing Cotton tensor. We will see later, as example, that they correspond to particular homogeneous but non-isotropic metrics on S^3. The coexistence of fixed points from different conformal classes of the metric make this flow particularly complex.

The driving terms of the Ricci–Cotton flow involve, in general, third-order derivatives in space coordinates (originating from the Cotton tensor), and, therefore, it is not possible to apply standard results from the mathematics literature to prove even the short-time existence of solutions. Nevertheless, the mini-superspace models that will be studied later show that these flow equations are well-behaved and the trajectories converge to fixed points after sufficiently long time.

Some special cases are worth noting, since they have already appeared in the literature for different reasons:

- $w_{CS} \to \infty$: the Cotton tensor contribution drops out and one obtains a variant of the Ricci flow on three-manifolds, which is second-order and well studied in the literature. Its trajectories describe solutions of $z = 2$ Hořava–Lifshitz gravity in $3 + 1$ dimensions, whereas the fixed points are Einstein metrics $R_{ij} = 2\Lambda_W g_{ij}$.
- $\kappa_W^2 \to \infty$: the Ricci and cosmological constant terms drop out and one obtains the pure Cotton flow that was recently introduced in the literature [36]. Its trajectories describe solutions of $z = 3$ Hořava–Lifshitz gravity in $3 + 1$ dimensions, in the limit under consideration. The fixed points are conformally flat metrics, $C_{ij} = 0$.

Even these simpler cases are impossible to solve in all generality. Mini-superspace models have been used to study the long time behavior of the Ricci and Cotton flows for homogeneous geometries [37, 36].

Apart from the Ricci and Cotton flows that will studied separately in the next section, there are also some other special cases of the combined Ricci–Cotton flow that are relatively easier to study. First, by considering that limiting case $\lambda \to -\infty$, which lies in the allowed range $\lambda < 1/3$, one obtains the normalized Ricci–Cotton flow, which is driven by a traceless tensor, and, thus, preserves the volume of space; the cosmological constant decouples in this case. It becomes relevant in the Carroll limit of Hořava–Lifshitz gravity, where the effective speed of light vanishes[4]. The effective

[4]When $\lambda \to -\infty$, the metric in superspace becomes singular as its inverse has zero eigenvalues. Yet the flow equations are well-defined and so is the potential term S_V of the gravity action. It is opposite to the case $\lambda = 1/3$ for which the metric in superspace has zero eigenvalues and its inverse becomes singular; the latter case corresponds to the limit of infinite speed of light, where the theory develops anisotropic Weyl invariance.

speed of light vanishes also when $\Lambda_W = 0$, irrespective of λ, and the corresponding flow equations will be studied separately. The general case, with arbitrary coefficients, is much more complex. The pattern of fixed points and specific trajectories will only be discussed for axially symmetric deformations of S^3, which correspond to solutions with $SU(2) \times U(1)$ isometry.

2.3 Entropy functional and action bound

From now on, and in all examples that will be studied later, we consider flows without the effect of space reparametrizations, setting $N_i = 0$. Also, we will take advantage of time reparametrizations to set $N(t) = 1$ for convenience. We will also assume that the spatial slices are compact spaces without boundary. Here, we provide an entropy functional for the geometric flows arising in Hořava–Lifshitz gravity in arbitrary dimensions. This functional is also be related to the lower bound of the Euclidean action S (rather than S') when boundary terms S'' are properly taken into account.

When the metric in superspace is positive-definite (choosing $\lambda < 1/D$ in D spatial dimensions), the superpotential functional W changes monotonically along the flow. This follows easily by considering

$$\frac{\mathrm{d}W}{\mathrm{d}t} = -2 \int \mathrm{d}^D x \sqrt{g} E^{ij} \partial_t g_{ij} = \pm 2\kappa^2 \int \mathrm{d}^D x \sqrt{g} E^{ij} \mathcal{G}_{ijk\ell} E^{k\ell} \,, \tag{2.32}$$

which is the integral of a quadratic quantity, and, therefore, increases or decreases monotonically depending on the overall sign. Thus, W is an entropy functional for the flows under consideration.

With this in mind, let us revisit the original Euclidean action S of the theory and its lower bound taking into proper account the boundary terms. Equations (2.24) and (2.10) yield

$$\begin{aligned} S &= \frac{2}{\kappa^2} \int \mathrm{d}t \mathrm{d}^D x \sqrt{g} K_{ij} G^{ijk\ell} K_{k\ell} + \frac{\kappa^2}{2} \int \mathrm{d}t \mathrm{d}^D x \sqrt{g} E^{ij} \mathcal{G}_{ijk\ell} E^{k\ell} \\ &= \frac{2}{\kappa^2} \int \mathrm{d}t \, \mathrm{d}^D x \, \sqrt{g} \left(K_{ij} \pm \frac{\kappa^2}{2} \mathcal{G}_{ijmn} E^{mn} \right) G^{ijk\ell} \left(K_{k\ell} \pm \frac{\kappa^2}{2} \mathcal{G}_{k\ell rs} E^{rs} \right) \\ &\quad \mp 2 \int \mathrm{d}t \mathrm{d}^D x \sqrt{g} K_{ij} E^{ij}. \end{aligned} \tag{2.33}$$

The first term in (2.33) is S', given in equation (2.25), and the last term is the advertised boundary contribution S''. For positive-definite superspace metric, the Euclidean ac-

tion S is bounded from below by the boundary term S'', because $S' \geq 0$. Thus,

$$S \geq \mp 2 \int \mathrm{d}t \mathrm{d}^D x \sqrt{g} K_{ij} E^{ij} = \mp \int \mathrm{d}t \mathrm{d}^D x \sqrt{g} E^{ij} \partial_t g_{ij} = \pm \frac{1}{2} \int \mathrm{d}t \frac{\mathrm{d}W}{\mathrm{d}t}, \tag{2.34}$$

having set $N(t) = 1$. The time integral of equation (2.32) shows that the lower bound of S is always positive, as expected.

The flow equations (2.26) provide time-dependent extrema of the action S'. They are actually its ground states, since they make S' vanish. Since S'' is a boundary term, these ground states are also extrema of S under appropriate boundary conditions that make the variational problem well-posed. This can be easily verified for the class of flows with finite action (i.e. finite S''). Note for this purpose that the fixed points of the flow are static solutions of both S and S', since they are, by construction, critical points of the D-dimensional action functional W sitting at the minima of the Hořava–Lifshitz potential. If different minima exist, they will be all degenerate with zero potential energy. Hence, time-dependent solutions that interpolate between any two fixed points are guaranteed to satisfy the equations of motion following from the Hořava–Lifshitz action S. These solutions have finite action, given by the value of the boundary term, and is natural to call them instantons as they interpolate between two different static minima, which are connected by trajectories of the geometric flow. Their action is simply given by

$$S_{\text{instanton}} = \frac{1}{2} |\Delta W| \,, \tag{2.35}$$

where ΔW is the difference of the corresponding values of W at the two critical points. Note that $\Delta W \neq 0$, in general, since W changes monotonically along the flow lines and the instanton action is finite. Then, this yields the standard description of instanton solutions of a point particle moving in Euclidean time, but the number of degrees of freedom is infinite now, as the evolution takes place in superspace.

Finally, let us consider the evolution of the volume of spatial slices under the flow. In general, it takes the form

$$\frac{\mathrm{d}}{\mathrm{d}t} \mathrm{vol}(\mathcal{M}_D) = \frac{1}{2} \int \mathrm{d}^D x \sqrt{g} g^{ij} \partial_t g_{ij} = \mp \frac{\kappa^2}{2(1-3\lambda)} \int \mathrm{d}^D x \sqrt{g} g_{ij} E^{ij} \tag{2.36}$$

and, therefore, the trace-free part of the driving curvature terms do not contribute to the evolution. Otherwise, the volume changes without definite sign. Thus, in principle, the volume can bounce along the flow. At the fixed points, where $g_{ij} E^{ij} = 0$, the volume reaches a local maximum or minimum depending on circumstances.

As an example, let us consider the Ricci–Cotton flow described by equation (2.29).

Then, since the Cotton tensor is traceless, the volume of space changes as

$$\frac{\mathrm{d}}{\mathrm{d}t}\mathrm{vol}(\mathcal{M}_3) = \frac{\kappa^2}{4(1-3\lambda)\kappa_W^2}\int \mathrm{d}^D x\sqrt{g}(R-6\Lambda_W) \tag{2.37}$$

and it can have either sign. Of course, it is possible to normalize this (or any other flow that arises in this context) by rescaling the metric with a function of time followed by a suitably chosen time reparametrization $t \to \tilde{t}(t)$ so that the volume is preserved in time $\tilde{t}$. This does not resolve the problem, however, since $\tilde{t}(t)$ is not a monotonic function of t in general. Thus, the volume does not provide an entropy functional.

Other entropy functionals might also exist for these flows, generalizing Perelman's functional for the Ricci flow [15], but we have not been able to find them.

3 Bianchi IX model geometry

All homogeneous space geometries in three dimensions provide consistent ansatz for the mini-superspace truncation of the Ricci and Cotton flows and their combination thereof. Such spaces follow the Bianchi classification, but for practical reasons we will only consider the case of Bianchi IX model geometries that describe homogeneous but generally non-isotropic metrics on S^3. The corresponding gravitational instantons of the four-dimensional Euclidean theory are special in that they admit an $SU(2)$ isometry group and they provide the simplest examples in our study. In this section, we set up the notation and present some useful formulas that will enable us to formulate the problem as an autonomous system of ordinary differential equations. The Ricci and Cotton flows are studied separately here for Bianchi IX geometries. Comparison with the gravitational instantons of ordinary gravity will also be made at the appropriate places.

3.1 Some basic facts

We consider four-dimensional Riemannian manifolds that are foliated by homogeneous three-dimensional spaces of the form

$$\mathrm{d}s^2 = \mathrm{d}t^2 + \sum_i \gamma_i(t)\left(\sigma^i\right)^2 , \tag{3.1}$$

setting $N = 1$ and $N_i = 0$. The coefficients γ_i are taken to depend only on t and σ^i are the left-invariant Maurer–Cartan one-forms of $SU(2)$

$$\begin{aligned} \sigma^1 &= \sin\vartheta \sin\psi \, \mathrm{d}\varphi + \cos\psi \, \mathrm{d}\vartheta \\ \sigma^2 &= \sin\vartheta \cos\psi \, \mathrm{d}\varphi - \sin\psi \, \mathrm{d}\vartheta \\ \sigma^3 &= \cos\vartheta \, \mathrm{d}\varphi + \mathrm{d}\psi \end{aligned} \tag{3.2}$$

with Euler angles ranging as $0 \leq \vartheta \leq \pi$, $0 \leq \varphi \leq 2\pi$, $0 \leq \psi \leq 4\pi$, which satisfy

$$\mathrm{d}\sigma^i + \frac{1}{2}\epsilon^i{}_{jk}\sigma^j \wedge \sigma^k = 0. \tag{3.3}$$

The three-dimensional leaves are, in general, homogeneous but non-isotropic three-spheres. The isometry group is enhanced to $SU(2) \times U(1)$ when any two γ_i's coincide by imposing axial symmetry. Full isotropy requires all γ_i's to be equal, in which case the symmetry of the model is promoted to $SU(2) \times SU(2)$. The volume of the three-sphere is

$$V = 16\pi^2\sqrt{\gamma_1\gamma_2\gamma_3} \tag{3.4}$$

and when all coefficients γ_i are equal to $L^2/4$ the volume is expressed in terms of the radius L as $V = 2\pi^2 L^3$.

The Ricci and Cotton tensors are diagonal for all homogeneous geometries and this ensures consistency of the reduced models. They take the following form for the Bianchi IX class,

$$R_{11} = \frac{1}{2\gamma_2\gamma_3}\left[\gamma_1^2 - (\gamma_2 - \gamma_3)^2\right] , \tag{3.5}$$

$$C_{11} = -\frac{\gamma_1}{2(\gamma_1\gamma_2\gamma_3)^{3/2}}\left[\gamma_1^2\left(2\gamma_1 - \gamma_2 - \gamma_3\right) - \left(\gamma_2 + \gamma_3\right)\left(\gamma_2 - \gamma_3\right)^2\right] , \tag{3.6}$$

and similarly for the other two components that follow by cyclic permutation of the indices. Also, the Ricci scalar curvature is given by

$$R = \frac{1}{2\gamma_1\gamma_2\gamma_3}\left[2\gamma_1\gamma_2 + 2\gamma_2\gamma_3 + 2\gamma_3\gamma_1 - \gamma_1^2 - \gamma_2^2 - \gamma_3^2\right] , \tag{3.7}$$

whereas the trace of the Cotton tensor vanishes, as it can be readily checked.

With these explanations in mind, we arrive at the following system of ordinary differential equations for the metric coefficients $\gamma_i(t)$

$$\frac{\mathrm{d}\gamma_i}{\mathrm{d}t} = -\frac{\kappa^2}{\kappa_W^2}\left(R_{ii} - \frac{2\lambda - 1}{2(3\lambda - 1)}R\gamma_i + \frac{\Lambda_W}{1 - 3\lambda}\gamma_i\right) + \frac{\kappa^2}{w_{\mathrm{CS}}}C_{ii} \tag{3.8}$$

as the Bianchi IX mini-superspace model of the combined Ricci–Cotton flow with general couplings.

3.2 Ricci flow

When $w_{\rm CS} \to \infty$ the Cotton term decouples and one arrives at a variant of the Ricci flow as the relevant equation for Hořava–Lifshitz gravity with anisotropy scaling parameter $z = 2$. In this case, the system becomes

$$\frac{\mathrm{d}\gamma_i}{\mathrm{d}t} = -\frac{\kappa^2}{\kappa_W^2}\left(R_{ii} - \frac{2\lambda - 1}{2(3\lambda - 1)} R\gamma_i + \frac{\Lambda_W}{1 - 3\lambda}\gamma_i\right) \tag{3.9}$$

and its properties resemble the ordinary Ricci flow on S^3

$$\frac{\mathrm{d}\gamma_i}{\mathrm{d}t} = -R_{ii}(\gamma)\,. \tag{3.10}$$

Formally, one follows from the other by rescaling the metric with a function of time and changing time variable by suitable reparametrization; in such case, the components of the Ricci tensor remain invariant and they assume the same form for the rescaled components of the metric.

The Ricci flow equations (3.10) for homogeneous geometries are well studied in the literature following the original work [37]. For Bianchi IX geometries they take the form

$$\begin{aligned}
\frac{2}{\gamma_1}\frac{\mathrm{d}\gamma_1}{\mathrm{d}t} &= \frac{1}{\gamma_1\gamma_2\gamma_3}\left[(\gamma_2 - \gamma_3)^2 - \gamma_1^2\right]\,, \\
\frac{2}{\gamma_2}\frac{\mathrm{d}\gamma_2}{\mathrm{d}t} &= \frac{1}{\gamma_1\gamma_2\gamma_3}\left[(\gamma_3 - \gamma_1)^2 - \gamma_2^2\right]\,, \\
\frac{2}{\gamma_3}\frac{\mathrm{d}\gamma_3}{\mathrm{d}t} &= \frac{1}{\gamma_1\gamma_2\gamma_3}\left[(\gamma_1 - \gamma_2)^2 - \gamma_3^2\right]
\end{aligned} \tag{3.11}$$

and coincide with the celebrated *Darboux–Halphen* system that was introduced by Darboux in the nineteenth century [38] and subsequently solved by Halphen [39][5]. In principle, solutions of these equations can be translated into solutions of the original system (3.9).

[5]For the comparison one must consider the variables $\omega_1 = \gamma_2\gamma_3$, $\omega_2 = \gamma_1\gamma_3$, $\omega_3 = \gamma_1\gamma_2$ and change the time coordinate to $\mathrm{d}T = \mathrm{d}t/\gamma_1\gamma_2\gamma_3$. Then, the equations take the equivalent form

$$\frac{\mathrm{d}\omega_1}{\mathrm{d}T} = \omega_2\omega_3 - \omega_1(\omega_2 + \omega_3)$$

with cyclic permutations for ω_2 and ω_3. The identification of the Ricci flow equations for Bianchi IX geometry with the Darboux–Halphen system has escaped attention in the mathematics literature.

It can be shown quite generally that for given initial data $\gamma_i^{(0)}$ the metric will evolve towards the configuration $\gamma_1 = \gamma_2 = \gamma_3 = 0$ by making S^3 rounder and rounder until the whole space collapses to a point. A particularly simple solution that exhibits this behavior is provided by

$$\gamma_1(t) = \gamma_2(t) = \gamma_3(t) = \frac{1}{2}(t_0 - t) \tag{3.12}$$

and describes an isotropic metric on S^3 whose radius evolves from infinitely large size to zero as t varies from $-\infty$ to t_0.

Actually, following the literature [37], the convergence of the flow lines is best described in terms of the normalized Ricci flow equation on S^3

$$\frac{\mathrm{d}\gamma_i}{\mathrm{d}t} = -R_{ii} + \frac{1}{3}R\gamma_i \,, \tag{3.13}$$

which follows directly from equation (3.9) in the limit $\lambda \to -\infty$, and which can be obtained from the ordinary Ricci flow by (yet another) suitable rescaling of the metric and time reparametrization. Then, the volume is preserved along the flow and the round metric (fully isotropic model with finite radius) arises as fixed point that is exponentially reached after infinitely long time, regardless of initial conditions. The normalized Ricci flow will also be in focus later in section 4 for different reasons.

The Darboux–Halphen system is not algebraically integrable when $\gamma_1 \neq \gamma_2 \neq \gamma_3$. All its solutions, however, can be expressed in terms of modular forms (see, for instance, [40]). The system becomes algebraically integrable when two γ_i's are equal. Then, the corresponding three-dimensional space is a three-sphere with axially symmetric metric. Setting $\gamma_1 = \gamma_2 \geq \gamma_3$, the system (3.11) simplifies and exhibits a first integral

$$\frac{1}{\gamma_3^2} - \frac{1}{\gamma_1\gamma_3} = \frac{1}{4m^2} \tag{3.14}$$

with arbitrary parameter m. The solution is subsequently described as

$$\frac{\gamma_1}{m} + \operatorname{arcsinh}\frac{\gamma_1}{m} = \frac{-t+t_0}{m} = \log\frac{2m+\gamma_3}{2m-\gamma_3} - 2m\left(\frac{1}{2m+\gamma_3} - \frac{1}{2m-\gamma_3}\right) \,, \tag{3.15}$$

using another integration constant t_0. The fully isotropic solution with $SU(2) \times SU(2)$ isometry is obtained by taking the limit $m \to \infty$.

Remarkably, the same system of equations arises in the description of a class of self-dual instantons with $SU(2)$ isometry in ordinary gravity [34], as well as in the description of the moduli space of $SU(2)$ BPS monopoles with magnetic charge 2 [41, 42]. In these two cases, which share many features with each other, the ansatz for the

Bianchi IX geometries takes the form

$$\mathrm{d}s^2 = \mathrm{d}t^2 + a^2(t)\left(\sigma^1\right)^2 + b^2(t)\left(\sigma^2\right)^2 + c^2(t)\left(\sigma^3\right)^2 \tag{3.16}$$

with $a(t) = \gamma_1(t)$, $b(t) = \gamma_2(t)$ and $c(t) = \gamma_3(t)$ satisfying the same system of equations (3.11) above. Then, the corresponding axially symmetric gravitational instanton with $\gamma_1 = \gamma_2$ is the self-dual Taub–NUT metric with NUT parameter m. It can be brought into standard form using a radial coordinate $r \geq m$ with $m\,\mathrm{arcosh}(r/m) + \sqrt{(r-m)(r+m)} = -t + t_0$ so that the solution (3.15) becomes

$$\gamma_1 = \gamma_2 = \sqrt{(r-m)(r+m)}\,, \quad \gamma_3 = 2m\sqrt{\frac{r-m}{r+m}}\,. \tag{3.17}$$

The fully anisotropic instantons of Einstein gravity with $SU(2)$ isometry correspond to the so called Atiyah–Hitchin metric [41, 42], which is also the metric on the moduli space of charge 2 BPS $SU(2)$ monopoles in general position. These metrics will be discussed further in section 6 while comparing instanton solutions of general relativity with those of Hořava–Lifshitz theory.

3.3 Cotton flow

Next, we consider the pure Cotton flow equations[6] that arise in the limit $\kappa_W \to \infty$. They describe solutions of $z = 3$ Hořava–Lifshitz theory when the volume of space is very small, i.e., in the deep ultra-violet regime where the Cotton term dominates and all subleading relevant operators can be safely dropped from the potential. Then, the equations for Bianchi IX geometries take the form

$$\begin{aligned}
\frac{2w_{\mathrm{CS}}}{\kappa^2\gamma_1}\frac{\mathrm{d}\gamma_1}{\mathrm{d}t} &= -\frac{1}{(\gamma_1\gamma_2\gamma_3)^{3/2}}\left[\gamma_1^2\left(2\gamma_1-\gamma_2-\gamma_3\right)-\left(\gamma_2+\gamma_3\right)\left(\gamma_2-\gamma_3\right)^2\right],\\
\frac{2w_{\mathrm{CS}}}{\kappa^2\gamma_2}\frac{\mathrm{d}\gamma_2}{\mathrm{d}t} &= -\frac{1}{(\gamma_1\gamma_2\gamma_3)^{3/2}}\left[\gamma_2^2\left(2\gamma_2-\gamma_3-\gamma_1\right)-\left(\gamma_3+\gamma_1\right)\left(\gamma_3-\gamma_1\right)^2\right],\\
\frac{2w_{\mathrm{CS}}}{\kappa^2\gamma_3}\frac{\mathrm{d}\gamma_3}{\mathrm{d}t} &= -\frac{1}{(\gamma_1\gamma_2\gamma_3)^{3/2}}\left[\gamma_3^2\left(2\gamma_3-\gamma_1-\gamma_2\right)-\left(\gamma_1+\gamma_2\right)\left(\gamma_1-\gamma_2\right)^2\right],
\end{aligned} \tag{3.18}$$

and clearly they are much more complicated than the Darboux–Halphen system. It is not known whether they are algebraically integrable when $\gamma_1 \neq \gamma_2 \neq \gamma_3$, but it can be easily shown that, under any initial data $\gamma_i^{(0)}$, they flow exponentially fast towards

[6]The Cotton flow was originally introduced in the literature [36] as an alternative to the Ricci flow for studying the existence of constant curvature metrics on three-manifolds. So far it has only been applied to homogeneous geometries and its general utility for proving the Poincaré conjecture remains questionable.

the fixed point which is the round metric on S^3 and it is conformally flat [36]. Since the Cotton tensor is odd under parity (because of the fully antisymmetric epsilon symbol appearing in its definition), there is always an ambiguity in the overall sign of the flow equations. Here, we have chosen the sign that takes any metric towards the fixed point rather than away from it when $w_{\rm CS} > 0$.

The behavior of the Cotton flow is similar to the normalized Ricci flow, as they both preserve the volume of space $V = 2\pi^2 L^3$, but the convergence rate is different. To compare the two it is sufficient to linearize the corresponding equations around the fixed point

$$\gamma_1 = \gamma_2 = \gamma_3 = \frac{L^2}{4} \tag{3.19}$$

by considering small perturbations of the metric coefficients

$$\gamma_1(t) = \frac{L^2}{4}\left(1 + \delta x(t)\right), \quad \gamma_2(t) = \frac{L^2}{4}\left(1 + \delta y(t)\right), \tag{3.20}$$

whereas $\gamma_3(t)$ changes accordingly,

$$\gamma_3(t) = \frac{L^2}{4}\left(1 - \delta x(t) - \delta y(t)\right), \tag{3.21}$$

so that the volume of space is preserved. Then, the autonomous system of Cotton flow equations (3.18) becomes to linear order

$$\frac{\mathrm{d}}{\mathrm{d}t}\begin{pmatrix}\delta x\\ \delta y\end{pmatrix} = -\frac{12\kappa^2}{w_{\rm CS}\, L^3}\begin{pmatrix}1 & 0\\ 0 & 1\end{pmatrix}\begin{pmatrix}\delta x\\ \delta y\end{pmatrix} \tag{3.22}$$

and the two eigenvalues are equal and negative for $w_{\rm CS} > 0$,

$$\zeta_1 = \zeta_2 = -\frac{12\kappa^2}{w_{\rm CS} L^3}\,, \tag{3.23}$$

ensuring stability in all directions around the fixed point.

The perturbations diminish exponentially fast, as

$$\delta x(t) = A\mathrm{e}^{-t/\tau_{\rm C}}\,, \quad \delta y(t) = B\mathrm{e}^{-t/\tau_{\rm C}}\,, \tag{3.24}$$

using arbitrary integration constants A, B and the characteristic time scale of dissipation

$$\tau_{\rm C} = \frac{w_{\rm CS} L^3}{12\kappa^2}\,. \tag{3.25}$$

Thus, when $w_{\rm CS}$ is very small compared to $\kappa_{\rm W}^2$ so that the Cotton tensor dominates the flow over the Ricci curvature and the cosmological constant terms, or equivalently

when L is very small so that the volume of space is tiny, τ_C is very small and the metric perturbations dissipate very fast at late times[7].

There is an additional fixed point, which is unique, up to permutation of the axes, that arises when $\gamma_1 = \gamma_2 = \infty$ and $\gamma_3 = 0$ (correlated limit with V held fixed). It corresponds to a squashed S^3 that is completely flattened and has zero Cotton tensor, as it can be explicitly checked. Although this configuration is degenerate in one principal direction, it has no curvature singularities and it is legitimate to consider.

Axisymmetric solutions of the Cotton flow can be constructed in closed form, as for the Ricci flow. Assuming

$$\gamma_1 = \gamma_2 \equiv x\frac{L^2}{4}\,, \quad \gamma_3 = \frac{L^2}{4x^2}\,, \tag{3.26}$$

so that the volume of space is held fixed to $V = 2\pi^2 L^3$, the Cotton flow equations (3.18) reduce to a single equation

$$\frac{\mathrm{d}x}{\mathrm{d}t} = \frac{4\kappa^2}{w_{\mathrm{CS}} L^3}\frac{1-x^3}{x^5}\,, \tag{3.27}$$

which is solved as follows,

$$\frac{-t+t_\star}{\tau_C} = x^3 - 1 + \log\left|x^3-1\right| \tag{3.28}$$

with integration constant $t_\star$.

This solution has two branches. For $x \geq 1$, $x(t)$ changes from $+\infty$ to 1 as t varies from $-\infty$ to $+\infty$; the three-sphere deforms starting from the singular configuration $\gamma_1 = \gamma_2 = \infty$, $\gamma_3 = 0$ and gradually becomes rounder until it reaches the isotropic fixed point after infinitely long time. For $x \leq 1$, $x(t)$ changes from 0 to 1 as t varies from $t_0 = t_\star + \tau_C$ to $+\infty$; in this case, the three-sphere evolves from the singular configuration $\gamma_1 = \gamma_2 = 0$, $\gamma_3 = \infty$ towards the isotropic fixed point.

Finally, we point out that there is no known solution for the fully anisotropic model geometry that is analogous to the general solution of the Darboux–Halphen system. It remains an open question whether the system is algebraically integrable and find its solution.

[7]We note here for completeness, and it will be used in the next section, that the normalized Ricci flow $\mathrm{d}\gamma_i/\mathrm{d}t = -R_{ii} + R\gamma_i/3$ can be similarly analyzed by considering small perturbations around the fully isotropic fixed point. The two eigenvalues also turn out to be equal and negative, but the corresponding characteristic time scale for dissipation depends quadratically on L as $\tau_R = L^2/4$ with respect to the appropriate time coordinate. Comparison with the dissipation rate of the Cotton flow will become relevant in section 4.

4 Normalized Ricci–Cotton flow

We will now investigate the combined Ricci–Cotton flow when the effective speed of light vanishes by letting $\lambda \to -\infty$. In this case, the flow equations take the following general form,

$$\partial_t g_{ij} = -\frac{\kappa^2}{\kappa_W^2}\left(R_{ij} - \frac{1}{3}Rg_{ij}\right) + \frac{\kappa^2}{w_{\rm CS}}C_{ij} \tag{4.1}$$

and they become independent of Λ_W. The driving curvature term is traceless and the deformations preserve the volume of space. Thus, the resulting normalized Ricci–Cotton flow is a superposition of the Cotton and the normalized Ricci flow with competing effects, in general, that depend on the sign of $w_{\rm CS}$.

4.1 The general system of Bianchi IX equations

Using the Bianchi IX ansatz for the three-dimensional geometry, the normalized Ricci–Cotton flow equations form an autonomous system of equations for the coefficients γ_1, γ_2, γ_3. Since the volume $V = 2\pi^2 L^3$ is conserved, it is convenient to use two independent variables $x(t)$ and $y(t)$,

$$\gamma_1 = \frac{xL^2}{4}, \quad \gamma_2 = \frac{yL^2}{4}, \quad \gamma_3 = \frac{L^2}{4xy}\,, \tag{4.2}$$

and also set

$$\tau = \frac{4\kappa^2}{\kappa_W^2 L^2}t\,, \quad \mu = \frac{w_{\rm CS}L}{\kappa_W^2}\,. \tag{4.3}$$

Then, the general system of Bianchi IX equations takes the form

$$\begin{aligned}\frac{{\rm d}x}{{\rm d}\tau} &= \frac{1}{\mu x^2 y^3}\Big\{\left(1+\frac{\mu}{3}xy+xy^2\right)\left(1-xy^2\right)^2 \\ &\quad + \left(\frac{\mu}{3}+x\right)\left(1+xy^2-2x^2y\right)x^3y^2\Big\}, \end{aligned}\tag{4.4}$$

$$\begin{aligned}\frac{{\rm d}y}{{\rm d}\tau} &= \frac{1}{\mu x^3 y^2}\Big\{\left(1+\frac{\mu}{3}xy+x^2y\right)\left(1-x^2y\right)^2 \\ &\quad + \left(\frac{\mu}{3}+y\right)\left(1+x^2y-2xy^2\right)x^2y^3\Big\}. \end{aligned}\tag{4.5}$$

It is not known whether this system of equations is integrable, in general. However, we will be able to characterize its fixed points and study their stability on general grounds in order to infer the qualitative behavior of the flow lines. Note that the individual components of our system, the normalized Ricci flow and the Cotton flow,

can compete with each other. When $\mu > 0$ ($w_{\rm CS} > 0$), they both work in the same direction, but when $\mu < 0$ ($w_{\rm CS} < 0$) they work against each other and can affect the form and stability properties of the fixed points.

It will also be seen later that these equations can be solved exactly in the axially symmetric case $x = y$. Actually, there are three curves of axial symmetry in the problem, but, in practice, it is sufficient to consider only one of these axially symmetric cases, since the other two follow by permutation of the principal axes of S^3. Thus, apart from $x = y$, we also have $x^2y = 1$ and $xy^2 = 1$, depending on the pair of γ_i's that become equal and reduce the flow equations to a single one. They correspond to metrics on S^3 with enhanced symmetry $SU(2) \times U(1)$ and they all intersect at the fully isotropic point $x = y = 1$. These curves are by themselves flow lines, which, however, cannot be crossed by other flow lines; if any two γ_i's become equal at a given (finite) time they will remain equal for ever. Therefore, these three curves provide the barriers for six regions in the (x, y) plane where the generic flow lines are confined depending on initial conditions. The maximal time range of any given flow line also depends on the region in which the flow is confined. Finally, the flow lines along the three curves of axial symmetry can reach the fully isotropic point but cannot continue running beyond it. The three curves of axial symmetry are depicted in figure 1, which is restricted to the first quadrant of the (x, y) plane so that the metric has physical signature, and they intersect at $(1, 1)$.

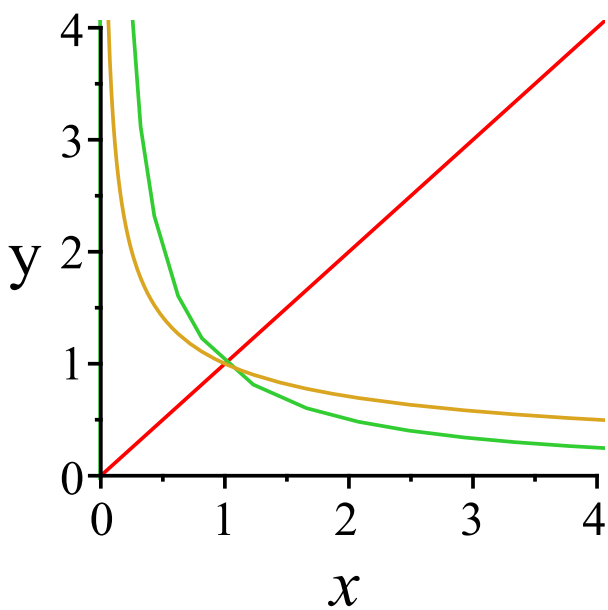

Figure 1: The lines of enhanced $SU(2) \times U(1)$ symmetry in the (x, y) plane.

These general qualitative remarks are sufficient to illustrate the evolution of any

given initial data on the (x, y) plane, provided that all fixed points are found and the arrows of flow lines around them are correctly identified by stability analysis. The same remarks apply equally well to the normalized Ricci and Cotton flows which can arise separately as special cases.

4.2 Classification of the fixed points

We are going now to classify all fixed points of the system (4.4) and (4.5) and find the critical values of μ that separate their behavior into different phases of stability.

The isotropic fixed point. The metric on the round sphere is a fixed point of the normalized Ricci–Cotton flow for all values of μ (positive and negative) and corresponds to the point

$$x_\star = y_\star = 1 \tag{4.6}$$

on the (x, y) plane. Its stability, however, depends on the values of the parameter μ.

By considering small perturbations around this fixed point, as

$$x(t) = x_\star + \delta x(t)\,, \quad y(t) = y_\star + \delta y(t)\,, \tag{4.7}$$

we find that the linearized system of equations takes the form

$$\frac{\mathrm{d}}{\mathrm{d}\tau}\begin{pmatrix}\delta x\\ \delta y\end{pmatrix} = -\left(1+\frac{3}{\mu}\right)\begin{pmatrix}1 & 0\\ 0 & 1\end{pmatrix}\begin{pmatrix}\delta x\\ \delta y\end{pmatrix}. \tag{4.8}$$

The two eigenvalues are equal

$$\zeta_1 = \zeta_2 = -\left(1+\frac{3}{\mu}\right) \tag{4.9}$$

and follow by linear superposition of the corresponding eigenvalues of the normalized Ricci and Cotton flows discussed in the previous section.

The fixed point is absolutely stable when μ satisfies the bound $3/\mu > -1$, i.e., $\mu > 0$ or $\mu < -3$. In these cases, the flow line converge towards the fixed point from all directions. Otherwise, for $-3 < \mu < 0$, the isotropic point is absolutely unstable and the flow lines diverge away from it in all directions. Finally, when $\mu = -3$, the eigenvalues are zero and all points in the vicinity of the fixed point are at equilibrium. Thus,

- $\mu > 0$ or $\mu < -3$: absolutely stable fixed point,

- $-3 < \mu < 0$: absolutely unstable fixed point.

These results are in exact agreement with the competition between the Ricci and Cotton components of the flow and can be understood by comparing the characteristic time scales $\tau_{\rm R}$ and $\tau_{\rm C}$ that govern metric perturbations at late times[8]. For $\mu > 0$ both components dissipate all metric perturbations exponentially fast, but for $\mu < 0$ the Cotton flow contributes differently leading to exponential growth of the perturbations. For the critical value $\mu = -3$, the dissipation of the normalized Ricci flow is canceled by the exponential growth of the Cotton flow, making zero the characteristic matrix of metric perturbations.

Anisotropic fixed points. For negative μ there are additional fixed points that correspond to particular axisymmetric metrics. As such, they appear in three copies related by permutation of the axes of S^3 and they are located on the lines of axial symmetry in the (x, y) plane. In particular, they arise

- on the diagonal $x = y$ with $x_\star = \sqrt{-3/\mu}$,
- on the branch $x^2 y = 1$ with $x_\star = \sqrt{-3/\mu}$,
- on the branch $xy^2 = 1$ with $y_\star = \sqrt{-3/\mu}$.

Note that all these points coalesce with the fully isotropic point when μ assumes the critical value $\mu = -3$.

It suffices to perform stability analysis around one of these fixed points, say the one located on the diagonal line, since the results will be identical for all of them by the symmetry of the problem. Using small fluctuations around the fixed point

$$x_\star = y_\star = \sqrt{-\frac{3}{\mu}}\,, \tag{4.10}$$

so that $x(t) = x_\star + \delta x(t)$ and $y(t) = y_\star + \delta y(t)$, the linearized system takes the form,

$$\frac{\mathrm{d}}{\mathrm{d}\tau}\begin{pmatrix}\delta x\\ \delta y\end{pmatrix} = \frac{1}{2}\begin{pmatrix}\zeta_1+\zeta_2 & \zeta_1-\zeta_2\\ \zeta_1-\zeta_2 & \zeta_1+\zeta_2\end{pmatrix}\begin{pmatrix}\delta x\\ \delta y\end{pmatrix}, \tag{4.11}$$

[8] According to definitions we have the following relations

$$\mu = \frac{w_{\rm CS} L}{\kappa_W^2} = 3\frac{\tau_{\rm C}}{\tau_{\rm R}} \quad \text{with} \quad \tau_{\rm C} = \frac{w_{\rm CS} L^3}{12\kappa^2}\,, \quad \tau_{\rm R} = \frac{\kappa_W^2 L^2}{4\kappa^2}\,.$$

The characteristic time scales $\tau_{\rm R}$ and $\tau_{\rm C}$ refer to the original time coordinate t but their ratio is the same in the time coordinate τ.

where

$$\zeta_1 = \frac{2}{3}\sqrt{-\frac{\mu}{3}}\left[\left(-\frac{\mu}{3}\right)^{3/2} - 1\right], \tag{4.12}$$

$$\zeta_2 = \frac{2}{3}\sqrt{-\frac{\mu}{3}}\left[\left(-\frac{3}{\mu}\right)^{3/2} - 1\right]\left[4\left(-\frac{3}{\mu}\right)^{3/2} - 1\right]. \tag{4.13}$$

The two eigenvalues are ζ_1 and ζ_2 and they are unequal offering various possibilities in general. They both vanish for $\mu = -3$. Otherwise, we have the following cases depending on the sign of the eigenvalues:

- $-3 < \mu < 0$: saddle fixed point with $\zeta_1 < 0 < \zeta_2$,
- $-6\sqrt[3]{2} < \mu < -3$: saddle fixed point with $\zeta_2 < 0 < \zeta_1$,
- $\mu < -6\sqrt[3]{2}$: absolutely unstable fixed point with $\zeta_i > 0$.

Thus, the axisymmetric fixed points are never absolutely stable. They are saddle or unstable depending on μ.

Totally anisotropic fixed points. It is not obvious from the beginning whether there are any fixed points with $\gamma_1 \neq \gamma_2 \neq \gamma_3$. Close inspection of the equations, assisted by numerical scanning, reveals the presence of two totally anisotropic fixed points that coexist with the axially symmetric anisotropic fixed point[9] when $\mu < -6\sqrt[3]{2}$. In fact, by the $\mathbb{Z}_3$ symmetry of the problem, there are six such additional fixed points, but we only focus attention on two of them appearing symmetrically left and right of the diagonal line $x = y$ in the lower two (out of the six disconnected) regions shown in figure 1; their presence should not be confused with the mirror images of the axially symmetric anisotropic fixed point discussed earlier.

The characteristic property of the totally anisotropic fixed points is that their Ricci scalar curvature vanishes and their location on the (x, y) plane is given by

$$x + \frac{1}{\sqrt{x}} = -\frac{\mu}{4} = y + \frac{1}{\sqrt{y}} \quad \text{with} \quad x \neq y\,. \tag{4.14}$$

Of course, one can always find Bianchi IX metrics with zero scalar curvature by imposing the appropriate algebraic condition on the metric coefficients, but these are not fixed points of the flow lines for general values of μ. Remarkably, they are real solutions of $\mathrm{d}x/\mathrm{d}\tau = 0 = \mathrm{d}y/\mathrm{d}\tau$ with $x \neq y$, which coexist with the axially symmetric

[9] We thank Christos Sourdis for pointing out the presence of these additional fixed points and thoroughly investigating their properties. This analysis was missed in a previous version of our paper and we are indebted to him for providing all the details. Similar results also appeared in [43].

anisotropic fixed point when $\mu < -6\sqrt[3]{2}$. They are not present when $\mu > -6\sqrt[3]{2}$, since there are no real solutions to equation (4.14) in that case. We also note that when $\mu = -6\sqrt[3]{2}$ the totally anisotropic fixed points coalesce with the axially symmetric anisotropic fixed point. Furthermore, there are no other fixed points in the problem.

The location of these fixed points is depicted in figure 2. Here, we plot the ratio x/y of the anisotropic fixed points as function of μ (actually $-\mu$). The horizontal line represents the axially symmetric anisotropic fixed point that exists below and above the critical value of μ.

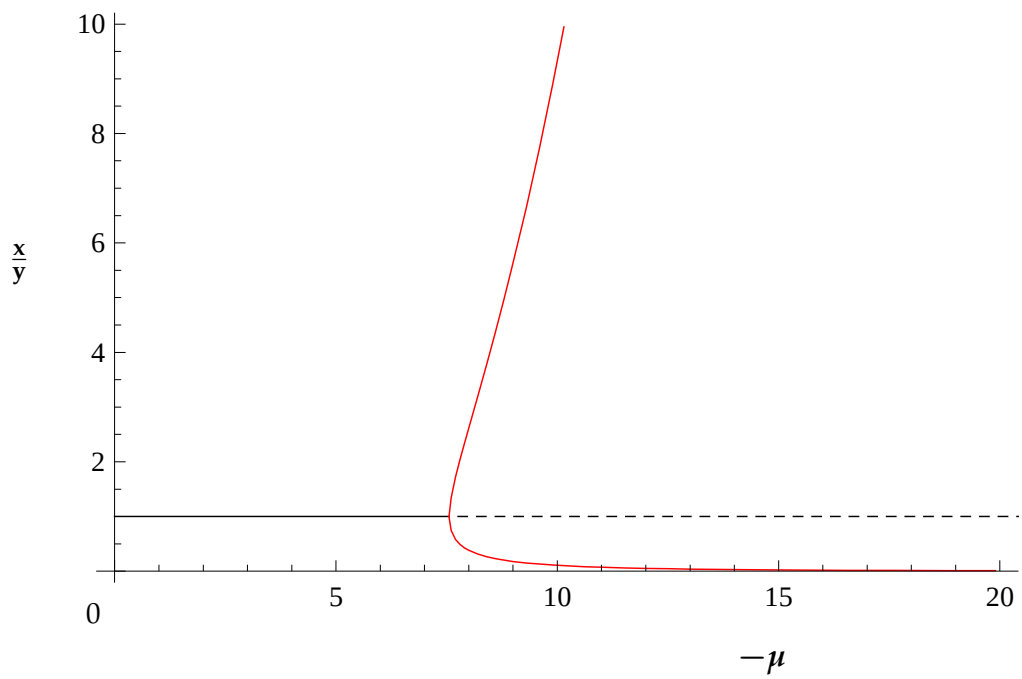

Figure 2: Relative location of all anisotropic fixed points for $\mu < 0$.

At this point, it is instructive to consider the Ricci scalar curvature of the axially symmetric anisotropic fixed point $x_\star = y_\star = \sqrt{-3/\mu}$, which turns out to be

$$R = -\frac{2\mu}{9L^2}\left(\mu + 12\sqrt{-\frac{3}{\mu}}\right) . \tag{4.15}$$

When $\mu = 0$ this point is at infinity and the curvature is zero. As μ varies from 0 to -3 the axially symmetric anisotropic fixed point is approaching the isotropic fixed point and the curvature increases monotonically. The curvature becomes maximal when these two points coincide at the critical value $\mu = -3$, and, then it decreases monotonically as μ varies from -3 to $-6\sqrt[3]{2}$. It becomes zero at the other critical value $\mu = -6\sqrt[3]{2}$, and, then, it turns negative for $\mu < -6\sqrt[3]{2}$. The value $\mu = -6\sqrt[3]{2}$ is also critical for the creation of the totally anisotropic fixed points, which pop out symmetrically from the diagonal and have zero curvature for all lower values of the

parameter μ.

These additional fixed points appear to be saddle points, as can be verified by numerical investigation for different values of μ. It is not easy to obtain closed formulas for the eigenvalues of the characteristic matrix describing small perturbations around them. However, their stability properties are important for constructing instanton solutions of Hořava–Lifshitz gravity, as will be seen in detail later in section 6. Another characteristic property of these points that will also be used later is the universal value of the gravitational Chern–Simons functional. Explicit calculation shows that $W_{\rm CS}$ for the fully anisotropic fixed points is

$$W_{\rm CS} = \frac{80\pi^2}{w_{\rm CS}}\,, \tag{4.16}$$

which is independent of μ! It actually coincides with the value of $W_{\rm CS}$ for the axially symmetric anisotropic fixed point when $\mu = -6\sqrt[3]{2}$ and it is ten times larger than the value of $W_{\rm CS}$ evaluated at the totally isotropic fixed point.

An important remark is in order at this point. The equations that determine the fixed points of the normalized Ricci–Cotton flow provide only the traceless part of the classical equations of motion of topologically massive gravity, leaving the trace undetermined. Then, depending on the value of their Ricci scalar curvature, these points also satisfy the trace equation $R = 6\Lambda_{\rm W}$ for appropriately chosen effective value of $\Lambda_{\rm W}$. Fixed points with positive, negative or zero Ricci scalar curvature are vacua of topologically massive gravity with positive, negative or zero cosmological constant, respectively. As a result, the fixed points of the Ricci–Cotton flow with general couplings, which are the vacua of topologically massive gravity, are expected to be less than the fixed points of the normalized flow, and, in fact, they can be obtained from them in certain ways[10]. This, however, does not make our analysis in section 5 redundant since their location, volume and stability properties also depend crucially on the flow equations we are considering in each case.

Summarizing the results for the normalized Ricci–Cotton flow, we note that the fully isotropic metric on S^3 is the unique fixed point for $\mu > 0$ that attracts all trajectories starting from any point in the first quadrant of the (x, y) plane. For $\mu < 0$, there are various possibilities that result to attractive or repelling directions around the fixed points. Note that the isotropic point becomes absolutely unstable when $-3 < \mu < 0$, in which case the anisotropic fixed point is a saddle that attracts partially the flow lines. For $-6\sqrt[3]{2} \leq \mu < 0$ there are four in total fixed points, including their $\mathbb{Z}_3$ mirrors, whereas for $\mu < -6\sqrt[3]{2}$ the total number of fixed points is ten.

[10]The mathematical problem one has to solve to determine the set of fixed points of massive gravity for given $\Lambda_{\rm W}$ is to fix R instead of the volume of the normalized fixed points, as functions of μ and L, and deduce from it the allowed range of μ for the selected set of fewer points.

4.3 Phase portraits of the flow

The qualitative behavior of the flow lines is illustrated by the phase portraits shown below for all possible values of μ.

For positive μ, which is qualitatively the same as for the normalized Ricci flow and the Cotton flow, the phase portrait is given in figure 3.

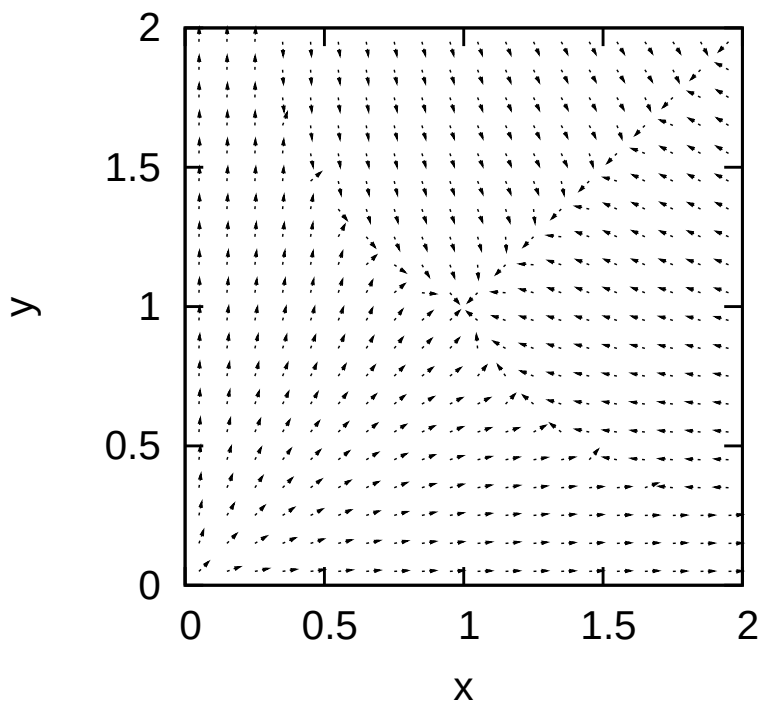

Figure 3: The flow lines for $\mu > 0$; here, $\mu = 2$.

For negative μ the stability properties of the fixed points is different in the intervals $-3 < \mu < 0$, $-6\sqrt[3]{2} < \mu < -3$ and $\mu < -6\sqrt[3]{2}$ and all these possibilities are represented in figures 4, 5 and 6, respectively. For later reference, it is important to realize the existence of trajectories interpolating between different fixed points. In figure 4 there is only one such flow line since one fixed point is unstable and the other a saddle. The same applies to figure 5 where the interpolating flow line connects a stable fixed point with a saddle. The picture changes drastically in figure 6 since there are infinitely many flow lines interpolating between an unstable and a stable fixed point. Also, in this case, there are additional fixed points away from the diagonal, which are saddle points. Figure 6 contains two such totally anisotropic fixed points located at $x \simeq 0.19$, $y \simeq 1.75$ (and $x \simeq 1.75$, $y \simeq 0.19$) for $\mu = -10 < -6\sqrt[3]{2} \simeq -7.56$. There are flow lines connecting these fixed points with the other two lying on the diagonal, but they are not easily seen on the phase portrait due to numerical deficiency.

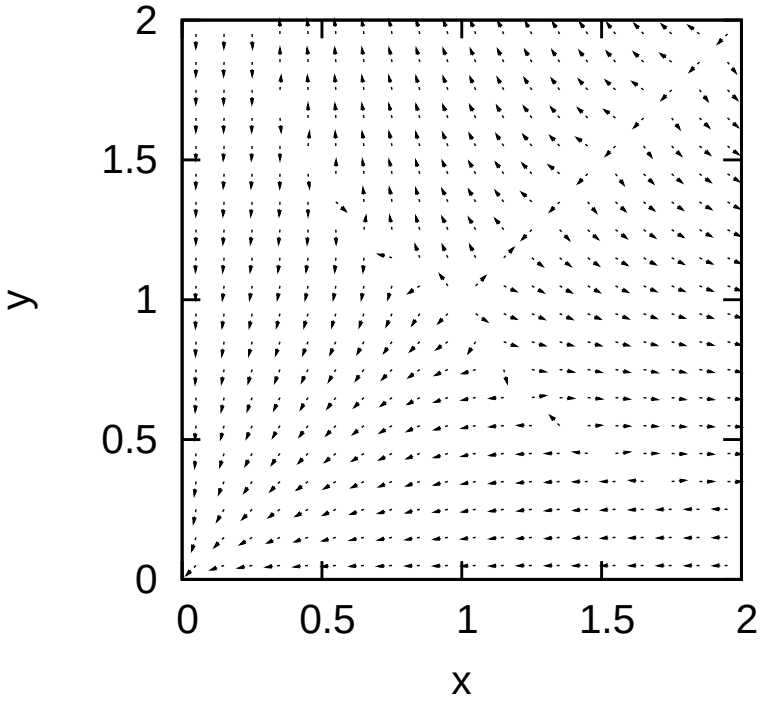

Figure 4: The flow lines for $-3 < \mu < 0$; here, $\mu = -2$.

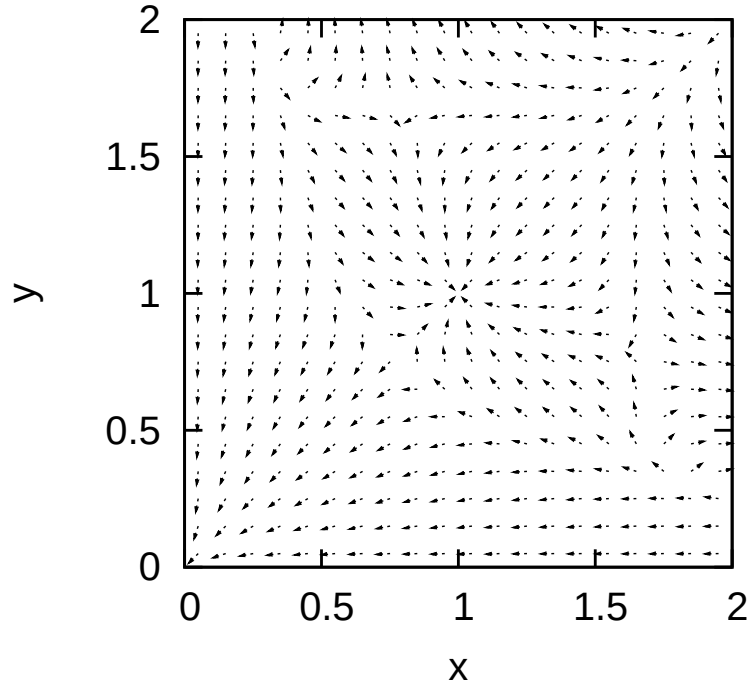

Figure 5: The flow lines for $-6\sqrt[3]{2} < \mu < -3$; here, $\mu = -5$.

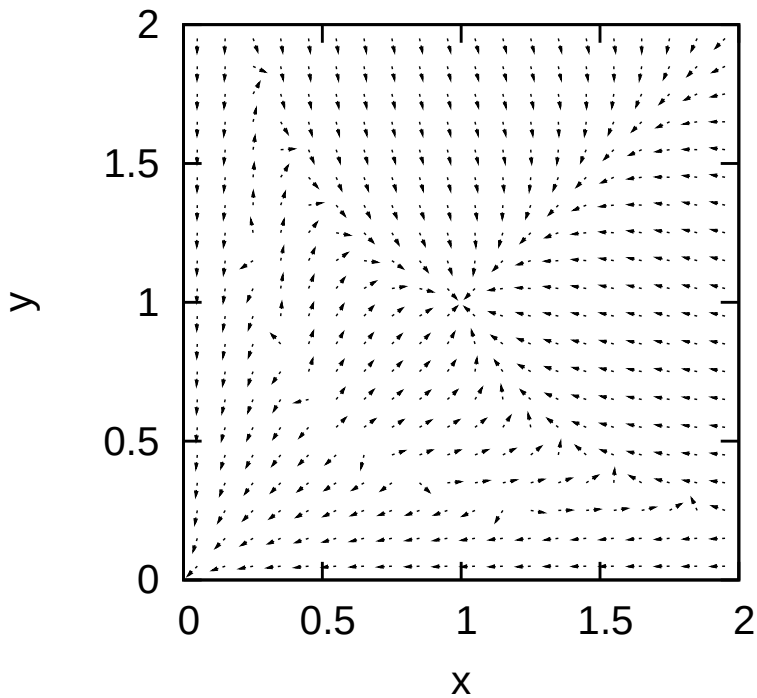

Figure 6: The flow lines for $\mu < -6\sqrt[3]{2}$; here, $\mu = -10$.

4.4 Axisymmetric solutions

Here, we present the exact axially symmetric solution of the normalized Ricci–Cotton flow, setting $x = y$. As such, it generalizes the axially symmetric solutions of the normalized Ricci and the Cotton flows discussed in the previous section. The system (4.4) and (4.5) reduces to a single equation

$$\frac{\mathrm{d}x}{\mathrm{d}\tau} = \frac{1}{\mu}\left(\frac{1}{x^3} - 1\right)\left(\frac{1}{x^2} + \frac{\mu}{3}\right), \tag{4.17}$$

and the flow takes place on the diagonal line of the (x, y) plane. The flow connects either the origin or infinity with a fixed point or it can extend between two different fixed points. These regions do not communicate with each other and the time interval that supports the solutions depends on μ and the choice of trajectory.

The behavior around $x = 0$ and $x \to \infty$ is universal and can be extracted directly from equation (4.17),

- $x \approx \left(\frac{6}{\mu}(\tau - \tau_0)\right)^{1/6}, \quad \text{as } x \to 0,$
- $x \approx -\frac{1}{3}\tau, \quad \text{as } x \to \infty.$

Around the fixed points the time dependence is exponential and determined by the eigenvalues ζ as $x - x_\star \approx \exp(\zeta\tau)$. The relevant eigenvalue for the isotropic point is given by (4.9) and for the anisotropic by (4.12).

Case I: $\mu > 0$**.** The solution behaves similarly for all positive values of μ, but it looks different on the two sides of the isotropic fixed point $x_\star = 1$. We find that

$\underline{x > 1}$: $\quad -\infty < \tau < +\infty$ as x decreases from $+\infty$ to 1 ,

$\underline{x < 1}$: $\quad \tau_0 < \tau < +\infty$ as x increases from $x(\tau_0) = 0$ to 1 .

The exact solution reads

$$\begin{aligned} \tau - \tau_\star \;=\; & -3x + \frac{\mu\,(\mu-6)}{2\,(\mu^2-3\mu+9)} \log\left(x^2+x+1\right) + \frac{\sqrt{3}\mu^2}{\mu^2-3\mu+9} \arctan\frac{2x+1}{\sqrt{3}} \\ & -\frac{\mu}{\mu+3}\log|x-1| + \frac{27\mu}{2\,(\mu^3+27)}\log\left(\mu x^2+3\right) \\ & +\frac{81}{\mu^3+27}\sqrt{\frac{3}{\mu}}\arctan\left(x\sqrt{\frac{\mu}{3}}\right) \end{aligned} \tag{4.18}$$

and it is represented by figure 7 with appropriately chosen integration constant $\tau_\star$.

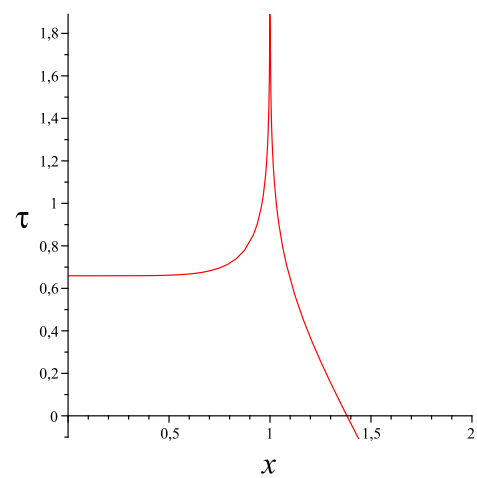

Figure 7: The dependence $\tau(x)$ for positive μ; here, $\mu = 1$.

Case II: $\mu < 0$. In this case the solution depends on the particular value of μ. First, we present the result for the critical value $\mu = -3$, which is simpler,

$$\begin{aligned}\tau - \tau_\star &= -3x + \frac{1}{2(x-1)} + \frac{1}{\sqrt{3}} \arctan \frac{2x+1}{\sqrt{3}} - \frac{7}{4} \log|x-1| \\ &\quad + \frac{3}{4} \log(x+1) + \frac{1}{2} \log\left(x^2 + x + 1\right) . \end{aligned} \tag{4.19}$$

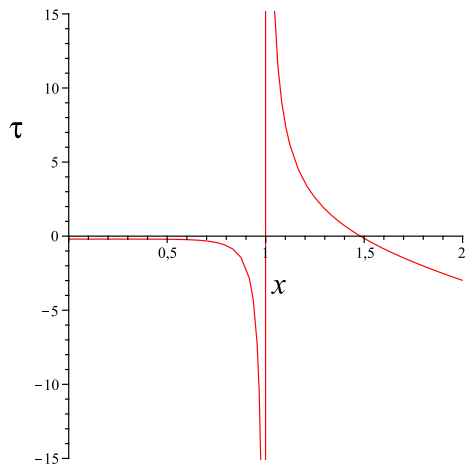

Figure 8: The dependence $\tau(x)$ for the critical value critical $\mu = -3$.

All fixed points coalesce to the isotropic and the eigenvalues vanish, so that there are no arrows infinitesimally close to this point. However, this behavior is lifted at second order in perturbation theory and there are arrows pointing from large to small values of τ. This particular case is depicted in figure 8, which also shows the range of τ in the two branches.

For $\mu \neq -3$ the expression becomes much more involved and reads

$$\begin{aligned}\tau - \tau_\star &= -3x + \frac{\mu(\mu-6)}{2(\mu^2 - 3\mu + 9)} \log\left(x^2 + x + 1\right) + \frac{\sqrt{3}\mu^2}{\mu^2 - 3\mu + 9} \arctan \frac{2x+1}{\sqrt{3}} \\ &\quad - \frac{\mu}{\mu+3} \log|x-1| + \frac{27\mu}{2(\mu^3+27)} \log\left|\mu x^2 + 3\right| \\ &\quad - \frac{81}{2(\mu^3+27)} \sqrt{-\frac{3}{\mu}} \left[\log\left|1 - x\sqrt{-\frac{\mu}{3}}\right| - \log\left|1 + x\sqrt{-\frac{\mu}{3}}\right|\right] . \end{aligned} \tag{4.20}$$

Then, depending on whether $-3 < \mu < 0$ or $\mu < -3$, the function $\tau(x)$ looks different. In all these cases the solution has three branches but the range of time is not the same. We have, in particular, the following behavior depending on μ:

- For $-3 < \mu < 0$ the two fixed points are ordered as $x_\star^{\rm iso} = 1 < x_\star^{\rm aniso} = \sqrt{-3/\mu}$ with the isotropic being repulsive and the anisotropic attractive. The exact solution is represented by figure 9.

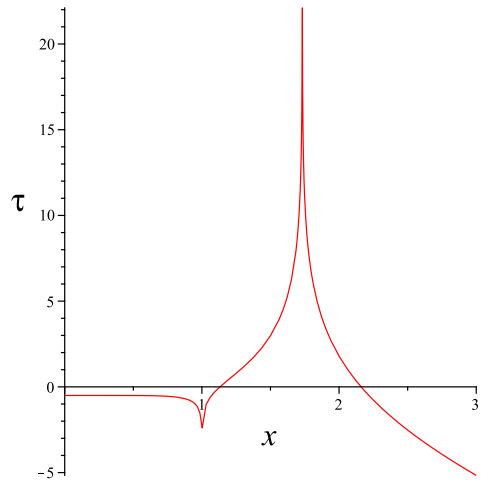

Figure 9: The dependence $\tau(x)$ for $-3 < \mu < 0$; here, $\mu = -1$.

- For $\mu < -3$ the two fixed points are ordered differently, as $x_\star^{\rm aniso} = \sqrt{-3/\mu} < x_\star^{\rm iso} = 1$. The isotropic point is now attractive whereas the anisotropic is repulsive. Then, the exact solution along the diagonal is represented by figure 10 and there is no essential difference for μ below or above the value $-6\sqrt[3]{2}$.

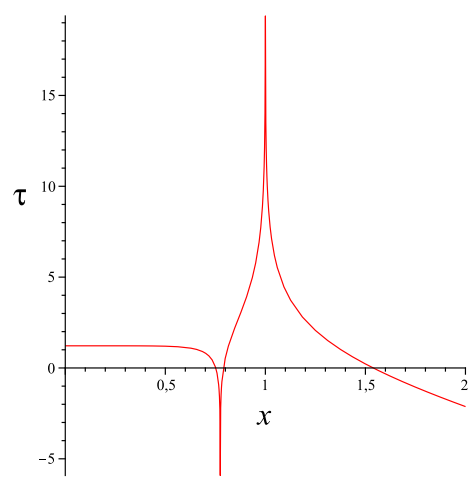

Figure 10: The dependence $\tau(x)$ for $\mu < -3$; here, $\mu = -5$.

Note that the three branches shown in figures 9 and 10 range differently: the first has support on a semi-infinite time interval, whereas the second and third to the right are eternal solutions that exist for all time $-\infty < \tau < +\infty$. (Despite ap-

pearances, caused by numerical deficiency, the spike at $x = 1$ extends to infinity in figure 9).

5 Ricci–Cotton flow with general couplings

Let us now examine the Ricci–Cotton flow equations for Bianchi IX model geometries with arbitrary couplings by letting λ and Λ_W take arbitrary values. The system of equations that needs to be studied is provided by (3.8)

$$\frac{\mathrm{d}\gamma_i}{\mathrm{d}\tau} = -R_{ii} + \frac{2\lambda - 1}{2(3\lambda - 1)} R\gamma_i + \frac{\Lambda_W}{3\lambda - 1}\gamma_i + \frac{1}{\mu} C_{ii} \tag{5.1}$$

with

$$\tau = \frac{\kappa^2}{\kappa_W^2} t \,, \qquad \mu = \frac{w_{\mathrm{CS}}}{\kappa_W^2} \,. \tag{5.2}$$

The definition of τ and μ resembles that for the normalized flow in section 4, but it does not include the rescaling by the characteristic length of space.

Since $\lambda < 1/3$, we will confine our discussion to the case of non-negative cosmological constant, $\Lambda_W \geq 0$, so that the effective speed of light is real, and investigate the structure of the fixed points and their stability properties. The choices $\Lambda_W > 0$ and $\Lambda_W = 0$ will be discussed separately, although the latter can be obtained as limiting case of the former. Mathematically it is also interesting to consider the more general situation, without imposing any restrictions on λ and Λ_W, but these cases will not be included here[11].

5.1 The axisymmetric Bianchi IX model

The flow of the metric coefficients $\gamma_i(t)$ does not preserve the volume of S^3 in this case, and, therefore, the three coupled equations are rather difficult to investigate in all generality with $\gamma_1 \neq \gamma_2 \neq \gamma_3$. Restricting attention to axially symmetric configurations simplifies matters without shadowing too much the rich structure of the system. Our analysis will be based on the qualitative theory of dynamical systems, as in previous sections, but because of the mathematical complexity of the equations it is not possible to obtain explicit solutions in closed form, apart from the isotropic solution. Also, the reader should be aware of the limitations: the fixed points can become unstable in other directions, when axial symmetry is relaxed, and the conclusions drawn here

[11] The nature of the corresponding fixed points changes drastically compared to the cases that are discussed in this paper. However, when $\Lambda_W < 0$ it is more appropriate to consider Bianchi type VIII model geometries rather than Bianchi IX.

may be altered and not be as general. Of course, this is part of a more general criticism for mini-superspace models compared to metric deformations with an infinite number of moduli taking place in the entire superspace.

With these explanations in mind, we are going to study the system of two equations

$$\frac{1}{\gamma_1}\frac{\mathrm{d}\gamma_1}{\mathrm{d}\tau} = -\frac{\sqrt{\gamma_1}}{\mu\,\gamma_2^3}(\gamma_1-\gamma_2) - \frac{8\lambda-3}{4(3\lambda-1)}\frac{\gamma_1}{\gamma_2^2} + \frac{2\lambda-1}{3\lambda-1}\frac{1}{\gamma_2} + \frac{\Lambda_W}{3\lambda-1}\,, \tag{5.3}$$

$$\frac{1}{\gamma_2}\frac{\mathrm{d}\gamma_2}{\mathrm{d}\tau} = \frac{\sqrt{\gamma_1}}{2\mu\,\gamma_2^3}(\gamma_1-\gamma_2) + \frac{4\lambda-1}{4(3\lambda-1)}\frac{\gamma_1}{\gamma_2^2} - \frac{\lambda}{3\lambda-1}\frac{1}{\gamma_2} + \frac{\Lambda_W}{3\lambda-1}\,, \tag{5.4}$$

which is obtained from (5.1) by setting $\gamma_2 = \gamma_3$. The existence and properties of the fixed points depends crucially on the values of μ, as in other examples considered so far. In particular, for $\mu < 0$, an anisotropic fixed point will coexist with the isotropic one.

There is an exact solution of these equations which is available for all $\Lambda_W \geq 0$ and describes the evolution of the isotropic metric on S^3. This possibility does not arise for the normalized Ricci–Cotton flow, since the isotropic metric is a fixed point. In particular, setting all $\gamma_i \equiv \gamma$, we have the following result:

$$\gamma(t) = A\exp\left(\frac{\Lambda_W}{3\lambda-1}\tau\right) + \frac{1}{4\Lambda_W} \quad \text{for } \Lambda_W > 0 \tag{5.5}$$

and

$$\gamma(t) = -\frac{1}{4(3\lambda-1)}(\tau-\tau_0) \quad \text{for } \Lambda_W = 0 \tag{5.6}$$

with A and τ_0 being arbitrary integration constant. Since $\lambda < 1/3$, the metric flows to the isotropic fixed point (to be discussed next in detail for more general trajectories) as $\tau \to +\infty$.

The difference between $\Lambda_W > 0$ and $\Lambda_W = 0$ is reflected in the life-time of the solutions. When $\Lambda_W > 0$ the solution has two branches: on the first branch $A > 0$ and the solution is eternal existing for all $-\infty < \tau < +\infty$; it describes a round sphere with infinite radius in the infinite past flowing towards a round sphere with radius set by Λ_W in the infinite future. The second branch corresponds to $A < 0$ in which case the solution exists for $\tau_\star \leq t < +\infty$, with appropriately chosen $\tau_\star$, so that the sphere starts from zero radius and reaches the fixed point as $t \to +\infty$. On the other hand, when $\Lambda_W = 0$, there is only one branch as the solution exists for $\tau_0 \leq \tau < +\infty$, interpolating between a fully collapsed configuration at $\tau = \tau_0$ to a sphere of infinite radius in the infinite future.

5.2 Classification of the fixed points

First, we consider the case of non-vanishing cosmological constant and reserve the last subsection to study $\Lambda_W = 0$ separately.

The isotropic fixed point. For $\Lambda_W > 0$, there is a natural length scale in the problem that gives rise to the isotropic fixed point of the flow, irrespective of the sign of μ,

$$\gamma_1 = \gamma_2 = \gamma_3 = \frac{1}{4\Lambda_W} \,. \tag{5.7}$$

This follows easily from the system of equations without assuming any restrictions on γ_1 and γ_2; it can also be shown that it is a fixed point of the more general system of equations with $\gamma_1 \neq \gamma_2 \neq \gamma_3$.

Linearizing around it as

$$\gamma_1(t) = \frac{1}{4\Lambda_W}\,\left(1 + \delta x(t)\right), \quad \gamma_2(t) = \frac{1}{4\Lambda_W}\,\left(1 + \delta y(t)\right), \tag{5.8}$$

we find that the small perturbations satisfy the characteristic matrix equation

$$\frac{\mathrm{d}}{\mathrm{d}\tau}\begin{pmatrix}\delta x\\ \delta y\end{pmatrix} = \Lambda_W \begin{pmatrix} -\frac{8}{\mu}\sqrt{\Lambda_W} - \frac{8\lambda-3}{3\lambda-1} & \frac{8}{\mu}\sqrt{\Lambda_W} + 2\frac{4\lambda-1}{3\lambda-1} \\ \frac{4}{\mu}\sqrt{\Lambda_W} + \frac{4\lambda-1}{3\lambda-1} & -\frac{4}{\mu}\sqrt{\Lambda_W} - 2\frac{2\lambda-1}{3\lambda-1} \end{pmatrix}\begin{pmatrix}\delta x\\ \delta y\end{pmatrix}. \tag{5.9}$$

The eigenvalues are

$$\zeta_1 = \frac{\Lambda_W}{3\lambda-1}, \quad \zeta_2 = -4\Lambda_W\left(1 + \frac{3}{\mu}\sqrt{\Lambda_W}\right) \tag{5.10}$$

and so $\zeta_1 < 0$ whereas ζ_2 can take all values, positive or negative, depending on μ.

Keeping Λ_W fixed and varying μ we obtain the following characterization of the isotropic fixed point:

- $\mu > 0$ or $\mu < -3\sqrt{\Lambda_W}$: absolutely stable,
- $-3\sqrt{\Lambda_W} < \mu < 0$: saddle point.

Note the emergence of a critical value, $\mu = -3\sqrt{\Lambda_W}$, where the two eigenvalues ζ_1 and ζ_2 vanish, separating stability from instability along the corresponding eigen-

directions[12]. Also note for completeness that if we were allowing $\lambda > 1/3$, the isotropic point would never be absolutely stable (it would be absolutely unstable or a saddle point in the respective intervals of the μ-line.).

Actually, one can go further and investigate whether the exact isotropic running solution $\gamma(t)$, given by (5.5), is stable against small fluctuations,

$$\gamma_i(t) = \gamma(t) + \delta\gamma_i(t) \,, \tag{5.11}$$

acting as *attractor* of nearby trajectories. Thus, given a small tube around the trajectory $\gamma(t)$, one is interested to know if any other trajectory with initial conditions inside this tube will remain there after some time and what is the size of tube that guarantees this attractor property. The differential equations for $\delta\gamma_i(t)$ are most conveniently stated using $\gamma(t)$ rather that t as flow time. Then, within the axially symmetric ansatz (5.3), the linearized equations take the following form,

$$\frac{\mathrm{d}}{\mathrm{d}\gamma(t)}\delta\gamma_1(t) = -\frac{2(\delta\gamma_1 - \delta\gamma_2)}{\gamma(4\Lambda_W\gamma - 1)}\left[\frac{2(3\lambda - 1)}{\mu\sqrt{\gamma}} + 4\lambda - 1\right] + \frac{4\Lambda_W\delta\gamma_1}{4\Lambda_W\gamma - 1} \,, \tag{5.12}$$

$$\frac{\mathrm{d}}{\mathrm{d}\gamma(t)}\delta\gamma_2(t) = \frac{\delta\gamma_1 - \delta\gamma_2}{\gamma(4\Lambda_W\gamma - 1)}\left[\frac{2(3\lambda - 1)}{\mu\sqrt{\gamma}} + 4\lambda - 1\right] + \frac{4\Lambda_W\delta\gamma_2}{4\Lambda_W\gamma - 1} \,, \tag{5.13}$$

generalizing the characteristic matrix equations of small perturbations around the isotropic fixed point. These equations apply for all Λ_W including the special case $\Lambda_W = 0$ that will be discussed separately.

Solutions of this system can be expressed as functions of t through $\gamma(t)$. Since $\delta\gamma_i$ are required to be small, for validity of the linearized analysis, the attractor property of the isotropic trajectory appears to be very limited. This behavior can be seen schematically in the phase portraits of the flow that will appear in the next two subsections.

Anisotropic fixed point. When $\mu < 0$, there is an additional fixed point associated with the axially symmetric metric with coefficients

$$\gamma_1 = \frac{36\mu^2}{(\mu^2 + 27\Lambda_W)^2}, \quad \gamma_2 = \gamma_3 = \frac{9}{\mu^2 + 27\Lambda_W}. \tag{5.14}$$

There are no other restrictions on the values of μ for the existence of this second fixed point.

[12]The critical value of μ is similar to that found for the normalized Ricci–Cotton flow; direct comparison can be made by replacing $\sqrt{\Lambda_W}$ with $1/L$ and rescaling μ with the characteristic length of space. In both cases, the critical value of μ occurs when the competing effects of the Ricci and Cotton deformations are balanced exactly.

Notice that this new fixed point and the isotropic one will coalesce if $\mu = -3\sqrt{\Lambda_W}$. For $-3\sqrt{\Lambda_W} < \mu < 0$, the anisotropic fixed point has $\gamma_1 < \gamma_2$, whereas for $\mu < -3\sqrt{\Lambda_W}$ it has $\gamma_1 > \gamma_2$. Thus, $-3\sqrt{\Lambda_W}$ appears as a critical value of μ.

By considering small perturbations around the anisotropic fixed point, as

$$\gamma_1(t) = \frac{36\mu^2}{(\mu^2 + 27\Lambda_W)^2}\left(1 + \delta x(t)\right), \quad \gamma_2(t) = \frac{9}{\mu^2 + 27\Lambda_W}\left(1 + \delta y(t)\right), \tag{5.15}$$

we find the characteristic matrix of the linearized system with respect to τ

$$\frac{1}{27(3\lambda - 1)}\begin{pmatrix} (9\lambda - 2)\mu^2 - 27\Lambda_W(3\lambda - 1) & -(18\lambda - 5)\mu^2 + 27\Lambda_W(6\lambda - 1) \\ -\frac{1}{2}(9\lambda - 5)\mu^2 + \frac{27}{2}\Lambda_W(3\lambda - 1) & (9\lambda - 4)\mu^2 - 27\Lambda_W(3\lambda - 2) \end{pmatrix}. \tag{5.16}$$

The corresponding eigenvalues are

$$\zeta_\pm = \frac{1}{18(3\lambda - 1)}\left[2(3\lambda - 1)\mu^2 - 27\Lambda_W(2\lambda - 1) \pm \sqrt{\Delta}\right], \tag{5.17}$$

where

$$\Delta = 6(3\lambda - 1)(2\lambda - 1)\mu^4 - 72\Lambda_W\mu^2(3\lambda - 1)^2 + 243\Lambda_W^2\left(12\lambda^2 - 6\lambda + 1\right). \tag{5.18}$$

The eigenvalues $\zeta_\pm$ are real[13]. Since their product is given by

$$\zeta_+\zeta_- = \frac{\left(\mu^2 - 9\Lambda_W\right)\left(\mu^2 + 27\Lambda_W\right)}{162(3\lambda - 1)}, \tag{5.19}$$

we note the appearance of a critical value μ, which is the same as for the isotropic fixed point, $\mu = -3\sqrt{\Lambda_W}$. Then, for $\mu < -3\sqrt{\Lambda_W}$ the anisotropic point is saddle. On the other hand, in order to examine the stability of this fixed point for $-3\sqrt{\Lambda_W} < \mu < 0$, we consider the sum of the two eigenvalues,

$$\zeta_+ + \zeta_- = \frac{1}{9(3\lambda - 1)}\left[2(3\lambda - 1)\mu^2 - 27\Lambda(2\lambda - 1)\right], \tag{5.20}$$

which is now negative. Therefore, for $-3\sqrt{\Lambda_W} < \mu < 0$, the anisotropic fixed point is absolutely stable. Summarizing all results obtained above, we have the following:

[13] It follows by noting that the two roots of Δ occur at

$$\mu_\pm^2 = \frac{3\Lambda_W}{2(3\lambda - 1)(2\lambda - 1)}\left[4(3\lambda - 1)^2 \pm \sqrt{2(3\lambda - 1)}\right]$$

and they are complex for $\lambda < 1/3$. Thus, Δ has the same sign as the coefficient of its μ^4-term, which is positive.

- An isotropic fixed point exists for all μ and it is absolute stable when $\mu > 0$ or $\mu < -3\sqrt{\Lambda_W}$. For $-3\sqrt{\Lambda_W} < \mu < 0$ it is a saddle point.
- An anisotropic fixed point exists for all $\mu < 0$. It is absolutely stable for $-3\sqrt{\Lambda_W} < \mu < 0$ and saddle for $\mu < -3\sqrt{\Lambda_W}$, which is reverse to the behavior of the isotropic fixed point.

As can be seen there are similarities as well as some differences with the classification of fixed points of the normalized Ricci–Cotton flow.

5.3 Phase portraits of the flow

A qualitative picture of the flow lines is provided by three consecutive phase portraits for different values of the parameter μ. In all drawings we choose $\Lambda_W = 0.25$ and $\lambda = 0.1$, and so the three regimes are $\mu > 0$ or $-1.5 < \mu < 0$ or $\mu < -1.5$. The isotropic fixed point appears at $\gamma_1 = \gamma_2 = 1/4\Lambda_W = 1$.

First, we consider the case $\mu > 0$ that exhibits only one (isotropic) fixed point, as shown in figure 11.

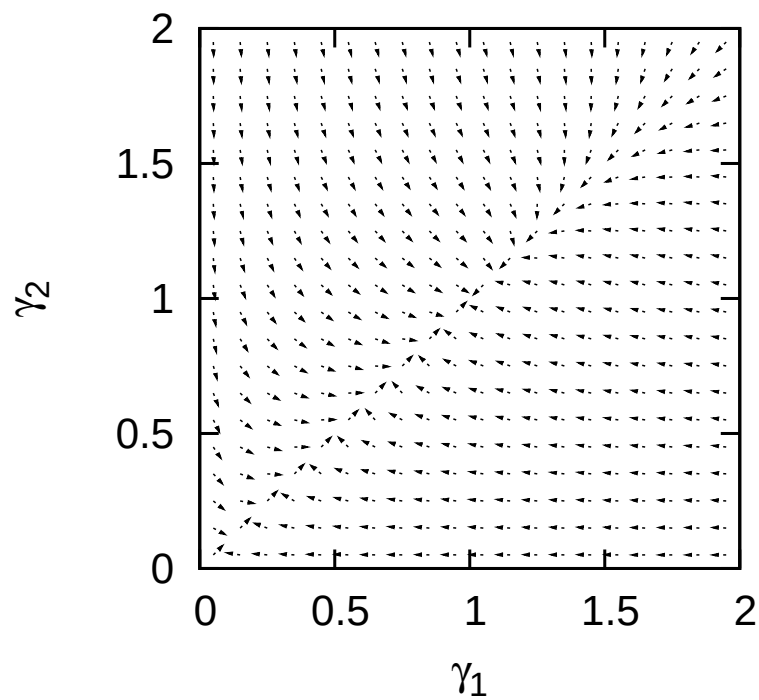

Figure 11: The flow lines for $\mu > 0$; here, $\mu = 1$.

Next, we consider the case $\mu < 0$ that exhibits an additional (anisotropic) fixed point and make the following choices for the plots shown in figures 12 and 13:

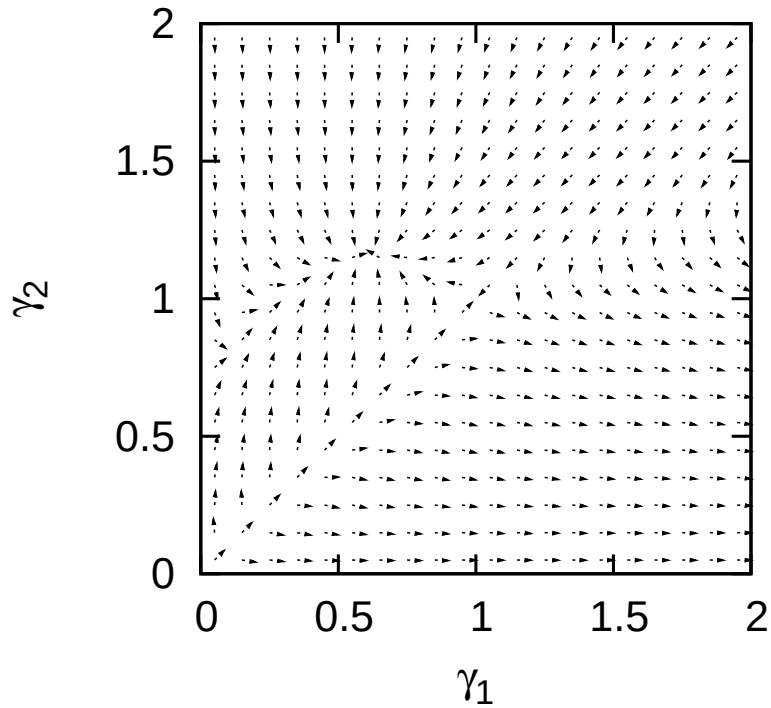

Figure 12: The flow lines for $-1.5 = -3\sqrt{\Lambda_W} < \mu < 0$; here, $\mu = -1$.

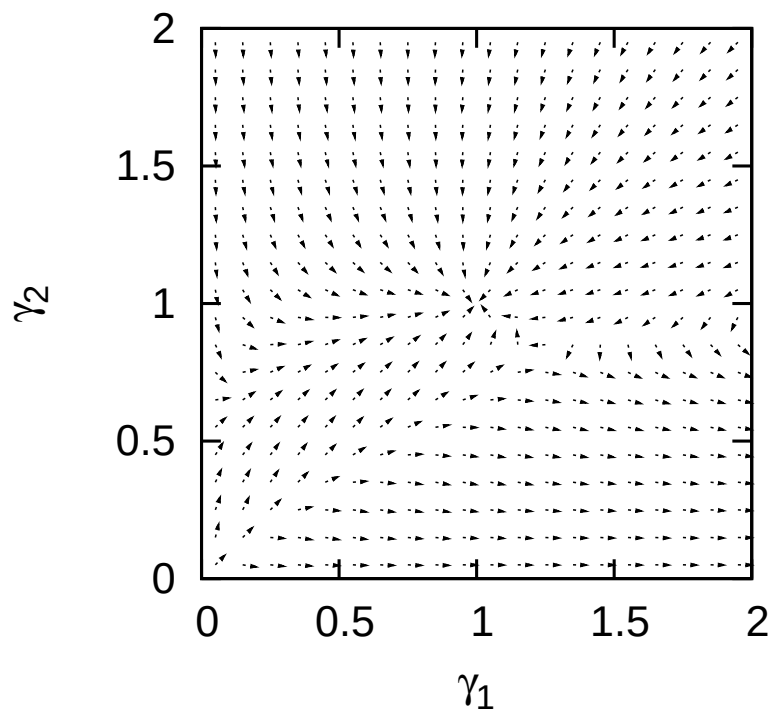

Figure 13: The flow lines for $\mu < -3\sqrt{\Lambda_W} = -1.5$; here, $\mu = -2$.

- $\mu = -1$: the anisotropic fixed point occurs at $\gamma_1 \simeq 0.60$, $\gamma_2 = \gamma_3 \simeq 1.16$.
- $\mu = -2$: the anisotropic fixed point occurs at $\gamma_1 \simeq 1.24$, $\gamma_2 = \gamma_3 \simeq 0.84$.

5.4 The special case $\Lambda_W = 0$

Setting $\Lambda_W = 0$ corresponds to taking the effective speed of light equal to zero, while keeping $\lambda < 1/3$ arbitrary. It should be contrasted with the normalized Ricci–Cotton flow, which is independent of Λ_W and has also zero effective speed of light.

The isotropic fixed point is now pushed to infinity and corresponds to a round S^3 with infinite radius. This is also apparent from the exact isotropic solution (5.6) that converges to it after infinitely long time. However, it is not strictly speaking a fixed point of the flow lines, since $\mathrm{d}\gamma_1/\mathrm{d}t$ and $\mathrm{d}\gamma_2/\mathrm{d}t$ do not vanish there when $\Lambda_W = 0$.

When $\mu < 0$ there is an anisotropic fixed point of the axially symmetric flow for

$$\gamma_1 = \frac{36}{\mu^2} = 4\gamma_2 = 4\gamma_3 \,. \tag{5.21}$$

This is always a saddle point because the corresponding eigenvalues of the characteristic matrix of small perturbations are real for $\lambda < 1/3$ and their product is negative. The results follow setting $\Lambda_W = 0$ in the expressions we had before (see e.g. (5.19)).

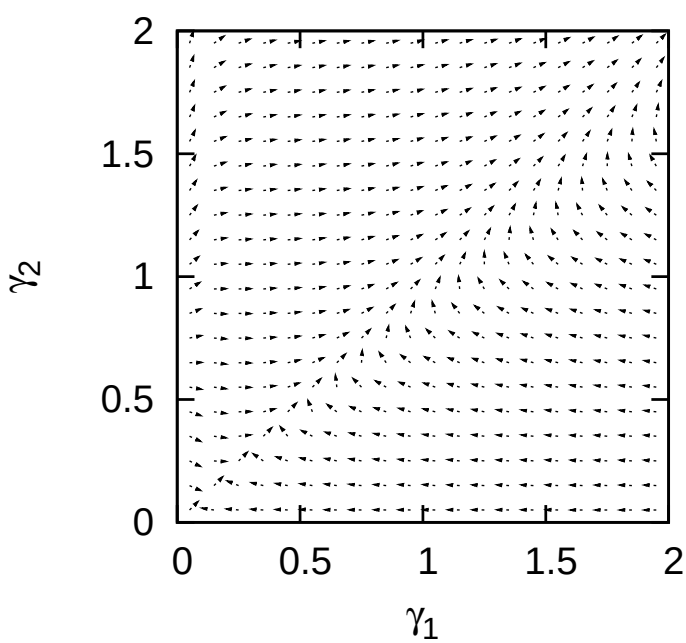

Figure 14: The flow lines for $\mu > 0$; here, $\mu = 1$.

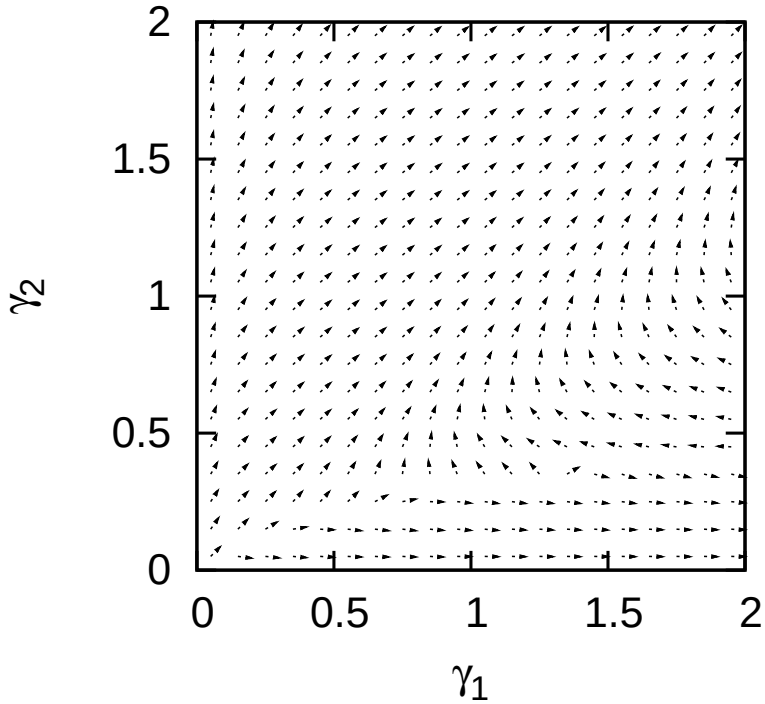

Figure 15: The flow lines for $\mu < 0$; here, $\mu = -5$.

We include two phase portraits of the flow lines that are characteristic for $\mu > 0$ and $\mu < 0$, respectively, choosing $\lambda = 0.1$. The case $\mu > 0$ is shown first in figure 14. Next, we consider the case $\mu < 0$ that exhibits an additional (anisotropic) fixed point and make the choice $\mu = -5$. The anisotropic fixed point occurs at $\gamma_1 \simeq 1.44$, $\gamma_2 = \gamma_3 \simeq 0.36$ as shown in figure 15.

Finally, concluding this section, we end up with an interesting observation that arose in our study of the flow lines. Along these lines, the volume of space changes, but the dependence on t is not monotonic in general. It is therefore interesting to inquire in this context for the existence of bouncing solutions for which the volume reaches a minimum and then increases in time. Although this behavior is not generic, it seems to arise along particular flow lines that can be found by numerical scanning. An example of this kind is provided in figure 16 for an appropriate choice of initial data and couplings. Cases with full anisotropy, but with initial conditions close to axial symmetry, also seem to lead to bounces, including minima with very small volume. Similar conclusions hold when $\Lambda_W > 0$, with or without axial symmetry, but we have not been able to obtain any quantitative characterization of the phenomenon so far.

The bouncing solutions can be regarded (in some sense) as the Euclidean space analogue of bouncing models in standard cosmology, which provide a viable alterna-

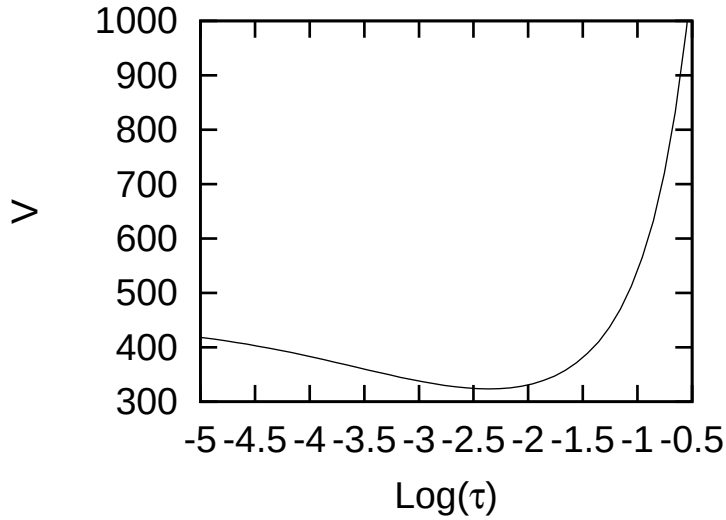

Figure 16: Bouncing solution with initial data $\gamma_1^{(0)} = 28$, $\gamma_2^{(0)} = \gamma_3^{(0)} = 4$ for $\lambda = 0.26$, $\Lambda_W = 0$ and $\mu = -5$.

tive to inflation. Matter bounces have already appeared in studies of Hořava–Lifshitz cosmology (see, for instance, [44, 45, 46]), but they are also non-generic. It remains to be seen whether they have any special meaning and implications for the models we study here, although their occurrence does not require any matter couplings, as they are purely geometric, and, hence, different from those arising in cosmology.

6 Space-time interpretation of the flow lines

The solutions of geometric flows are shown as flow lines in the various phase portraits that have been drawn. Explicit solutions were obtained in special cases, whereas more general solutions can only be described pictorially. The problems that will be addressed in this section are the selection of flow lines that can qualify as regular gravitational-instanton solutions in four dimensions and the completeness of the corresponding space-time metrics. It will also be useful in this context to compare $SU(2)$ instanton solutions of Hořava–Lifshitz theory with those of ordinary Einstein gravity.

According to the analysis of section 2.3, only the flow lines that interpolate between two fixed points (when more than one fixed point is present in our models) qualify as instantons. They are indeed finite-action solutions, and this property is sufficient to determine the global structure of space–time and its asymptotic behavior, and render the corresponding metrics complete. Our main result in a nut-shell is that all gravitational instantons with $SU(2)$ isometry are globally $\mathbb{R} \times S^3$ describing a smooth deformation of S^3 as t runs from $-\infty$ to $+\infty$, without ever encountering a

singularity. The details are given below together with the *complete classification* of gravitational instantons with $SU(2)$ isometry in Hořava–Lifshitz gravity with anisotropy parameter $z = 3$. We will also compute their Euclidean action and determine their moduli spaces. In most cases we have explicit solutions. There are also a few other solutions that are shown to exist, but we have not (yet) been able to obtain expressions for their metric in closed form.

The variant of the theory with anisotropy parameter $z = 2$ will not be especially discussed, since it is clear that it exhibits no instanton solutions (of the type we are considering here) with $SU(2)$ isometry. Recall in this case that the relevant equations are provided by the Ricci flow on S^3, which takes the form (3.9) in proper time with arbitrary parameters $\lambda < 1/3$ and $\Lambda_W > 0$. Its fixed points are determined by the equations

$$R_{ii} - \frac{2\lambda - 1}{2(3\lambda - 1)} R\gamma_i + \frac{\Lambda_W}{1 - 3\lambda}\gamma_i = 0\,, \quad i = 1, 2, 3 \tag{6.1}$$

and clearly there is a unique solution given by the constant-curvature metric with $R = 6\Lambda_W$. The absence of other fixed points, which is also implied on more general grounds by Poincaré's conjecture for S^3, shows that there can be no finite-action instanton solutions in this case.

Thus, in the following, we focus on instanton solutions of the $z = 3$ theory and explain their properties, as outlined above.

6.1 Global structure and completeness of the metrics

First of all we examine the occurrence of singularities that can appear at finite proper time t (or τ, since the two are simply related by rescaling) and render the Euclidean space–time manifold incomplete. Singularities arise when some or all of the metric coefficients of the Bianchi IX model geometry vanish and they are classified, in general, as *nuts* and *bolts*. Such singularities are intimately related to the fixed points of Killing vector fields by geometrical reasoning and they are independent of the gravitational equations. Following [47, 33] we recall that the structure of the fixed point set of a Killing vector field ξ_μ acting on any four-dimensional Riemannian manifold with metric $g_{\mu\nu}$ is determined by the rank of the 4×4 matrix $\nabla_\mu \xi_\nu$. This is an anti-symmetric matrix (since its symmetric part vanishes identically by definition of a Killing vector) which can have rank 4 or 2; rank 0 is excluded for, otherwise, the vector field vanishes everywhere. In the former case there are no directions left invariant at the tangent space of the fixed point, which, thus, appears to be isolated and it is called nut. In the latter case only a two-dimensional subspace of the tangent space at the fixed point remains invariant under the action of the Killing vector field, whereas the two-dimensional orthogonal complement rotates into itself. Then, the fixed point set

is provided by this invariant two-dimensional subspace and it is naturally called bolt (it is typically a two-sphere, as in Bianchi IX geometries).

Nuts and bolts lead to incomplete manifolds, in general, but in certain cases the apparent singularities can be removed and provide regular and complete metrics with no curvature singularities. It all depends on the form of the metric as these singularities are approached. A removable nut singularity contributes one unit to the Euler number χ of the four–manifold and a removable S^2 bolt singularity contributes two units [47], following the theorems on fixed points. This counting applies to compact four–manifolds without boundary, but it also generalizes to non-compact spaces when the Killing vector field is either everywhere tangential to the boundary (as in space–times with homogeneous spatial sections that we are considering here) or is everywhere transverse. Thus, if $\chi \neq 0$, any Killing vector field will have at least one fixed point. No fixed points imply that $\chi = 0$. Instanton solutions of Einstein and Hořava–Lifshitz gravity are quite different in this respect, as will be seen shortly, having important implications for their global topological structure.

Let us briefly review when such singularities can be removed from a Riemannian four-manifold without referring to any specific theory or any solutions at the moment. Using locally the Bianchi IX form of the metric (3.16)

$$\mathrm{d}s^2 = \mathrm{d}t^2 + a^2(t)\left(\sigma^1\right)^2 + b^2(t)\left(\sigma^2\right)^2 + c^2(t)\left(\sigma^3\right)^2 , \tag{6.2}$$

we suppose that a singularity (nut or bolt) occurs at some finite proper distance, say $t = 0$. It is well known that the metric has a *removable nut singularity* provided that near $t = 0$ all metric coefficients vanish as

$$a^2(t) = b^2(t) = c^2(t) = \frac{1}{4}t^2 \quad \text{as} \quad t \to 0 . \tag{6.3}$$

In this case we have a coordinate singularity of the polar coordinate system in $\mathbb{R}^4$ centered at $t = 0$, which is simply removed by changing to a local Cartesian coordinate system near the point $t = 0$ and adding it to the manifold. Also, it is well known that the metric has a *removable bolt singularity* provided that near $t = 0$ two of the metric coefficients (say a^2 and b^2) become equal and the third vanishes as

$$a^2(t) = b^2(t) = \text{finite} , \quad c^2(t) = \frac{1}{4}n^2t^2 \quad \text{as} \quad t \to 0 \quad \text{with} \quad n \in \mathbb{Z} . \tag{6.4}$$

Then, $a^2 = b^2 = R_0^2$ implies $a^2(\sigma^1)^2 + b^2(\sigma^2)^2 = R_0^2(\mathrm{d}\vartheta^2 + \sin^2\vartheta \mathrm{d}\varphi^2)$, which is the canonical S^2 metric, while the $\mathrm{d}t^2 + c^2(\sigma^3)^2$ part of the four-dimensional metric becomes $\mathrm{d}t^2 + (n^2t^2/4)\mathrm{d}\psi^2$ near $t = 0$, keeping ϑ and φ constant. In this case, the topology of the manifold is locally $\mathbb{R}^2 \times S^2$ and the $\mathbb{R}^2$ factor shrinks to a point on S^2

as $t \to 0$. By adjusting the range of ψ so that $n\psi/2$ runs from 0 to 2π, the apparent singularity at $t = 0$ becomes a coordinate singularity of the polar system in $\mathbb{R}^2$ and can be removed as before. In all other cases the singularities cannot be removed and the manifold is incomplete.

The above reasoning is purely geometrical without reference to any field equations. Thus, different gravitational theories for Euclidean space–times of the form (6.2) may or may not lead to removable singularities at the fixed points of a Killing vector field. This depends on the way that the metric coefficients approach zero in the vicinity of a singularity and it is sensitive to the dynamics. The space–time singularities of Euclidean Einstein and Hořava–Lifshitz gravity (if they are present) will follow different power-law behavior, which, in turn, will affect the completeness of the corresponding metrics. Thus, the absence of non-removable singularities provides a natural selection for the physically admissible solutions in those theories.

In Euclidean Hořava–Lifshitz gravity, a singularity can only arise if an eligible flow line reaches the boundaries – including the origin – of the physical parameter space, namely the two wedges of the first quadrant in the (x, y) (or (γ_1, γ_2)) plane used in the phase portraits. Then, the flow becomes extinct as it cannot be continued beyond that point. Such singularities, if they are present, will arise at finite proper time (say $t = t_0$, but we can always set $t_0 = 0$ without loss of generality). This is obviously so because such singular points can also act as initial data for the time-reversed flow at a given finite instance of (proper) time[14]. Such possibilities should be ruled out by the theory, unless the singularities are removable nuts or bolts, for, otherwise, the space–time metric will be singular. Using the Bianchi IX form of the metric (6.2) with $a^2 = \gamma_1$, $b^2 = \gamma_2$ and $c^2 = \gamma_3$ (like in (3.1)), which is the appropriate choice in this case, we may set (as in nuts)

$$\gamma_1 = \beta_1 t^{p_1} \,, \quad \gamma_2 = \beta_2 t^{p_2} \,, \quad \gamma_3 = \beta_3 t^{p_3} \tag{6.5}$$

or alternatively (as in bolts)

$$\gamma_1 = \beta_1 \,, \quad \gamma_2 = \beta_2 \,, \quad \gamma_3 = \beta_3 t^{p_3} \tag{6.6}$$

and determine the allowed values of the coefficients β_i and the exponents p_i as $t \to 0$. In all cases we find that the first-order system of Bianchi IX equations for Hořava–Lifshitz gravity with general couplings does not lead to removable nuts or bolts. Only non-removable singularities can arise along the flow lines and they seem trouble-

[14]Proving finiteness of extinction time for the solutions of geometric flow on certain three-manifolds is an intricate mathematical problem that will not be addressed in all generality, since we are only considering homogeneous geometries on S^3. It is a key point in Perelman's proof of the Poincaré conjecture based on Ricci flow [15] and it is not yet clear how it may generalize to the Ricci–Cotton flow.

some[15]. Recall, however, that instanton solutions are rather restrictive, since they are described only by those trajectories that interpolate between two fixed points. Therefore, their metrics would be singular if any one of the fixed points were singular. But this is a contradiction of terms and cannot happen, since a fixed point, unlike a singularity, is only reached at infinite proper time, $t \to \pm\infty$ (with sign that depends on the direction of the flow), and not at at finite time[16]. Thus, the instanton solutions protect themselves from the singularities that may otherwise arise by moving along generic flow lines. Whenever instanton solutions exist, their spaces will be always complete without any singularities.

In Euclidean Einstein gravity nuts and bolts are important elements in the theory of gravitational instantons, since all known solutions exist thanks to their presence. In this case, there is a certain class of gravitational instantons (6.2) that follows from the Ricci flow equations (3.11) in proper time t with $\gamma_1 = a$, $\gamma_2 = b$ and $\gamma_3 = c$, as explained in section 3.2. They include the trivial flat–space metric associated with the isotropic solution (3.12), having $a^2 = b^2 = c^2 = t^2/4$ everywhere (with $t_0 = 0$), as well as the Taub–NUT metric as the next non-trivial example with an additional axial symmetry $a(t) = b(t)$ and a removable nut singularity at the origin[17]. The Atiyah–Hitchin metric provides an even more complicated solution, which is fully anisotropic and complete [41, 42]. It exhibits a removable bolt singularity at the origin, where $b = -c$ and it comes asymptotically close to Taub–NUT metric with $a = b$ as $t \to \infty$; we skip the details as they are not important for the present work. It turns out that these are the only complete gravitational instantons with $SU(2)$ isometry that satisfy the Ricci flow equations (3.11); there is another complete metric with $SU(2)$ isometry, the Eguchi–Hanson instanton, which has $a = b$ everywhere and a removable bolt singularity at the origin, but its coefficients satisfy a different system of first-order equations. Finally, we note for completeness, that exactly the same reasoning applies to gravitational instantons of Einstein gravity with cosmological constant [47, 33] that have removable nut and bolt singularities (e.g., $\mathbb{C}P^2$ as a gravitational instanton).

Thus, on the one hand, in Euclidean Einstein gravity the instanton spaces have non-vanishing Euler number and, in many cases, they also have non-vanishing signature (given roughly, but without any further explanation here, by the number of

[15]The power-law behavior of solutions as the flow lines approach the origin can also be read off from the exact solutions we have presented in various cases.

[16]This is also implied by the stability analysis around the fixed points, which shows that the time dependence of small fluctuations varies exponentially as t goes to infinity.

[17]The gravitational field equations determine the Taub–NUT metric in the form shown in section 3.2,

$$\frac{a(t)}{m} + \operatorname{arcsinh}\frac{a(t)}{m} = \frac{-t+t_0}{m} = \log\frac{2m+c(t)}{2m-c(t)} - 2m\left(\frac{1}{2m+c(t)} - \frac{1}{2m-c(t)}\right) .$$

Setting $t_0 = 0$ for convenience, the power-law behavior of the coefficients close to the origin $t = 0$ turns out to be $a^2(t) = b^2(t) = c^2(t) = t^2/4$ and describes a removable nut singularity.

nuts minus the number of anti-nuts [47] that may be present). On the other hand, the instanton solutions of Hořava–Lifshitz gravity are globally $\mathbb{R} \times S^3$ having zero Euler number and signature. They simply describe the evolution of a three-sphere from $t = -\infty$ to $t = +\infty$ which deforms geometrically by the flow without ever becoming singular along the way; as such they resemble closer the behavior of ordinary instantons in particle theories rather than the instantons of Einstein gravity. This is not surprising in retrospect, since consistency of the Hořava–Lifshitz gravity is not questionable in the projectable case for space–times with global cross-product foliation structure. In either case, the corresponding metrics are regular everywhere and complete and their Euclidean gravitational action is finite – though the reasoning is different for each theory. The finiteness of the action, which will be discussed more extensively shortly, makes these solutions mostly relevant in the quantum theory using, for instance, the path integral approach.

Let us also discuss the asymptotic structure of the solutions and compare them to those of ordinary gravity, since there are also important differences between the two theories. In Einstein gravity, the physical boundary conditions are largely determined by the positive-action conjecture that requires that the action of any asymptotically Euclidean four-metric be positive, vanishing if and only if the space is flat [48, 33, 34]. Then, using the Bianchi IX form of the metric (6.2), the following possibilities arise at infinite proper distance t: either there is a Euclidean infinity

$$a^2(t) = b^2(t) = c^2(t) = \frac{1}{4}t^2 \quad \text{as} \quad t \to \pm\infty \tag{6.7}$$

when $0 \leq \psi \leq 4\pi$ (it is a conical infinity when $0 \leq \psi \leq 2\pi$) or a Taubian infinity

$$a^2(t) = b^2(t) = t^2\,, \quad c^2 = \text{finite} \quad \text{as} \quad t \to \pm\infty \tag{6.8}$$

that encompasses the Taub–NUT metric. Combining all distinct boundary conditions that are available at $t = 0$ and $t = \pm\infty$, one ends up with a few viable solutions that provide the list of all complete gravitational instanton metrics with $SU(2)$ isometry. Similar considerations may apply to solutions with cosmological constant.

In Hořava–Lifshitz theory the situation is different. The Euclidean action is always positive-definite (at least for $\lambda < 1/3$ that we are considering here) and vanishes when the three-dimensional metrics are vacua of topologically massive gravity without any time dependence. Thus, there are no a priori conditions on the asymptotic structure of instantons other than the mere existence of multiple vacua in three dimensions that serve as fixed points of the flow. Then, the asymptotic structure of space–time as $t \to \pm\infty$ is simply determined by the specific form of the metric coefficients γ_1, γ_2 and γ_3 at the initial and final fixed points, respectively. Their time

dependence is exponential and it is completely determined by the eigenvalues of the characteristic matrix of small fluctuations around these fixed points. The departure from usual asymptotics (with zero or positive cosmological constant) is inherited to the solutions from the detailed balance condition and seems to be rather universal. It inflicts other classes of solutions, such as the construction of black-hole solutions whose right asymptotic structure requires departure from detailed balance using more general couplings [49, 50, 51] (otherwise there is no match with observations at large distances). This is also closely related to the problem of obtaining ordinary gravity by arguing (naively) that all higher-order curvature terms are suppressed in the infrared regime of the theory[18]. However, it is not necessarily a big problem in the ultra-violet regime relevant to early time cosmology, where our discussion is applicable keeping $\lambda < 1/3$. Abandoning detailed balance will ruin our general construction of instanton solutions.

6.2 The action and moduli of $SU(2)$ instanton metrics

Let us now give some examples of instantons, based on the results described in previous sections, and compute their action $S_{\text{instanton}} = |\Delta W|/2$ in each case separately (see (2.35)). In general, the superpotential consists of two terms $W = W_{\text{CS}} + W_{\text{EH}}$, which are given by the following expressions for Bianchi IX model geometries,

$$W_{\text{CS}} = \frac{16\pi^2}{w_{\text{CS}}}\left[1 + \frac{1}{2\gamma_1\gamma_2\gamma_3}(\gamma_1+\gamma_2-\gamma_3)(\gamma_1-\gamma_2+\gamma_3)(\gamma_1-\gamma_2-\gamma_3)\right] \tag{6.9}$$

and

$$W_{\text{EH}} = -\frac{16\pi^2}{\kappa_W^2}\left[\frac{1}{\sqrt{\gamma_1\gamma_2\gamma_3}}(\gamma_1^2+\gamma_2^2+\gamma_3^2-2\gamma_1\gamma_2-2\gamma_2\gamma_3-2\gamma_3\gamma_1)+4\Lambda_W\sqrt{\gamma_1\gamma_2\gamma_3}\right] \tag{6.10}$$

and will be used next to evaluate the instanton action.

The cases below refer to instantons constructed from interpolating trajectories of the Ricci–Cotton flow for different couplings, changing as the complexity of the equations increases.

[18]For the same reason we cannot obtain the instantons of Einstein gravity from those of Hořava–Lifshitz theory. The first arise by dropping all higher-curvature terms and setting $\lambda = 1$, whereas the latter exist in the full theory only for $\lambda < 1/3$. Bianchi type IX models may offer a glimpse at this problem since the gravitational potential is derived from a superpotential in both cases (see, for instance, [34] for the derivation of the superpotential that governs $SU(2)$ instantons in ordinary gravity; this reference also provides a neat qualitative picture for the completeness of their metrics using Hamiltonian methods). It should be easier to explore the renormalization of the coefficients of the superpotential and the parameter λ for this class of mini-superspace models, as the theory is taken from the ultra-violet to the infrared domain.

Cotton flow. For the pure Cotton flow treated in section 3.3 there are two fixed points: the isotropic point with $\gamma_1 = \gamma_2 = \gamma_3 = L^2/4$ and the anisotropic fixed point with $\gamma_1 = \gamma_2 = xL^2/4$, and $\gamma_3 = L^2/4x^2$ that arises for $x = \infty$; two more anisotropic fixed points are obtained from it by permuting the three principal axes of S^3. The corresponding instanton, which is given in closed form by (3.28), describes the evolution of a fully squashed (flattened) sphere towards the round sphere as t varies from $-\infty$ to $+\infty$; the anti-instanton follows by reversing the time direction.

Note that a natural entropy function associated with the volume-preserving deformation of S^3 (other than W) can be defined in this case[19]. It is important for the mathematics of the Cotton flow, but, unlike W that determines the action of the instanton, this entropy has no deeper meaning in space–time (as far as we can tell now). Also, there is no (yet) known analogue of it for the combined Ricci–Cotton flow.

The instanton solution has enhanced isometry $SU(2) \times U(1)$, since the deformation line possesses axial symmetry. Also, since the interpolating trajectory is unique, the instanton has no moduli other than the radius of the sphere at the fixed point. In this case, $W = W_{\rm CS}$ and one finds that the superpotential takes the following values at the two fixed points,

$$W^{\rm iso} = \frac{8\pi^2}{w_{\rm CS}}\,, \qquad W^{\rm aniso} = \frac{16\pi^2}{w_{\rm CS}}\,. \tag{6.11}$$

Therefore, the action is

$$S_{\rm instanton} = \frac{4\pi^2}{|w_{\rm CS}|} \tag{6.12}$$

and it is independent of the modulus L. Obviously, there are no other instantons derived from the Cotton flow equations.

[19]For Bianchi IX model geometries one can define in general an additional function (other than W) that changes monotonically under the Cotton flow. We consider

$$F(t) = \frac{1}{\gamma_1^2} + \frac{1}{\gamma_2^2} + \frac{1}{\gamma_3^2}\,,$$

which is bounded from below by $3/(\gamma_1\gamma_2\gamma_3)^{2/3} = 3(16\pi^2/V)^{4/3}$ for a three-sphere with volume V. The lower bound is attained in the fully isotropic case $\gamma_1 = \gamma_2 = \gamma_3$. $F(t)$ becomes infinite when the sphere is completely squashed in one or more directions; as such, it is a measure of the "shape entropy" of S^3. Using the Cotton flow (3.18), we obtain

$$\frac{{\rm d}F}{{\rm d}t} = -\frac{\kappa^2}{w_{\rm CS}(\gamma_1\gamma_2\gamma_3)^{3/2}}\left[\frac{(\gamma_2+\gamma_3)(\gamma_2-\gamma_3)^2}{\gamma_1^2} + \frac{(\gamma_3+\gamma_1)(\gamma_3-\gamma_1)^2}{\gamma_2^2} + \frac{(\gamma_1+\gamma_2)(\gamma_1-\gamma_2)^2}{\gamma_3^2}\right]$$

and, therefore, $F(t)$ changes monotonically. For $w_{\rm CS} > 0$, these properties of $F(t)$ suffice to prove the convergence of the flow lines to the fully isotropic fixed point regardless of initial conditions [36].

Normalized Ricci–Cotton flow. The normalized Ricci–Cotton flow has more than one fixed points when $\mu < 0$, in which case there are instantons with $SU(2)$ isometry interpolating between them as t varies for $-\infty$ to $+\infty$.

Let us first consider the instantons connecting the two axially symmetric fixed points. Recall that the isotropic fixed point appears at $\gamma_1 = \gamma_2 = \gamma_3 = L^2/4$ and the anisotropic point at $\gamma_1 = \gamma_2 = L^2/4a$ and $\gamma_3 = a^2L^2/4$ (up to permutations of the axes of S^3), setting for notational convenience

$$a = \sqrt{-\frac{\mu}{3}}\,. \tag{6.13}$$

Then, explicit calculation shows that $W = W_{\rm CS} + W_{\rm EH}$ (with $\mu = w_{\rm CS}L/\kappa_W^2$) takes the following form at the two fixed points,

$$W^{\rm iso} = \frac{8\pi^2}{w_{\rm CS}}\left(1 - 9a^2 + 3a^2\Lambda_W L^2\right) \tag{6.14}$$

and

$$W^{\rm aniso} = \frac{8\pi^2}{w_{\rm CS}}\left(2 + 4a^6 - 14a^3 + 3a^2\Lambda_W L^2\right)\,. \tag{6.15}$$

Although Λ_W does not appear in the normalized Ricci–Cotton flow equations, it enters into W by contributing the same at all points (recall that the volume V is preserved in this case). Consequently, the instanton action takes the value

$$S_{\rm instanton} = \frac{4\pi^2}{|w_{\rm CS}|}(a-1)^2\left(4a^4 + 8a^3 + 12a^2 + 2a + 1\right) \tag{6.16}$$

and it is independent of L, as expected. Notice that it vanishes when $a = 1$ ($\mu = -3$), as required, since the two fixed point coalesce and there is no instanton in this case. The action is non-zero and positive for all other values $\mu < 0$.

The axisymmetric solutions of the normalized Ricci–Cotton flow have been constructed explicitly in section 4.4, but one should only use those branches that interpolate between the two fixed points. The stability analysis performed in section 4.2 shows that for $-3 < \mu < 0$ the isotropic fixed point is absolutely unstable and the anisotropic is a saddle point. Therefore, there can be only one flow line interpolating between the two fixed points (corresponding to the axisymmetric solution we obtained) and the instanton has no moduli other than L. Exactly the same conclusion holds for $-6\sqrt[3]{2} < \mu < -3$, since the isotropic fixed point is now absolutely stable and the anisotropic is a saddle point. The absence of moduli in these cases can also be seen schematically in figures 4 and 5, respectively. Thus, for all $-6\sqrt[3]{2} < \mu < 0$ the instantons have enhanced $SU(2) \times U(1)$ isometry. The situation changes dras-

tically when $\mu < -6\sqrt[3]{2}$, since the isotropic fixed point is absolutely stable and the anisotropic is absolutely unstable. In this case, we have several flow lines interpolating between the two fixed points, as can also be seen schematically in figure 6, and the instantons have an additional (real) modulus that labels these trajectories. The physical interpretation of this modulus is nothing else but the geometric shape of S^3 (there is only one shape modulus, since the volume of space is held fixed by specifying L). Of course, the instanton action is independent of all moduli.

The axisymmetric solution we have obtained in this case has enhanced $SU(2) \times U(1)$ isometry, whereas the other ones should only have an $SU(2)$ isometry group. They all correspond to regular and complete metrics on $\mathbb{R} \times S^3$, but we have not been able to find them in closed form. They should be the analogue of the Atiyah–Hitchin metric for Hořava–Lifshitz gravity when $\lambda = -\infty$. Their explicit construction is an interesting open mathematical problem.

Finally, we turn to instantons that owe their existence to the presence of totally anisotropic fixed points in the problem when $\mu < -6\sqrt[3]{2}$. They have no moduli (other than their volume) since they connect a saddle point with a stable or an unstable fixed point. These instantons also have $SU(2)$ isometry but no higher symmetry.

The value of the superpotential for the totally anisotropic fixed points (see also section 4.2) turns out to be

$$W^{\text{total aniso}} = \frac{8\pi^2}{w_{\text{CS}}}(10 + 3a^2\Lambda_W L^2) \,. \tag{6.17}$$

Therefore, the instanton that interpolates between these points and the totally isotropic fixed point has action

$$S_{\text{instanton}} = \frac{72\pi^2}{|w_{\text{CS}}|}(a^2 + 1) \,. \tag{6.18}$$

It never becomes zero because these points cease to exist before they have the chance to meet with the isotropic point. Similarly, the instanton that interpolates between the totally anisotropic and the axially symmetric anisotropic fixed points has action

$$S_{\text{instanton}} = \frac{16\pi^2}{|w_{\text{CS}}|}(a^3 - 4)(2a^3 + 1) \,. \tag{6.19}$$

The latter vanishes when $a^3 = 4$ ($\mu = -6\sqrt[3]{2}$), as the end-points coalesce in this case, and it is positive definite otherwise.

General Ricci–Cotton flow. The Ricci–Cotton flow with general couplings (provided that $\lambda < 1/3$ and Λ_W is non-negative) was found to exhibit two fixed points when $\mu < 0$, in which case there are instanton solutions in Hořava–Lifshitz gravity. Recall

that the isotropic point appears at $\gamma_1 = \gamma_2 = \gamma_3 = 1/4\Lambda_W$ and the anisotropic point at $\gamma_1 = 36\mu^2/\left(\mu^2 + 27\Lambda_W\right)^2$ and $\gamma_2 = \gamma_3 = 9/\left(\mu^2 + 27\Lambda_W\right)$, assuming the presence of an axial symmetry $\gamma_2 = \gamma_3$ for all time.

Taking $\mu < 0$, we define, for notational convenience, the non-negative number

$$a = -\frac{\mu}{3\sqrt{\Lambda_W}} \tag{6.20}$$

and evaluate the superpotential $W = W_{\rm CS} + W_{\rm EH}$ at the two fixed points. Using $\mu = w_{\rm CS}/\kappa_W^2$, as defined in section 5, we obtain the following results

$$W^{\rm iso} = \frac{8\pi^2}{w_{\rm CS}}(1-6a)\,, \quad W^{\rm aniso} = \frac{16\pi^2\left(5a^4 - 54a^2 + 9\right)}{w_{\rm CS}\left(a^2+3\right)^2}\,. \tag{6.21}$$

Therefore, the instanton action turns out to be

$$S_{\rm instanton} = \frac{12\pi^2}{|w_{\rm CS}|}\frac{(a-1)^2}{\left(a^2+3\right)^2}\left(2a^3 + 7a^2 + 24a + 3\right)\,. \tag{6.22}$$

Note that the action is manifestly positive-definite, as required, and vanishes when $a = 1$ ($\mu = -3\sqrt{\Lambda_W}$), in which case the two fixed points coalesce and there is no instanton.

Even in the presence of axial symmetry, which was used to simplify the analysis of the general Ricci–Cotton flow equations, we have not been able to obtain the interpolating solutions in closed form. Nevertheless, it is clear that a unique solution exists in this case, for all $\mu < 0$, which interpolates between the two fixed points. For $0 < a < 1$ ($-3\sqrt{\Lambda_W} < \mu < 0$) the isotropic fixed point is saddle and the anisotropic is absolutely stable, and, therefore, there is a single flow line that connects the two. For $a > 1$ ($\mu < -3\sqrt{\Lambda_W}$) the isotropic fixed point is now absolutely stable and the anisotropic is a saddle point and, therefore, the interpolating flow line is again unique. This can also be seen by inspecting figures 12 and 13.

The solutions at hand have no moduli at all[20]. They correspond to instantons with $SU(2) \times U(1)$ isometry. It will be very interesting to construct them explicitly. Also, other more general solutions with strict $SU(2)$ isometry are expected to exist in the general case, with $\gamma_1 \neq \gamma_2 \neq \gamma_3$, but their investigation will not be pursued in the present work. We only note here that all anisotropic fixed points of the Ricci–Cotton flow equations with general couplings seem to be axially symmetric even when $\gamma_1 \neq \gamma_2 \neq \gamma_3$ at generic points. Thus, we expect to have instanton so-

[20]Even the size of S^3 at the isotropic fixed point is not free, as L was free to vary in the normalized flow, but it is determined by the parameters of the differential equations. Thus, it is not surprising that the instanton action depends on Λ_W (through a) in this case.

lutions without axial symmetry that interpolate between these fixed points, serving as the Hořava–Lifshitz analogue of the Atiyah–Hitchin metric. They should depend only on one free parameter.

The special case $\Lambda_W = 0$. Finally, note that as Λ_W is taken to zero, while keeping μ fixed in the general system of Ricci–Cotton flow equations, W^{iso} blows up to infinity, whereas W^{aniso} remains finite, tending to the value $80\pi^2/w_{\text{CS}}$. Consequently, $S_{\text{instanton}}$ becomes infinite and one may consider it a problem, since instantons must have finite action. However, in this case, there is no contradiction, since the isotropic configuration ceases to be (strictly speaking) a fixed point when it is pushed away to infinity by setting $\Lambda_W = 0$ and, therefore, the flow line that interpolates between the two points (see figure 15) does not qualify as instanton solution of the theory. In conclusion, there are no instanton solutions when $\Lambda_W = 0$.

This completes our analysis of $SU(2)$ gravitational instantons of Hořava–Lifshitz theory with anisotropy scaling parameter $z = 3$. We have obtained complete classification of all explicit and implicit solutions that exist for all different couplings of the theory satisfying the detailed balance condition, provided that $\lambda < 1/3$ and $\Lambda_W > 0$. By the same token, the variant of the theory with scaling parameter $z = 2$ does not exhibit any such instanton solutions. The results are on par with the classification of instantons with $SU(2)$ isometry in Einstein gravity. The only missing technical part is the explicit construction of some of these instanton metrics.

We end this section with some general remarks concerning the existence and description of instanton metrics in Hořava–Lifshitz gravity without relying on isometry groups, such as $SU(2)$. According to definition, they should be trajectories of the Ricci–Cotton flow equations interpolating between any two solutions of three-dimensional topologically massive gravity that provide the fixed points. The landscape of vacua of topologically massive gravity is not known completely[21] and, therefore, it is difficult to make explicit general constructions. Also, it is rather difficult to investigate the general behavior of the flow equations by standard mathematical techniques, since they are third-order in space derivatives and even the short-time existence of solutions is difficult to establish in all generality. The formation and characterization of singularities is another related general open problem for these flow equations. Addressing these issues successfully will lead to further advances.

[21]Note, however, the recent work [52] that develops techniques to solve the field equations of topologically massive gravity (and other massive-gravity models) for three-dimensional geometries admitting a Killing vector field. Older results in this direction are neatly summarized in [53] although most of them focus on vacua with negative cosmological constant.

7 Generalization to higher dimensions

In this section we make a few remarks concerning higher-dimensional generalizations of Hořava–Lifshitz theory and the correspondence of its instanton solutions to the theory of higher-order geometric flows.

7.1 Hořava–Lifshitz gravity in $4+1$ dimensions

The general aspects have been reviewed in section 2 for all space–time dimensions. The theory is power-counting renormalizable when $z = D$ using the appropriate superpotential W. Let us concentrate on $D = 4$ for definiteness, so that W is the action of four-dimensional gravity with higher-order corrections of the general form [7]

$$W[g] = \int \mathrm{d}^4x \sqrt{g} \left(\alpha C_{ijk\ell} C^{ijk\ell} + \beta R^2 + \gamma (R - 2\Lambda_W) \right). \tag{7.1}$$

Here, $C_{ijk\ell}$ is the Weyl tensor and R is the Ricci scalar curvature of a four-dimensional Riemannian metric g that describes the geometry of spatial slices in a five-dimensional space–time with topology $\mathcal{M}_5 = \mathbb{R} \times \mathcal{M}_4$. Here, there is no need to include the term $R_{ij}R^{ij}$ because it can be removed by a Gauss–Bonnet topological term, adjusting the coefficients α and β.

Thus, Hořava–Lifshitz gravity in $4+1$ dimensions with anisotropic scaling $z = 4$ is defined by the action

$$S = \frac{2}{\kappa^2} \int \mathrm{d}t\, \mathrm{d}^4x\, \sqrt{g} N K_{ij} G^{ijk\ell} K_{k\ell} - \frac{\kappa^2}{8} \int \mathrm{d}t\, \mathrm{d}^4x\, \sqrt{g} N \left(\frac{1}{\sqrt{g}} \frac{\delta W}{\delta g_{ij}} \right) \mathcal{G}_{ijk\ell} \left(\frac{1}{\sqrt{g}} \frac{\delta W}{\delta g_{k\ell}} \right) \tag{7.2}$$

using the extrinsic curvature K_{ij} of $\mathcal{M}_4$ and the metric $G^{ijk\ell}$ of superspace with parameter λ. Also, following the general discussion of section 2, we will also take $\lambda < 1/4$ so that the Euclidean counterpart of this action is manifestly bounded from below.

The theory with detailed balance is completely specified by the choice of $W[g]$. It is given by the general expression (7.1) in $D = 4$; other appropriate choices of W should be made in higher dimensions to render the theory power-counting renormalizable. We also note for completeness that if higher-order curvature functionals are chosen in D spatial dimensions so that $z > D$, the resulting gravitational theory will be power-counting superenormalizable [7]. Such generalizations will not be considered at all in the present work.

Next, we illustrate the structure of the resulting equations by considering the simplest higher-dimensional case with $z = D = 4$.

7.2 Bach flow and its variants

Solutions of the Euclidean five-dimensional Hořava–Lifshitz gravity can be obtained from the geometric-flow equation

$$\frac{1}{N(t)}\partial_t g_{ij} = \pm\frac{\kappa^2}{2\sqrt{g}}\mathcal{G}_{ijk\ell}\frac{\delta W[g]}{\delta g_{k\ell}} + \nabla_i\xi_j + \nabla_j\xi_i \tag{7.3}$$

that describes deformations of the four-dimensional Riemannian metric g_{ij}. The lapse function $N(t)$ can be set equal to 1 by time redefinition.

The details can be worked out using the following identity, which is well known among people working in conformal Weyl gravity,

$$B^{ij} = -\frac{1}{\sqrt{g}}\frac{\delta W_{\text{Weyl}}}{\delta g_{ij}}\,, \tag{7.4}$$

where

$$W_{\text{Weyl}} = \int \mathrm{d}^4x\sqrt{g}\; C_{ijk\ell}C^{ijk\ell} \tag{7.5}$$

is the quadratic Weyl tensor action functional and

$$B^{ij} = \nabla_k\nabla_\ell C^{ikj\ell} + \frac{1}{2}R_{k\ell}C^{ikj\ell} \tag{7.6}$$

is the so called *Bach tensor* [54]. It is a fourth-order symmetric and traceless tensor that clearly vanishes when the four-dimensional metric is conformally flat. The Bach tensor provides the analogue of the Einstein tensor in the field equations of conformal Weyl gravity, and, as such, it is also covariantly conserved.

Thus, for this particular choice of superpotential W, the corresponding geometric flow takes the form

$$\partial_t g_{ij} = \mp\frac{\kappa^2}{2}B_{ij} + \nabla_i\xi_j + \nabla_j\xi_i\,, \tag{7.7}$$

and it can be naturally called Bach flow. Its fixed points (modulo reparametrizations) are the vacuum solutions of conformal Weyl gravity and include the isotropic (constant curvature) metric on S^4. It is mathematically more interesting to pick the sign that drives the evolution towards the fixed points rather that away from them. Although this is a higher-order flow, it is better behaved mathematically than the third-order Cotton flow. Thus, one should investigate it in detail and attempt to construct solutions. It is a new geometric flow that has not appeared in the mathematics literature before, to the best of our knowledge. By restricting it to Kähler manifolds, it might be also interesting to compare it (and the variants which are discussed below) with other well known geometric flows of fourth-order, such as the Calabi flow [55].

If there is an additional contribution to W given by the quadratic Ricci scalar curvature action,

$$W_{R^2} = \int \mathrm{d}^4x \sqrt{g}\, R^2 \,, \tag{7.8}$$

it will account for the gradient term

$$H^{ij} = -\frac{1}{\sqrt{g}} \frac{\delta W_{R^2}}{\delta g_{ij}} \tag{7.9}$$

with

$$H^{ij} = 2g^{ij}\nabla_k\nabla^k R - 2\nabla^i\nabla^j R - 2RR^{ij} + \frac{1}{2}g^{ij}R^2 \,. \tag{7.10}$$

This tensor is symmetric but not traceless. Then, the complete flow equation will be a variant of the Bach flow receiving contributions from B^{ij} and H^{ij}, which are both fourth-order. Of course, in the general case, there will also be subleading curvature terms associated with the Einstein tensor G^{ij} by adding the four-dimensional Einstein–Hilbert action (possibly with a cosmological constant) to the superpotential W.

Instanton solutions will correspond to flow lines interpolating between different vacua of four-dimensional conformal Weyl gravity (and its deformations thereof), but again it seems rather difficult to derive explicit general results. Using four-dimensional model geometries may provide some simple and tractable mini-superspace models that are worth studying in the future.

Similar considerations apply to all higher-dimensional generalizations of Hořava–Lifshitz gravity. In $D+1$ dimensions, the non-relativistic gravitational theory becomes power-counting renormalizable when the anisotropic scaling parameter is $z = D$. Then, for the appropriate choice of W, we obtain geometric flows of order D that describe instanton-like configurations of the Euclidean $(D+1)$-dimensional theory when $\lambda < 1/D$. This framework hosts very naturally a whole hierarchy of geometric flows and provides a reason to study them.

8 Conclusions and discussion

We examined the Euclidean version of Hořava–Lifshitz gravity satisfying the detailed balance condition and described its instanton solutions as flow lines interpolating between different fixed points of a new class of geometric evolution equations, which are first-order in time. Although the specific couplings implied by detailed balance are rather restrictive (and sometimes appear to be problematic), the general connection between instanton solutions and geometric flows is rather interesting in many respects. Focusing to $3+1$ dimensions, where the potential term is derived from a superpotential W given by the action functional of three-dimensional topologically mas-

sive gravity and the anisotropy scaling parameter of the theory is $z = 3$, the driving curvature terms are provided by a certain combination of the Cotton and Ricci tensors as well as the cosmological constant term. The geometric-flow equations, called Ricci–Cotton flow, were shown to exhibit an entropy functional that is given by W and can be used to put a lower bound on the Euclidean Hořava–Lifshitz gravitational action.

Our construction requires $\lambda < 1/3$ and $\Lambda_W > 0$, but otherwise the parameters of the theory can be arbitrary within the class of detailed balance couplings. Fixed points of the flow are provided by classical solutions of the three-dimensional topologically massive gravity and they correspond to static solutions of the $(3+1)$-dimensional theory. As such, they include constant-curvature isotropic metrics in three dimensions as well as anisotropic configurations obtained by balancing the deformation effect of the Cotton and Ricci tensors. Since there is no general classification of these metrics, the landscape of fixed points remains largely unexplored to the best of our knowledge. Running solutions represent genuine time-dependent configurations, but they are even more difficult to investigate in exact terms. Thus, the Ricci–Cotton flow appears to be a rather complex system of equations that deserves proper mathematical study on general grounds. Addressing these problems in all generality remains out of reach at the moment, but some simple mini-superspace truncations of the equations help to obtain concrete results in simple cases that are interesting both physically and mathematically.

We found that the homogeneous model geometries on three-manifolds provide consistent truncation of the Ricci–Cotton flow equations. In particular, focusing on the Bianchi IX model geometries on S^3, so that the corresponding gravitational instantons exhibit $SU(2)$ group of isometries, we were able to classify the fixed points of the flow (isotropic as well as anisotropic) and study their stability properties for a variety of different couplings. Some special solutions with axial symmetry (associated with $SU(2) \times U(1)$ isometry group) were constructed explicitly and their space–time interpretation was discussed in analogy with the gravitational instanton solutions of ordinary gravity. In particular, we have arrived at complete classification of the instanton solutions with $SU(2)$ isometry. It remains to be seen whether more general running solutions can be constructed explicitly beyond their qualitative description based on the phase portraits of the flow. Also, it will be interesting to find other consistent reductions of the flow equations beyond the class of homogeneous geometries, but we have not yet been able to obtain any concrete results in this direction.

Another possibility that has not been discussed at all in this paper is to consider super-renormalizable versions of Hořava–Lifshitz gravity in $3+1$ dimensions with anisotropic scaling $z = 4$. These are generated by a superpotential W – other than the action functional of topologically massive gravity – which contains higher-order Ricci

curvature terms such as $R_{ij}R^{ij}$ and R^2 on top of the cosmological Einstein–Hilbert action in three dimensions [7]. In this case, the instanton solutions will be described by geometric flows in three dimensions with fourth-order derivatives in their driving curvature terms. The resulting equations appear to have some nice mathematical properties (compared to the third-order Ricci–Cotton flow) and they also seem to admit consistent reduction to an autonomous system of ordinary differential equations for homogeneous model geometries. A particular choice of such W is provided by the action of the so called "new massive gravity" in three dimensions that contains both terms $R_{ij}R^{ij}$ and R^2 with relative coefficient $-3/8$ [56]. We intend to investigate elsewhere the corresponding fourth-order flows [57], together with the associated instanton solutions, and examine the privileged role (if any) of new massive gravity in this context.

Higher-dimensional generalizations were also briefly discussed. It was pointed out that instanton solutions exist in all dimensions and their defining equations provide new classes of geometric-flow equations, such as the Bach flow in four dimensions. In general, the driving curvature terms of such flows contain spatial derivatives of order z (equal to the anisotropy scale parameter that renders the higher-dimensional Hořava–Lifshitz gravity power-counting renormalizable) and they describe metric deformations on spatial slices of dimension $D = z$. The hierarchy of such flows has not been considered in the literature before and they certainly pose several interesting questions that are worth studying in the details. They should also be of interest to the mathematics community working on geometric analysis. In all cases, the non-relativistic theory of gravity provides a general framework to embed geometric evolution equations. The situation should be compared to general relativity and string theory, where such embedding is only possible in some very special cases, such as the Ricci flow on homogeneous three-geometries that can be interpreted as self-dual gravitational instantons in four dimensions or using some appropriately chosen higher-dimensional plane-wave gravitational backgrounds.

The off-shell formulation of string theory based on the world-sheet renormalization group equations provides a natural framework for the appearance of the Ricci flow (and other closely related geometric-flow equations) in gravitational physics. In this context, closed string tachyon condensation is described by transitions from one fixed point to another more stable fixed point. Thus, the lines of the Ricci flow resemble instanton transitions among different vacua of the string landscape. In Hořava–Lifshitz gravity, on the other hand, the Ricci flow (and its variants) describe the instantons of the theory when the anisotropic scaling is $z = 2$. Therefore, it seems interesting to investigate further this aspect while searching for possible embedding of the non-relativistic theory of gravity into a more fundamental theory. Likewise, non-relativistic theories of gravity with higher anisotropic scaling, in particular $z = D$, and

their instanton solutions may admit a similar description and interpretation in terms of a more fundamental theory. It is not yet known, however, whether the geometric evolution equations we are considering here can also arise as renormalization-group equations in a class of quantum field theories.

Finally, another interesting problem is the use of instantons for the quantization of Hořava–Lifshitz gravity. One possible line of work in this direction is the path integral approach over Euclidean space–times with applications to quantum cosmology in the spirit of Hartle–Hawking proposal. The quantization of mini-superspace models appears to be tractable, at least for homogeneous (but generally non-isotropic) geometries, and requires special attention. They can also provide some non-perturbative information about the quantum theory and a testing bed for comparison with the quantization of ordinary gravity.

It remains to be seen whether the non-relativistic theory of gravity is a viable alternative to Einstein gravity at very short distances. However, the simplified version of the theory with detailed balance can also play another role in physics, serving as landscape explorer of the vacuum structure of relativistic field theories determined by W (with topologically massive gravity being just an example). It provides an effective particle model to describe transitions among different vacua through instantons. It also offers a dynamical principle for vacuum selection that is worth exploring further in all generality using the powerful tools of geometric flows and associated entropy functions. Advocating this point of view introduces a new twist to the subject and departs from the idea (and the problems that seem to accompany it) that Hořava-Lifshitz gravity is the ultra-violet completion of a fundamental theory. It could have also been used from the very beginning as an alternative motivation for the present work.

We hope to return to these topics elsewhere in the near future.

Acknowledgements

The authors would like to thank G. Huisken, A. Petkou, C. Sourdis and M. Taylor for stimulating discussions. Many of the ideas developed in the present work were triggered during the 2009 GGI workshop *New Perspectives in String Theory*. I. Bakas, F. Bourliot and M. Petropoulos would like to thank the LMU for kind hospitality. This research was supported by the Cluster of Excellence *Origin and the Structure of the Universe* in Munich, Germany, the French Agence Nationale pour la Recherche, contract 05-BLAN-NT09-573739 *String Cosmology*, the ERC Advanced Grant 226371 *Mass Hierarchy and Particle Physics at the TeV Scale*, the ITN programme PITN-GA-2009-237920 *Unification in the LHC Era* and the GRC APIC PICS-Grèce 3747.

References

[1] E.M. Lifshitz, "On the theory of second order phase transitions I & II", Zh. Eksp. Teor. Fiz. 11 (1941) 255 & 269.

[2] S. Chadha and H.B. Nielsen, "Lorentz invariance as a low-energy phenomenon", Nucl. Phys. B217 (1983) 125.

[3] J. Iliopoulos, D.V. Nanopoulos and T.N. Tomaras, "Infrared stability or anti grand unification", Phys. Lett. 94B (1980) 141.

[4] I. Antoniadis, J. Iliopoulos and T. Tomaras, "On the infrared stability of gauge theories", Nucl. Phys. B227 (1983) 447.

[5] M. Petrini, "Infrared stability of N = 4 super Yang–Mills theory", Phys. Lett. B404 (1997) 66 [arXiv:hep-th/9704004].

[6] P. Hořava, "Membranes at quantum criticality", JHEP 0903 (2009) 020 [arXiv:0812.4287 [hep-th]].

[7] P. Hořava, "Quantum gravity at a Lifshitz point", Phys. Rev. D79 (2009) 084008 [arXiv:0901.3775 [hep-th]].

[8] D. Orlando and S. Reffert, "On the renormalizability of Hořava–Lifshitz-type gravities", Class. Quant. Grav. 26 (2009) 155021 [arXiv:0905.0301 [hep-th]].

[9] F.-W. Shu and Y.-S. Wu, "Stochastic quantization of the Hořava gravity" [arXiv:0906.1645 [hep-th]].

[10] C. Charmousis, G. Niz, A. Padilla and P.M. Saffin, "Strong coupling in Hořava gravity", JHEP 0908 (2009) 070 [arXiv:0905.2579 [hep-th]].

[11] M. Li and Y. Pang, "A trouble with Hořava–Lifshitz gravity", JHEP 0908 (2009) 015 [arXiv:0905.2751 [hep-th]].

[12] D. Blas, O. Pujolas and S. Sibiryakov, "On the extra mode and inconsistency of Hořava gravity", JHEP 0910 (2009) 029 [arXiv:0906.3046 [hep-th]]; "A healthy extension of Hořava gravity" [arXiv:0909.3525 [hep-th]]; "Comment on strong coupling in extended Hořava–Lifshitz gravity" [arXiv:0912.0550 [hep-th]].

[13] K. Koyama and F. Arroja, "Pathological behavior of the scalar graviton in Hořava–Lifshitz gravity" [arXiv:0910.1998 [hep-th]].

[14] R. Hamilton, "Three-manifolds with positive Ricci curvature", J. Diff. Geom. 17 (1982) 255.

[15] G. Perelman, "The entropy formula for the Ricci flow and its geometric applications" [math.DG/0211159]; "Ricci flow with surgery on three-manifolds" [math.DG/0303109]; "Finite extinction time for the solutions to the Ricci flow on certain three-manifolds" [math.DG/0307245].

[16] H.-D. Cao, B. Chow, S.-C. Chu and S.-T. Yau eds., *Collected Papers on Ricci Flow*, Series in Geometry and Topology, 37, International Press, Somerville, 2003.

[17] J.W. Morgan and G. Tian, *Ricci Flow and the Poincaré Conjecture*, Clay Mathematics Monographs, Amer. Math. Soc., Cambridge, 2007 [math.DG/0607607].

[18] D.H. Friedan, "Nonlinear models in two + epsilon dimensions", Phys. Rev. Lett. 45 (1980) 1057; "Nonlinear models in two + epsilon dimensions", Ann. Phys. 163 (1985) 318.

[19] C. Schmidhuber and A.A. Tseytlin, "On string cosmology and the RG flow in 2-d field theory", Nucl. Phys. B426 (1994) 187 [arXiv:hep-th/9404180].

[20] I. Bakas, D. Orlando and P.M. Petropoulos, "Ricci flows and expansion in axion-dilaton cosmology", JHEP 0701 (2007) 040 [arXiv:hep-th/0610281].

[21] M. Cvetic, G.W. Gibbons, H. Lu and C.N. Pope, "Cohomogeneity one manifolds of Spin(7) and $G(2)$ holonomy", Phys. Rev. D65 (2002) 106004 [arXiv:hep-th/0108245]; I. Bakas and K. Sfetsos, unpublished work (2004); G.W. Gibbons, private communication (2005).

[22] F. Bourliot, J. Estes, P.M. Petropoulos and Ph. Spindel, "Gravitational instantons, self-duality and geometric flows" [arXiv:0906.4558 [hep-th]].

[23] J.B. Hartle and S.W. Hawking, "Wave function of the universe", Phys, Rev. D28 (1983) 2960.

[24] C.W. Misner, "Mixmaster universe", Phys. Rev. Lett. 22 (1969) 1071; "Quantum cosmology 1", Phys. Rev. 186 (1969) 1319.

[25] V.A. Belinskii, I.M. Khalatnikov and E.M. Lifshitz, "Oscillatory approach to a singular point in the relativistic cosmology", Adv. Phys. 19 (1970) 525; "A general solution of the Einstein equations with a time singularity", Adv. Phys. 31 (1982) 639.

[26] J.D. Barrow, "Chaotic behaviour in general relativity", Phys. Rept. 85 (1982) 1.

[27] I. Bakas, F. Bourliot, D. Lüst and M. Petropoulos, "Mixmaster universe in Horava–Lifshitz gravity", Class. Quant. Grav. 27 (2010) 045013 [arXiv:0911.2665 [hep-th]].

[28] Y.S. Myung, Y.W. Kim, W.S. Son and Y.J. Park, "A non-chaotic mixmaster universe in the $z = 2$ Hořava–Lifshitz gravity" [arXiv:0911.2525 [gr-qc]].

[29] L. Carroll, *Alice's Adventures in Wonderland*, MacMillan, London, 1865.

[30] C.W. Misner, K.S. Thorne and J.A. Wheeler, *Gravitation*, Freeman, San Francisco, 1973.

[31] M. Henneaux, A. Kleinschmidt and G. Lucena Gomez, "A dynamical inconsistency of Hořava gravity" [arXiv:0912.0399 [hep-th]].

[32] S. Deser, R. Jackiw and S. Templeton, "Topologically massive gauge theories", Ann. Phys. 140 (1982) 372; Erratum-ibid. 185 (1988) 406; "Three-dimensional massive gauge theories", Phys. Rev. Lett. 48 (1982) 975.

[33] T. Eguchi, P.B. Gilkey and A.J. Hanson, "Gravitation, gauge theories and differential geometry", Phys. Rept. 66 (1980) 213.

[34] G.W. Gibbons and C.N. Pope, "The positive action conjecture and asymptotically Euclidean metrics In quantum gravity", Commun. Math. Phys. 66 (1979) 267.

[35] R.S. Hamilton, "The Ricci flow on surfaces" in *Mathematics and General Relativity*, Contemp. Math. 71, p. 237–262, Amer. Math. Soc., Providence, 1988.

[36] A.U.O. Kisisel, O. Sarioglu and B. Tekin, "Cotton flow", Class. Quant. Grav. 25 (2008) 165019 [arXiv:0803.1603 [hep-th]].

[37] J. Isenberg and M. Jackson, "Ricci flow of locally homogeneous geometries on closed manifolds", J. Diff. Geom. 35 (1992) 723.

[38] G. Darboux, "Mémoire sur la théorie des coordonnées curvilignes et des systèmes orthogonaux", Ann. Ec. Normale Supér. 7 (1878) 101.

[39] G.-H. Halphen, "Sur un système d'équations différentielles", C.R. Acad. Sc. Paris 92 (1881) 1001; "Sur certains systèmes d'équations différentielles", C.R. Acad. Sc. Paris 92 (1881) 1004.

[40] L.A. Takhtajan, "A simple example of modular forms as tau functions for integrable equations", Theor. Math. Phys. 93 (1992) 1308.

[41] M.F. Atiyah and N.J. Hitchin, "Low energy scattering of non-abelian monopoles", Phys. Lett. A107 (1985) 21; *The Geometry and Dynamics of Magnetic Monopoles*, Porter Lectures, Princeton University Press, Princeton, 1988.

[42] G.W. Gibbons and N.S. Manton, "Classical and quantum dynamics of BPS monopoles", Nucl. Phys. B274 (1986) 183.

[43] Y. Nutku and P. Baekler, "Homogeneous, anisotropic three–manifolds of topologically massive gravity", Ann. Phys. 195 (1989) 16.

[44] G. Calcagni, "Cosmology of the Lifshitz universe", JHEP 0909 (2009) 112 [arXiv:0904.0829 [hep-th]].

[45] E. Kiritsis and G. Kofinas, "Hořava–Lifshitz cosmology", Nucl. Phys. B821 (2009) 467 [arXiv:0904.1334 [hep-th]].

[46] R. Brandenberger, "Matter Bounce in Hořava–Lifshitz Cosmology", Phys. Rev. D80 (2009) 043516 [arXiv:0904.2835 [hep-th]].

[47] G.W. Gibbons and S.W. Hawking, "Classification of gravitational instanton symmetries", Commun. Math. Phys. 66 (1979) 291.

[48] G.W. Gibbons, S.W. Hawking and M.J. Perry, "Path integrals and the indefiniteness of the gravitational action", Nucl. Phys. B138 (1978) 141.

[49] A. Kehagias and K. Sfetsos, "The black hole and FRW geometries in non-relativistic gravity", Phys. Lett. B678 (2009) 123 [arXiv:0905.0477 [hep-th]].

[50] H. Lu, J. Mei and C.N. Pope, "Solutions to Hořava gravity", Phys. Rev. Lett. 103 (2009) 091301 [arXiv:0904.1595 [hep-th]].

[51] E. Kiritsis and G. Kofinas, "On Hořava–Lifshitz black holes" [arXiv:0910.5487 [hep-th]].

[52] M. Gürses, "Killing vector fields in three dimensions: a method to solve massive gravity field equations" [arXiv:1001.1039 [gr-qc]].

[53] D.K. Chow, C.N. Pope and E. Sezgin, "Classification of solutions in topologically massive gravity" [arXiv:0906.3559 [hep-th]].

[54] R. Bach, "Zur Weylschen Relativitätstheorie und der Weylschen Erweiterung des Krümmungsbegriffs", Math. Zeitschr. 9 (1921) 110.

[55] E. Calabi, "Extremal Kähler metric" in *Seminar on Differential Geometry*, ed. S.-T. Yau, Annals of Mathematical Studies, 102, Princeton University Press, Princeton, 1982.

[56] E.A. Bergshoeff, O. Holm and P.K. Townsend, "Massive gravity in three dimensions", Phys. Rev. Lett. 102 (2009) 201301 [arXiv:0901.1766 [hep-th]].

[57] I. Bakas and C. Sourdis, work in progress.

Bibliographie

[1] R.M. Wald, "General Relativity" (University of Chicago, 1984) ; S.W. Hawking et G.F.R. Ellis, "The large-scale structure of space-time" (Cambridge, 1973).

[2] J. Polchinski, "String Theory", Vol. 1 & 2, (Cambridge University press, 2001)

[3] A. Perez, "Introduction to loop quantum gravity and spin foams", gr-qc/0409061 ; C. Rovelli, "Quantum Gravity" (Cambridge Monographs on Mathematical Physics, 2005)

[4] A. Connes, "Noncommutative Geometry", Academic Press, San Diego, CA, 1994

[5] D. Joyce, "Lectures on Calabi-Yau and special Lagrangian geometry", arXiv :math/0108088

[6] P. Ginsparg, "Applied Conformal Field Theory", arXiv :hep-th/9108028

[7] A. W. Peet, “TASI lectures on black holes in string theory,” arXiv :hep-th/0008241.

[8] J. M. Maldacena, *Prepared for Theoretical Advanced Study Institute in Elementary Particle Physics (TASI 2002) : Particle Physics and Cosmology : The Quest for Physics Beyond the Standard Model(s), Boulder, Colorado, 2-28 Jun 2002*

[9] F. Bourliot, *work in progress*

[10] J. Zuntz, T. Zlosnik, P.G. Ferreira, G. Starkman et F. Bourliot, " Vector field models of modified gravity adn the dark field sector," arXiv :1002.0849 [astro-ph.CO]

[11] F. Bourliot, P. G. Ferreira, D. F. Mota, C. Skordis, "The cosmological behavior of Bekenstein's modified theory of gravity", Phys.Rev.D **75** :063508,2007

[12] F. Bourliot, C. Kounnas and H. Partouche, "Attraction to a radiation-like era in early superstring cosmologies," Nucl. Phys. B **816** (2009) 227 [arXiv :0902.1892 [hep-th]].

[13] F. Bourliot, J. Estes, C. Kounnas and H. Partouche, "Cosmological Phases of the String Thermal Effective Potential,” Nucl. Phys. B **830** (2010) 330 [arXiv :0908.1881 [hep-th]].

[14] F. Bourliot, J. Estes, C. Kounnas and H. Partouche, "Thermal and quantum induced early superstring cosmology," arXiv :0910.2814 [hep-th], *accepted for publication by NOVA publishers.*

[15] F. Bourliot, J. Estes, P. M. Petropoulos and Ph. Spindel, "Gravitational instantons, self-duality and geometric flows," Phys. Rev. D **81** (2010) 104001 [arXiv :0906.4558 [hep-th]].

[16] F. Bourliot, J. Estes, P. M. Petropoulos and Ph. Spindel, "G3-homogeneous gravitational instantons," Class. Quant. Grav. **27** (2010) 105007 [arXiv :0912.4848 [hep-th]].

[17] P. Horava, "Membranes at Quantum Criticality", JHEP **0903**, 020 (2009) [arXiv :0812.4287, hep-th] ; P. Horava, "Quantum Gravity at a Lifshitz Point", Phys. Rev. D **79** (2009) 084008 [arXiv :0901.3775, hep-th]

[18] I. Bakas, F. Bourliot, D. Lust and M. Petropoulos, "Mixmaster universe in Horava-Lifshitz gravity," Class. Quant. Grav. **27** (2010) 045013 [arXiv :0911.2665 [hep-th]].

[19] I. Bakas, F. Bourliot, D. Lust and M. Petropoulos, "Geometric flows in Horava-Lifshitz gravity," JHEP **1004** (2010) 131 [arXiv :1002.0062 [hep-th]].

[20] J. Moffat, "Reiventing Gravity", (HarperCollins, 2008)

[21] P. Fayet, S. Ferrara, "Supersymmetry", Phys.Rept.32 :249-334,1977

[22] A. Bilal, "Introduction to Supersymmetry", hep-th/0101055, J. wess & J. Bagger "Supersymmetry and Supergravity" (Princeton, 1992)

[23] J. Scherk et J. H. Schwarz, "Spontaneous breaking of supersymmetry through dimensional reduction", Phys. Lett. B **82** (1979) 60 ; C. Kounnas et B. Rostand, "Coordinate dependent compactifications and discrete symmetries", Nucl. Phys. B **341** (1990) 641.

[24] F. Gliozzi & al., "Supersymmetry, Supergravity Theories And The Dual Spinor Models", Nucl. Phys. B122, 253-290, 1977

[25] D. Gross, J. Harvey, E. Martinec et R. Rohm, Nucl.Phys. **B256** (1985) 253 ; ibid. **B267** (1986) 75.

[26] T. Clifton et P.G. Ferreira, "Archipelagian Cosmology", astro-ph.CO :0907.4109

[27] S. Perlmutter et al., "Measurements of Omega and Lambda from 42 High-Redshift Supernovae", Astrophysical Journal, 517, 565-586 (1999), astro-ph/9812133 ; A.G. Riess et al., "Observational Evidence from Supernovae for an Accelerating Universe and a Cosmological Constant", Astronomical Journal, 116, 1009-1038 (1998), astro-ph/9805201

[28] J. J. Atick et E. Witten, "The Hagedorn transition and the number of degrees of freedom of string theory", Nucl. Phys. B **310** (1988) 291.

[29] R.H. Brandenberger, "String Gas Cosmology", Progress of Theoretical Physics, Vol. 111, No. 4, 2004

[30] E. Kiritsis, "String Theory in a Nutshell" (Princeton, 2007)

[31] L.Dixon & al. "Moduli dependence of string loop corrections to gauge coupling constants", Nuclear Physics B, Vol. **355**, (1991), 649-688

[32] C. Kounnas, H. Partouche, "Instanton transition in thermal and moduli deformed de Sitter cosmology," Nucl. Phys. B **793** (2008) 131 [arXiv :0705.3206 [hep-th]] ; C. Kounnas, H. Partouche, "Inflationary de Sitter solutions from super-

strings," Nucl. Phys. B **795** (2008) 334 [arXiv :0706.0728 [hep-th]] ; T. Catelin-Jullien, C. Kounnas, H. Partouche and N. Toumbas, "Thermal/quantum effects and induced superstring cosmologies," Nucl. Phys. B **797** (2008) 137 [arXiv :0710.3895 [hep-th]] ;

T. Catelin-Jullien, C. Kounnas, H. Partouche and N. Toumbas, "Thermal and quantum superstring cosmologies," Fortsch. Phys. **56** (2008) 792 [arXiv :0803.2674 [hep-th]] ;

T. Catelin-Jullien, C. Kounnas, H. Partouche and N. Toumbas, "Induced superstring cosmologies and moduli stabilization," Nucl. Phys. B **820** (2009) 290 [arXiv :0901.0259 [hep-th]].

[33] V.V. Gorbatsevich, "Three dimensional homogeneous spaces", Sibirskii Matematicheskii Zhurnal, Vol. 18, No. 2, 280 – 293, March-April, 1977.

[34] P. Scott, "The geometries of 3-manifolds," Bull. London Math. Soc. **15** (1983) 401.

[35] W. Thurston, "Three-dimensional manifolds, Kleinian groups, and hyperbolic geometry," Bull. Amer. Math. Soc. (N.S.) **6** (1982) 357.

[36] J. Isenberg and M. Jackson, "Ricci flow of locally homogeneous geometries on closed manifolds," J. Differential Geometry **35** (1992) 723.

[37] L. Bianchi, "On three-dimensional spaces which admit group of motions," Mem. Soc. It. Della Sc. (Dei XL) **11** (1897) 267.

[38] M.P. Ryan and L.C. Shepley, "Homogeneous Relativistic Cosmologies," (Princeton series in Physics, 1975)

[39] A.A. Belavin et al. "Pseudoparticle Solutions of the Yang-Mills Equations" Phys. Lett. 76B. 433-435.

[40] G.W. Gibbons and C.N. Pope, "The positive action conjecture and asymptotically Euclidean metrics In quantum gravity," Commun. Math. Phys. **66** (1979) 267.

[41] T. Eguchi, P.B. Gilkey and A. J. Hanson, "Gravitation, gauge theories and differential geometry," Phys. Rept. **66** (1980) 213.

[42] C.W. Gibbons et S.W. Hawking, "Classification Of Gravitational Instanton Symmetries" Commun. Math. Phys. **66**, 291-310 (1979)

[43] I. Bakas, D. Orlando et P.M. Petropoulos, "Ricci flows and expansion in axion-dilaton cosmology", hep-th/0610281 ; K. Sfetsos, *u.w*

[44] V.A. Belinskii & al. ,"Asymptotically Euclidean Bianchi IX Metrics in Quantum Gravity", Phys. Lett., Vol 76B, No 4, (1978)

[45] G. Darboux, "Mémoire sur la théorie des coordonnées curvilignes et des systèmes orthogonaux," Ann. Ec. Normale Supér. **7** (1878) 101.

[46] G.-H. Halphen, "Sur un système d'équations différentielles," C.R. Acad. Sc. Paris **92** (1881) 1001.

[47] G.-H. Halphen, "Sur certains systèmes d'équations différentielles," C.R. Acad. Sc. Paris **92** (1881) 1004.

[48] M. F. Atiyah and N. J. Hitchin, Phys. Lett. 107A (1985), 21 ; Phil. Trans. R. Soc. London 315A (1985), 459.

[49] G. Perelman, "The entropy formula for the Ricci flow and its geometric applications," math/0211159[math.DG].

[50] A.U.O Kisişel, Ö. Sarioğlu et B. Tekin, "Cotton Flow," Class. Quant. Grav. **25** (2008) 165019 [arXiv :0803.1603 [hep-th]].

[51] Numerical Recipes, *http ://www.nr.com/*

[52] D. Lorenz, "Gravitational Instanton Solutions for Bianchi types I-IX " Acta Physica Polonica **B**, Vol. B14 (1983)

[53] A.H. Taub, "Empty space-times admitting a three parameter group of motions," Annals Math. **53** (1951) 472.

[54] B. Chow and D. Knopf, "The Ricci flow : an introduction," Mathematical Surveys and Monographs **110** (2004) 630.

[55] T. Eguchi and A.J. Hanson, "Asymptotically flat selfdual solutions to Euclidean gravity," Phys. Lett. **74B** (1978) 249.

[56] T. Eguchi and A.J. Hanson, "Selfdual solutions to Euclidean gravity," Annals Phys. **120** (1979) 82.

[57] S. Carlip, "Quantum Gravity in 2+1 Dimensions : The Case of a Closed Universe"
`http://www.livingreviews.org/lrr-2005-1`

[58] C. Charmousis, G. Niz, A. Padilla and P.M. Saffin, "Strong coupling in Horava gravity," arXiv :0905.2579 [hep-th].

[59] C.W. Misner, "Mixmaster universe", Phys.Rev.Lett. 22 (1969) 1071.

[60] M. Milgrom, "A modification of the Newtonian dynamics - Implications for galaxies," *ApJ*, **270**, 365 (1983)

[61] J.D. Bekenstein, "Relativistic gravitation theory for the MOND paradigm," *Phys. Rev. D* **70**, 083509 (2004)

[62] N.E. Mavromatos, M. Sakellariadou & M.F. Yusaf, "Can TeVeS avoid Dark Matter on galactic scales ?" Phys. Rev. D 79, 081301(R) (2009)

[63] T.G Zlosnik, P.G Ferreira, G.D Starkman, "Modifying gravity with the Aether : an alternative to Dark Matter," Phys.Rev.D75 :044017,2007

[64] M. Milgrom, "New Physics at Low Accelerations (MOND) : an Alternative to Dark Matter", arXiv :0912.2678 [astro-ph.CO]